eman ta zabal zazu

Universidad del País Vasco

Euskal Herriko Unibertsitatea

Departamento de Fisiología

Facultad de Medicina y Enfermería

The role of TREM2 receptor in cholestasis and fibrosis-associated hepatocellular carcinoma (HCC)

Tesis presentada por

IBONE LABIANO CIRIZA

Donostia-San Sebastián

2020

The role of TREM2 receptor in cholestasis and fibrosis-associated hepatocellular carcinoma (HCC)

Tesis presentada por

Ibone Labiano Ciriza

Para la obtención del título de doctor en

Investigación Biomédica **por la**

Universidad del País Vasco/Euskal Herriko Unibertsitatea

Tesis dirigida por

Dra. Dña. María Jesús Perugorria Montiel

Dr. D. Jesús María Bañales Asurmendi

Ibone Labiano Ciriza was funded by the Gobernment of the Basque Country (PRE_2016_1_0152) for the entire PhD duration. Additionally, she received founding for the short stay by the “Egon Labur” program, also from the Basque Government (EP_2019_1_0005).

Universidad del País Vasco Euskal Herriko Unibertsitatea

NAZIOARTEKO BIKAINTASUN CAMPUSA
CAMPUS DE EXCELENCIA INTERNACIONAL

TESI ZUZENDARIAREN BAIMENA TESIA AURKEZTEKO	AUTORIZACIÓN DEL/LA DIRECTORA/A DE TESIS PARA SU PRESENTACIÓN

Zuzendariaren izen-abizenak /Nombre y apellidos del/la director/a:

Dra. María Jesús Perugorria Montiel

IFZ /NIF: **33441140-Z**

Tesiaren izenburua / Título de la tesis:

The role of TREM2 receptor in cholestasis and fibrosis-associated HCC

Doktorego programa / Programa de doctorado:

Programa de Doctorado en Investigación Biomédica

Doktoregaiaren izen-abizenak / Nombre y apellidos del/la doctorando/a: **Ibone Labiano Ciriza**

Unibertsitateak horretarako jartzen duen tresnak emandako ANTZEKOTASUN TXOSTENA ikusita, baimena ematen dut goian aipatzen den tesia aurkez dadin, horretarako baldintza guztiak betetzen baititu.

Visto el INFORME DE SIMILITUD obtenido de la herramienta que a tal efecto pone a disposición la universidad, autorizo la presentación de la tesis doctoral arriba indicada, dado que reúne las condiciones necesarias para su defensa.

Tokia eta data / Lugar y fecha: **Donostia-San Sebastian a 26 octubre 2020**

Sin. / Fdo.: Tesiaren zuzendaria / El/La director/a de la tesis

Universidad del País Vasco Euskal Herriko Unibertsitatea

NAZIOARTEKO BIKAINTASUN CAMPUSA
CAMPUS DE EXCELENCIA INTERNACIONAL

TESI ZUZENDARIAREN BAIMENA TESIA AURKEZTEKO	AUTORIZACIÓN DEL/LA DIRECTORA/A DE TESIS PARA SU PRESENTACIÓN

Zuzendariaren izen-abizenak /Nombre y apellidos del/la director/a:

Dr. Jesús María Bañales Asurmendi

IFZ /NIF: **72698733-B**

Tesiaren izenburua / Título de la tesis:

The role of TREM2 receptor in cholestasis and fibrosis-associated HCC

Doktorego programa / Programa de doctorado:

Programa de Doctorado en Investigación Biomédica

Doktoregaiaren izen-abizenak / Nombre y apellidos del/la doctorando/a: **Ibone Labiano Ciriza**

Unibertsitateak horretarako jartzen duen tresnak emandako ANTZEKOTASUN TXOSTENA ikusita, baimena ematen dut goian aipatzen den tesia aurkez dadin, horretarako baldintza guztiak betetzen baititu.

Visto el INFORME DE SIMILITUD obtenido de la herramienta que a tal efecto pone a disposición la universidad, autorizo la presentación de la tesis doctoral arriba indicada, dado que reúne las condiciones necesarias para su defensa.

Tokia eta data / Lugar y fecha: **Donostia-San Sebastian a 26 octubre 2020**

Sin. / Fdo.: Tesiaren zuzendaria / El/La director/a de la tesis

AUTORIZACION DEL TUTOR/A DE TESIS

PARA SU PRESENTACION

Dr/a. como Tutor/a de la Tesis Doctoral: **The role of TREM2 receptor in cholestasis and fibrosis-associated hepatocellular carcinoma (HCC)** realizada en el **Programa de Doctorado en Investigación Biomédica** por el Doctorando Don/ña. **Ibone Labiano Ciriza**, y dirigida por la **Dra. María Jesús Perugorria Montiel y** el **Dr. Jesús María Bañales Asurmendi** autorizo la presentación de la citada Tesis Doctoral, dado que reúne las condiciones necesarias para su defensa.

En _____ a _____ de _____ de

EL/LA TUTOR/A DE LA TESIS

Fdo.:

AUTORIZACIÓN DE LA COMISIÓN ACADÉMICA DEL PROGRAMA DE DOCTORADO

La Comisión Académica del **Programa de Doctorado en Investigación Biomédica** en reunión celebrada el día _____ de _____ de 20___,

ha acordado dar la conformidad a la presentación de la Tesis Doctoral titulada: **The role of TREM2 receptor in cholestasis and fibrosis-associated hepatocellular carcinoma (HCC)** dirigida por la **Dra. María Jesús Perugorria Montiel y el Dr. Jesús María Bañales Asurmendi** y presentada por Dña. **Ibone Labiano Ciriza** adscrita al Departamento de **Fisiología**.

En _____a _____de _____de _____

EL/LA RESPONSABLE DEL PROGRAMA DE DOCTORADO

Fdo.: _____

AUTORIZACIÓN DEL DEPARTAMENTO

CONFORMIDAD DEL DEPARTAMENTO

El Consejo del Departamento de **Fisiología**

en reunión celebrada el día ___ de _____ de _____ ha acordado dar la conformidad a la

admisión a trámite de presentación de la Tesis Doctoral titulada: **The role of TREM2 receptor in cholestasis and fibrosis-associated hepatocellular carcinoma (HCC)** dirigida por **la Dra. María Jesús Perugorria Montiel y el Dr. Jesús María Bañales Asurmendi.**

---

y presentada por **Doña Ibone Labiano Ciriza** ante este Departamento.

En _____ a _____ de _____ de _____

VºBº DIRECTOR/A DEL DEPARTAMENTO

SECRETARIO/A DEL DEPARTAMENTO

Fdo.: _____

Fdo.: _____

ACTA DE GRADO DE DOCTOR O DOCTORA

ACTA DE DEFENSA DE TESIS DOCTORAL

DOCTORANDO/A DON/DÑA. Ibone Labiano Ciriza

TITULO DE LA TESIS: **The role of TREM2 receptor in cholestasis and fibrosis-associated hepatocellular carcinoma (HCC)**

El Tribunal designado por la Comisión de Postgrado de la UPV/EHU para calificar la Tesis Doctoral arriba indicada y reunido en el día de la fecha, una vez efectuada la defensa por el/la doctorando/a y contestadas las objeciones y/o sugerencias que se le han formulado, ha otorgado por_____la calificación de:

unanimidad ó mayoría

SOBRESALIENTE / NOTABLE / APROBADO / NO APTO

Idioma/s de defensa (en caso de más de un idioma, especificar porcentaje defendido en cada idioma):

Castellano _____

Euskera _____

Otros Idiomas (especificar cuál/cuales y porcentaje) _____

En _____a _____de _____de _____

EL/LA PRESIDENTE/A,

Fdo.:

Dr/a: _____

EL/LA SECRETARIO/A,

Fdo.:

Dr/a: _____

VOCAL 1º,

Fdo.:

Dr/a: _____

EL/LA DOCTORANDO/A,

Fdo.: _____

ACKNOWLEDGMENTS

I would like to thank the University of the Basque Country (UPV-EHU) and the Basque Government for giving me the opportunity, and also for the funding that enabled me to perform this PhD.

The process of fulfilling a PhD is a long and challenging adventure. Fortunatelly, I was never alone this time and I had the opportunity to learn both professionally and personally from all the people that accompanied me. I want to take this opportunity to thank all of them, because nothing would have been possible without their constant support, understanding and love.

First of all, I would like to thank my directors, Dr. María Jesús Perugorría, ***Matxus****, and Dr. Jesús María Bañales,* ***Txus****, for giving me the opportunity to perform this PhD under your supervision. I want to thank both of you for teaching, guiding and supporting me always during these years. Thank you* ***Matxus****, for all of the hours that we shared in the lab. We lived hard-times together with the revision of the first and the second "Gut", with always one experiment more to do, one graph more to align and one word more to change, but also the excitement and the satisfaction of the well done work after finally publishing both of the papers. I want to thank you for sharing your commitment to science with me and involving me in all your projects, and for always understanding and staying close personally. To you* ***Txus****, I want to thank your endless passion and enthusiasm for science, for always going one step further with all of the ideas that you propose, always trying to make the projects a bit better each day. You translate this energy to the entire group, and you are always good at seeing the best of what each of us can give to the lab, you have created an amazing scientific and human group. Thank you, also, because you are always ready to promote and support all of the members of the lab. I also want to thank Dr. Luis Bujanda,* ***Luis****, for being always ready to help and provide ideas and for trying to keep the clinic and basic areas together.*

I would like to thank very especially all of the members of the ***"Hepato" lab*** *for being part of this adventure from the very beginning to the end. You are an incredible human group and I could never imagine a better team to share all of the good and also not so good moments of the PhD.*

We lived amazing moments during these years, I will never forget all of the hours that we shared in the lab, with the best hits, as you know "sí con nosotros pasas el rato, vas a ser feliz, feliz en Hepato", coffe and lunch times, Friday afternoons in the lab, when everything could happen, and it did indeed happen, all of the jokes, tales and laughter that made a bad day look better. Our endless conversations trying to make things better in the lab and in the world generally, hypothesizing about our experiments and our projects, I want to thank you all for that, because there is probably a bit of all of you in this PhD manuscript. But we also shared so many moments out of the lab, so many beers, pintxopotes, dinners and also some dances to celebrate and sometimes forget. Our weekend trips to Salamanca, Asturias or Belgium, our sportive moments with the rebufo, the kayak, the bowling afternoon or the paddle surf. All of our trips to visit members of the lab to Paris, Padua, Aachen, the congresses in Oslo, Madrid, Vienna, Lisbon, Prague…and an endless list of memories that could go on and on for pages, thank you for sharing all of this with me.

*Thanks to **Bikinis**, Laura, Paula and Ainhoa. I think you are the soul and the backbone that maintains the lab together and alive. Thank you for organizing the lab, for being the everyday strength and for always wanting to make things a bit better. Because we laughed, cried and grew up together during these years. Thank you for listening when I needed to talk and for understanding when I was suffering, for all of your support words. I will never forget the crazy Fridays, and you telling me the gossips, sometimes I was not the last one to know thanks to you. **Laura**, we shared many hours in the last months in the pecera, I admire you so much for your resilience and your capacity to learn and find your way to manage with everything. I think you have become a referent for everybody in the lab, to me, you have transmitted your strength and motivation in the last weeks of the PhD, and I thank you for helping me to maintain my confidence. **Paula**, we have shared every moment in this adventure, as we started and finished at the same time, thank you for having always the right answer, for sharing your impressions and emotions with me when we felt we were alone against the PhD, and for being the mirror to look at. **Ainhoa**, thank you for living and sharing everything with us, for your intensity, for giving everything you have to the lab and to us, for always being ready to leave whatever you were doing to listen and give a hug in a bad moment.Thank you also for the moments that we shared in the congreses, they were much more fun thanks to you, for your creativity in the jokes, the thesis gifts and the choreographies you taught us, anyway I think I need 4 years more to master break dance xD.*

***Aloña,** it has been a pleasure to work with you, I will miss so much having you by my side. I will miss the fun part of working with you, all of your stories and gossips about the Basque celebrities ;P, all of the contests we participated in Gaztea mornings, and for wanting to bring me hiking to Txindoki or any other Mountain, even in the last months of the PhD, when I kept saying no to everything and everybody. I was supposed to teach you in the lab, but I think I learnt much more from you than you did from me during these years. I will also miss working with you because we formed a good team professionally, I will miss confirming things together, discussing about immunology, sharing our impressions after a meeting, you asking me questions that I could never answer, and you being so patient with me in the last months. I know that, at some moments, things may look complicated and also frustrating during the PhD, but you are an excellent professional and a better person, and I know everything will work well for you. Thank you for everything =)*

*Arkaitz, **Pedro**, I am so glad that we managed to do things on time for your first contract. Since then, you have become an essential support for me in the lab. I will miss the hours that we shared training for the sleeping beauty, your expertise and your passion in science, which helped me staying motivated when experiments were not working as expected. But above everything, I want to thank you for your friendship, for always being ready to share and listen, for being so patient with me and for all of the fun we had in total training. Thank you also for introducing me to the "UEG family, engatusando" I learnt a lot rehearsing for the presentations and had much fun that year in Vienna.*

Javi, thank you for all of your jokes, I think you managed to make me laugh everyday in the lab. Thank you also, for sharing your good taste in music, in those Friday afternoons with Tina Turner, Temptations and Pink Floyd. I also want to thank you for your support words, and for sometimes showing me another point of view that made things look different.

Irene, my dear influenzer x). I will miss so much when you tried to update me in the social media and the new vocabulary. Thank you for being always ready to accept new challenges, and for wanting to contribute to make things a bit better in the lab.

Nuno, tahnk you for being so calm and patient and for being always ready to help. It was always a pleasure to work with you and, although your photos were too artistic, I had much fun with you in that trip to Italy!

Anne, thank you for being patient with me in the last monts of the PhD, and for being ready to help with the experiments every time I needed. I am sure you will have a fruitful experience in the lab.

Many of the members of the lab that helped and supported me during this adventure already left to continue with other profresional projects elsewere. I want to thank very specially Aitor, because we shared more tan 2 years of this adventure, it was amazing working by your side, we shared countless moments in the animal facility, in the histology hood, writing reviews... I learned new things from you everyday and I really miss the way you managed to keep relaxed in the worst moments, which always helped to balance my stress. But I specially want to thank you for your friendship during these years, for taking care of me and for the moments that we shared outside the lab. Alvaro, when we knew you were leaving I could not imaging the lab without you, we have survived, more or less, but I miss you every day, your jokes and your humor, you managed to make the lab, the working place, I place to have fun and enjoy every day work. I miss sharing congresses with you and having you there, as a person to whom you could ask anything and would always look for an answer. Oihane, you left the lab 3 years ago, but you still are, and always will be, a referent for everybody. We still look through your lab books when we do not know the answer. You taught me everything in the lab, and although many times I felt exhausted after 4 hours in the cell culture room, I always enjoyed so much working by your side. Thank you for your patience, for being and excellent teacher and for your friendship. Ander, for your revolutionary spirit, because you always kept trying to change the world and resisted to accept that the world could change you. I miss the endless conversations with you trying to fix the world. Puyi, I miss the times when you learnt Spanish and we all wanted to help, it was fun, thank you for the moments that we shared. I also want to thank Patri for building the lab and teaching me when I first arrived. Finally, I want to thank people that were in the lab for short periods, Mirian, Elisa, Nerea, Mariana, Francesca you also contributed to the good atmosphere in the lab and I thank you for your kindness and support.

I also want to take this opportunity to thank people from other laboratories and areas of the Biodonostia health research institute, especially, thanks to Jaione, Garazi, Jon,

Ander, Mikel, Claudia, Alba, Ana Aiastui, Lucia, Sandra, the animal facility staff, *and all of PhD students, because our research centre is small and we are always in constant contact, I feel that you have also been part of this PhD. Thank you for always been ready to help and for your kindness, because all of you make Biodonostia a nice place to work at.*

I would like to thank the ***group of Dr. Tomm Luedde*** *in Uniklinik Aachen for hosting me during my international stay, I want to thank all of the group for making me feel at home and for including me in everything since the very first day. To* ***Dr. Luedde***, ***Tom***, *for making things easy for me and for sharing his enthusiasm for research and all of his excellent ideas with me. To* ***Mihael*** *for answering all of my, sometimes stupid, questions and for all of his jokes. Thanks to* ***Katrin***, *for all of our endless conversation about science and life, for the coffees we shared in the "Cafe Grün". To* ***Jakob***, *probably one of the most brilliant scientists I have ever met, I enjoyed very much jogging with you and the conversation. I hope you both can visit here sometime, in better times.*

But of course, the PhD period is much more than laboratory life, and I also want take this opportunity to specially thank all of the people outside the lab that supported me and shared these adventure with me.

First of all I want to thank my family. ***My parents, aita, ama,*** *my sister,* ***Josune*** *,my brother,* ***Xabi*** *and* ***Sarai****. This PhD would not have been possible without your support and love, for being always there, even when you did not understand any of what was going on with the lab and the PhD. Thank you for being patient and understanding, and because you never stopped trying to help. For taking care of me, for visiting me in Donosti and in Aachen every time I needed to feel you close, even when I was too stubborn to accept your care. I love you so much, in all of you I find the strength to keep going on in the hard times. I also want to thank all of my family, the* ***familia Ciriza****, for their interest in what I was doing, because I always felt their strength when I needed and because they are a very important part of my support. Very especially I want to thank my Grandmother,* ***amatxi****, for being the reason that keeps us all together, for being there, after 88 years, loving us, taking care of all of us and never feeling tired. Thank you for your "comidicas", that made me feel closer to home when I spent the weekend working in Donosti. But specially, for teaching me to be happy and appreciate the small things in life, and to take care of everything and everybody that we love. Everybody that I met during this PhD knows how proud I am of you and being your grandaughter, amatxi, and how you have been one the most important supports during this PhD. I love you.*

I would also like to take this opportunity to rember ***Begoña****, she was the first one who talked to me about women in science, and I will always remember her for the joy and the love with which she shared this ideas.*

Thank you to my ***flatmates****,* ***Markel, Julene, Laura*** *and* ***Leire****. You shared with me different moments of this process but you always have made of the flat a shelter and a home. With all of you I laughed, cried and talked, talked and talked, about life, society,*

science, relationships…I want to believe we fixed the world just a little bit, after all of these years trying. Especially to Julene, for being my other sister, I love you.

To pottokak ;P, ***Irene, Garazi*** *and* ***Leire****, you have been my family in Donosti, you were always ready to listen and help and you were the door to knock at, every time I felt something was not working well, and, somehow, you always managed to find the right words to make me feel better. I also had so much fun with you during these years, I enjoyed so much the short travels and trips that we made and I am so looking forward to Iceland :). Specially, I want to thank* ***Irene****, I think we could fill years with all of the audio messages that we shared during these years. I love you so much, thank you for everything, for being the perfect friend, for giving me so much and teaching me so much.*

To my ***kuadrilla*** *from Iruña, in these strange times I miss so much when we all met for San Fermin, lunch, korrika or any other celebration…Saturday dinners with you were the moment to disconnect from the lab, to leave everything behind and laugh with the gossips you were always ready to tell. I also want to thank your interest in what I was doing; I will never forget how you listened to my rehersal just before my first oral communication in a congress. You made me smile and keep motivated and feel that you were there supporting, every year, when the Nobel Prize was announced and you kept saying I was next x) Maitane even dreamt about it! The great date of the 30th Birthday is getting closer and I promise, now with the PhD finished, I will concentrate in trying to organize our desired trip to celebrate it xD Thank you for loving and supporting me all this time. I also want to thank* ***Sara, Itsaso, Olano****, although we only had the opportunity to meet from time to time, you always made me feel you were there, and I want to thank you for your friendship and your love during all of these years. Thanks also to* ***Iñaki****, you shared part of this adventure with me, took care of me and made me disconnect and forget about everything when I needed.*

I also want to thank ***Joseba Urzela****i for helping me with the version in Basque of this dissertation.*

Quisiera agradecer muy especialmente a mi familia, ***ama, aita, Josune, Xabi y Sarai.*** *Gracias por cuidar de mi y estar ahi siempre que os he necesitado, por que esto no hubiera sido possible sin vosotros. Por todo vuestro amor y por darme mimos, por darmelos aunque últimamente haya sido difícil. Os he echado de menos cada día durante la tesis cuando llegaba al piso de Donosti y no estabais allí. Menos mal que los findes cuando iba a casa siempre conseguiais que cargara pilas, con las comidicas buenas en casa, las salidas de compras, algun que otro intento de escalada, y las salidas al monte, a Tenerife, a Burdeos, a Donosti, a Aachen, nunca habeis dejado de visitarme aunque fuera para verme 10 minutos. Quiero agradeceros también todos vuestros esfuerzos por apoyarme e intentar entender cómo funciona este mundo de la investigación en el que os ha tocado meteros de rebote. Por aguantar y escuchar mi matraca explicandoos la carrera investigadora, predoc, posdoc, jefe de grupo, becas, proyectos, publicaciones, revisions... Gracias especialmente por este ultimo año, con el confinamiento de por medio, gracias, por aguantarme en casa, por las sesiones de hit, total training, Zumba y Taichi, por todas las videollamadas y por mimarme como se pudo en mi cumpleaños confinado. Os quiero muchisimo, asko maite zaituztet.*

También quiero agradecer al resto de mi familia, la ***gran familia Círiza*** *x). Gracias por vuestro interés en lo que hacía, por las Navidades, las comidas y juegos en Anoz y las salidas al monte que hemos compartido. Soys una parte muy importante de mi apoyo y siempre haceis que sienta vuestra fuerza empujándome hacia delante. Eskerrik asko familia maite zaituztet!*

Amatxi, *eres la que nos mantiene a todos unidos. Después de 88 años sigues queriéndonos, animándonos, apoyándonos y mimándonos, y nunca te cansas. Tus comidicas me hacían sentirte cerca, como en casa, cada vez que me quedaba el fin de semana en Donosti trabajando. Has sido uno de los pilares más importantes para mi durante esta tesis y quería agradecerte todo lo que me has transmitido y enseñado durante estos años, a ser feliz con las pequeñas cosas en la vida y a cuidar siempre de la gente que quieres, a ser humilde y sensible, y por trasmitirme esas ganas y energía para afrontarlo todo. Cualquiera que me haya acompañado durante esta aventura sabe lo orgullosa que estoy de ser tu nieta. Te quiero muchisimo, amatxi.*

También quisiera aprovechar esta ocasion para acordarme de ***Begoña****, por que siempre la he tenido muy presente durante esta aventura. Begoña fue la primera persona a la que oí hablar de la mujer en ciencia, de la mujer donde quisiera estar, de la fuerza de las chicas. Por su espíritu luchador, que compartía y trasladaba a todos con su cariño, su amor y su alegría, gracias Begoña por transmitirme todo esto que siempre llevo conmigo.*

Azkenik, eskerrak eman nahi dizkiet nire ***lagun guztiei****, tesiko garaietan irribarrea atera didatelako eta behar nuenean nire ondoan egoteagatik, ni ulertzen eta behar nituen hitzak esaten.*

Iruñako kuadrilari*, oraingo garai arrarotan inoiz baino gehiago faltan botatzen dut elkarrekin planak libre egiten genituenean. San ferminak, bazkariak, mendira ateraldiren bat, herri eta auzoetako jaiak, Luzaide eta ingurura eskapatzen ginean... Larunbateko afarietan tesiko momenturik okerrenetaz deskonektatzea lortzen zenuten, zuen anekdota eta kotilleo guztiekin. Eskerrik asko nire lehenenngo kongresua baino lehen nire ensaioa entzun nahi izateagatik, eta urtero Nobel saria ateratzen zenean, ea ni noizko galdetzen zenutenean, irribarrea ateratzen zenidaten beti, eta jarraitzeko gogoa piztu. Asko maite zaituztet eta asko eskertzen dut zuek beti gertu sentitzea.*

Eskerrak Pottokei, Donostiko lagunak, ***Irene, Garazi, Leire****, nire familia izan zarete Donostin. Zaindu nauzue, entzun eta lagundu abentura honetan. Pirineotara eta Iparraldera egin genituen ateraldietan konpartitu genuen guztiarengatik eta egin genituen barreengatik. Ze gogo Islandiara joateko =). Bereziki* ***Ireneri*** *eskertu nahi diot bere laguntasuna, karreran ezagutu ginenetik pack bat izan garelako, eta gure audio guztiekin urtetako irrati programa bat bete zitekeelako. Ezinbesteko euskarria izan zara niretzat tesi guztian zehar eta eskerrrak eman nahi dizkizut ematen eta irakasten didazun guztiarengatik bueltan ezer eskatu gabe, maite zaitut.*

Pixukideei, ***Julene, Markel, Laura*** *eta* ***Leireri****, momentu desberdinetan kointziditu dugu pixuan, baina denekin bizikidetza ezin hobea izan da. Pixua babesleku egin duzue, egunero iluntzean heldu eta onak eta txarrak partekatzeko tokia. Bizitzaz, zientziaz, gizarteaz eta harremanez hizketan orduak eta orduak egin ditugu eta zuengandik izugarri ikasi dut. Hainbeste saiatu eta gero pentsatu nahi dut mundua pixka bat konpotzea, pixka bat hobea egitea, lortu dugula.*

Bereziki ***Juleneri*** *eman nahi dizkiot eskerrak, nire beste ahizpatxoari =). Elkarrekin bizi izan ditugun lasterketa, bidaia, elkarrizketa, negar eta irribarre guztiengatik. Mila esker beti prest egoteagatik edozertarako, zure indarrarengatik eta momentu zailetan transmititu didazun lasaitasunarengatik. Asko maite zaitut ahizpatxo!*

Mila esker era bai, ***Itsaso, Sara, Olanori,*** *noizbehinka bakarrik kointziditu ahal izan dugu baina beti sentitu zaituztet gertu. Eskerrik asko baita* ***Iñakiri****, elkarrekin bizitakoagatik, ni zaintzeagatik eta deskonektatzen laguntzeagatik behar nuenean.*

Azkenik, ***Joseba Urzelairen*** *laguntza eskertu nahiko nuke, eskerrik asko euskarazko bertsioarekin emandako aholkuengatik.*

ABBREVIATIONS

AASLD	American Association for the Study of the Liver
Abx	Antibiotics
Acta2	Actin alpha 2, smooth muscle
AD	Alzheimer´s disease
aHSCs	Activated hepatic stellate cells
AKT	RAC-alpha serine/threonine-protein kinase
ALS	Amyotrophic lateral sclerosis
ALT	Alanine aminotransferase
ANIT	Alpha-naphtylisothiocyanate
ALP	Alkaline phosphatase
***α*SMA**	Alpha-smooth muscle actin
AST	Aspartate aminotransferase
AU	Arbitrary units
BA	Bile acid
BDL	Bile duct ligation
BSA	Bovine serum albumin
CA	Cholic acid
$CaCl_2$	Calcium chloride
CCA	Cholangiocarcinoma
CEEA	*Comité ético de experimentación animal*
CCL	Chemokine (C-C motif) ligand
CCl_4	Carbon tetrachloride
CD	Cluster of differentiation
CDCA	Chenodeoxycholic acid
cDNA	Complementary deoxyribonucleic acid
CETP	Cholesteryl ester transfer protein
CK19	Cytokeratin 19
Cl-Casp3	Cleaved caspase 3
CNS	Central nervous system
CO_2	Carbon dioxide
COL1A1	Collagen type 1 alpha 1
COPD	Chronic obstructive pulmonary disease
CTGF	Connective tissue growth factor
CXCL1	Chemokine (C-X-C motif) ligand 1
DAB	3,3'-Diaminobenzidine
DAMP	Danger associated molecular pattern
DAP12/ TYROBP	DNAX Adaptor Protein 12 /TYRO protein tyrosine kinase-binding protein
DCA	Deoxycholic acid
DDC	3,5-Diethoxycarbonyl-1,4-dihydrocollidine
DDR	Discoidin domain receptor
DEN	Diethylnitrosamine
dH_2O	Distilled water
DMEM	Dulbecco´s modified eagle medium
DNA	Deoxyribonucleic acid

dNTP	Deoxynucleotide triphosphate
DRC	Ductular reactive cell
DTT	Dithiothreitol
EASL	European Association for the Study of the Liver
ECM	Extracellular matrix
ECL	Enhanced chemiluminescence
EDTA	Ethylenediaminetetraacetic acid
EMT	Epithelial mesenchymal transition
ESI	Electrospray inonization
EtOH	Ethanol
FBS	Fetal bovine serum
FGF15/19	Fibroblast growth factor
FMT	Faecal microbial transplant
FXR	Farnesoid X receptor
GAPDH	Glyceraldehyde-3-phosphate dehydrogenase
GDCA	Glycodeoxycholic acid
GR	Glucocorticoid receptor
GSH	Glutathione
H_2O_2	Hydrogen peroxyde
HBV	Hepatitis B virus
HCC	Hepatocellularcarcinoma
HCl	Hydrogen chloride
HCV	Hepatitis C virus
HDL	High density lipoprotein
Hepes	4-(2-Hydroxyethyl)-1-piperazineethanesulfonic acid
H&E	Haematoxylin and eosin
Hh	Hedgehog
Hmox	Heme oxygenase
HNa_2PO_4	Sodium diphosphate
HPLC	High performance liquid chromatography
HPRT1	Hypoxanthine phosphoribosyltransferase 1
HRP	Horseradish peroxydase
HSCs	Hepatic stellate cells
ICAM1	Intercellular adhesion molecule 1
IHC	Immunohistochemistry
IF	Immunofluorescence
IL	Interleukin
IL6	Interleukin 6
IL8	Interleukin 8
IL17	Interleukin 17
IL33	Interleukin 33
INFγ	Interferon gamma
IgG	Immunoglobulin G
IRAK-M	Interleukin-1 receptor-associated kinase-M
ITAM	Immunoreceptor tyrosine-based activation motif
ITIM	Immunoreceptor tyrosine-based inhibitory motif

IU	International units
JNK	c-Jun N-terminal kinase
KCl	Potassium chloride
KCs	Kupffer cells
LPS	Lipopolysacharide
LSECs	Liver sinusoidal endothelial cells
MAPK	Mitogen-activated protein kinase
MCA	Muricholic acid
MCP1	Monocyte chemoattractant protein 1
Mdr2	Multidrug resistance 2
MELD	Model for end stage liver disease
MMP2	Matrix metalloprotease 2
MyD88	Myeloid differentiation primary response 88
NaCl	Sodium chloride
NAFLD	Non-alcoholic fatty liver disease
NEAA	Non-essential aminoacids
NF-kB	Nuclear factor – kappa B
NOS2	Nitric oxide synthase 2
NLR	NB-LRR-related gene family
NTPD	Nucleoside triphosphate subunit D2
O/N	Overnight
O.Oil	Olive oil
oxLDL	Oxydized low density lipopotrein
PAMP	Pathogen-associated molecular pattern
PBC	Primary biliary cholangitis
PBS	Phosphate buffered saline
PCNA	Proliferating cell nuclear antigen
PCR	Polymerase chain reaction
PDGF	Platelet-derived growth factor
PDL1	Programmed death-ligand 1
PI3K	Phosphoinositide 3 kinase
PLOSL	Lipomembranous osteodysplasia with sclerosing leukoencephalopathy
PM	Portal myofibroblast
PMA	Phorbol 12-myristate 13-acetate
pMLKL	Phosphorylated multilineage kinase like
PRR	Pattern recognition receptor
PSC	Primary sclerosing cholangitis
qRT-PCR	Quantitative reverse transcription polymerase chain reaction
RIP3	Receptor-interacting serine/threonine-protein kinase 3
RIPA	Radioimmunoprecipitation assay
RNA	Ribonucleic acid

RPMI	Roswell park memorial institute medium
RT	Room temperature
S100A4	S100 calcium-binding protein A4
SDS	Sodium dodecyl sulfate
SDS-PAGE	SDS polyacrylamide gel electrophoresis
SEM	Standard error of the mean
SHP	Small heterodimer partner
SHP1	Src homology region 2 domain-containing phosphatase 1
SIGIRR	Single Ig IL1R-related molecule
SR-A	Scavenger receptor A
sTREM	Soluble triggering receptor expressed in myeloid cells
TAA	Thioacetamide
TCA	Taurocholic acid
TDCA	Taurodeoxycholic acid
TGFβ	Transforming growth factor beta
TIMP	Tissue inhibitor of metalloproteinase
TLRs	Toll like receptors
TNF	Tumour necrosis factor
TREM	Triggering receptor expressed in myeloid cells
TREM1	Triggering receptor expressed in myeloid cells 1
TREM2	Triggering receptor expressed in myeloid cells 2
TREML	Triggering receptor expressed in myeloid cells like
TREML1	Triggering receptor expressed in myeloid cells like 1
TREML2	Triggering receptor expressed in myeloid cells like 2
TREML4	Triggering receptor expressed in myeloid cells like 4
***Trem2*$^{-/-}$**	*Trem2* deficient
T-TBS	Tris-buffered saline with 0.1% Tween-20
TUDCA	Tauroursodeoxycholic acid
Tv	Tumour volume
TWEAK	TNF-related weak inducer of apoptosis
UDCA	Ursodeoxycholic acid
USA	United States of America
VEGF	Vascular endothelial growth factor
VLDL	Very low density lipoprotein
WNT	Wingless
WT	Wild type
YAP	Yes-associated protein

TABLE OF CONTENTS-
EDUKIEN TAULA

INTRODUCTION

I.1. Liver physiology and anatomy

The liver is the biggest solid organ in the human body and the most important one in the maintenance of the metabolic homeostasis. This organ carries out essential functions including the synthesis, metabolism, storage and redistribution of a great variety of nutrients. In this regard, thousands of enzymes expressed in the liver are responsible for carbohydrate, lipid, amino acid and nitrogen metabolism. It also serves as a storage site for glucose, lipids, iron and vitamin A. In addition, the liver is responsible for bile production and secretion, as well as for the synthesis and secretion of most of the plasma proteins, including albumins, apolipoproteins, transferrins and fibrinogen. Owing to its anatomical location, the liver is exposed to a wide range of xenobiotics, and it plays a key role in the detoxification of these molecules (1, 2).

The anatomical, functional and structural subunit of the liver is named "the hepatic lobule" (**Figure I.1.**). The hepatic lobule is roughly hexagonal in shape and consists of portal triads and hepatocytes that are arranged radially forming rows around the central vein. The portal triad is located in the vertex of the hepatic lobule and is formed by a branch of the hepatic artery, a branch of the portal vein and a bile duct. Blood carrying nutrients and oxygen drains from the portal triad to the central vein through the hepatic sinusoids; which are located between the hepatocyte rows. Hepatic sinusoids are lined by liver sinusoidal endothelial cells (LSECs), and, in their lumen, they harbour the liver resident macrophage population, named as Kupffer cells (KCs). By contrast, bile is drained in the opposite direction to blood, from the perivenous hepatocytes to the portal triad. The perisinusoidal space or space of Disse is composed of reticular fibres and blood plasma and it is located between hepatocytes and the hepatic sinusoids. The space of Disse is also the location for hepatic stellate cells (HSCs). Here, the metabolic exchange between hepatocytes and blood plasma occurs (1).

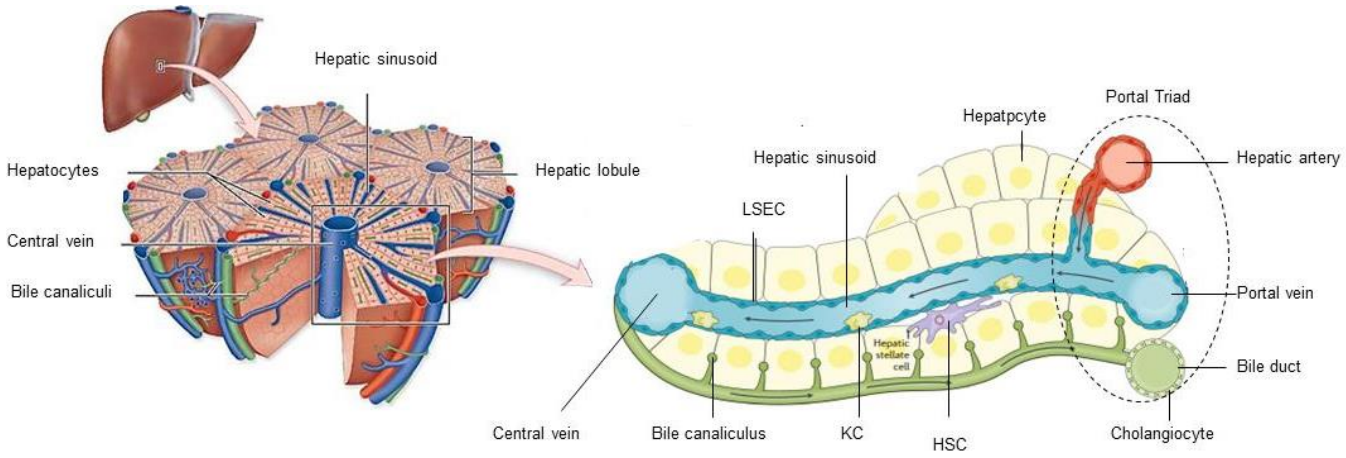

Figure I.1. Anatomical, functional and structural subunit of the liver. The anatomical, functional and structural subunit of the liver, the hepatic lobule, consists of hepatocyte rows organised concentrically towards the central vein and of portal triads. In the vertex of the hepatic lobule the portal triad is found, which consists of a branch of the hepatic artery, a branch of the portal vein, and a bile duct. Blood drains from the portal triad to the central vein via the sinusoids in between the hepatocyte rows. The hepatic sinusoids are lined by LSECs, while KCs are located in the luminal side of the sinusoids. HSCs are found in the space of Disse, the space between the hepatocyte rows and the sinusoids. KC, kupffer cells, HSCs, hepatic stellate cells, LSEC, liver sinusoidal endothelial cells. *[Adapted from Miyajima A et al, 2014 (3)]*.

I.1.1. Parenchymal cells and cholangiocytes

The liver is composed of two types of epithelial cells: hepatocytes and cholangiocytes. Hepatocytes, also named liver parenchymal cells, are hexagonally shaped cells, quiescent in the healthy liver and often bi-nucleated. They constitute the 70-80% of the total liver volume, and account for most of the metabolic and detoxifying functions of the liver (1). Hepatocyte functions are heterogeneously distributed along the hepatic lobule in a phenomenon termed liver zonation (4). Differential accessibility to nutrients, oxygen and morphogens results in the spatial regulation of more than 50% of the genes expressed on hepatocytes, which show a zonated expression pattern.

Cholangiocytes are the cells lining the bile ducts, and represent the 3-5% of the total liver volume, yet these cells account for up to the 30-40% of the total bile flow and participate in its alkalinisation and fluidisation (5). In order to fulfil these functions, cholangiocytes express a wide variety of receptors and transporters (6). Importantly, many of these receptors are found in the primary cilium. This sensory organelle protrudes into the bile duct lumen detecting changes in bile flow and composition and subsequently transmitting these signals into the cell, to further regulate bile composition (7).

I.1.2. Bile formation and drainage

Bile formation and drainage is the result of a complex interplay between hepatocytes, cholangiocytes and intestinal cells and microbiota. Bile is a vital biofluid composed of water, bile salts, bilirubin, lipids, electrolytes, proteins and xenobiotics (8). Bile is produced in the liver and it fulfils important functions including the emulsion of dietary fat, the immunological protection from gut-derived bacteria and the excretion of toxic lipophilic substances (6).

The most important components in bile are bile salts or bile acids (BAs). BAs are synthesised in a complex enzymatic network involving the liver and the intestinal microbiota (9). (**Figure I.2.**). BA synthesis initiates mainly in pericentral hepatocytes with the conversion of cholesterol into primary BAs. The rate limiting enzyme in this pathway is cytochrome P450 7A1 (CYP7A1) and its activity is tightly controlled in response to physiological and pathological fluctuations of BA concentrations (10). Free BAs show an amphipathic structure, which enables them to diffuse across cellular membranes (11). But free BAs can be subjected to conjugation with glycine or taurine into peroxisomes. BA conjugation increases their hydrophobicity, preventing their passive diffusion across cellular membranes. In humans, most of the BAs are conjugated with glycine and taurine in a 3:1 relation, while in mice taurine-conjugated BAs are the most abundant conjugated species (9, 12).

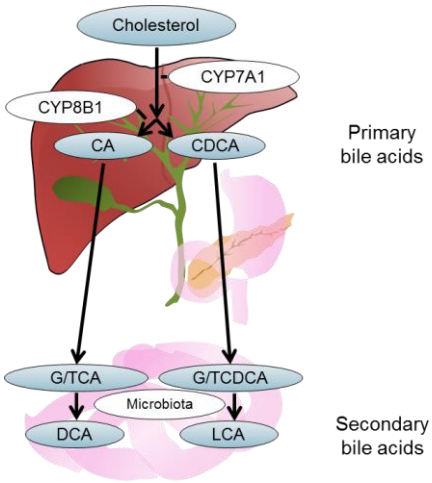

Human		Mouse	
Primary, free	**Secondary, free**	**Primary, free**	**Secondary, free**
CA, CDCA	DCA, LCA, UDCA	CA, α and βMCA, CDCA, UDCA	DCA, ωMCA
Primary, conjugated	**Secondary, conjugated**	**Primary, conjugated**	**Secondary, conjugated**
G/TCA, G/TCDCA	G/TDCA, G/TLCA, G/TUDCA	TCA, α and βTMCA, TCDCA, TUDCA	TDCA, ωTMCA

Figure I.2. BAs biosynthetic pathway and most common BA species in human and mouse. *Right panel*. Cholesterol is the molecular precursor of BAs, which is converted into the primary BAs CA and CDCA, being CYP7A1 the main rate limiting enzyme of the pathway. Primary BAs are then subjected to conjugation with glycine or taurine in the human liver and mainly with taurine in the mouse liver. Once on the intestine, microbiota further modifies these BAs to form secondary BAs, which upon reabsorption can also be conjugated in the liver. *Left panel*. Classification of the most abundant BA species in human and mouse. CA, cholic acid; CDCA, chenodeoxycholic acid; CYP7A1, cytochrome P450 family 7 subfamily A member 1; CYP8B1, cytochrome P450 family 8 subfamily B member 1; DCA, deoxycholic acid; G/TCA, glyco/taurocholic acid; G/TCDCA glyco/taurochenodeoxycholic acid; G/TLCA, glycol/tauro lithocholic acid; G/T, glycol/tauroursodeoxycholic acid; LCA, lithocholic acid; MCA, muricholic acid; TMCA, tauromuricholic acid; UDCA, ursodeoxycholic acid *[Adapted from Qi Y et al, 2015(13) , and Li J et al, 2019(12)]*.

Both conjugated and unconjugated primary BAs are secreted through the hepatocyte canaliculi, located between adjacent hepatocytes. Then they are drained through the canals of Hering, which represent the connection between the hepatocyte canaliculi and the biliary tree and the niche of hepatic progenitor cells (HPCs) (14). Thereafter, bile enters the biliary tree, which is lined by cholangiocytes and extends from the canals of Hering to the main bile duct. From the canals of Hering to the common bile duct, the segment of the biliary tree increases and cells lining the bile ducts also vary in morphology and function (15). Overall, the biliary tree is composed of both intra and extrahepatic bile ducts (**Figure I.3.**) (8).The intrahepatic bile ducts include those from the canals of Hering until the segmental bile ducts, while the extrahepatic bile ducts comprise the hepatic ducts, the gallbladder and the common bile duct (16).

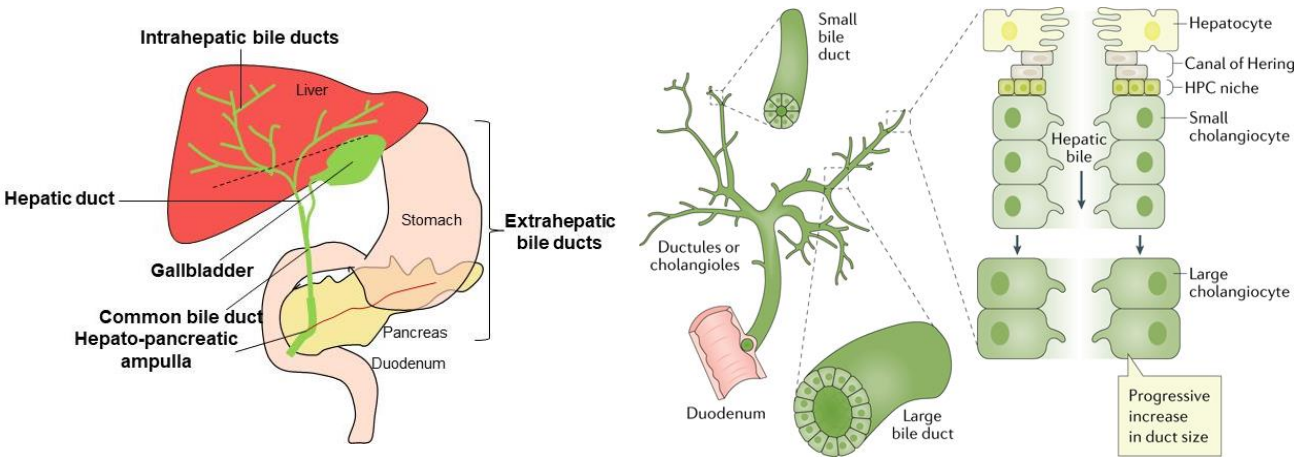

Figure I.3. The anatomy of the biliary tree. *Left panel***.** Bile drains from the hepatocyte canaliculi to the duodenum via the biliary tree. Intrahepatic ducts extend from the canaliculi to the common hepatic bile duct, while extrahepatic bile ducts comprise the hepatic ducts, the gallbladder and the common bile duct. *Right panel*. The canals of Hering represent the connecting structure between hepatocytes and bile ducts. The biliary tree is a complex structure lined by cholangiocytes. Bile ducts augment in segment from the canals of Hering to the common bile duct and cholangiocytes lining them also vary in morphology and function. HPC, hepatic progenitor cell *[Adapted from Banales JM et al, 2019 (6)]*.

Once in the intestine, most bile components, including BAs, are reabsorbed in the terminal ileum and transported back to the hepatocytes via the portal vein. This process is known as the "enterohepatic circulation" and accounts for the recycle of around 95% of total BAs (17). Only 5% of the newly synthesised BAs reach the colon, where they are exposed to intestinal microbiota, which further modify their structure, thereby generating the secondary BAs and contributing to the plethora of BA species naturally occurring in different organisms (18). In the colon, BAs can be reabsorbed and reenter the circulating BA pool or be excreted in faeces (19) BAs can also be recycled via the "cholehepatic shunt", a process by which cholangiocytes reabsorb BAs that are then further uptaken by hepatocytes, to be again secreted into bile (20).

Besides their action as fat emulsifiers, BAs also fulfil other critical functions including immunological protection from gut-derived bacteria; additionally, they also regulate diverse pathophysiological processes owing to their ability to bind and activate specific receptors (21). In this regard, BAs bind to and activate nuclear receptors including farnesoid X receptor (FXR, encoded by *NR1H4*), pregnane X receptor (PXR, encoded by *NR1I2*), vitamin D_3 receptor (VDR, encoded by *NR1I3*) and constitutive androstane receptor (CAR, encoded by *NR1I3*). Additionally, BAs can also bind the plasma membrane G protein coupled receptor TGR5 (21).

BAs regulate their own synthesis in hepatocytes. In the presence of augmented BA concentration in the intestine, BAs that are reabsorbed by the enterohepatic circulation enter hepatocytes and bind to FXR, which induces the expression of short heterodimer partner (SHP), which acts as a transcriptional inhibitor of CYP7A1 and, therefore, diminishes BA synthesis (10). FXR activation by chenodeoxycholic acid (CDCA), cholic acid (CA) as well as synthetic agonists, exerts cytoprotective and anti-cholestatic responses in cholangiocytes (22). Moreover, FXR is expressed in enterocytes, upon BA binding, enterocytes produce and secrete fibroblast growth factor 15 (in rodents)/19 (in human) (FGF15/19) which acts as a hormone in hepatocytes to down-regulate CYP7A1 (**Figure I.4**). (23) Of note, selective activation of intestinal FXR is sufficient to protect the liver from different forms of cholestasis (24) and hepatocarcinogenesis (25).

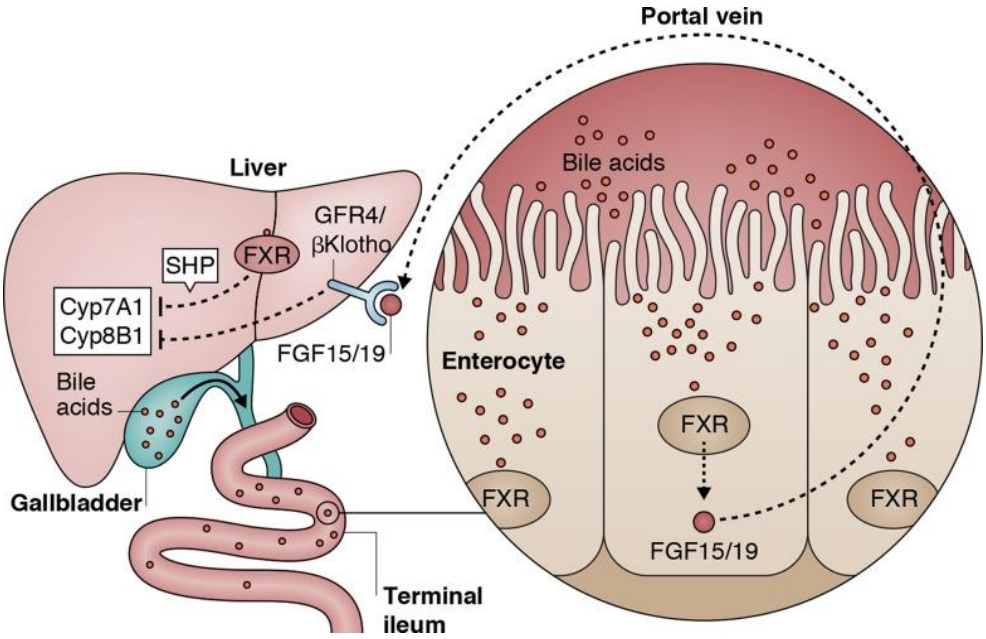

Figure I.4. BA-mediated regulation of their own synthesis. BAs regulate their own synthesis by their action in the nuclear receptor FXR. BAs reabsorbed via the enterohepatic circulation bind to FXR in the liver thereby inhibiting their synthesis by the promotion of the expression of SHP, which downregulates CYP7A1 expression. FXR is also expressed in enterocytes and, upon BA binding to intestinal FXR, FGF15/19 is produced, which acts as a hormone in the liver inhibiting CYP7A1 expression. CYP7A1, cytochrome P450 Family 7 Subfamily A Member 1; CYP8B1, cytochrome P450 family 8 subfamily B member 1; FGF15/19, fibroblast growth factor 15/19; FXR, farnesoid X receptor *[Adapted from, Shapiro H et al, 2018 (26)]*.

I.1.3. Non-parenchymal cells

The non-parenchymal liver cell populations include LSECs, KCs and HSCs as well as intrahepatic lymphocytes. These cells cooperate with liver parenchymal cells and cholangiocytes, fulfilling complementary functions that help to maintain the homeostasis of the organ. Of note, liver non-parenchymal cells become paramount during liver injury and disease, as they orchestrate mechanisms of inflammation, wound-healing response and regeneration (27).

I.1.3.1. KCs and macrophages

Liver macrophages can be divided into two main populations: KCs (i.e. liver resident macrophages), and monocyte-derived macrophages. Both populations cooperate in the immune surveillance of the liver and represent the first line of defence mechanisms against harmful pathogens (28). Although many of the surface markers overlap between KCs and monocyte-derived macrophages, specific markers distinguish both cells in mouse and human. Mouse KCs are characterised by F4/80, CD68, CLEC4F, TLRs and the absence of monocyte-derived markers such as CX3CR1 (29), while monocyte-derived macrophages express LY6C$^{+/-}$, CX3CR1^{+} and CCR2^{+} among other markers (28). Specific cell surface markers are less well described in human macrophages; common strategies to identify KCs focus on CD68^{+}, CD14^{+} and the absence of CX3CR1, while monocyte-derived macrophages are distinguished by CD14^{+}, CCR2^{+} and CD16$^{+/-}$ (30).

KCs constitute the 15% of the total liver volume (31) and are regarded as the largest tissue-fixed resident macrophage population in the organism (32). KCs reside in the hepatic sinusoid, a strategic location that enables them to detect, opsonise and phagocytise pathogens and dying epithelial cells. In order to fulfil this task, these cells express a plethora of receptors including scavenger receptors, toll like receptors (TLRs), complement receptors and Fc receptors (32).

In a healthy liver, KCs show a tolerogenic phenotype, given the anatomical location of the liver, in direct contact with gut-derived products; the liver is exposed to a large amount of agents. KCs respond to these agents as professional phagocytes and prevent any undesired immune reaction (33), for instance by the activation of T regulatory cells (Tregs) (34). KCs are also important in the metabolism of iron and cholesterol. In this

regard, they are able to remove damaged erythrocytes and haemoglobin waste products from the blood (35, 36). In addition, they express the scavenger receptors cluster of differentiation 36 (CD36) and scavenger receptor-A (SR-A) for the recognition of oxidised low density lipoproteins (oxLDL) (37) and express cholesteryl ester transfer protein (CETP) which regulates plasma levels of high-density lipoprotein (HDL) and very low-density lipoprotein (VLDL) (38).

KCs also constitute the first line of defence in the liver. KCs are able to sense tissue damage and harmful pathogens by the recognition of danger associated molecular patterns (DAMPs) or pathogen associated molecular patterns (PAMPs), respectively. Upon stimulation of specific receptors, KCs activate the transcription of a wide range of inflammatory cytokines and chemokines, thus directly reacting to the harmful pathogen and also warning other immune cells about the presence of dangerous agents (**Figure I.5.**) (28). KC-mediated responses range from the release of pro-inflammatory cytokines such as tumour necrosis factor (TNF), interleukin 6 (IL6), inflammasome activation and subsequent interleukin 1β (IL1β) and interleukin 18 (IL18), production of reactive oxygen and nitrogen species (ROS and NOS), release of chemotactic signals for the recruitment of monocyte-derived macrophages or T cells, among others, as well as anti-inflammatory or regulatory signals such as interleukin 10 (IL10) production and Treg recruitment (39). Each response is tightly fine-tuned depending on the triggering stimuli. In this line, one of the best examples of KCs-orchestrated immune response is the reaction to lipopolysaccharide (LPS). LPS binds to toll like receptor 4 (TLR4) in KCs and elicits the activation of c-Jun N-terminal kinase (JNK), mitogen-activated protein kinase (MAPK) and nuclear factor-κappa B (NF-kB) pathways, which finally results on the production of TNF, interleukins (IL1, IL6, IL12, IL18, IL10) and interferon-gamma (IFN-γ) (40).

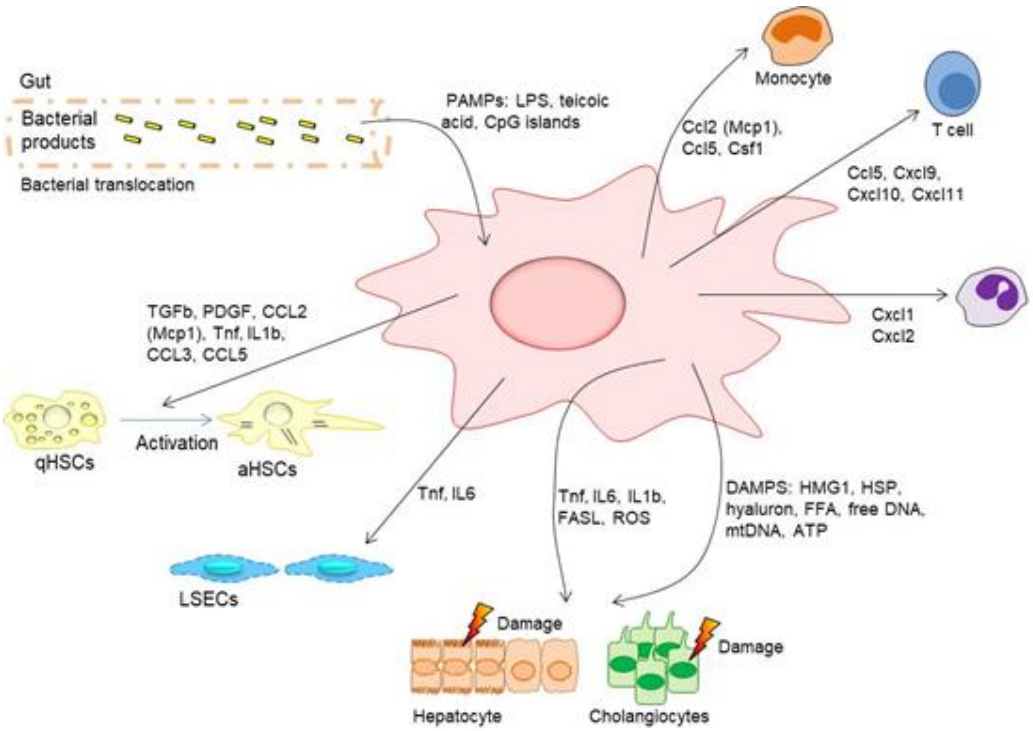

Figure I.5. KC activation in response to liver injury. Upon liver injury, DAMPs and PAMPs are recognised by the plethora of receptors expressed on KC surface, which leads to the activation of these cells. KC activation encompasses the production of a wide range of pro-inflammatory cytokines and chemokines, which maintain their activated state and enable them to communicate with other cell types including monocyte-derived macrophages, T cells, neutrophils and hepatic stellate cells *[Based on Krenkel O et al, 2017 (28)]*.

Monocyte-derived macrophages are also important players in liver immunology. In a healthy liver, they are found in the portal triad, where they participate in cooperation with KCs in the metabolism of iron and cholesterol (41). Upon liver damage, large amounts of monocytes are recruited to the liver, where they differentiate to macrophages (42). In the liver, monocyte-derived macrophages act in a complementary fashion with KCs, showing a high phagocytic activity, which is linked to the production of pro and anti-inflammatory mediators depending on the eliciting stimuli (43).

I.1.3.2. HSCs

HSCs are located in the space of Disse or perisinusoidal space; in a healthy or physiological state, they exhibit a quiescent phenotype, serving as the main storage for retinoids or vitamin A in the organism (44). In response to liver injury, these cells become the main fibrogenic cell in the liver and account for the synthesis and secretion of large amounts of extracellular matrix (ECM) proteins (45). In order to fulfil this function, HSCs lose their quiescent phenotype in a process named trans-differentiation or activation, after which they become myofibroblasts-like activated HSCs and acquire pro-inflammatory, proliferative, fibrogenic and contractile properties (44).

However, the myofibroblast population in the liver is complex, and may also derive from different cell types. Portal fibroblasts (PFs) and circulating fibrocytes have also been reported to trans-differentiate into myofibroblasts (46). Nevertheless, cell-tracing experiments have shown that HSCs contribute to the ~90% of the myofibroblasts population in various mouse models (47). Similar approaches revealed that liver epithelial cells (hepatocytes and cholangiocytes) are not able to trans-differentiate into myofibroblasts, and therefore do not contribute to this population (48-50).

HSCs activation has two main steps, a pre-inflammatory stage characterised by a rapid gene induction, followed by a perpetuation stage in which the activated phenotype is maintained and amplified (51). During their activation process, HSC response to a myriad of stimuli derived from damaged liver epithelial cells and inflammatory cells recruited to the liver.

The LSECs-derived fibronectin is one of the first factors directing HSC activation (52). After these primary stimuli, HSCs respond to reactive oxygen species, hedgehog ligands, nucleotides and cell death signals released from death hepatocytes and cholangiocytes, all of which contribute to the activation of HSCs (53). In addition, HSCs can detect and engulf apoptotic bodies, and this event also promotes their activation (54, 55). Macrophages are regarded as key mediators of HSC activation; of note, depletion of these cells in mice leads to decreased HSC activation and reduced liver fibrosis. The main HSC activator molecules derived from macrophages include transforming growth factor beta (TGFβ), platelet derived growth factor (PDGF), TNF, IL1β, monocyte chemoattractant protein 1 (MCP1) and chemokine (C-C motif) ligands CCL3 and CCL5 (51). Finally, platelets are also known to produce PDGFβ and TGFβ, essential factors that promote HSC activation (51).

HSCs also sense changes in ECM, they express integrins and discoidin domain receptors (DDRs), through which they react to ECM components and regulate cellular responses, including differentiation, proliferation and migration (56, 57). Importantly, HSC express different TLRs. In this line, bacterial products translocated from the gut, bind to these TLRs and affect HSCs behaviour. One of such examples includes the LPS-TLR4 signalling; specifically, LPS binds to TLR4 thereby increasing pro-fibrogenic mediators including TGFβ and inducing HSC trans-differentiation (58).

All of these stimuli induce behavioural changes in HSCs, in this regard, the activation process is characterised by genetic and epigenetic changes that finally lead to autophagy and retinoid loss, proliferation, contractility and chemotaxis and ECM protein production (**Figure I.6.**) (52). The main target genes of these genetic and epigenetic changes are type I collagen (α_1- and α_2-chains), TGFβ1 and TGFβ receptors, matrix metalloproteinase 2 (MMP2), tissue inhibitor of metalloprotease 1 and 2 (TIMPs 1 and 2), and alpha-smooth muscle actin (αSMA) (52). Perpetuation of the activated state and fibrotic response is achieved via autocrine and paracrine signals that further promote HSC proliferation while maintaining their activated phenotype.

Yet, as many recent publications have suggested, fibrosis seems to be a reversible response, and mechanisms that reverse HSC activation have been lately described (**Figure I.6.**). Activated HSCs also acquire the expression of death receptors, which upon engagement promote their death by apoptosis (27). Moreover, activated HSCs may also become senescent, a process that results in reduced ECM and increased MMP expression (59). Finally, cell-tracing experiments have reported that half of the activated HSC are able to revert the expression of fibrogenic genes and reacquire a quiescent-like phenotype (60, 61).

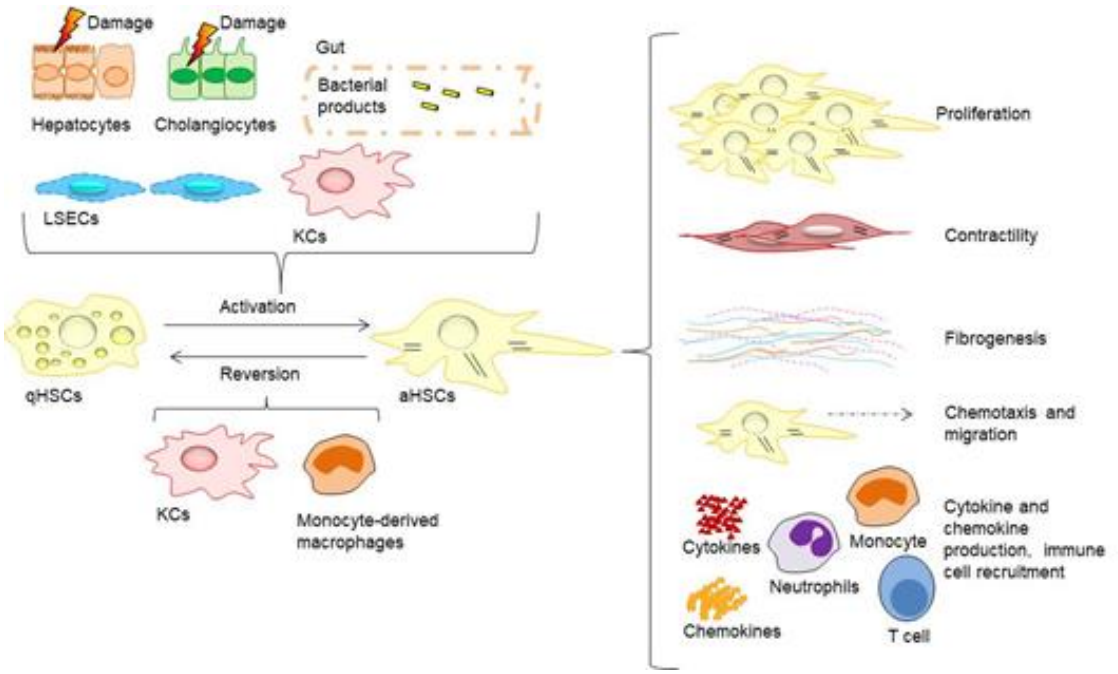

Figure I.6. Trans-differentiation of HSCs. Upon liver injury, HSCs transdifferentiate or activate to become the main ECM producing cells in the liver. In this process, HSCs acquire myofibroblasts-like features, with increased proliferation, contractility, ECM production and inflammatory cytokine and chemokine release, which lead to the recruitment of immune cells. This process can be reversed by HSCs apoptosis aided by innate immune cells or reversion to a quiescent-like phenotype. aHSCs, activated hepatic stellate cells; KCs, Kupffer cells; qHSCs, quiescent hepatic stellate cell *[Based on Tsuchida T et al, 2017 (51)*].

I.2. Chronic liver diseases

As aforementioned, the liver is a highly complex organ with multiple cell types working in an orchestrated manner to maintain the metabolic homeostasis of the whole body. Given its highly complex nature, the liver is also the target of a variety of diseases which can arise from diverse origins. Diseases affecting the liver primarily target its epithelial compartment. In this regard, hepatocellular and biliary diseases can be distinguished (62).

Diseases that target the hepatocellular compartment of the liver include hepatitis B and C virus (HBV, HCV) infection (63, 64), alcoholic liver disease (65), non-alcoholic fatty liver disease (NAFLD) (66) drug-induced liver injury (67) autoimmune hepatitis (68) and hepatocellular carcinoma (HCC) (69). Hepatocellular diseases represent a world-wide challenge, as an example, it is estimated that NAFLD affects 24% of the global population (70). On the other hand, diseases that primarily target intra or extrahepatic cholangiocytes are named cholangiopathies (71). Cholangiopathies can be classified as

genetic, infectious, immune-mediated, drug-induced, idiopathic, malignant and vascular alterations (**Table I.1.**) (72). As individual entities, cholangiopathies are rare diseases, but grouped together, they show considerable morbidity and mortality rates (6), being liver transplantation the only curative option in many cases (73).

Table I.1. Cholangiopathies. *[Adapted from Cheung A-C et al, 2017 (72).*.

Genetic
Allagile´s syndrome
Caroli´s syndrome
Cystic fibrosis
MDR3 deficiency
Polycystic liver disease (ADPLD, ADPKD, ARPKD)
Immune-mediated
Acute allograft rejection
Chronic allograft rejection
Graft versus host disease
Primary biliary cholangitis
Primary sclerosing cholangitis
Idiopathic
Biliary atresia
Idiopathic childhood adulthood ductopenia
IgG4 cholangiopathy
Sarcoidosis

Infectious
AIDs cholangiopathy (e.g. viral cholangitis)
Bacterial cholangitis (e.g. *Escherichia coli*, *Klebsiella*)
Parasitic cholangitis (e.g. *Opisthorchis viverrini*)
Malignant
Cholangiocarcinoma
Other
Drug-induced
Vascular/ischemic

ADPLD, autosomal dominant polycystic liver disease; ADPKD, autosomal dominant polycystic kidney disease; ARPKD, autosomal recessive polycystic kidney disease; MDR3, multidrug resistance protein 3.

I.2.1. Cholestatic diseases

Cholestasis is a multifactorial pathologic condition commonly observed in cholangiopathies of diverse origins, inculuding genetic, drug-induced, obstructive or immune-associated biliary diseases (74). Cholestasis is characterised by a decreased or stopped bile flow and the subsequent accumulation of BAs and other bile-derived toxic substances within the liver (75). Primary biliary cholangitis (PBC) and primary sclerosing cholangitis (PSC) stand out as the two most common chronic cholestatic diseases in adults, and they are associated with auto-immune phenomena targeting the biliary tree (74). Progression of cholestatic diseases leads to clinical consequences that include pruritus, fatigue or osteoporosis but it can also further evolve to cirrhosis, portal hypertension and the development of liver malignancies (74) **(Figure I.8.)**.

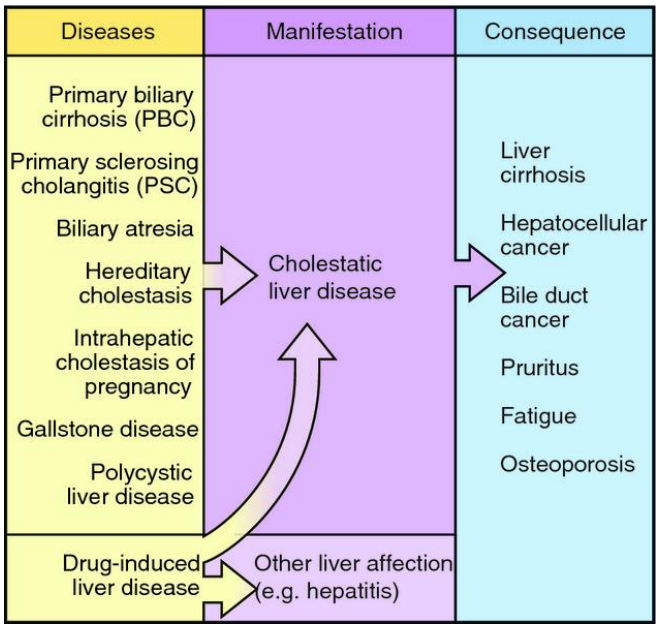

Figure I.8. Cholestasis and its clinical manifestations. Cholestasis is a clinical manifestation common in cholangiopathies of diverse origins, including adult and paediatric diseases; among these, PBC and PSC stand out as the two most common adult cholestatic diseases. Cholestatic liver diseases lack satisfactory therapeutic options and commonly progress to advanced stages of liver disease such as the development of liver cirrhosis, an augmented risk for hepatobiliary malignancies and disease-associated symptoms including, pruritus and osteoporosis. PBC, primary biliary cholangitis; PSC, primary sclerosing cholangitis *[Adapted from Karlsen TH et al, 2014 (74)]*.

I.2.1.1. PBC

PBC, previously named primary biliary cirrhosis, is a rare chronic cholestatic disease characterised by auto-immune phenomena targeting the small and intermediate intrahepatic bile ducts, which can lead to fibrosis, cirrhosis and liver failure (76). PBC is considered a rare disease as its prevalence in Europe is estimated to be around 35 per 100,000 individuals, with a female/male ratio of 10/1 (77).. The serological hallmark of PBC patients is the presence of anti-mitochondrial antibodies (AMA) against the E2 component of the pyruvate dehydrogenase complex (PDC-E2) in serum, which are present in ~95% of the patients (78, 79).

The aetiology of PBC remains unknown and its biology is obscure, including genetic predispositions, epigenetic changes and environmental factors that affect the homeostasis of cholangiocytes and their crosstalk with the immune system (**Figure I.9.**). One of the key steps in PBC pathogenesis is the loss of tolerance to mitochondrial antigens, namely PDC-E2. The loss of tolerance characteristic of PBC is thought to be

mediated by molecular mimicry. In this regard, urinary tract infections by *Escherichia coli* (*E. coli*) as well as fungal and viral infections have been associated with increased PBC risk (80). A general multilineage dysregulation of the immune response accounts for disease progression in PBC. This is characterised by genetic alterations in the human leukocyte antigen (HLA) locus and other immune pathways, including antigen presentation, lymphoid cell differentiation and B cell function (81). In this regard, patients with PBC display infiltration of cluster of differentiation 4 positive (CD4+) T cells and cluster of differentiation 8 positive (CD8+) T cells as well as boosted pro-inflammatory and insufficient immune regulatory mechanisms (82-84).

Cholangiocytes are also the target of molecular alterations of different natures in PBC (80). An epigenetic alteration specific to PBC involves the microRNA 506 (miR-506), which targets chloride/bicarbonate anion exchanger 2 (AE2). miR-506 is upregulated in patients with PBC, leading to decreased expression of AE2. Therefore, the alkalisation of bile is impaired, and the bicarbonate umbrella becomes weakened, rendering cholangiocytes more susceptible to toxic BA-mediated apoptosis (85). Moreover, these cells express TLRs, which activate upon binding of bacterial products contributing to the pro-inflammatory microenvironment and boosting auto-immune responses (86, 87).

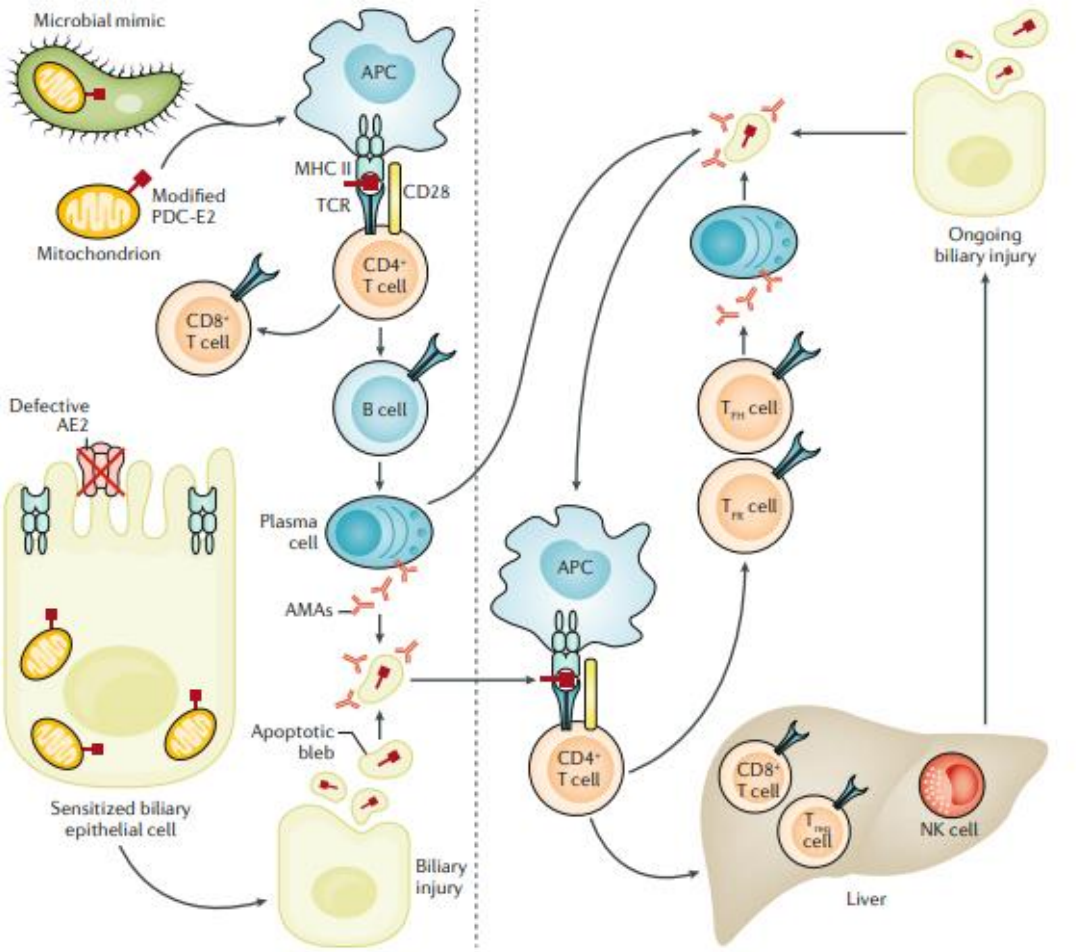

Figure I.9. Pathobiology of PBC. PBC is a chronic cholestatic disease characterised by an aberrant immune response to PDC-E2 through the production of AMAs. Molecular mimicry is thought to underlie the autoimmune response on these patients. Besides, an overall dysregulation of the immune compartment is detected and this is characterised by increased number and activation of effector T cells and NK cells and dampened immune regulatory mechanisms, such as a decrease in intrahepatic and circulating T regulatory cells. Alterations in cholangiocytes are also detected in patients with PBC; AE2 expression is diminished, affecting the bicarbonate umbrella, and thus, making cells sensitive to BA-mediated apoptosis. AE2, anion exchanger 2; AMAs, antimitochondrial antibodies; APC, antigen presenting cell; CD28, cluster of differentiation 28; MHC II, major histocompatibility complex II; TCR, T cell receptor *[Adapted from Gulamhusein A et al, 2020 (81)]*..

I.2.1.2. PSC

PSC is a rare disease with an estimated prevalence in Northern Europe and the United States (US) of about 1 per 10,000, (88, 89), while in Spain is estimated in 0.022 (90). PSC is a chronic cholestatic disease characterised by multifocal bile duct strictures and persistent biliary inflammation. Importantly, PSC is a risk factor to develop cholangiocarcinoma (CCA), i.e. tumours of the biliary tree (91). PSC diagnosis is

achieved based on imaging criteria by magnetic resonance cholagiography and exclusion of other known causes of possible secondary sclerosing cholangitis (92).

From a pathological point of view, the liver of patients with PSC presents the typical onion-skin-like concentric fibrosis around bile ducts (92). The aetiology of PSC still remains obscure, yet a series of genetic and environmental factors have been associated with the disease (91) **(Figure I.10.)**. In this regard, the most prominent finding derived from genome-wide association studies, identified the HLA locus as a susceptibility factor for PSC (93, 94). Besides, the contribution of unknown environmental factors, which may trigger some aspects of disease pathogenesis is now arising as an important factor in this disease (91). In this regard, PSC patients exhibit alterations in the gut microbiota, mainly a reduction in microbiota diversity (95). Additionally, cholangiocytes show an aberrant phenotype in patients with PSC (96). This is believed to act as the underlying phenomena of the peribiliary fibrosis and cirrhosis, due to the intercellular interaction between cholangiocytes and HSC or portal myofibroblasts (47, 97).

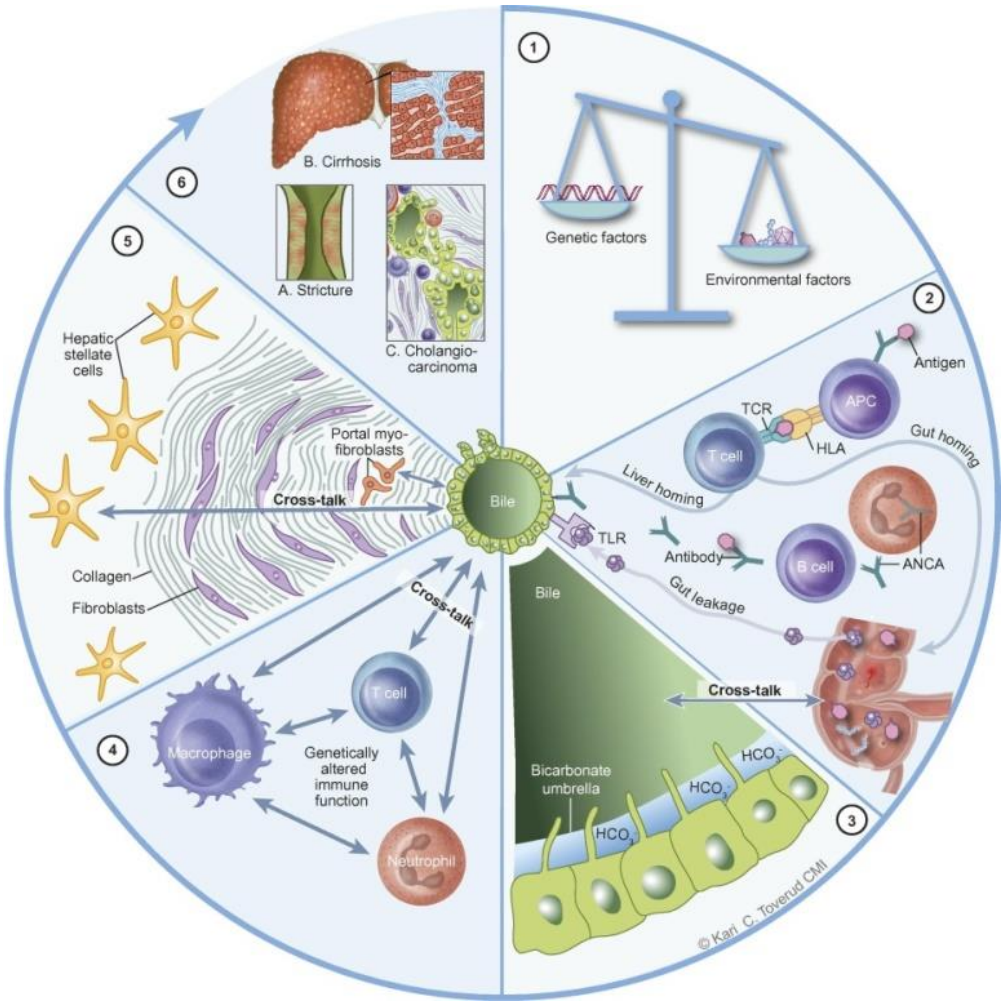

Figure I.10. Pathophysiology of PSC. (1) PSC develops as a result of the cooperation of genetic and environmental alterations**. (2-4)** Genetic alterations associated to PSC target manly the HLA locus, resulting in aberrant antigen presentation, the gut liver axis, via gut dysbiosis and translocation of gu-derived bacterial products to the liver also contributes to this pathology. Additionally, bile homeostasis and cholangiocyte physiology are altered due to the immune attack to cholangiocytes, resulting in cholangiocyte activation and a strong crosstalk between altered cholangiocyte and the immune compartment. **(5-6)** All of these phenomena result in the activation of HSCs or PMs, driving biliary fibrosis and advanced stages of the disease, including bile duct strictures, cirrhosis and potential CCA development. *[Adapted from Karlsen TH et al, 2017(91)]*.

1.2.1.3. Therapeutic strategies for PBC and PSC

Despite the important auto-immune component of PBC and PSC, immunossuppressive drugs have failed to show beneficial effects in these patients (76, 98). In turn, Ursodeoxycholic acid (UDCA), an endogenous choleretic BA, was reported to exert beneficial effects in cholestatic diseases and is still regarded as the reference treatment option for several of these diseases (22). Currently, UDCA represents the first line therapy for PBC. In this regard, UDCA effects on patients with PBC are linked to its

choleretic nature, leading to a reduction in the hydrophobic BA-mediated attack to hepatocytes and cholangiocytes (99). Additionally, UDCA is also able to exert anti-apoptotic effects in cholangiocytes (100) and mediate anti-inflammatory responses due to its action on glucocorticoid receptor (GR) (101). Yet, around 30% of the patients with PBC show an incomplete biochemical response to UDCA, and this percentage rises to 50% in patients younger than 40 years old (102). Importantly, these patients are at risk of developing end-stage liver disease, finally needing liver transplantation (98). Regarding PSC, UDCA was shown to improve serum enzymes and liver histology in these patients (103). and it is currently used in some centres to treat this disease. However, controversy exist about its efficacy as some studies report adverse outcomes after high-dose UDCA treatment in patients with PSC (104). Therefore, the European Association for the Study of the Liver (EASL) accepts its use for these patients, while the American Association for the Study of Liver Diseases (AASLD) recommends against it use (105).

Novel therapeutic strategies to treat PBC and PSC have been developed during the last years. Among them, nuclear receptor agonists, mainly, obeticholic acid (OCA), have gained attention for PBC treatment (106-108), while the antibiotic vancomycin showed the most beneficial effects for patients with PSC (109). Nevertheless, overall, cholestatic diseases represent an unmet clinical challenge as therapeutic options for these patients are scarce and in many cases, disease progresses to end stage liver disease.

I.2.2. The progression of chronic cholestatic diseases

Despite having a heterogeneous origin, the progression of liver disease shares virtually common features (27) (**Figure I.11.**). The initial harmful agents mainly target the epithelial components of the liver (i.e. hepatocytes and cholangiocytes) inducing epithelial cell death (110). The death of liver parenchymal cells and cholangiocytes triggers the so called wound-healing response, a coordinated response comprising different epithelial and non-epithelial compartments of the liver that mediate inflammatory and regenerative mechanisms in an effort to restore the lost liver tissue (111).

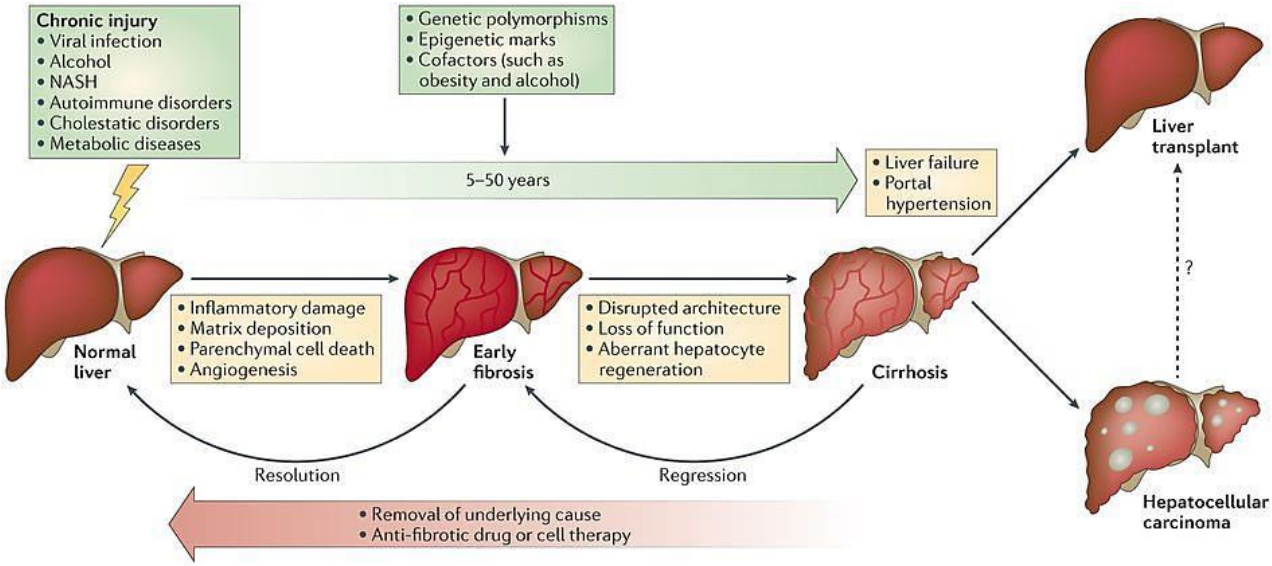

Figure I.11. Progression of chronic liver diseases. Progression of chronic liver diseases shares common features, despite specific phenomena linked to certain diseases may also exist. Overall, after injury, disease progression initiates with an inflammatory and regenerative response to the harmful stimuli. However, when the damaging stimulus is maintained over time, this response is overwhelmed, with sustained inflammation and hepatitis that then progresses to fibrosis, cirrhosis and eventually carcinogenesis *[Adapted from Pellicoro A et al, 2014, (27)]*

When the primary harmful stimulus is transient the wound-healing response is a tightly controlled and beneficial mechanism that will help activating the regeneration process of the damaged liver (112). However, in the scenario of sustained liver injury, the wound-healing response is exacerbated and perpetuated, becoming one of the main events promoting chronic liver disease progression (111). Despite presenting common features, the regenerative responses to chronic liver injury differ with disease nature. In this regard, chronic cholestatic diseases of diverse origins share a similar course with the development of biliary fibrosis, which can further evolve to cirrhosis, portal hypertension and the development of liver malignancies(74).

I.2.2.1. Damage initiation in cholestatic diseases

As most cholestatic diseases have an unknown aetiology, there is controversy when identifying the first trigger of epithelial cell damage in these diseases. Cell death induced by different mechanisms including, apoptosis, necroptosis or autophagy among others, has been identified in the liver of patients with cholestatic diseases including PBC and PSC (113). The initial stimulus that trigger epithelial cell death seems to be a

combination of the aberrant immune response detected in this diseases as well as BA-mediated direct and indirect effects. Importantly, PBC and PSC are associated with autoimmune phenomena targeting the biliary tree; specifically, T cells are recruited to biliary structures where they mediate cytotoxic effects and induce cholangiocyte cell death (114). Moreover, in the classical hypothesis, BAs are regarded as a direct cytotoxic agent owing to their membranolytic properties. Indeed, BAs are able to disrupt cellular membranes and therefore induce apoptotic and necroptotic cell death, as well as senescence (115-117). Mechanisms of BA-induced cell death include JNK activation, Fas/Fas ligand (FasL) engaging and mitochondrial membrane disruption (118). Nevertheless, this hypothesis is largely discussed currently, as BA concentrations used for *in vitro* studies are in the milimolar range, hence exceeding pathophysiological concentrations usually found in cholestatic conditions (119, 120).

Additionally, BAs have lately been proposed as strong pro-inflammatory mediators (119). Incubating mouse hepatocytes with taurocholic acid (TCA) or glycodeoxycholic acid (GDCA) at concentrations reached in cholestatic conditions (i.e. 20-200 µM) elicits the expression of pro-inflammatory cytokines and chemokines (121, 122). In addition, BAs induce the expression of osteopontin, a chemoattractant for immune cells (123) and also promote the proliferation of cholangiocytes (124). Both hepatocyte-derived chemokines and osteopontin, function to recruit neutrophils to the liver. These immune cells are characterised by a strong cytotoxic response, with the release of ROS and regarded as the main mediators of cholestatic liver injury in different mouse models (125-127). In line with this, human cholestatic injury correlates with neutrophil content, and also with intercellular adhesion molecule 1 (ICAM1), the main neutrophil attractant protein which is upregulated in these patients (128, 129).

I.2.2.2. Ductular reaction

Following the primary harmful stimuli, a specific wound-healing response termed as "ductular reaction" is triggered in cholestatic diseases, this response is identified in human cholestatic diseases (including PBC and PSC) (130, 131), and in mouse models of cholestasis (i.e. the obstructive cholestasis model based on bile duct ligation (BDL), the chemical cholestasis model based on the diet supplemented with 3,5-diethoxycarboncyl-1,4-dihydrocollidine (DDC) and the genetic model based on multidrug resistance 2 deficiency (*Mdr2*$^{-/-}$)) (131). Ductular reaction is believed to develop as an effort to augment the biliary surface to excrete the accumulating bile, and thus maintain the physiological functions of the biliary compartment (132).

Despite being classically defined as the expansion and branching of biliary structures due to cholangiocyte proliferation, ductular reaction is now regarded as a complex response orchestrated by diverse cell types and their cross-talk (15, 131). Hence, ductular reaction comprises immune cell infiltration, (133) biliary expansion and changes in the ECM composition (134) and the liver microvasculature (135).

Different cellular sources have been proposed to account for the expansion of biliary structures characteristic of ductular reaction (131, 136). In this line, ductular expansion can be explained by the proliferation of cholangiocytes. In a healthy liver, cholangiocytes are in a mitotically inactive state, but upon damage, they acquire a reactive phenotype (137) with cellular traits reminiscent of early developmental stages, featuring increased proliferation and an altered secretory activity (6, 138). HPCs have the ability to differentiate into reactive biliary-like cells (139). Interestingly, activation of this cellular compartment has been described in ductular reactions of diverse origins (130). Moreover, lineage-tracing studies have unravelled the ability of hepatocytes to trans-differentiate to biliary reactive cells in a setting of severe cholangiocyte injury (140, 141). This phenomenon has been described in mice; although whether this finding can be translated to human diseases is still far from clear (131).

As aforementioned, in the presence of a persisting damage, wound-healing reactions become uncontrolled and are the main trigger of disease progression. In line with this, regardless of their origin, ductular reactive cells (DRCs), also regarded as "reactive cholangiocytes", proliferate and accumulate in chronic cholestasis, as an indication of maladaptive regeneration (**Figure I.12**) (6, 136). DRCs are biliary-like cells, but they display differential features in comparison to healthy cholangiocytes, and are characterised by certain cellular plasticity and a strong secretory phenotype (136). Among the factors able to induce this DRC phenotype TNF, TNF-related weak inducer of apoptosis (TWEAK), TGFβ, hepatocyte growth factor (HGF), vascular endothelial growth factor (VEGF), sonic Hedgehog (Hh), and Wingless (Wnt)/β-catenin have been described (142, 143). In this process, DRCs gain expression of mesenchymal markers, including S100 calcium-binding protein A4 (S100A4), vimentin, snail and MMP2, whilst reducing the expression of the epithelial markers E-cadherin and cytokeratin 19 (CK19), as shown in patients with PBC and PSC (144) and in mouse models of cholestasis (145). It is important to bear in mind that the objective of ductular reaction is to restore the biliary architecture, as such, Notch and yes-associated protein 1 (YAP) pathways get activated to direct biliary morphogenesis (146, 147).

DRCs are also characterised by a strong secretory phenotype (148). Indeed, inflammation is central to ductular reaction and directs the cellular cross-talk enabling immune cell recruitment and activation, as well as the fibrogenic response (**Figure I.12**). DRCs activate KCs and release macrophage (149) and neutrophil chemoattractants (150), as well as connective tissue growth factor (CTGF), to promote expansion of these type of cells (151). Importantly, interleukin 8 (IL8), a major neutrophil chemoattractant, is upregulated in serum and in liver tissue of patients with PBC and PSC (152, 153). Recruited macrophages and neutrophils can in turn perpetuate DRCs phenotype and proliferation by the production of pro-inflammatory mediators (6, 154). IL6 can also be secreted by damaged cholangiocytes acting in an autocrine and paracrine fashion, to perpetuate cholangiocyte proliferation and potentiate the immune crosstalk (6, 96) Notably, bile ducts were reported to have their own vasculature, which is maintained during injury (135).. Indeed, biliary expansion is accompanied by angiogenesis, which can be elicited by DRC-derived VEGF, endothelin-1, nitric oxide (NO) and PDGF-BB (154).In this line, increased vascular structures and expression of VEGF and other angiogenic factors were described in PBC samples (155). DRCs are also known to provoke fibrogenic responses, as will be discussed in the following section. In sum, ductular reaction results in a strong pro-inflammatory microenvironment, characterised by an expansion of biliary structures, immune cell recruitment, angiogenesis and scarring.

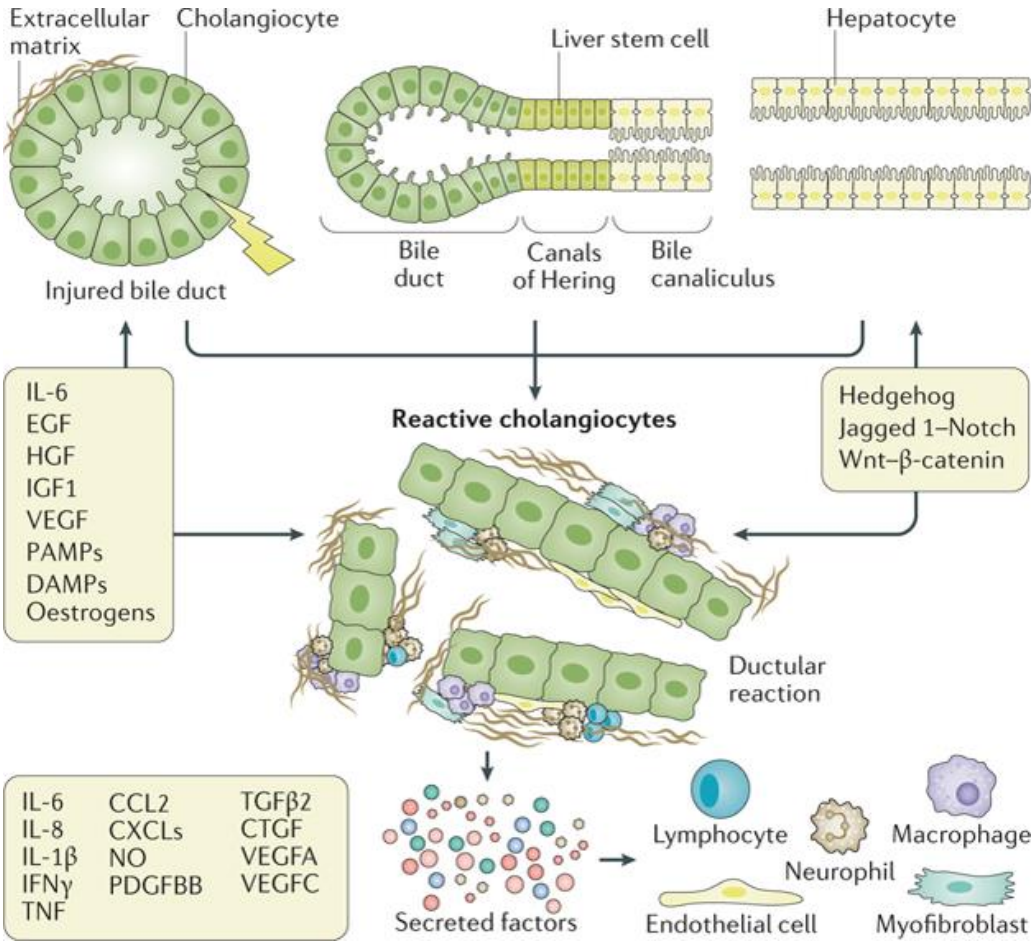

Figure I.12. Ductular reaction and ductular reactive cells. Upon biliary damage, expansion of biliary structures occurs in an effort to secrete accumulating BAs and restore the lost biliary mass. Ductular reactive cells may arise from different cellular compartments including differentiated cholangiocytes, hepatic progenitor cells or hepatocytes under trans-differentiation in response to cytokines, PAMPs, DAMPs and morphogens. DRCs have a partial biliary-like phenotype but with marked des-differentiation and a strong secretory phenotype, thus, releasing inflammatory cytokines and growth factors to maintain their population and to activate immune cells, endothelial cells and HSCs or myofibroblasts. CCL2, chemokine (C-C motif) ligand 2; CTGF, connective tissue growth factor; CXCLs, C-X-C motif chemokine ligand 2; DAMPs, danger associated molecular patterns; EGF, epithelial growth factor; HGF, hepatocyte growth factor; IFNγ, interferon gamma; IGF, insulin growth factor; IL, interleukin; NO, nitric oxide; PAMPs, pathogen-associated growth factor; PDGFBB, platelet-derived growth factor BB; TGFβ2, transforming growth factor beta 2; TNF, tumour necrosis factor; VEGF, vascular endothelial growth factor; VEGFA, vascular endothelial growth factor A; VEGFC, vascular endothelial growth factor C *[Adapted from Banales JM et al 2019 (6)]*.

I.2.2.3. Biliary fibrosis

The intense cellular cross-talk and inflammatory microenvironment established during ductular reaction represents the ideal scenario for the development of biliary fibrosis. Biliary fibrosis is characterised by an excessive accumulation of ECM proteins as well as qualitative changes in ECM composition (156). Biliary fibrosis starts to develop in

the periportal space and continues to expand commonly following a portal to portal pattern (148). As chronic disease progresses, fibrosis extends to lobular areas involving hepatocytes and can evolve to bridging fibrosis and eventually cirrhosis, end-stage liver disease and carcinogenesis (157).

Long has been discussed about the main mesenchymal compartment involved in biliary fibrosis and this issue is still far from clear (120, 136). Overall, HSCs are regarded as the main fibrogenic cell in the liver and their contribution to fibrogenic responses, also in biliary diseases, has extensively been reported. In this regard, it has been demonstrated that most mesenchymal cells derive from HSCs in biliary fibrosis and cirrhotic animal models (47, 158). However, one of these studies missed the early stages of biliary injury and only analysed the cellular responses in cirrhotic stages (136, 158). Moreover, the other study describes the presence of PMs as a different entity from HSCs, suggesting they may play a specialised role in cholestatic injury (47). Indeed, PMs were first described in relation to biliary injury and fibrosis (159-161). Since then, owing to their anatomical location in portal spaces, PMs were described as the primary mesenchymal cell responding to biliary injury (162). They could in turn participate in the recruitment and activation of HSCs that display their fibrogenic potential extending the scarring process to lobular areas (120, 162).

Biliary fibrogenesis is characterised by the strong interplay between DRCs and mesenchymal cells, which is established due to the coordinated expression of ligands and cognate receptors (136) (**Figure I.13.**). In this line, DRCs are known to secrete TGFβ2 (163) , IL6 (164) PDGF-BB (165), MCP1 (166), CTGF and osteopontin (167), , which directly induce mesenchymal cell activation but can also act as indirect factors, thereby, as aforementioned, recruiting macrophages which, in turn, may also act as a potent source of pro-fibrogenic factors (136). Mesenchymal cells express BA receptors, which, although controversial, have been reported in some studies to promote activation of these cells upon engagement (168). In turn, mesenchymal cells respond to these stimuli and are thus able to affect DRCs behaviour. Portal fibroblasts express hyaluronic acid, which is especially important in biliary fibrosis as it potentiates biliary proliferation (169). Moreover, Wnt, Hh and Notch signalling pathways play a crucial role in the DRCs-mesenchymal cell interplay, as they may act in both directions, amplifying biliary expansion and fibrogenesis (136). In this regard, Notch signalling induces HPCs differentiation to DRCs by a mechanism involving Jag-1 expression in portal myofibroblasts and its engagement in Notch-expressed HPCs (136, 146). Disruption of Hh signalling is reported in chronic cholestatic diseases; noteworthy, an

increase in the Hh ligands Sonic and Indian, as well as Gli1 and Patched was shown in DRCs of patients with PBC (170). Hh ligands induce proliferation and mesenchymal traits in DRCs (145), and at the same time promote myofibroblast activation (171). Several components of the Wnt/β-catenin pathway have been found upregulated in PBC and PSC (172, 173). Interestingly, Wnt ligands have been related to DRCs expansion (174) and also to mesenchymal cell activation (175).

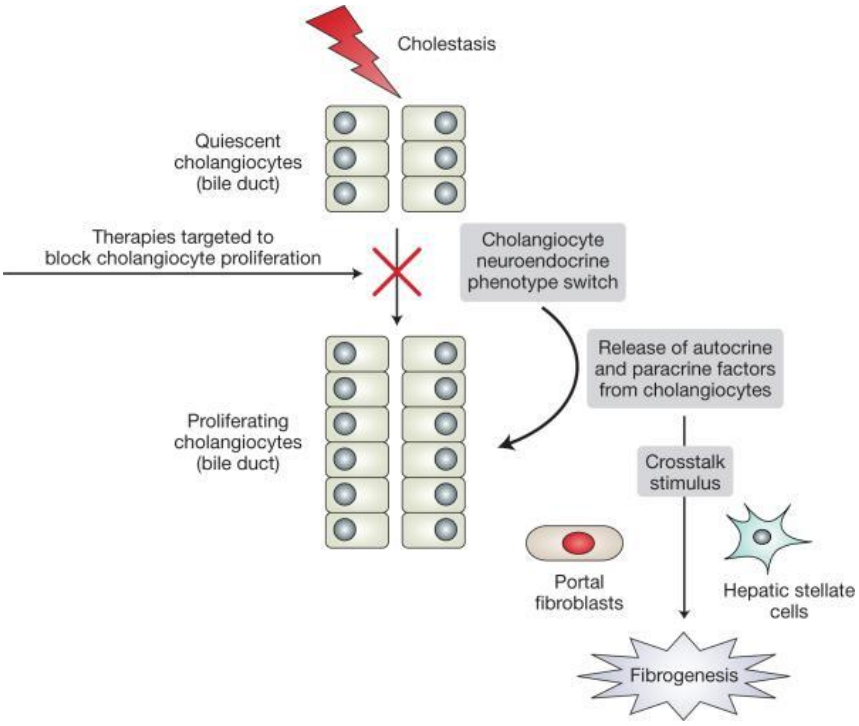

Figure I.13. Biliary fibrosis. Cholestasis leads to the activation and proliferation of DRCs. DRCs release factors that bind to and activate portal fibroblasts and HSCs to promote fibrogenesis. Conversely, activated portal fibroblasts and HSCs also affect DRCs, with the release of factors that maintain DRC phenotype and promote their proliferation. *[Adapted from Glaser S et al, 2009 (176)]*.

I.2.2.4. Advanced stages of chronic cholestasis and cirrhosis

Liver cirrhosis is regarded as the final stage of fibrosis and develops in virtually all chronic liver diseases regardless of their aetiology (177). In the context of biliary fibrosis, cirrhosis develops in advanced stages, when the initial periportal lesion extends to lobular spaces involving the hepatic sinusoids and impairing hepatocyte function (157). Cirrhosis is characterised by the massive production of ECM that extends replacing the parenchymal space of the liver. Remaining hepatocytes occupy regenerative nodules that are surrounded by fibrotic tissue. The deposition of ECM fibres results in the hardening of the organ and gives to the liver a scar-like appearance

(177). The anatomical derangement of the liver has a direct impact on its functionality, and hardening of the organ disrupts liver irrigation resulting in portal hypertension (178). Other extrahepatic complications of cirrhosis include, oesophageal variceal bleeding, liver encephalopathy and ascites (179). Overall, liver cirrhosis is regarded as an end-stage condition as it provides the ideal niche for the development of liver malignancies, and it is also the major indication for liver transplantation in adults (180).] In line with this, a significant proportion of patients with PBC and PSC develop end-stage liver disease and need organ transplantation. Specifically, in the period between 2002 and 2016, 36% of the patients with PBC and 50% of the patients with PSC were subjected to liver transplantation, representing around the 10% of the total liver transplantations in Europe (181).

I.2.2.5. Hepatobiliary carcinogenesis

Chronic cholestasis and inflammation are intimately linked to hepatobiliary carcinogenesis (182). This association has been shown both in patients and in diverse experimental models of cholestasis and hepatobiliary diseases. Patients with PBC can ultimately develop HCC (183), whereas patients with PSC display a higher risk of developing cholangiocarcinoma (CCA), (184, 185) HCC, gallbladder and colorectar cancer (186). Indeed, the risk (adjusted odds ratio) to develop CCA in patients with PSC was reported as 171 compared with controls in USA (187)and 160-fold increase compared to control population in Northern Europe (188).

I.2.2.5.1. HCC

HCC develops due to the malignant transformation of hepatocytes. It represents the sixth most common cancer worldwide and the fourth leading cause of cancer-related deaths (69). Around 80% of the HCCs arise in cirrhotic livers. Hence, most of the patients with HCC present an underlying chronic liver disease, which is mainly triggered by viral infections (HBV or HCV), alcohol abuse or obesity (189), among others The high rate of deaths related to this cancer (190) is due, at last in part, to the lack of early, accurate, non-invasive diagnostic biomarkers and their refractory nature to chemotherapy (191).

HCC development involves the coordination of many multi-step processes. Tumour generation initiates with hepatocyte death, which is accompanied by inflammation, fibrosis and compensatory proliferation (192). In this environment, mitogenic factors

are overexpressed in order to sustain initial compensatory proliferation. Yet, when persistent in time, mitogenic stimuli perpetuate liver damage and establish autocrine mechanisms of uncontrolled hepatocyte proliferation (193). This scenario also favours the appearance and accumulation of mutations (194).

Somatic mutations in oncogenes and tumour suppressor genes are the main triggers of hepatocyte transformation into malignant cells. Although this cancer is highly heterogeneous, some genes stand out as the most commonly mutated in HCC (195). Specifically, due to these mutations, several developmental pathways, that are normally dormant in the adult liver, reactivate during hepatocarcinogenesis (196). In this regard, mutations in the telomerase reverse transcriptase (*TERT*) are present in about 60% of the HCCs, and members of the Wnt/β-catenin signalling pathway (*CTNNB* 18%, *AXIN1* 8%) are also commonly found mutated in this type of cancer. Mutations in the *TP53* (25-30%) are also common (192, 195). Other cancer-related pathways frequently found altered in in this tumour include, chromatin remodelling and epigenetic abnormalities, as well as oxidative stress regulators. Similarly, the Notch, Hedgod, NF-κB, PI3K/AKT/mTOR, Ras/RAf/MEK/ERK and JAK/STAT pathways are also found deregulated in HCC tumours (195).

I.2.2.5.2. HCC therapy

Benefits of HCC therapy are tightly linked to a proper stratification of these patients. Different stratification approaches have been proposed, but the Barcelona Clinic Liver Cancer (BCLC) is the most widely used and the only one that has been prospectively validated (197). The BCLC staging system combines tumour stage with the evaluation of liver function and cancer-related symptoms, and proposes an optimal clinical management strategy for each stage (191). Only certain patients with early stage HCCs are amenable for curative resection or transplantation (198), while others at early to middle stages receive locoregional (199) and/or systemic chemotherapies based on multikinase inhibitors (e.g. sorafenib) (200). Additionally, combined onco-immunotherapy is showing benefits in advanced stages of HCC as shown in recent reports (201).

I.2.3. The gut-liver axis

The human gut harbours 100 trillion of bacteria, which live in symbiosis and are important for a number of metabolic functions of the organism (202). Therefore, the

organism has developed a series of measures to maintain tolerance to endogenous microorganisms and commensal bacteria (203). Due to its anatomical location, the liver is the first organ to be connected with the gut via the portal vein, and thus represents a central organ in the interaction between the microbiome and the organism (204, 205).

I.2.3.1. Pathological bacterial translocation

During chronic liver disease, mechanisms that maintain the normal symbiotic status between the host and gut microbiota fail at different levels. As a consequence, the intestinal epithelia loses its normal architecture, with the disruption of tight junctions, thickening of mucus, a decrease in defensin secretion, and an overall insufficient immune response to bacteria that invade the epithelial layer (202). In parallel, there is dysbiosis of the microbiota, with an overgrowth of the pathological bacterial strains. All of these phenomena enable the translocation of bacteria, mainly bacterial products, from the gut to the liver (206).

Pathological bacterial translocation from the gut to the liver results in the presence of PAMPs such as LPS, teichoic acid, or bacterial DNA in the liver (207). PAMPs are recognised by pathogen associated pattern recognition receptors (PPRs) (208), which include two main families: TLRs and NB-LRR-related gene family (NLRs). The family of TLRs is the most extensively studied; upon ligand binding, TLRs signal through the myeloid differentiation primary response 88 (MyD88) adaptor and initiate the transcription of pro-inflammatory genes (209). Of note, PRRs and particularly, TLRs can also be activated by DAMPs which are released by damage epithelial cells in response to injury (111, 210). Thus, TLRs drive tissue reparative responses upon infection or damage, which makes them a key player in the setting of liver diseases (210). Within the liver, TLRs are mainly expressed on KCs and HSCs (**Figure I.14.**). Activation of toll like receptor 2 (TLR2), TLR4 and toll like receptor 9 (TLR9) in these cells was demonstrated to boost inflammatory responses and chronic liver disease progression (58, 211, 212) and TLR4 deficient mice are protected from various forms of liver injury (213-215). Moreover, genetic polymorphisms in *TLR2*, *TLR4* and *TLR9* result in the alteration of the inflammatory responses to translocating bacteria, thus leading to complications in liver cirrhosis (216).

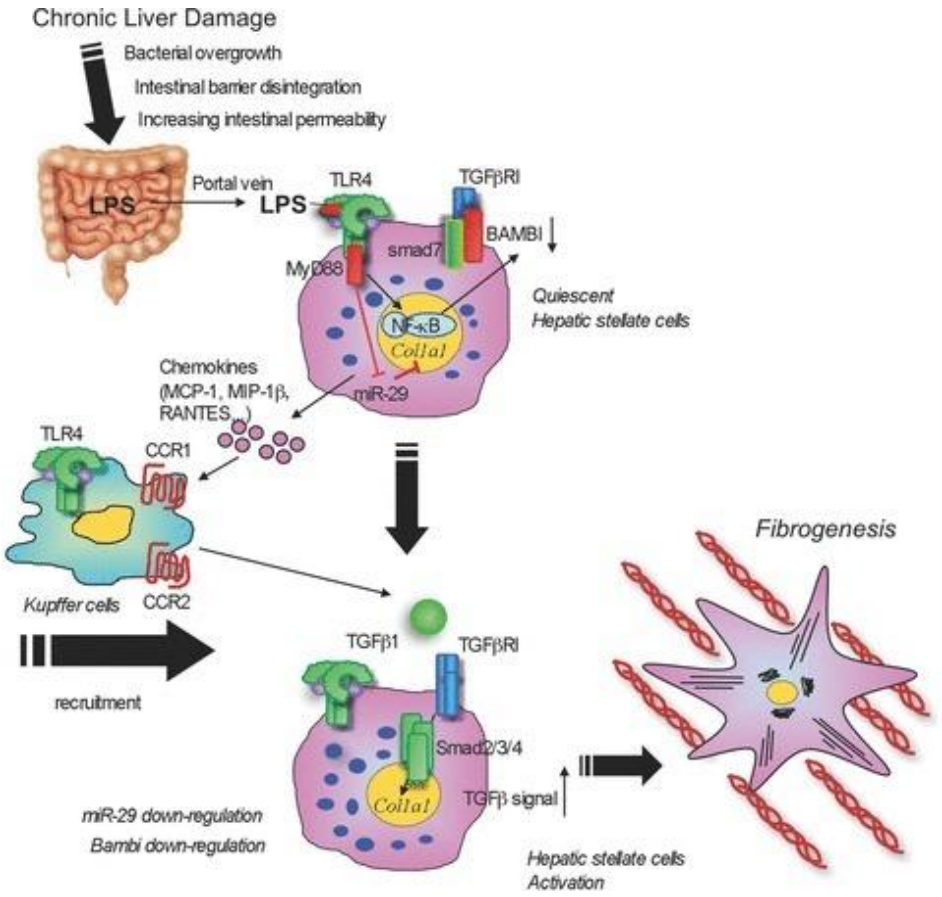

Figure I.14. Pathological gut-liver bacterial translocation and its effects in KCs and HSCs. Chronic liver injury leads to translocation of bacterial products, mainly LPS, to the liver. In the liver, bacterial products bind to TLRs, mainly TLR4, which are expressed in KCs and HSCs. Upon binding to TLR4, LPS promotes KC and HSC activation, leading to inflammation and fibrogenesis. BAMBI, BMP and activin membrane bound inhibitor; CCR, chemokine (C-C motif) receptor; COL1A1, collagen type 1 alpha 1; MAPK, mitogen-activated protein kinases; MCP1, monocyte chemoattractant protein 1; Mip-1β (CCL4), C-C motif chemokine ligand 4; Myd88, myeloid differentiation primary response gene 88; NF-κB, nuclear factor kappa B; LPS, lipopolysaccharide; RANTES (CCL5), C-C motif chemokine ligand 5; TGFβ, transforming growth factor β 1; TGFβR, transforming growth factor β receptor; TLR, toll-like receptor. *[Adapted from Seki E et al, 2012 (217)]*.

I.2.3.2. Pathological bacterial translocation in chronic liver diseases

During cholestasis, due to the disruption of the biliary architecture, bile accumulates within the liver and cannot properly reach the intestine. Therefore, bile cannot exert anti-microbial effects on the intestine, which facilitates certain bacterial overgrowth and translocation to the liver (218). In line with this, bacterial translocation is particularly important in cholestatic liver diseases such as PBC and PSC (204). Different studies have reported qualitative and quantitative alterations in the gut microbiota of patients with PBC and PSC, which are characterised by bacterial overgrowth and decreased biodiversity (95, 219). Moreover, elevated LPS-binding protein and cluster of

differentiation 14 (CD14) (markers related to microbial translocation) in serum are associated with worse prognosis in PBC and PSC (220, 221). Autoantibodies found in PBC and PSC patients could also cross-react with bacterial components and promote processes as molecular mimickry (222).

There is a large body of evidence also supporting the role of the gut-liver axis in hepatocarcinogenesis (205). *Tlr4* deficient mice are protected from HCC development. Specifically, TLR4 signalling promotes HCC through various cellular effects, including NF-κB activation in HSCs and expression and release of epiregulin from these cells, which induces hepatocyte proliferation and inhibition of hepatocyte apoptosis (213). In KCs, LPS-TLR4 signalling promotes IL6 and TNF expression, which again trigger compensatory hepatocyte proliferation and mediate inflammation-related HCC (223). Likewise, LPS challenge promotes hepatocyte proliferation *in vivo* and *in vitro* in HCC cell lines (224). Metabolites derived from microbiota metabolism were also shown to impact hepatocarcinogenesis. Dysbiosis leads to augmented concentration of the secondary BA deoxycholic acid (DCA), which promotes the HSCs secretory phenotype resulting in inflammatory and pro-tumourigenic factor secretion (225). Similarly, the accumulation of cholesterol and secondary BAs in a mouse model of NAFLD-related HCC was suggested to accelerate liver carcinogenesis (226).

I.2.3.3. Regulation of the gut liver axis-mediated signalling

Regulation of the gut liver axis at different levels seems crucial in the inhibition of the progression of chronic liver disease. Importantly, antibiotic pre-treatment has shown to limit inflammation and liver damage after transplantation in both mice and humans (227). Similarly, limiting PAMP-derived signalling by antibiotic or probiotics had beneficial effects in different settings of liver injury (213-215). Faecal microbial transplant (FMT) form cirrhotic patients induces neuroinflammation in mice, while this effect is reduced when the colonization is performed with stools of cirrhotic patients previously subjected to FMT from healthy donors (228). This was also proven in patients with hepatic encephalopathy to whom FMT improves hepatic encephalopathy by reducing inflammation and cognition scores (229). Interestingly, a particular bacterial strain, *Bifidobacterium pseudocatenulatum* CECT7765 was shown to induce an anti-inflammatory phenotype in macrophages and KCs under chronic liver damage (230).

TLR signalling regulation is extremely complex and is subjected to a myriad of control systems including TLR folding and trafficking, regulatory proteins that bind at their ectodomains as well as post-translational modifications and adaptor proteins that regulate TLR-mediated intracellular signalling (231). TLR signalling regulation impacts liver disease progression. In this regard, single Ig IL1R-related molecule (SIGIRR) was shown to compete for an adaptor protein of toll like receptor 3 (TLR3), thus inhibiting its signalling and reducing liver inflammation in response to polyinosinic-polycytidylic acid [poly(I:C)] stimulation (232). A20 is another intracellular regulator of TLR-mediated signalling, it inhibits NF-κB signalling and has been reported to protect the liver from HCV and HBV infection (233). Interleukin-1 receptor associated kinase M (IRAK-M) binds to MyD88 to inhibit TLR-mediated signalling, in a model of alcoholic liver disease, IRAK-M deficiency lead to enhanced liver injury and enhanced pathological bacterial translocation from the gut (234). In summary, fine-tuning of the TLR-driven inflammation seems critical in the development of liver injury and carcinogenesis of diverse aetiologies.

I.3. The triggering receptor expressed on myeloid cell (TREM) family

I.3.1. TREM receptor family members and genomic location

The family of TREM receptors was discovered in 2000 (235, 236), since then, different members have been described and, owing to their ability to modulate inflammatory signalling, they have gained considerable interest in different diseases. The genes encoding for TREM family members are located in the human chromosome 6p21.1 where the main TREM receptors *TREM1* and *TREM2* are encoded. Here, the TREM-like (TREML) genes *TREML1*, *TREML2* and *TREML*4 and the pseudogenes *TREML3P* and *TREML5P* are also found. In mice, the TREM family is encoded in chromosome 17C and is composed by *Trem1*, *Trem2*, *Trem3*, *Treml1*, *Treml2* and *Treml4* (**Figure I.15.**).

TREM receptors are characterised by a single V-type extracellular immunoglobulin-like domain, a trans-membrane domain and a short cytoplasmic tail. Both human and mouse TREMs are unable to transduce intracellular signals, as they lack any intracellular signalling motif. In turn, TREMs couple to DNAX Adaptor Protein 12 (DAP12) also known as TYRO protein tyrosine kinase-binding protein (TYROBP), which transduces the signal intracellularly based on its immunoreceptor tyrosine-based activation motif (ITAM) that phosphorylates upon activation (237).

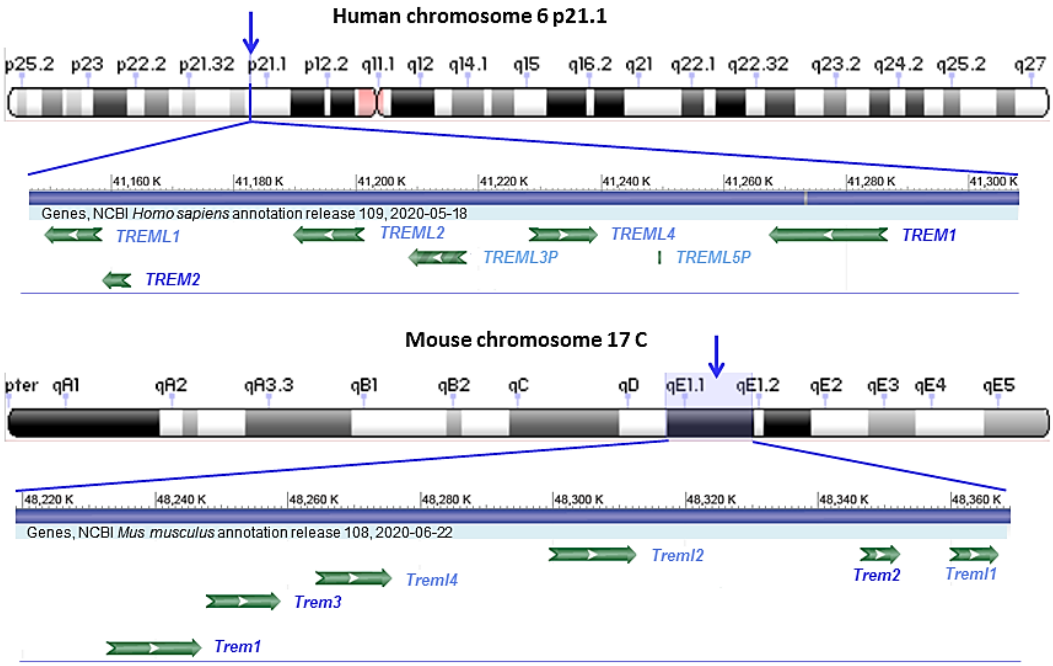

Figure I.15. Human and mouse genomic location of TREM family genes. In human, the TREM family of genes includes *TREM1*, *TREM2*, *TREML1*, *TREML2*, *TREML4* genes and *TREML3P* and *TREML5P* pseudogenes which cluster on chromosome 6. In mouse, *Trem* family members are encoded in chromosome 17 and include *Trem1*, *Trem2*, *Trem3*, *Treml1*, *Treml2 and Treml4*. TREM, triggering receptor expressed on myeloid cells; TREML, triggering receptor expressed on myeloid cells like *[Adapted from NCBI Gene database, NCBI, https://www.ncbi.nlm.nih.gov/gene]*.

The TREML receptors present the same V-type extracellular immunoglobulin-like domain, but in contrast to TREM members, they do present intracellular signal-transducer domains. Human TREML1 and mouse Treml1, Treml2 and Treml4 present a cytoplasmic immunoreceptor tyrosine-based inhibitory motif (ITIM) domain while human TREML2 possesses a SH3 binding domain for intracelular signalling (238). Alternative splicing or cleavage results in the generation of soluble forms of the TREM receptors. In this regard, soluble forms of TREM1, TREM2, TREML1 and TREML2 (sTREM1, sTREM2, sTREML1 and sTREML2) have been described. Although their role is still far from clear, they have been reported to compete with the full form of the receptors to negatively regulate their signalling (237).

I.3.2. Signal transduction

TREM-related signalling is a complex process, largely tissue and context dependent. The ligands for these receptors are still unknown, although some endogenous and exogenous agents have been suggested, overall anionic molecules or lipids (239, 240).

Upon ligand binding, TREM receptors couple to DAP-12 receptor, which becomes tyrosin phosphorylated and is able to attract different mediators, resulting in different signalling outcomes (241). Indeed, TREM1 and TREM2 have been shown to exert antagonic effects on TLR-mediated signalling. Although cell and tissue specific effects exist, TREM1 is generally believed to act as an enhancer of TLR-mediated inflammation, as it was reported to amplify inflammatory gene transcription upon TLR activation. By contrast, TREM2 is generally regarded as an anti-inflammatory receptor; due to its reported ability to inhibit TLR-mediated inflammatory gene transcription (242) (**Figure I.16.**). The specific inflammatory mediators modulated by TREM1 and TREM2 receptors will be discussed in detail in the next sections.

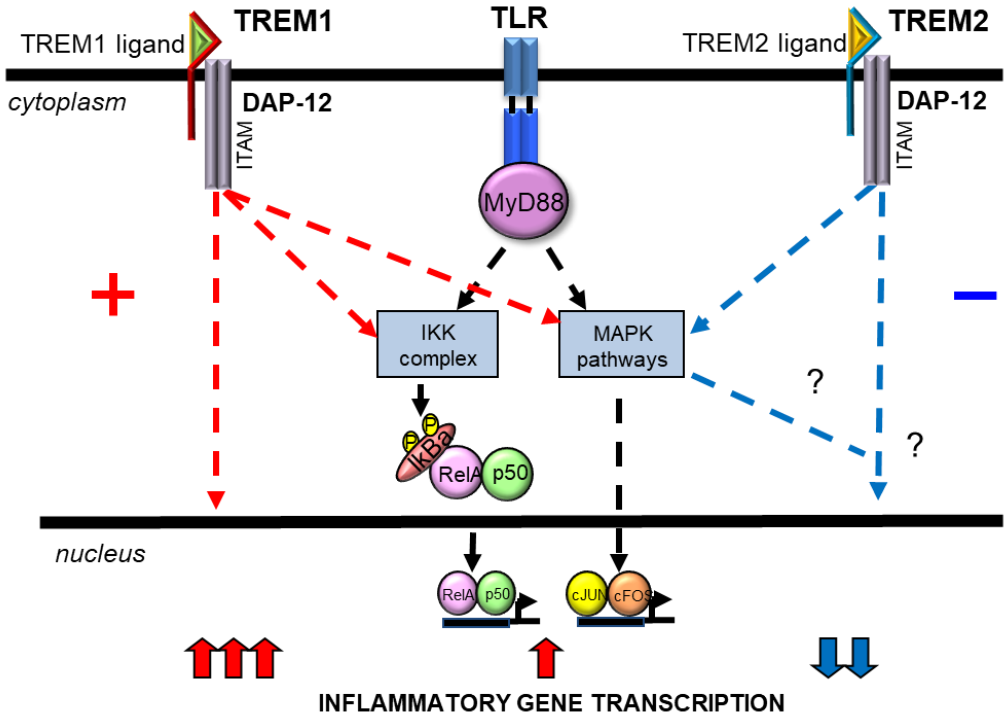

Figure I.16. TREM1 and TREM2 modulate TLR-mediated signalling. TREM receptors lack any signalling motif, thus, upon ligand binding, they both signal through the ITAM motif of DAP-12. Of note, the ligands for TREM1 and TREM2 are yet to be identified. TREM1 has been reported to amplify TLR-mediated signalling, as such, TREM1 activation results in ERK1/2 phosphorylation and increased nuclear levels of the NF-κB transcription factor, finally leading to the upregulation of inflammatory gene transcription. TREM2 is believed to dampen TLR-mediated signalling. TREM2 signaling shows differences compared to TREM1, upon ligand binding, TREM2 activation results in ERK1/2 phosphorylation while no effects are detected on the NF-kB pathway; ERK1/2, extracellular signal-regulated kinases 1/2; IκBα, NF-kappa-B inhibitor alpha; IKK, IκB kinase; ITAM, immunoreceptor tyrosine-based activation motif; MAPK, mitogen-activated protein kinases; Myd88, myeloid differentiation primary response gene 88; NF-κB, Nuclear factor kappa B; TLR, toll-like receptor; TREM, triggering receptor expressed on myeloid cells *[Adapted from Sharif O et al, 2008 (239)*].

Different theories have arisen to address the issue of how activation of the same adaptor molecule can give rise to antagonic cellular responses (240, 241, 243) (**Figure I.17.**). Regarding the first and the most widely accepted of these theories, downstream signalling effects of TREM receptor activation depend on the ligand eliciting such response. The so called high avidity ligands would lead to the total phosphorylation of DAP-12 and the recruitment of activatory molecules and activatory effects downstream of TREM1/TREM2 signalling, while low avidity ligands may lead to the partial phosphorylation of DAP12, and the recruitment of the Src homology region 2 domain-containing phosphatase 1 (SHP1), which would in turn dephosphorylate, and thus, direct to degradation the downstream mediators of TREM2 activatory response (240, 241, 243). Another theory suggests that some of the secondary mediators of TREM2-derived signalling may exert inhibitory signals in down-stream mediators of TLR signalling (241, 243). The last theory has mainly been described in dendritic cells, where the subcellular location of the receptor would dictate the outcome of the signalling (243).

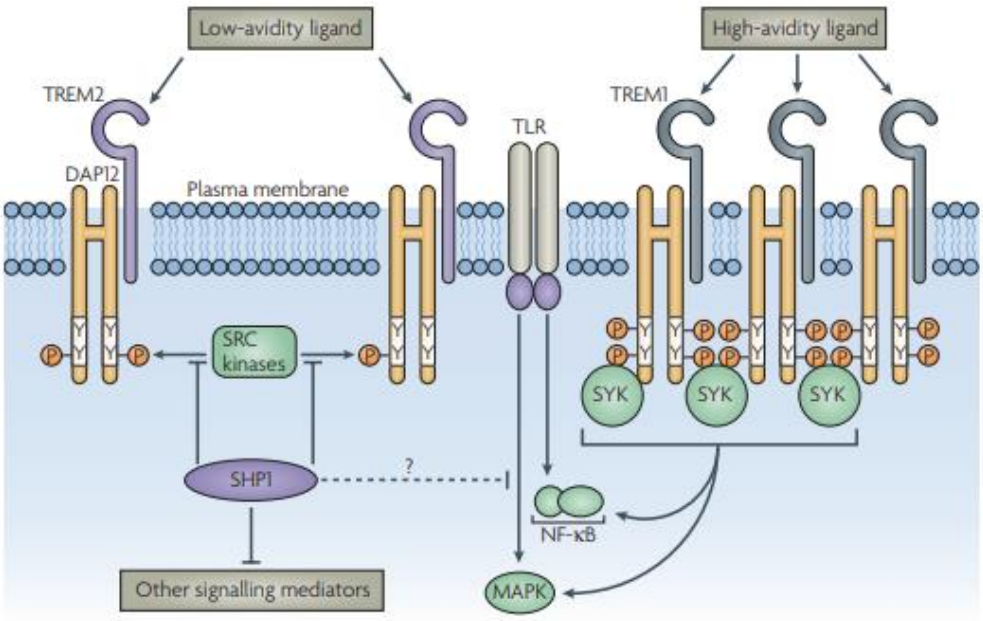

Figure I.17. Theory of low and high avidity ligands in TREM1 and TREM2 signalling transduction. Despite signalling through the same adaptor molecule, TREM1 and TREM2 activation leads to differentiated cellular responses. The low and high avidity ligand is the most accepted theory to explain this phenomenon. In this regard, binding of high avidity ligands to TREM1/TREM2 would lead to the total phosphorylation of DAP-12 and the recruitment of activatory molecules. By contrast, low avidity ligand binding to TREM2 would result in the partial phosphorylation of DAP-12, finally leading to the recruitment of inhibitory mediators. DAP12, DNAX-activation protein 12; MAPK, mitogen-activated protein kinases; NF-κB, Nuclear factor kappa B; P, phosphate; SHP1, Src homology region 2 domain-containing phosphatase-1; SRC, Proto-oncogene tyrosine-protein kinase; Syk; spleen tyrosine kinase; TLR, toll like receptor; TREM1, triggering receptor expressed in myeloid cells 1; TREM2, triggering receptor expressed on myeloid cells 2; Y, tyrosin *[Adpted from Turnbull I et al, 2007 (241)*].

I.3.3. TREM1

TREM1 was the first member of the TREM family of receptors to be discovered (235). Since then, TREM1 has been widely described as a pro-inflammatory receptor, as it enhances TLR mediated signalling in various tissues and contexts. Overall, TREM1 activation in myeloid cells results in an exacerbated innate immune response with increased expression of inflammatory mediators including IL1β, IL6, IL8, IL10, TNF and MCP1 (235, 244-247). This pro-inflammatory effect results in the progression of different inflammation-related diseases such Chron and ulcerative cholitis (248) atherosclerosis (249) or rheumatoid arthritis (250).. TREM1 is also implicated in different cancers. In this regard, *Trem1*$^{-/-}$ mice are protected from intestinal inflammation related cancer (251) and inhibition of TREM1 delays lung cancer xenograft growth (252).

In the liver, TREM1 is expressed in LSECs, KCs, HSCs and HCC cells (253-255)and it is also implicated in various forms of liver diseases. In this regard, owing to its effects as an activator of inflammatory responses in KCs and myeloid cells, TREM1 promotes progression of chronic liver diseases produced by viral infections (256, 257), alcohol (258), NAFLD (259) as well as liver injury and fibrosis (260).

In HCC, TREM1 promotes cancer cell proliferation and invasion and its expression correlates with increased recurrence and shorter survival in patients (255).. Furthermore, TREM1 regulates KCs responses to liver damage promoting the activation of NF-κB and the JNK signalling pathways and the subsequent expression of the inflammatory markers IL6, IL1β, TNF, CCL2, and CXCL10 upon administration of the hepatotoxic diethylnitrosamine (DEN). In an HCC mouse model based on the exposure to the same hepatotoxic, TREM1 promotes liver tumourigenesis (261). Moreover, TREM1 regulates immunosuppression and directs resistance to anti-programmed death-ligand 1 (PDL1) therapy (262).

I.3.4. TREM2

TREM2 is expressed on myeloid cells including alveolar, bone, central nervous system (CNS), and/or liver macrophages, this receptor is also expressed in dendritic cells, and endothelial cells (239). TREM2 loss of function mutations were identified as causative for a rare neurodegenerative disease termed Nasu–Hakola or lipomembranous osteodysplasia with sclerosing leukoencephalopathy (PLOSL) (236). This disease is

characterised by bone cysts that lead to fractures and dementia. Regarding disease pathobiology, TREM2 may be involved in osteoclast (macrophages in the bone) differentiation from myeloid cells, which is impaired in patients with PLOSL (263).

Since its association with PLOSL, TREM2 has been linked to diseases of the CNS due to its key role in the regulation of the homeostasis of microglia, the macrophage population of the CNS. In line with this, TREM2 was first discovered to play opposite effects to TREM1, as it was shown to suppress production of the inflammatory cytokines TNF and IL6 in macrophages upon TLR stimulation with different ligands (264, 265). The TREM2 variant R47H (rs75932628) is associated with increased risk of Alzheimer´s disease (AD) (266). Moreover, genetic variants of TREM2 are also associated with other neurodegenerative disorders such as amyotrophic lateral sclerosis (ALS) (267) and fronto-temporal dementia (268). Defects in microglial function have been reported in *Trem2* deficient (*Trem2*$^{-/-}$) mice, or mice harbouring genetic variants of *Trem2,* subjected to different forms of neurodegenerative diseases. The phnotype observed in these mice is characterised by microglial activation, increased apoptosis, failure to clear myelin or Aβ plaques, and failure to sense and response to lipids (269-271).

TREM2 also plays important roles in myeloid populations outside the central nervous system (240). This receptor was shown to promote phagocytosis in peritoneal and bone marrow derived macrophages, as well as in neutrophils (272, 273). By contrast, in the lung, TREM2 inhibits bacterial opsonisation and phagocytic activity in alveolar macrophages (274). In a model of virus-induced chronic obstructive pulmonary disease (COPD), TREM2 promotes survival and proliferation of M2 macrophages, which finally results in the progression of the disease (275). TREM2 also impacts gut macrophage homeostasis, as it was shown to promote wound-healing by directing macrophages to an M2 phenotype upon intestinal damage (276). In a model of chemically induced colitis TREM2 induced the opposite effects, promoting inflammation and exacerbating mucosal damage (277) Therefore, it is important to note that TREM2 effects may be disease and cell-type specific. More recently, TREM2 has been linked to metabolic homeostasis in obesity. In this context, TREM2 drives the differentiation of a particular macrophage subset, named as lipid associated macrophages (LAMs) in a mouse model of obesity based on HFD. In *Trem2*$^{-/-}$ mice, the myeloid compartment on the adipose tissue response fails and the LAM population is lost, which is associated with the disruption of the expression profile characteristic of

this type of macrophages. The loss of LAMs finally leads to the development of adipocyte hypertrophy, hypercholesterolemia and glucose intolerance (278).

Uncovering the role of TREM2 in the liver has been the objective of our research group and others in the last years. Initially, TREM2 and other TREM family members were shown to be expressed in liver macrophages and LSECs (253). Moreover, TREM2 expression in KCs was shown to modulate the response of these cells to the malaria inducing parasite *Plasmodium Berghei* (279). More recently, high throughput techniques such as single cell RNA sequencing (scRNAseq) have revealed particular TREM2 expressing macrophage subsets that associate with NAFLD (280) and cirrhosis (281).TREM2 expression was also detected in liver dendritic cells, where it protects the liver from acute ischemia/reperfusion injury (282). Importantly, the expression of this receptor is upregulated in various types of cancers (283-286). During hepatocarcinogenesis TREM2 is able to inhibit HCC cell growth, migration and invasion in a mechanism involving the phosphoinositide 3 kinase (PI3K)/RAC-alpha serine/threonine-protein kinase (AKT)/β-catenin signalling axis (287).

I.3.5. The role of TREM2 during the progression of liver injury: previous data from our group

Previous studies of our research group have focused on unravelling the role of TREM2 in acute and chronic hepatocellular injury and during hepatocarcinogenesis (**Figure I.18.**) (288, 289). First, we described that in human, TREM2 expression is enhanced in patients with liver cirrhosis regardless of the aetiology and also in livers of patients with HCC compared to controls. Moreover, *TREM2* expression positively correlates with the expression of different markers of liver inflammation (*IL1β*, *IL6*, *IL8* and *TNF*) and fibrosis (Collagen type 1 alpha 1 (*COL1A1*) and actin alpha 2, smooth muscle (*ACTA2*) in patients with HCC. This tendency is conserved in mouse models of acute and chronic liver injury and HCC, where an increase in *Trem2* expression is detected compared to control conditions. Importantly, TREM2 expression is mainly restricted to KCs and HSCs compared to hepatocytes in human and mouse. Experiments performed in *Trem2*$^{-/-}$ mice show that this receptor acts as a protecting agent against hepatocellular injury and malignant transformation to HCC, due to its anti-inflammatory effects in KCs and HSCs. In this line, *Trem2*$^{-/-}$ mice subjected to chronic administration of carbon tetrachloride (CCl_4) show an exacerbated phenotype with increased hepatocellular injury and cell death compared to wild type (WT) mice. This is explained by the action of this receptor in the acute phases of liver injury. Thus, in acute models of liver injury

(CCl_4 and acetaminophen (APAP) administration), *Trem2*$^{-/-}$ mice show enhanced serum aspartate aminotransferase (AST) and alanine aminotransferase (ALT) levels, inflammatory gene transcription, oxidative stress and immune infiltration into the liver. Of note, *Trem2*$^{-/-}$ display shorter survival times after a lethal dose of acetaminophen. As aforementioned, TREM2 is mainly expressed in KCs and HSCs, the main cellular types orchestrating the wound-healing response to liver injury. In this regard, KCs and HSCs derived from *Trem2*$^{-/-}$ mice exhibit enhanced expression of the inflammatory cytokines *Il1β*, *Il6* and *Tnf* and the chemokines *Mcp1* and *Cxcl1* upon LPS-mediated TLR stimulation (288).

Hepatocarcinogenesis is regarded as the final step of chronic liver disease progression. In this regard, the anti-inflammatory effects of TREM2 also impact the transformation to the malignant phenotype. In acute phases of hepatocarcinogenesis, *Trem2*$^{-/-}$ mice display exacerbated liver and DNA damage as well as increased oxidative stress and inflammatory marker expression. TREM2 also exerts an effect in hepatic regeneration, upon partial hepatectomy, *Trem2*$^{-/-}$ animals exhibit increased expression of proliferative markers and inflammation. Importantly, *Trem2*$^{-/-}$ mice develop more tumours after 30 or 40 weeks of DEN administration, with enhanced hepatocyte proliferation and DNA damage. These effects seem to be mediated by the interplay between HCC and HSC cells. *TREM2* overexpressing human HSCs show reduced expression of inflammatory mediators and Wnt ligands. Moreover, HCC spheroids grow less when cultured in presence of *TREM2* overexpressing HSC conditional media, as compared to control plasmid transfected HSCs-derived conditioned media. Moreover, these effects are dependent on Wnt/β-catenin signalling (289).

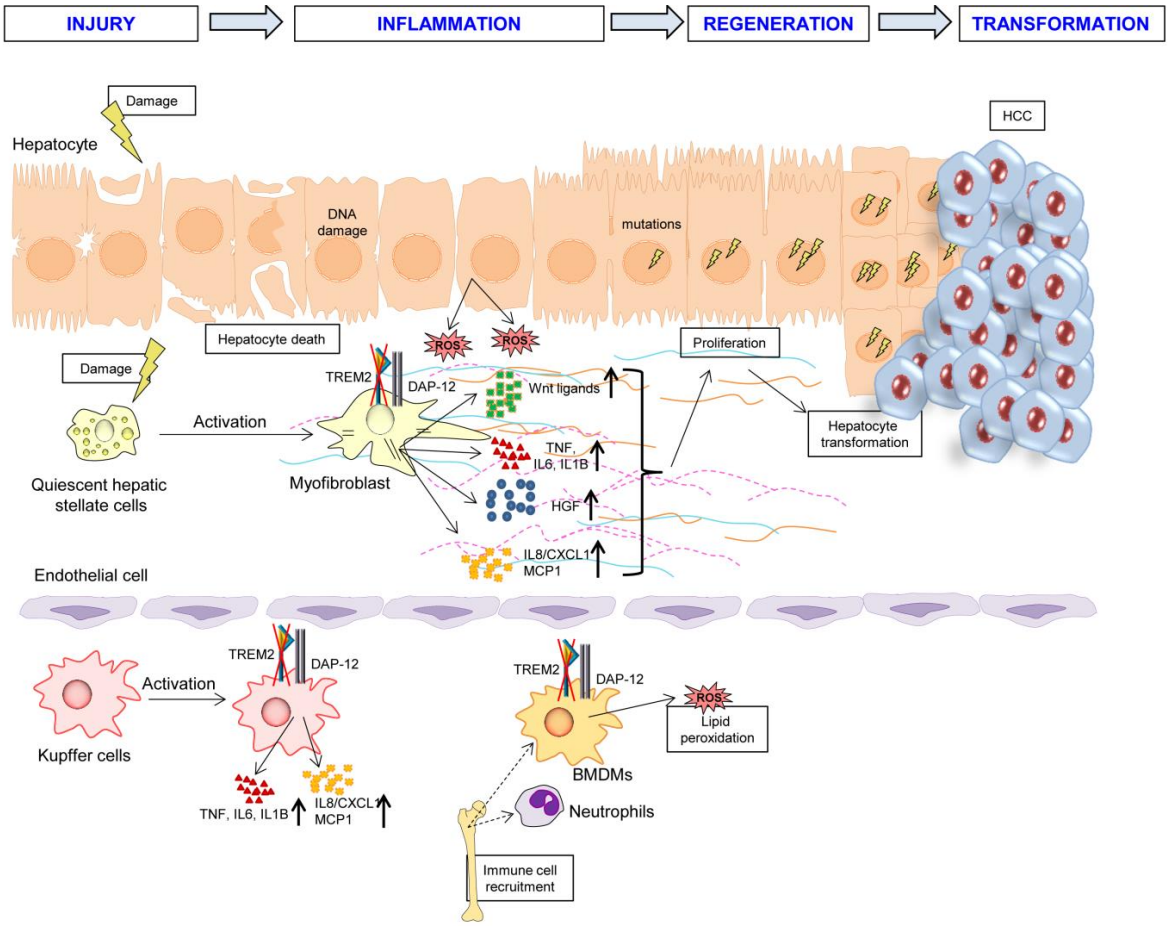

Figure I.18. Working model of TREM2 actions under chronic liver damage and hepatocarcinogenesis. After liver injury, in the absence of *Trem2*, hepatocyte damage and death are increased. This is associated with increased ROS production, augmented cytokine, chemokine, growth factor, WNT ligand expression and DNA damage. In addition, in the absence of *Trem2*, immune cell recruitment to the liver is enhanced and ROS production in BMDMs is increased, which is associated with increased lipid peroxidation in the liver. On the other hand, during liver regeneration, an increase in early phase inflammatory cytokine and growth factor expression is observed, which is associated with enhanced hepatocyte proliferation in the absence of *Trem2*. This pro-inflammatory microenvironment may favour the appearance of mutations in the proliferating hepatocytes, promoting their transformation and the development of HCC. BMDMs, bone-marrow derived macrophages; CXCL, C-X-C Motif Chemokine Ligand; DAP-12, DNAX-activation protein 12; HGF, hepatocyte growth factor; IL, interleukin; MCP1, monocyte chemoattractant protein 1; TNF, tumour necrosis factor; TREM2, triggering receptor expressed in myeloid cells 2 *[Adapted from Esparza-Baquer A et al, Gut 2020, (289)]*.

HYPOTHESIS AND OBJECTIVES

TREM2 was already reported to play a crucial role in the regulation of inflammatory responses during both, acute and chronic hepatocellular damage, and also during hepatocarcinogenesis by previous studies of our research group (288, 289). Taking these data into account, here, we hypothesised that TREM2 may also participate in the regulation of inflammatory responses during chronic cholestasis and fibrosis-associated HCC. Thus, In order to prove our hypothesis, we propose the following specific aims:

1. Evaluate *TREM2* expression in the liver of patients with cholestatic disease in comparison to healthy and cirrhotic livers of diverse aetiologies.

2. Evaluate the expression levels of *Trem2* in animal models of cholestasis.

3. Characterise the role of TREM2 in the development of biliary injury in an obstructive cholestasis model.

4. Determine the contribution of signals derived from bacterial translocation to the TREM2 mediated phenotype in an obstructive cholestasis model.

5. Characterise the role of TREM2 in the development of biliary injury in a chemically-induced cholestasis model.

6. Address the role of TREM2 as a novel mediator of the effects of UDCA treatment in non-parenchymal liver cells.

7. Characterise the specific immune subpopulations expressing TREM2 in HCC tumours in patients.

8. Determine the role of TREM2 during fibrosis-associated hepatocellular carcinogenesis.

MATERIALS AND METHODS

M.1. Human liver tissue samples

M.1.1. San Sebastian/Warsaw cohort of patients

In order to assess *TREM2* gene expression levels in human cholestasis, we obtained liver tissue samples from control individuals, patients with cirrhosis of different aetiologies and patients with PBC or PSC. Patient characteristics and clinical parameters are presented in **Table M.1**. Healthy liver tissue samples were derived from control individuals with colorectal metastasis on the liver. Here, healthy liver tissue was obtained by selecting non-neoplastic tissue located furthest away from tumour mass lesions. Control (n=18) and cirrhotic (n=35) samples were provided by the Basque Biobank and were processed according to standard procedures approved by the Clinical Research Ethics Committees of the Basque Country and the Donostia University Hospital. An informed consent was obtained from all subjects. Samples derived from patients with PBC or PSC were provided by Dr. P. Milkiewicz from the Medical University of Warsaw, Warsaw (Poland) and Dr. M. Milkiewicz from the Pomeranian Medical University, Szczecin (Poland). All patients included in the study underwent liver transplantation (LT) at the Department of General, Transplant and Liver Surgery (Warsaw, Poland) between June 2014 and November 2016. A total of 20 samples from explanted livers (PBC n=10, and PSC n=10) were either immediately frozen in liquid nitrogen for subsequent analysis of mRNA. Total RNA was extracted from 50-mg tissue samples using the RNeasy Mini Kit according to the manufacturer's instructions (Qiagen, Hilden, Germany). Isolated RNA quantity and quality was determined using Epoch™ Microplate Spectrophotometer (BioTek Vermont, USA). Procedures were approved by the Research Ethics Committe of the Medical University of Warsaw.

Table M.1. Patients and clinical characteristics of the San Sebastian/Warsaw study cohort.

Variable	Control (n=18)	Cirrhotic (n=35)	PBC (n=10)	PSC (n=10)
Age, (years)	66.26 ± 7.54	63.46 ± 8.9	59 ± 6.28	28.5 ± 12.15
Gender, n (%)				
Male	13 (72.22)	33 (94.28)	1 (10)	7 (70)
Female	5 (27.78)	2 (5.17)	9 (90)	3 (3)
Aetiology, n (%)				
Alcoholic	-	11 (31.43)	-	-
HCV	-	9 (25.71)	-	-
Idiopathic	-	6 (17.14)	-	-
HCV+HBV	-	3 (8.57)	-	-
HBV	-	2 (5.71)	-	-
HCV+HIV	-	1 (2.86)	-	-
HCV+HBV+HIV	-	1 (2.86)	-	-
HBV+EtOH	-	1 (2.86)	-	-
Hemochrom.	-	1 (2.86)	-	-
Histological staging, n (%)				
F1-F2	-	-	1 (10)	4 (40)
F3-F4	-	35 (100)	9 (90)	6 (60)
Serum biochemistry,				
ALT, (IU/l)	20.5 ± 7.22	31 ± 28.16	60 ± 43.32	54 ± 102.68
AST, (IU/l)	23 ± 6.24	36 ± 29.49	65 ± 61.35	78.5 ±47.87
GGT, (IU/l)	-	96 ±201.90	84 ± 52.91	204 ± 613.21
Alkaline phosphatase, (IU/l)	-	78 ± 32.29	216 ± 333.1	366 ± 595.3
Bilirubin	0.55 ± 0.18	0.6 ± 0.27	6.16 ± 7.18	2.25 ± 10.06

Data are shown as median ± SD.
ALT, alanine aminotransferase; AST, aspartate transaminase; HBV, hepatitis B virus; GGT, gamma glutamil transferase; HCV, hepatitis C virus; Hemochrom., hemochromatosis; HIV, human immunodeficiency virus; IU, international units; PBC, primary biliary cholangitis; PSC, primary sclerosing cholangitis; SD, standard deviation.

M.1.2. GSE79850 cohort of patients

To analyse TREM2 in additional cohort of PBC patietns, we downloaded the GSE79850 array data set, which contains 24 liver tissue samples, including control (n=8), low-risk PBC (n=7) and high-risk PBC (n=9) samples, RNA samples were obtained from FFPE tissue at the time of biopsy and prior to treatment; controls from the donor liver transplant recipients were included (290). In this study, low-risk PBC

patients are defined according to the following criteria: 1) Fully responsive to UDCA according to Paris 1 criteria; 2) Remained well and in full UDCA response after a minimum of 15 years follow up; 3) Did not require liver transplantation. Whereas high-risk PBC patients were defined as: 1) Non-responders to treatment with UDCA at one year of treatment at a dose of 13–15 mg/Kg using Paris 1 criteria; 2) Requiring liver transplantation for prognostic reasons for their PBC during subsequent follow-up.

M.1.3. Cohort of patients included in the IHC studies

TREM2 expression was analysed by IHC in the liver of patients with HCC of different aetiologies and in healthy liver tissue of control individuals with colorectal or mamary metastasis on the liver. Patient characteristic and clinical parameters are presented in **Table M.2**. These samples were provided by the Basque Biobank and were processed according to standard procedures approved by the Clinical Research Ethics Committees of the Basque Country and the Donostia University Hospital. An informed consent was obtained from all subjects.

Table M.2. Patients and clinical characteristics of the cohor of patients included in the IHC studies.

Variable	**Control** (n=4)	**HCC** (n=10)
Age, (years)	61.5 ± 11.79	59.2± 7.38
Gender, n (%)		
Male	0 (0)	10 (100)
Female	4 (100)	0 (0)
Aetiology, n (%)		
Alcoholic	-	1 (10)
HBV	-	2 (20)
HCV	-	3 (30)
HCV+HBV	-	1 (10)
Hemochrom.	-	1 (10)
Idiophatic	-	2 (20)
Serum biochemistry,		
ALT, (IU/l)	27.5 ± 14.36	31.10 ± 9.86
AST, (IU/l)	30.75 ± 17.48	29.00 ± 9.97

Data are shown as median ± SD.
ALT, alanine aminotransferase; AST, aspartate transaminase; HBV, hepatitis B virus; HCC, hepatocellular carcinoma; HCV, hepatitis C virus; Hemochrom., hemochromatosis; IU, international units; SD, standard deviation.

M.1.4. GSE125449 cohort of patients and scRNAseq analysis

sgRNAseq data from 9 human HCC tumours was obtained from the publicly available GSE125449 (291). Clinical information on the HCC patients and the pipeline for scRNAseq including quality control have already been described in the original publication (291). Briefly, filtering for high quality cells included keeping cells with at least 500 features detected, with a percent of mitochondrial RNA less than 20%. Data was log-normalised and scaled to factor 10000. From 18274 genes, 4655 genes were selected for the analysis, based on whether they were detected in at least 10 % of the cells in each group under comparison. Genes with highest differences between groups were defined as having average logFC >1 and adjusted p-value < 0.01. PCA clustering was performed on 2244 most variable features. Clustered data was visualised using t-distributed Stochastic Neighbor Embedding (t-SNE) through the Seurat R package. Differential expression analysis between TREM2 expressing TAMs (cluster 1 and 2) and the rest of the TAMs was implemented with Seurat. For identification of enriched gene signatures, we used gene set enrichment analysis (GSEA) implemented in the clusterProfiler R package and Molecular Signatures Database (MSigDB) v7.

M.2. Mouse models of cholestasis and hepatocarcinogenesis

Experiments with animals were performed in WT and *Trem2*$^{-/-}$ mice. Age-matched male WT and *Trem2*$^{-/-}$ mice (both of C57BL/6 genetic background) were bred at the animal facility of the Biodonostia Health Research Institute. *Trem2*$^{-/-}$ mice were obtained from Dr. Marco Colona from the Department of Pathology and Immunology, Washington University School of Medicine, St. Louis (USA) and were backcrossed onto a >98% C57BL/6 background and generated as previously described (264). All experiments were performed under the approval of the Animal Experimentation Ethics Committee of Biodonostia Health Research Institute (CEEA15/001, CEEA15/020, CEEA18/21, CEEA19/002, CEEA19/004).

At the indicated time points for each experiment, mice were humanely killed under general isoflurane-based anaesthesia. After measuring their body weight, blood was collected by cardiac puncture. Blood was then centrifuged at 1500 g for 20 minutes at 4ºC for serum extraction. Serum ALT, aspartate aminotransferase AST, alkaline phosphatase (AP), and bilirubin levels were measured at the Donostia University Hospital in a Cobas 8000 c702 (Roche) analyser. In parallel, the liver was extracted and weighted. The liver was further processed; that is, 3 pieces from different lobules were

fixed in paraformaldehyde 4% (Merck) for histological analysis. The remaining liver was stored at -80ºC for further processing.

Cholestasis is a pathological condition characteristic of cholangiopathies of diverse origins. This condition can manifest in different clinical situations and follows a complex pathobiological process (74). Therefore, a single mouse model fails to recapitulate the full picture of this condition (292); as a consequence, we chose to perform different models of cholestasis to recapitulate different aspects of the disease. Patients with chronic cholestatic diseases are at a higher risk of developing hepatobiliary carcinogenesis (183-185). In order to assess the role of TREM2 in liver carcinogenesis associated to fibrosis, we also carried out different HCC models in WT and *Trem2*$^{-/-}$ mice. Similar to chronic cholestasis, HCC is also a complex and highly heterogeneous disease (195), of note, around 80% of the HCCs arise in cirrhotic livers (191). Therefore, we also chose to perform different models of fibrosis-associated HCC.

M.2.1. BDL-based obstructive cholestasis model

The BDL model was employed to provoke obstructive cholestasis. In this model, the common bile duct is ligated, therefore stopping bile flow and leading to increased concentration of BAs and other bile-derived products in the liver. After BDL, mice develop biliary obstruction, ductular reaction and biliary fibrosis in the liver (293). In parallel, heavy alterations are also detected in the gut. Of note, in this model bacterial products translocate from the gut to the liver is detected (294). BDL was performed as previously described (293). Briefly, 10-12 week old WT and *Trem2*$^{-/-}$ mice were used; a 2 cm excision was made in the abdomen of the mice to expose the common bile duct. This was ligated in two points using 6-0 non absorbable surgical silk. Then, the peritoneum was rinsed with sterile phosphate buffered saline (PBS) and chlorhexidine, the muscle was sutured with 6-0 non absorbable surgical silk and the skin with 3-0 non absorbable surgical silk. Sham operated mice were used as control, in these mice the same protocol was followed except for common bile duct ligation. Analgesic treatment based on meloxicam (Boeringher Ingelheim) was given to mice when needed. Mice were humanely killed at 7 days after surgical procedure.

M.2.2. α-naphthylisothiocyanate (ANIT)-based model of chemical cholestasis

ANIT is a chemical compound which is initially metabolised in hepatocytes by conjugation with glutathione (GSH) and is secreted in bile via multidrug resistance-associated protein 2 (MRP2). The ANIT-GSH complex is unstable in bile and dissociates, thus exposing cholangiocytes to high concentrations of this compound. Additionally, ANIT undergoes various cycles of secretion-reabsorption by hepatocytes, where it is always conjugated with GSH, therefore depleting glutathione and, thus, also producing hepatocellular toxicity (295). When administered at a high-single dose by oral gavage, ANIT produces severe cholangiocyte destruction leading to intrahepatic cholestasis (295, 296). To perform this model, 8 week old WT and *Trem2*$^{-/-}$ mice were administered 50mg/kg of ANIT (Sigma-Aldrich) dissolved in olive oil (O.Oil) (Sigma-Aldrich) by oral gavage, control animals were administered O.Oil by the same procedure. Mice were sacrificed 48 hours after the administration of ANIT or O.Oil.

M.2.3. DDC-based model of chemical cholestasis

As another alternative model of cholestasis, the chemical cholestasis model based on a diet supplemented with DDC was performed. DDC inhibits ferrochelatase, the enzyme that produces the Heme group from protoporphyrin in the liver (297). When this enzyme is inhibited, protoporphyrins accumulate in the liver. Protoporphyrins can only be secreted in bile, thus, in the presence of DDC, the accumulating protoporphyrins cannot be properly secreted and provoke biliary obstruction and hepatocellular damage (298). Subsequently, a phenotype of xenobiotic-induced cholestasis is developed in the liver, which is characterised by cholangiocyte proliferation, pericholangitis and biliary fibrosis in both, intra and extrahepatic bile ducts (299). The DDC model was performed in 8 week old WT and *Trem2*$^{-/-}$ mice which were fed a 0.1% DDC diet (Ssniff) for 4 weeks. Control mice were fed the same diet without DDC (Ssniff). All mice were humanly killed 4 weeks after the diet initiation.

M.2.4. BDL-based obstructive cholestasis model with gut sterilisation by an antibiotic (Abx) cocktail

To evaluate the involvement of gut-liver axis in the TREM2-associated phenotype, the BDL-based model was performed in mice subjected to gut sterilisation. The combination of Abx was the following: 1 g/l ampicillin (Sigma-Aldrich), 1 g/l neomycin (Gibco), 1 g/l metronidazole (Acros Organics) and 500 mg/l vancomycin

(Pfizer). This combination of Abx was administered in drinking water as previously described, being this a valuable method for gut sterilization (58). Abx treatment was given in drinking water for a total of 4 weeks, and in the 3rd week of Abx administraton, BDL was performed; then, mice were humanely killed 7 days after the BDL surgery.

M.2.5. DEN+CCl_4-based model of fibrosis associated-HCC

Fibrosis-associated HCC was induced in WT and *Trem2*$^{-/-}$ male mice by combining DEN administration with CCl_4 injections, based on previously reported approaches (213). DEN is a potent hepatocarcinogen in mice; it is metabolised by cytochrome P450 CYP2E1 to produce unstable metabolites that cause DNA damage. When administered during active hepatocyte proliferation, as in the postnatal period, DEN induced mutations are transmitted to daughter cells leading, in the long term, to the generation of HCC tumours (300). Additionally, CCl_4 is metabolised in the liver to form the CCl_3 radical, which leads to lipid and protein peroxidation, subsequently inducing hepatocyte death and activation of an overwhelmed repair process, that finally results in liver fibrosis (301). To perform this combination model, WT and *Trem2*$^{-/-}$ male mice were injected with 30mg/kg DEN at 15 days postpartum, thereafter, 10 weekly injections (1 injection once a week) of CCl_4 at 2 µl/g body weight (CCl_4/O.Oil 1:3 [volume:volume]) were performed, starting at 4 weeks of age (2 weeks after DEN injection). Mice were humanely killed 30 weeks after DEN injection, in the sacrifice, tumours were manually counted and size was recorded.

M.2.6. Thioacetamide (TAA)-based model of fibrosis-associated HCC

As a second approach to perform a fibrosis-associated HCC model, we administered TAA to mice. TAA is commonly used to generate liver fibrosis and it was also shown to produce spontaneous hepatocarcinogenesis in the long term in mice (302). When metabolised in the liver, TAA-derived metabolites induce oxidative stress and centrilobular necrosis, provoking a defective reparative response and liver fibrosis, which can also lead to tumour formation (301) . To perform this model, 8 week-old WT and *Trem-2*$^{-/-}$ male mice were administered 0.03% weight/volume (w/v) TAA (Sigma Aldrich) in drinking water for 40 weeks. Mice were humanely killed 40 weeks after treatment initiation, in the sacrifice, tumours were manually counted and size was recorded, tumour volume was calculated using the formula: (Tumour volume = Wide^2 X Long)/2); Tv = ($W^2 \times L$)/2 (303).

M.3. Mouse primary cell isolation, culture and treatment

M.3.1. *In situ* mouse liver perfusion for primary cell isolation

With the aim of extracting different liver cell types, first an *in situ* liver perfusion step, a common protocol for the extraction of all cell types, was performed. During the entire procedure, mice were maintained under general anaesthesia based on isoflurane (Abbvie) in inhaling oxygen. First, the abdomen was opened and the internal organs were exposed. Thereafter, the portal vein was cannulated using a 22G cannula (BD Insyte), the tubing was connected to the catheter and the perfusion solution was pumped by a perfusion pump at a flow of 5 ml/minute. The inferior vena cava was cut below the liver, thus, enabling perfusion solutions to enter the liver and exit through the inferior vena cava. Regarding the perfusion solutions, the liver was first washed with a perfusion buffer containing 10 mM 4-(2-hydroxyethyl)-1-piperazineethanesulfonic acid (Hepes), 2.7 mM potassium chloride (KCl), 135 mM sodium chloride (NaCl) and 250 μM sodium diphosphate (HNa_2PO_4) (all from Sigma-Aldrich). Next, the liver was perfused with 50 ml of perfusion buffer containing 60 mg of Collagenase type IV (Gibco) and 10 mM calcium chloride ($CaCl_2$) and flow was decreased to 3 ml/minute, thus achieving the digestion of the liver. During this step, the inferior vena cava was clamped above the diaphragm in order to direct the solutions to the liver and to prevent the perfusion of other organs. For the isolation of KCs and HSCs, an additional intermediate step was performed before the collagenase-based digestion. Specifically, 100 μl of 200 mg/ml pronase (Roche) were added to 50 ml of F-12 media (Gibco) and the liver was perfused at 3 ml/minute. Finally, the liver was carefully removed. For KCs and HSCs isolation, a minimum of 3 mouse livers are necessary to yield enough cells and, in this case, livers were kept in ice until all the livers were perfused.

M.3.2. Isolation of mouse hepatocytes

Mouse hepatocytes were isolated by our group as previously described (304). Briefly, after *in situ* perfusion livers were homogenised and filtered with a 70 μm cell strainer (Falcon) to eliminate undigested tissue remnants. Three consecutive washing steps were carried out by centrifuging the cell suspensions at 800 g for 6 minutes at 4ºC and resuspending them in William's medium E (Sigma-Aldrich) supplemented with 10% heat-inactivated foetal bovine serum (FBS) (Gibco), 1% penicillin-streptomycin (P/S) (Gibco) and 1% MEM Non-essential amino acids (NEAA) (Gibco). After the last centrifugation, the cell suspensions were resuspended in 25 ml of supplemented

William's medium E. Next, a Percoll-based (Sigma-Aldrich) density gradient solution was prepared by adding 2.4 ml of PBS 10X to 21.6 ml Percoll, and the cell suspension was added to the top of the density gradient. The gradient was centrifuged for 10 minutes at 1500 g at 4ºC without brake. Isolated hepatocytes were cultured in thin collagen-coated plates with William's medium E supplemented with 10% FBS, 1% penicillin-streptomycin and 1% NEAA. Thin collagen was prepared adding glacial acetic acid (500 µL, Corning) to sterile MilliQ water (500 mL). Rat tail collagen type I (354236, BD) was added to a final concentration of 50 mg/L and the mix was filtered through a 0.22 µm pore size filter (Corning).

M.3.3. Isolation of mouse cholangiocytes

Normal mouse cholangiocytes (NMCs) were isolated by our group as previously described (305). For mouse cholangiocyte isolation, *in situ* perfusion was performed following the same protocol, but different perfusion solutions were employed. First, the liver was perfused with Hanks solution A containing 120mM NaCl, 5mM KCl, 0.4 mM KH_2PO_4, 0.2 mM Na_2HPO_4, 25mM $NaHCO_3$, (all from Sigma-Aldrich) 0.1% D-Glucose (Sigma-Aldrich), 0.095% EGTA (Sigma-Aldrich) and 4 units of heparin at a flow of 5 ml/minute. Then, perfusion was continued with Hanks solution B containing 120mM NaCl, 5mM KCl, 0.4 mM KH_2PO_4, 0.2 mM Na_2HPO_4, 25mM $NaHCO_3$, 0.82mM $MgSO_4$, 1.07mM $MgCl_2$, 4mM $CaCl_2$, (all from Sigma-Aldrich) 0.1% D-Glucose, 5.1 µg/ml soybean trypsin inhibitor (STI) (Gibco), 0.025% Collagenase type IV. After *in situ* perfusion, the liver was extracted and washed with Dulbecco's modified eagle medium (DMEM) (Gibco) discarding the liver capsule. Then the biliary tree was isolated with tweezers and the rest of the parenchyma containing the hepatocytes was discarded. Once the biliary tree was isolated, it was further digested with 20 ml of Pronase solution containing 1% BSA (Sigma Aldrich), 0.025% Collagenase type IV, 0.034% pronase , 0.006% DNase, 1% penicillin/streptomycin (P/S) (Gibco) at 37ºC for 30 minutes with shake at 140 rpm. After incubation, the cholangiocyte solution was filtered through a 100 µm filter. Newly isolated NMCs were cultured in the enriched flask medium in thick collagen coated plates. Flask medium consists on DMEM/F12 supplemented with 5% FBS (Gibco) 1% NEAA (Lonza), 1% lipid mixture (Sigma), 1% MEM vitamine solution (Gibco), 1% P/S (Gibco), 1% Insulin Transferrin Selenium (Gibco), 0.05 mg/ml STI (Gibco), 30 µg/ml Bovine Pituitary Extract (Gibco), 393 ng/ml Dexamethasone (Sigma), 3.4 µg/ml 3, 3' 5-triiodo-L-thyronine (T3) (Sigma), 25 ng/ml Epidermal Growth Factor (EGF) (Gibco) and 4.11 mg/ml Forskolin (Ascent-Scientific).

Thick collagen was prepared adding acetic acid (50 µL, Corning) to sterile MilliQ water (50 mL) and rat tail collagen type I (354236, BD) to a final concentration of 1.5 mg/ml.

M.3.4. Isolation of KCs and HSCs

After *in situ* perfusion, livers were further digested *in vitro* for 30 minutes at 37ºC in F-12 media supplemented with 10 µl of 200 mg/ml pronase and 50 µl of 2 mg/ml DNase (Roche). Livers were homogenised, filtered through a 70 µm cell strainer and washed twice by centrifugation at 800 g for 6 minutes at room temperature (RT), and then resuspended in MEM media (Gibco). Next, a Nycodenz-based (Sigma-Aldrich) gradient solution was prepared (11% over 16.5%) and the cell suspension was added to the top of the gradient. The gradient was centrifuged at 1500 g at RT for 22 minutes without brake. After centrifugation, cells were carefully obtained from the appropriate layers. Due to their differences in density, KCs are collected from the16.5% layer while HSCs are present in the 11% layer. Thereafter, KCs were plated at a density of 10^6 cells/ml in 6 well plates (Corning) and were cultured in roswell park memorial institute medium 1640 (RPMI) (Gibco) supplemented with 10% FBS and 1% P/S. KCs were left for 20 minutes to allow them to adhere and plates were then washed thoroughly to remove the contaminating endothelial cells. Purity of KCs was established by measuring liver cell type specific markers and all the experiments were carried out 24 hours after cell isolation. HSCs were plated at an approximate density of 10^5cells/well in 6 well plates and cultured in DMEM supplemented with 10% FBS and 1% P/S. Purity of HSCs was assessed by autoflorescence one day after the isolation, and was always higher than 95%. Experiments in activated HSCs were carried out by culturing these cells in DMEM supplemented with 10% FBS and 1% penicillin-streptomycin tissue culture plastic for 7 days at 37ºC and 5% of CO_2. KCs were stimulated with 100 ng/ml LPS (Sigma-Aldrich), and/or with 100 µM or 200 µM UDCA for several time points. Following treatment, cells were processed for RNA extraction and stored at -80ºC.

M.4. Liver histology and staining

Tissue samples were collected and fixed in 4% formaldehyde for 24 hours. Then, tissues were processed using the MTM tissue processor (Slee Medical GmbH), embedded in paraffin (Thermo Fisher scientific) and cut using the HM355S microtome (Thermo Fisher scientific) in sections at a thickness of 4-5 µm.

M.4.1. Haematoxylin and eosin (H&E) staining and histology scoring

H&E staining was performed with the aim of analysing tissue morphology. First, sections were de-paraffined and rehydrated by incubating for 2 minutes in xylene (VWR) (2 incubations) and for 5 minututes in ethanol solutions of decreasing concentrations (100%, 96%, 70%, 50%), with a final washing step in PBS. Thereafter, slides were incubated in Harris Haematoxylin (Merck) for 5 minutes, washed in tap water, incubated in Eosin (Merck) for 5 minutes and washed in tap water again. Slides were then dehydrated with ethanol solutions of increasing concentrations (50%, 70% and 100%) for 5 minutes and xylene (2 incubations) for 2 minutes. Finally, slides were mounted with Pertex (Sigma-Aldrich) and analysed under an Eclipse 80i (Nikon) microscope. Liver histology scoring was performed by an experienced pathologist from the Department of Animal Medicine and Surgery, Veterinarian faculty, Complutense University, Madrid (Spain). In brief, liver inflammation score was established as 0= no inflammation; 1= light: isolated inflammatory cells without defined inflammatory foci; 2= moderate: inflammatory cells forming foci; 3=severe: abundant inflammatory cells forming a mass or multiple layers. Liver necrosis was evaluated as previously published (306) as 0=no necrosis; 1= isolated cellular necrosis; 2= necrotic areas < 5%; 3= necrotic areas 5-10% and 4= necrotic areas >10%. Finally, biliary expansion was evaluated and scored blindly in the H&E sections being 0= no biliary expansion and 5= the section with the highest degree of biliary expansion.

M.4.2. Sirius red staining

Sirius red staining was performed in paraffin embedded slides for collagen visualisation. Slides were de-paraffined and rehydrated as described in the previous section. After rehydration, slides were stained with 2% phosphomolybdic acid (Sigma-Aldrich) for 2 minutes and washed with dH_2O. Collagen was stained by incubation of the slides in 0.1% sirius red F3BA (Gibco) for 3 hours. Finally, slides were incubated with 0.01 N hydrogen chloride (HCl) (Merck) for 2 minutes and dehydrated and mounted as described in the previous section.

M.4.3. IHC and image analysis

IHC was performed in formalin-fixed and paraffin embedded mouse and liver tissue slides. First, slides were de-paraffined and rehydrated as described in the haematoxylin and eosin section. Endogenous peroxidase activity was blocked by incubating slides in

0.6% hydrogen peroxide (H_2O_2) in methanol for 15 minutes. Next, slides were subjected to the appropriate antigen retrieval method (**Table M.3.**). After cooling, tissue slides were mounted into the sequenza system. Avidin and biotin blocking (Vector laboratories) for 20 minutes at RT was performed when needed. Then slides were blocked with the corresponding blocking serum, which was derived from the animal species where the secondary antibody was generated, for 30 minutes at RT. Primary antibodies were incubated at the appropriate concentrations overnight (O/N) at 4ºC (**Table M.3.**). The next day, slides were washed with 1X PBS and incubated with the corresponding secondary antibodies, which were biotinylated (**Table M.3.**), afterwards, the ABC tertiary reagent was employed to amplify the signal (Vector laboratories). IHC were developed with 3,3'-Diaminobenzidine (DAB) (Vector laboratories). Thereafter, slides were counterstained with Mayer´s Haematoxylin (Sigma-Aldrich), dehydrated and mounted with DPX (Sigma-Aldrich).

Immunostained cells were manually counted in 15 (10X, 20X or 40X) high power fields of each slide and the mean number of positive cells was calculated. On the other hand, image analysis of 15 fields (10X or 20X) per slide was performed using NIS-Elements software for necrotic area measurement and CK19, αSMA, and F4/80. Representative pictures were taken in an Eclipse 80i (Nikon) microscope using the Digital sight DS-U2 camera controller (Nikon) using NIS-Elements.

Table M.3. Antibodies used for IHC.

Antibody	*Company*	*Reference*	*Dilution*	*Antigen retrieval*
Rabbit polyclonal anti-CK19	Abcam	ab84632	1/200	Citrate buffer pH6 (Vector laboratories)
Mouse monoclonal anti-aSMA	Sigma-Aldrich	F3777	1/200	Citrate buffer pH6
Rat monoclonal anti-NIMP-R14	Abcam	ab2557	1/100	Citrate buffer pH6.0 followed by 2% trypsin in PBS 1X
Rat monoclonal anti-F4/80	Abcam	Ab6640	1/100	Proteinase K-EDTA pH 8
Rabbit monoclonal anti-CD3	Thermo scientific	RM-9107	1/500	EDTA pH 9
Rabbit polyclonal anti-Cl-Casp3	Cell Signaling	9661	1/750	EDTA pH 9
Swine anti-rabbit IgG biotinylated secondary antibody	Dako	E0353	1/200	-
Goat anti-rat IgG biotinylated secondary antibody	Serotec	STAR80B	1/200	-
Rabbit polyclonal anti-FITC HRP conjugate	Dako	P5100	1/200	-

αSMA, alpha smooth muscle actin; CD3, cluster of differentiation 3; Cl-Casp3, cleaved caspase 3; CK19, cytokeratin 19; EDTA, ethylenediaminetetraacetic acid; FITC, fluorescein isothiocyanate; HRP, horse radish peroxidase; IgG, immunoglobulin G; IHC, immunohistochemistry; PBS, phosphate buffered saline; PCNA, proliferating cell nuclear antigen.

M.5. BAs measurement

BAs from the total liver and serum collected from WT and *Trem2*$^{-/-}$ mice subjected to BDL or sham operated were analysed using high performance liquid chromatography-tandem mass spectrometry using an adaptation (307) of a previously reported method (308) in a 6410 Triple Quad LC/MS (Agilent Technologies, Santa Clara, CA) equipment employing MS2Scan to select the precursor ions, (i.e. the molecular ion in each case). This procedure was carried out by the group of Prof. José J. G. Marin at the University of Salamanca, Salamanca (Spain).

BAs were determined in serum after acetonitrile precipitation/extraction (309). Approximately 150 mg of liver were homogenised in 3 volumes of water. Nor-DCA was added and liver homogenates were incubated at 65ºC with 2 volumes of absolute ethanol for two periods of 2 hours. Ethanolic extracts obtained by centrifugation after each incubation were pooled together and mixed (1:4 volume:volume) with 0.1 N NaOH before being applied to Silica-based bonded phase cartridges (C18 Sep Pack cartridges, Waters-Millipore). After washing the cartridge with subsequent water, 10% acetone and water, BAs were eluted with methanol and brought to dryness. For serum samples, 200 µl of serum were mixed with acetonitrile (1:3, vol:vol), mixture was

vigorously vortexed for 1 minute and centrifuged at 13 000 x G for 15 minutes at 4ºC. After collecting supernatant, this process was repeated with the pellet. Finally, both supernatants were mixed and evaporated until dryness.

HPLC was carried out using a *Zorbax Eclipse XDB-C18* column (150 mm x 4.6 mm, 5 µm). The chromatographic conditions were as follows: *i*) solvents were methanol and water, both containing 5 mM ammonium acetate and 0.01% formic acid at a final pH 4.6; *ii*) chromatography was kept at 35ºC and the flow rate was 0.5 ml/minutes; and *iii*) the chromatography was started at 73:27 methanol/water, and the proportion of methanol was increased linearly up to 93:7 over 10 minutes and then returned to 73:27 in 1 minunte. Negative electrospray ionization (ESI) was performed with the following conditions: gas temperature 350ºC, gas flow 11 l/minute, nebulizer 45 psi, capillary voltage 2500 V. Precursor ions were then filtered and further fragmented in multiple-reaction monitoring (MRM) mode for using the product ions (80.2 m/z for taurine-conjugated bile acids, 74.0 m/z for glycine-conjugated bile acids and their own precursor ions for unconjugated bile acids) to measure the abundance of the indicated compounds. Nor-deoxycholic acid was used as internal standard. The transition followed for this bile acid was 377.0 m/z to 331.3 m/z. Standard bile acids (purity higher than 95%) were purchased from Sigma-Aldrich. All other reagents were of analytical grade.

M.6. Determination of chemokine expression by the Bio-Plex assay

MCP1 and CXCL1 chemokine expression were analysed in the liver of WT and *Trem2*$^{-/-}$ subjected to sham or BDL in collaboration with the group of Dr. Tom Luedde at the Uniklinik Aachen, Aachen (Germany); using the custom-made Bio-Plex assay kit (Bio-Rad) and a FACS-Canto II System (BD) and following manufacturer´s instructions. For the chemokine analysis, samples were prepared at a concentration of 0.9 µg/µl in sample diluent with 0.5 % BSA.

M.7. Determination of protein expression by immunoblot

M.7.1. Protein extraction from liver tissue

Liver tissue (~20 mg) was homogenised in 400 µl of radioimmunoprecipitation assay (RIPA) buffer containing: 150 mM NaCl, 50 mM Tris pH 7.5, 0.1% sodium dodecyl sulfate (SDS), 1% triton X100, 0.5% sodium deoxycholate, protease inhibitors

(Complete; Roche) and phosphatase inhibitors (1 mM ortovanadate, 10 mM sodium fluoride (NaF), 100 mM β-glycerophosphate). Homogenates were then incubated in a rotator (Stuart) for 30 minutes at 4ºC to facilitate homogenization. Subsequently, tissue homogenates were sonicated (JP Selecta) twice for 15 seconds and centrifuged for 10 minutes at 18000 g at 4ºC. Supernatant was then transferred into a new tube, thus obtaining protein homogenates.

M.7.2. Total protein concentration determination

Protein content was measured in tissue and cell lysates by using the Pierce Bicinconic acid kit (Thermo Scientific) following manufacturer´s instructions. In brief, an aliquot of each sample was diluted 1/40 for tissue lysates with dH_2O. In parallel, a reference standard curve was prepared with bovine serum albumin (BSA). 25 µl of standard curve and samples were placed in a 96-well plate (Corning). A and B reagents were mixed at 50/1 relation and 200 µl of the mix was added to each well, the plate was incubated for 30 minutes at 37ºC in darkness and absorbance was determined at 570 nm in a Haloled 96 (Dynamica) spectophotometer. Protein concentration was thereafter determined by extrapolation from the standard curve.

M.7.3. SDS polyacrylamide gel electrophoresis (SDS-PAGE) and immunoblotting

For protein separation, the required amount of total protein (Ranging from 60-100 µg depending on the protein to be detected) was loaded into 10 or 12.5% SDS-PAGE and then transferred onto nitrocellulose membranes (Bio-Rad). After confirmation of successful transference by Ponceau staining (Sigma-Aldrich), membranes were blocked in Tris-buffered saline with 0.1% Tween-20 (T-TBS) containing 5% skim milk for 1 hour. The appropriate primary antibodies were prepared by dilution in the corresponding blocking solution and incubated O/N at 4ºC (**Table M.4.**). The next day, membranes were washed with T-TBS and incubated for 1 hour with the corresponding HRP-conjugated secondary antibodies at 1:5000 dilution (**Table M.4.**). After the incubation with the secondary antibody, membranes were washed with T-TBS and proteins were visualised by enhanced chemiluminescence (ECL) HRP Chemiluminiscent Substrate Reagent Kit (Invitrogen) in an iBright FL1000 (Invitrogen) biomolecular imager, glyceraldehyde-3-phosphate dehydrogenase (GAPDH) was used as a protein loading control.

Table M.4. Antibodies used for immunoblotting.

Antibody	*Company*	*Reference*	*Dilution*
Rabbit-polyclonal anti-RIP3	Pro Sci	2283	1/2000
Rabbit-polyclonal anti-Cleaved caspase-3 (Asp-175)	Cell signaling	9661	1/2000
Rabbit polyclonal anti-MLKL	Biorbyt	Orb32399	1/2000
Mouse-monoclonal anti-GAPDH	AbD Serotec	MCA-4739	1/2000
Anti-rabbit IgG HRP-linked antibody	Cell signaling	7074	1/5000
Anti-mouse IgG HRP-linked antibody	Sigma-Aldrich	A4416	1/5000

Asp, aspartate; GAPDH, glyceraldehyde-3-phosphate dehydrogenase; HRP, horse raddish peroxidase; IgG, immunoglobulin G;MLKL, mixed lineage kinase domain like; RIP3 receptor interacting protein 3; Thr, threonine.

M.8. RNA isolation and quantitative real time polymerase chain reaction (qRT-PCR) analysis

M.8.1. Total RNA extraction from liver tissue

Liver tissue (~20 mg) was homogenised in 1 ml of Tri-reagent® (Sigma-Aldrich) and subjected to a freeze-thaw cycle at -80ºC to facilitate digestion. For total RNA extraction, 200 µl of chloroform (Merck) were added and samples were thoroughly mixed and incubated for 15 minutes at RT. Thereafter, samples were centrifuged for 15 minutes at 18000 g at 4ºC and the upper phase was transferred into a new tube. For RNA precipitation, 500 µl of isopropanol (AppliChem Panreac) were added and samples were mixed by inverting several times, incubated for 10 minutes at RT and centrifuged for 15 minutes at 18000 g at 4ºC. After this step the RNA pellet was formed, supernatant was discarded and pellets were washed by addition of 1 ml of 75% Ethanol and centrifugation for 15 minutes at 18000 g at 4ºC. Supernatant was again discarded and pellets were left to dry. Final RNA pellets were resuspended in 300-200 µl of Ultrapure™ DNase/RNase-free distilled water (Gibco). RNA concentration was determined with a NanoDrop® ND-1000 apparatus (Thermo-Fisher Scientific).

M.8.2. Reverse transcription of RNA derived from human tissue samples and primary isolated mouse cells

The SuperScript® VILO™ cDNA Synthesis Kit (Life technologies) was used for RNA derived from human tissue and primary isolated mouse cells. Reverse transcription was performed following manufacturer´s instructions. Briefly, 2 µl of 10X SuperScript® Enzyme Mix, 4 µl of 5X VILO™ Reaction Mix and DNase/RNase-free distilled water to a total volume of 20 µl was added to 200-500 ng of total RNA of each sample. RT was performed in a Verity 96 well thermal cycler (Applied biosystems) using a 3 step protocol: *i*) 10 minutes at 25ºC, *ii*) 1 hour at 42ºC and *iii*) 5 minutes at 85ºC. DNase/RNase-free distilled water was added to the newly synthetised complementary DNA (cDNA) for a final concentration of 12.5 ng/µl.

M.8.3. Reverse transcription of RNA derived from mouse tissue samples

1 µg of extracted RNA was subjected to DNase incubation to remove genomic DNA by adding 1 µl of DNase I Amplification Grade (Invitrogen) and 1 µl of 10X DNase I Reaction Buffer (Invitrogen) and incubating for 20 minute at 37°C. Next, 1 µl of 25 mM ethylenediaminetetraacetic acid (EDTA) (Invitrogen) was added to chelate magnesium and stop DNase activity and samples were incubated for 10 minutes at 65°C, 1 minute at 90°C and kept at 4°C. The cDNA synthesis step was performed by adding 30 µl of RT Mix [8 µl Buffer 5X, 4 µl Random primers 100 ng/µl, 4 µl Deoxy-nucleotide-triphosphate mix (dNTPs), 2 µl 1,4-dithiothreitol (DTT), 1.2 µl RNase OUT, 1.2 µl M-MLVRT (all from Invitrogen) and 9.6 µl DNase/RNase-free distilled water] to samples and reaction was performed by incubating the tubes for 60 minutes at 37°C, 1 minute at 95°C and cooled at 4°C. Finally, the newly synthesised cDNA was diluted to a final concentration of 12.5 ng/µl with DNase/RNase-free distilled water.

M.8.4. Gene expression analysis by qRT-PCR

Gene expression analysis was performed using SYBR technology and specific primers. The qRT-PCR reaction mix was prepared with 10 µl of iQ™ SYBR® Green Supermix (Bio-Rad), 0.6 µl of 10 µM appropriate forward and reverse primers (**Table M.5.** and **Table M.6.**) and DNase/RNase-free distilled water to a final volume of 17 µl per sample. Mix was placed in Hard-Shell PCR plates 96-well (Bio-Rad), and then 2-3 µl of the desired cDNA sample at 12.5 ng/ul were added to each well and the plate was sealed with Microseal “B” seal (Bio-Rad). A CFX 96 apparatus (Bio-Rad) was employed for

RT-qPCR reaction and detection of DNA amplification following an iQ™ SYBR® Green Supermix standard protocol. Briefly, cDNA denaturation and enzyme activation were achieved by an initial step of 10 minutes at 95°C. Thereafter, DNA amplification was performed by 40 cycles of 3 steps including 15 seconds at 95ºC for DNA denaturation, 30 seconds at 60ºC for primer binding and 45 seconds at 72ºC for extension. A dissociation curve to confirm primer specificity was obtained by gradually increasing the temperature from 60°C to 93ºC. Expression levels of *GAPDH* or Hypoxanthine phosphoribosyltransferase 1 (*HPRT1*) were used as housekeeping control. Relative gene expression levels of the desired gene was determined using ΔCT calculation, mRNA levels are expressed as arbitrary units (AU) or relative to the control condition when indicated.

Table M.5. Human primers for qRT-PCR-based gene expression analysis.

Gene	*Forward primer sequence (5´-3´)*	*Reverse primer sequence (5´-3´)*
ACTA2	CGGGACTAAGACGGGAATCCT	GTCACCCACGTAGCTGTCTT
CD9	CAACAAGCTGAAAACCAAGGA	CAAACCACAGCAGTTCAACG
COL1A1	GATGGCTGCACGAGTCACAC	AACGTCGAAGCCGAATTCCT
GAPDH	CCAAGGTCATCCATGACAAC	TGTCATACCAGGAAATGAGC
HPRT1	TATGGCGACCCGCAGCCCT	CATCTCGAGCAAGACGTTC
IL6	AAAGAGGCACTGGCAGAAAA	AGCTCTGGCTTGTTCCTCAC
IL8	GTGCAGTTTTGCCAAGGAGT	ACTTGTCCACAACCCTCTGC
IL33	TTAATGGTAACCCTGAGTCC	TATGAAGGACAAAGAAGGCC
MCP1	CAGCCAGATGCAATCAATGCC	TGGAATCCTGAACCCACTTCT
TNF	CCTGCTGCACTTTGGAGTGA	CAGCTTGAGGGTTTGCTACA
TREM2	ACGAGATCTTGCACAAGGCA	GGTAGAGACCCGCATCATGG

Acta2, actin alpha 2, smooth muscle; *COL1A1*, collagen type 1 alpha 1;*GAPDH*, glyceraldehyde 3-phosphate dehydrogenase; *HPRT1*, hypoxanthine-guanine phosphoribosyltransferase; *IL*, interleukin; *MCP1*, monocyte chemoattractant protein 1; *TNF*, tumour necrosis factor; *TREM2* triggering receptor expressed on myeloid cells 2.

Table M.6. Mouse primers for qRT-PCR-based gene expression analysis.

Gene	*Forward primer sequence (5´-3´)*	*Reverse primer sequence (5´-3´)*
Acta2	CTCAGCGCCTCCAGTTCCT	AAAAAAAACCACGAGTAACAAATCAA
Col1a1	TTCACCTACAGCACGCTTGTG	GATGACTGTCTTGCCCCAAGTT
Ck7	AGGAGTCAACCGACGCAC	GTCTCGTGAAGGGTCTTGAGG
Ck19	GGGGGTTCAGTACGCATTGG	GAGGACGAGGTCACGAAGC
Cxcl1	CTGGGATTCACCTCAAGAACATC	CAGGGTCAAGGCAAGCCTC
Cyp7a1	GGGATTGCTGTGGTAGTGAGC	GGTATGGAATCAACCCGTTGTC
Fxr	GGCTGAAAGGTTTCTTCG	CAGCCAACATCCCATCTCT
GAPDH	GCACAGTCAAGGCCGAGAAT	GCCTTCTCCATGGTGGTGAA
Hmox	AAGCCGAGAATGCTGAGTTCA	GCCGTGTAGATATGGTACAAGGA
Il6	TAGTCCTTCCTACCCCAATTTCC	TTGGTCCTTAGCCACTCCTTC
Mcp1	TTAAAAACCTGGATCGGAACCAA	GCATTAGCTTCAGATTTACGGGT
Nos2	GTTCTCAGCCCAACAATACAAGA	GTGGACGGGTCGATGTCAC
Tnf	CCCTCACACTCAGATCATCTTCT	GCTACGACGTGGGCTACAG
Trem1	ATGACCTAGTGGAGGGCCAG	GCACAACAGGGTCATTCGGAG
Trem2	TTGCTGGAACCGTCACCATC	CACTTGGGCACCCTCGAAAC

Acta2, actin alpha 2, smooth muscle; *Ck*, cytokeratin; *Col1a1*, collagen type 1 alpha 1; *Cxcl1*, C-XC motif ligand 1; *Cyp7a1*, cytochrome P450 family 7 subfamily A Member 1; *Fxr*, farnesoid X receptor; *Gapdh*, glyceraldehyde 3-phosphate dehydrogenase; *Hmox1*, heme oxygenase 1; *Hprt1*, hypoxanthine-guanine phosphoribosyltransferase; *Il*, interleukin; *Mcp1*, monocyte chemoattractant protein 1; *Nos2*, nitric oxide synthase 2; *Shp*, small heterodimer partner; *Tnf*, tumour necrosis factor; *Trem1*, triggering receptor expressed on myeloid cells 1; *Trem2*, triggering receptor expressed on myeloid cells 2.

M.9. Statistical analysis

GraphPad Prism 6.00 (GraphPad Software) was used to perform the statistical analysis. Firstly, normality of the data set was assessed by Shapiro-Wilk test. Parametric tests were employed for normally distributed and corresponding non-parametric tests for non-normally distributed data. For comparisons of two independent groups parametric Student's *t*-test or non-parametric Mann Whitney test were employed. When more than two groups were compared parametric one-way analysis of variance with Tukey's post hoc test or non-parametric Kruskal-Wallis test followed by Dunn's multiple comparison test were used. For correlation analysis parametric Pearson´s test or non-parametric Spearman's correlation test were used. Data are expressed as mean ± standard error of the mean (SEM). Statistically significant data is represented in figures by * or # codes which are used to distinguish the different comparisons specified in each figure. * or #, ** or ##, *** or ###, **** or #### denote a *p* value of <0.05, <0.01, < 0.001 and < 0.0001, respectively. In correlation analysis, correlation coefficient and exact *p* values are shown.

RESULTS

R.1. *TREM2* expression is upregulated in the liver of patients with cholestasis

R.1.1. *TREM2* expression is upregulated in the liver of patients with PBC and PSC and positively correlates with markers of disease progression in the San Sebastian/Warsaw cohort of patients

We have previously observed an upregulation of the expression of TREM2 in liver tissue of patients with cirrhosis regardless of their aetiology (288), and also in patients with HCC (289) in comparison to healthy-control liver tissue. Here, we assessed the expression of TREM2 in human cholestasis.

First, *TREM2* mRNA expression was analysed in the San Sebastian/Warsaw cohort, in which healthy (n=18) and cirrhotic liver tissue of diverse aetiologies (n=35) of patients recruited in San Sebastian, and liver tissue from patients with PBC and PSC (PBC n=10 and PSC n=10) recruited in Warsaw are included. Patient and clinical characteristics of the study cohort are shown in **Table M.1**. As previously described (288), here we confirmed that *TREM2* gene expression is upregulated in the livers of patients with cirrhosis compared to healthy-control liver tissue. Interestingly, *TREM2* expression increased in the liver of patients with PBC and PSC compared to control individuals. Moreover, *TREM2* mRNA expression was also higher in the liver tissue of patients with PBC or PSC compared to patients with cirrhosis of different aetiologies including alcoholic, HCV and/or HBV infection and idiopathic (**Figure R.1A**).

Next, in order to analyse the correlation levels of liver *TREM2* mRNA expression in patients with cholestasis with different markers of liver inflammation and fibrosis, data from patients with PBC and PSC were grouped together. In this regard, *TREM2* mRNA levels positively correlated with the mRNA expression levels of inflammatory cytokines such as *IL6*, *IL8* and *IL33*, with the KC marker *CD68*, and with *CD9*, a macrophage marker that identifies a $TREM2^{+}CD9^{+}$ macrophage subpopulation recently described in cirrhotic liver tissue (281). Moreover, *TREM2* mRNA expression also positively correlated with the mRNA expression of the fibrosis marker *COL1A1* in patients with different chronic cholestatic diseases including PBC and PSC (**Figure R.1B**).

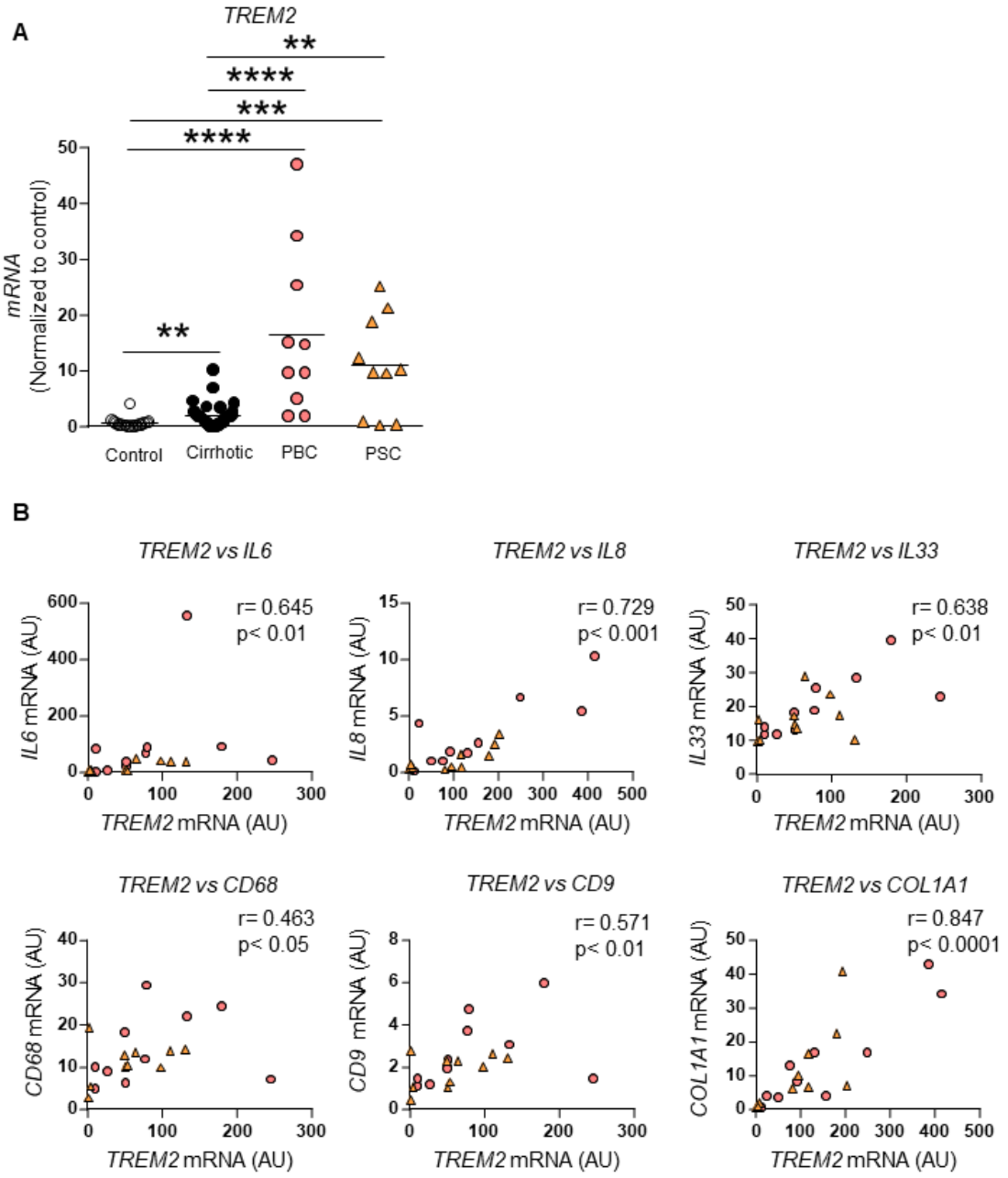

Figure R.1. *TREM2* mRNA expression in the liver of patients with cholestasis. (A) *TREM2* mRNA expression in the liver of control individuals (n=18) patients with cirrhosis (n=35) and with the chronic cholestatic diseases PBC (n=10) or PSC (n=10). (**B**) Correlation of *TREM2* mRNA expression with the mRNA expression of *IL6*, *IL8*, *IL33*, *CD68*, *CD9* and *COL1A1* in the liver of patients with chronic cholestatic diseases (PBC and PSC). (**A**) Non-parametric Mann Whitney test was used. (**B**) Non-parametric Spearman correlation test was used and correlation coefficient (r) and *p* value are shown. **, *** and **** represent a *p* value of <0.01, <0.001 and <0.0001, respectively. AU, arbitrary units; *CD9*, cluster of differentiation 9; CD68, cluster of differentiation 68; *COL1A1*, collagen type 1 a 1; *IL6*, interleukin 6; *IL8*, interleukin 8; *IL33*, interleukin 33; PBC, primary biliary cholangitis; PSC, primary sclerosing cholangitis; *TREM2*, triggering receptor expressed on myeloid cells.

Taking into account that PBC and PSC represent two different diseases with particular pathobiological characteristics, we analysed the correlation of *TREM2* mRNA expression with different markers of disease progression separately in each disease. In this regard, *TREM2* gene expression positively correlated with the levels of different serological markers of liver injury, including AST, ALT and also with bilirubin, a marker of cholestasis; in patients with PBC (**Figure R.2A**). Similarly, we also observed a positive correlation between *TREM2* and model for end-stage liver disease (MELD) score in patients with PBC (**Figure R.2A**). These results were associated with a positive correlation between *TREM2* mRNA expression and the mRNA expression of the markers of inflammation *IL8* and *IL33*, as well as the marker of fibrosis *COL1A1* in the liver of patients with PBC. In the liver of patients with PSC, a positive correlation was observed between the mRNA expression levels of *TREM2* and the inflammatory markers *IL6* and *IL8*, and also the fibrotic marker *COL1A1* (**Figure R.2B**).

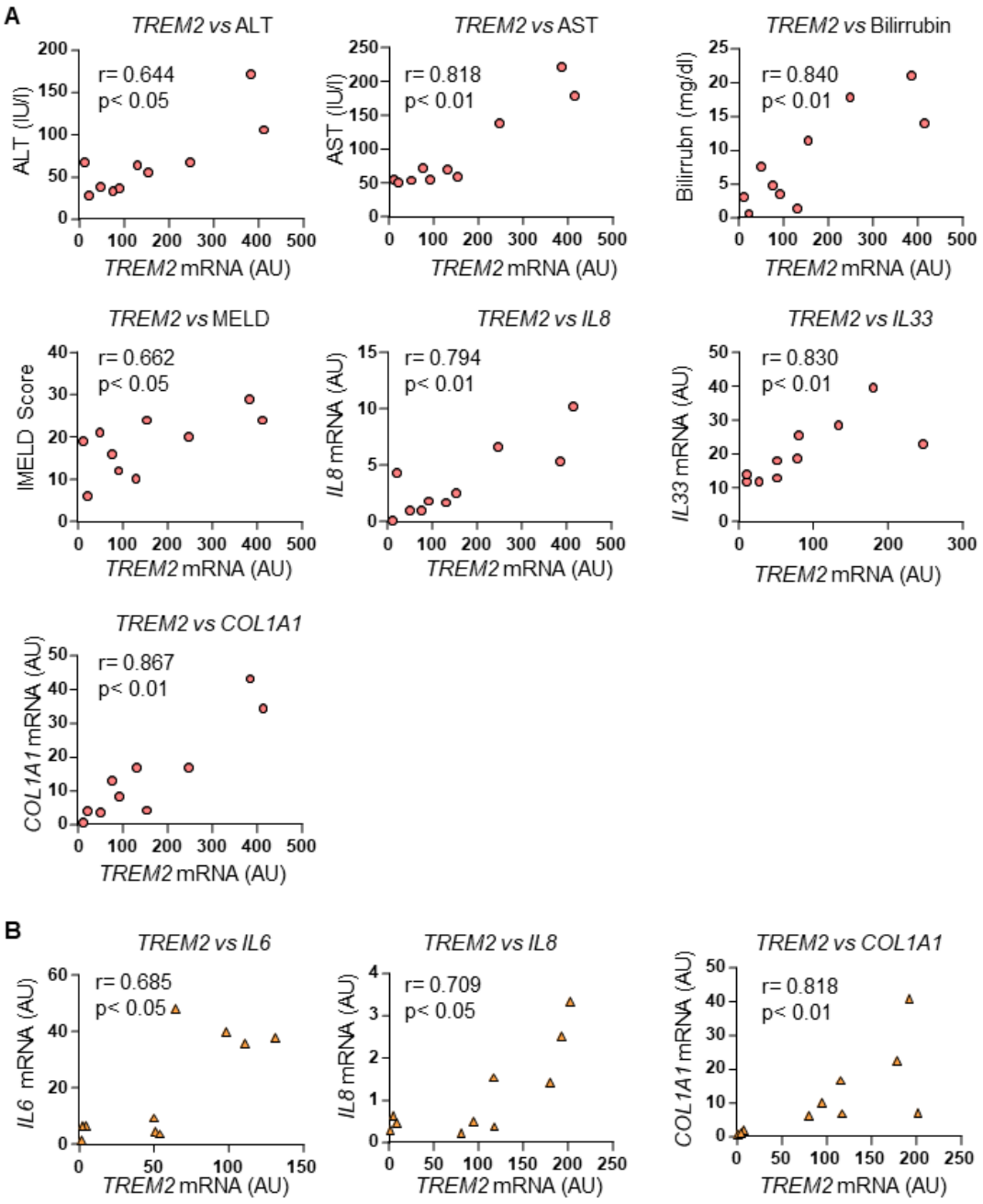

Figure R.2. Correlation of *TREM2* mRNA expression in the liver of patients with PBC or PSC with markers of cholestatic disease progression. (A) Correlation of liver *TREM2* mRNA expression with serum levels of ALT, AST and bilirubin, MELD score, and mRNA expression levels of inflammatory markers such as *IL8*, *IL33* and the fibrotic marker *COL1A1* in the liver of patients with PBC (n=10). (**B**) Correlation of *TREM2* mRNA expression with liver expression levels of inflammatory markers such as *IL6*, *IL8* and the fibrosis marker *COL1A1* in the liver of patients with PSC (n=10). Parametric Pearson (*TREM2*-Bilirrubin and *TREM2*-MELD) and non-parametric Spearman correlation test were used, correlation coeficient (r) and *p* value are shown. ALT, alanine aminotransferase; AST, aspartate aminotransferase; AU, arbitrary units; *COL1A1*, collagen type 1 a 1; *IL6*, interleukin 6; *IL8*, interleukin 8; *IL33*, interleukin 33; MELD, model for end-stage liver disease; PBC, primary biliary cholangitis; PSC, primary sclerosing cholangitis; *TREM2*, triggering receptor expressed on myeloid cells.

R.1.2. *TREM2* expression is upregulated in the liver of patients with high-risk PBC and positively correlates with markers of disease progression in the GSE79850 cohort of patients

Next, we utilised publicly available data from the Gene Expression Omnibus (GEO) database to evaluate *TREM2* expression in an independent cohort of patients with PBC. In this cohort, samples were obtained from patients with low and high-risk PBC and healthy controls at the time of biopsy, prior to treatment (290). Low-risk PBC patients are defined according to the following criteria: 1) Fully responsive to UDCA according to Paris 1 criteria; 2) Remained well and in full UDCA response after a minimum of 15 years follow up; and 3) Did not require liver transplantation. Whereas high-risk PBC patients were defined as: 1) Non-responders to treatment with UDCA at one year of treatment at a dose of 13–15 mg/Kg using Paris 1 criteria, and 2) Requiring liver transplantation for prognostic reasons for their PBC during subsequent follow-up.

Interestingly, *TREM2* mRNA expression was upregulated in the liver of patients with high-risk PBC compared to both control liver tissue and liver from patients with low-risk PBC, while no differences were detected between control liver tissue and the liver of patients with low-risk PBC (**Figure R.3A**). With the aim of analysing the correlation between the mRNA expression levels of *TREM2* and markers of disease progression included in the GSE79850 data base, patients with low-risk and high-risk PBC were grouped together. Similarly to our observations in the San Sebastian/Warsaw cohort, in these samples, *TREM2* also positively correlated with the expression levels of the inflammatory markers *CXCL1* and *IL6*, and with *CD9*, which as aforementioned,was recently described to identify a new population of scar associated $TREM2^{+}CD9^{+}$ macrophages in patients with cirrhosis (**Figure R.3B**) (281). Lastly, liver *TREM2* mRNA expression also positively correlated with the mRNA expression levels of the fibrosis-associated marker *COL3A*1.

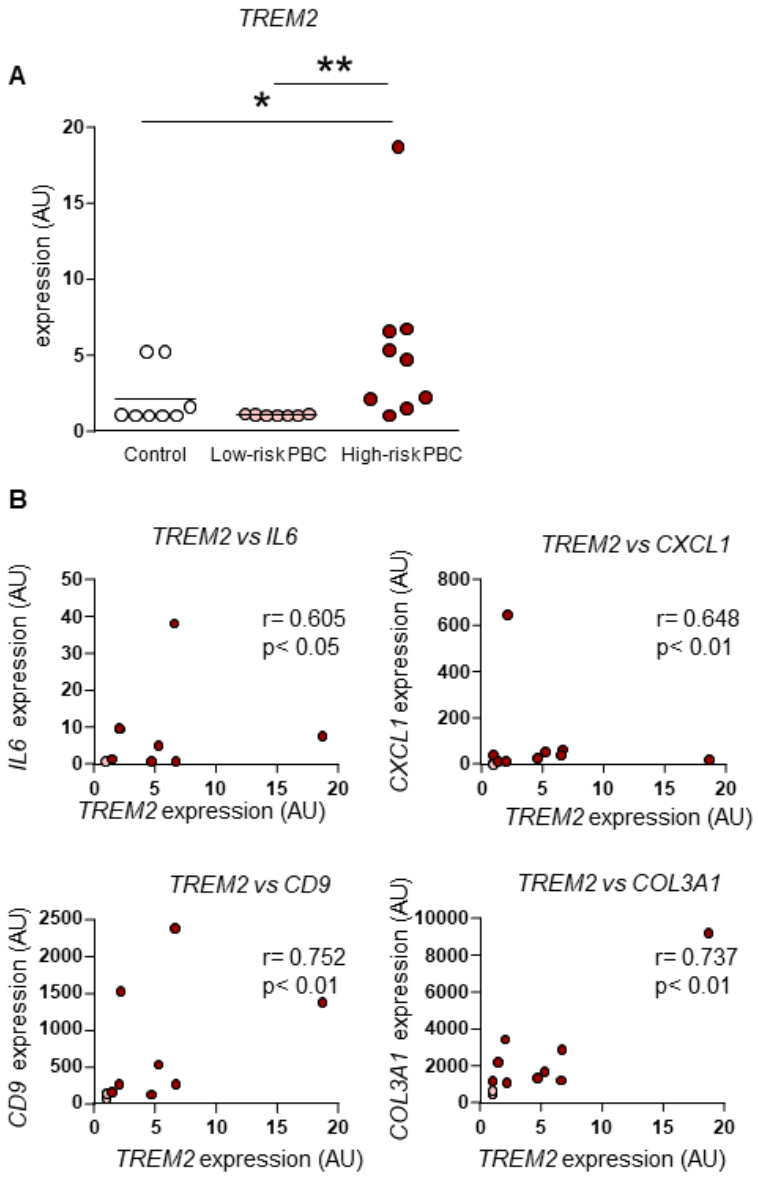

Figure R.3. Correlation of the expression of *TREM2* and inflammatory or fibrotic markers in the GSE79850 liver samples. (**A**) *TREM2* mRNA expression levels in livers of control individuals (n= 8), and patients with PBC, low risk PBC (n= 7) and high risk PBC (n= 9). (**B**) Correlation of *TREM2* mRNA expression levels with the mRNA expression levels of markers of liver inflammation (*IL6* and*CXCL1*), a macrophage marker (*CD9*) and a marker of fibrosis (*COL3A1*) in patients with PBC (low and high risk grouped together). (**A**) Non-parametric Mann Whitney test and (**B**) Spearman´s correlation test were used, correlation coeficient (r) and p value are shown. * and ** represent a *p* value of <0.05 and <0.01, respectively. AU, arbitrary units; *CD9*, cluster of differentiation 9; *COL3A1*, collagen type 3 a 1; *CXCL1*, *Cxcl1*, C-X-C Motif Chemokine Ligand 1; *IL6*, interleukin 6; PBC, primary biliary cholangitis;*TREM2*, triggering receptor expressed on myeloid cells.

Overall, these data indicate that TREM2 expression is upregulated in the livers of patients with chronic cholestasis, and thus, this receptor may play a role in the development and/or progression of this condition.

R.2. *Trem2* expression is upregulated in mouse models of cholestasis

In order to establish if TREM2 upregulation is a conserved phenomenon in human and mouse cholestasis, we studied *Trem2* mRNA expression in mice. First, we analysed *Trem2* expression in different cell types isolated from healthy mice. Confirming previous data reported by our group (288, 289), *Trem2* mRNA expression was minimal on the epithelial compartment of the liver, while it was markedly increased in the non-parenchymal cells such as KCs and activated HSCs (**Figure R.4A**). In order to evaluate the relevance of this receptor in experimental cholestasis, we then analysed *Trem2* expression in three different models of cholestasis to cover different settings of the condition. Specifically, *Trem2* mRNA expression increased in the liver of mice subjected to BDL-based obstructive cholestasis as compared to sham-operated mice (**Figure R.4B**). Similarly, *Trem*2 mRNA levels were also upregulated in the liver of mice with chemically-induced cholestasis based on ANIT or DDC administration, in comparison to control conditions based on O.Oil and control diet administration, respectively (**Figure R.4C,D**). Hence, hepatic *Trem2* expression was upregulated in all the models of cholestasis here analysed, regardless of the underlying cause, in comparison to control conditions. These results suggest that TREM2 upregulation is a general event in cholestasis.

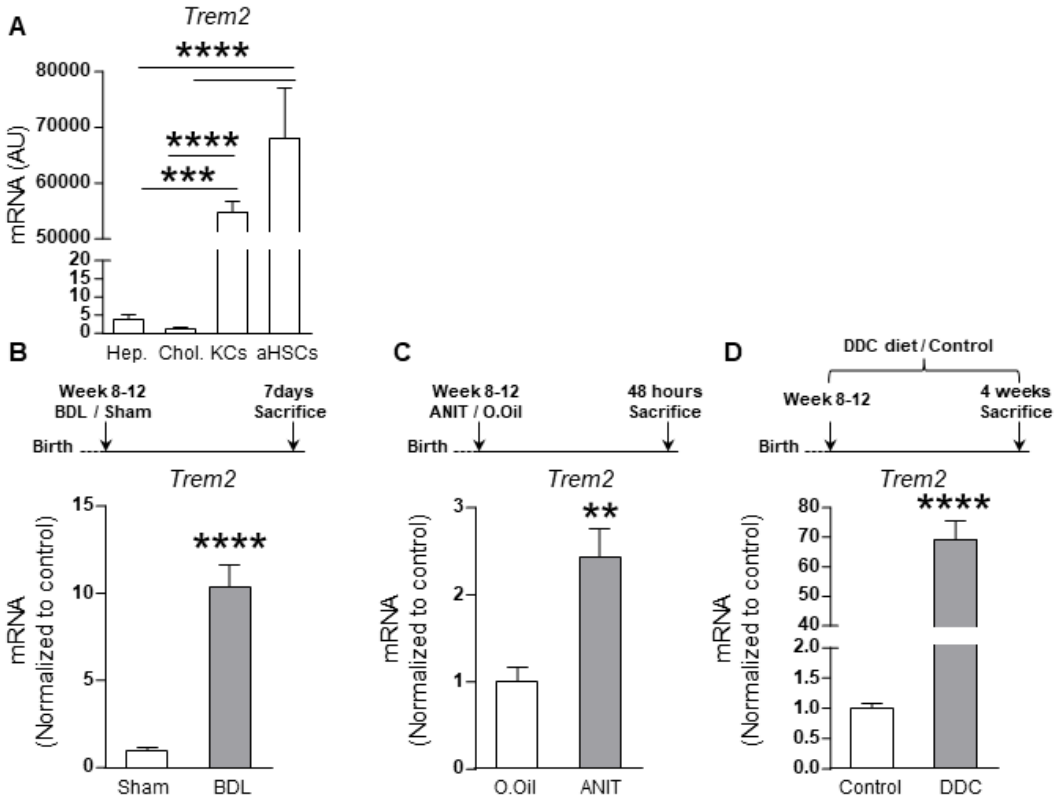

Figure R.4. *Trem2* mRNA expression in different cell types of the liver and in mouse models of cholestasis. (**A**) *Trem2* mRNA expression in primary mouse liver cells including, hepatocytes (n=8), cholangiocytes (n=6), KCs (n=6) and activated HSCs (n=5) derived from control healthy mice. (**B-D**) Liver Trem2 mRNA expression in the liver of different models of cholestasis compared to control conditions, (**B**) bile duct ligation (n=6-9), (**C**) ANIT feeding (n=9-10) and (**D**) DDC- supplemented diet feeding (n=9-11). (**A**) Parametric Student´s *t*-test and non-parametric Mann Whitney test were used. (**B**, **C**) Parametric Student´s *t*-test was used. (**D**) Non-parametric Mann Whitney test was used **, *** and **** represent a p value of <0.01, <0.001 and <0.0001, respectively. ANIT, α-Naphthylisothiocyanate; AU, arbitrary units; BDL, bile duct ligation; DDC, 3,5-Diethoxycarbonyl-1, 4-Dihydrocollidine; Trem2: triggering receptor expressed on myeloid cells 2.

Similarly to the results observed in patients with cholestasis, liver *Trem*2 mRNA expression in the BDL-based obstructive cholestasis model also positively correlated with markers of disease progression. Particularly, *Trem*2 mRNA expression levels in the liver positively correlated with the mRNA expression of the biliary markers *Ck19* and Ck7 (**Figure R.5A**). A positive correlation between the mRNA expression levels of *Trem*2 and *Acta*2, as well as *Trem2* and *Col1a*1 was also observed (**Figure R.5B**), being *Acta2* the gene that encodes for αSMA, the main marker of HSCs activation, and *Col1a1* the main type of fibre that usually accumulates during liver fibrosis.

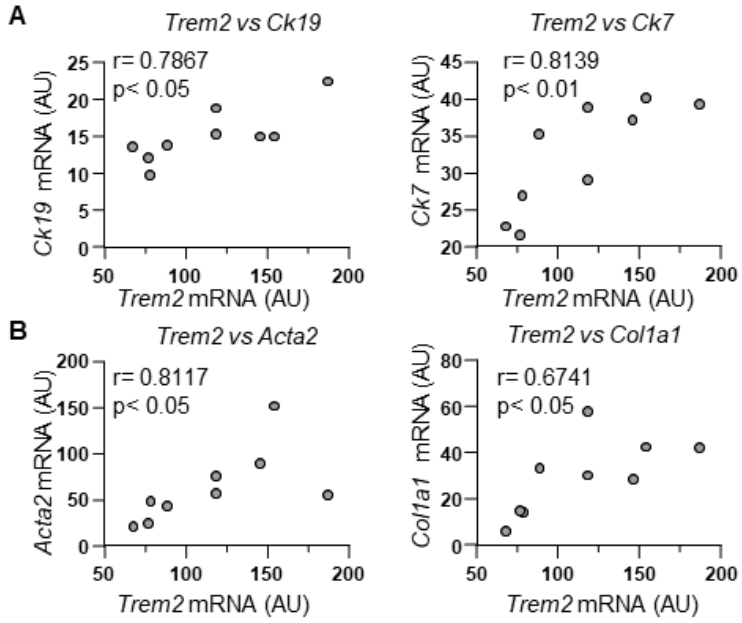

Figure R.5. Correlation of *Trem2* mRNA expression with markers of disease progression in the liver of mice subjected to BDL. (**A**) Correlation with the biliary markers *Ck19* and *Ck7* and (**B**) the markers of liver fibrosis *Acta2* and *Col1a1* in the liver of WT mice after BDL surgery (n=9). (**A**) Parametric Pearson´s correlation test and (**B**) Non-parametric Spearman´s correlation test (*Trem2* vs *Acta2*) and parametric Pearson´s correlation test (*Trem2* vs *Col1a1*) were used. In correlation coeficient (r) and *p* value are shown. *Acta2*, actin alpha 2; AU, arbitrary units; BDL, bile duct ligation; *Ck7*, cytokeratin 7; *Ck19*, cytokeratin 19; *Col1a1*, collagen type 1a 1; *Trem2*: triggering receptor expressed on myeloid cells 2.

In sum, we conclude that TREM2 expression is induced during human and experimental cholestasis, suggesting a potential role for this receptor in the pathobiology of this condition. Our results further indicate that mice represent a suitable setting to study the role of TREM2 in the context of cholestasis.

R.3. *Trem2*$^{-/-}$ mice exhibit exacerbated injury and inflammation after bile duct ligation

R.3.1. Increased liver damage scores, biliary expansion and cell death in *Trem2*$^{-/-}$ compared to WT mice after BDL

In order to determine the role of TREM2 in cholestasis, we first used the obstructive cholestasis model based on BDL. With the aim of comparing their responses to cholestasis-induced liver injury, we subjected WT and *Trem2*$^{-/-}$ mice to BDL and sacrificed animals 7 days after the surgery. We employed mice subjected to sham surgery as controls (**Figure R.6A**).

BDL induced a notable increase in serum markers of cholestatic injury, including alkaline phosphatase and bilirubin, in both genotypes (**Figure R.6B**). Serum markers of hepatocellular injury also increased in BDL mice compared to sham operated mice, in both genotypes of mice (**Figure R.6B**). Nevertheless, except for an increase in ALT in sham operated *Trem2*$^{-/-}$ mice compared to WT mice, no significant differences were detected in the levels of serum makers of cholestatic and hepatocellular injury between genotypes, either in sham operated mice or after BDL (**Figure R.6B**).

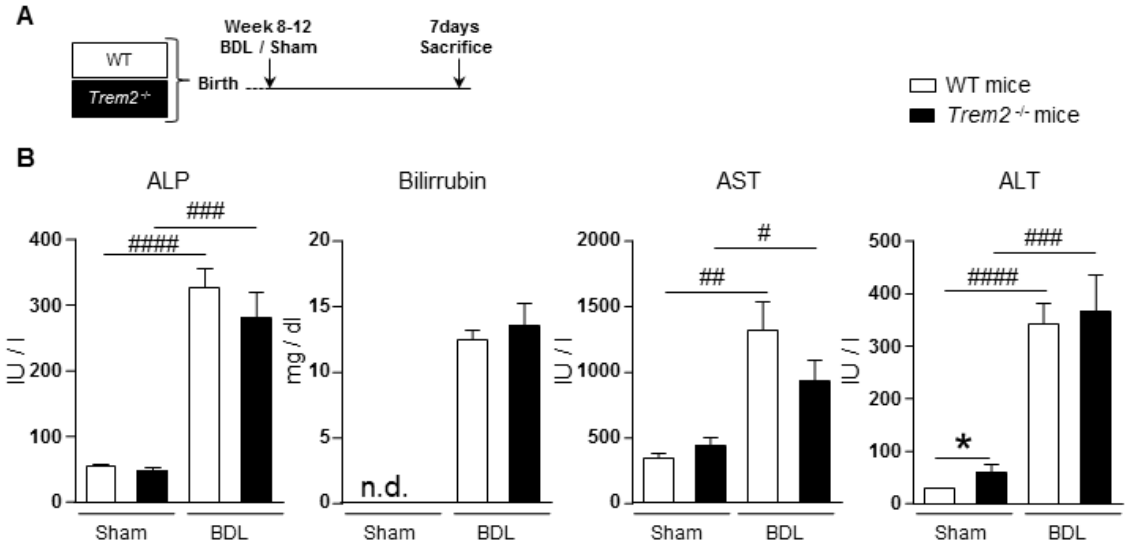

Figure R.6. Serum markers of biliary and hepatocellular injury in WT and *Trem2* $^{-/-}$ mice after BDL. (A) WT and *Trem2* $^{-/-}$ mice were subjected to BDL (WT n=9; *Trem2* $^{-/-}$ n=8) or sham (WT n=6; *Trem2* $^{-/-}$ n=7) and sacrificed 7 days after surgery. (**B**) Serum levels of liver enzymes and bilirrubin were analysed. (**B**) Parametric Student´s *t*-test and non-parametric Mann-Whitney test were used * represents *p* values of <0.05 in comparison to WT mice following the same experimental conditions. #, ##, ### and #### represent *p* values of <0.05, <0.01, <0.001 and <0.0001 in comparison to sham operated mice of the same genotype. ALP, alkaline phosphatase; ALT, alanine aminotransferase; AST, aspartate aminotransferase; AU, arbitrary units; BDL, bile duct ligation; IU, international units; n.d., non-detected; *Trem2*, triggering receptor expressed on myeloid cells; WT, wild type.

Histological analysis of the H&E stained liver sections depicted an exacerbated cholestatic injury in response to BDL-based obstructive cholestasis particularly in the *Trem2*$^{-/-}$ mice. This exacerbated response was characterised by increased scores of inflammatory infiltration and necrosis, as well as by augmented biliary expansion (**Figure R.7A**). Next, we assessed changes related to the biliary expansion in more detail. In association with the aforementioned data, *Trem2*$^{-/-}$ mice showed enhanced CK19 staining in the liver (**Figure R.7B**). By mRNA analysis, we observed that *Ck19* and *Ck7* expression increased in both genotypes after BDL, compared to sham operated mice (**Figure R.7C**). mRNA data further confirmed the IHQ results, as *Ck19* and *Ck7*

expression augmented in the liver of *Trem2*$^{-/-}$ mice compared to WT mice after BDL (**Figure R.7C**).

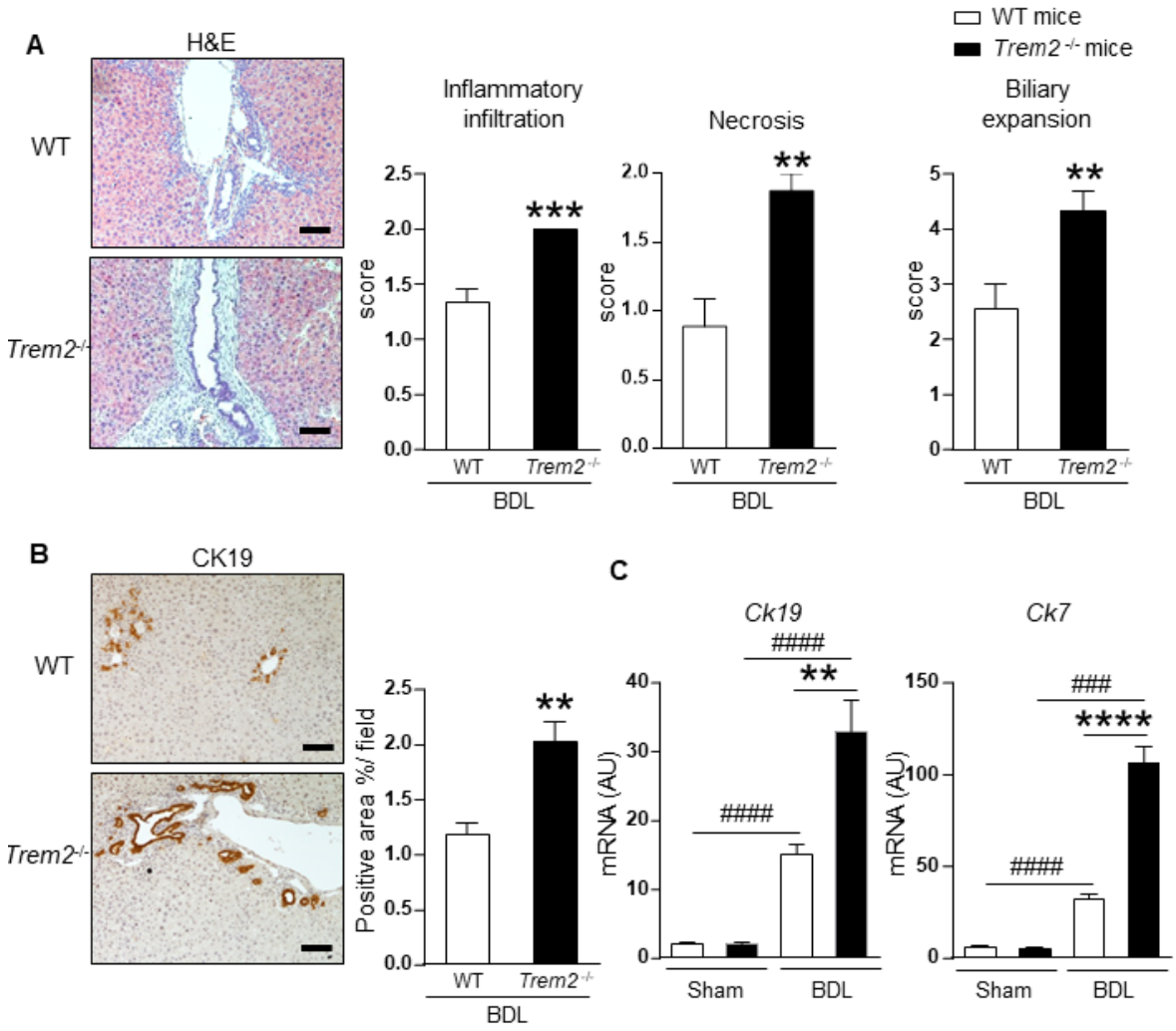

Figure R.7. Liver injury and biliary expansion in response to BDL in WT and *Trem2*$^{-/-}$ mice. (A) Liver H&E staining was evaluated by an experienced pathologist, representative images and inflammatory infiltration, liver necrosis and biliary expansion scores are shown. (**B**) IHC for the cholangiocyte marker CK19, representative images and quantification are shown. (**C**) Liver mRNA expression of the cholangiocyte markers *Ck19* and *Ck*7. Scale bar in (**A** and **B**) represents 100 µm. (**A**) Non-parametric Mann-Whitney test was used. (**B**) Parametric Student´s *t*-test was used (**C**) Parametric Student´s *t*-test and non-parametric Mann-Whitney test were used. **, *** and **** represent *p* values of <0.01, <0.001 <0.0001, respectively in comparison to WT mice following the same experimental conditions; ### and #### represent *p* values of <0.001 and <0.0001, respectively in comparison to sham operated mice of the same genotype. AU, arbitrary units; BDL, bile duct ligation; *Ck7*, cytokeratin 7; *Ck19*, cytokeratin 19; H&E, hematoxylin and eosin; *Trem2*, triggering receptor expressed on myeloid cells; WT, wild type.

Livers of *Trem2*$^{-/-}$ mice also showed enhanced necrotic areas compared to the livers of WT mice after BDL (**Figure R.8A**). This was accompanied by increased hepatic expression of the oxidative stress markers heme oxygenase (*Hmox*) and nitric oxide

synthase 2 (*Nos2*), which were induced in both genotypes under BDL compared to sham operated mice, and were further increased in *Trem2*$^{-/-}$ compared to WT mice after BDL(**Figure R.8B**). To assess the specific cell death mechanisms responsible for this phenomenon, markers of apoptosis and necroptosis were evaluated. We detected low levels of the apoptotic marker cleaved caspase3 (Cl-Casp3) both by IHC (a positive control of mice challenged with LPS was included) and immunoblotting, with no differences between genotypes (**Figure R.9A,B**). By contrast, a strong tendency towards and upregulation was observed in the expression of the marker of necroptosis, receptor-interacting protein kinase 3 (RIP3) in livers of *Trem2*$^{-/-}$ mice following BDL compared to WT mice. Concomitantly, the expression of the main effector protein in necroptosis, MLKL, was also upregulated in the livers of *Trem2*$^{-/-}$ mice compared to WT mice (**Figure R.9C**).

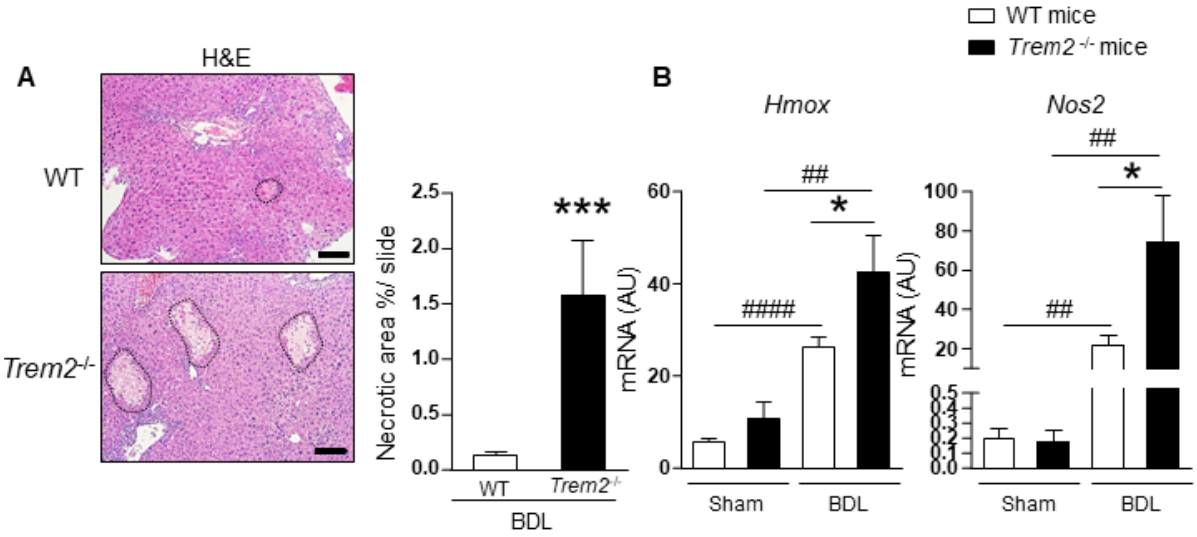

Figure R.8. Cell death in response to BDL in the liver of WT and *Trem2* $^{-/-}$ mice. (**A**) Necrotic areas were measured in the H&E slides; representative images and quantification are shown. (**B**) Liver mRNA expression of oxidative stress markers *Hmox* and *Nos2*. Scale bar in (**A**) represents 100 µm. (**A**) Parametric Student´s *t* -test was used. (**B**) Parametric Student´s *t*-test and non-parametric Mann Whitney test were used. * and *** represent *p* values of <0.05 and <0.001, respectively in comparison to WT mice following the same experimental conditions; ## and ### represent *p* values of <0.01 and <0.001, respectively in comparison to sham operated mice of the same genotype. AU, arbitrary units; BDL, bile duct ligation; H&E, haematoxylin and eosin; *Hmox*, heme oxygenase; *Nos2*, nitric oxide synthase 2; *Trem2*, triggering receptor expressed in myeloid cells 2; WT, wild type.

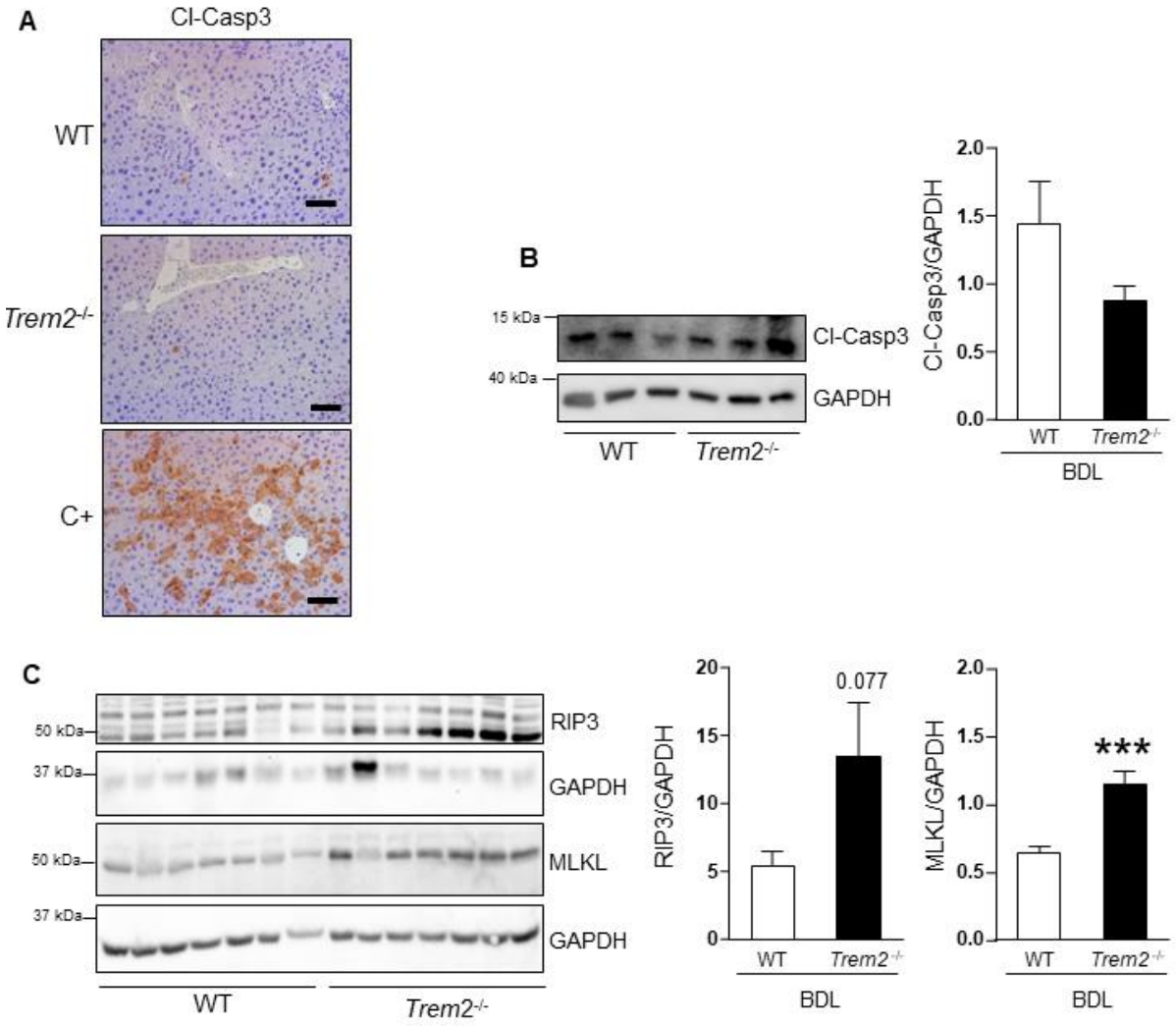

Figure R.9. Expression of apoptotic and necroptotic markers in response to BDL in the liver of WT and *Trem2*$^{-/-}$ mice. (**A**) IHC for Cl-Casp3 in WT and *Trem2*$^{-/-}$ mice after BDL and in a positive control; representative images are shown. (**B**) Immunoblot for the apoptosis marker Cl-Casp3; a representative blot and quantification relative to GAPDH are shown. (**C**) Immunoblot for the necroptosis RIP3 and MLKL a representative blot and quantification relative to GAPDH are shown. Scale bar in (C) represents 50 µm. (**B,C**) Parametric Student´s *t* -test was used. *** represents a *p* value of <0.001 in comparison to WT mice following the same experimental conditions. AU, arbitrary units; BDL, bile duct ligation; Cl-Casp3, cleaved caspase 3; GAPDH, glyceraldehyde-3-phosphate dehydrogenase; RIP3, receptor-interacting protein kinase 3; *Trem2*, triggering receptor expressed in myeloid cells 2; WT, wild type.

R.3.2. Changes in serum and liver BA concentrations in WT and *Trem2*$^{-/-}$ mice after BDL

BAs are regarded as the first triggers of cholestatic liver injury, either due to their direct cytotoxic effects (119) or because of their action in boosting inflammatory responses (117). Taking this into account, we analysed the BA profile in serum and liver of mice subjected to BDL or sham (control group) by mass spectrometry.

It is important to mention that glycine conjugated BAs were not included in the analysis, owing to their negligible contribution to the total BA pool in mice (12). As expected, we observed a dramatic increase in the BA concentration in serum after BDL both in WT and *Trem2*$^{-/-}$ mice compared to control, sham operated mice (**Figure R.10.**). The increase in the total BA concentration in serum is mainly explained by the augmentation in the concentration of the primary BAs (**Figure R.10A**) defined as the family of BAs synthesised by the action of the hepatic enzymes only, which in mice includes CA, QDCA, alpha-muricholic acid (αMCA), beta-muricholic acid (βMCA) and their taurine-conjugated species (8, 12). The concentration of di-hydroxylated toxic BA species (i.e. DCA, QDCA and their taurine conjugates) (310) also increased in both genotypes after BDL (**Figure R.10B**). Similarly, the family of the choleretic BA UDCA (i.e. UDCA and TUDCA); which is regarded as secondary in human and primary in mice, was also higher in response to BDL compared to sham operated mice (12). By contrast, the concentration of the secondary BA species generated by the action of intestinal microbial metabolism, which includes DCA LCA, and their corresponding taurine-conjugated species (8, 12), decreased after BDL in both genotypes of mice (**Figure R.10B**). No significant differences were detected in the BA concentration in serum between WT and *Trem2*$^{-/-}$ mice either in sham operated controls or after BDL (**Figure R.10.**).

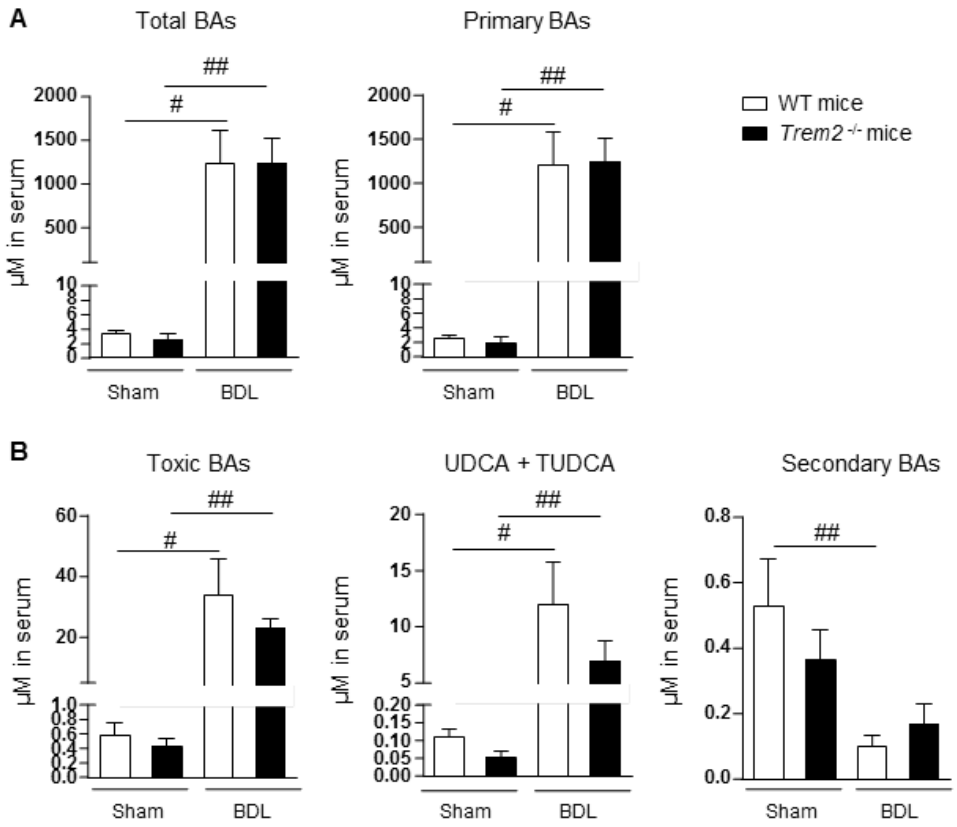

Figure R.10. Serum BA concentration in WT and *Trem2*$^{-/-}$ mice after BDL. Serum concentration of BAs (Sham: WT n=5; *Trem2*$^{-/-}$ n=6 / BDL: WT n=7; *Trem2* $^{-/-}$ n=6) were analysed in WT and *Trem2*$^{-/-}$ mice after BDL or sham. **(A)** Serum concentration of total and primary BAs. (**B**) Serum concentration of toxic, UDCA and TUDCA and secondary BAs. Parametric Student´s *t*-test and non-parametric Mann Whitney test were used. # and ## represent *p* values of <0.05 and <0.01, respectively in comparison to sham operated mice of the same genotype. AU, arbitrary units; BAs, bile acids; BDL, bile duct ligation; TUDCA, tauroursodeoxycholic acid; *Trem2*, triggering receptor expressed on myeloid cells; UDCA, ursodeoxycholic acid; WT, wild type.

In the liver, changes in BA concentration followed the same trend as what we observed in serum. In this regard, BA concentration also markedly increased in the liver of both genotypes after BDL compared to sham operated mice (**Figure R.11A**). This is also mainly explained by an increase in the concentration of the primary BAs species (**Figure R.11A**). The concentration of the toxic BAs species and the UDCA family also increased after BDL in WT and *Trem2*$^{-/-}$ livers (**Figure R.11B**). On the contrary, secondary BAs concentration decreased after BDL in both genotypes of mice (**Figure R.11B**). By contrast to our observations in serum, concentrations in BAs in the liver were indeed different between WT and *Trem2*$^{-/-}$ animals. In this regard, sham operated *Trem*2$^{-/-}$ animals showed an overall reduction of the BA concentration in their liver compared to WT mice (**Figure R.11.**). These differences were no longer detectable after BDL, and BA concentrations reached comparable levels in the liver of WT and *Trem*2$^{-/-}$ mice. Nevertheless, it is important to note that the fold-change of the total BA, primary

BA and toxic BA concentrations induced by BDL, was more prominent in *Trem2*$^{-/-}$ compared to WT mice (**Figure R.11.**).

In an effort to explain the differences observed between WT and *Trem2*$^{-/-}$ mice in the hepatic BA concentration in the control, sham operated mice; we assessed the expression levels of the crucial genes involved in the hepatic BA metabolism. In this regard, liver *Cyp7a*1 mRNA expression showed a marked tendency towards a reduction in *Trem2*$^{-/-}$ compared to WT in sham operated mice, and increased in both genotypes after BDL (**Figure R.11C**). In parallel, the mRNA expression levels of the main negative regulator of *Cyp7a1*, *Fxr*, showed a marked tendency towards an upregulation in sham operated *Trem2*$^{-/-}$ mice in comparison to sham operated WT mice (**Figure R.11C**).

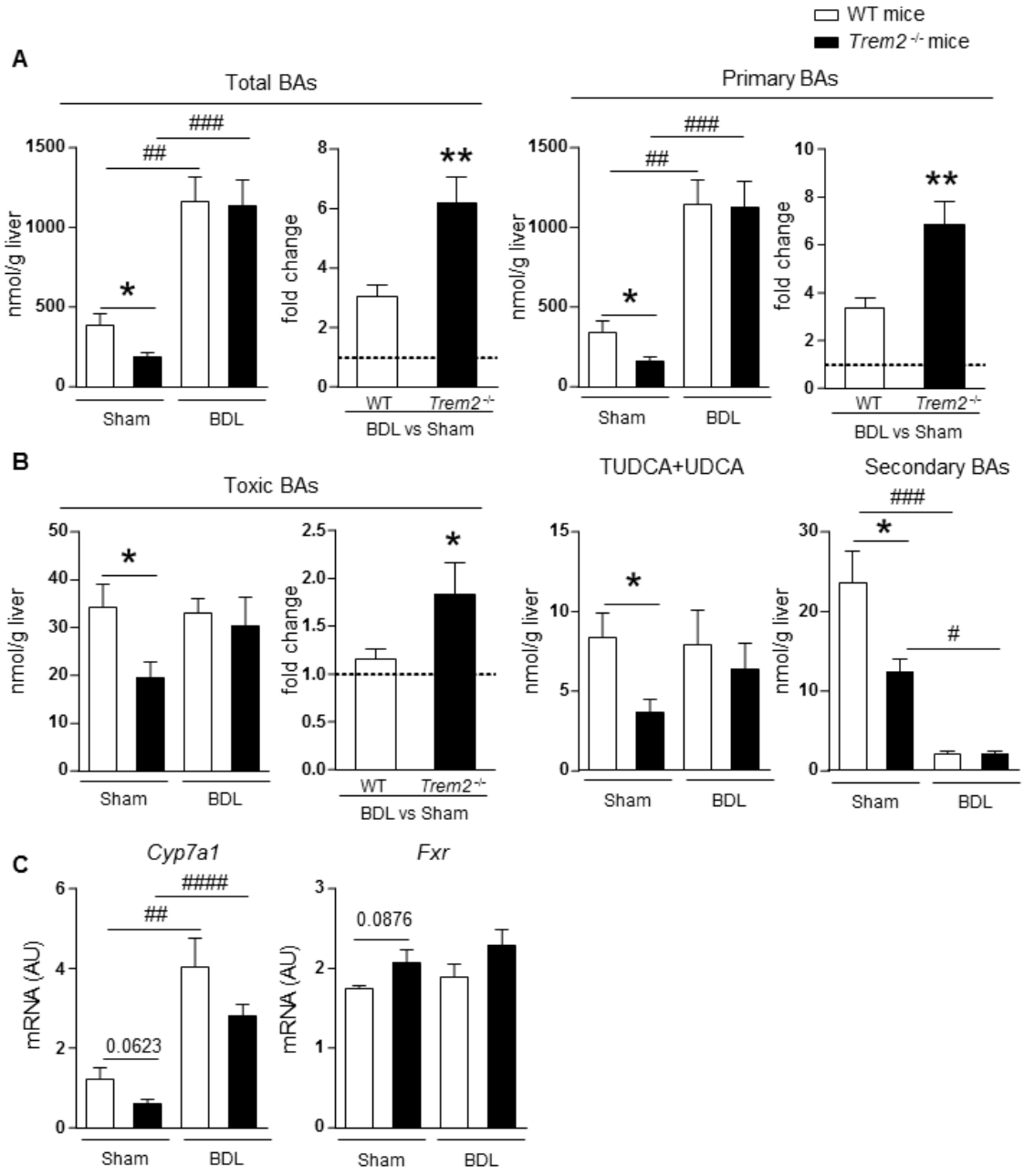

Figure R.11. Liver BA concentration and the expression levels of genes involved in hepatic BA metabolism in WT and *Trem2* $^{-/-}$ mice after BDL. Concentrations of BAs in the liver of WT and *Trem2* $^{-/-}$ mice after BDL or sham operation (Sham: WT n=5; *Trem2* $^{-/-}$ n=6 / BDL: WT n=7; *Trem2* $^{-/-}$ n=6) (**A**) Liver content of total BAs and primary BAs, concentrations and fold change induction from sham to BDL in WT and *Trem2* $^{-/-}$ are shown. (**B**) Liver content of toxic BAs, UDCA+TUDCA and secondary BAs, in WT and *Trem2* $^{-/-}$ after sham and BDL, for toxic BAs concentrations and the fold change induction from sham to BDL in WT and *Trem2* $^{-/-}$ are shown. (**C**) Liver *Cyp7a1* and *Fxr* mRNA expression. (**A**) Parametric Student´s *t*-test was used (**B**) Parametric Student´s *t*-test and non-parametric Mann-Whitney tests were used. (**C**) Parametric Student´s *t*-test was used. * and ** represent *p* values of <0.05 and <0.01, respectively in comparison to WT mice following the same experimental conditions; ##, ### and #### represent *p* values of < 0.05, <0.001 and <0.0001, respectively in comparison to sham operated mice of the same genotype. AU, arbitrary units; BAs, bile acids; BDL, bile duct ligation; *Cyp7a1*; Cytochrome P450 family 7 subfamily A member 1; *Fxr*, farnesoid X receptor; *Trem2*, triggering receptor expressed on myeloid cells; TUDCA, tauroursodeoxycholic acid; UDCA, ursodeoxycholic acid.

R.3.3. *Trem2*$^{-/-}$ mice display exacerbated inflammation in the liver after BDL

Inflammatory mediators play a central role in the progression of chronic biliary diseases in general and, specifically, in chronic cholestatic diseases. These mediators enable intercellular communication, and thus coordinate the wound-healing response which is characteristic of these diseases (6, 154). Accordingly, inflammatory mediators are also central to the phenotype observed in the BDL mouse model, which is characterised by increased inflammatory mediators and the recruitment of immune cells into the liver (293).

Overall, BDL induced the mRNA expression of the inflammatory cytokines *Il6, Tnf* and *Il33*, as well as the pro-inflammatory chemokines *Mcp1* and *Cxcl1*, which are involved in monocyte and neutrophil recruitment to the liver, respectively, in both genotypes of mice compared to sham operated control mice (**Figure R.12.**). Moreover, our results depict increased mRNA expression levels of the inflammatory cytokines *Il*6, *Tnf and Il33* as well as the chemokines *Mcp1* and *Cxcl1* in the livers of *Trem2*$^{-/-}$ mice compared to WT mice after BDL (**Figure R.12A,B**). We corroborated these results at protein level, as the expression of the chemokines MCP1 and CXCL1 in the liver increased with BDL compared to sham operated mice in both genotypes, and this expression was further enhanced in *Trem2*$^{-/-}$ mice in comparison to WT mice after BDL (**Figure R.12C**).

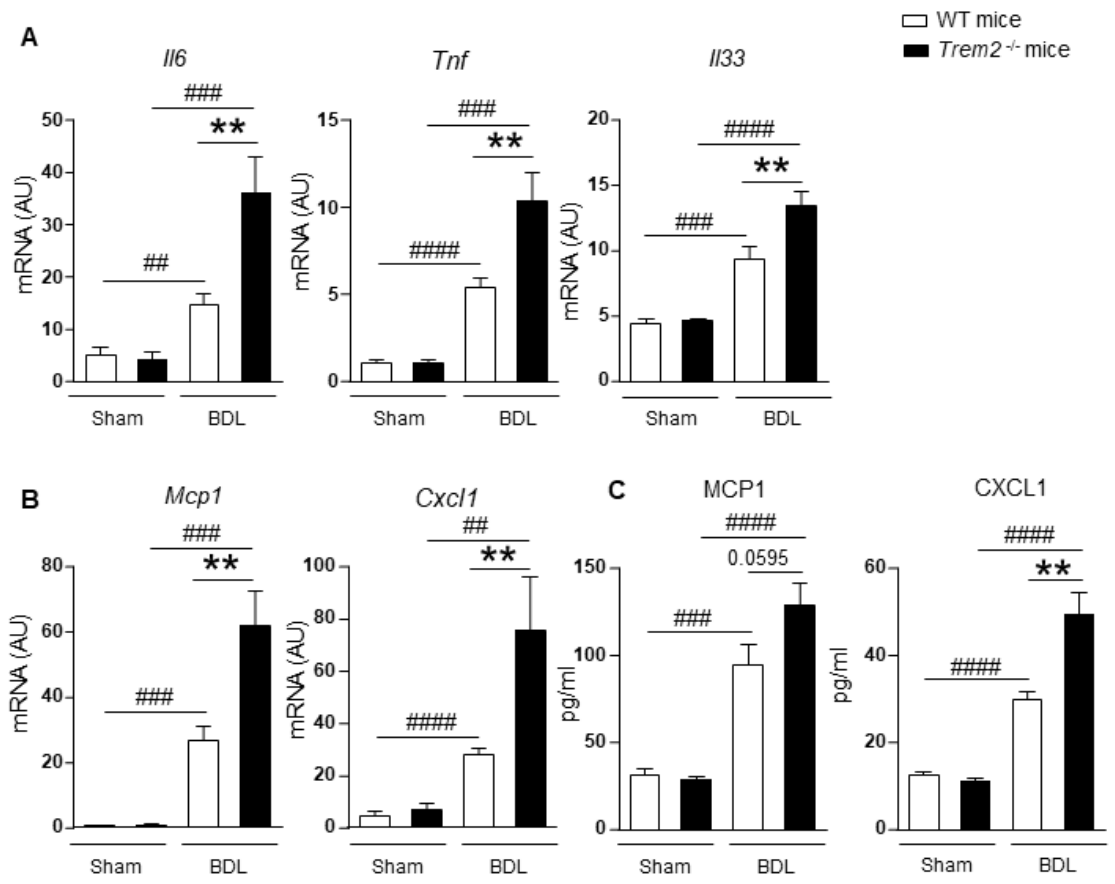

Figure R.12. Liver inflammatory cytokine and chemokine expression after BDL in WT and *Trem2*$^{-/-}$ mice. (A) mRNA expression of the inflammatory cytokines *Il6*, *Tnf* and *Il33* and (**B**) the chemokines *Mcp1* and *Cxcl1* in the liver. (**C**) Protein expression of the inflammatory chemokines MCP1 and CXCL1 in the liver. Parametric Student´s *t*-test was used. ** represent *p* values of <0.01, in comparison to WT mice following the same experimental conditions; ##, ### and #### represent *p* values of < 0.05, <0.001 and <0.0001, respectively in comparison to sham operated mice of the same genotype. AU, arbitrary units; BDL, bile duct ligation; *Cxcl1*, C-X-C motif chemokine ligand 1; *Il6*, interleukin 6; *Il33*, interleukin 33; *Mcp1*, monocyte chemoattractant protein 1; *Tnf*, tumour necrosis factor; *Trem2*, triggering receptor expressed on myeloid cells; WT, wild type.

Neutrophils are regarded as the main innate immune cells to mediate cytotoxic responses during cholestasis, both in human diseases and also in mouse models (125-127). Of note, increased *Cxcl1* mRNA expression levels in the liver of *Trem2*$^{-/-}$ mice after BDL were associated with increased hepatic neutrophil content in these mice compared to WT mice after BDL, as shown by IHC of the neutrophil marker NIMP-R14 (**Figure R13A**). No significant differences were detected between WT and *Trem2*$^{-/-}$ mice in the hepatic content of macrophages and T lymphocytes as assessed by IHC for the F4/80 and CD3 markers in response to BDL, respectively (**Figure R.13B,C**).

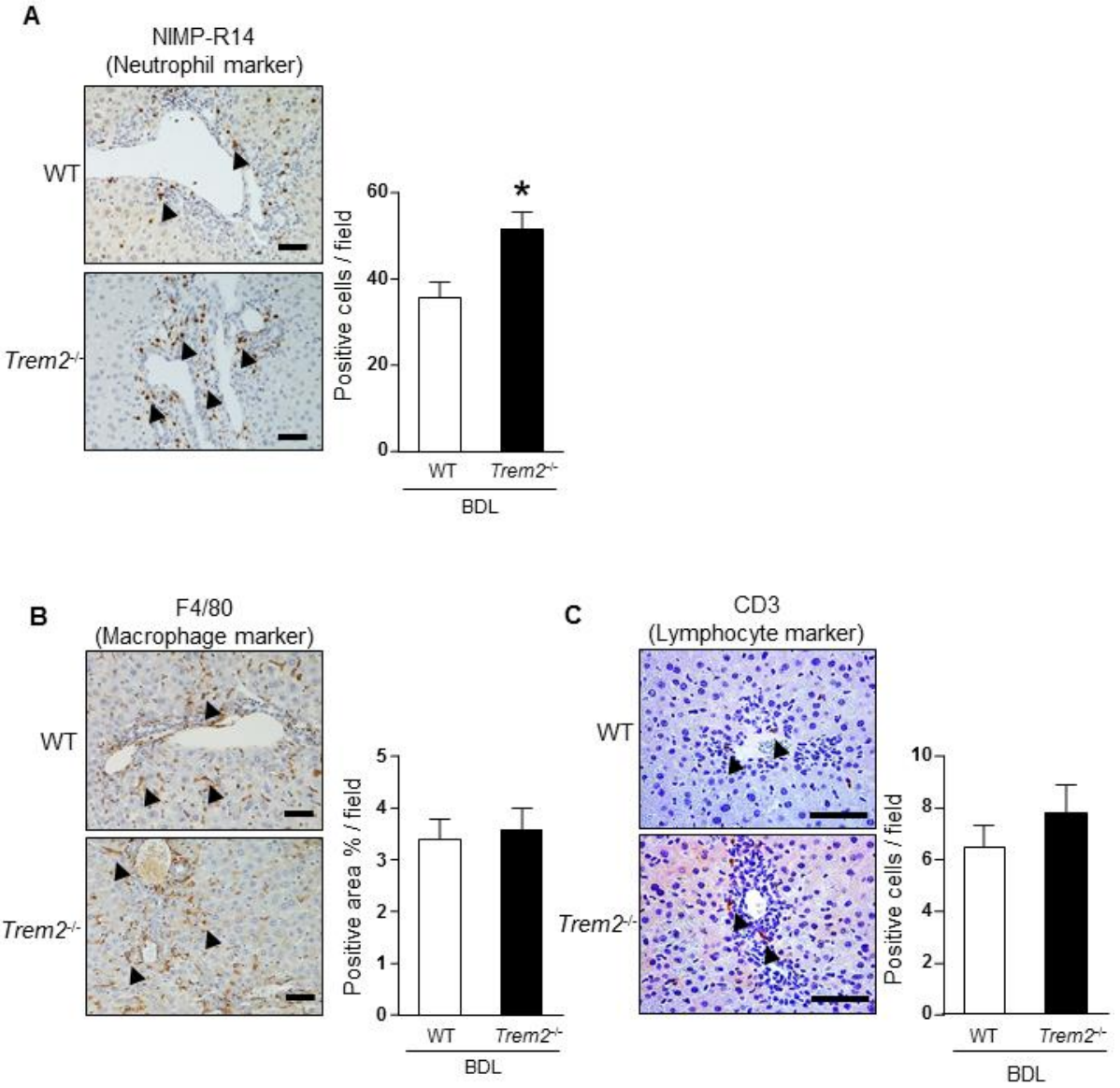

Figure R.13. Liver immune cell recruitment after BDL in WT and *Trem2*$^{-/-}$ mice. (A) IHC for the neutrophil marker NIMP-R14, representative images and quantification are shown (**B**) IHC for the macrophage markers F4/80, representative images and quantification are shown. (**C**) IHC for the lymphocyte marker CD3, representative images and quantification are shown. Scale bar in (**A,B**) represents 50 µm and in (**C**) 10 µm, back arrows indicate stained cells. Parametric Student´s *t*-test and was used. * represents a *p* value of <0.05 to WT mice following the same experimental conditions. AU, arbitrary units; BDL, bile duct ligation; CD3,cluster of differentiation 3; *Hmox*, heme oxygenase; *Nos2*, nitric oxide synthase 2; *Trem2*, triggering receptor expressed on myeloid cells; WT, wild type.

R.3.4. *Trem2*$^{-/-}$ mice display increased HSC activation but no differences in liver fibrosis compared to WT mice following BDL

As aforementioned, inflammatory mediators serve as intercellular communication factors during ductular reaction. In this regard, one of the most important outcomes of this intercellular communication is HSC or PM recruitment and activation, which are important players contributing to the inflammatory response, and are also the main cell types responsible of ECM production and liver fibrosis (136, 176). Thus, our results showing exacerbated hepatic inflammation in the *Trem2*$^{-/-}$ mice compared to WT mice after BDL, prompted us to study liver fibrosis.

First, we detected increased expression of the main marker of HSC activation, aSMA, both at mRNA (coding gene *Acta2*) and protein levels in the liver of *Trem2*$^{-/-}$ mice compared to WT mice after BDL (**Figure R.14AB**). Both *Acta2* and *Col1a1* mRNA expression levels were enhanced with BDL in comparison to sham operated controls in both genotypes of mice and *Col1a1* mRNA levels were also enhanced in the liver of *Trem2*$^{-/-}$ mice compared to WT mice after BDL (**Figure R.14B**). Conversely, no differences were detected in Sirius red staining between WT and *Trem2*$^{-/-}$ mice after BDL (**Figure R.14C**).

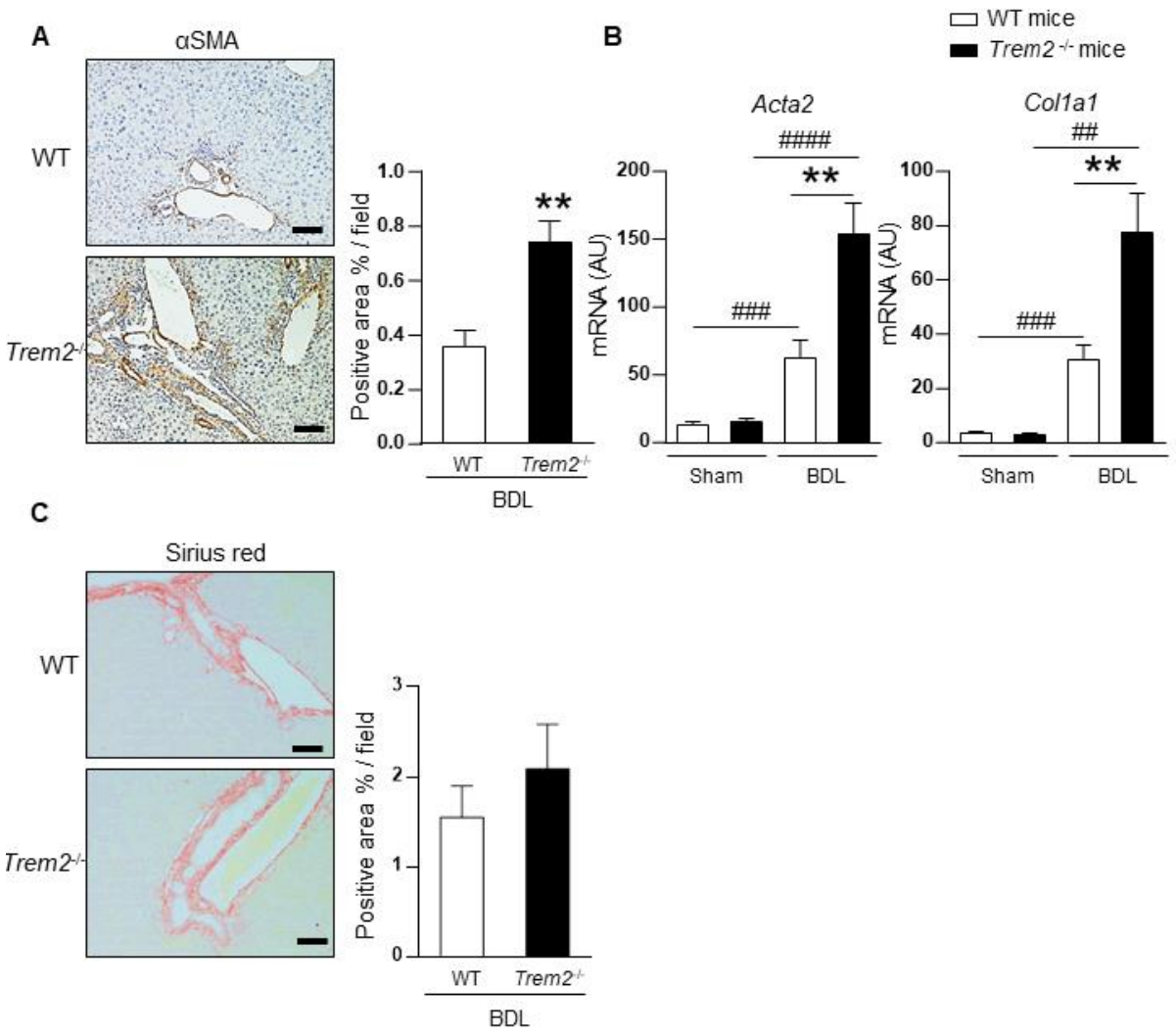

Figure R.14. Liver fibrotic responses after BDL in WT and *Trem2*$^{-/-}$ mice. (A) IHC of the hepatic stellate cell activation marker αSMA, representative images and quantification are shown. (**B**) mRNA expression of *Acta2* and *Col1a1* in the liver. (**C**) Sirius red staining, representative images and quantification are shown. Scale bar in (**A, C**) represents 100 µm. (**A,C**) Parametric Student´s *t*-test was used. (**B**) Parametric Student´s *t*-test and non-parametric Mann Whitney test were used. ** represent *p* values of <0.01 in comparison to WT mice following the same experimental conditions; ##, ### and #### represent *p* values of < 0.05, <0.001 and <0.0001, respectively in comparison to sham operated mice of the same genotype. *Acta2*, actin alpha 2, smooth muscle; αSMA, alpha smooth muscle actin; AU, arbitrary units; BDL, bile duct ligation; *Col1a1*, collagen type 1 A 1; *Trem2*, triggering receptor expressed on myeloid cells; WT, wild type.

Overall, these results pinpoint for a role of TREM2 as a negative regulator of inflammatory responses during cholestatic injury in mice, which finally results in a diminished wound-healing response and a less pronounced cholestasis-associated phenotype.

R.4. Abx treatment rescues some of the TREM2-associated changes in BDL

Advanced chronic cholestatic diseases may induce portal hypertension and gut disbiosis, finally resulting in the translocation of bacteria and bacterial products from the gut to the liver via the portal vein. This phenomenon is known as the gut-liver axis and is now regarded as one of the sources of inflammatory signals, and therefore, disease progression in chronic cholestasis (204). Bacterial product translocation is also identified during BDL as early as 24 hours after the surgery (294). It is important to bear in mind that TREM2 has been reported by us and others to act as a negative regulator of TLR-related signalling (264, 265, 288, 289).

In order to test the contribution of gut microbiota as one of the triggering factors of the TREM2-mediated phenotype in cholestasis, we treated WT and *Trem2*$^{-/-}$ mice with an Abx cocktail for 4 weeks and, in the third week of Abx treatment, we conducted the BDL surgery and continued the Abx treatment until the sacrifice, 7 days after BDL (**Figure R.15A**). Interestingly, Abx rescued some of the differences observed after BDL between WT and *Trem2*$^{-/-}$ mice.

Abx treatment did not result in differences in the score of inflammatory infiltration or necrosis after Abx treatment after BDL in any of the genotypes (**Figure R.15B**). However, the differences between WT and *Trem2*$^{-/-}$ mice following BDL were no longer observed after Abx treatment, and the fold change observed in the necrotic score in BDL between WT and *Trem2*$^{-/-}$ actually decreased. In line with this, liver mRNA expression of the oxidative stress marker *Nos2* was reduced in *Trem2*$^{-/-}$ mice after Abx treatment and in the case of *Hmox* a strong tendency towards a reduction was detected. The differences detected in *Nos2* and *Hmox* mRNA expression between WT and *Trem2*$^{-/-}$ mice following BDL disappeared after Abx treatment. Additionally, the fold-change of *Nos2* observed in BDL between WT and *Trem2*$^{-/-}$ was reduced after Abx treatment and in the case of *Hmox* a strong tendency towards a reduction was observed (**Figure R.16.**).

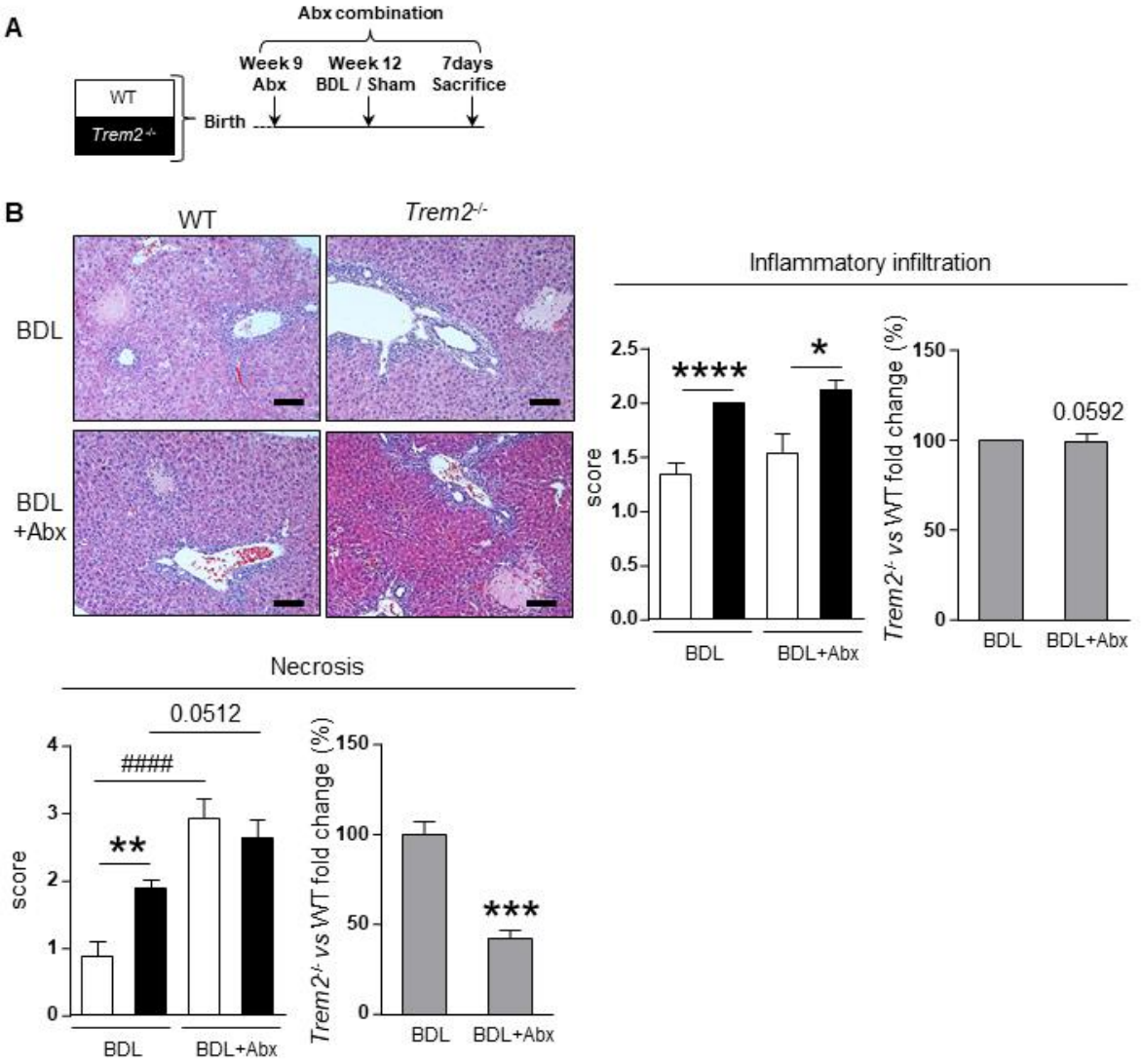

Figure R.15. Liver injury in response to BDL or BDL+Abx in WT and *Trem2*$^{-/-}$ mice. (A) WT and *Trem2*$^{-/-}$ mice were treated with an antibiotic cocktail for three weeks, then subjected to BDL and sacrificed 1 week after the surgery (WT n=13; *Trem2*$^{-/-}$ n=8). The groups subjected to sham operation (WT n=6; *Trem2*$^{-/-}$ n=7) and BDL only (WT n=9; *Trem2*$^{-/-}$ n=8) are included for comparison. (**B**) Liver H&E staining was evaluated by an experienced pathologist; representative images, inflammatory infiltration and necrosis scores and fold change of *Trem2*$^{-/-}$ vs WT in BDL and Abx+BDL are shown. Scale bar in (**B**) represents 100 µm. (**B**) Non-parametric Mann Whitney test was used. *, **, *** and **** represent *p* values of <0.05, <0.01, <0.001, <0.0001 in comparison to WT mice following the same experimental condition (or in comparison to the fold change observed in BDL); #### represent p values of <0.0001, respectively in comparison to sham operated mice of the same genotype. Abx, antibiotics; AU, arbitrary units; BDL, bile duct ligation; *Trem2*, triggering receptor expressed on myeloid cells; *vs*, versus; WT, wild type. *Data in sham and BDLgroups are the same as the presented in figures R.6. and R.7.*

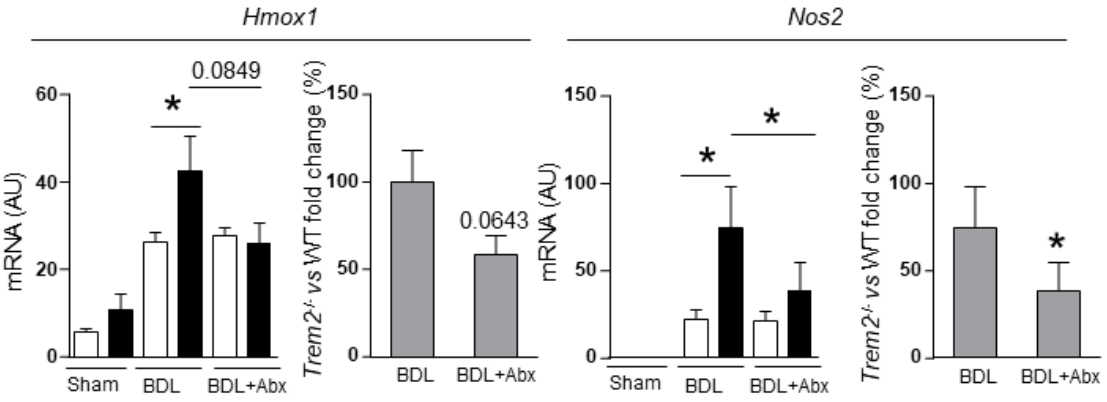

Figure R.16. Oxidative stress marker expression in the liver of WT an *Trem2*$^{-/-}$ subjected to BDL or BDL+Abx. Liver mRNA expression of the oxidative stress markers *Hmox1* and *Nos2;* total values and fold change of *Trem2*$^{-/-}$ *vs* WT in BDL and Abx+BDL are shown. Parametric Student´s *t*-test and non-parametric Mann Whitney test was used. * represents a *p* value of <0.05 in comparison to WT mice following the same experimental condition (or in comparison to the fold change observed in BDL). Abx, antibiotics; AU, arbitrary units; BDL, bile duct ligation; *Hmox*, heme oxygenase; *Nos2*, nitric oxide synthase 2 *Trem2*, triggering receptor expressed on myeloid cells; *vs*, versus; WT, wild type. *Data in sham and BDL groups are the same as the presented in figures R.6. and R.7*.

When changes related to biliary expansion were assessed, we observed diminished liver protein expression levels of the biliary marker CK19 in both genotypes after the treatment with Abx, compared to BDL only. Importantly, this expression was no longer different between WT and *Trem2*$^{-/-}$ mice after Abx treatment; consequently, the fold-change between WT and *Trem2*$^{-/-}$ observed in BDL showed a marked tendency towards a reduction after Abx (**Figure R.17A**). The mRNA expression levels of the biliary marker *Ck7* diminished in the liver of *Trem2*$^{-/-}$ after Abx treatment compared to BDL only, while mRNA expression levels of *Ck19* did not change with Abx treatment, compared to BDL only. Nevertheless, the fold change between WT and *Trem2*$^{-/-}$ mice showed a tendency towards a downregulation in *Ck19*, which was significant in the case of *Ck7* (**Figure R.17B**).

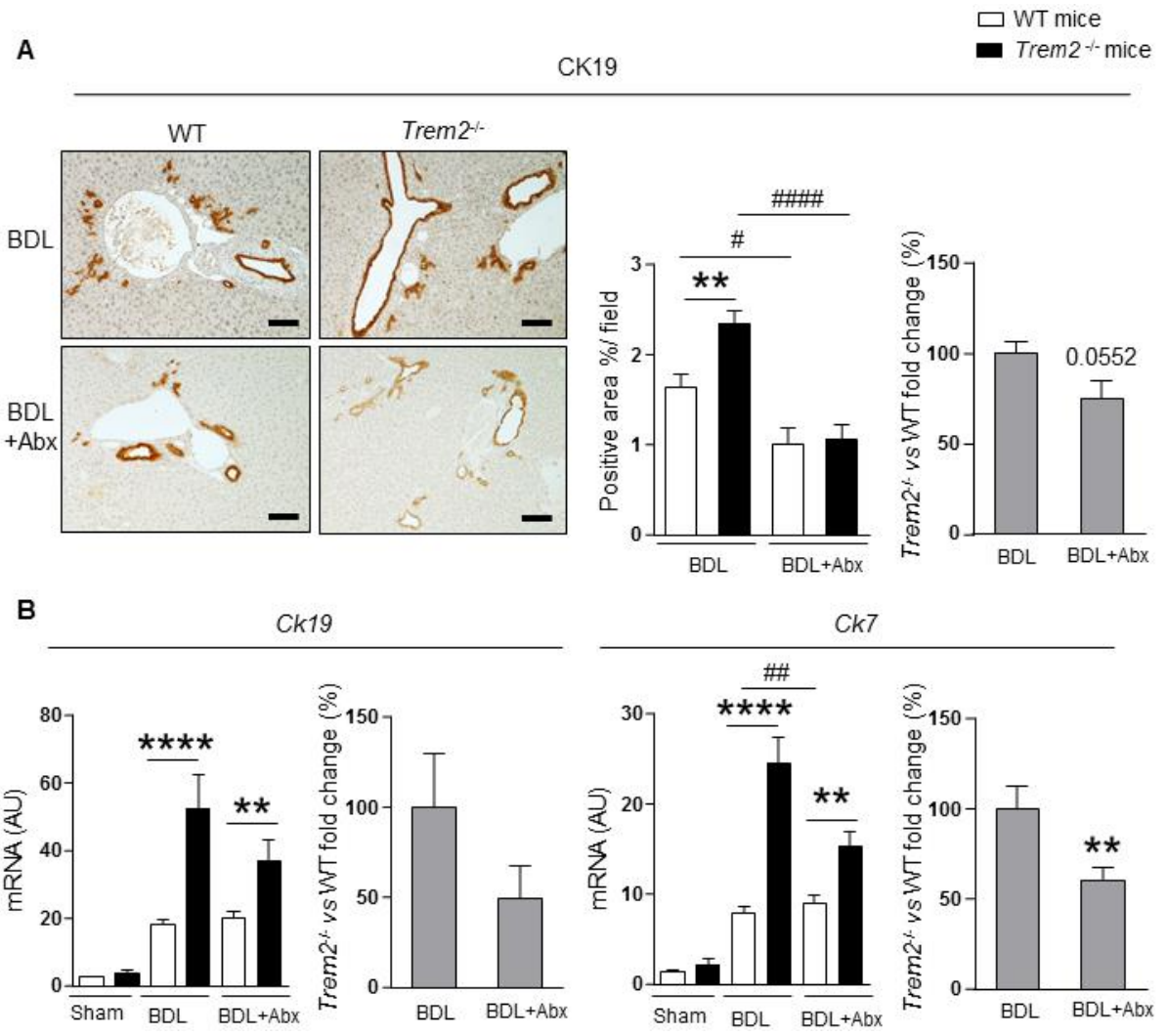

Figure R.17. Biliary expansion in response to BDL or BDL+Abx in WT and *Trem2* $^{-/-}$ mice. (A) Liver IHC for the cholangiocyte marker CK19, representative images, quantification and fold change of *Trem2* $^{-/-}$ *vs* WT are shown. (**B**) mRNA expression levels of the biliary markers *Ck19* and *Ck7* in the liver; total values and fold change of *Trem2*$^{-/-}$ *vs* WT are shown. Scale bar in (**A**) represets 100 µm. (**A**) Parametric Student´s *t*-test was used (**B**) Parametric Student´s *t*-test and non-parametric Mann Whitney test were used. **and **** represent *p* values of <0.01 and <0.0001 in comparison to WT mice following the same experimental conditions (or in comparison to the fold change observed in BDL); #, ## and #### represent *p* values of <0.05, <0.01 and <0.0001, respectively in comparison to sham operated mice of the same genotype. Abx, antibiotics; AU, arbitrary units; BDL, bile duct ligation; *Ck7*, cytokeratin 7; *Ck19*, cytokeratin 19; *Trem2*, triggering receptor expressed on myeloid cells; vs, versus; WT, wild type. *Data in sham and BDL groups are the same as the presented in figure R.6., IHC same data, qPCRs, different qPCR but same samples*.

Liver expression of several inflammatory markers induced under BDL was reduced by Abx treatmen compared to BDL only, such as *Tnf* and *Mcp1* in WT mice and *Mcp1* was also reduced in the *Trem2*$^{-/-}$. On the other hand, other markers including *Cxcl1*, *Il6* and *Il33* were not affected by the treatment with Abx (**Figure R.18.**). Analysis of the fold-change between WT and *Trem2*$^{-/-}$ revealed that Abx did not impact the differences observed in the hepatic expression levels of these pro-inflammatory cytokines and chemokines between WT and *Trem2*$^{-/-}$ after BDL only, except for a reduction in the fold-change of *Il33* (**Figure R.18.**).

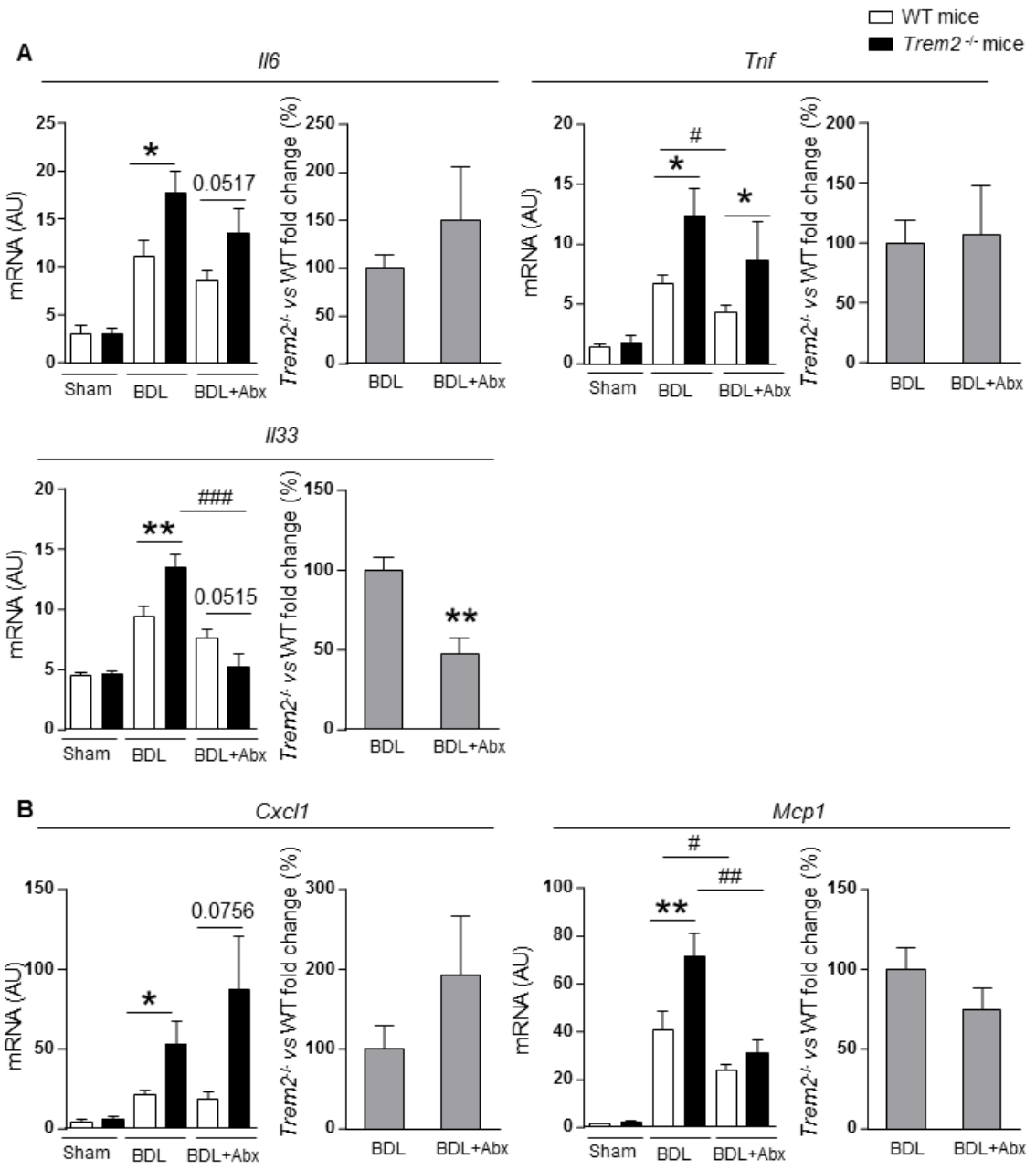

Figure R.18. Inflammatory cytokine and chemokine expression in the liver of WT and *Trem2* $^{-/-}$ mice in response to BDL or BDL+Abx. (A) mRNA expression of inflammatory cytokines *Il6*, *Tnf* and *Il33*; total values and fold change of *Trem2*$^{-/-}$ *vs* WT in BDL and Abx+BDL are shown. (**B**) The chemokines *Mcp1* and *Cxcl1* total values and fold change of *Trem2*$^{-/-}$ *vs* WT are shown. Parametric Student´s *t*-test and non-parametric Mann Whitney test were used. *and ** represent *p* values of <0.05 and <0.01 in comparison to WT mice following the same experimental conditions (or in comparison to the fold change observed in BDL); #, ## and ### represent *p* values of <0.05, <0.01 and <0.001, respectively in comparison to sham operated mice of the same genotype. Abx, antibiotics; AU, arbitrary units; BDL, bile duct ligation; *Cxcl1*, C-X-C motif chemokine ligand 1; *Il6*, interleukin 6; *Il33*, interleukin 33; *Mcp1*, monocyte chemoattractant protein 1; *Tnf*, tumour necrosis factor; *Trem2*, triggering receptor expressed on myeloid cells; *vs*; versus; WT, wild type. *Data in sham and BDL groups are the same as the presented in figure R.10, IL6, Tnf, Mc1, Cxcl1 same samples, different qPCR, Il33 same samples and same qPCR.*

Neutrophil recruitment showed a marked tendency towards an increase in WT with Abx-BDL compared to BDL only, while it was not affected in *Trem2*$^{-/-}$ mice (**Figure R.19.**). When we analysed the fold-change between WT and *Trem2*$^{-/-}$ mice, we noted that Abx induced a reduction of the differences observed after BDL between WT and *Trem2*$^{-/-}$ mice, in the hepatic content of neutrophils (**Figure R.19.**).

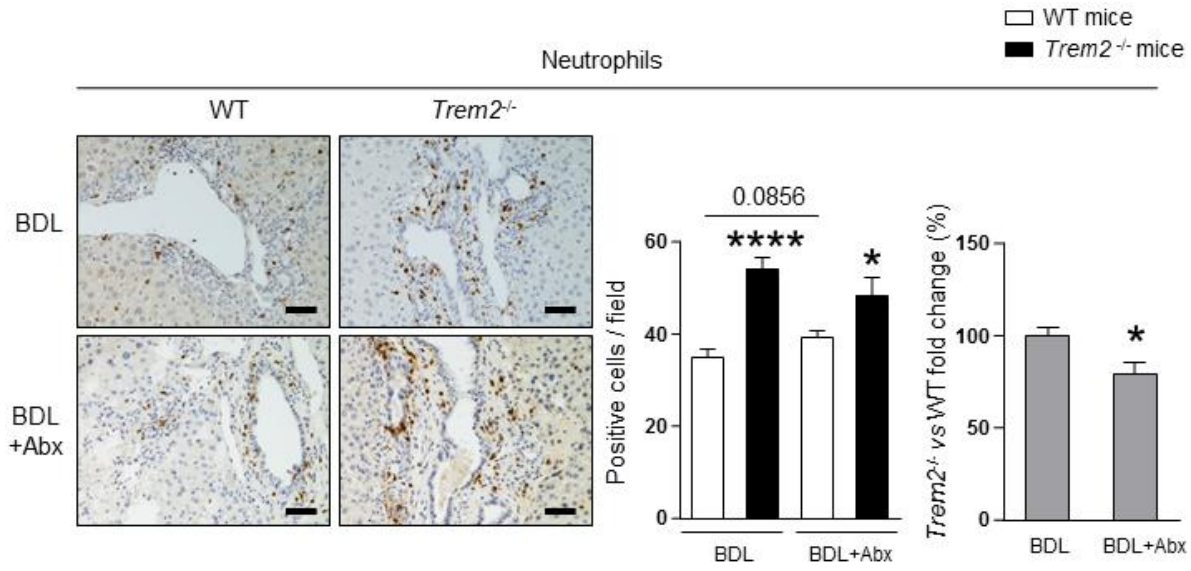

Figure R.19. Neutrophil recruitment to the liver after BDL and BDL+Abx in WT and *Trem2*$^{-/-}$ mice. IHC for the neutrophil marker NIMP-R14; representative images, the quantification and the fold change of *Trem2*$^{-/-}$ *vs* WT in BDL and Abx-BDL are shown. Scale bar represents 50 µm. Parametric Student´s *t*-test and non-parametric Mann Whitney test were used. *and **** represent p values of <0.05 and<0.0001, respectively in comparison to WT mice following the same experimental conditions (or in comparison to the fold change observed in BDL). Abx, antibiotics; BDL, bile duct ligation; Trem2, triggering receptor expressed on myeloid cells; *vs*, versus; WT, wild type. Data in BDL is the same as presented in figure R.11.

R.5. *Trem2*$^{-/-}$ mice show exacerbated liver damage and inflammation in a chemically-induced model of cholestasis based on ANIT administration

R.5.1. Increased liver damage in *Trem2*$^{-/-}$ mice in a chemically-induced model of cholestasis based on ANIT administration

The results obtained in the BDL model, together with the observation that *Trem2* mRNA expression is upregulated in the liver of mice subjected to different models of cholestasis regardless of their origin, prompted us to investigate the role of TREM2 in an additional model of chemically-induced cholestasis. We selected the ANIT-based model of chemically-induced cholestasis due to its action in cholangiocytes, where administered in a high-single dose by oral gavage, produces severe cholangiocyte

destruction leading to intrahepatic cholestasis (295, 296). To perform this model, we administered ANIT at a dose of 50mg/kg or the vehicle O.Oil to WT and *Trem2*$^{-/-}$ mice and sacrificed them 48 hours after the administration (**Figure R.20A**).

Comparable levels of the serum marker of cholestasis, ALP, and the serum markers of hepatocellular injury ALT and AST, between O.Oil and ANIT-treated mice, suggested that ANIT at the dose of 50 mg/kg was unable to induce liver damage in WT mice. Nevertheless, *Trem2*$^{-/-}$ mice display enhanced levels of these markers compared to O.Oil treated mice and also compared to WT mice after ANIT administration (**Figure R.20B**).

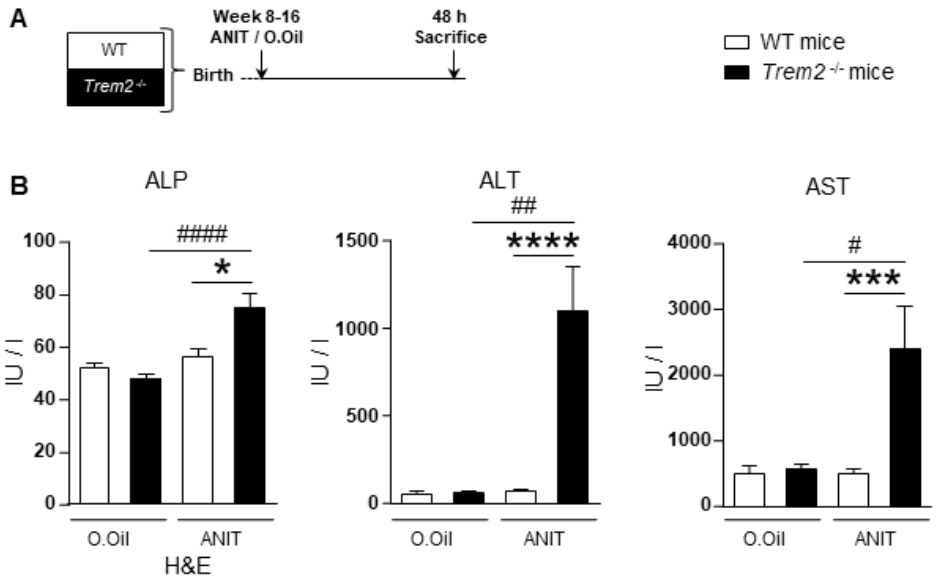

Figure R.20. Serum markers of biliary and hepatocellular injury after chemically-induced cholestasis, based on ANIT administration in WT and *Trem2*$^{-/-}$ mice. (**A**) WT and *Trem2*$^{-/-}$ mice were administered O.Oil (WT n=8; *Trem2*$^{-/-}$ n=8) or ANIT (WT n=11; *Trem2*$^{-/-}$ n=12) by oral gavage and sacrificed 48 hours after the administration. (**B**) Serum levels of liver enzymes. (**B**) Parametric Student´s *t*-test and non-parametric Mann Whitney test were used. *, ***, **** represent *p* values of <0.05, <0.001 and <0.0001, respectively in comparison to WT mice following the same experimental conditions; #, ## and #### represent *p* values of < 0.05, <0.01 and <0.0001, respectively in comparison to O.Oil administered mice of the same genotype. ALP, alkaline phosphatase; ALT, alanine aminotransferase; ANIT, α-naphthylisothiocyanate; AST, aspartate aminotransferase; AU, arbitrary units; BDL, bile duct ligation; H&E, haematoxylin and eosin; O.Oil, olive oil; *Trem2*, triggering receptor expressed on myeloid cells; WT, wild type.

Accordingly, livers of *Trem2*$^{-/-}$ mice displayed enhanced necrotic areas after ANIT compared to livers of WT mice (**Figure R.21A**), which was accompanied by increased mRNA expression of the oxidative stress markers *Hmox* and *Nos2*, which increased in both genotypes of mice after ANIT administration and were further enhanced in *Trem2*$^{-/-}$ mice compared to WT mice (**Figure R.21B**). Hepatic mRNA expression of the biliary

markers *Ck7* and *Ck19* was upregulated in both genotypes of mice under ANIT administration, but at a higher extent in *Trem2*$^{-/-}$ mice *vs* WT mice (**Figure R.21C**).

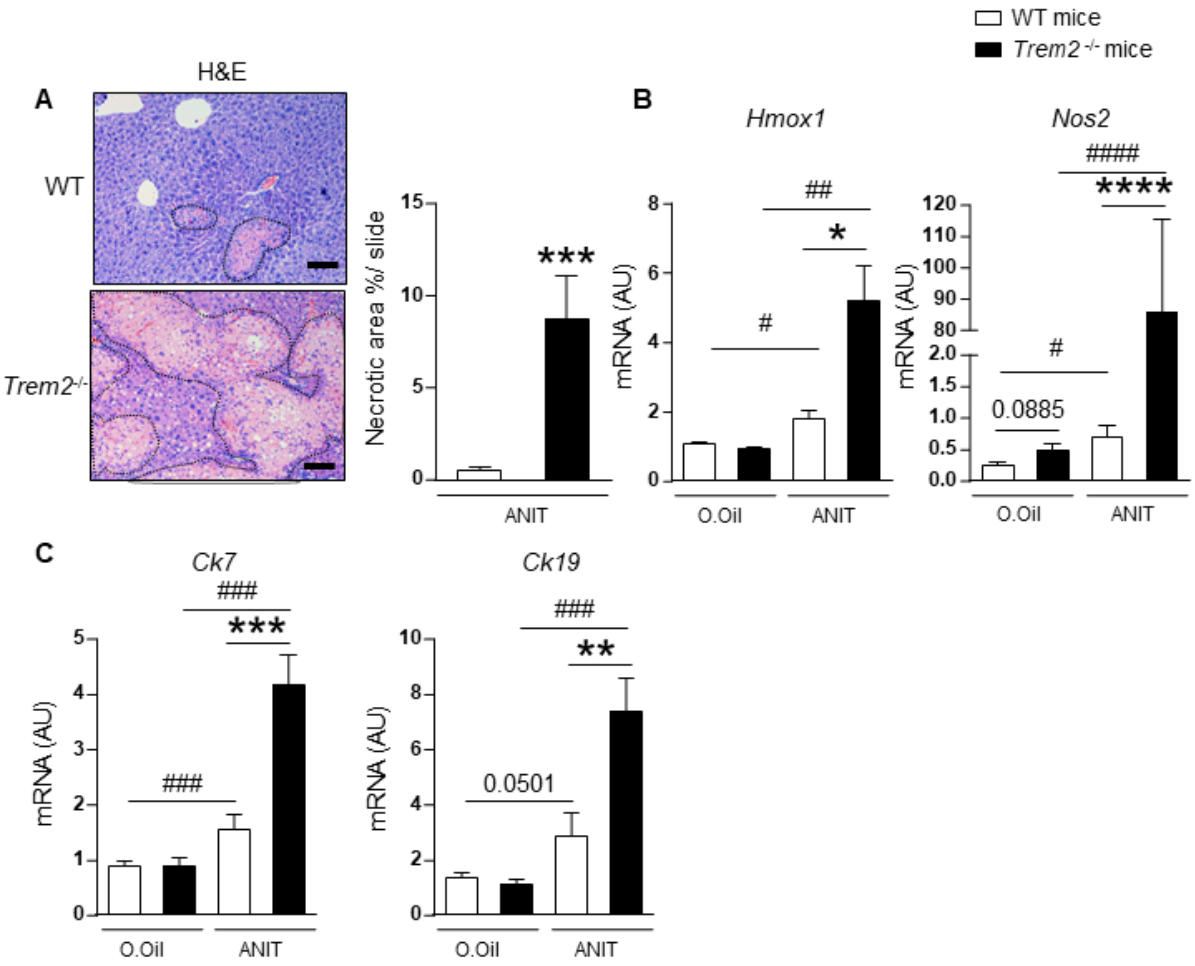

Figure R.21. Liver injury after chemically-induced cholestasis, based on ANIT administration in WT and *Trem2*$^{-/-}$ mice. (**A**) Necrotic areas were measured in H&E slides; representative images and the quantification are shown. (**B**) mRNA expression levels of the oxidative stress markers *Hmox1* and *Nos2* in the liver. (**C**) mRNA expression of the cholangiocyte markers *Ck19* and *Ck7* in the liver. Scale bar in (**A**) represents 100 µm. (**B,C**) Non-parametric Mann Whitney test was used. *, **, ***, **** represent *p* values of <0.05, <0.01,<0.001 and <0.0001, respectively in comparison to WT mice following the same experimental conditions; #, ##, ### and #### represent *p* values of < 0.05, <0.01,<0.001 and <0.0001, respectively in comparison to O.Oil administered mice of the same genotype. ANIT, α-naphthylisothiocyanate; AU, arbitrary units; BDL, bile duct ligation; *Ck7*, cytokeratin 7; *Ck19*, cytokeratin 19; H&E, haematoxylin and eosin; O.Oil, olive oil; *Trem2*, triggering receptor expressed on myeloid cells; WT, wild type.

R.5.2. Exacerbated inflammation in *Trem2*$^{-/-}$ mice in a chemically-induced model of cholestasis based on ANIT administration

Akin to our results in the BDL model, *Trem2*$^{-/-}$ mice also showed exacerbated inflammation in response to chemically-induced cholestasis based on ANIT administration. In this line, *Trem2*$^{-/-}$ displayed enhanced mRNA expression of the pro-inflammatory cytokines *Il1β*, *Il6*, *Il33* and *Tnf* as well as the chemokine *Mcp1* compared to WT mice after ANIT administration (**Figure R.22.**). Of note, ANIT administration did not affect the expression of these pro-inflammatory markers in WT mice compared to O.Oil administered mice, while it did induce the expression of all of them in the liver of *Trem2*$^{-/-}$ mice (**Figure R.22.**). Similarly, mRNA expression levels of *Acta2* showed a strong tendency towards upregulation after ANIT administration in WT mice, and this upregulation was significant in the case of *Trem2*$^{-/-}$ mice. *Acta2* expression was further increased in *Trem2*$^{-/-}$ mice compared to WT mice after ANIT administration (**Figure R.22.**).

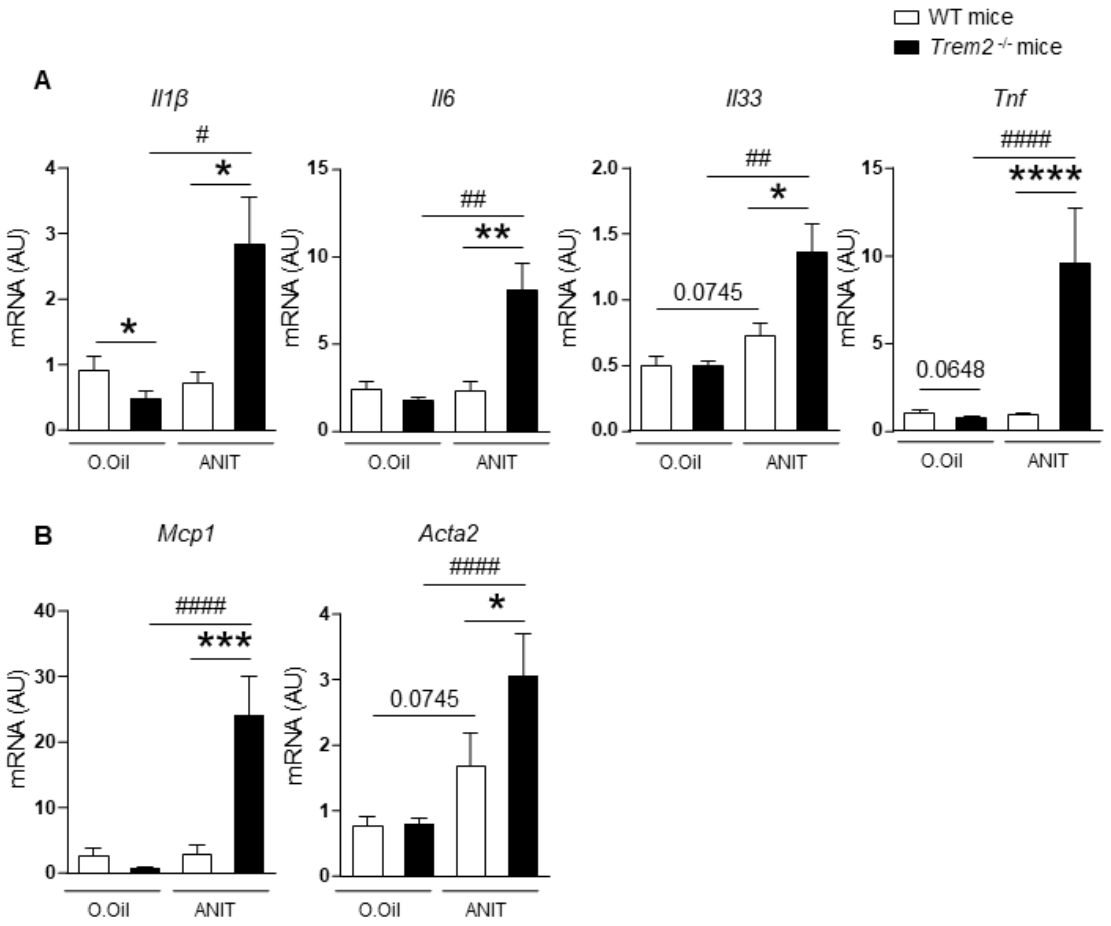

Figure R.22. Hepatic levels of inflammatory cytokines and chemokines after chemically-induced cholestasis based on ANIT administration in WT and *Trem2*$^{-/-}$ mice. (A) mRNA expression of the inflammatory cytokines *Il1β*, *Il6*, *Il33* and *Tnf* (**B**) the chemokine *Mcp1* and (**C**) the HSCs activation marker *Acta2*. Parametric Student´s *t*-test and non-parametric Mann Whitney test were used. *, **, ***, **** represent *p* values of <0.05, <0.01, <0.001 and <0.0001, respectively in comparison to WT mice following the same experimental conditions; #, ## and #### represent *p* values of <0.05, <0.01 and <0.0001, respectively in comparison to O.Oil administered mice of the same genotype. *Acta2*, actin alpha 2, smooth muscle; ALT, alanine aminotransferase; ANIT, α-naphthylisothiocyanate; AP, alkaline phosphatase; AST, aspartate aminotransferase; AU, arbitrary units; BDL, bile duct ligation; *Cxcl1*, C-X-C motif chemokine ligand 1; *Il6*, interleukin 6; *Il33*, interleukin 33; *Mcp1*, monocyte chemoattractant protein 1; O.Oil, olive oil; *Tnf*, tumour necrosis factor; *Trem2*, triggering receptor expressed on myeloid cells; WT, wild type

Taking together, our results in the BDL and the ANIT models suggest that TREM2 is able to protect the liver from excessive injury and inflammation in the context of cholestasis regardless of its origin.

R.6. UDCA regulates TREM1 and TREM2 expression in isolated KCs

As aforementioned, KCs are the key cellular players that orchestrate the wound-healing response during cholestasis (27, 131). Moreover, as shown in section R.2. (**Figure R.4.**) of this dissertation, and in our previous publications (288, 289), TREM2 is mainly expressed in these cellular compartments in the liver. TREM1 and TREM2 play opposite effects, as TREM1 mainly acts as a promoter of TLR-mediated inflammation, while TREM2 negatively regulates this pathway (242). The opposite effects of these receptors are evident in hepatocarcinogenesis, where TREM1 promotes disease progression (261), while TREM2 shows multifactorial protective effects (289).

First, we analysed *Trem1* and *Trem2* mRNA expression in isolated WT KCs in response to LPS at different time points. Interestingly, we observed that LPS induced a rapid overexpression of *Trem1*, which was maintained until 12 hours, and this was then slightly decreased 24 hours after the treatment. By contrast, *Trem2* expression was progressively downregulated upon LPS administration (**Figure R.23.**).

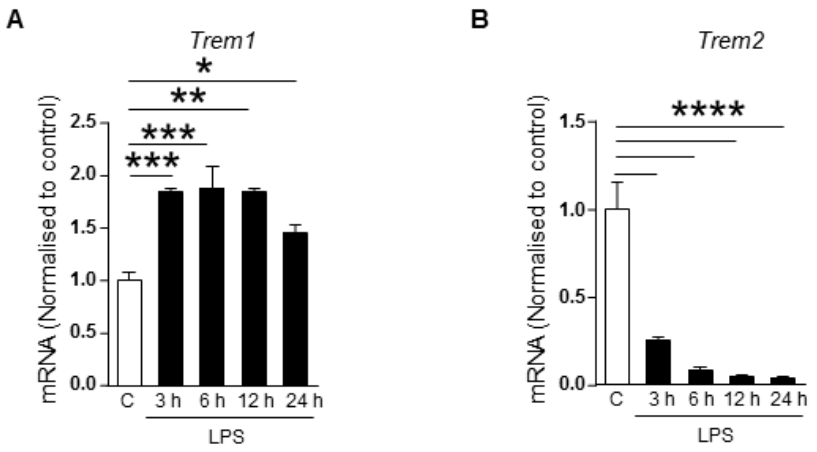

Figure R.23. *Trem1* and *Trem2* mRNA expression in response to LPS in isolated mouse WT KCs. (**A**) *Trem1* and (**B**) *Trem2* mRNA expression levels in isolated mouse WT KCs cells at 3, 6, 12 and 24 hours after LPS incubation compared to control cells (n=3-5). Parametric ANOVA and Tukey´s post hoc test were used. *, **, ***, **** represent *p* values of <0.05, <0.01, <0.001 and <0.0001, respectively compared to control condition. AU, arbitrary units; h, hours; LPS, lipopolysaccharide; *Trem1*, triggering receptor expressed on myeloid cells 1; *Trem2*, triggering receptor expressed on myeloid cells 2.

The endogenous choleretic BA, UDCA, represents the first line therapy for PBC and it is also currently used to treat patients with PSC in some centres. UDCA therapeutic benefits beyond choleresis, include anti-apoptotic, induction of biliary bicarbonate secretion and anti-inflammatory effects, but its specific mechanisms of action are still

far from clear (311). Strikingly, around 30% of the patients with PBC treated with UDCA present an incomplete response and are, therefore, at higher risk of developing end-stage liver disease and need of liver transplantation (22). A deeper understanding of the molecular mechanisms mediating UDCA effects in cholestasis may shed light into this issue and also enable optimised therapeutic strategies for these patients. In line with this, our next step was so investigate whether UDCA could impact inflammatory responses in KCs via TREM2 dependent mechanisms.

Confirming our previous results, LPS incubation at 6 hours induced *Trem1* mRNA expression in WT KCs (**Figure R.24A**). Interestingly, at this time point, UDCA alone was able to downregulate *Trem1* expression compared to control KCs. The combination of LPS with UDCA was able to reduce *Trem1* mRNA expression compared to LPS alone (**Figure R.24A**). We next analysed *Trem2* mRNA expression at a longer time point, when *Trem2* downregulation upon LPS incubation was most prominent. As previously shown, *Trem2* expression was reduced 24 hours after LPS incubation. Interestingly, UDCA at a dose of 200 μM augmented *Trem2* expression compared to the control group. The addition of UDCA to the LPS treated KCs, slightly increased *Trem2* expression compared to LPS incubation alone (**Figure R.24B**). This effect was not significant with the ANOVA+Tukey´s post hoc test, but when only the two groups were compared with Student´s *t* test, the increase in *Trem2* expression produced by the combination of LPS with UDCA was statistically significant.

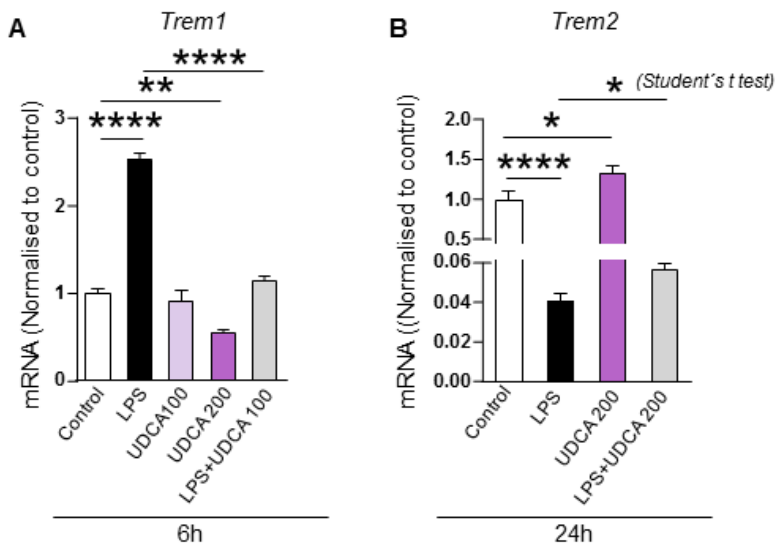

Figure R.24. Effects of UDCA in the mRNA expression levels of *Trem1* and *Trem2* in isolated mouse KCs. *Trem1* and *Trem2* mRNA expression levels in isolated KCs 6 hours and 24 hours after the incubation with LPS and/or UDCA (n=5-6) Parametric ANOVA and Tukey´s post hoc test and parametric Student´s *t*-test were used. *, **, ***, **** represent *p* values of <0.05, <0.01, <0.001 and <0.0001, respectively. AU, arbitrary units; LPS, lipopolysaccharide *Trem1*, triggering receptor expressed on myeloid cells 1; *Trem2*, triggering receptor expressed on myeloid cells 2; UDCA, ursodeoxycholic acid.

R.7. TREM2 arises as a novel mediator of UDCA therapeutic effects in non-parechymal liver cells

Next, we aimed to investigate if the modulation of *Trem1* and *Trem2* expression induced any functional changes in KCs. With this purpose, we isolated KCs from WT and *Trem2*$^{-/-}$ mice and incubated them with LPS and/or the combination of LPS and UDCA. As previously reported, LPS strongly induced the mRNA expression of the inflammatory cytokines *Il6*, *Tnf* and the chemokine *Cxcl1* in KCs of both genotypes, and this induction was enhanced in *Trem2*$^{-/-}$-derived KCs compared to WT KCs (288) (**Figure R.25**). Importantly, in the presence of LPS, the addition of UDCA, reduced the expression of these inflammatory mediators in WT KCs compared to LPS alone, while no changes were observed in *Trem2*$^{-/-}$ KCs (**Figure R.25**). These results indicate that UDCA reduces LPS-induced inflammatory gene transcription expression, at least in part, via a *Trem2* dependent mechanism.

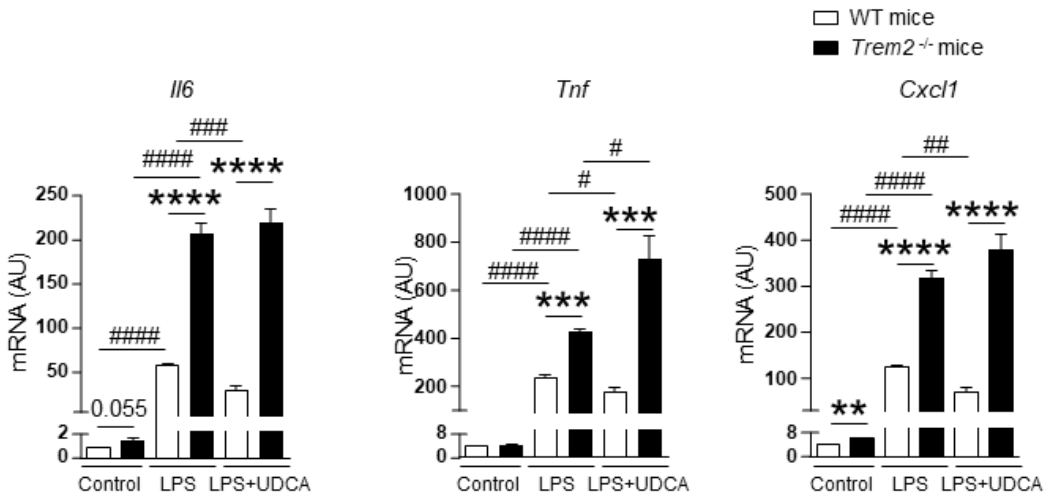

Figure R.25. Effects of UDCA in the LPS-induced mRNA expression of *Il6* in WT and *Trem2*$^{-/-}$ KCs. *Il6* mRNA expression levels in WT and *Trem2* $^{-/-}$ KCs 3 hours after incubation with LPS and the combination of LPS and UDCA (n=3-5). Parametric Student´s *t*- test was used. **, ***and **** represent *p* values of <0.01, <0.001 and <0.0001, respectively in comparison to WT KCs following the same experimental conditions; #, ##, ### and #### represent *p* values of <0.05, <0.01, <0.001 and <0.0001, respectively in comparison to control or LPS incubated KCs of the same genotype. AU, arbitrary units; *Cxcl1*, C-X-C motif chemokine ligand 1, *Il6*, interleukin 6; *Tnf*, tumour necrosis factor; *Trem1*, triggering receptor expressed on myeloid cells 1; *Trem2*, triggering receptor expressed on myeloid cells 2; UDCA, ursodeoxycholic acid.

R.8. TREM2 expression is mainly found in resident and infiltrating macrophages in HCC tumours

As previously mentioned, cholestasis and intrahepatic accumulation of BAs is intimately linked to hepatobiliary carcinogenesis (182). Patients with chronic cholestatic diseases at advanced stages are at a higher risk to develop hepatobiliary carcinogenesis. In this regard, patients with PBC can develop HCC (183) and patients with PSC show an increased risk to develop both HCC and CCA (184-186). Carcinogenesis develops in advanced stages of the disease when biliary fibrosis and cirrhosis have already established (180). In a recently published study, we have reported that TREM2 protects the liver from hepatocarcinogenesis (289). We found that *TREM2* expression is upregulated in the human HCC tumours compared to healthy control tissue in two independent cohorts of patients (289).

R.8.1. TREM2 expression is found in macrophage-resembling cells in HCC tumours

First, we analysed TREM2 expression by IHC in human healthy liver and in the liver of patients with HCC tumors of variable etiologies, patients characteristics of the study cohort are shown in **Table M.2**. In agreement with our previous results (289), TREM2 expression was more extensive in diseased liver compared with healthy liver (**Figure R.26.**). In the HCC samples, we analysed TREM2 staining in surrounding cirrhotic liver tissue and within the tumour. TREM2 staining intensity was similar between the tumour and the surrounding cirrhotic tissue. Importantly, overall, we did not detect TREM2 staining in transformed hepatocytes. In the surrounding cirrhotic tissue, TREM2 staining was observed in inflammatory periportal areas and adjacent tissue to the fibrotic septa. Witin the tumour, TREM2 staining was observed in infiltrating or resident cells, TREM2 stained cells morphologically resembled macrophages (**Figure R.26.**).

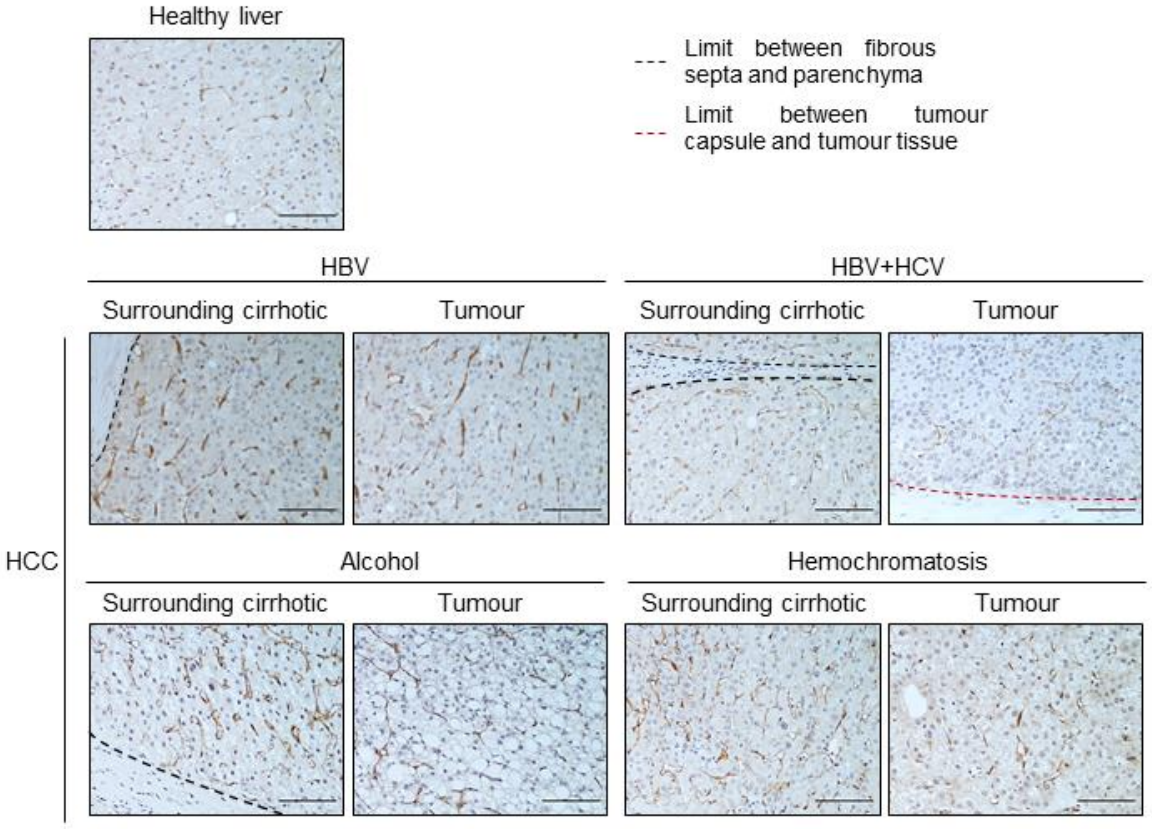

Figure R.26. TREM2 expression in human HCC and surrounding cirrhotic tissue. IHC for TREM2 in healthy liver tissue and in the liver of patients with HCC of different aetiologies, representative images are shown. For the HCC tissues, images of surrounding cirrhotic liver tissue and from the tumour are included. Scale bar represents 100 µm.

R.8.2. TREM2 expression is most prominent in resident and infiltrating macrophages in HCC tumours of the GSE125449 cohort of patients

In order to extend these findings and gain insight into the specific cell types that express TREM2 in human HCC, we analysed publicly available scRNAseq data from 9 HCC livers (291). After processing, data was visualised using t-distributed Stochastic Neighbor Embedding (t-SNE) through the Seurat R package. In particular, 6 different clusters were identified, including, T cells, B cells, cancer-associated fibroblasts (CAFs), tumour-associated macrophages (TAMs), tumour-associated endothelial cells (TECs), and hepatic progenitor like (HPC-like) cells (**Figure R.27A**). HCC malignant cells clustered together with HPC-like cells and were annotated based on RNA-seq derived large-scale chromosomal copy-number variations (CNVs) prediction from the original work (291). Among these clusters, *TREM2* expression was mainly found in the TAMs (**Figure R.27B**) cluster, while the expression was minimal in all the other

clusters of cells. Thus, confirming our observations in HCC tissue sections by IHC (289).

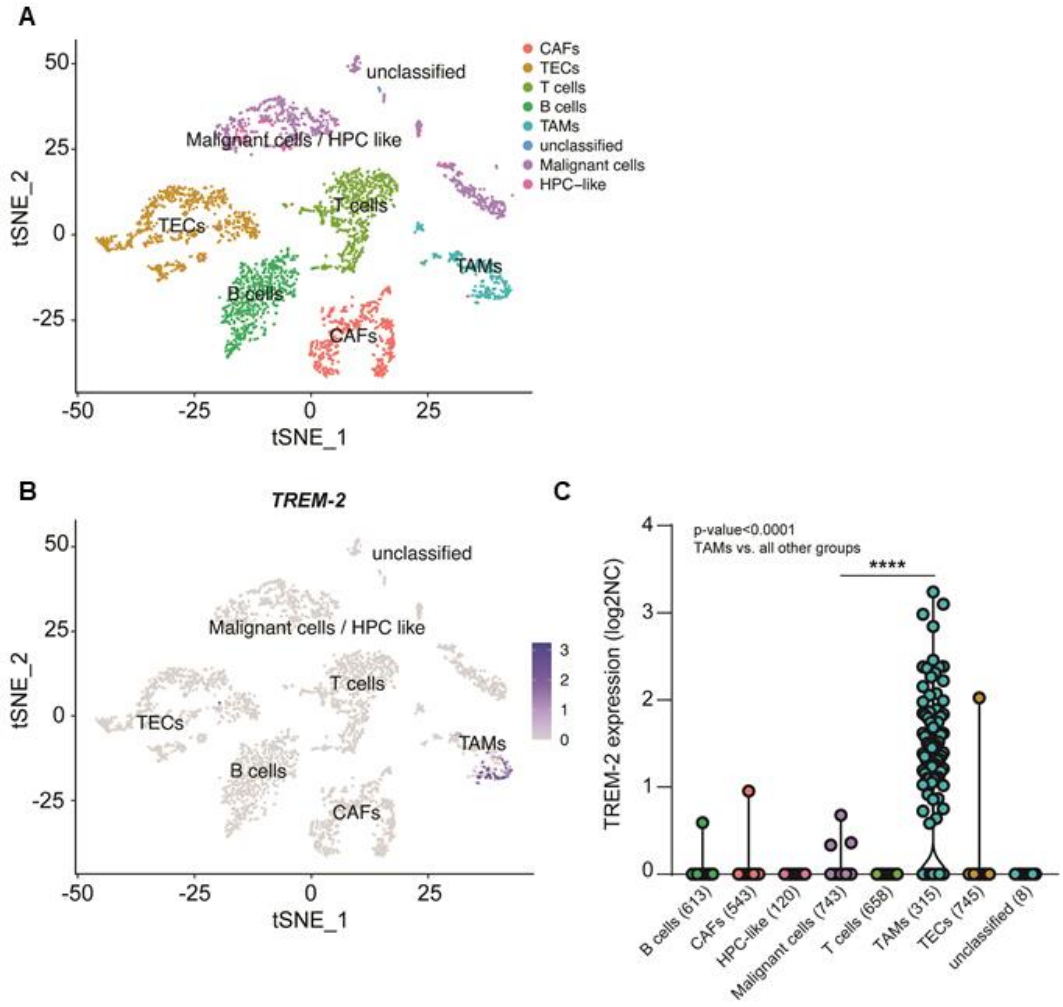

Figure R.27. *TREM2* expression in different cell populations within HCC tumours. Publicly available scRNAseq data from HCC tumours (n=9) was used to analyse TREM2 expression. (**A**) t-SNE projection depicting cellular composition of human HCC tumours. Cells that share similar transcriptome profiles are grouped by colors and were annotated using lineage specific markers. (**B**) t-SNE plot depicting *TREM2* expression in TAMs. (**C**) Corresponding Log2 normalised counts (Log2NC) *TREM2* expression values for all tumour infiltrating cells types. The numbers of cells analysed for each cell type post data processing are shown in brackets. (**C**) One-way ANOVA followed by Tukey's post-test was used. **** denote a P value of <0.0001 respectively.CAFs, cancer associated fibroblasts; HPC-like, hepatic progenitor cell-like; TAMs, tumour associated macropghages; TECs, tumour associated endothelial cells; TREM2, triggering receptor expressed on myeloid cells; tSNE_2, t-distributed Stochastic Neighbor Embedding.

Each of the 6 identified cluster annotated to a specific cell type according to cell lineage specific marker gene expression enrichment. In this regard, T cells were characterised by receptor complex CD2 and CD3D, B cells by B cell receptor (BCR) signalling components CD79A and Fc receptor like 5 (FCRL5), TECs are enriched for expression

of the endothelial markers von Willebrand factor (VWF) and cadherin 5 (CDH5), TAMs express macrophage markers CD163 and CSFR1 and CAFs are characterised by the expression of the markers COL3A1 and decorin (DCN) (**Figure R.28**). On the other hand, malignant hepatocytes/HCC progenitor cells clustered together with HPC-like cells and were enriched in the expression of typical markers of transformed hepatocytes possessing stem/progenitor properties including alpha-fetoprotein (AFP), albumin (ALB), cluster of differentiation 24 (CD24), cytokeratin 19 (KRT19) and SRY-box transcription factor 9 (SOX9) (**Figure R.29**).

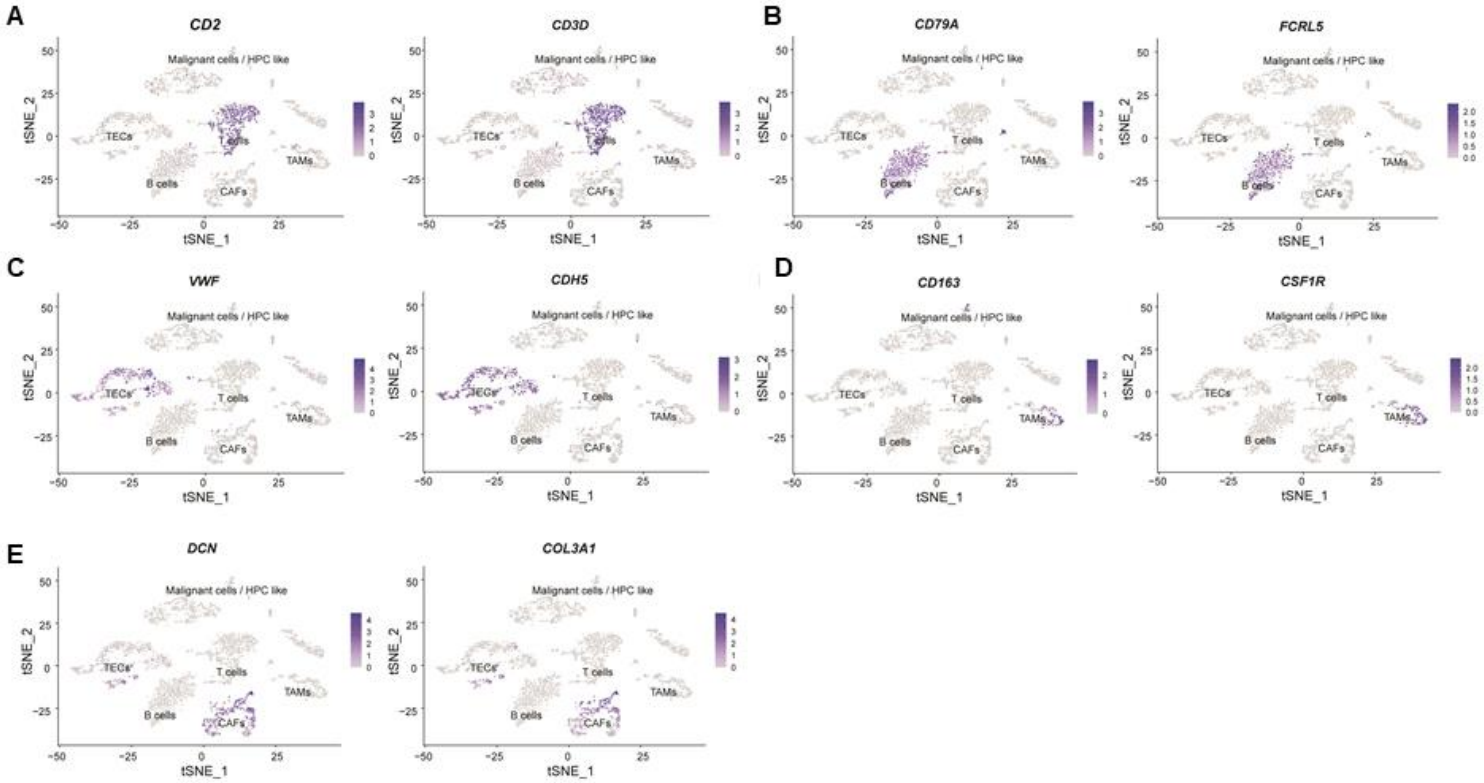

Figure R.28. Lineage specific markers demonstrate annotation of single cell RNA sequencing data. (**A**) T cells are enriched for expression of components of the T cell receptor complex CD2 and CD3D. (**B**) B cells are enriched for expression of the BCR signalling components CD79A and FCRL5. (**C**) TECs are enriched for expression of the endothelial markers VWF and CDH5. (**D**) TAMs are enriched for expression of the macrophage markers CD163 and CSFR1. (**E**) CAFs are enriched for expression of the markers COL3A1 and DCN. CAFs, cancer associated fibroblasts; CD, cluster of differentiation; CDH5, cadherin 5; ; COL3A1, collagen type III alpha 1 chain; CSFR1, colony stimulating factor 1 receptor; DCN, decorin; FCRL5, Fc receptor like 5; VWF, von Willebrand factor; TAMs, tumour-associated macrophages; TECs, tumour-associated endothelial cells; t-SNE_2, t-distributed stochastic neighbour embedding.

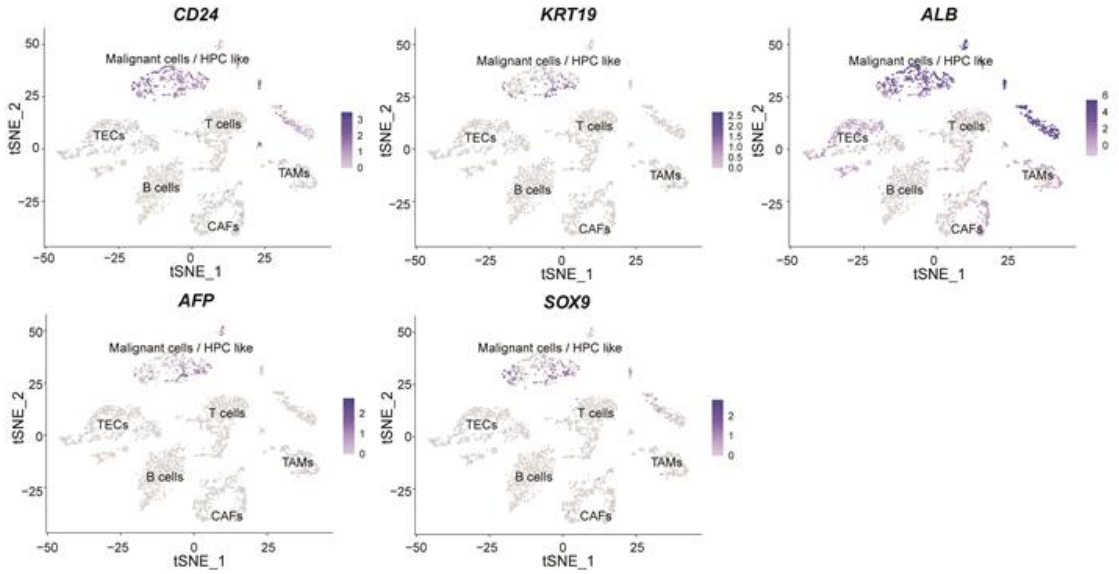

Figure R.29. The Malignant/HCC progenitor cell t-SNE cluster is enriched for markers associated with transformed hepatocytes Expression of markers typical of transformed hepatocytes possessing stem/progenitor properties including *AFP*, *ALB*, *CD24*, *KRT19* and *SOX9* are specifically found in this cluster. *AFP*, alpha-feto protein; *ALB*, albumin; *CD24*, CD24 molecule, *KRT19*; keratin 19; *SOX9*, SRY-box transcription factor 9; t-SNE_2, t-distributed stochastic neighbour embedding.

Moreover, we next analysed the TAMs cluster in more detail, and performed refined clustering, identifying 5 different TAMs subpopulations. Here, *TREM2* expression was most prominent in clusters 1 and 2 (**Figure R.30A**), which were also enriched in the expression of the KCs marker *CD68* and the monocyte marker *CD14*. Of note, clusters 1 and 2 were also characterised by the expression of *CD9* (**Figure R.30B**), in agreement with a recent study describing a novel subpopulation of $TREM2^{+}CD9^{+}$ monocyte derived scar associated macrophages in human cirrhotic livers (281). Then we performed gene set enrichment analysis (GSEA) in the *TREM2* expressing TAMs subpopulations, and found enrichment in TLR signalling and lysosome-associated pathways (**Figure R.30C**).

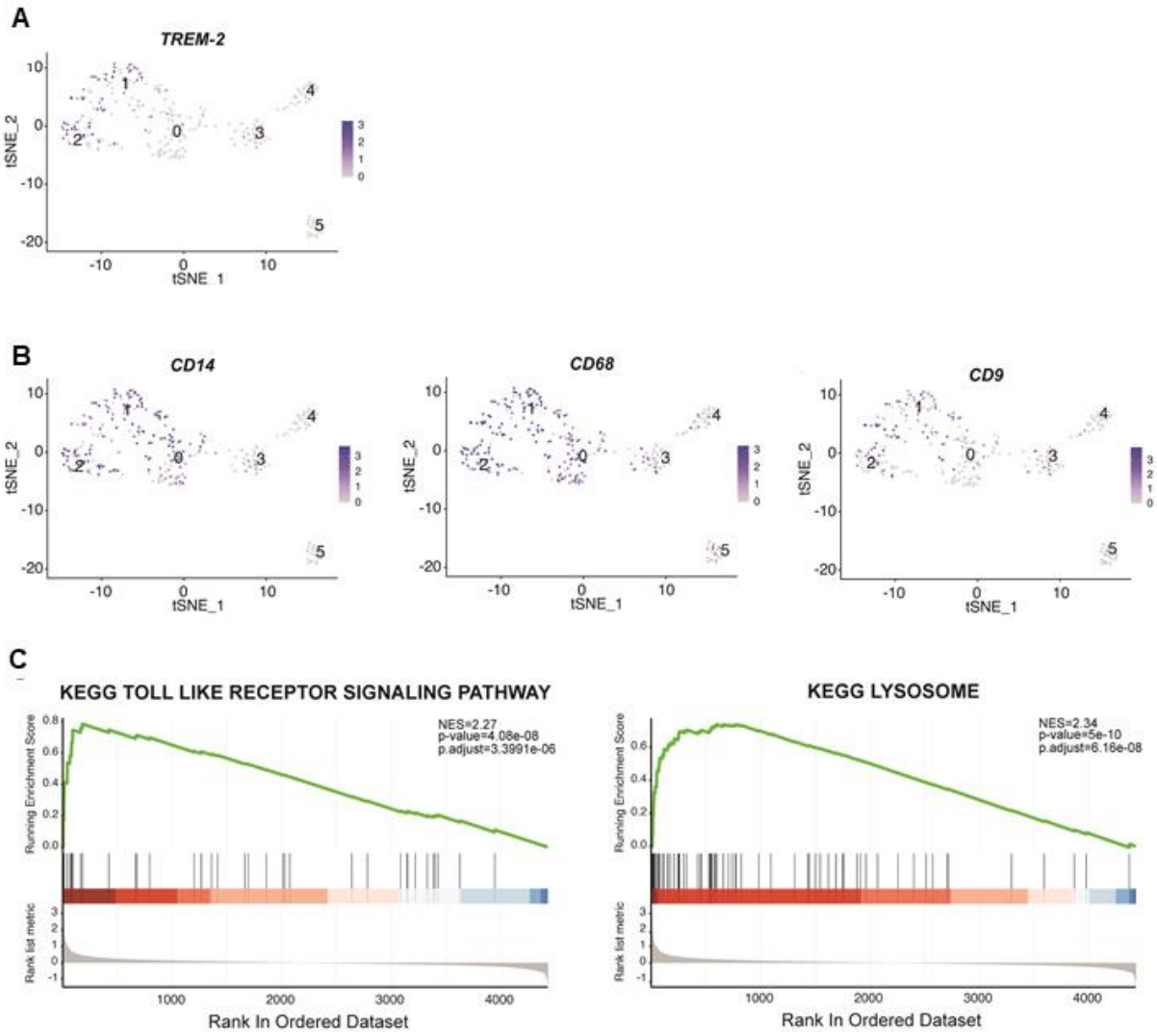

Figure R.30. Refined TAMs clustering and characterization. (**A,B**) t-SNE projection post re-clustering of TAMs and (**A**) *TREM2* and (**B**) *CD14*, *CD68* and *CD9* expression therein. (**C**) GSEA plots depicting enrichments in TLR signalling and lysosome pathways within TREM-2 expressing TAMs. The y-axis represents the enrichment score (ES) and vertical black lines on the x-axis shows where genes annotated to the respective pathways appear in the ranked list of genes. The colored band represents the ES values (red for positive and blue for negative). CD, cluster of differentiation; KEGG, Kyoto encyclopedia of genes and genomes; t-SNE_2, t-distributed Stochastic Neighbor Embedding.

R.9. TREM2 plays a protective role in fibrosis-associated liver carcinogenesis

In order to strengthen our hypothesis about the protective effects of TREM2 in chronic cholestasis progression and to examine its potential impact on fibrosis-associated hepatocarcinogenesis, we next performed two different models of fibrosis-associated HCC.

R.9.1. Augmented carcinogenesis is detected in *Trem2*$^{-/-}$ mice in an experimental fibrosis-associated HCC model based on DEN+CCl_4 administration

CCl_4 induces hepatic fibrosis and is frequently combined with the hepatocarcinogen DEN to study fibrosis-associated HCC (300). Thus, we combined DEN administration with weekly injections of CCl_4 to perform a fibrosis-associated HCC model in WT and *Trem2*$^{-/-}$ mice (**Figure 31A**). DEN plus CCl_4 administration led to increased numbers of small (≤ 2mm) tumours in *Trem2*$^{-/-}$ mice *vs* WT mice at 30 weeks, while it did not impact the presence of bigger tumours (**Figure R.31B**). Evaluating fibrosis using Sirius red staining, demonstrated that despite the enhanced tumourigenesis in *Trem2*$^{-/-}$ mice compared to WT mice, these animals displayed less fibrosis (**Figure R.31C**). Furthermore, we detected increased proliferating cell nuclear antigen (*Pcna*) mRNA levels in DEN plus CCl_4 administered *Trem2*$^{-/-}$ compared to WT animals (**Figure R.31D**).

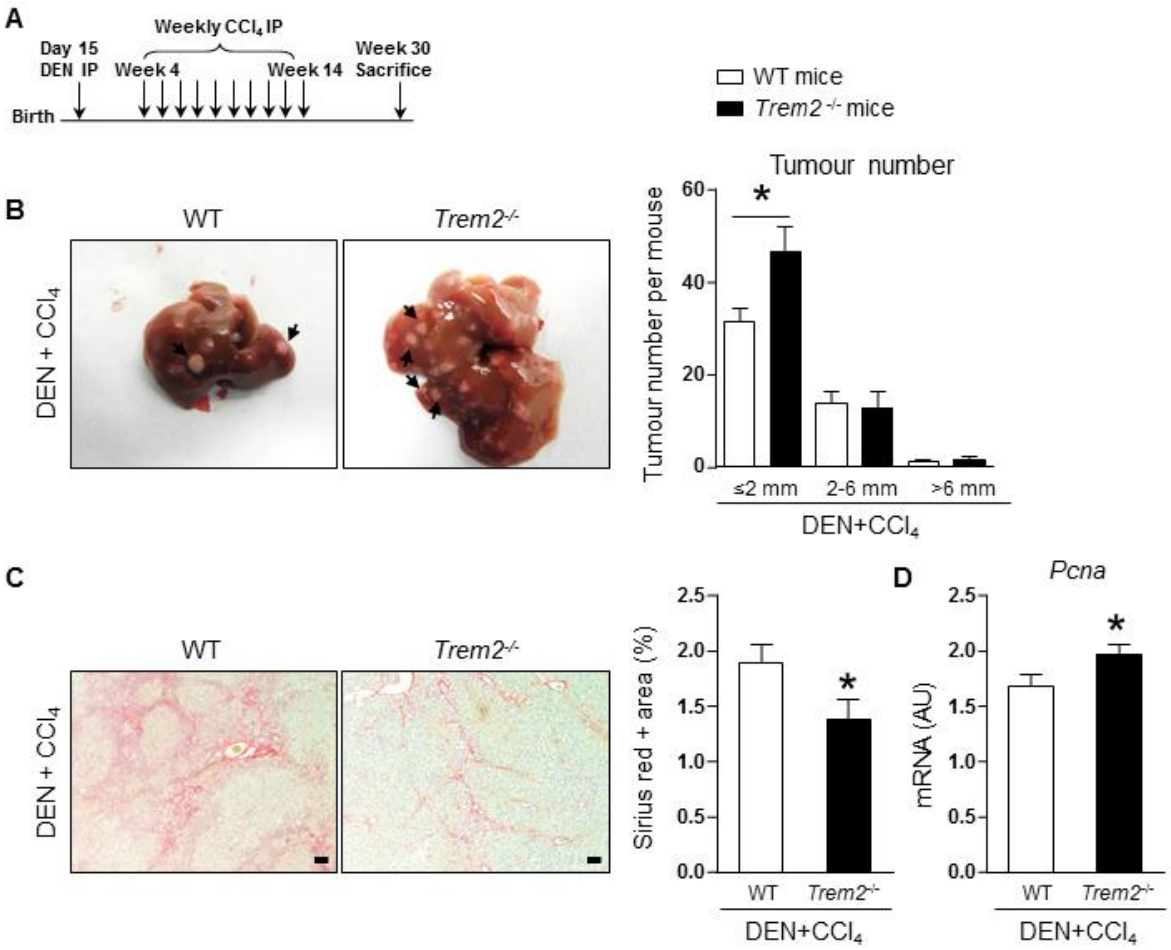

Figure R.31. Fibrosis-associated hepatocarcinogenesis in the DEN plus CCl_4 model in WT and *Trem2*$^{-/-}$ mice. (A) WT and *Trem2*$^{-/-}$ were injected with 30mg/kg of DEN at 15 days post-partum, thereafter, 10 weekly injections of CCl_4 were performed and mice were humanely killed 30 weeks after DEN administration (WT n=13;*Trem2*$^{-/-}$ n=14). (**B**) Liver tumour numbers classified by size; representative liver images and the quantification are shown. (**C**) Sirius red staining, representative images and the quantification are shown. (**D**) mRNA expression of *Pcna* in the liver. Scale bar in (**C**) represents 100 µm. (**A**) Parametric Student´s *t*-test and non-parametric Mann-Whitney test were used. (**B**,**C**) Parametric Student´s *t*-test was used. * represents $p<0.05$. AU, arbitrary units; CCl4 carbon tetrachloride; DEN, diehylnitrosamine; IP, intraperitoneal; *Pcna*, proliferating cell nuclear antigen; *Trem2*, Triggering receptor expressed on myeloid cells; WT, wild type.

R.9.2. Augmented carcinogenesis is detected in *Trem2*$^{-/-}$ mice in an experimental fibrosis-associated HCC model based on TAA administration

As an alternative model of fibrosis-associated HCC, TAA was administered to WT and *Trem2*$^{-/-}$ mice in drinking water for 40 weeks (302). (**Figure R.32A**). *Trem2* deficient animals exhibited an increased tumoural volume in comparison to WT animals after TAA administration (**Figure R.32B**). Similarly to the DEN plus CCl_4 model, *Trem2*$^{-/-}$ mice also showed attenuated fibrosis after TAA administration as compared to WT mice

(**Figure R.32C**). Additionally, increased *Pcna* levels were also detected in the *Trem-2*$^{-/-}$ mice as compared WT mice (**Figure R.32D**).

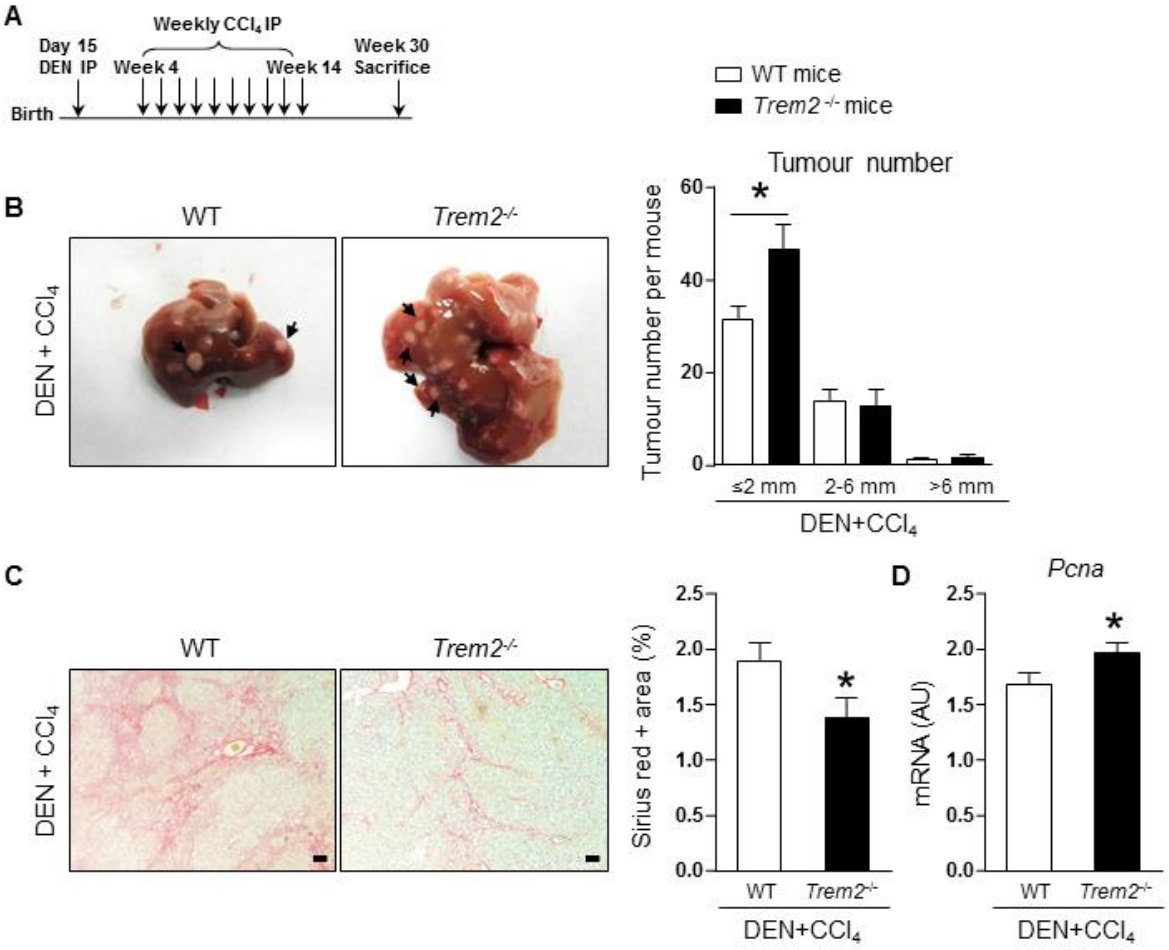

Figure R.32. Fibrosis associated hepatocarcinogenesis in the TAA-based model in WT and *Trem2*$^{-/-}$ mice. (A) WT and *Trem2*$^{-/-}$ mice received TAA in drinking water for 40 weeks (WT n=9; *Trem2*$^{-/-}$ n=9). (**B**) Liver tumour volume, representative liver images and the quantification are shown. (**C**) Sirius red staining, representative images and the quantification are shown. (**D**) mRNA expression levels of *Pcna* in the liver. Scale bar in (**C**) represents 100 µm. (**A**) Non-parametric Mann-Whitney test was used. (**B**,**C**) Parametric Student´s *t*-test was used. * represents p<0.05. AU, arbitrary units; *Pcna*, proliferating cell nuclear antigen; TAA, thioacetamide; *Trem2*, triggering receptor expressed on myeloid cells; WT, wild-type.

Together, all these data encompassing different murine models demonstrate that TREM2 halts chronic cholestatic disease progression as well as hepatocarcinogenesis in fibrosis-associated HCC.

DISCUSSION

Cholestasis is a pathological condition shared in different cholangiopathies, including PBC and PSC, the two most common chronic cholestatic diseases in adults (74). Chronic cholestasis evolves in different steps including inflammation, ductular reaction, fibrosis, cirrhosis, and may also result in liver carcinogenesis (312). Inflammation is a central phenomenon in this progression as it directs intercellular communication, thus becoming the fuel that fires the mal-adaptive wound-healing response and, consequently, disease progression (136). Cholestatic diseases represent an unmet clinical challenge, as therapeutic strategies for these patients are scarce and in many cases, disease progresses to critical stages where liver transplantation is the only curative option (181). In parallel, hepatocarcinogensis, arising mainly in cirrhotic livers, as the last step of chronic liver disease progression, also represents a clinical challenge, as the high heterogenicity and chemoresistance of this tumours hinder its treatment (192). Therefore, there is a critical need for research strategies focused on studying the molecular mechanisms governing chronic cholestasis progression and hepatocarcinogenesis, which will potentially unravel novel therapeutic targets for these diseases.

Among the different processes involved in the pathobiology of cholestasis, the gut-liver axis is now regarded as an important phenomenon in the progression of cholestatic diseases (204) and hepatocarcinogenesis (205). In this regard, bacterial products translocated from the gut to the liver bind to TLR receptors expressed in KCs, HSCs and recruited immune cells, and potentiate inflammatory gene transcription (217). Interestingly, interfering with the gut-liver axis at different levels have showed beneficial effects in diverse settings of liver injury (213, 232-234). In this regard, the family of TREM receptors was described as modulators of TLR mediated signalling (235, 236). Overall, TREM1 is believed to potentiate TLR mediated signalling, whereas TREM2 dampens TLR mediated inflammatory gene transcription (235, 264, 265). Our previous studies have unveiled that TREM2 is expressed in KCs, HSCs and recruited macrophages in the liver, were it acts as an anti-inflammatory receptor to defend the liver from acute and chronic hepatocellular injury and also hepatocarcinogenesis (288, 289). Taking all this data into account, in this study, we hypothesised that TREM2 may also regulate inflammatory responses in cholestasis and also in fibrosis-associated HCC, thus representing a potential therapeutic target for these patients.

D.1. TREM2 expression is upregulated in human and experimental cholestasis

In this study, we have shown an upregulation of the expression of TREM2 in the liver of patients with chronic cholestatic diseases compared to healthy liver tissue, and observed the same tendency in the livers of mice subjected to experimental cholestasis. To our knowledge, this is the first study assessing TREM2 expression in human and mouse cholestasis. Importantly, our results are in line with previous studies, in which we have reported an upregulation of TREM2 expression in the liver of patients with inflammation-driven hepatocellular diseases of diverse origins, and also in related mouse models (288, 289) . Interestingly, our results show that *TREM2* mRNA levels are also higher in the liver of patients with cholestasis in comparison to the liver of patients with cirrhosis of other origins.

We have previously reported that *TREM2* expression correlates with disease progression, as higher *TREM2* expression positively correlates with serum transaminase levels, liver inflammation and fibrosis (288, 289). This study confirms this finding also in cholestasis, where *TREM2* expression positively correlates with diverse markers of disease progression in two independent cohorts of patients. It is important to note, that in the San Sebastian/Warsaw study cohort, patients with cholestasis (both PBC and PSC) showed enhanced levels of liver transaminases, ALP and bilirubin, in comparison to patients with cirrhosis of other origins. This may reflect a more advanced stage of the underlying disease and also explain higher *TREM2* expression levels in the liver of patients with PBC and PSC when compared to patients with cirrhosis of other origins. Moreover, in the GSE79850 cohort, *TREM2* expression is differentially upregulated in the liver of patients with high-risk PBC compared to controls and to patients with low-risk PBC. Patients with high-risk PBC included in this cohort were characterised by an overall worse disease phenotype at the time of diagnosis, and also display increased expression levels of genes involved in T-cell activation and apoptosis, as well as INF-γ signalling and leukocyte migration, in comparison to patients with low-risk PBC (290), suggesting that the overexpression of TREM2 receptor may be an indicator of disease progression in cholestasis. These data indicate that TREM2 expression is upregulated in inflammation-driven diseases regardless of the triggering stimuli. Moreover, TREM2 expression is further upregulated with disease progression, thus we hypothesise that TREM2 expression may be induced as a compensatory mechanism to mild down inflammation in the context of advanced disease.

As aforementioned, *TREM2* mRNA upregulation was evident in the livers of patients with different cholestatic diseases including PBC and PSC, in two independent cohorts of PBC patients, and also in experimental cholestasis induced by obstructive (BDL model) as well as chemical (ANIT and DDC models) triggers, suggesting TREM2 overexpression is a general event during cholestasis. Although the aetiology of both diseases is still obscure, both PBC and PSC are strongly associated with autoimmunity, and as such, innate and adaptive immune pathways play an essential role in their pathogenesis (81, 91). In line with this, a recent study investigated genetic alterations as well as alterations in tissue expression levels shared by the main cholangiopathies including PBC, PSC and the pediatric disease biliary atresia (BA), and thus identified the connectome of these diseases. In this study, the involvement of inflammation/immunity related genes, including TNF, IL10, forkhead box P3 (FOXP3), TGFB1, IL2, IL17A, NFKB1, signal transducer and activator of transcription 3 (STAT3), TP53, SMAD3, hypoxia inducible factor 1 A (HIF1A), prostaglandin-endoperoxide synthase 2 (PTGS2), IL6 and TLR4 is highlighted, as the core genes found altered in the three cholangiopathies (313). Interestingly, as aforementioned, TREM2 is a modulator of TLR mediated signalling (242) and specifically regulates the expression of some of these factors, including IL6 and TNF as shown here and in previous reports (288, 289). Therefore, based on these data, we hypothesized that TREM2 may be a novel important entity in the genomic connectome of at least PBC and PSC.

In isolated mouse cells, we detect that, *Trem2* expression is highly upregulated in KCs ad HSCs compared to hepatocytes and cholangiocytes. These findings are in line with previous observations showing that TREM2 expression is restricted to the non-parenchymal compartment in the liver (253, 279, 288, 289). Chronic cholestasis is driven by sustained inflammation and is characterised by innate immune cell recruitment to the liver as wells as KCs and HSCs activation and proliferation (131). Therefore, TREM2 upregulation and its correlation with markers of disease progression in cholestasis may be explained by two parallel events. On the one hand, upon liver injury TREM2 expressing cells are recruited to the liver and proliferate, thus accounting for the upregulation of TREM2 expression. On the other hand, upon KCs, HSCs and monocyte-derived macrophage activation, TREM2 expression may be induced as a compensatory mechanism to halt excessive inflammatory gene transcription triggered by sustained activation of these cells.

We are aware that the small sample size employed for our analysis in patients, especially in the case of the patients with cholestasis, represents a limitation. The limited availability of liver tissue from patients with cholestasis is explained by the overall tendency to reduce biopsies in these patients, as diagnosis is now achieved by the combination of serological parameters and liver imaging techniques (77, 92). Nevertheless, our results are confirmed at least in two independent cohorts of patients and also corroborated in different mouse models of cholestasis, strongly indicating that TREM2 upregulation is a general and conserved event during cholestasis.

Sophisticated techniques of single cell RNA sequencing are starting to unravel specific cell subpopulations that play key roles in the pathobiology of chronic liver diseases. Indeed, recently published scRNAseq studies have identified specific TREM2 expressing macrophage subpopulations in patients with obesity (278), NAFLD (280), and cirrhosis (281). Our data show that *TREM2* overexpression is a central event during cholestasis, yet, due to the difficulties to obtain liver tissue from patients with PBC and PSC and the lack of sophisticated techniques, we could not analyse in detail the specific immune cellular subpopulations expressing TREM2. Thus, this type of studies may be of particular interest in the setting of cholestatic diseases where innate and adaptive immune compartment play a prominent role in disease pathogenesis and hypothetically, TREM2 expressing cellular compartments associated with cholestasis may arise.

D.2. TREM protects the liver from cholestasis-induced liver damage

Our results depict that TREM2 expression is increased in the liver of patients with cholestasis, and that this phenomenon is conserved in mice, as TREM2 expression is also enhanced in the liver of mice subjected to different forms of cholestasis. These findings prompted us to study the role of TREM2 in the pathogenesis of cholestasis in mouse models of the disease.

Importantly, this study reveals a critical role for TREM2 as a negative regulator of inflammatory responses in cholestatic conditions of diverse origins. Here, we have analysed the role of TREM2 in two different mouse model of cholestasis, specifically, after BDL surgery and ANIT administration. BDL is an obstructive cholestasis model, characterised by inflammation, biliary obstruction, ductular reaction and biliary fibrosis (293), while acute ANIT administration results in an extensive loss of cholangiocytes mainly affecting intrahepatic cholangiocytes, reminiscent of some aspects of PBC (296). Therefore, these findings reinforce the hypothesis that the protective effects of

TREM2 may be a general event in cholestasis regardless of its aetiology. Here, we detect an exacerbated response to cholestatic injury in *Trem2*$^{-/-}$ mice subjected to BDL or after ANIT administration, the phenotype observed in both of these models overlaps while also presenting specific features.

We are aware that this study shows a limitation in the ANIT-based model of chemically-induced cholestasis. In this regard, ANIT administration at the selected dose did not impact most the levels of the markers of liver damage and inflammation in the WT mice, were only upregulation, or marked tendency towards upregulation, of the expression of the biliary markers *Ck19* and *Ck7*, oxidative markers *Hmox* and *Nos2* and the HSCs activation marker *Acta2* was detected, while all other parameters remained unchanged compared to the O.Oil administered mice. There is controversy when choosing the most suitable dose for the ANIT-based model, with published studied ranging from 50mg/kg to 100mg/kg (295, 296, 314-316). For our study, we decided to choose the minimum dose reported to induce biliary damage, since we expected that *Trem2*$^{-/-}$ mice would show an exacerbated phenotype and did not want to overwhelm the model and loose the potential differences between WT and *Trem2*$^{-/-}$ mice.

In terms of the phenotypic parallels between ANIT and BDL, we show increased epithelial cell death in *Trem2*$^{-/-}$ mice in both of the models, this is accompanied by increased necroptotic but not apoptotic marker expression in the BDL model, and also by increased levels of serum markers of hepatic injury in the case of the ANIT model. In line with these observations, necroptosis was previously detected as the main contributor to cell death in cholestatic patients with PBC and also in mice subjected to BDL (317, 318). Furthermore, RIP3, the main molecular mediator of necroptosis, was shown to promote cholestatic liver injury in mice (317) (319). Necroptotic cell death may be triggered by inflammatory mediators such as TNF (320), which is upregulated in *Trem2*$^{-/-}$ after BDL and ANIT administration compared to WT mice. We also observed upregulated expression of *Tnf* in *Trem2*$^{-/-}$ mice in acute phases of hepatocarcinogenesis after DEN exposure; nevertheless, we do not observe differences in the expression levels of the markers of necroptosis in the long-term DEN model (289). Interestingly, cholangiocytes have been reported to be more prone to necroptotic cell death, as they express higher levels of RIP3 (321), therefore suggesting that the enhanced necroptotic marker expression may be derived from cholangiocyte death.

BAs fulfil a key role in the progression of cholestatic diseases. In this regard, intrahepatic accumulation of BAs may exert direct cytotoxic effects on liver epithelial

cells (119) and also initiate and boost inflammatory responses (117). In the context of the BDL model, our results reveal lower BA content in livers of *Trem2*$^{-/-}$ mice in the sham operated control condition in comparison to livers of WT mice. These results are accompanied by a marked tendency to a downregulation of the expression of the BA rate limiting enzyme in the BA biosynthetic pathway, *Cyp7a1*, and upregulation of its inhibitor *Fxr*. These findings suggest that *Trem2*$^{-/-}$ mice may have developed a mechanism to maintain low BAs levels in the liver. The dramatic increase in BAs induced by BDL may overwhelm this mechanism, thus after BDL, hepatic BA concentrations reach similar levels in WT and *Trem2*$^{-/-}$ mice. Of note, the increase of the BA liver content from sham to BDL condition is higher in *Trem2*$^{-/-}$ mice compared to WT mice, which is associated to enhanced cell death in *Trem2*$^{-/-}$ mice after BDL, suggesting *Trem2*$^{-/-}$ mice may be sensitised to BA-mediated cell death.

Indeed, the link between TREM2 and nuclear receptors has already been established, as *Trem2*-deficient microglia show enhanced CE accumulation, which can be reversed upon treatment with LXR agonists (322). Moreover, TLR activity has been shown to regulate FXR expression in the intestine. In this regard, activation of TLR2,4,5 and 6 downregulate, while TLR3,7,8 and 9 upregulate FXR and SHP expression (323). Thus, we hypothesise that the effects of TREM2 on TLR signalling may also impact FXR expression and/or activity and, therefore, affect BA metabolism. The molecular mechanisms linking TREM2 with BA metabolism and its potential implication in liver disease progression is still far from clear and pose an interesting research opportunity.

Both intrahepatic BA accumulation and cell death are associated with the induction of inflammatory responses. Particularly, necroptosis is intimately linked to inflammation (111), indeed, DAMPs released by necroptotic epithelial cells can contribute to the pro-inflammatory microenvironment in an autocrine and paracrine manner. Moreover, RIP3 may also directly induce inflammatory cytokine expression by the activation of NF-κB (324). As aforementioned, intrahepatic accumulation of BAs triggers inflammatory responses (117). Therefore, the exacerbated phenotype observed in *Trem2*$^{-/-}$ mice under BDL or ANIT-induced cholestasis, which is characterised by increased cell death and by the increased fold-change of accumulating BA concentrations may be associated with increased inflammatory responses.

Indeed, the pro-inflammatory microenvironment is exacerbated in *Trem2*$^{-/-}$ mice both after BDL and ANIT administration. Upregulated inflammatory mediators include the general ones induced upon liver injury, such as, *Il1β*, *Il6*, *Tnf*, *Il33 Mcp1* and *Cxcl1*.

These findings are in agreement with previous observations where elevated expression levels of *Il6*, *Tnf*, *Mcp1* and *Cxcl1* were observed in *Trem2*$^{-/-}$ mice subjected to acute and chronic hepatocellular injury as well as in acute phases of hepatocarcinogenesis and regeneration (288, 289) and suggest that TREM2 dampens liver inflammation regardless of the triggering stimuli. Moreover, these inflammatory mediators play key roles in the progression of cholestatic diseases in human and in experimental cholestasis (325). Their expression is upregulated in patients with PBC (164, 326) and PSC (327) and they are also identified as key mediators in the inflammatory microenvironment derived from DRCs (6). Moreover, IL6 and TNF are among the core genes identified in the connectome of PBC, PSC and BA (313). Interestingly, peripheral monocytes derived from patients with PBC show an exacerbated reaction to LPS, featuring increased secretion of IL1β, IL6, IL8 and TNF among others (328). On the other hand, IL33 promotes cholangiocyte proliferation in murine models of biliary injury and repair (329) and is found upregulated in the serum of patients with PBC (330). Similarly, IL8, regarded as the human homologue to Cxcl1 in most of each functions (331), is found upregulated in bile of patients with PSC and it also promotes primary cholangiocyte proliferation *in vitro* (153). Thus, TREM2 downregulates expression of all of these cytokines and chemokines, suggesting this receptor may exert a protective role in the progression of cholestatic liver injury.

Our results have evidenced that enhanced expression of inflammatory mediators in the liver of *Trem2*$^{-/-}$ mice is translated into increases in the recruitment of neutrophils, while recruitment of macrophages and T lymphocytes was similar in both genotypes. As previously shown, these results suggest that differences in the immune cell recruitment to the liver may be model and disease specific (39). Noteworthly, neutrophils are particularly important in cholestasis, where they are regarded as the primary cytotoxic cell (125-127). The CXCL1-CXCR2 axis, which drives neutrophil recruitment to the liver, and plays a pivotal role in cholestasis, as *Cxcr2*$^{-/-}$ mice are protected from BDL-mediated injury (332). In this regard, TREM2 was previously shown to modulate neutrophil recruitment in the lungs (274). Additionally, the diversity on specific macrophage sub-populations is starting to be discovered (333). Therefore, it cannot be ruled out that after BDL, even with the same number of the overall macrophage content in WT and *Trem2*$^{-/-}$ mice, specific differences in the macrophage subtype recruited to the liver may exist. In this regard, different TREM2-expressing macrophage subtypes associated with adipose tissue and obesity (278) , liver cirrhosis (281) and NAFLD (280) development have been described. Therefore, as aforementioned, research

strategies focused on elucidating in detail differential cholestasis associated macrophage subpopulations may be of interest.

During the wound healing response after liver injury, both regenerative and fibrotic responses are activated in order to restore the lost tissue (111) Inflammation and exacerbated cell death-derived products promote hepatocyte and cholangiocyte proliferation (111). Accordingly, we observe exacerbated cell death in *Trem2*$^{-/-}$ mice in response to cholestasis, which is accompanied by enhanced biliary expansion after BDL and also increased expression of biliary markers after ANIT administration. Regarding the role of TREM2 in cholestasis-mediated fibrogenic responses, enhanced HSCs activation is detected in *Trem2*$^{-/-}$ mice after BDL, presumably as a consequence of the increased presence of inflammatory mediators. Yet, liver fibrosis, mainly measured by the intrahepatic collagen content, is not changed between WT and *Trem2*$^{-/-}$ mice after BDL. This phenomenon may be explained by the time point selected for this study; indeed, changes in liver collagen content were not detected until 14 days after BDL in a time-course analysis (334, 335).

In terms of the molecular mechanisms responsible of the effects of TREM2 during cholestasis, the gut-derived bacterial products are now regarded as crucial mediators of liver injury in different settings. In cholestasis, this idea was already established as an important contributor to disease progression (204) and continues to be strengthened. Lately, gut-derived bacterial products were shown to sensitize hepatocytes to BA-induced injury, and are needed to establish cholestatic damage in two experimental models of cholestasis (316). TREM2 is regarded as an inhibitor of TLR mediated signalling and, in line with this, antibiotic-based gut sterilization rescued some of the differences observed between WT and *Trem2*$^{-/-}$ mice after cholestasis. This is in agreement with our previous results, where effects of TREM2 in CCl_4 induced liver injury were shown to be triggered by gut derived PAMPs (288). Nevertheless, in this study, some parameters were not rescued after the treatment with antibiotics, suggesting TREM2´s effects on cholestasis might also occur due to binding of alternative TLR ligands beyond PAMPs, which include DAMPs released from dying epithelial cells (111, 210). Alternatively, TREM2 might also exert its protective effects in cholestasis in a TLR-independent mechanism. Of note, TREM2 has been reported to sense lipids that are exposed in apoptotic neurons (269) and to trigger intracellular signalling mechanisms in response to these stimuli (336). Therefore, these data suggest that TREM2 may regulate inflammatory responses via a TRL-independent mechanism.

D.3. TREM2 arises as novel mediator of UDCA effects in non-parenchymal cells

The endogenous choleretic BA, UDCA, represents the first line therapy for PBC. For the treatment of PSC, the therapeutic benefits of UDCA are not so well defined, and there is no general consensus in its use, in this regard, the EASL accepts its use, while the AASLD recommends against UDCA-based treatment for patients with PSC (105). UDCA effects beyond choleresis include anti-apoptotic, induction of biliary bicarbonate secretion and anti-inflammatory effects, but its specific mechanisms of action are still far from clear (311). Strikingly, around 30-40% of the patients with PBC treated with UDCA present an incomplete response and are, therefore, at a higher risk to develop end-stage liver disease and need of liver transplantation (22). A deeper understanding on the molecular mechanisms mediating UDCA effects in cholestasis may shed light into this issue and also enable optimised therapeutic strategies for these patients. As previously mentioned, the non-parenchymal liver cells KCs and HSCs are paramount in the progression of cholestatic diseases (131) and therapeutic strategies focused on these cellular compartments may exert pleiotropic effects on disease progression.

In this context, little is known on the potential beneficial effects of UDCA on KCs and HSCs. Currently, UDCA treatment has been reported to diminish liver fibrosis *in vivo* in a CCl_4-based model, this is associated with its effects *in vitro*, in the HSCs cell line LX2 counteracts the effects of TGFβ1, thereby diminishing activation and increasing cell death (337). Effects of UDCA in liver fibrosis are associated to its action as a modulator of Mast cell activation (338). Moreover, an UDCA-lysophosphatidylethanolamide (UDCA-LPE) conjugate inhibits LPS-induced inflammatory cytokine production in KCs and *in vivo* in a mouse model of liver failure induces by galactosamine and LPS treatment. Additionally, conditioned media from UDCA-LPE treated KCs inhibits fibrosis in HSCs (339). Moreover, recently published studies reveal that UDCA may affect signals derived from intestinal microbiota. In this regard, during cholestasis of pregnancy, UDCA was shown to enrich the microbiome with *Bacteroidetes* strains, which facilitates hepatoprotective effects due to increased FGF15/19-FXR signalling (340). Similarly, in a small study with NAFLD patients, UDCA was shown to modulate the microbiome and metabolic pathways that finally lead to an improved liver function (341).

In this dissertation, we report a novel mechanism by which UDCA impacts non-parenchymal liver cell biology. Our results suggest that UDCA is able to counteract

LPS effects on KCs and HSCs; in particular, upon LPS incubation, UDCA downregulates the expression of the pro-inflammatory receptor *Trem1*, while upregulating its anti-inflammatory partner, *Trem2* in comparison to cells incubated with LPS alone. Importantly, UDCA alone is also able to downregulate *Trem1* and upregulate *Trem2* expression in KCs. To our knowledge, this is the first study assessing the effects of UDCA on TREM1 and TREM2 expression. Interestingly, our results also indicate that some of the anti-inflammatory effects of UDCA on KCs may be TREM2-dependent, as UDCA reduced the LPS-induced expression of *Il6*, *Tnf* and *Cxcl1* in comparison to LPS alone, and this effect was not detected in *Trem2*$^{-/-}$ KCs.

Importantly, IL6, TNF and CXCL1 are key pro-inflammatory mediators in the development of cholestatic diseases. As previously mentioned, these mediators are found upregulated in the liver of patients with PBC (164, 326) and also in cholangiocytes derived from the liver of patients with PSC (327, 342) as well as in the microenvironment of DRCs (6). Additionally, IL6 and TNF show mitogenic properties in cholangiocytes (343) and hepatocytes (344) and CXCL1 is key in the recruitment of neturophils, the main cytotoxic cell in cholestasis (332) Moreover, the UDCA-LPE conjugate inhibits IL6 and TNF production in KCs (339). These results suggest that UDCA treatment may induce changes in TREM1 and TREM2 expression, which may underlie the response of patients to this treatment. In this regard, it would be interesting to analyse TREM1 and TREM2 expression in UDCA-treated patients, focusing on differences between those patients with a total and a partial response to UDCA. In summary, these findings unravel a new mechanism by which UDCA exerts its effects on KCs, and thus pose new research opportunities in the field of UDCA treatment for patients with chronic liver diseases.

D.4. In HCC tumours, TREM2 is mainly expressed in resident and infiltrating macrophages

We have previously reported that TREM2 is upregulated in the liver of patients with HCC compared to healthy control liver (289) Here, we analysed this expression in detail, in order to unravel the specific cell type responsible for TREM2 overexpression in HCC. Our IHC results suggest that TREM2 is not expressed in transformed hepatocytes, while TREM2 staining is evident in macrophage resembling cells in the surrounding cirrhotic tissue and within the tumour. Importantly, our scRNAseq analyses confirm this data, demonstrating that TREM2 expression is most prominent in liver resident and infiltrating TAMs. These findings coincide with recent single cell RNA

sequencing work demonstrating TREM2^{+} expressing macrophage populations in NAFLD (280), human and murine liver cirrhosis (281) and obese adipose tissue (278). Moreover, TREM2^{+} expressing TAMs are also characterised by the expression of CD9 and CD68, suggesting they resemble scar associated macrophages identified in human and murine liver cirrhosis (281). Accordingly, the *Trem2*^{high} population predominating in nonalcoholic steatohepatitis (NASH) is characterised by the upregulation of CD9 expression (280). Moreover, our data show that TREM2 expressing TAMs are enriched in TLR signalling and lysosome associated pathways, suggesting that these TAMs cooperate in the regulation of TLR mediated inflammatory responses (288). Accordingly, *Trem2*^{high} KCs described in NASH models are also characterised by the enrichment in lysosome associated pathways (280).

D.5. TREM2 protects the liver from enhanced fibrosis-associated carcinogenesis

The exacerbated response to cholestatic damage observed in *Trem2*$^{-/-}$ mice is characterised by increased cell death, inflammation and neutrophil recruitment. All of these processes can provoke a vicious cycle of inflammation and cell death that in the long term may lead to the malignant transformation of epithelial cells and the development of HCC (192) and CCA (185).

In this regard, our results depict increased expression levels of the inflammatory cytokines *Il6* and *Tnf* in *Trem2*$^{-/-}$ mice in response to cholestasis. Interestingly, these mediators are also upregulated in *Trem2*$^{-/-}$ mice in response to acute and chronic hepatocellular damage (288) as well as in early phases of carcinogenesis, as shown after an acute DEN administration (289). Both IL6 and TNF are able to promote cholangiocyte proliferation (343), indeed, IL6 is differentially overexpressed in patients with CCA arising from PSC background compared to patients with PSC without malignant transformation (345). Importantly, TNF and IL6 are also pivotal cytokines in hepatocarcinogenesis, as they establish a molecular link between inflammation and cancer development (346, 347). Under the effect of mutagenic stimuli such as DEN or TAA, enhanced proliferation and sustained inflammation may aid hepatocyte transformation (348). Indeed, we observed increased hepatocarcinogenesis in the *Trem2*$^{-/-}$ mice after DEN+CCl_4 and TAA-based fibrosis-associated HCC models, which also display enhanced expression of the proliferative marker *Pcna*.

Additionally, although similar levels of intrahepatic BA concentration are detected in WT and *Trem2*$^{-/-}$ mice after BDL, their fold change is more pronounced in *Trem2*$^{-/-}$

animals. BA accumulation promotes deleterious effects in the liver, including DNA damage, oxidative stress and inflammatory autocrine and paracrine loops, all of which aid HCC and CCA development (349). Recently, BAs were shown to promote hepatocarcinogenesis by the regulation of NKT cell recruitment to the liver (350). In CCA, conjugated BAs induce AKT and ERK1/2 signalling in the tumour cells, finally resulting in CCA growth and invasiveness (351). BAs are also associated with carcinogenesis by their action on FXR signalling. In this regard, BA accumulation can lead to FXR downregulation (352), of note, *Fxr*$^{-/-}$ mice develop spontaneous HCC (353), but in this process, *Fxr* loss itself is not sufficient to induce carcinogenesis, and this is dependent on intrahepatic BA accumulation (354). On the other hand, FXR activation protects the liver from HCC (25) and CCA development (355). In summary, BAs are regarded as co-carcinogenic factors, and thus may also represent the link between the exacerbated response to cholestasis and subsequent fibrosis-associated carcinogenesis in *Trem2*$^{-/-}$ mice.

Liver collagen content as measured by Sirius red staining, is reduced in *Trem2*$^{-/-}$ mice in long term, fibrosis-associated HCC models. Although generally believed as a driver of liver carcinogenesis, fibrosis and HCC development may also be dissociated in some contexts (356). In this line, TREM2 has been suggested to play a pro-fibrogenic role in TREM2 expressing scar associated macrophages (281). Therefore, TREM2 may exert uncoupled effects on HSC activation and fibrogenesis, which may be explained by different mechanisms. In the one hand, macrophages phagocytise fibrotic fibres, thereby contributing to fibrosis resolution (357). TREM2 has been linked to phagocytosis in different macrophage subpopulations with context-specific findings. In the CNS macrophages, TREM2 promotes phagocytosis of apoptotic bodies (358, 359), while in alveolar macrophages TREM2 dampens bacterial opsonisation and clearance (274). We hypothesise that TREM2 may also impact the phagocytosis of fibrotic fibres, in liver resident or infiltrating macrophages, and thus modulate liver fibrosis, albeit this hypothesis still needs to be explored. Interestingly, a recent publication suggests that TREM2 may exert its anti-inflammatory and phagocytic effects via independent intracellular signalling pathways (360), suggesting that TREM2 may distinctly regulate inflammation and phagocytosis, which may also result in unexpected effects on the deposition of fibrotic fibres. Indeed, macrophages play an essential role in liver fibrosis resolution, and specialised macrophage subpopulations seem to direct this response (361). As aforementioned, a detailed dissection of the effects of TREM2 in the recruitment of distinct macrophage populations to the liver is still awaiting and may

shed light into the specific molecular mechanisms underlying the link between TREM2 and fibrosis.

D.6. TREM2 activation represents a novel potential therapeutic strategy for patients with cholestasis and HCC

In conclusion, cholestatic damage triggers the wound healing response, in which epithelial and non-epithelial cells collaborate in an effort to restore the lost liver parenchyma and its functions. In this context, bacterial products derived from the intestinal compartment bind to TLRs, mainly in KCs and HSCs, and here, boost the expression of inflammatory gene transcription. Inflammatory mediators act in an autocrine and paracrine fashion, inducing epithelial cell death and perpetuation of the inflammatory response. In the long term, these alterations favour hepatocyte transformation and fibrosis-associated HCC. In the absence of TREM2, the natural break to TLR-mediated signalling disappears; therefore, TLR-mediated inflammatory gene transcription in KCs and HSCs is amplified, resulting in an exacerbated response to cholestasis and hepatocarcinogenesis (**Figure D.1**). Limiting the contribution of the gut-derived products by the treatment with Abx shows that TREM2 effects depend, at least in part, on the regulation of this pathway. Moreover, TREM2 arises as possible mediator of UDCA anti-inflammatory effects in non-parenchymal liver cells.

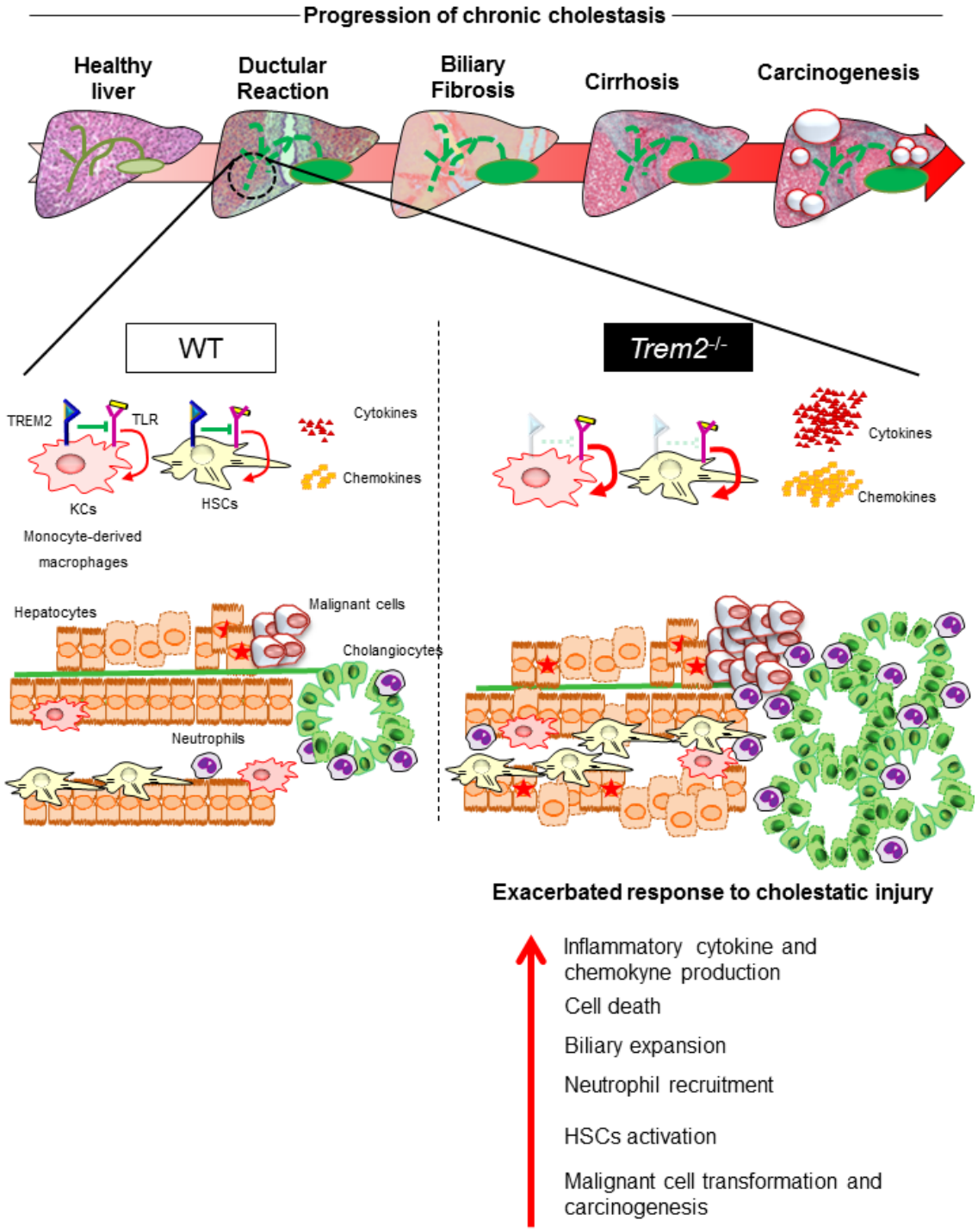

Figure D.1. Working model on the role of TREM2 in response to cholestatic injury. Chronic cholestatic diseases progress in different steps including ductular reaction, fibrosis, cirrhosis and may also lead to carcinogenesis. During this progression PAMPs and DAMPs bind to TLRs in the non-parenchymal cells KCs, monocyte derived macrophages and HSCs, thereby promoting pro-inflammatory cytokine and chemokine production. In the absence of TREM2, the natural break for TLR-mediated signalling disappears, which results in increased inflammatory cytokine and chemokine production and subsequently leads to an exacerbated response to cholestatic injury characterised by enhanced cell death, biliary expansion, neutrophil recruitment, HSC activation and fibrosis-associated hepatocarcinogenesis. KCs, kupffer cells; HSCs, hepatic stellate cells; TLR, toll like receptors; TREM2, triggering receptor expressed on myeloid cells 2; WT, wild type.

Importantly, inflammation is central in the progression of almost all liver diseases. This concept and the novel findings on the anti-inflammatory role of TREM2 in the liver presented here and in our previous studies (288, 289), suggest that this receptor may act as a central regulator of the wound-healing response in liver diseases of different origins. This confers an added value to this pathway, as a therapeutic strategy potentiating TREM2 signalling on the liver may be beneficial to a wide range of patients.

Although small molecules aimed at activating TREM2 signalling and its anti-inflammatory effects are yet to be developed, other strategies to boost TREM2 signalling are starting to be discovered in the setting of CNS diseases, mainly in AD. In this regard, soluble TREM2 was shown to promote microglial functions in AD models and thus improve disease progression (362). Recent studies have evaluated the efficacy of TREM2 activating strategies in the context of AD. In one of the studies, a monoclonal antibody was employed to prevent TREM2 shedding and stabilize it in the cell surface, this induced a beneficial AD-associated phenotype in microglia (363). However, this strategy also led to a reduction in sTREM2, which may trigger counteractive effects in microglial activation. In an additional strategy, intracranial administration of, AL002a, an antibody that recognizes the extracellular portion of TREM2 and triggers its signalling, leads to beneficial effects on microglia, which ultimately translate to reduced amyloid deposition and improved cognition (364). In sum, although novel promising strategies are being developed, additional knowledge on TREM2 and sTREM2 is still needed in order to design an optimal strategy to promote TREM2 signalling. In this regard, as previously mentioned, UDCA upregulated TREM2 expression in KCs, and some of the beneficial effects of this choleretic BA in cholestasis may be triggered via TREM-dependent mechanisms.

Owing to its ability to fine-tune inflammatory and immune responses, TREM2 is gaining interest in the context of tumour immunology. In this regard, two recent studies report the role of this receptor as a modulator of the immune compartment and its response to tumour growth (365, 366). One of the studies identifies two distinct populations of *Arg1* and *Trem2* expressing suppressive myeloid cells. Specifically, *Arg1*$^{+}$ *Trem2*$^{+}$ myeloid regulatory cells (Mreg) and *Arg1*$^{+}$ *Trem2*$^{+}$ TAMs are identified in the tumour microenvironment of the fibrosarcoma cell line MCA205-derived tumours in mice. Interestingly, in the absence of *Trem2* the Mreg cell population decreases substantially and less CD8+ dysfunctional cells are detected, while cytotoxic responses against the tumour are reactivated, including increased natural killer cells

(NKs) and cytotoxic T cells. This results in the reactivation of cytotoxic responses against the tumour and the regression of its growth (365). Similar results were obtained in another study, where the genetic ablation of *Trem2*, or its inhibition by a specific antibody to its extracellular ectodomain, restrains tumour growth in different syngeneic models including fibrosarcoma, colorectar carcinoma and mammary tumours. A more detailed analysis of the mechanisms retraining tumour growth in *Trem2*$^{-/-}$ mice, reveals that the absence of this receptor shapes the tumour infiltrating immune compartment. In this regard, the tumour microenvironment of *Trem2*$^{-/-}$ mice is characterised by a decreased representation of immune suppressive myeloid subpopulations and increased representation of immune stimulatory myeloid subpopulations. In parallel, NK cells and T cells are enriched in *Trem2*$^{-/-}$ mice, and CD4+ and CD8+ T cells express more PD1, which is associated with improved responsiveness to anti-PD1 therapy. Similar results are also confirmed by the use of a TREM2 inhibitory antibody in WT mice. Besides, TREM2 expression is assessed in a variety of human tumours, were the expression of this receptor is mainly found in tumour infiltrating macrophages (366).

These findings suggest that the outcome of TREM2-mediated modulation of inflammatory and immune responses may be context and time dependent. In this regard, TREM2 is a natural break for sustained inflammation; consequently, TREM2 agonism would presumably attenuate inflammation both in non-parenchymal hepatic stromal cells and in infiltrating monocyte derived macrophages, during chronic liver disease. Thus, TREM2 activation would exert protective effects in the progression of cholestatic diseases and fibrosis-associated hepatocarcinogenesis (**Figure D.2**). In turn, once the tumour is established, TREM2 activation may be associated with the suppression of immune responses that target the tumour, and may therefore be detrimental. In this context, inhibition of TREM2 may shape the myeloid and lymphoid immune subpopulations in a manner that enables the immune attack against the tumour and halts tumour gowth (**Figure D.2**). Specifically, genetic absence of *Trem2* or its inhibition by a specific antibody, results in decreased immune suppressive subpopulations and increased immune stimulatory myeloid and lymphoid cells, and it is also associated with increased PD1 expression and responsiveness to immune-therapy. Thus, a deeper understanding on the specific role of TREM2 in each of the cellular subtypes of the liver is still needed in order to unravel the full picture of TREM2-mediated immune modulation in the context of hepatobiliary disease progression.

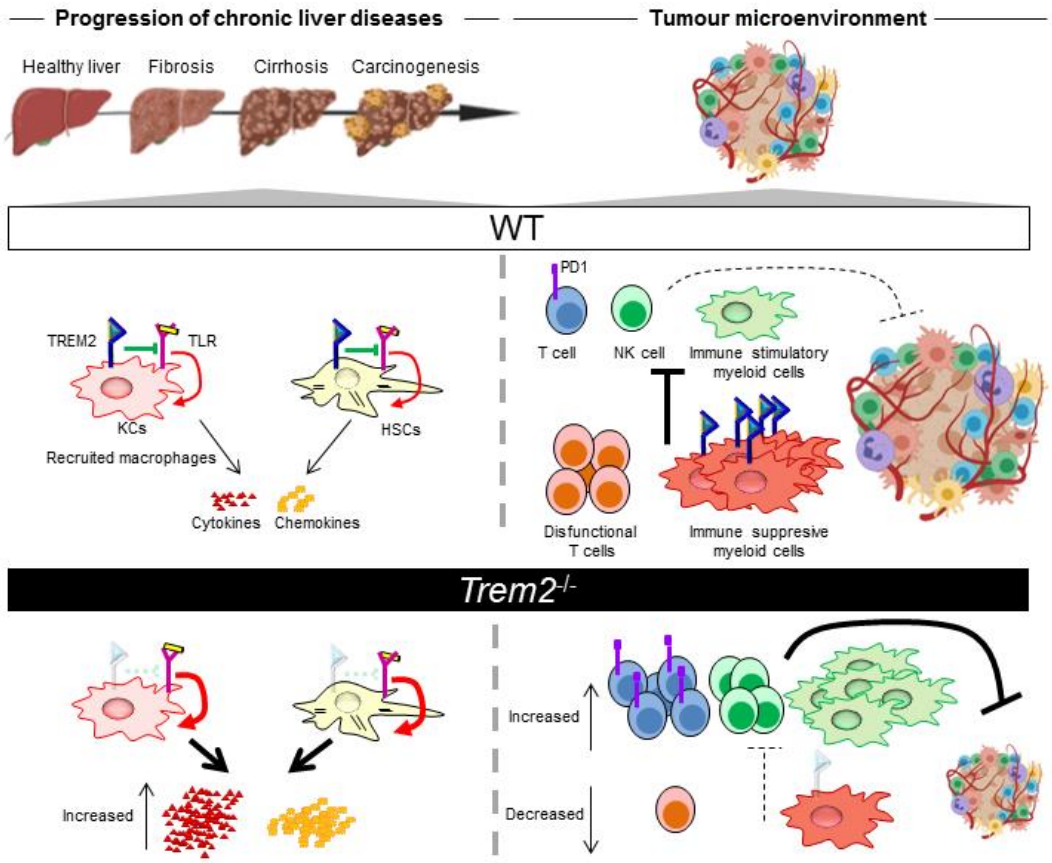

Effects observed upon genetic ablation or inhibition of TREM2	
Chronic liver disease progression	**Tumour microenvironment**
Increased cytokine and chemokine production	Increased number of stimulatory myeloid cells and decreased number of suppressive myeloid cells
Increased cell death and oxidative stress	Increased number and activation of cytotoxic cells, increased PD1 expression
Exacerbated liver damage	Improved responsiveness to immune therapy
Enhanced Hepatocarcinogenesis	Decreased tumour growth

Figure D.2. Effects observed upon genetic ablation or inhibition of TREM2 in the progression of chronic liver diseases and in immune responses against the tumour. *Left panel*. The progression of chronic liver diseases is characterised by different stages including fibrosis, cirrhosis and hepatobiliary carcinogenesis. During this progression, the non-parenchymal cells including KCs, recruited macrophages and HSCs, orchestrate mechanisms of inflammation, wound-healing response and regeneration. In this context, TREM2 acts as a natural break for TLR-mediated signalling, thereby regulating inflammatory gene transcription. In the absence of *Trem2*, TLR-mediated inflammatory gene transcription is amplified, resulting in an exacerbated response to liver damage and hepatocarcinogenesis. *Right panel*. Different immune stimulatory and suppressive populations are found within the tumour microenvironment and their interplay determines tumour growth. TREM2 is mostly expressed in immune suppressive myeloid cells, which negatively modulate cytotoxic responses against the tumour mediated by T cells, NK cells and stimulatory myeloid cells. In the absence of *Trem2*, or by using inhibitory antibodies for this receptor, the balance between stimulatory and suppressive mechanisms shifts, resulting in increased stimulatory myeloid cells, cytotoxic T and NK cells and decreased *Trem2* expressing myeloid suppressive cells as well as dysfunctional T cells. Additionally, increased expression of PD1 is detected in lymphoid cells, which results in an enhanced responsiveness to immune-therapy (blockade of PD1).

CONCLUSIONS

1. *TREM2* mRNA expression is upregulated in the liver of patients with chronic cholestatic diseases including PBC and PSC, compared to healthy liver tissue.

2. *TREM2* mRNA expression positively correlates with the mRNA expression of inflammatory and fibrotic markers in the liver of patients with chronic cholestatic diseases including PBC and PSC.

3. In patients with PBC, *TREM2* mRNA expression also positively correlates with serological levels of liver damage biomarkers and with liver disease progression scores.

4. In the mouse liver, *Trem2* mRNA is minimally expressed in epithelial cells (including hepatocytes and cholangiocytes) while the expression of this receptor is markedly upregulated in the non-parenchymal cells such as KCs and activated HSCs.

5. *Trem2* mRNA expression is induced in the liver of mice subjected to different models of cholestasis.

6. *Trem2*$^{-/-}$ mice display an exacerbated response to obstructive cholestatic injury induced by BDL, this exacerbated response is characterised by increased biliary expansion and cell death.

7. *Trem2*$^{-/-}$ mice show a baseline alteration of the BA metabolism in the liver, with reduced levels of hepatic BAs and a trend towards altered expression of genes involved in BA metabolism.

8. The exacerbated response of *Trem2*$^{-/-}$ to BDL-based cholestatic injury is associated with increased inflammation and neutrophil recruitment to the liver.

9. The treatment with Abx rescues some of the differences observed between WT and *Trem2*$^{-/-}$ mice after BDL. Therefore, the protective effects of TREM2 in obstructive cholestasis are partially mediated by the regulation that TREM2 exerts on the effects of translocation of gut-derived bacterial products in the liver.

10. TREM2 also performs a protective role in chemically induced cholestasis, as *Trem2*$^{-/-}$ mice display enhanced liver injury, cell death and inflammation in the ANIT-based model.

11. UDCA downregulates *Trem1* while upregulates *Trem2* expression in mouse isolated KC cells.

12. UDCA rescues LPS-mediated effects in KCs, thereby downregulating the expression of the pro-inflammatory receptor *Trem1* and upregulating the expression of the anti-inflammatory receptor *Trem2*.

13. UDCA reduces de expression of the inflammatory mediators *Il6*, *Tnf* and *Cxcl1* in mouse isolated KCs in a TREM2 dependent mechanism.

14. *TREM2* is expressed in liver resident and recruited TAMs in HCC tumours.

15. *TREM2*$^{+}$ TAMs are characterised by the expression of *CD68*, *CD14* and *CD9*, as well as by the enrichment in TLR signalling and lysosome associated pathways.

16. TREM2 protects the liver from fibrosis associated hepatocellular carcinogenesis, which is associated with reduced expression of proliferative markers and enhanced liver fibrosis.

In summary, TREM2 arises as a novel regulator of inflammatory responses in cholestasis and a protector against fibrosis-associated hepatocellular carcinogenesis. Therefore, activation of TREM2 could represent a promising therapeutic strategy for patients with cholestasis. Moreover, some of the therapeutic benefits of UDCA supplementation in cholestasis may be mediated by the regulation of TREM1 and TREM2 expression in non-parenchymal liver cells. Nevertheless, although TREM2 activation may prevent cholestatic injury and also hepatocarcinogenesis, it might also be associated with unwarranted effects on liver fibrosis and regulation of immune responses to tumour growth once developed.

VERSION OF THE THESIS IN BASQUE
TESIAREN BERTSIOA EUSKARAZ

SARRERA

S.1. Gibelaren fisiologia eta anatomia

Gibela gorputzeko organorik handiena da eta homeostasi metabolikoa mantentzeko garrantzitsuena. Gibela elikagaien sintesiaz, metabolismoaz, biltegiratzeaz eta hauen birbanaketaz arduratzen da. Hori horrela, gibelean adierazten diren milaka entzimek karbohidratoen, lipidoen, aminoazidoen eta nitrogenoaren metabolismoa burutzen dute. Era berean, organo hau, glukosa, lipido, burdina eta A bitaminaren biltegiratze tokia da. Horrez gain, gibelean odol plasmako proteina gehienak ekoitzi eta jariatzen dira, hala nola, albumina, apolipoproteinak, transferrina eta fibrinogenoa. Bere kokapen anatomikoa dela eta, gibelera askotariko molekula toxikoak hel daitezke, beraz, organo honek funtsezko papera betetzen du toxina hauen detoxifikazioan (1, 2).

Gibelaren azpiunitate anatomikoa, egiturazkoa eta funtzionalak gibel lobulua izena hartzen du (**S.1. Irudia**). Gibel lobuluak forma hexagonala du eta zain zentralaren inguruan erradialki kokaturik dauden hepatozito ilarek eta hirukote portalek osatzen dute. Hirukote portala gibel lobuluaren erpinetan kokatzen da eta gibel arteriaren, porta zainaren eta behazun hodien adar banaz osatuta dago. Elikagaiak eta oxigenoa dakartzan odola hirukote portaletik zain zentralera drainatzen da gibel sinusoidetan zehar eta, azkenekoak, hepatozitoen ilaren artean kokatzen dira. Sinusoidea gibeleko zelula endotelialez estalita dago (liver sinusoidal endothelial cells LSECs) eta bere lumenean gibeleko bertako makrofagoak, Kupffer zelulak (Kupffer cells, KCs) izenez ere ezagutzen direnak, kokatzen dira. Behazuna ,aldiz, odolaren kontrako zentzuan drainatzen da, zain zentralaren inguruan dauden hepatozitoetatik (hepatozito peribenosoak) hirukote portalera. Espazio perisinusoidala, Disse-ren espazioa ere deitzen dena, zuntz erretikularrez eta odol plasmaz osatuta dago eta hepatozito eta gibel sinusoideen artean kokatzen da. Bertan, hepatozito eta odol plasmaren arteko elkartruke metabolikoa gertatzen da. Disseren espazioa gibeleko zelula estelareen (hepatic stellate cells, HSCs) kokalekua ere bada (1).

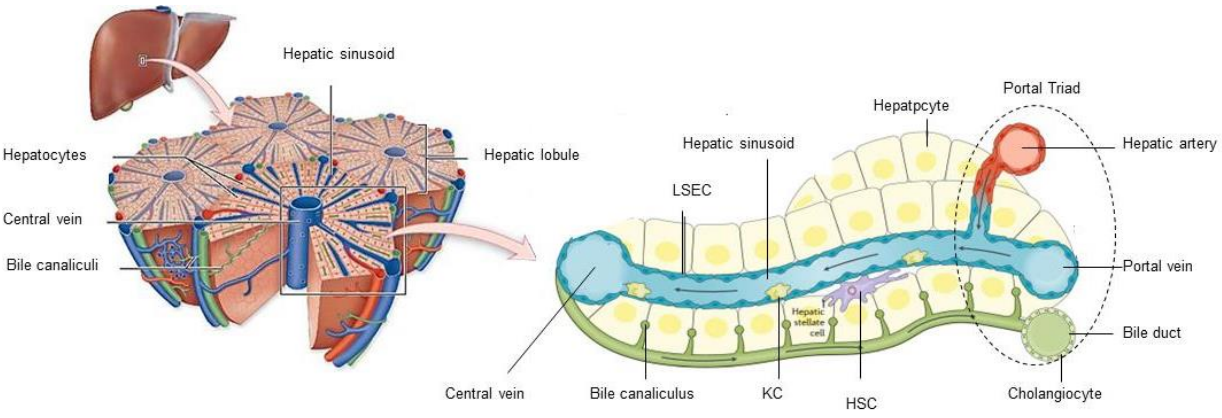

S.1. Irudia. Gibelaren azpiunitate anatomikoa, egiturazkoa eta fntzionala. Gibelaren azpiunitate anatomiko, funtzional eta egiturazkoa , gibel lobulua, zain zentralaren inguruan ilaretan antolatzen diren hepatozitoek eta hirukote portalek osatzen dute. Gibel lobuluaren erpinean hirukote portala kokatzen da, hau porta zainaren, gibeleko arteriaren eta behazun hodiaren adar banak osatzen dute. Odola hirukote portaletik zain zentralera drainatzen da, hepatozitoen ilaren arteko sinusoideetan zehar. Gibeleko sinusoideak LSEC-ez estalita daude, KC-ak, aldiz, sinusoidearen lumenean kokatzen dira. HSC-ak Disse espazioan kokatzen dira, hau, hepatozito ilaren eta sinusoiedeen arteko espazioa da. KC, kupffer cells, HSCs, hepatic stellate cells, LSEC, liver sinusoidal endothelial cells. *[Miyajima A et al, 2014 (3) artikulutik egokitua]*.

S.1.1. Gibeleko zelula epitelialak

Gibela bi motako zelula epitelialez osatuta dago: hepatozitoak eta kolangiozitoak. Hepatozitoak edo gibeleko zelula parenkimalak, hexagono forma duten zelulak dira, gibel osasuntsuan egoera kieszentean mantentzen dira eta askotan bi nukleo izaten dituzte. Gibelaren bolumen osoaren %70-80 hartzen dute eta organoaren funtzio metaboliko eta detoxifikazio funtzioen gehiengoa burutzen dituzte (1). Hepatozitoek betetzen dituzten funtzioak era heterogeneoan banatzen dira gibel lobuluan zehar, gibel zonifikazioa deituriko prozesu batean (4). Horrela, elikagai, oxigeno eta morfogenoen eskuragarritasun diferentzialak gibeleko geneen %50-aren tokiaren araberako erregulazioa dakar, ondorioz, gene hauek adierazpen zonifikatua erakusten dute.

Kolangiozitoak behazun hodiak estaltzen dituzten zelulak dira, gibelaren bolumen osoaren %3-5 inguru soilik hartzen badute ere, behazun fluxu osoaren %30-40 bideratzen dute zelula hauek eta behazunaren alkalinizazio eta fluidifikazioan ere parte hartzen dute (5). Funtzio hauek bete ahal izateko, kolangiozitoek hainbat hartzaile eta garraiatzaile adierazten dituzte. Kontuan hartzekoa da hartzaile eta garraiatzaile hauetako asko kolangiozitoaren zilio primarioan topatzen direla (6). Organulu berezi hau behazun hodien argira luzatzen da, horrela, behazunean sortzen diren eraldaketak

detektatu ditzake eta seinale hauek zelula barrura bideratu ditzake, prozesu hau dela medio, kolangiozitoek behazunaren konposizioa erregulatzen dute (7).

S.1.2. Behazunaren sorrera eta drainatzea

Behazunaren sorrera eta drainatzea hepatozito, kolangiozito, hesteetako zelulen eta hesteetako mikrobiotaren arteko elkarekintza konplexuaren emaitza da. Behazuna bizitzarako ezinbesteko biojariakina da, eta urez, behazun azido edo gatzez (bile acids, BAs), bilirrubinaz, lipidoez, elektrolitoez, proteinez eta konposatu xenobiotikoez osatuta dago (8). Behazuna gibelean ekoizten da eta funtzio garrantzitsuak betetzen ditu, besteak beste, dietan hartutako gantzaren liseriketa, hesteetako bakteriekiko babes immunologikoa eta substantzia lipofiliko toxikoen kanporaketa (6).

Behazunaren osagairik garrantzitsuenak BA-k dira. BA-k entzima sare konplexu baten bidez sintetizatzen dira, zeinetan gibelak eta hesteetako mikroorganismoek parte hartzen duten (9) **(S.2. Irudia)**. Sintesi prozesu hau hepatozito perizentraletan hasten da, hemen kolesteroletik eratorritako BA primarioak sortzen dira. Bidezidor honen entzima mugatzailea, zitokromo P450 7A1 (Cyp7a1) da, eta bere aktibitatea kontrol zorrotz baten menpean dago, BA-en kontzentrazioen aldaketa fisiologiko zein patologikoei erantzuna emanez (10). BA askeek egitura anfipatikoa dute, eta ezaugarri honek zelularen mintza zeharkatzeko gaitasuna ematen die (11). Hala ere, sintetizatu berri diren BA-k taurina edo glizinarekin konjugatu daitezke, peroxisometan. Prozesu honen bidez beren hidrofobizitatea emendatzen da eta zelulen mintzekiko iragazgaitzak bilakatzen dira. Gizakietan BA gehienak glizinarekin konjokatzen dira, erlazio hau 3:1 (glizina:taurina) izanik. Saguetan, aldiz, BA gehienak taurinarekin konjokatzen dira (9, 12).

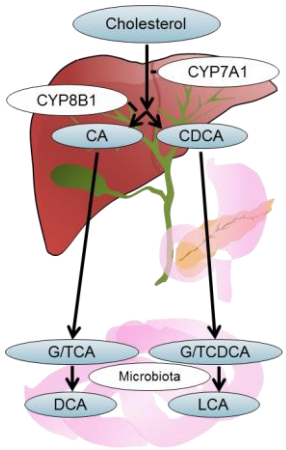

Gizakia		Sagua	
Primario, aske	**Sekundario, aske**	**Primario, aske**	**Sekundario, aske**
CA, CDCA	DCA, LCA, UDCA	CA, α and βMCA, CDCA, UDCA	DCA, ωMCA
Primario, konjokatu	**Sekundario, konjokatu**	**Primario, konjokatu**	**Sekundario, konjokatu**
G/TCA, G/TCDCA	G/TDCA, G/TLCA, G/TUDCA	TCA, α and βTMCA, TCDCA, TUDCA	TDCA, ωTMCA

S.2. Irudia. BA-en bidezidor biosintetikoa eta gizaki eta saguetan aurkitzen diren BA espezie nagusiak *Eskuineko irudia*. Kolesterola BA-en aurrekari molekularra da, hau, CA eta CDCA BA primarioetan bilakatzen da, bidezidor honen entzima mugatzailea CYP7A1 izanik. Ondoren, BA primarioak taurina edo glizinarekin konjokatzen dira giza gibelean eta nagusiki taurinarekin saguen gibelean. Behin hesteetan, mikrobiotak gehiago eraldatzen ditu BA hauek, BA-en espezie sekundarioak sortuz, hauek bir-xurgatu eta berriz gibelean konjokatu daitezke. *Ezkerreko taula*. Gizakian eta saguan aurkitzen diren BA espezie nagusiak. CA, cholic acid; CDCA, chenodeoxycholic acid; CYP7A1, cytochrome P450 Family 7 Subfamily A Member 1; CYP8B1, cytochrome P450 Family 8 Subfamily B Member 1; DCA, deoxycholic acid; G/TCA, glyco/taurocholic acid; G/TCDCA glyco/taurochenodeoxycholic acid; G/TLCA, glycol/tauro lithocholic acid; G/T, glycol/tauroursodeoxycholic acid; LCA, lithocholic acid; MCA, muricholic acid; TMCA, tauromuricholic acid; UDCA, ursodeoxycholic acid *[Qi Y et al, 2015, (13) eta Li J et al, 2019 (12) artikuluetatik egokitua]*.

BA ez-konjokatuak (edo askeak) zein BA konjokatuak, zuhaitz biliarrera jariatzen dira elkarren ondoan dauden hepatozitoen artean aurkitzen diren hepatozitoen kanalikuluen bitartez. Hering kanala hepatozito kanalikulua eta behazun zuhaitza konektatzen dituen egitura da, eta, gibeleko zelula progenitoreen (hepatic progenitor cell, HPC) kokalekua ere bada (14). Hemendik aurrera, behazuna behazun zuhaitzean zehar garraiatzen da hesteetara iritsi arte. Zuhaitz biliarra egitura heterogeneoa da, kolangiozitoz estalitakoa eta Hering kanaletatik behazun hodi nagusiraino hedatzen dena. Hering kanaletatik behazun hodi komunera, zuhaitz biliarraren segmentua emendatzen doa eta behazun hodiak estaltzen dituzten kolangiozitoen morfologia eta funtzioa ere aldatzen dira (15). Behazun zuhaitza gibel-barneko eta gibel-kanpoko kolangiozitoek osatzen dute. (**S.3. Irudia**) (8). Gibel barneko behazun hodiak Hering kanaletatik behazun hodi segmentalerainokoak dira. Gibel kanpoko behazun hodiek, aldiz, gibeleko hodiak, behazun maskuria, hodi zistikoa eta behazun hodi nagusia hartzen dituzte (16).

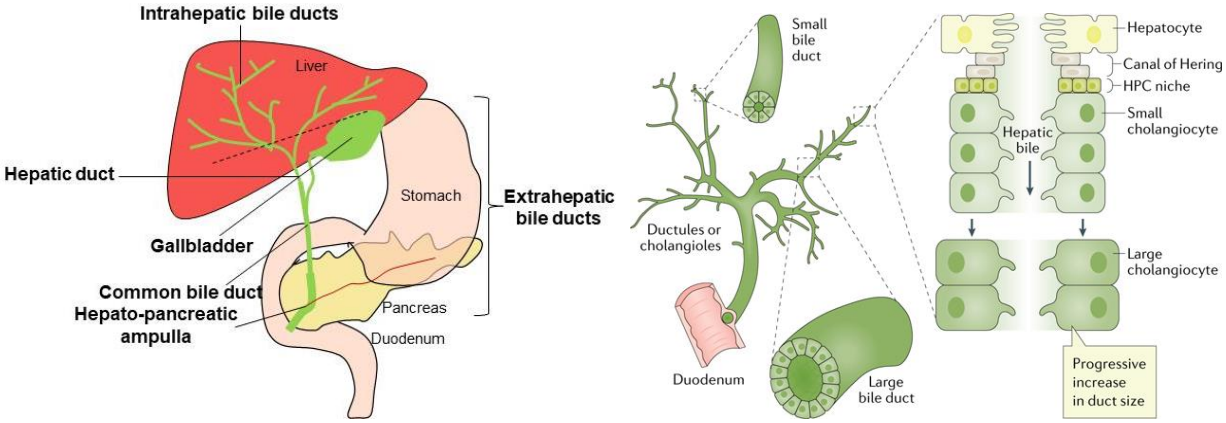

S.3. Irudia. Behazun zuhaitzaren anatomia. Ezkerreko irudia. Behazuna hepatozitoen kanalikulutik duodenora drainatzen da behazun zuhaitzean zehar. Gibel barneko behazun hodiak kanalikulutik gibeleko behazun hodi komunera hedatzen dira. Gibel kanpoko behazun hodiak, aldiz, behazun hodi komuna, behazun maskuria eta gibel-are anpula hartzen dituzte. Eskuineko irudia. Hering kanala hepatozitoak eta behazun hodiak konektatzen dituen egitura da. Behazun zuhaitza kolangiozitoez estalitako egitura konplexua da. Honen segmentua handitzen doa Hering kanaletatik behazun hodi komunera eta hauek estaltzen dituzten kolangiozitoen morfologia eta funtzioa ere aldatzen doa egituran zehar. HPC, hepatic progenitor cell. *[Banales JM et al, 2019 (6) artikulutik egokitua]*.

Behin hesteetara heltzen direnean, behazunaren osagai gehienak, BA-k barne, birxurgatzen dira ileo terminalean, eta hepatozitoetara garraitzen dira bueltan porta zainaren bidez. Prozesu honi zirkulazio enterohepatikoa izena ematen zaio, eta BA guztien %95a birziklatzeko gai da (17). Sintetizatu berri diren BA-en %5-a bakarrik heltzen da kolonera, bertan, hesteetako mikroorganismoek eragindako eraldaketak jasan ditzakete, horrela, BA sekundarioak sortuz. BA primario zein sekundario, konjokatu zein konjokatu gabekoek osatzen dute naturalki organismoetan aurki daitezkeen BA espezieen sorta anitza (18). Kolonean, BA-ak birxurgatu daitezke zirkulazioan dauden BA-en parte izateko berriz, edo gorotzetan kanporatu daitezke (19). Deribazio kolehepatikoa BA-ak birziklatzeko beste mekanismo bat da, honetan, kolangiozitoek BA-ak bixurgatu ditzakete behazun hodietatik, hemendik berriz hepatozitoetara pasa eta berriz behazunean jariatzeko (20).

Gantzaren liseriketan betetzen duten funtzioaz gain, BA-ek organismorako ezinbestekoak diren beste funtzio batzuetan ere parte hartzen dute. Hauen artean, hesteetatik eratorritako bakterien aurkako babes immunologikoa ematen dute, gainera, hartzaile espezifikoetara lotzeko duten gaitasuna dela eta, hainbat prozesu fisiopatologiko erregulatzen dituzte (21). Ildo honetan, BA-ak FXR, (farnesoid X respetor, NR1H4 geneak kodetzen duena), PXR (pregnane X receptor, NR112 geneak kodetzen duena), VDR (vitamin D3 receptor, NR113 geneak kodetzen duena, CAR

(constitutive andrstane receptor, NRII3 geneak kodetzen duena) hartzaile nuklearretara lotzen dira. Era berean, zelularen mitnzean kokatzen den G proteinari lotutako hartzaile bati, hain zuzen ere, TGR5-ri lotzeko gaitasuna ere badute (21).

BA-ek beren buruaren sintesia erregulatzeko gai dira hepatozitoetan. Hesteetan BA-en kontzentrazioa altua denean, BA-ak birxurgatu eta zirkulazio enterohepatikoaren bidez hepatozitoetara heltzen dira. Hepatozitoetan, FXR (farnesoid X receptor) hartzailera lotzen dira. FXR hartzaileak SHP (transcriptional repressor partner) aktibatzen du, eta SHP-k CYP7A1 inhibitzen du, ondorioz BA-en sintesia ere geldiaraziz (10). Azido kenodeoxikoliko, (chenodeoxicholic acid, CDCA), azido koliko (cholic acid, CA) eta agonista sintetikoen bidezko FXR-ren aktibazioak efektu zito-babesleak eta anti-kolestatikoak ditu kolangiozitoetan (22). FXR hartzailea hesteetako zelula epitelialetan, enterozitoetan, ere adierazten da, hauetan, BA-ak FXR hartzaileari lotzen zaizkionean, enterozitoek FGF15/19 (fibroblast growth factor 15 (karraskarietan)/19 (gizakian)) ekoitzi eta jariatzen dute, FGF15/19-ek hormona bat bezala jokatzen du hepatozitoetan, CYP7A1 entzimaren adierazpena murriztuz (23) (**S.4. Irudia**). Ikerketa lan batek agerian utzi duenez, hesteetako FXR-aren aktibazio selektiboa nahikoa da gibela kolestasi mota desberdinez (24) eta hepatokartzinogenesiaz (25) babesteko.

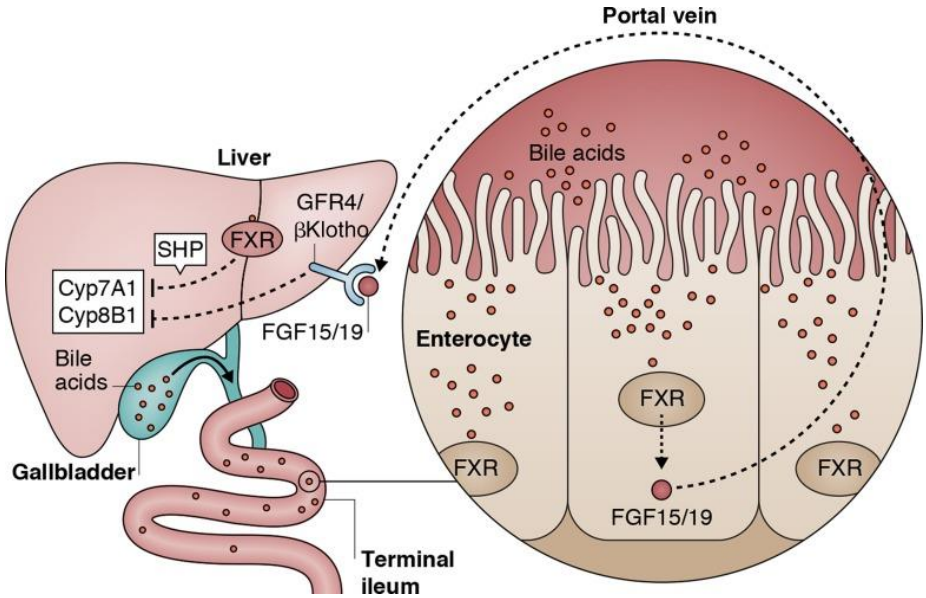

S.4 Irudia. BA-ak beren sintesia erregulatzeko gai dira. BA-ek bere sintesia modulatzen dute FXR hartzaileari lotzeko duten gaitasuna dela eta. Zirkulazio enterohepatikoan birxurgatzen diren BA-ak FXR-ari lotzen zaizkie gibelean, honela, beren sintesia inhibitzen dute SHP-ren adierazpena emendatuz, CYP7A1 inhibitzen duena, hain zuzen ere. FXR hesteetan ere adierazten da, hemen, BA-en loturaren ondorioz, FGF15/19-ren ekoizpena ematen da, honek hormona baten papera betetzen du eta gibeleko CYP7A1 inhibitzeko gai da. CYP7A1, cytochrome P450 Family 7 Subfamily A Member 1; CYP8B1, cytochrome P450 Family 8 Subfamily B Member 1; FGF15/19, fibroblast growth factor 15/19; FXR, farnesoid X receptor *[Shapiro H et al, 2018 (26) artikulutik egokitua.]*..

S.1.3. Gibeleko zelula ez-parenkimalak

Gibeleko zelula ez-eparenkimalen artean ondorengoak bereizten dira: LSEC-ak, KC-ak, HSC-ak eta gibel-barneko linfozitoak. Gibel osasuntsu batean, zelula hauek funtzio osagarriak betetzen dituzte, eta gibeleko zelula epitelialekin elkarlanean, organoaren homeostasia mantentzen laguntzen dute. Gibeleko kalte edo gaixotasunak sortzen direnean ordea, zelula ez-parenkimalek berebiziko garrantzia hartzen dute, inflamazioa, zauri-sendatze eta birsortze prozesuak bideratuz (27).

S.1.3.1. KC-ak eta makrofagoak

Gibeleko makrofagoak bi populazio nagusitan bana daitezke: KC-ak (hots, gibeleko, bertako makrofagoak), eta monozitoetatik eratorritako makrofagoak. Bi populazio hauek gibeleran babes immunologikoan elkarrekiten dute, patogeno kaltegarrien aurkako lehengo defentsa-mekanismoa osatuz (28).

Bi populazio hauek azaleko markatzaile gehienak partekatzen dituzten arren, KC-en eta monozitoetatik eratorritako makrofagoen arteko bereizketa ahalbidetzen duten markatzaile batzuk ere identifikatu dira. Saguen KCs-etan F4/80, CD68, CLE4F eta TLR-ak agertzen dira, monozitoetatik eratorritako makrofagoen markatzaile den CX3CR1-a aurkitzen ez den bitartean. Monozitoetatik eratorritako makrofagoek, ordea, bestelako markatzaileen artean, $LY6C^{+/-}$, $CX3CR1^{+}$ and $CCR2^{+}$ fenotipoa dute (29). Gizakien kasuan, zelula hauek bereizteko markatazileak ez dira hain ezagunak, hauetan, KCs-ak identifikatzeko $CD68^{+}$, $CD14^{+}$ eta CX3CR1-ren gabezia erabiltzen dira, eta monozitoetatik eratorritako makrofagoek $CD14^{+}$, $CCR2^{+}$, $CD16^{+/-}$ markatzaileak adierazten dituzte (30).

KC-ak gibelaren bolumenaren %15-a hartzen dute (31) eta, organo batean aurkitzen den makrofago populaziorik handiena dira organismoan (32). KC-ak gibel sinusoidean aurkitzen dira, eta kokapen estrategiko honek patogenoak eta hildako zelulak detektatu, opsonizatu eta fagozitatzeko aukera paregabea ematen die. Helburu hau betetzeko, KC-ek hainbat hartzaile adierazten dituzte, besteak beste, scavenger hartzaileak, TLR (toll like receptors) hartzaileak konplementuaren hartzaileak eta antigorputzen hartzaileak (32).

Gibel osasuntsu batean, KC-ek fenotipo tolerogenikoa dute. Hau da, bere kokapen anatomikoa dela eta, gibela kontaktu zuzenean dago hesteekin, eta, hortaz, hesteetatik

eratorritako askotariko molekulen eraginpean. KC-ek erantzuna ematen diete molekula hauei, hauek fagozitatuz eta erreakzio immunologiko kaltegarriak ekidinez (33). Hau T zelula erregulatzaileak aktibatuz egiten dute, besteak beste (34). Gainera, KC-ak garrantzizkoak dira burdina eta kolesterolaren metabolismoan. Honela, odola kaltetutako eritrozito eta hemoglobinaren hondakin produktuez garbitzen dute (35, 36). Era berean, CD36 (cluster of cluster of differentiation 36) eta SR-A (scavenger receptor-A) hartzaileak adierazten dituzte, hauen bitartez, oxidatutako lipoproteinak ezagutzen dituzte (37) eta CETP (cholesteryl ester transfer proteina) ere adierazten dute, dentsitate handiko eta dentsitate oso baxuko lipoproteinen plasmako mailak kontrolatzen dituena (38).

Nahiz eta egoera osasuntsuan fenotipo tolerogenikoa izan, KC-ak gibelaren immunologian lehengo defentsa maila ere babadira. Zelula hauek ehuneko kaltea eta patogeno kaltegarriak detektatzeko gai dira, kaltearekin lotutako patroi molekularrak, (danger associated molecular patterns, DAMPs-ak) eta patogenoekin lotutako patroi molekularrak (patogen associated molecular patterns, PAMPs-ak) ezagutzen baitituzte. Hauek ezagutu ostean, KCs-ak zitokina eta kemokina ugari ekoitzi eta jariatzeko gai dira, horrela, molekula kaltegarri hauen aurka zuzenean erreakzionatuz eta bestelako zelula inmuneei agente kaltegarrien berri emanez (**S.5. Irudia**) (28). KCs-ek bideratutako erantzunak askotarikoak dira, eta zitokina pro-inflamatorioen ekoizpenetik hasita (hauen artean TNF, IL6), inflamasomaren, eta ondorioz IL1β eta IL18-ren, ROS eta NOS-en ekoizpenera, monozitoetatik eratorritako makrofagoen eta T zelulen erakarpenera eta baita IL10 bezalako zitokina anti-inflamatorioen eta zelula T erregulatzaileen erakarpeneraino doaz (39). Estimulu bakoitzari eman beharreko erantzuna estuki kontrolatzen da eta estimulu zehatzaren araberakoa da. Hori horrela, KC-ek eragindako erantzun immune baten adibiderik argiena LPS-arekiko (lipopolisacharide) sortzen den erantzuna da. LPS-a TLR4 hartzaileari lotzen zaio KC-etan. Horrela, JNK (c-Jun N-terminal kinase), MAPK (mitogen-activated protein kinase) eta NF-κB (nuclear factor-κB) bidezidorrak pizten ditu, azkenik TNF (tumor necrosis factor) , IL1, IL6, IL12, IL18, IL10 (interleukins 1,6,12,18,10), eta IFNγ (interferon-gamma) zitokinen ekoizpena eraginez (40).

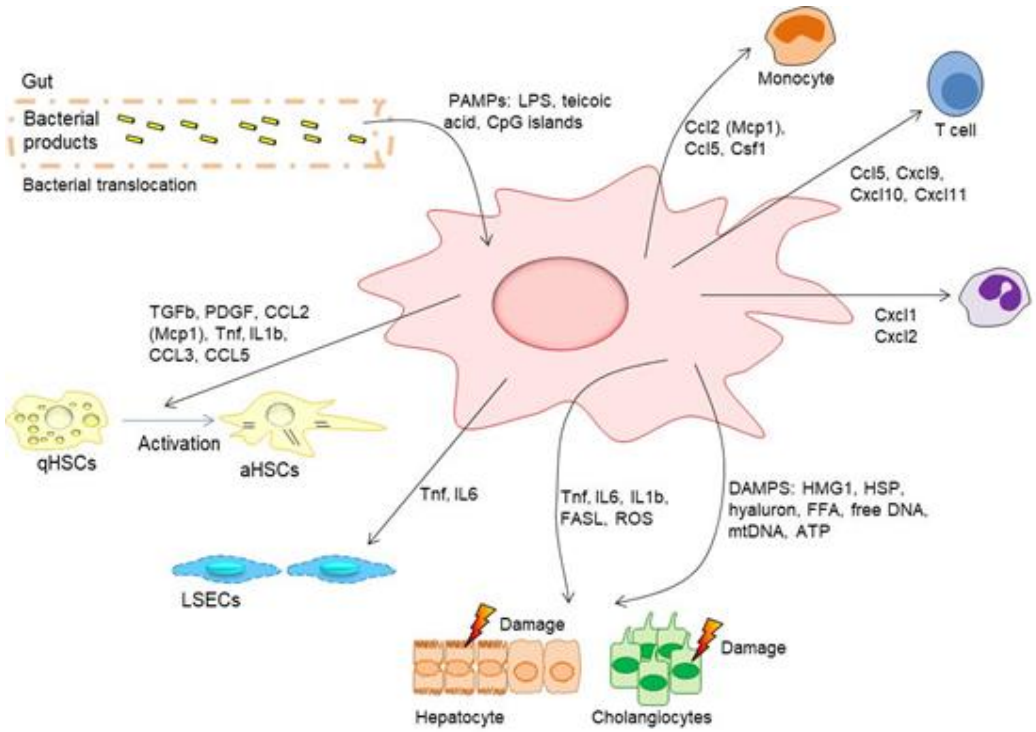

S.5. Irudia. Gibel kaltearen ondoriozko KC-en aktibazioa. Gibeleko kaltearen ondorioz KC-en azalean adierazten diren hainbat hartzailek, DAMP eta PAMP-ak ezagutzen dituzte eta honek zelula hauen aktibazioa dakar. KC-en aktibazioak zitokina eta kemokina pro-inflamatorioen ekoizpena dakar, bitartekari huek egoera aktibatua mantentzen dute eta, aldi berean, T linfozio, neutrofilo eta HSC-ekin komunikazioa ahalbidetzen dute. *[Krenkel O et al, 2017 (28) artikuluan oinarritua]*.

Monozitoetatik eratorritako makrofagoak ere funtsezko zelulak dira gibeleko immunologian. Gibel osasuntsuan, hirukote portalean aurkitzen ditugu, bertan, KC-ekin elkarlanean, burdina eta kolesterolaren metabolismoaz arduratzen dira (41). Gibeleko kaltearen ondorioz, ordea, monozito ugari erakartzen dira gibelera, bertan, zelularen diferentziazioaren ondorioz, makrofago bilakatuko direnak (42). Behin gibelean, monozitoetatik eratorritako makrofago hauek KC-ekin batera elkarlanean aritzen dira. Zitokina anti- eta pro-inflammatorioen ekoizpenari lotutako aktibitate fagozitikoa dute, erantzun hau anti edo pro-inflammatorioa izatea kasuan kasuko estimuluaren araberakoa izanik (43).

S.1.3.1. HSC-ak

HSC-ak Disse zonaldean edo zonalde perisinusoidalean kokatzen dira, gibel osasuntsuan, fenotipo kieszentea dute, eta, beren funtzio nagusia A bitamina edo erretinoideak biltegiratzea da. Izan ere, zelula hauetan dago organismoko A bitamina biltegirik handiena (44). Gibeleko kaltearen ondorioz, berriz, zelula hauek zelula

kanpoko matrizeko (extracellular matrix, ECM) proteinak ekoitzi eta jariatzen dituzte, horrela, HSC-ak gibeleko zelula fibrogeniko garrantzitsuenak bilakatzen dira (45). Funtzio hau bete ahal izateko, HSC-ak aktibatu edo trans-diferentziazio prozesu bat jasaten dute, honen bidez, fenotipo kiszentea galdu eta miofibroblasto motako zelulak bihurtzen dira, ezaugarri pro-inflamatorio, proliferatibo, fibrogeniko eta uzkurkorrak bereganatuz (44) (**S.6. Irudia)**.

Gibeleko miofibroblastoen populazioa konplexua da, miofibroblastoen jatorri izan daitezkeen hainbat zelula mota identifikatu baitira. Horrela, fibroblasto portalak (PFs) eta zirkulazioko fibrozitoak ere miofibroblastoetara trans-diferentziatu daitezke (46). Hala eta guztiz ere, zelulen jarraipeneko esperimentuetan HSC-ak miofibroblastoen ~90% osatzen dutela ikusi da, hainbat sagu eredutan (47). Era berean, antzeko estrategiek agerian utzi dute gibeleko zelula epitelialak (hots, hepatzito zein kolangiozitoak) ez direla miofibroblasto bilakatzeko gai, eta beraz ez dira populazio honen parte (48-50).

HSC-en aktibazioan bi fase bereizten dira: lehenik urrats aurre-inflamatorio bat, hainbat generen indukzio azkarra ezaugarri duena, eta, jarraian, mantentze edo perpetuazio urrats bat dator, non fenotipo aktibatua mantendu eta zelula kopuruaren hazkuntza gertatzen den (51) . Aktibazio prozesuan zehar, HSC-ak kaltetutako zelula epitelialetatik eta gibelera erakarritako sistema immuneko zeluletatik eratorritako askotariko estimuluei erantzuten diete.

LSEC-etatik eratorritako fibronektina HSC-en aktibazioa zuzentzen duen lehenengo faktoretako bat da (52). Lehenengo faktore honen ondoren, hildako hepatozito edota kolangiozitoek oxigeno espezie erreaktiboak, hedgehog ligandoak, nukleotidoak eta hildako zelulen seinaleak jariatzen dituzte, hauek denak HSC-en aktibatzioa eragiteko gai izanik (53). Horrez gain, HSC-ek gorputz apoptotikoak detektatu eta barneratu ditzakete, eta, honek, euren aktibazioa bultzatzen du (54, 55). Makrofagoak ere zelula gakoak dira HSC-en aktibazioan. Kontuan hartzekoa da, zelula hauen deuseztatzeak HSC-en aktibazioaren eta fibrosiaren murrizpena dakarrela saguetan. Makrofagoetatik eratorritako HSC-en aktibatzaile nagusiak honakoak dira: TGFβ (transforming growth factor β), PDGF (platelet derived growth factor), TNF (tumour necrosis factor), IL1β (interleukin 1β), MCP1 (monocyte chemoatractant protein), CCL3 and CCL5 (chemokine (C-C motif) ligands 3 and 5) (51). Plaketak ere garrantzitsuak dira HSC-en aktibazioan, izan ere, PDGFβ eta TGFβ-a jariatzen dituzte, HSC-en aktibazio eta hazkuntzan ezinbestekoak direnak (51).

Era berean, HSC-ek ECM-an gertatutako eraldaketak ere antzeman ditzakete. Horretarako, integrinak eta DDR-ak (discoidin domain receptor) adierazten dituzte, hauen bitartez, ECM-aren osagaiak detektatu eta hauei erantzun desberdinak ematen dizkiete. Hau da, ECM-en osagaien aldaketen arabera, HSC-ak diferentziatu, hazi edo migratu dezakete (56, 57). Azpimarragarria da HSC-ek TLR hartzaile desberdinak adierazten dituztela. Ildo honetan, hesteetatik gibelera translokatutako bakterietatik eratorritako produktuak, TLR-etara lotu eta HSC-etan eragina izan dezakete. LPS-a, hain zuzen ere, TLR4-ra lotu eta faktore pro-fibrogenikoen adierazpena emendatzen du, TGFß-ren adierazpena barne, hortaz, HSC-en trans-diferentziatzioa eraginez (58).

Estimulu hauek denek, HSC-en portaera aldarazten dute. Honela, aktibazio prozesuan eraldaketa genetiko eta epigenetikoak gertatzen dira. Eraldaketa hauen ondorioz, autofagia, erretinoideen galera, hazkuntza, uzkurkortasuna, kemotaxia eta ECM-ko proteinen ekoizpen eta jariapena bideratzen dira HSCs-etan (52). Aktibazioan edo trans-diferentziatioan ematen diren eraldaketa genetiko eta epigenetikoen itu nagusiak I motako kolagenoa, TGF-β1 eta TGF-β hartzaileak, MMP2 (matrix metaloprotease2), TIMPs 1 eta 2 (tissue inhibitors of matrix metalloproteases 1 eta 2) eta aSMA (alpha-smooth muscle actin) dira (52). Egoera aktibatuaren eta erantzun fibrotikoaren mantenua seinale autokrino eta parakrinoen bidez lortzen da, hauek HSC-en hazkuntza bultzatzen dute euren fenotipo aktibatua mantentzen duten bitartean.

Hala ere, azken urteotan argitaratutako lanek iradokitzen dutenez, fibrosia prozesu itzulgarria da eta HSC-en aktibazioa itzultzen duten mekanismoak deskribatzen hasi dira. Ildo honetan, aktibazio prozesuan zehar HSC-etan zelulen heriotzaren hartzaileen adierazpena ere ematen da, euren ligandoak lotu ondoren, hartzaile hauek zelulen apoptosi bidezko heriotza dakarte (27). HSC-en aktibazioa itzultzeko beste mekanismo bat seneszentzia litzake, honen bitartez ECM-eko proteinen adierazpena murriztu eta MMP-ena emendatzen da (59). Azkenik, zelulak jarraitzen dituzten esperimentuei esker ikusi ahal izan da, aktibatutako HSC-en erdiak gene fibrogenikoak isilarazi eta kieszente antzeko fenotipoa berreskuratu dezaketela (60, 61).

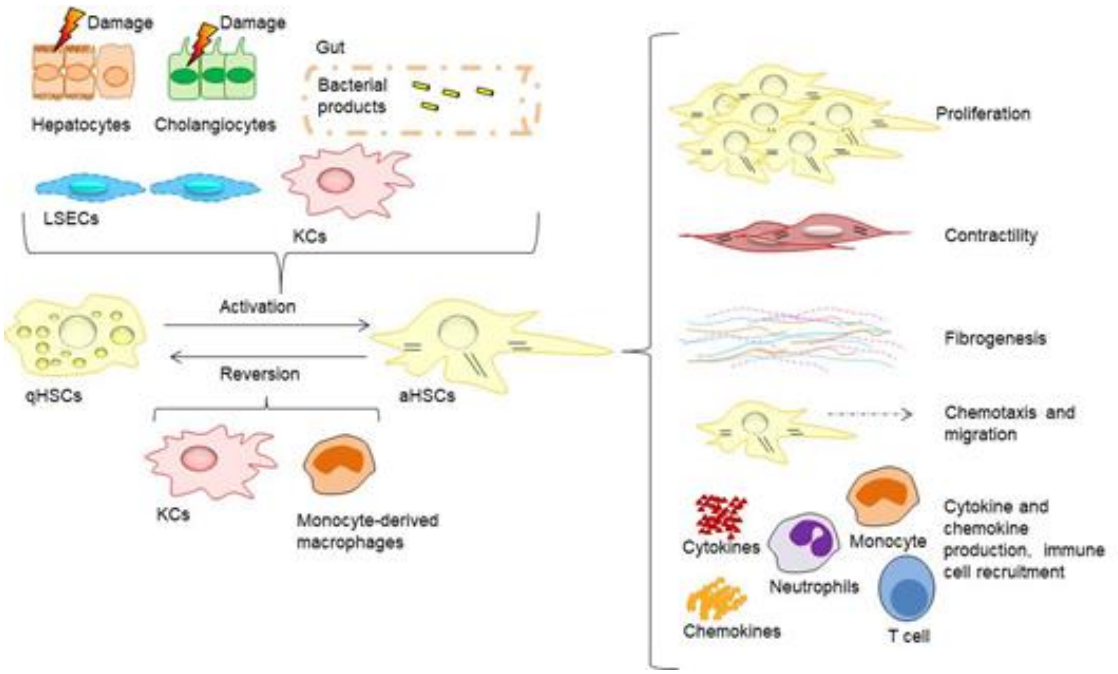

S.6. Irudia. HSC-en trans-diferentziazio prozesua. Gibeleko kaltearen ondorioz, HSC-ak trans-diferentziatu edo aktibatzen dira eta ECM ekoizten duten gibeleko zelula nagusiak bilakatzen dira. Prozesu honetan, HSC-ek miofibroblasto antzeko ezaugarriak bereganatzen dituzte, besteak beste, zelula hazkuntzaren emendioa, uzkurkortasuna edota ECM eta zitokina eta kemokina pro-inflamatorioen ekoizpena. Azken hauek, sistema immuneko zelulen erakarpena bideratzen dute. Prozesu hau itzulgarria da, sistema immune innatoko zelulek lagundutako HSCsen apoptosiaren bidez, edo kieszente antzeko fenotipo batera bueltatu daitezkeelako HSC-ak. aHSCs, activated hepatic stellate cells; KCs, kupffer cells; qHSCs, quiescent hepatic stellate cell *[Tsuchida T et al, 2017 (51) artikuluan oinarritua]*.

S.2. Gibeleko gaixotasun kronikoak

Aurreko ataletan aipatu bezala, gibela organismoaren homeostasi metabolikoa mantentzeko elkarlanean jarduten duten hainbat zelula motaz osatuta dagoen organo konplexua da. Bere konplexutasuna dela eta, gibela jatorri anitzetatik eratorri daitezkeen hainbat gaixotasunen itu da. Gibeleko gaixotasunek, organo honen zelula epitelialak dituzte itu nagusitzat. Horrela, gaixotasun hepatozelularrak, hots, hepatozitoak itu dituztenak, eta behazun hodietako gaixotasunak, hau da, kolangiozitoak itu dituztenak, bereizi daitezke (62).

Alde batetik, gaixotasun hepatozelularren artean, hainbat aurki ditzakegu, hepatitis B eta C birusek (HBV eta HCV) eragindako infekzioak (63, 64), gibeleko gaixotasun alkoholikoa (65), gibeleko gaixotasun ez-alkoholikoa (NAFLD) (66), drogek eragindako gibeleko kaltea (67), hepatitis autoimmunea (68) eta hepatokartzinoma (HCC), besteak beste (69). Gaixotasun hepatozelularrak mundu mailako osasun erronka plazaratu dute, honen erakusle da, NAFLD gaixotasuna munduko biztanleriaren %24-k

pairatu dezakeela uste dela (70). Bestalde, behazun hodietako gaixotasunak edo gibel barneko eta kanpoko kolangiozitoak itu dituzten gaixotasunak, kolangiopatia izenez ezagutzen dira (71). Kolangiopatiak honela sailka daitezke, gaixotasun genetikoak, infekziosoak, immunitateak edo drogak eragindakoak, idiopatikoak, malignoak edo baskularrak (72). Kolangiopata nagusiak (**S.1. Taula**) taulan ikus daitezke. Era indibidualean kolangiopatiak gaixotasun arraroak dira, baina taldekatuta, morbilitate eta heriotza tasa esanguratsuak eragiten dituzte (6), eta gaixo hauetako askorentzat gibeleko transplantea da sendatzeko aukera bakarra (73).

S.1. Taula. Kolangiopatiak. *[Cheung A-C et al, 2017 (72) artikuluan oinarritua]*

Genetikoak
Allagile-ren sindromea
Caroli-ren sindromea
Fibrosi kistikoa
MDR3-ren gabezia
Gibeleko gaixotasun polikistikoak (ADPLD, ADPKD, ARPKD)
Immunitateak eragindakoak
Alo-transplantearen errefusa akutua
Alo-transplantearen errefusakronikoa
Transplantea hartzailearen kontra gaixotasuna
Kolangitis biliar primarioa
Kolangitis esklerosante primarioa
Idiopatikoak
Atresia biliarra
Haurtzaro edo helduaroko duktopenia idiopatikoa
IgG4 kolangiopatia
Sarkoidosia

Infekziosoak
HIESA-ren kolangiopatia (e.g. kolangitis birikoa)
Kolangitis bakterianoa (e.g. *E. coli, Klebsiella*)
Kolangitis parasitarioa (e.g. *Opisthorchis viverrini*)
Malignoak
Kolangiokartzionma
Bestelakoak
Drogek eragindakoak
Baskularrak edo iskemikoak

ADPLD, autosomal dominant polycystic liver disease; ADPKD, autosomal dominant polycystic kidney disease; ARPKD, autosomal recessive polycystic kidney disease; MDR3, multidrug resistance protein 3.

S.2.1. Gaixotasun kolestatikoak

Kolestasia egoera patologiko multifaktoriala da, jatorri anitzetako kolangiopatietan garatu daitekeena. Honela, gaixotasun kolestatikoek askotariko etiologia dute, haien artean, genetikoak, toxinek edo drogek eragindakoak, buxadurazkoak edo immunitatearekin lotutako gaixotasun kolestasikoak aurkitu daitezke (74). Kolestasiaren ezaugarri nagusia behazun fluxuaren murrizketa edo gelditzea da, honen ondorioz, BA-en eta behazuneko beste molekula toxikoen metaketa gertatzen da gibelean (75).

Kolangitis biliar primarioa (primary biliary cholangitis, PBC) eta kolangitis esklerosante primarioa (primary sclerosing cholangitis, PSC), helduetan sortzen diren gaixotasun kolestatiko kronikoen artean ohikoenak dira. Bai PBC bai PSC, behazun hodiak itu dituzten prozesu auto-immuneekin lotuta daude (74). Gaitz kolestatikoen garapenean pruritoa, nekea eta osteoporosia agertzen dira, baina gaixotasunaren garapenari lotutako egoera larriagoak ere sor daitezke, hauen artean zirroisia, hipertentsio portala eta gibeleko minbizien garapena (74) **(S.8. Irudia)**.

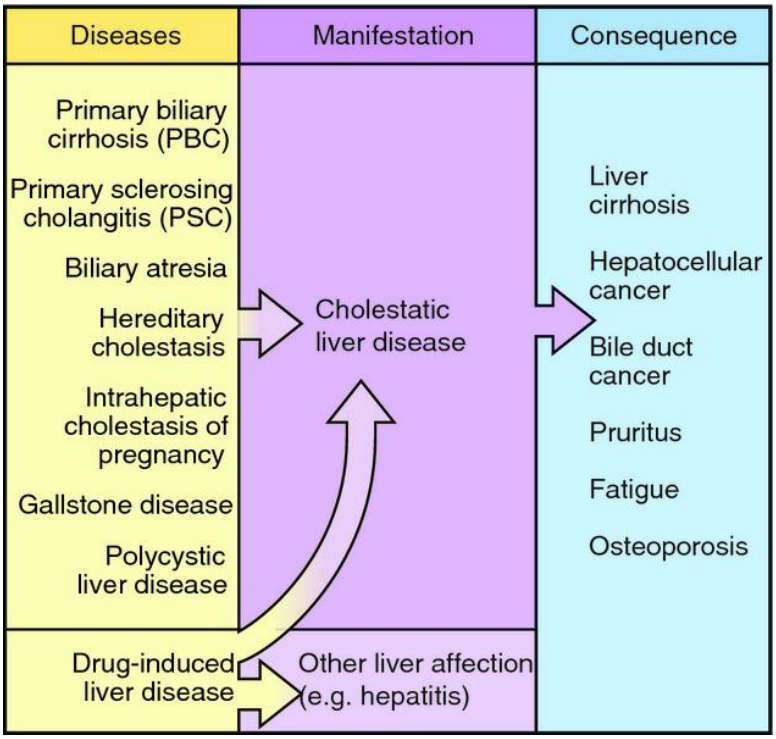

S.8. Irudia. Kolestasia eta bere agerpen klinikoak. Kolestasia jatorri desberineko hainbat kolangiopatietan garatzen den agerpen klinikoa da, hauen artean, PBC eta PSC helduetan ematen diren gaixotasun kolestatiko kroniko ohikoenak dira. Gaixotasun hauekin lotutako sintomen artean nekea, pruritoa eta osteoporosia daude, besteak beste. Egun, ez dago gaixotasun kolestatikoekiko estrategia terapeutiko egokirik eta kasu askotan, gaixotasun hauek aurrera egiten dute gibeleko zirrosia edo gibel zein behazun zuhaitzeko minbiziak garatu daitezkeelarik. *[Karlsen TH et al, 2014 (74) artikulutik egokituta]*.

S.2.1.1. PBC

PBC-a gaixotasun kolestatiko kroniko arraroa da, gaixotasun honen ezagarri nagusia da behazun hodi txiki eta tamaina ertainekoen kontrako fenomeno autoimmuneak garatzen direla, epe luzean fibrosia, zirrosia eta gibelaren funtzionamenduaren galera ekar dezaketenak (76). PBC-a gaixotasun arrarotzat hartzen da, bere prebalentzia Europan

100 000 biztanletik 35 kasukoa dela kalkulatzen baita eta bere emakume/gizon ratioa 10/1-ekoa da (77). PBC-dun pazienteen serumeko markatzaile nagusia PDC-E2 konplexua itu duten antigorputz antimitokondrialen (antimitochondrial antibody, AMA) agerpena da, PBC-dun pazienteen ~%95-ean aurkitzen direnak (78, 79).

PBC-ren fisiopatologia konplexua da eta honetan kolangiozito eta sistema immuneko zelulen arteko elkarrekintzaren homeostasia eraldatzen duten faktore genetiko, epigenetiko eta ingurunekoek parte hartzen dute (**S.9. Irudia**). PBC-aren patogenesian funtsezko urrats bat da antigeno mitokondrialekiko tolerantziaren galera da, batik bat, PDC-E2-rekikoa. Tolerantziaren galera hau, antzekotasun molekularreko mekanismoek eragin dezaketela uste da. Honela, *Escherichia coli-k* (*E. coli*) eragindako gernu sistemaren infekzioak, bai eta onddo edota birus bidezko infekzioak PBC-a jasateko arrisku handiagoarekin lotzen dira (80). Gainera, sistema immuneko hainbat zelula talderen derregulazio orokorra dago PBC-aren garapenaren atzean. Hau, HLA (human leukocyte antigen) lokusaren eta bestelako sistema immuneko bidezidorren geneetan aurkitu diren eraldaketekin lotzen da (81). Ildo honetan, PBC-dun gaixoek CD4+ T zelulen eta CD8+ T zelulen erakarpena aurkezten dute gibelean, hau bidezidor proinflamatorioen gehiegizko aktibazioaren eta mekanismo erregulatzaileen funtzionamendu akastunarekin bat dator (82-84).

Halaber, kolangiozitoak ere hainbat eraldaketa molekularren itu dira gaixotasun honetan (80). PBC-aren ezaugarri bereizgarri den eraldaketa epigenetiko batean AE2 (anion exchanger 2) itu duen mikroRNA 506 (miR-506) da protagonista nagusia. miR-506 gainadierazita dago PBC-dun gaixoetan, honek AE2-ren adierazpenaren murrizketa dakar, eta, ondorioz, behazunaren alkalinizazio akastuna eta bikarbonato aterkiaren ahulezia behatzen dira. Honek denak kolangiozitoak BA-bidezko apoptosiarekiko sentikorrago bihurtzen ditu (85). Are gehiago, kolangiozitoek TLR-ak adierazten dituzte, hauek bakterietatik eratorritako produktuen loturaren ondorioz aktibatu eta mikroingurune pro-inflamatorioa eta erantzun auto-immuneak sustatzen dituzte (86, 87).

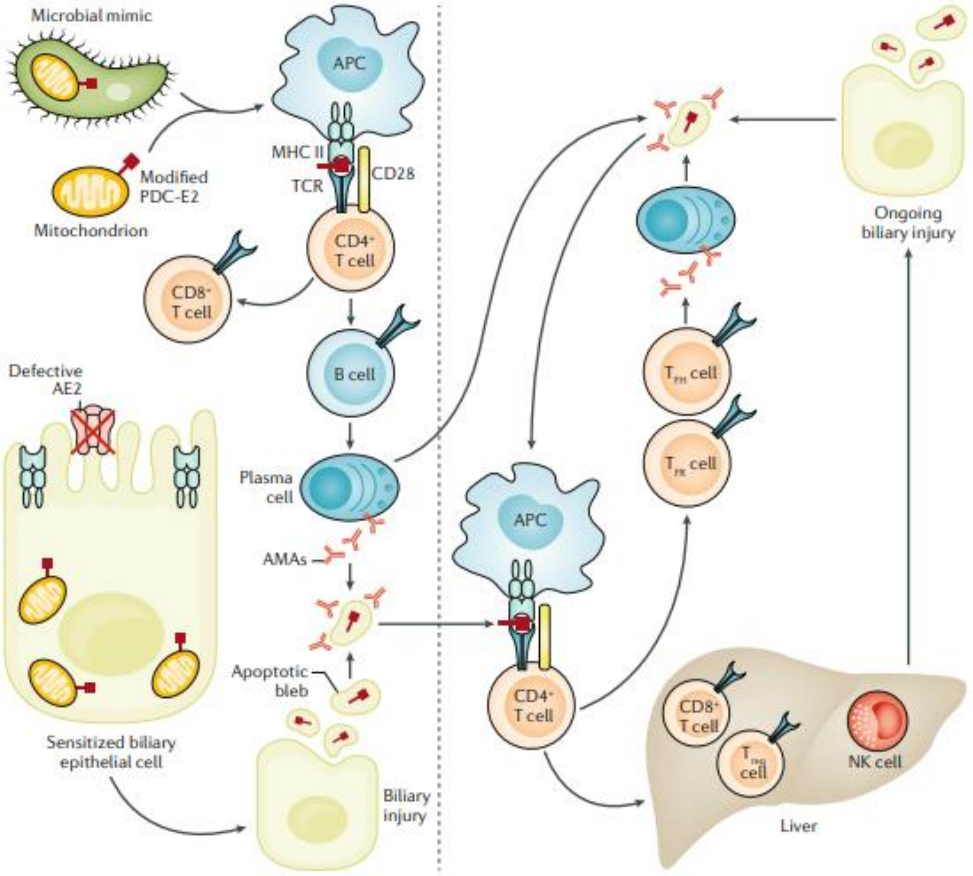

S.9. Irudia. PBC-aren fisiopatologia. PBC-an PDC-E2-rekiko AMA-en ekoizpena ezaugarri duen erantzun immune akastuna ikusten da. Gaixo hauetan ikusten diren erantzun autoimmuneen atzean antzekotasun molekularra dagoela uste da. Honez gain, sistema immunearen eraldaketa orokorra ere aurkezten dute gaixo hauek, honetan, T zelula efektoreen eta NK zelulen emendioa eta hauen gehiegizko aktibazioaz gain, T zelula erregulatorioen murrizketa behatzen da. Kolangiozitoak ere hainbat eraldaketen itu dira, hauetan AE2-ren adierazpenaren murrizketa ikusten da eta bikarbonato aterkia ahulagoa da, zelulak apoptosiaren bidezko heriotzarekiko sentikorrago bihurtuz. AE2,anion exchanger 2; AMAs, antimitochondrial antibodies; APC, antigen presenting cell; CD28,cluster of differentiation 28; MHC II, major histocompatibility complex II; TCR, T cell receptor *[Gulamhusein A et al, 2020(81) artikulutik egokitua]*.

S.2.1.2. PSC

PSC gaixotasun arraro bat da, Iparraldeko Europa eta Estatu Batuetan (AEB) 10 000 binztanleko 1-eko prebalentzia duena (88, 89), Espainian, aldiz, bere prebalentzia bajuagoa da, 10 000 binztanleko 0.022 kasukoa (90). PSC gaixotasun kolestatiko kroniko bat da, behazun hodiko estutze-gune multi-fokalak eta behazun zuhaitzeko inflammazio iraunkorra ezaugarri dutuena (91). Gainera, PSC gaixotasuna behazun zuhaitzeko minbizia, hau da CCA (cholangiocarcinoma) garatzeko arrisku faktore bat da (91). Gaixotasun honen diagnostikoa erresonantzia magnetikozko kolangiografiaren

irudi tekniken bidez, eta bestelako bigarren mailako kolangitis esklerosantearen kausa ezagunen esklusioaren bidez burutzen da (92).

PSC-aren patologiari dagokionez, gaixo hauek gibelean tipularen azalaren itxura duen behazun hodien ingurko fibrosi kontzentrikoa aurkezten dute (92). Bere etiologia oraindik ezezaguna den arren, faktore genetiko zein inguruneko faktore batzuk gaixotasun honekin lotu izan dira (91) (**S.10. Irudia**). Ildo honetan, "genoma-wide association" ikerketetatik eratortzen den aurkikuntza nabarmenenean, HLA lokusa PSC-a pairatzeko arrisku faktore bezala identifikatu da (93, 94) . Gainera, inguruneko faktore ezezagunen parte hartzea ere garrantzitsua da gaixotasun honen garapenean, honela, gaixotasuaren patogenesiaren aspektu batzuk bideratu ditzakete faktore hauek (91). Ildo honetan, PSC-dun gaixoek hesteetako mikrobiotan eraldaketak aurkezten dituzte, oro har, mikrobiotaren aniztasunaren murrizketa behatzen da (95). Gainera, PSC-dun gaixoen kolangiozitoek ere fenotipo akastuna dute (96). Hau, behazun hodien inguruko fibrosi eta zirrosiaren atzean egon daitekeela uste da, kolangiozito eta HSCs edota PM-en arteko elkarrekintza eraldatuz (47, 97).

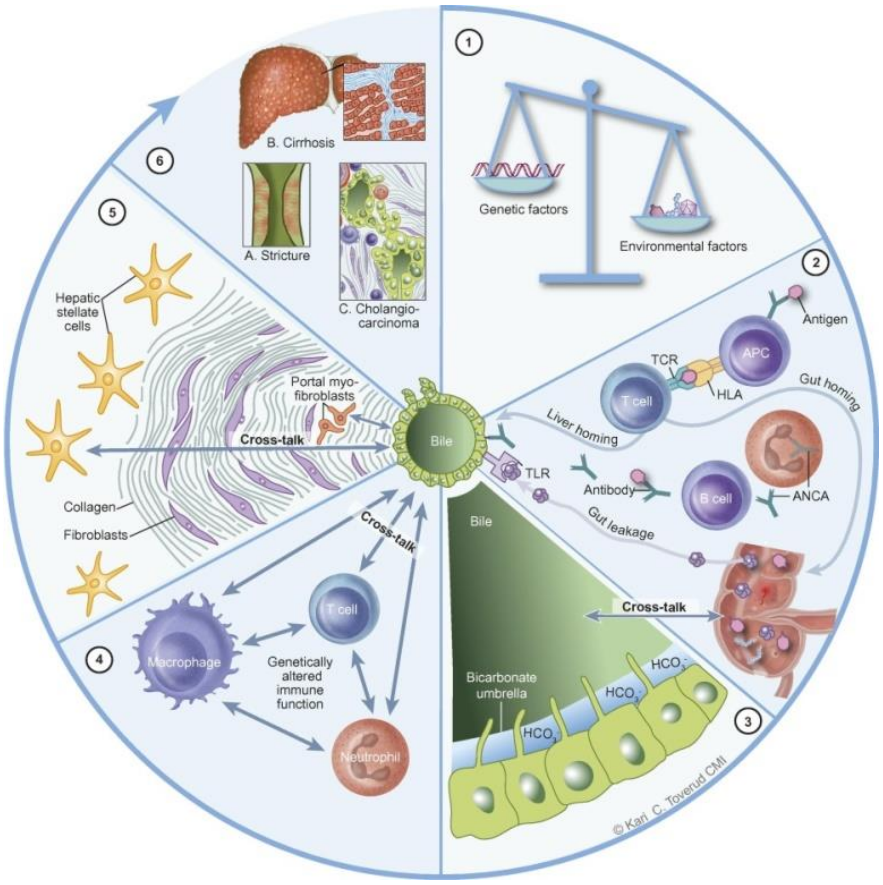

I.10. Irudia. PSC-aren fisiopatologia. (1) PSC-a eraldaketa genetikoen zein inguruneko eraldaketen ondorioz garatzen da. **(2-4)** PSC-arekin lotzen diren eraldaketa genetikoak batez ere HLA lokusean ematen dira eta antigenoaren aurkezpen akastuna dakarte. Gibel-heste ardatza, hesteetako disbiosia dela eta, bakterietik eratorriko produktuak TLR-etara lotzean, erantzun autoimmuneak areagotzeko gai dira. Behazunaren homeostasia eta kolangiozitoen fisiología ere eraldatuta daude kolangiozitoen kontrako sistema immunearen erasoa dela eta, honela, kolangiozitoak aktibatu eta sistema immuneko zelulekin elkarrekintza estua eratzen dute. **(5-6)** Prozesu hauek, guztiak, HSCs-en aktibazioa dakarte, zelula hauek fibrosia eta gaixotasunaren egoera larriagoak zuzentzen dituzte, behazun hodien estutze guneak, zirrosia eta baita CCA-ren garapena erraztuz *[Karlsen TH et al, 2017 (91) artikulutik egokitua]*.

S.2.1.3. PBC eta PSC-a tratatzeko aukera terapeutikoak

PBC eta PSC gaixotasunetan faktore autoimmuneek berebiziko garrantzia duten arren, immunosupresoreetan oinarritutako aukera terapeutikoek ez dute efektu onuragarririk ekarri paziente hauetan (76, 98). UDCA (ursodeoxycholic acid), BA endogeno eta koloretiko batek, kolestasidun gaixoetan eragin onuragarriak izan zitzakeela ikusi zenetik, erreferentziazko tratamendutzat hartzen da gaixotasun hauetan (22). Egun, UDCA lehen mailako terapia da PBC-dun gaixoentzat. UDCA-ak PBC-dun gaixoetan eragiten dituen efektuak bere ezaugarri koleretikoekin lotzen dira, honela, BA hidrofobikoek heapatozito eta kolangiozitoen kontra eragiten duten erasoa murrizten da

(99). Horrez gain, UDCA-k efektu anti-apoptotikoak eragiten ditu kolangiozitoetan (100) eta erantzun anti-inflamatorioak zuzendu ditzake GR-an (glucocorticoid receptor) duen eraginaren ondorioz (101). Hala ere, PBC-dun gaixoen %30 inguruk UDCA-rekiko erantzun ez-egokia erakusten du, eta portzentaia hau %50-era igotzen da 40 urtetik beherako gaixoen artean (102). Kontuan hartzekoa da, UDCA-rekiko erantzun ez-egokia erakusten duten paziente hauek gaixotasunari lotutako egoera larriagoak garatzeko arrisku handiagoa dutela, beraz, azkenean gibel trasplantearen beharra izan dezakete (98). PSC gaixotasunari dagonionez, UDCA-an oinarritutako tratamendua serumeko entzimen mailak eta gibelaren histologia hobetzeko gai zela ikusi zen (103). Egun, PSC-dun gaixoak tratatzeko UDCA-ren erabilera zabalduta dago zentro batzuetan (103). Hala ere, eztabaida dago UDCA-k PSC-dun gaixoetan izan dezakeen eraginkortasunaren inguruan, ikerlan batzuetan PSC-dun gaixoak UDCA-ren dosi altuekin tratatzeak ondorio larriak izan dezakeela behatu baitute (104). Hori horrela, gibelaren ikerketarako Europako elkarteak (European Association for the Study of the Liver, EASL) UDCA-ren erabilera onartzen du PSC-aren tratamendurako, Amerikako elkartea (American Association for the Study of Liver Disease, AASLD), aldiz, bere erabilpenaren aurkakoa da (105).

Azken urteotan PBC eta PSC-a tratatzeko estrategia terapeutiko berriak garatu dira. Hauen artean, hartzaile nuklearren agonistak, nagusiki OCA (obeticholic acid), PBC-aren tratamendurako eraginkorra izan daitekeela adierazi da hainbat ikerlanetan (106-108). PSC-aren tratamendurako, ordea, vancomycina antibiotikoak eragin onuragarriak ditu gaixo hauetan (109). Hala ere, orokorrean, gaixotasun kolestatikoek erantzunik gabeko erronka klinikoa plazaratu dute, izan ere, gaixo hauentzako aukera terapeutikoak murritzak dira eta kasu askotan, gaixotasunak aurrera egiten du egoera larriagoen garapena ekarriz.

S.2.2. Gaixotasun kolestatiko kronikoen garapena

Gibeleko gaixotasunen jatorria desberdina izan arren, bere progresioak antzeko ezaugarriak partekatzen ditu (27) **(S.11. Irudia)**. Hasierako estimulu kaltegarriek gibelaren osagai epitelialak dituzte itu nagusi bezala (hots, hepatozitoak eta kolangiozitoak) zelula hauen heriotza eraginez (110). Hepatozito eta kolangiozitoen heriotzak zauri-sendatze erantzuna pizten du. Honetan, gibelaren osagai epitelialek eta ez-epitelialek parte hartzen dute era koordinatu batean, mekanismo inflamatorio eta birsortzaileak martxan jarriz, galdutako gibel ehuna berreskuratzeko ahaleginean (111).

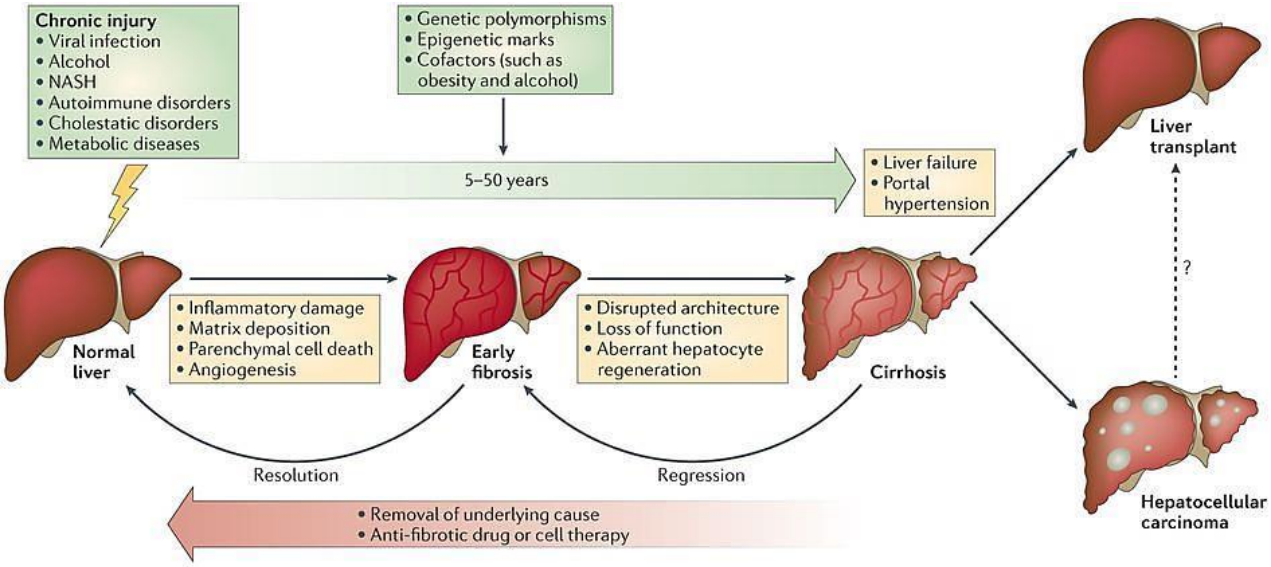

S.11. Irudia. Gibeleko gaixoatasun kronikoen garapena. Gibeleko gaixotasun kronikoen garapenak ezaugarri komunak ditu, baina gaixotasun zehatz bakoitzarekin lotutako fenomeno espezifikoak ere ager daitezke. Orokorrean, garapena hasierako estimulu kaltegarriarekiko erantzunarekin hasten da, estimulua denboran mantentzen denean, erantzun hau gehiegizkoa da eta inflamazio eta hepatitis iraunkorrak, fibrosia, zirrosia eta kartzinogenesiaren garapena ekar dezakete. *[Pellicoro A et al, 2014 (27) artikulutik egokitua]*.

Hasierako estimulu kaltegarria aldi baterakoa denean, zauri-sendatze erantzuna onuragarria da, kaltetutako gibelaren birsortzean laguntzen duelako (112). Kaltea iraunkorra denean, ordea, zauri-sendatze erantzunaren kontrola galdu eta denboran mantentzen da, gaixotasunaren progresioaren eragile nagusi bilakatuz (111). Antzeko ezaugarriak partekatzen dituzten arren, gibeleko gaixotasun kronikoekiko erantzunak gaixotasunaren jatorriaren araberakoak dira. Hau da, jatorri desberdineko gaixotasun kolestatiko kronikoek antzeko garapena dute, fibrosi biliarrarekin eta egoera larriagoen garapenarekin, horrela, zirrosia, hipertentsio portala eta gibeleko minbiziak ere agertu daitezke (312).

S.2.2.1. Kaltearen hastapenak gaixotasun kolestatikoetan

Gaixotasun kolestatikoetan gibeleko kaltearen hastapena eragiten duen faktorearen identifikazioa argitu gabeko gaia da oraindik. Mekanismo desberdinek eragindako zelularen heriotza behatzen da gaixotasun kolestatikodunen gaixoen gibelean, besteak beste, apoptosia, nekroposia edo autofagia behatu izan dira (113). Zelularen heriotza eragiten duen hasierako estimulua gaixotasun hauetan agertzen den gehiegizko erantzun immunearen eta BA-en eragin zuzen eta zeharkakoen konbinazioa dela uste da.

Gaarantzitsua da gogoan izatean PBC eta PSC gaixotasunak behazun hodiak itu dituzten fenomeno auto-inmuneekin lotzen direla. Auto-inmunitate honen ondorioz, T zelulak behazun hodietara erakartzen dira eta hemen kolangiozitoen aurkako eraso zitotoxikoak bideratzen dituzte (114). Are gehiaho, hipotesi klasikoaren arabera, BA-ak agente zitotoxiko zuzentzat hartzen dira, bere ezaugarri membranolitikoak direla eta. Berez, BA-ak zelulen mintza hondatzeko gai dira, hortaz, apoptosi eta nekroptosi bidezko zelularen heriotza eta baita zelulen seneszentzia ere eragin ditzakete (115-117) . BA-ek eragindako zelulen heriotzan parte hartzen duten mekanismoen artean JNK aktibazioa, FasL/Fas lotura eta mitokondrioen mintzaren hondatzea daude (118). Hala ere, hipotesi hau asko eztabaidatzen da gaur egun, *in vitro* erabili izan diren BA kontzentrazioak egoera kolestatikoetan aurkitutako kontzentrazioak baino altuagoak direlako (119, 120).

Gainera, BA-ak bitartekari pro-inflamatorio bezala joka dezaketela proposatu izan da azken aldian (119). Saguen hepatozitoak egoera kolestatikoetan lortzen diren TCA (taurocholic acid) eta GDCA (glycochenodeoxycholic acid) BA-en kontzentrazioekin (hots, 20-200 µM inguru) inkubatzeak, zitokina eta kemonika pro-inflamatorioen adierazpena sustazen du (121, 122). Are gehiago, BA-ek sistema immuneko kimio-erakarlea den (123) eta kolangiozitoen hazkuntza bultzatzen duen (124). osteopontinaren adierazpena eragiten dute. Hepatozitoetatik eratorritako zitokinak zein osteopontinak neutrofiloak erakartzen dituzte gibelera. Sistema inmuneko zelula hauek erantzun zitotoxiko indartsua bideratu dezakete eta kolestasiaren animalia eredu desberdinetan gibeleko kaltearen bitartekari nagusi bezala deskribatu izan dira (125-127). Gizakian, kalte kolestasikoaren eta gibeleko neutrofilo kopuruaren arteko korrelazioa dago eta, ICAM-I-en (intercellular adhesion molecule 1), hots, neutrofiloak gibelera erakartzen dituen proteinaren, adierazpena emendatuta dago paziente hauetan (128, 129).

S.2.3.2. Erreakzio duktularra

Hasierako estimulu kaltegarriek eraginda, zauri-sendatze erantzun bereizgarri bat pizten da gaixotasun kolestatikoetan. Erantzun honi erreakzio duktularra izena ematen zaio eta PBC eta PSC bezalako giza gaixotasun kolestatikoetan (130, 131), zein kolestasiaren animalia ereduetan, hauen artean, BDL-an oinarritutako buxadurazko kolestasikoan, kolestasi kimikoko DDC dietan oinarriturikoan eta *Mdr2* gabeko eredu genetikoan, behatu izan da erantzun hau (131). Erreakzio duktularra behazun hodien azalera emendatzeko ahalegin bat dela uste da, horrela, gibel barruan metatzen den behazuna kanporatu eta behazun hodien funtzio fisiologikoak mantendu ahal izateko (132).

Klasikoki kolangiozitoen hazkuntzaren ondorioz soilik ematen den behazun hodien hedapen eta adarkatzea bezala definitu den arren, egun, erreakzio duktularra hainbat zelula moten elkarrekintzaren ondorioz ematen den erantzun konplexua bezala ulertzen da (131, 136). Honela, erreakzio duktularrak bere gain hartzen ditu sistema inmuneko zelulen erakarpena (133), behazun hodien hedapena eta ECM-aren (134) eta gibelaren mikro baskulaturaren eraldaketa (135) **(I.12. Irudia)**.

Hainbat iturri zelular proposatu dira erreakzio duktularrean ematen den behazun hodien hedapena azaltzeko (131, 136). Alde batetik, erreakzio duktularra kolangiozitoen hazkuntzaren bidez azaldu daiteke. Gibel osasuntsuan, kolangiozitoak mitotikoki inaktiboak dira, baina kalte bat suertatu eta gero, fenotipo erreaktibo bat bereganatzen dute (137). Fenotipo honetan, zelulek garapeneko fase goiztiarren antzeko ezaugarriak aurkezten dituzte, hazkuntzaren emendioa eta jariapenaren aktibitate eraldatuak direla medio (6, 138). Gibeleko zelula progenitoreak ere zelula erreaktibo biliar-antzeko bilakatzeko gaitasuna dute (139). Zelula hauen aktibazioa jatorri anitzetako erreakzio duktularretan detektatu da (130). Gainera, zelulen jarraipeneko teknikaz egindako ikerketek azaleratu dutenez, hepatozitoek ere zelula erreaktibo biliar-antzeko bilakatzeko gaitasuna dute, kolangiozitoekiko kalte larria sortzen denean (140, 141). Fenomeno hau saguetan identifikatu da, baina horrelako prozesua gizakian ere eman daitekeen oraindik argitzeke dago (131).

Aurreko ataletan aipatu bezala, estimulu kaltegarria denboran mantentzen denean zauri-sendatze erreakzioa deskontrolatu egiten da eta gaixotasunaren garapenaren eragile nagusi bilkatzen da. Ildo honetan, bere jatorria edozein izanik ere, kolestasi kronikoan zelula duktular erreaktiboak (ductular reactive cells, DRCs) hazi eta metatzen dira, birsortze-prozesu akastun baten seinale (**S.12. Irudi**) (6, 136). DRC-ak behazun zuhaitzeko antzeko zelulak dira, baina kolangiozito osasuntsuekin alderatuz ezaugarri bereizgarriak adierazten dituzten, honela, zelularen nolabaiteko plastizitatea eta fenotipo jariatzaile nabarmena dute ezaugarri nagusitzat (136). DRC fenotipoa sustatzeko gai diren faktoreen artean, TNF, TWEAK (TNF-related weak inducer of apoptosis), TFGβ, HGF (hepatocyte growth factor), VEGF (vascular endothelial growth factor), Hh (sonic Hedgehog) eta Wnt/β-catenin bidezidorra deskribatu dira (142, 143). Prozesu honetan, DRCs-etan markatzaile mesenkimalen adierazpena emendatu eta markatzaile epitelialena murrizten dela ikusi da PBC eta PSC-dun gaixoetan (144) eta baita kolestasiaren animalia ereduetan ere (145). Horien artean, S100A4 (S100 calcium-binding protein A4), vimentina, snail eta MMP2-ren adierazpena emendatu eta E-

cadherina, era CK19-ren (cytokeratin 19) adierazpena murrizten da. Kontuan hartzekoa da erreakzio duktularraren helburua behazun hodien egitura mantentzea dela, eta, hortaz, behazun hodien morfogenesia zuzentzen duten Notch eta YAP (yes-associated protein 1) bezalako bidezidorren aktibazioa ere ematen da (146, 147).

DRC-en beste ezaugarrietako bat euren fenotipo jariatzailea da (148). Izan ere, inflamazioak berebiziko garrantzia du erreakzio duktularrean, zelulen arteko komunikazioa zuzentzen baitu. Honela, inflamazioak sistema inmuneko zelulen erakarpen eta aktibazioa eta erantzun fibrogenikoa zuzentzen ditu. DRC-ek KC-ak aktibatu eta makrofago (149) eta neutrofiloen (150) erakarpena eragiten duten kemo-erakartzaileak jariatzen dituzte, aldi berean, euren hazkuntza eta hedapena bermatzen dute CTGF (151) faktorearen jariapenaren bidez. IL8-ren, hots, neutrofiloen kemo-erakartzaile garrantzitsuenetako baten adierazpena handituta dago PBC eta PSC-dun pazienteen gibelean era serumean (152, 153). Gibelera erakarritako makrofago eta neutrofiloek, halaber, DRCs-en fenotipoa eta hazkuntza mantendu dezakete bitartekari inflamatorien ekoizpenaren ondorioz (6, 154). Kaltetutako kolangizitoek IL6 jariatu dezakete, honek funtzio autokrino eta parakrinoak ditu, aldi berean kolangiozitoen hazkuntza eta elkartruke inmunea sustatzen dituelako (6, 96). Gainera, behazun hodiak bere odol hodi sistema propioa dutela eta kalte egoeretan hau mantentzeko gai direla ikusi da (135). Horrela, behazun hodien hedapenarekin batera, angiogenesia ematen da, hau DRCs-etatik eratorritako VEGF, endothelin-1, oxido nitrikoak eta PDGF-BB faktoreek sustatu dezakete (154). Ildo honetan, odol hodi sistemako egituren emendioa eta VEGF eta beste faktore angiogenikoen adierazpena deskribatu da PBC-dun gaixoen laginetan (155). DRCs-ak erantzun fibrogenikoak sustatzeko gai dira, hau zehaztasun handiagoz azalduko da hurrengo atalean. Laburbilduz, erreakzio duktularraren ondorioz ingurune pro-inflamatorio indartsua sortzen da, behazun hodien hedapena, sistema inmuneko zelulen erakarpena, angiogenesia eta orbaindura ezaugarri dituena.

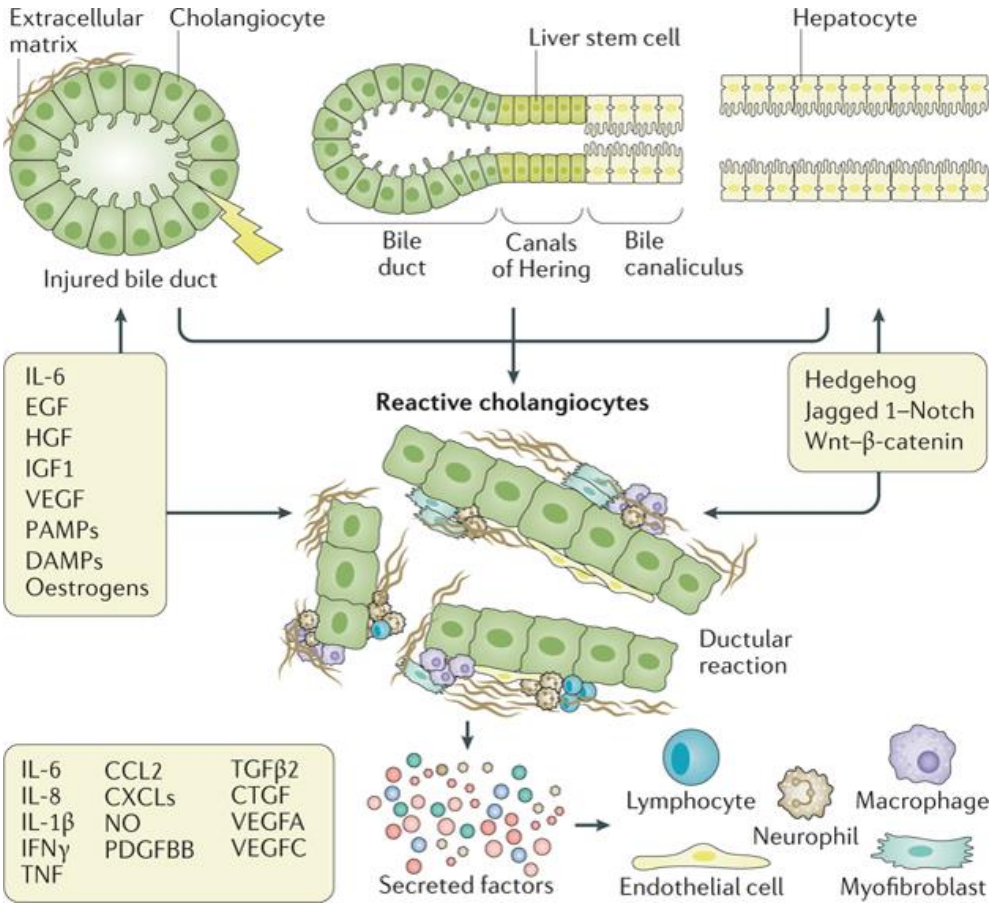

S.12. Irudia. Erreakzio duktularra eta zelula duktular erreaktiboak. Behazun zuhaitzeko kaltea eta gero, behazun zuhaitzeko egituren hedapena gertatzen da, metaturiko BAak kanporatu eta galdutako behazun zuhaitzeko masa berreskuratzeko ahaleginean. Zelula duktular erreaktiboak hainbat jatorrietatik eratorri daitezke, besteak beste, zitokina, DAMP, PAMP eta morfogenoei erantzunez kolangiozitoak, gibeleko zelula progenitoreak eta hepatozitoak zelula duktular erreaktibo bilakatu daitezke. Zelula hauek behazun zuhaitzeko zelulen antzeko fenotipoa dute baina des-diferentziazio nabarmenarekin eta fenotipo jaiatzaile nabarmenarekin. Hori horrela, beraien hazkuntza mantentzeko eta sistema immuneko zelulak, zelula endotelialak eta HSC-ak aktibatzeko zitokina inflamatorioak eta hazkuntza faktoreak jariatzen dituzte. CCL2, chemokine (C-C motif) ligand 2; CTGF, connective tissue growth factor; CXCLs, C-X-C Motif Chemokine Ligand 2; DAMPs, danger associated molecular patterns; EGF, epithelial growth factor; HGF, hepatocyte growth factor; IFNγ, interferon gamma; IGF, insulin growth factor; IL, interleukin; NO, nitric oxide; PAMPs, pathogen associated growth factor; PDGFBB, platelet derived growth factor BB; TGFβ2, transforming growth factor beta 2; TNF, tumour necrosis factor; VEGF, vascular endothelial growth factor; VEGFA, vascular endothelial growth factor A; VEGFC, vascular endothelial growth factor C *[Banales JM et al 2019 (6) artikulutik egokitua]*.

S.2.3.3. Fibrosi biliarra

Erreakzio duktularrean sortzen den mikro-ingurune inflamatorioak eta zelulen arteko komunikazio handiak, fibrosi biliarra sortzeko egoera egokia plazaratzen dute. Fibrosi biliarrean gehiegizko ECM-ko proteinen metaketa eta ECM-aren osagaien eraldaketa kualitatiboa ematen dira (156). Fibrosi biliarra porta-inguruko guneetan sortzen hasten

da eta portatik-portarako patroia jarraituz hedatzen da (148). Gaixotasun kronikoa garatzen den heinean, fibrosia gune lobularretara hedatzen da hepatozitoak bere gain hartuz, azkenean zirrosia, eta minbizia ere garatu ditzakete gaixo hauek (157).

Fibrosi biliarrean parte hartzen duen zelula mesenkimalen jatorriaren inguruan eztabaida dago oraindik (120, 136). Orokorrean HSC-ak gibeleko zelula fibrogeniko nagusia dira eta lan askotan deskribatu da haien parte hartzea erantzun fibrogenikoetan. Honela, fibrosi eta zirrosi biliarreko animalia ereduetan zelula mesenkimal gehienak HSC-etatik eratortzen direla frogatu da (47, 158). Hala ere, lan horietako batean fase zirrotikoak bakarrik aztertu zituzten, eta ez fibrosi biliarreko fase goiztiarrak (136, 158). Are gehiago, beste lanean, miofibroblasto portalak HSC-etatik bereizitako zelula mota bezala identifikatu dira, honek iradokitzen du miofibroblasto portalek paper berezia bete dezaketela kolestasian (47). Hain zuzen ere, miofibroblasto portalak behazun hodietako kaltearen testuinguruan identifikatu ziren lehenengo aldiz (159-161). Orduztik, euren espazio portaletako kokapen anatomikoa dela eta, miofibroblasto portalak behazun hodietako kalteari erantzuten dion lehenengo zelula mesenkimalak bezala deskribatu ziren (162). Hortaz, miofibroblasto portalak HSC-en aktibazio eta erakarpenean ere parte har lezakete, eta, ondoren, HSCs-ek euren gaitasun fibrogenikoaren ondorioz fibrosia gune lobularretara hedatuko lukete (120, 162).

Fibrogenesi biliarra DRCs-en eta zelula mesenkimalen arteko elkarlan estua du ezaugarri nagusitzat, hau ligando eta hartzaile baliokideen adierazpenaren bidez lortzen da (136) **(S.13. Irudia)**. Ildo honetan, DRCs-ek TFGβ2 (163), IL6 (164), PDGF-BB (165), MCP1 (166), CTGF eta osteopontina (167) jariatzen dituzte. Faktore hauek, zelula msenkimalen aktibazio zuzena eragiteaz gain, zeharkako faktore bezala ere funtzionatu dezakete, horrela, makrofagoak erakartzen dituzte, eta, hauek, faktore fibrogenikoen iturri garrantzitsua dira (136). Zelula mesenkimalek BA-en hartzaileak adirazten dituzte, gai hau eztabaidapean dagoen arren, lan batzuk adierazi dute BA-en hartzaileek, euren ligandoen loturaren ondorioz, zelula mesenkimalen aktiboazioa eragin dezaketela (168). Halaber, zelula mesenkimalek ere DRC-en portaera eraldatu dezakete. Fibroblasto portalek azido hialuronikoa adierazten dute, fibrosi biliarrean bereziki garrantzitsua dena eta behazun hodien proliferazioa bultzatzen duena (169). Ildo honetan, Wnt, Hh eta Notch bidezidorrek paper garrantzitsua betetzen dute DRC eta zelula mesenkimalen arteko komunikazioa, behazun zuhaitzeko egituren hedapena eta fibrogenesia sustatuz (136). Notch bidezidorrak HPC-en DRC-rako diferentziazioa eragiten du, miofibroblasto portalen Jag-1 eta HPC-en Notch-en arteko elkarkintza behar duen mekanismo baten bidez (136, 146). Gaixotasun kolestatiko kronikoetan, Hh

bidezidorraren eraldaketa behatu da, Hh-ren Sonic eta Indian ligandoen eta Gli1 eta patched-en emendioa ikusi da PBC-dun pazienteen DRCs-etan (170). Hh ligandoek hazkuntza eta ezaugarri mesenkimalak sustatzen dituzte DRC-etan (145), era berean miofibroblastoen aktibazioa eraginez (171). Wnt/β-catenin bidezidorreko hainbat kideren gainadierazpena ere ikusi da PBC eta PSC-dun gaixoetan (172, 173). Wnt-ligandoak DRCs-en hedapenarekin (174) eta zelula mesenkimalen aktibazioarekin lotzen dira (175).

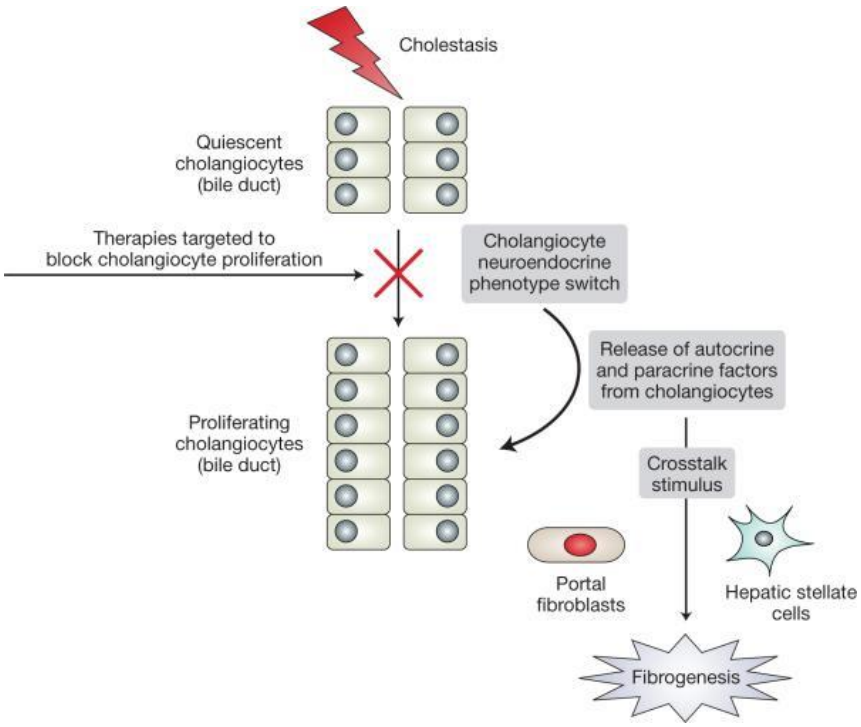

S.13. Irudia. Fibrosi biliarra. Kolestasiak kolangiozitoen aktibazioa eta hazkuntza eragiten ditu. DRC-ak PM-etara eta HSC-etara lotu eta hauek aktibatzen dituzten faktoreak jariatzen dituzte, honela fibrogenesia eraginez. Bestalde, PM-ek eta HSC-ek DRC-en fenotipoa mantendu eta beren hazkuntza sustatzen duten faktoreak jariatu ditzakete. *[Glaser S et al, 2009(176) artikulutik egokitua]*.

S.2.3.4. Kolestasi kronikoaren fase aurreratuak eta zirrosia

Gibeleko zirrosia fibrosiaren azkeneko fasetzat hartzen da eta gibeleko gaixotasun kroniko gehienetan ematen da, euren etiologia edozein izanda ere (177). Fibrosi biliarraren kasuan, zirrosia fase aurreratuetan garatzen da, hasierako gune portalen inguruko fibrosia, gune lobulerrata hedatzen denean, sinusoideak hartuz eta hepatozitoen funtzioa murriztuz (157). Zirrosian ECM-ren ekoizpen masiboa gertatzen da eta ECM hau gibelaren espazio parenkimala hartuz hedatzen da. Bizirik geratzen diren hepatozitoak ehun fibrosoaz inguratutako birsortze noduluetan antolatzen dira.

ECM zuntzen metaketak organoaren gogortzea dakar, gibelari orban moduko itxura emanez (177). Era berean, gibelaren desegituratze anatomikoak eragin zuzena du bere funtzioetan, gainera, organoaren gogortzeak odol hodien eraldaketa dakar, eta, ondorioz, hipertentsio portala garatzen da (178). Zirrosiaren beste konplikazioen artean esofagoetako barizeen odol galera, gibel entzefalopatia eta aszitisa daude (179). Orokorrean, zirrosia muturreko egoera bezala hartzen da eta gibeleko minbizia garatzeko ingurune egokia plazaratzen du, aldi berean, gibeleko transplanterako arrazoirik ohikoena da gaixo helduetan (180). Horrela, PBC eta PSC-dun gaixoen proportzio esanguratsu batek muturreko egoerak garatzen ditu, eta gibeleko transplantea behar izaten du. Zehatz esanda, 2002 eta 2016 urteen artean PBC-dun gaixoen %30-ak eta PSC-dunen %50-ak transplantea behar izan zuten, eta Europan egindako transplante guztien %10-a gaixotasun hauen ondoriozkoak izan ziren (181)

S.2.2.5. Gibeleko eta behazun zuhaitzeko minbizien garapena

Kolestasia eta gibel barruko BA-en metaketa estuki lotuta daude minbizi hepatobiliarrarekin (182). Lotura hau gaixoetan zein kolestasi eta bestelako gaixotasun hepatobiliarren animalia ereduetan behatu izan da. PBC-dun gaixoek HCC garatu dezakete gaixotasunaren azken faseetan (183), ildo berean, PSC-dun gaixoek kolangiokartzinoma (CCA) (184, 185), HCC, behazun maskuriko minbizia eta minbizi kolorektala garatzeko arrisku handiagoa dute (186). PSC eta CCA gaixotasunen arteko lotura estuaren erakusle, PSC gaixotasuna, CCA garatzeko arrisku faktore bezala identifikatu da AEB-n (kontrolek baino 171 aldiz arrisku handiagoa) (187) eta Ipar-Europan (kontrolek baino 160 aldiz arrisku handiagoa) (188).

S.2.2.5.1. Hepatokartzinoma

HCC-a hepatozitoen eraldaketa malignoaren ondorioz garatzen da. Munduko seigarren minbizi ohikoena da eta minbiziaren ondoriozko heriotzak eragiten laugarrena (190). HCC-en %80 inguru, gibel zirrotikoetan agertzen dira. Beraz, gaixo gehienek gibeleko gaixotasun kronikoren bat aurkezten dute, gehienetan, birusek eragindako infkezioek (HBV edo HCV), akoholak, edo obesitateak eragindakoak (189). Minbizi mota honekin lotutako heriotza kopuru handiaren atzean, bere izaera kimio-erresistentea eta diagnostiko goiztiarra buruzeko zailtasunak daude (191).

HCC-aren garapena urrats ugariko prozesu askoren koordinazioaren ondorioz ematen da. Hepatokartzinogenesia hepatozitoen heriotzarekin hasten da, honekin batera

inflamazioa, fibrosia eta hazkunza konpentsatoria garatzen dira (192). Testuinguru honetan, hasierako hazkuntza konpentsatorioa ahalbidetzeko, faktore mitogenikoen gainadierazpena ematen da. Faktore mitogenikoen adierazpena iraunkorra denean, gibeleko kaltea areagotu eta kontrolik gabeko hazkuntza bideratzen duen mekanismo autokrinoak eratzen dituzte (193) . Egoera honek mutazioen sorrera eta metaketa ere laguntzen ditu (194).

Onkogene eta tumore supresoreetan ematen diren mutazio somatikoek hepatozitoen eraldaketa malignoa bideratzen dute. HCC-aren ezaugarri bereizgarri bat bere heteregeneitate handia bada ere, gene batzuk maiztasun handiz agertzen dira mutatuta minbizi mota honetan (195). Mutazio hauen ondorioz, egoera normalean gibel helduan isilarazita dauden bidezidor asko ber-aktibatzen dira minbiziaren garapenean (196). Horrela, TERT-en (telomerase reverse transcriptase) mutazioak HCC-en %60-ean aurkitzen dira, Wnt/β-Catenin bidezidorreko geneak (CTNNB 18%, AXIN1 8%) eta TP53 (25-30%) genea ere askotan agertzen dira mutatuta (192, 195) . Minbiziarekin lotutako beste bidezidor batzuk ere eraldatuta daude tumore hauetan, hauen artean kromatinaren remodelazioa eta eraldaketa epigenetikoak bideratzen dituzten bidezidorrak edota estress oxidatiboaren erregulatzaileak. Era berean, Notch, Hedgod, NF-κB, PI3K/AKT/mTOR, Ras/RAf/MEK/ERK eta JAK/STAT bidezidorrak ere eraldatuta egoten dira paziente hauetan (195).

S.2.2.5.2. HCC-rentzako terapia

HCC-arentzako terapiaren onurak gaixoen taldekatze egokiarekin estuki lotuta daude. Hainbat taldekatze aukera proposatu izan diren arren, BCLC (Barcelona Clinic liver cancer) aukera da zabalduen dagoena eta era prospektiboan balioztatu den bakarra (197). BCLC mailakatze sistemak tumorean egoera, eta gibelaren funtzioaren eta minbiziarekin lotutako sintomen azterketa konbinatzen ditu, maila bakoitzeko estrategia kliniko egokiak proposatuz (191) . Maila goiztiarrean dauden HCC-dun paziente gutxi batzuk bakarrik dira resekzio sendatzailerako edo transplanterako egokiak (198), baina maila goiztiar zein ertaineko HCC-ak dituzten gaixo gehienak terapia loko-regionalen bidez tratatzen dira (199). Maila aurreratuko HCC-ak dituzten gaixoentzat, aldiz, multikinasen inhibitzaileetan (adibidez, sorafenib) oinarritutako terapiak dira aukera bakarra (200). Honez gain, onko-immunoterapia konbinatua erabiltzen duten estrategiek, maila aurreratuko HCC-ak dituzten gaixoetan onura batzuk ekartzen dituztela behatzen hasi da azken aldian (201).

S.2.3. Heste-gibel ardatza

Gizakiaren hesteetan 100 triloi bakteria bizi dira, hauek gizakiarekin sinbiosian bizi dira eta organismoaren hainbat funtzio metaboliko behar bezala burutzeko ezinbestekoak dira (202). Hori dela eta, giza organismoak elikagaietako bakteriekiko eta mikroorganismo endogenoekiko tolerantzia mantentzeko hainbat neurri garatu ditu (203) . Bere kokapen anatomikoa dela eta, gibelak kontaktu zuzena du hesteekin, porta zainaren bidez, hortaz, mikrobioma eta organismoaren arteko elkarrekintzan berebiziko garrantzia du gibelak (204, 205).

S.2.3.1. Bakterien lekualdaketa patologikoa

Gibeleko gaixotasun kronikoetan organismoa eta hesteetako mikrobiotaren arteko elkarrekintza sinbiotikoa bermatzen duten mekanismoek huts egiten dute. Ondorioz, hesteetako epitelioak bere egitura galtzen du, honela, lotura hertsien galera, mukiaren eraldaketa, denfensinen jariapenaren murrizpena eta, orohar, geruza epiteliala hartzen duten bakteriekiko erantzun immune murriztua behatzen dira (202). Aldi berean, mikrobiotaren disbiosia gertatzen da, bakterien andui patlogikoen gehiegizko hazkuntza ematen da, alegia. Fenomeno hauek, guztiek, bakteria eta bakterietatik eratorritako produktuen hestetik-gibelerako lekualdaketa ahalbidetzen dute (206).

Hesteetatik gibelerako bakterien lekualdaketa patogokikoaren ondorioz, gibelean hainbat PAMP agertzen dira, besteak beste LPS, azido teikoikoa edota bakterien DNA (207).. PRR (pattern recognition receptors) hartzaileek PAMP hauek ezagutzen dituzte (208). PRRs-en artean bi familia nagusi ezagutzen dira: TLR-ak eta NLR-ak (NB-LRR-related). TLR-en familia da gehien aztertu eta ezagutzen dena, ligandoaren loturaren ondorioz, TLR-ek MyD88 (myeloid differentiation primary response 88) adaptatzailearen bidez seinaleztatzen dute, eta gene pro-inflammatorioen transkripzioa sustatu (209). Kontuan hartzekoa da PRR-ak eta, bereziki, TLR-ak gibeleko kaltearen ondorioz, hiltzen diren zelula epitelialetatik eratorritako DAMP-en bidez ere aktibatu daitezkeela (111, 210). Beraz, TLR-ek infekzio zein kalteari erantzunez pizten diren zauri-sendatze prozesuak bideratzen dituzte, gibeleko gaixotasunen testuinguruan garrantzi berezia hartuz (210). Gibelean TLR-ak KC eta HSC-etan adierazten dira nagusiki (**S.14. Irudia**). TLR2, TLR4 eta TLR9-ren aktibazioak erantzun inflammatorioak, eta hortaz, gibeleko gaixotasunen garapena areagotzen dituela behatu da (58, 211, 212). Era berean, TLR4-rik gabeko saguak gieleko kalteaz babestuta daude, hainbat kontestutan (213-215) eta TLR2, TLR9 eta TLR4 geneen polimorfismoek

lekualdatutako bakteriekiko erantzun inflammatorioetan eragiten dute, gibeleko zirrosiarekin lotutako konplikazioak sortuz (216).

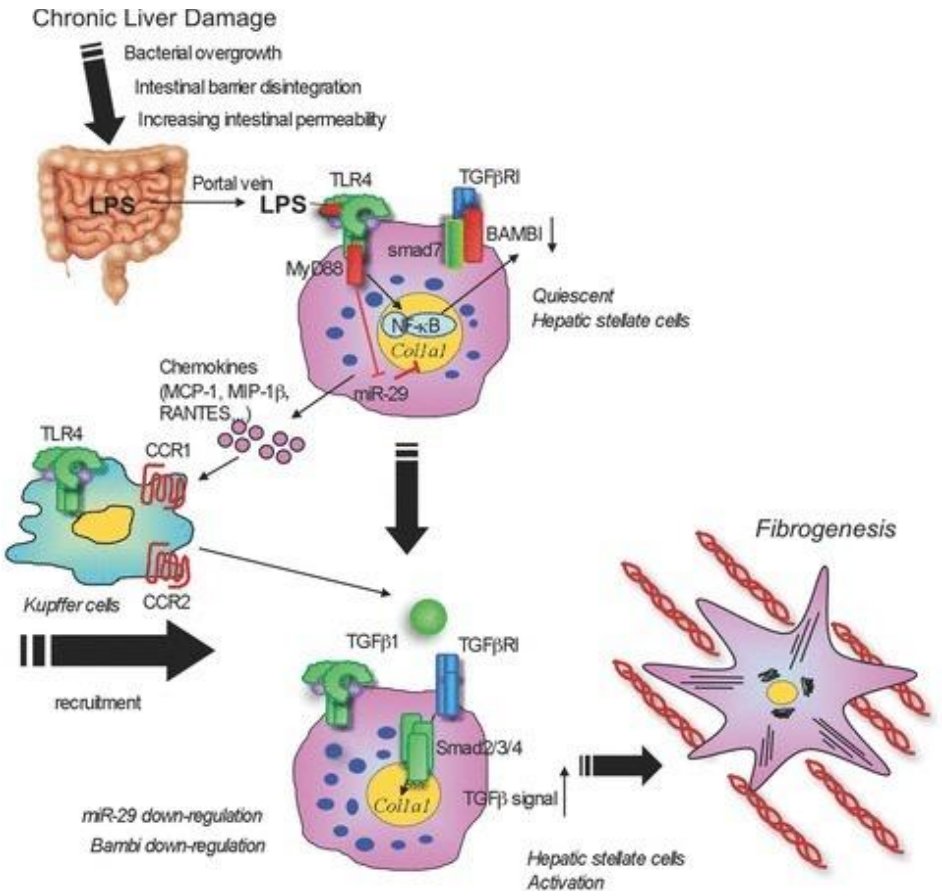

S.14. Irudia. Bakterien lekualdaketa patologikoak KC eta HSC-etan dituen eraginak. Gibeleko kalte kronikoak bakterietatik eratorritako produktuen, batez ere, LPS, hesteetatik gibelerako lekualdaketa eragiten du. Gibelean, bakterietatik eratorritatko produktuek TLR-ei lotzen zaizkie, batez ere TLR4-ari, KC-etan eta HSC-etan adierazten direnak. TLR4-ari lotu ondoren, LPS-ak KC-en eta HSC-en aktibazioa eragiten du. Honek, azkenean, fibrogenesiaren garapena dakar. BAMBI, BMP and activin membrane bound inhibitor; CCR, chemokine (C-C motif) receptor; COL1A1, collagen type 1 alpha 1; MAPK, mitogen-activated protein kinases; MCP1, monocyte chemoattractant protein 1; Mip-1β (CCL4), C-C motif chemokine ligand 4; Myd88, myeloid differentiation primary response gene 88; NF-κB, nuclear factor kappa B; LPS, lipopolysaccharide; RANTES (CCL5), C-C motif chemokine ligand 5; TGFβ, transforming growth factor β 1; TGFβR, transforming growth factor β receptor; TLR, toll-like receptor. *[Seki E et al, 2012 (217) artikulutik egokitua]*

S.2.3.2. Bakterien lekualdaketa patologikoa gibeleko gaixotasun kronikoetan

Kolestasian, behazun zuhaitzaren egituraren galera dela eta, behazuna gibelean metatzen da eta ezin da hesteetara heldu. Hori dela eta, behazunak ezin ditu bere efektu anti-mikrobianoak burutu hesteetan, eta honek, bakterien gehiegizko hazkuntza eta gibelerako lekualdaketa errazten ditu (218). Ildo honetan, bakterien lekualdaketak

garrantzi handia hartzen du PBC eta PSC bezalako gaixotasun kolestatikoetan (204). Hainbat ikerlanek deskribatu dutenez, bakterien gehiegizko hazkuntza eta bioaniztasunaren murrizketa ezaugarri duten mikrobiotaren eraldaketa kualitatibo eta kuantitatiboak gertatzen dira PBC eta PSC-dun gaixoetan (95, 219). Are gehiago, serumean LPS-a lotzen duen proteinaren eta CD14-ren (cluster of differentiation 14) maila altuak izateak (biak bakterien lekualdaketarekin lotutako markatzaileak izanik) prognostiko okerragoarekin lotzen dira PBC eta PSC-dun gaixoetan (220, 221). Are gehiago, PBC eta PSC-dun gaixoetan aurkitzen diren auto-antigorputzak bakterietatik eratorritako osagaiekin errakzionatu litzakete eta antzekotasun molekularreko prozesuak sustatu (222).

Era berean, hepatokartziongenesian heste-gibel ardatzaren garrantzia azaleratzen da hainbat lanetan (205). *Tlr4*-rik gabeko saguak HCC-aren garapenaz babestuta daude. Zehatz esanda, TLR4-ren seinaleztapenak HCC-ren garapena sustatzen du zeluletan eragiten dituen hainbat efektuen bidez, honela HSC-etan NF-κB-ren aktibazioa eta epiregulinaren adierazpena eta jariapena bultzatzen ditu. Era berean, honek hepatozitoen hazkuntza eta apoptosiaren inhibizioa dakar (213). KC-etan, LPS-TLR4 seinaleztapenak IL6 eta TNF-ren adierazpena sustatzen ditu, eta faktore hauek hepatozitoen hazkuntza eta inflamazioari lotutako HCC-aren garapena dakarte (223). LPS-aren tratamenduak HCC-zelulen hazkuntza sustatzen du *in vitro* eta *in vivo* (224). Mikrobiotaren metabolismotik eratorritako metabolitoek ere, eragina dute hepatokartzinogenesian. Disbiosiak DCA (deoxycholic acid) BA sekundarioaren kontzentrazioaren emendioa dakar, DCA-k, berriz, HSC-en fenotipo jariatzailea handitzen du, faktore inflammatorio eta pro-tumorigenikoen jariapena ondorio duena (225). NAFLD-arekin lotutako HCC sagu eredu batean, kolesterola eta BA sekundarioen metaketak hepatokartzinoenesia azkartzen duela uste da (226).

S.2.3.3. Heste-gibel ardatzaren seinaleztapenaren erregulazioa

Aurreko atalean adierazi bezala, gaixotasun kronikoaren garapenean, ezinbestekoa da heste-gibel ardatzaren erregulazio estua, honetatik eratorritako seinaleek gaixotasunaren garapenean parte hartzen duten hainbat erantzun pizten baitituzte. Hori horrela, antibiotikoetan oinarritutako aurre-tratamenduak gibel transplantearen ondorengoko inflamazioa eta gibel kaltea mugatzen dituela ikusi da saguetan zein gizakieta (227). Halaber, PAMP-etatik eratorritako TLR-en bidezko seinaleztapena antibiotikoen bidez mugatzea, eragin onuragarriak dakartza hainbat jatorriko gibel kaltean (213-215). Zirrosidun gaixoen gorotzetako mikroorganismoen transplanteak (fecal microbial

transplant, FMT) neuroinflamazioa eragiten du saguetan. Aitzitik, neuroinflazioaren murrizpen bat ikusi da, sagu zirrotiko hauei, aurretik sagu osasuntsuen FMT-a egin bazaie (228). Kontzeptu bera gizakietan ere frogatu da, FMT-ak gibel entzefalopatia hobetzen du hauetan, inflamazioa murriztuz eta kognizio balioak hobetuz (229). Beste estrategia baten ikerketan, emaitza interesgarriak lortu dira bakteria andui berezi batekin, *Bifidobacterium pseudocatenulatum* CECT7765, honek fenotipo anti-inflamatorio baten garapena bultzatzen du makrofago eta KC-etan gibel kalte kronikoko egoeretan (230).

TLR-en seinaliztapenaren erregulazioa oso konplexua da eta kontrol sistema desberdinen bidez lortzen da. Kontrol sistema hauen artean aurkitzen ditugu, TLR-en tolesdura eta zelula barruko garrioa, bere ektodomeinuetara lotzen diren proteina erregulatzaileak, itzultze ondoko eraldaketak eta zelula barruko seinaleztapena erregulatzen duten proteina adaptatzaileak (231). TLR-en seinaleztapenaren erregulazioak eragina du gibeleko gaixotasunen garapenean. Ildo honetan, SIGIRR (single Ig IL1R-related molecule), TLR3 hartzailearen proteina adaptatzaile batekin lehiatzen da, ondorioz TLR3-aren bidezko seinaleztapena eta poly(I:C)-arekiko gibel inflamazioa murriztuz (232). A20 TLR-en bidezko seinaleztapenaren zelula barneko beste erregulatzaile bat da, zeinak NF-κB bidezko seinaleztapena inhibitzen duen eta gibela HCV eta HBV infekzioetatik babesteko gai dela ikusi den (233). IRAK-M (Interleukin-1 receptor associated kinase M) MyD88 proteina adaptatzaileari lotzen zaio TLR-en bidezko seinaleztapena inhibitzeko. Alkoholak eragindako gibel gaixotasunaren sagu eredu batean, IRAK-M-ren galerak gibeleko kaltearen eta translokazio bakterianoaren emendioa dakar (234). Laburbilduz, TLR-etatik eratorritako inflamazioaren erregulazio fina ezinbestekoa da jatorri anitzetako gibeleko kaltean eta kartzinogenesian.

S.3. TREM (triggering receptor expressed on myeloid cell)-en familia

S.3.1.TREM familiako kideak eta kokapen genomikoa

TREM hartzaileen familia 2000. urtean aurkitu zen, eta, orduztik, familiaren kide desberdinak deskribatu dira (235, 236) . Seinaleztapen inflamatorioa modulatzeko duten gaitasuna dela eta, familia honetako kideen gaineko interesa handitu da azken urteotan. Gizakian, TREM familiako kideak kodetzen dituzten geneak 6p21.1 kromosoman kokatzen dira. Hemen familiako kide garrantzitsuenak, hots, TREM1 eta TREM2 kokatzen dira, baina baita TREM-antzeko geneak (TREM-like, TREML): TREML1,

TREML2 eta TREML4 eta TREML3P eta TREML5P pseudogeneak ere. Saguetan, TREM familia 17C kromosoman kokatzen da eta Trem1, Trem2, Trem3, Treml1, Treml2 and Treml4 kideek osatzen dute (**S.15. Irudia**)[Gene database from the NCBI, https://www.ncbi.nlm.nih.gov/gene)].

TREM hartzaileak V-motako, zelulaz kanpoko, immunoglobulina motako domeinu bakarraz, zelula mintzeko domeinu batez, eta isats zitoplasmatiko motz batez osatuta daude. Ez giza, ez sagu TREM hartzaileek, ez dute zelula barruko seinaleak bideratzeko gaitasunik. Hori dela eta, TREM hartzaileek, DAP12 (DNAX Adaptor Protein 12 , TYRO protein tyrosine kinase-binding protein (TYROBP) izenaz ere ezagutzen dena) proteina adaptatzaileaz baliatzen dira zelula barruko seinaleak bideratzeko bere ITAM motiboaren bitartez, aktibazioaren ondorioz fosforilatzen dena (237).

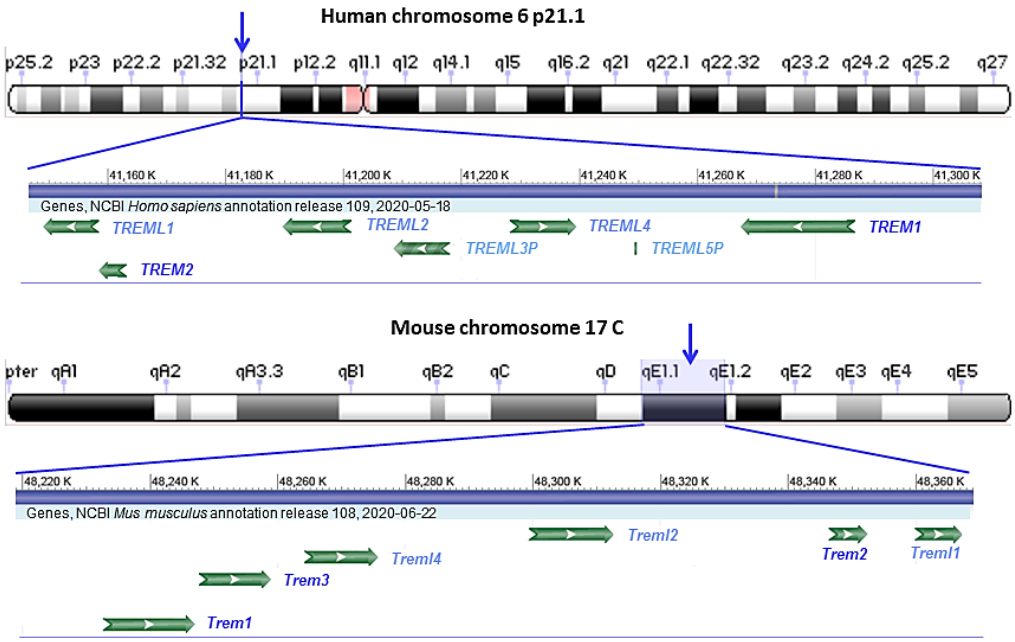

Figure S.15. TREM geneen familiaren kokapena gizakiaren eta saguaren genoman. A) Gizakian, TREM geneen familiak *TREM1*, *TREM2*, *TREML1*, *TREML2* eta *TREML4* geneak eta *TREML3P* eta *TREML5P* pseudogeneak ditu, hauek denak 6. kromosoman taldekatzen dira. B) Saugan, aldiz, *Trem1*, *Trem2*, *Trem3*, *Treml1*, *Treml2* eta *Treml4* geneak aurkitu dira, hauek denak saguaren 17. kromosoman kodetzen dira. TREM, triggering receptor expressed on myeloid cells; TREML, triggering receptor expressed on myeloid cells like. *[NCBI Gene database, NCBI, https://www.ncbi.nlm.nih.gov/gene datubasetik egokitua]*.

TREML hartzaileek, aldiz, zelula kanpoko, V-motako, immunoglobulina antzeko, domeinu berdina duten arren, badituzte zelula barruko sinaleak bideratzeko domeinuak. Giza TREML1 eta sagu Treml1, Treml2 eta Treml4 hartzaileek ITIM domeinua dute,

giza TREML2 hartzaileak SH3-lotzen duen domeinua duen bitartean (238). Splicing alternatiboaren ondorioz TREM hartzaileen forma disolbagarriak eratzen dira. Horrela, TREM1, TREM2, TREML1 eta TREML2 hartzaileen forma disolbarriak deskribatu dira jadanik. Forma hauek betetzen duten funtzioa ez da argitu oraindik, baina euren hartzaileen forma osoekin lehiatzeko gai direla uste da, modu honetan forma osoaren bidezko seinaleztapena negatiboki erregulatuz (237).

S.3.2. Seinalearen transdukzioa

TREM hartzaileen bidezko seinaleztapena prozesu konplexua da, hein handi batean ehun eta testuinguru espeziko bakoitzaren araberakoa. Hartzaile hauentzako ligandoak oraindik ezezagunak dira. Hala ere, ligando bezala joka dezaketen faktore endogeno eta exogeno batzuk proposatu izan dira, gehien bat, molekula anionikoak edo lipidoak (239, 240). Ligandoaren lotura eta gero, TREM hartzaileak DAP12 proteinarekin uztartzen dira, azkenekoa, tirosinetan fosforilatzen da, eta seinaleztapenaren emaitza desberdinak ekarriko dituzten bitartekariak erakartzeko gai da (241). Izan ere, TREM1 eta TREM2 hartzaileek efektu antagonikoak eragiten dituzte TLR-en bidezko seinaleztapenean. Zelula eta ehunaren araberako efektu espezifikoak dauden arren, orokorrean, TREM1-ek TLR-bidezko inflamazioaren bultzatzaile bezala jokatzen du. Honela, TLR-en aktibazioaren ondoriozko gene inflamatorioen transkripzioa emendatzeko gai dela ikusi da. TREM2 hartzailea, berriz, orokorrean hartzaile anti-inflamatoriotzat hartzen da, TLR-ek eragindako gene inflamatorioen transkripzioa inhibitzeko gaitasuna baitu (242) (**S.16. Irudia**). TREM1 eta TREM2-k erregulatzen dituzten bitartekari inflamatorio zehatzen inguruko infomazioa hurrengo ataletan aurkeztuko da.

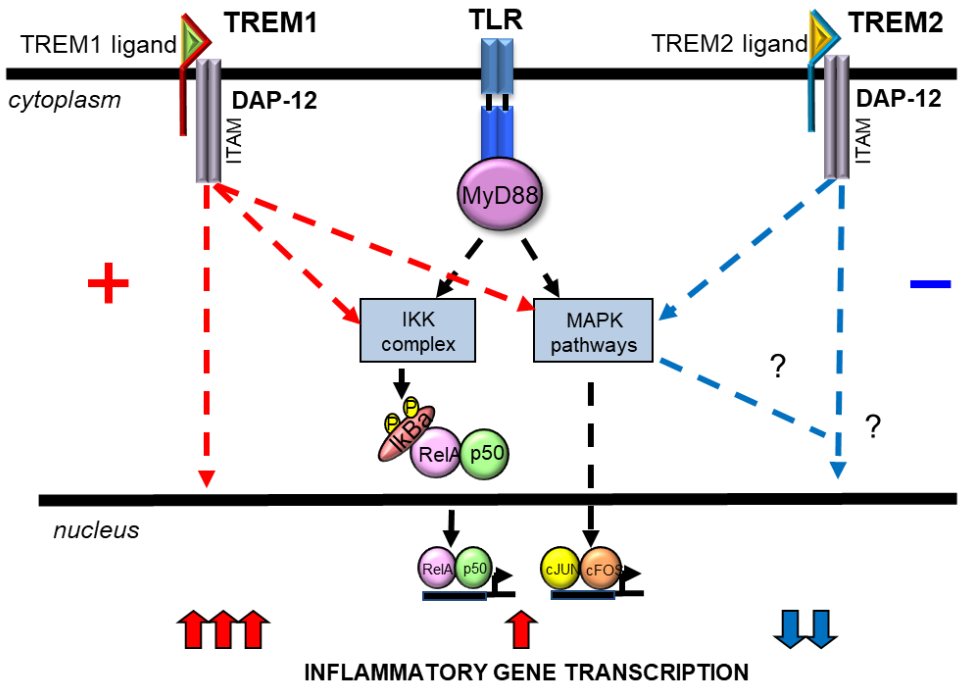

S.16 Irudia. TREM1 eta TREM2-k TLR-en bidezko seinalezapena modulatzen dute. TREM hartzaileek ez dute zelula barruko seinaleztapen motiborik, hortaz, ligandoaren lotura eta gero, biek DAP12 adaptatzailearen ITAM motiboaren bidez bideratzen dituzte zelula barruko seinaleak. TREM1 eta TREM2 hartzaileen ligandoak identifikatzeke daude oraindik. TREM1 TLR-en bidezko seinaleztapena sustatzeko gai dela ikusi izan da, honela, TREM1-en aktibazioak ERK1/2 eta NF-κB transkripzio faktorearen aktibazioa dakar, azkenean gene inflamatorioen transkripzioa emendatuz. TREM2, aldiz, TLR-en bidezko seinaleztapena murrizteko gai dela uste da. Ligandoaren loturaren ondorioz, TREM2-ren aktibazioak ERK1/2-ren fosforilazioa dakar, baina ez da efekturik ikusten NF-κB bidezidorrean. DAP-12, DNAX-activation protein 12; ERK1/2, extracellular signal-regulated kinases 1/2; IκBα, NF-kappa-B inhibitor alpha; IKK, IκB kinase; ITAM, immunoreceptor tyrosine-based activation motif; MAPK, mitogen-activated protein kinases; Myd88, myeloid differentiation primary response gene 88; NF-κB, Nuclear factor kappa B; TLR, toll-like receptor; TREM, triggering receptor expressed on myeloid *cells [Sharif O et al, 2008 (239) artikuluan oinarritua]*.

Teoria desberdinak proposatu dira azaltzeko nola, proteina adaptatzaile berdinaren bidez seinaleztatzen duten bi hartzaileek, erantzun zelular antagonikoak eragin ditzaketen (240, 241, 243) (**S.17. Irudia**). Teoria hauen artean aztertu eta onartuenak dio, TREM hartzailearen ondorengo efektuak, erantzuna piztu duen estimuluaren araberakoak izango direla. Honela, afinitate handiko ligandoek TREM1/TREM2-ren bidezko efektu aktibatzaileak eragingo lituzkete. Afinitate txikiko ligandoek, ordea, DAP12-ren fosforilazio partziala eragin dezakete eta ondorioz SHP1 (Src homology region 2 domain-containing phosphatase 1) erakarri, honek era berean, TREM2 hartzailearen erantzun aktibatorioa eragiten duten bitartekariak defosforilatu, eta proteasoma bidezko degradaziora zuzenduko lituzke (240, 241, 243). Beste teoria baten arabera, TREM2-tik eratorritako seinaleztapenaren bitartekari batzuek efektu inhibitorioa izan dezakete TLR-en ondorengo bitartekarietan (241, 243). Azkeneko teoria zelula dendritikoetan

behatu da, honetan, hartzailearen kokapen azpi-zelularraren araberakoa izango litzateke seinaleztapenaren ondorioa (243).

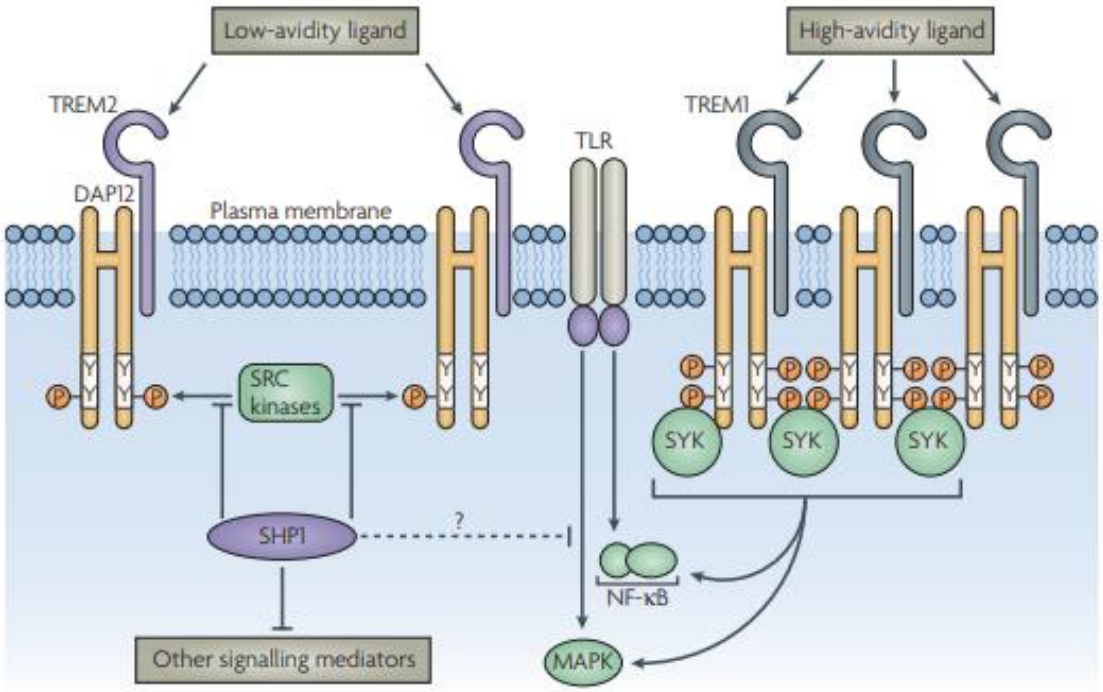

S.17. Irudia. TREM1 eta TREM2-ren afinitate txikiko eta afinitate handiko ligandoen teoria. Zelula barruko seinaleak molekula adaptatzaile berdinaren bidez bideratzen dituzten arren, TREM1 edo TREM2-ren aktibazioak zelulan erantzun bereizgarriak eragiten ditu. Afinitate txikiko eta handiko ligandoen teoria fenomeno hau azaltzeko onartuena da. Honen arabera, afinitate handiko ligandoen loturak TREM1/TREM2-ri, DAP12-ren fosforilazio totala, eta, beraz, molekula aktibatzaileen erakarpena eragingo luke. Afinitate txikiko ligandoen loturak, ordea, DAP12-ren fosforilazio partziala eragingo luke, ondorioz, bitartekari inhibitorioen erakarpena gertatuz. DAP12, DNAX-activation protein 12; MAPK, mitogen-activated protein kinases; NF-κB, Nuclear factor kappa B; P, phosphate; SHP1, Src homology region 2 domain-containing phosphatase-1; SRC, Proto-oncogene tyrosine-protein kinase; Syk; spleen tyrosine kinase; TLR, toll like receptor; TREM1, triggering receptor expressed in myeloid cells 1; TREM2, triggering receptor expressed on myeloid cells 2; Y, tyrosin *[Turnbull I et al, 2007 (241) artikuluan oinarritua]*.

S.3.3. TREM1

TREM1 izan zen aurkitu zen TREM familiako lehenengo kidea (235). Bere aurkikuntzaz geroztik, TREM1 hartzaile pro-inflamatorio bat bezala deskribatu da, TLR-en bidezko seinaleztapena emendatzeko gai baita testuinguru eta ehun desberdinetan. Orokorrean, TREM1-en aktibazioak erantzun immune innatoa areagotzen du, bitartekari inflamatorioen adierazpenaren emendioaren bidez, hauen

artean, IL1β, IL6, IL8, IL10, TNF eta MCP1 (235, 244-247). Efektu honen ondorioz, TREM1-en aktibazioak inflamazioarekin lotutako gaixotasun desberdinen progresioa eragiten du. Gaixotasun hauen artean, Chron-en gaixotasuna eta kolitis ultzeratiboa (248), aterosklerosia (249) edo arthritis erreumatoidea daude (250). TREM1 hartzailea minbizi mota desberdinekin ere lotu izan da. Ildo honetan, *Trem1*$^{-/-}$ saguak hesteetako inflamazioarekin lotutako minbiziaz babestuta daude (251), eta TREM1-en inhibizioak biriketako minibizien xenograft-en hazkuntza atzeratzen du (252).

Gibelean, TREM1, LSEC, KC, HSC eta HCC-ren zeluletan adierazten da (253-255). eta gibeleko hainbat gaixotasunetan parte hartzen du. Honela, KC-etan eta zelula mieloideetan inflamazioaren aktibazioa eragiten duenez gero, TREM1-ek infekzio biralen (256, 257)**,** alkoholaren (258)**,** eta NAFLD-ren (259) ondoriozko gibeleko gaixotasun kronikoen eta baita gibeleko fibrosiaren (260) progresioa ere sustatzen ditu.

Halaber, TREM1-ek HCC zelulen hazkuntza eta inbasioa eragiten ditu, are gehiago, TREM1-en adierazpenak minbiziaren ber-agerpenarekin eta gaixo hauen biziraupen motzagoarekin korrelazionatzen du (255). Gainera, TREM1-ek KC-en gibel kaltearekiko erantzuna erregulatzen du, NF-κB eta JNK bidezidorrak sustatuz eta, ondorioz, IL6, IL1β, TNF, CCL2 eta CXCL10 markatzaile inflamatorioen adierazpena sustatzen ditu DEN (diethylnitrosamine) hepatotoxikoaren administrazioaren ondorioz. Molekula honen administrazioan oinarritutako HCC-aren sagu eredu batean, TREM1-ek gibeleko tumorigenesia sustatzen du. (261) TREM1-ek immunosupresioa eta anti-PDL1 terapiarekiko erresistentzia ere erregulatzen ditu (262).

S.3.4.TREM2

TREM2 TREM familiako kide bat da, zelula mieloidetan adierazten dena, hauen artean, makrofago albeolarretan, hezur, nerbio sistema zentral (central nervous system CNS) eta gibeleko makrofagoetan aurkitzen da TREM2. Eta berean, zelula dendritiko eta endotelialek ere hartzaile honen adierazpena aurkezten dute (239). TREM2-ren funtzioaren galera dakarten mutazioek Nasu–Hakola edo PLOSL (lipomembranous osteodysplasia with sclerosing leukoencephalopathy) izeneko gaixotasun neurodegeneratibo arraro bat sortzen dute (236). Gaixotasun honen ezaugarri nagusiak hausturak eragiten dituzten hezurretako kisteak eta dementzia dira. Gaixotasunaren fisiopatologiari dagokionez, TREM2 hezurreko makrofagoen, hots osteoklastoen, diferentziazio prozesuan parte har lezake, hain zuzen ere, prozesu hau urrituta dago PLOSL-dun pazienteetan (263).

PLOSL gaixotasunarekin lotu zenetik, TREM2 CNS-eko makrofagoen, hau da, mikrogliaren homeostasiaren erregulazioan funtsezko papera betetzen duela ikusi da. Beraz, CNS-arekin lotura estua du hartzaile honek. Ildo honetan, TREM2-k TREM1-en kontrako funtzioak betetzen zituela behatu zen, hain zuzen ere, mikroglian TLR-arekiko erantzunean TNF eta IL6 bezalako zitokina inflamatorioen adierazpena murrizteko gaitasuna baitu (264, 265). TREM2-ren R47H (rs75932628) aldaera genetikoa Alzheimer gaixotasuna garatzeko arriskuarekin lotzen da (266). Halaber, TREM2-ren beste aldaera genetiko batzuk ere beste gaixotasun neurodegeneratibo batzuekin uztartzen dira, ALS-arekin (amyotrophic lateral sclerosis) (267) eta dementzia fronto-temporalarekin (268), hain zuzen ere. Lan desberdinetan azaleratu da *Trem2*$^{-/-}$ eta *Trem*2-ren aldaera genetikoak dituzten saguek mikrogliaren funtzioan akatsak erakusten dituztela. Zentzu honetan, mikrogliaren aktibazioaren murrizpena, apoptosiaren emendioa, mielina edo Aβ plaken garbiketan eta lipidoak ezagutu eta hauei erantzuteko akatsak behatu dira sagu hauetan (269-271).

Hala ere, TREM2-k funtzio garrantzitsuak betetzen ditu CNS-etik kanpoko zelula mieloideetan ere (240). Lan batean ikusi da TREM2 fagozitosia sustatzeko gai dela makrofago peritonealetan, hezur muinetik eratorritako makrofagoetan, eta neutrofiloetan (272, 273). Aitzitik, biriketan, TREM2-k bakterien opsonizazioa eta makrogafo albeolarren aktibitate fagozitikoa inhibitzen ditu (274). Birus batek eragindako biriketako gaixotasun kroniko obstruktiboko eredu batean, TREM2-k M2 motako makrofagoen biziraupena eta hazkuntza sustatzen ditu, azkenean gaixotasunaren garapena dakarrena (275). TREM2-k hesteetako makrofagoen homeostasian ere eragina du, hemen, hesteetako kaltearen ondoriozko zauri-sendatze prozesua bultzatzen du, makrofagoak M2 motako fenotipo batera bideratuz (276). Kimikoki sorturiko kolitisaren eredu batean, aldiz, TREM2-k kontrako efektuak eragiten ditu, inflamazioa sustatuz eta mukosako kaltea areagotuz (277). Hori dela eta, kontuan hartzekoa da TREM2-ren efektuak gaixotasun eta zelula-motaren araberakoak izan daitezkeela. Berriki, TREM2 homeostasi metabolikoarekin lotu da obesidadearen kontestuan. Hemen, HFD-an oinarritutako obesidadearen sagu eredu batean, TREM2-k makrofago azpi-populazio berezi baten diferentziazioa bideratzen du, LAMs (lipid associated macrophages) izenez ezagutzen direnak. *Trem2*$^{-/-}$ saguetan ehun adipotsuaren zelula mieloideen erantzuna akastuna da eta LAM populazioa eta makrofago mota honen bereizgarri den adierazpen profila galtzen dira. Populazio honen galerak, azkenean, adipozitoen hipertrofia, hiperkolesterolemia eta glukosarekiko intolerantzia garatzea dakartza (278).

TREM2-k gibelean betetzen duen funtzioa hein handi batean ezezaguna da oraindik eta hau argitzea gure ikerketa taldea eta beste talde batzuen helburua izan da azken urteotan. Hasiera batean, TREM2 eta TREM familiako beste kide batzuk gibeleko makrofago eta LSEC zeluletan adierazten zela ikusi zen (253). Gainera, TREM2-ren adierazpenak, malaria eragiten duen *Plasmodium Berghei* parasitoarekiko erantzuna modulatzen du KCs-etan (279). Etekin handiko tekniken bidez, TREM2 adierazten duten, eta NAFLD (280) edo zirrosiarekin (281) lotzen diren, makrofagoen azpi-populazioak aurkitu dira. TREM2-ren adierazpena gibeleko zelula dendritikoetan ere deskribatu da, hauetan, iskemia/bir-perfusioak eragindako kalteaz babesten du gibela (282). Halaber, hartzaile honen adierazpena emendatuta dago minbizi mota desberdinetan (283-286). HCC-n ere bere papera betetzen du TREM2-k, hemen, HCC zelulen hazkuntza, migrazioa eta inbasioa inhibitzen ditu, PI3K/AKT/β-catenin (phosphoinositide 3 kinase/ RAC-alpha serine/threonine-protein kinase/ β-catenin) seinaleztapen ardatzaren bidezko mekanismo batez (287).

S.3.5.TREM2-ren papera gibeleko kaltearen garapenean: gure ikerketa taldearen aurrekariak

Gure ikerketa taldean, esperientzia dugu TREM2 hartzailearen azterketan, eta hartzaile honek gibeleko kalte hepatozelular akutu eta kronikoan, zein HCC-an betetzen duen funtzioa deskribatu dugu azken urteotan (**S.18 Irudia**). Gibeleko gaixotasun hepatozelularretan, euren jatorria edozein izanda ere, eta baita HCC-dun gaixoen gibeletan ere emendatu egiten da hartzaile honen adierazpena, gibel ehun osasuntsuarekin konparatuz. Are gehiago, *TREM2*-ren mRNA adierazpenak korrelazio positiboa du gibeleko inflamazioaren *(IL1β, IL6, IL8 and TNF*) eta fibrosiaren markatzaileekin (*COL1A1* eta actin alpha 2, smooth muscle (*ACTA2*) HCC-dun gaixoetan. Joera bera behatzen da gibel kalte akutu zein kronikoaren eta HCC-aren sagu ereduetan kontrol egoerarekin alderatuz. Adierazpen hau, KCs eta HSCs-etan aurkitzen da batez ere, hepatozitoek hauekin konparatuta oso adierazpen maila baxuak erakusten baitituzte. *Trem2*$^{-/-}$ saguetan burututako esperimentuetan ikusi ahal izan dugu gibeleko gaixotasun akutu zein kronikoetan eta transformazio malignoan, TREM2-k inflamazioa mugatu eta gibela babesten dituela, KCs eta HSCs-etan dituen efektuak direla eta. Ildo honetan, CCl_4-az kronikoki tratatutako *Trem2*$^{-/-}$ saguek kalte hepatozelular eta zelulen heriotzaren emendioa aurkezten dituzte WT (wild type) saguekin konparatuz. Hau, hartzaile honek kaltearen fase akutuetan dituen efektuen bidez azaltzen da, non, CCl_4 akutu eta APAP-ren trataenduan oinarritutako sagu ereduetan, *Trem2*$^{-/-}$ saguek AST (aspartate aminotransferase) eta ALT-ren (alanine aminotransferase) serumeko mailen,

gene inflamatorioen transkripzioaren, estress oxidatiboaren eta sistema immuneko zelulen gibelerako erakarpenaren emendioa aurkezten duten. Azpimarratzekoa da, *Trem2*$^{-/-}$ saguek biziraupen motzagoa dutela APAP drogan oinarritutako gaindosi sagu-eredu batean. Aurretik aipatu bezala, TREM2 KCs eta HSCs-etan adierazten da batez ere, hauek gibeleko kaltearekiko erantzunak bideratzen dituzten zelula mota nagusiak izanik. Ildo honetan, *Trem2*$^{-/-}$ saguetatik eratorritako KC and HSC zelulek *Il1β*, *Il6*, *Tnf*, *Mcp1* eta *Cxcl1* bitartekari inflamatorioen emendioa erakusten dute, TLR4-en aktibatzaile den LPS-rekin tratatzerakoan (288).

Hepatokartzinogenesia gibeleko gaixotasun kronikoen azkeneko urrats bezala hartzen da, modu honetan, TREM2-ren efektu anti-inflamatorioek heaptozitoen eraldaketa malignoan ere eragina dute. Hepatokartzinogenesiaren fase akutuetan, *Trem2*$^{-/-}$ saguetan gibelaren gehiegizko kaltea, DNA-ren kaltea eta extres oxidatiboaren eta inflamazioaren markatzaileen adierazpenaren emendioa behatzen dira. TREM2-k efektu garrantzitsua du gibelaren birsortzean ere, hemen, hepaktetomia partzialaren sagu eredu batean, *Trem2*$^{-/-}$ saguek zelularen hazkuntzaren eta inflamazioaren markatzaileen adierazpenaren emendioa aurkezten dute. Gainera, *Trem2*$^{-/-}$ saguek gibeleko tumore gehiago garatzen dituzte DEN-aren administraziotik 30 edo 40 asteetara. Azkenik, TREM2-k eragindako efektuak HCC eta HSC zelulen arteko elkarrekintzan suertatzen diren eraldaketen ondoriozkoak direla behatu dugu. TREM2-ren gainadierazpenak Wnt ligandoen eta biartekari inflamatorioen adierazpenaren murrizpena dakar giza HSC-etan. Are gehiago, HCC esferoideak gutxiago hazten dira, TREM2-ren gainadierazpena duten HSC-en medioan, plasmido kontrolarekin transfektatutako HSC-en medioarekin konparatuz. Efektu hauek Wnt/β-catenin seinaleztapenaren menpekoak dira (289).

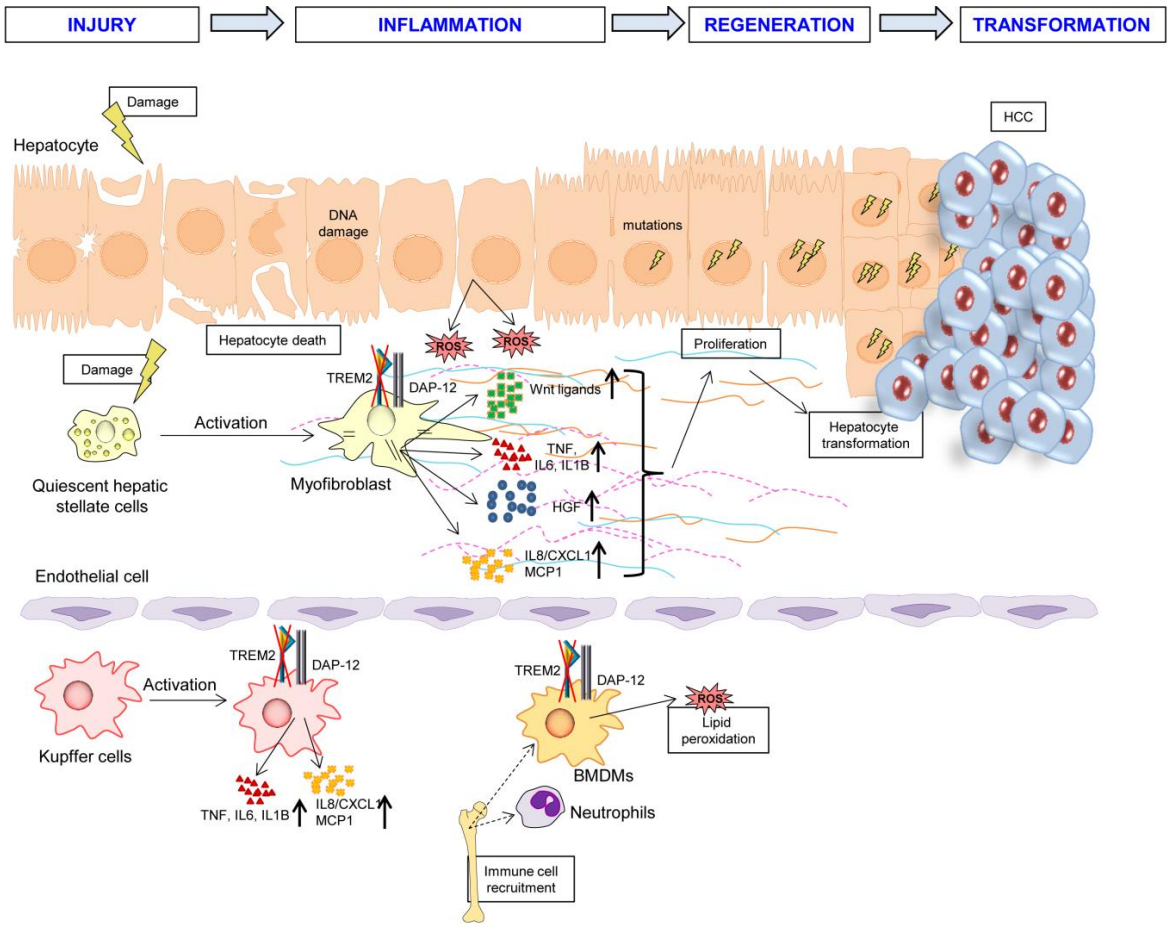

S.18. Irudia. TREM2-k gibeleko kalte kronikoan eta hepatokartzinogenesian betetzen duen paperaren inguruko proposamena. Gibeleko kaltea eta gero, *Trem2*-ren ezean, hepatozitoen kaltea eta heriotza emendatzen dira. Hau ROS-en ekoizpenaren, zitokina, kemokina, hazkuntza faktore eta Wnt ligandoen adierazpenaren eta DNA-ren gaineko kaltearen emendioarekin batera behatzen da. Gainera, *Trem2*-ren ezean, sistema immuneko zelulen gibelerako erakarpena emendatzen da eta BMDM-ek ere ROS gehiago ekoizten dute, era berean, hau gibeleko lipidoen peroxidazio handiago batekin lotzen da. Bestalde, gibeleko birsortzean, fase goiztiarretako zitokina inflammatorioen eta hazkuntza faktoreen adierazpenaren emendioa behatzen da, hepatozitoen hazkuntzarekin lotzen dena, *Trem2*-ren ezean. Mikroingurune pro-inflamatorio honek hazkuntza prozesuan dauden hepatozitoetan mutazioak sortzea errazten du, zelula hauen transformazioa eta HCC-aren garapena sustatuz. BMDMs, bone-marrow derived macrophages; CXCL, C-X-C Motif Chemokine Ligand; DAP-12, DNAX-activation protein 12; HGF, hepatocyte growth factor; IL, interleukin; MCP1, monocyte chemoattractant protein 1; TNF, tumour necrosis factor; TREM2, triggering receptor expressed in myeloid cells 2 *[Esparza-Baquer A et al, 2020 (289) atikulutik egokitua]*.

HIPOTESIA ETA HELBURUAK

Gure ikerketa taldearen aurreko lanetan, TREM2-k gibeleko kalte akutu zein kronikoan, eta hepatokartzinogenesian, erantzun inflamatorioen erregulazioan funtsezko papera betetzen duela ikusi dugu (288, 289). Datu hauek kontuan hartuta, ikerlan honetan hipotetizatzen dugu, TREM2-k kolestasi eta fibrosiarekin lotutako HCC-aren garapenean ere paper garrantzitsua bete lezakeela, testuinguru hauetan ere erantzun inflamatorioak erregulatuz. Hipotesi hau frogatzeko bidean, hurrengo helburu espezifikoak plazaratu genituen:

1. *TREM2* hartzailearen adierazpen maila aztertzea kolestasidun gaixoen gibeletan, gibel osasuntsu eta hainbat etiologiatako gibel zirrotikoekin alderatuz.

2. *Trem2* hartzailearen adierazpena aztertzea kolestasiaren animalia eredueta.

3. Buxadurazko kolestasiaren sagu eredu batean, TREM2-k behazun hodietako kaltean betetzen duen papera deskribatzea.

4. Hesteetatik geibelerako bakterien lekualdaketak TREM2-k kolestasian eragiten duen fenotipoan betetzen duen papera zehaztea.

5. Kimikoki eragindako kolestasiko sagu eredu baten testuinguruan, TREM2-k behazun hodietako kaltean betetzen duen papera deskribatzea.

6. UDCA-k zelula ez-parenkimaletan sortzen dituen efektuen berritasunak aztertzea: TREM2-ren bidezko efektu anti-inflamatorioak aztertzea.

7. Giza HCC tumoreetan TREM2 adierazten duten sistema immuneko azpipopulazioak zeintzuk diren zehaztea.

8. TREM2-ren papera fibrsoiarekin lotutako HCC-an aztertzea.

MATERIALAK ETA METODOAK

M.1. Gizakietatik eratorritako gibeleko ehun laginak

M.1.1. San Sebastian/Warsaw gaixo taldea

TREM-ren adierazpen mailak giza kolestasian aztertzeko asmoz, gibeleko ehuna indibiduo kontroletatik, jatorri desberdinetatik sortutako zirrosidun pazienteetatik eta PBC eta PSC-dun pazienteetatik lortu genuen. Gaixoen ezaugarriak eta parametro klinikoak **M.1. Taula**-n aurkezten dira. Gibel ehun osasuntsuaren laginak minbizi kolorrektalaren ondoriozko gibeleko metastasia zuten indibiduo kontroletatik lortu ziren. Gibel ehun osasuntsua tumore-masa lesioetatik urrunen kokatutako gibel ehun osasuntsua aukeratuz lortu zen. Kontrol laginak (n=18) eta zirrotikoak (n=35) Euskadiko Biobankoak eman zituen eta prozesamendua egiteko Euskadiko eta Donostia Unibertsitate Hospitaleko Ikerketa Klinikoko Etika Komitearen onespena jaso zen. PBC eta PSC-dun pazienteen laginak P.Milkiewicz (Medical University of Warsaw, Warsaw, Poland) eta M. Milkiewicz (Pomeranian Medical University, Szczecin, Poland) doktoreek ema zituzten. Lan honetan aztertutako gaixo (zeinetatik laginak eratorri ziren) guztiek gibeleko transplantea izan zuten Warsaw, Poland-eko "Department of General, Transplant and Liver Surgery"-ean 2014ko ekaina eta 2016ko azaroa bitartean. Guztira 20 lagin aztertu ziren (PBC n=10 eta PSC n=10), hauek segituan nitrogeno likidotan izoztu ziren RNA-ren azterketarako. RNA totala gibel ehuneko 50 mg-tatik erauzi zen Rneasy Mini Kit-a erabiliz (Qiagen), ekoizleak gomendatutako argibeak jarraituz. Erauzitako RNA-ren kantitatea eta kalitatea Epoch™ Microplate Spectrophotometer (BioTek) batean neurtu zen. Prozedura guztiek Medical University of Warsaw-eko "Research Ethics Committee"-aren onespena jaso zuten.

M.1. Taula. San Sebastian/Warsaw gaixo taldearen ezaugarriak eta aldagai klinikoak.

Aldagaia	**Kontrol** (n=18)	**Zirrotiko** (n=35)	**PBC** (n=10)	**PSC** (n=10)
Adina, (urteak)	66.26 ± 7.54	63.46 ± 8.9	59 ± 6.28	28.5 ± 12.15
Generoa, n (%)				
Gizonak	13 (72.22)	33 (94.28)	1 (10)	7 (70)
Emakumeak	5 (27.78)	2 (5.17)	9 (90)	3 (3)
Etiologia, n (%)				
Alkoholikoak	-	11 (31.43)	-	-
HCV	-	9 (25.71)	-	-
Idiopatikoak	-	6 (17.14)	-	-
HCV+HBV	-	3 (8.57)	-	-
HBV	-	2 (5.71)	-	-
HCV+HIV	-	1 (2.86)	-	-
HCV+HBV+HIV	-	1 (2.86)	-	-
HBV+EtOH	-	1 (2.86)	-	-
Hemochrom.	-	1 (2.86)	-	-
Mailakatze histologikoa, n (%)				
F1-F2	-	-	1 (10)	4 (40)
F3-F4	-	35 (100)	9 (90)	6 (60)
Serumeko biokimika,				
ALT, (IU/l)	20.5 ± 7.22	31 ± 28.16	60 ± 43.32	54 ± 102.68
AST, (IU/l)	23 ± 6.24	36 ± 29.49	65 ± 61.35	78.5 ±47.87
GGT, (IU/l)	-	96 ±201.90	84 ± 52.91	204 ± 613.21
Fosfatasa alkalinoa, (IU/l)	-	78 ± 32.29	216 ± 333.1	366 ± 595.3
Bilirubin	0.55 ± 0.18	0.6 ± 0.27	6.16 ± 7.18	2.25 ± 10.06

Datuak mediana ± SD bezala adierazten dira.
ALT, alanine aminotransferase; AST, aspartate transaminase; HBV, hepatitis B virus; GGT, gamma glutamil transferase; HCV, hepatitis C virus; Hemochrom., hemochromatosis; HIV, human immunodeficiency virus; IU, international units; PBC, primary biliary cholangitis; PSC, primary sclerosing cholangitis; SD, standard deviation.

M.1.2. GSE79850 gaixo taldea

GSE79850 array datu taldea deskargatu genuen, honetan gibel ehunaren 24 lagin daude, hauen artean kontrolak (n=8), arrisku bajuko PBC-dunak (n=7) eta arrisku altuko PBC-dunak (n=9) daude. RNA, tratamendua jaso aurretik, biopsioren momentuko FFPE ehunetatik erauzi zen; kontrolak gibel transplante hartzaileren gibel emaileetatik lortu ziren (290). Jatorrizko ikerlanean, arrisku bajuko PBC-dun gaixoak hurrengo irizpideen bidez definitzen dira: 1) Paris 1 irizpideen arabera, UDCA-rekiko erantzulea; 2) Osasun

egoera onean egotea eta UDCA-rekiko erabateko erantzuna izaten jarraitzea 15 urte eta gero; 3) Ez zuen gibeleko transplatnterik behar izan. Bestalde, arrisku altuko PBC-dun gaixoek hurrengoak bete behar zituzten: 1) Paris 1 irizpidearen arabera UDCA-ren 13-15mg/Kg-ko dosiko tratamenduarekiko ez erantzuleak, 2) jarraipen denboran zehar, gibeleko transplantea behar izan zuten arrazoi prognostikoak zirela eta.

M.1.3. IHC azterketan erabilitako gaixo taldea

TREM2-ren adierazpena IHC bidez aztertu zen jatorri anitzetako HCC-dun gaixoen gibelean eta minbizi kolorrektala edo bularreko minbiziaren ondoriozko gibeleko metastasia duten kontrol indibiduoen gibel osasuntsuan. Gaixoen ezaugarriak eta aldagai klinikoak (**M.2. Taulan)** jasotzen dira. Lagin hauek Euskadiko Biobankoak eman zituen eta prozesamendua egiteko Euskadiko eta Donostia Unibertsitate Hospitaleko Ikerketa Klinikoko Etika Komitearen onespena jaso zen.

M.2. IHC azterketan erabilitako gaixo taldearen ezaugarriak eta aldagai klinikoak

Aldagaia	**Kontrol** (n=4)	**HCC** (n=10)
Adina, (urteak)	61.5 ± 11.79	59.2± 7.38
Generoa, n (%)		
Gizonak	0 (0)	10 (100)
Emakumeak	4 (100)	0 (0)
Etiologia, n (%)		
Alkoholikoak	-	1 (10)
HBV	-	2 (20)
HCV	-	3 (30)
HCV+HBV	-	1 (10)
Hemochrom.	-	1 (10)
Idiophatic	-	2 (20)
Serumeko biokimika,		
ALT, (IU/l)	27.5 ± 14.36	31.10 ± 9.86
AST, (IU/l)	30.75 ± 17.48	29.00 ± 9.97

Datuak mediana ± SD bezala adierazten dira.
ALT, alanine aminotransferase; AST, aspartate transaminase; HBV, hepatitis B virus; HCC, hepatocellular carcinoma; HCV, hepatitis C virus; Hemochrom., hemochromatosis; IU, international units; SD, standard deviation.

M.1.4. Zelula bakarreko RNA sekuentziazio (single cell RNA sequencing, scRNAseq) gaixo taldea eta azterketa

9 HCC tumoreen scRNAseq datuak publikoki eskuragarri dagoen GSE125449 datu basetik lortu ziren (291). Gaixo talde honi dagokion informazio klinikoa eta scRNAseq egiteko jarraitutako bidea, kalitatearen kontrola ere kontuan hartuta, jatrrizko ikerlanean aurki daitezke (291). Laburbilduz, kalitate altuko zelulak filtratzeko, behintzat 500 ezaugarri identifikatu izana eta RNA mitokondriala %20-a baino gutxiago izatea kontuan hartu zen. Datuak log-normalizatu ziren eta 10000 faktore batera eskalatu ziren. Identifikatutako 18274 geneetatik 4655 gene hautatu ziren analisirako, zelula talde batean barruan, zelulen %10-ean behintzat behatzea oinarritzat hartuta. Taldeen arteko desberdintasun handienak aurkezten zituzten geneak bataz besteko logFC >1 eta egokitutako *p* balorea < 0.01 aintzat hartuta definitu ziren. PCA taldekatzea 2244 ezaugarri aldagarrienetan egin zen. Ondoren, taldekatutako datuak t-SNE (t-distributed Stochastic Neighbor Embedding) grafiken bidez ikustarazi ziren Seurat R paketearen bidez. TREM2 adierazten zuten TAM (1 eta 2 taldeak) eta gainerako TAM-en arteko geneen adierazpen diferentzialaren azterketa egin zen Seurat-en bidez. Aberastutako geneen profila identifikatzeko GSEA analisiak burutu genituen clusterProfiler R paketea eta Molecular Signatures Database (MsigDB) v7 datubasea erabiliz.

M.2.Kolestasi eta fibrosiarekin lotutako HCC-aren sagu ereduak

Animalietan oinarritutako esperimentuak burutzeko sagu basatiak (wild type, WT) eta *Trem2* generik gabeko (*Trem2*$^{-/-}$) saguak erabili ziren. Pareko adina zuten WT eta *Trem2*$^{-/-}$ sagu arrak erabili ziren esperimentu guztietan. Sagu hauek Biodonostia osasun ikerketa insititutoan hazi ziren, bi sagu motek C57BL/6 jatorri genetikoa dute. *Trem2*$^{-/-}$ saguak Marco Colona ikerlariarengandik lortu ziren, eta aldez aurretik deskribatutako prozesu baten bidez sortu ziren, >98% C57BL/6 jatorri genetikoa lortu arte bir-gurutzatuz (264). Esperimentu guztietarako Biodonostia Osasun Ikerketa Institutoko Animalia Ikerketaren Komite Etikoaren onespena jaso zen (CEEA15/001, CEEA15/020, CEEA18/21, CEEA19/002, CEEA19/004).

Esperimentu bakoitzean zehaztutako denbora puntuetan, saguak isofluranoan oinarritutako anestesiapean sakrifikatu ziren. Gorputzeko pisua neurtu ondoren, odola bildu zen bihotzeko ziztadaren bidez. Odola 1500 g-tan 4ºC-tara zentrifugatu zen 20 minutuz. Sueroko alanine aminotransferasa (ALT), aspartato aminotransferasa (AST), fosfatasa alkalina (alkaline phosphatase, AP) eta bilirrubina mailak neurtu ziren

Donostia Uniberstsitate Ospitalean Cobas 8000 c702 (Roche) aparatuaren laguntzaz. Bitartean, gibela erauzi eta pisatu zen. Ondoren, gibela hurrengo moduan prozesatu zen: lobulu desberdinetatik eratorritako 3 zati %4 paraformaldeidotan (Merck) fixatu ziren azterketa histologikorako. Gainerako gibela -80 ºC-tara gorde zen ondoren beharrezko helburuaren metodologiaren arabera prozesatzeko.

Kolestasia kolangiopatia desberdinek partekatzen duten egoera patologikoa da. Era berean, egoera patologiko honek prozesu fisioopatologiko konplexua jarraitzen du eta egoera kliniko desberdinak azaleratu ditzake (74). Hori dela eta, sagu eredu bakar batean ezin dira bildu egoera patologiko honen zehaztasun guztiak (292). Arazo honi aurre egiteko, kolestasiaren sagu eredu desberdinak burutu genituen, honela, gaixotasunaren alderdi desberdinen inguruko informazioa jasotzeko. Kolestasi kronikodun gaixoak gibeleko mibizia jasateko arrisku handiagoa dute (183-185). TREM2-k gibeleko minbiziaren garapenean duen papera aztertzeko asmoz, HCC-ko eredu desberdinak burutu genituen WT eta *Trem2*$^{-/-}$ saguetan. Kolestasi kronikoan gertatzen den bezala, HCC ere gaixotasun konplexua da eta heterogeneotasun maila altua da minbizi honen ezaugarri bereizgarrietako bat (195). Kontuan hartzekoa da HCC-en %80 inguru gibel zirrotikoetan agertzen direla (191). Beraz, kasu honetan ere HCC-ren eredu desberdinak burutzea erabaki genuen, bereziki, fibrosiarekin lotutako HCC sagu ereduak aztertu ditugu ikerlan honetan.

M.2.1.BDL-an oinarritutako buxadurazko kolestasiaren sagu eredua

BD-an oinarritutako eredua erabili zen buxadurazko kolestasia sortzeko. Sagu eredu honetan, behazun hodi komuna lotzen da, horrela, behazunaren fluxua geldiaraziz. Honen ondorioz, BA-en eta behazunetik eratorritako bestelako produktu toxikoen metaketa ematen da gibelean. BDL-aren ondoren, saguek behazuneko hodietako bucadura, erreakzio duktularra eta fibrosi biliarra garatzen dituzte gibelean (293). Era berean, hesteetan ere, eraldaketa sakonak gertatzen dira sagu eredu honetan, honen erakusle da, hesteetatik gibelerako bakterien translokazio esanguratsua behatzen dela eredu honetan (294). BDL-a, aurretik literaturan deskribatu denari jarriki burutu zen (293). 10-12 asteetako adina zuten WT eta *Trem2*$^{-/-}$ saguak erabili ziren prozedura honetan. Laburbiduz, hasteko, 2 cm-tako irekigunea zabaldu zen saguen sabelaldean, behazun hodi komuna agerian uzteko. Behazun hodia bi puntu desberdinetan lotu zen, 6-0-tako zeta kirurgiko xurgagaitza erabiliz. Ondoren, peritoneoa PBS eta klorexidinaz garbitu zen, giharra 6-0tako zeta kirurgiko xurgagaitzaz eta azala 3-0-tako zetako kirurgiko xurgagaitzaz josi ziren. Kontrol moduan erabilitako saguei, “sham” edo

itxurazko ebakuntza egin zitzaien, horretarako BDL-aren protokolo berdina jarraitu zen, baina kasu hoentna, behazun hodiaren lotura egin gabe. Beharrezko kasuetan, meloxicam (Boeringher Ingelheim) sendagaiean oinarritutako tratemendu analgesikoa eman zitzaien saguei. Animaliak ebakuntzatik 7 egunetara sakrifikatu ziren.

M.2.2. ANIT-aren (alpha-naphthylisothiocyanate) adminsitrazioan oinarritutako kolestasi kimikoaren eredua

ANIT hepatozitoetan metabolizatzen den konposatu kimikoa da. Hasiera batean, ANIT-a glutationarekin (GSH) konjokatzeb da hepatozitoetan, eta behazunean jariatzen da MRP2 (multidrug resistance-associated protein 2) garraiatzailearen laguntzaz. ANIT-GSH konplexua ezegonkorra da behazunean, eta beraz, bertan banatzen da, kolangiozitoak ANIT kontzentrazio altuen menpean jarriz. Gainera, ANIT-ak hainbat jariapen-birxurgatze ziklo jasaten ditu hepatozitoetan, ziklo hauetako bakoitzean ANIT-a glutationarekin konjokatzen da, honela, hepatozitoen glutation biltegiak agortuz eta kalte hepatozelularra eraginez (295). Ahotik hartzeko ANIT dosi altu batek, kolangiozitoen suntsiketa larria dakar, ondorioz, gibel barruko kolestasia sortuz (295, 296). Sagu eredu hau burutzeko, 8 asteko adina zuten WT eta *Trem2*$^{-/-}$ saguei ANIT-a (Sigma-Aldrich) ahoz eman zitzaien 50mg/kg-ko dosian eta oliba oliotan (Sigma-Aldrich) disolbatuta. Kontrol animaliei oliba olioa eman zitzaien prozedura berdina jarraituz. Saguak, ANIT edo oliba olioa eman ondoren 48 ordutara sakrifikatu ziren.

M.2.3. DDC-an oinarritutako kolestasi kimikoaren sagu eredua

Kolestasiaren beste eredu alternatibo bat bezala, DDC-a gehigarri duen dietan oinarritutako kolestasi kimikoko eredua erabili zen. DDC-ak ferrokelatasa inhibitzeko gaitasuna du, zeinak protoporfirinetatik abiatuta, hemo taldea sortzen duen gibelean (297). Ferrokelatasaren aktibitatea inhibitzen denean, protoporfirinak gibelean metatzen dira eta hauek behazunetik bakarrik kanporatu daitezke. Hortaz, protoporfirinen kontzentrazioaren emendioak behazun hodietako buxadura eta kalte hepatozelularra eragiten ditu (298). Ondorioz, gibelean xenobiotikoek eragindako kolestasiaren fenotipoa garatzen da. Fenotipo honen ezauagrri dira kolangiozitoen hazkuntza, perikolangitisa eta fibrosi biliarra gibel barneko zein kanpoko behazun hodietan (299). DDC eredua 8 asteko adina zuten WT and *Trem2*$^{-/-}$ saguetan egin zen, saguok %0.1 DDC-dun dieta (Ssniff) batez elikatu ziren 4 astez. Kontrol saguak DDC-rik gabeko (Ssniff) dieta berdinaz elikatu ziren, sagu guztiak dietarekin hasi eta 4 aste geroago sakrifikatu ziren.

M.2.4. BDL-an oinarritutako buxadurazko kolestasiaren eredua antibiotikoen bidezko hesteen esterilizazioarekin

Heste-gibel ardatzak TREM2-rekin lotutako fenotipoan betezen duen papera aztertzeko, BDL-an oinarritutako eredua, aurretik hesteen esterilizazioa egin zitzaien saguetan burutu zen. Aurretik argitaratutako lanetan behatu da, antibiotikoen konbinazio jakin bat edateko uretan ematea, saguen hesteen esterilizaziorako metodo baliagarria dela. Konbinazio hau hurrengo antibiotikoez osatzen da: 1 g/l ampicillin (Sigma-Aldrich), 1 g/l neomycin (Gibco), 1 g/l metronidazole (Acros Organics) and 500 mg/l vancomycin (Pfizer) (58). 4 astez, antibiotiko konbinazio hau edateko uretan eman zitzaien WT eta *Trem2*$^{-/-}$ saguei, tratamenduaren 3. astean BDL ebakuntza burutu zen eta animaliak ebakuntzatik 7 egunetara sakrifikatu ziren.

M.2.5. DEN+karbono tetrakloruran (CCl_4)-an oinarritutako fibrosiari lotutako HCC-ren sagu eredua

Fibrosiarekin lotutako HCC-a WT eta *Trem2*$^{-/-}$ saguetan eragin zen DEN eta karbono tetrakloruroaren konbinazioaz, lehenago argitaratutako estrategietan oinarrituz (213). DEN hepatokartzinogeno indartsua da saguetan, zitokromo P450 familiako CYP2E1-k metabolizatzen du DEN, DNA-ko kaltea sortzen duen metabolito ezegonkorra sortuz. Hepatozitoen hazkuntza aktiboa gertatzen denean ematen bada, jaio ondorengo faseetan bezala, DEN konposatuak eragindako mutazioak zelula-alabetara pasatzen dira, epe luzean HCC tumoreen sorrera dakarrena (300). Honez gain, CCl_4 gibelean metabolizatzen da, CCl_3 erradikala sortuz, honek lipido eta proteinen peroxidazioa eragiten ditu, ondorioz hepatozitoen heriotza eta birsortze prozesu akastuna sustatzen dira, eta azkenean gibeleko fibrosia garatzen da (301). Konbinazio modelo hau burutzeko, WT eta *Trem2*$^{-/-}$ sagu arrak 30mg/kg DEN-ekin ziztatu ziren jaio ondotik 15 egun zituztenean. Honen ondoren, (CCl_4/olive oil (O.Oil) 1:3 [vol:vol]) disolbatutako 2 µl/g CCl_4-ko 10 ziztada egin ziren, ziztadok astean behin egin ziren saguak 4 astetako adina zutenean hasita (DEN-en ziztada eta 2 aste ondoren). Saguak DEN-en ziztadatik 30 astetara sakrifikatu ziren. Tumore kopurua eskuz kontatu zen eta hauen tamaina neurtu zen sakrifizioaren unean.

M.2.6. Tioazetamida (TAA)-ren administrazioan oinarritutako fibrosiarekin lotutako HCC-ren sagu eredua

Fibrosiarekin lotutako HCC-ren bigarren sagu eredua egiteko, saguak TAA-z tratatu genituen. TAA gibeleko fibrosia eragiteko erabiltzen da orokorrean, baina epe luzera gibeleko minbiziaren garapen espotaneoa sortzeko gai dela behatu da (302). Gibelean metabolizatu ondoren, TAA-tik eratorritako metabolitoek estres oxidatiboa eta lobuluaren erdigunean hasten den nekrosia eragiten dute. Honek, birsortze mekanismo akastuna aktibatzen du, aldi berean, gibeleko fibrosia eta tumoreen garapena ere dakarrena (301). Sagu eredu hau burutzeko, 8 asteko adina zuten WT and *Trem-2*$^{-/-}$ sagu arrei %0,03 TAA zuen edateko ura eman zitzaien 40 astez. Saguak tratamendua hastetik 40 astetara sakrifikatu ziren, sakrifizioaren unean tumoreak eskuz kontatu ziren eta hauen tamaina neurtu zen. Tumoreek betetzen zuten bolumena kalkulatzeko ondorengo formula erabili zen: $Tv = (W^2 \times L)/2$ (303).

M.3. Saguetatik eratorritako zelula primarioen isolamendua, hazkuntza eta tratamendua

M.3.1. Zelula primarioen isolamendurako gibelaren *in situ* perfusioa

Gibeleko zelula mota desberdinak isolatzeko asmoarekin, hasteko, gibelaren *in situ* perfusio pauso bat burutu genuen, zeina zelula mota guztien isolamendurako protokoloan amankomuna den. Prozesu guztian zehar, animaliak arnastutako oxigenotan nahastutako isofluranoan (Abbvie) oinarritutako anestesia orokorpean mantendu ziren. Lehenik, sabelaldean irekigune bat zabaldu zen barne-organoak agerian uzteko. Ondoren, porta zaina kanulatu zen 22G-tako kanula bat erabiliz (BD Insyte), hodi-sistema kateterrera konektatu zen eta perfusiorako erabilitako disoluzioak hodi-sisteman zehar 5-7 ml/minutuko abiaduraz ponpatu ziren, perfusio ponpa baten lagutzaz. Azpiko kaba zaina gibelaren azpitik moztu zen, modu honetan, perfusioko disoluzioak gibeletik sartu eta azpiko kaba zainetik atera zitezen. Perfusio medioei dagokionez, lehenik gibela 10mM hepes (4-(2-hydroxyethyl)-1-piperazineethanesulfonic acid), 2,7 mM potasio kloruro (KCl), 135 mM sodio kloruro (NaCl) eta 250 µM sodio difosfatoz (HNa2PO4) osatutako medioaz garbitu zen (denak Sigma-Aldrich-enak). Ondoren, 60 mg kolagenasa IV (Gibco) eta 10 mM kaltzio kloruro ($CaCl_2$, Sigma-Aldrich) gehitu zitzaizkion perfusio medioari eta perfusio fluxua 3ml/minutuko abiadurara jeitsi zen, honela, gibelaren liseriketa bideratuz. Pauso honetan zehar, azpiko kaba zaina diafragmaren gainetik itxi zen, honen bidez perfusio medioak beste organoetan galtzea ekidin eta gibelean kontzentratzea lortzen da. KC eta HSC-en isolamendurako, kolagenasan oinarritutako liseriketaren aurretik, pauso gehigarri bat beharrezkoa da. Pauso gehigarri honetan, 200mg/ml-ko pronasaren 100 µl gehitu zitzaizkion F-12

medioaren (Gibco) 50 ml-ri eta gibela 3ml/minutuko abiadurara perfunditu zen. Azkenean gibela kontu handiz erauzi zen. KC eta HSC-en isolamendurako, behintzat 3 saguren gibelak behar dira zelula kantitate nahikoa lortzeko, kasu honetan, gibelak izotzetan gorde ziren perfusio guztiak bukatu arte.

M.3.2. Saguetatik eratorritako hepatozitoen isolamendua

Saguen hepatozitoen isolamendua gure ikerketa taldeak burutu zuen aurretik deskribatu bezala (304). *In situ* perfusioaren ondoren, gibela homogenizatu eta 70 μm zelula-prentsa batez filtratu zen, digeritu gabeko ehun soberakinak garbitzeko. Honen ostean, 3 garbiketa burutu ziren bat bestearen atzetik, hauetan zelula suspentsioak 800 g-tan 4 ºC-tara 6 minutuz zentrifugatu eta %10 FBS-ez (fetal bovine serum), %1 P/S-ez (penicilin-streptomicyn) (Gibco) eta %1 MEM aminoazido ez-esentzialez (Gibco) aberastutako William's E medioan (Sigma-Aldrich) birsuspenditu ziren. Azkeneko zentrifugazioaren ondoren, zelulak aberastutako William's E medioaren 25 ml-tan bersuspenditu ziren. Dentsitate gradiente bat prestatu zen 2.4ml 10X PBS eta 21.6 ml Percoll (Sigma-Aldrich) nahastuz, zelula suspentsioa dentsitate grandientearen gainean gehitu zen. Gradientea zentrifugatu zen 1500 g-tan 4ºC-tara 10 minutuz balaztarik gabe eta hemendik hepatozitoak lortu ziren. Isolatutako hepatozitoak kolageno finaz estalitatko plaketan hazi ziren %10 FBS, %1 P/S-az eta %1 NEAA-az aberastutako William´s E mediotan. Kolageno fina prestatzeko azido azetiko glaziala (500 μl, Corning) MiliQ urarekin (500 ml) nahastu zen. Arratoiaren isatseko I motako kolagenoa (BD) gehitu zen 50 mg/l-ko kontzentrazioan eta nahastea 0.22 μm poro tamaina zuen filro batean (Corning) zehar filtratu zen.

M.3.3. Saguetatik eratorritako kolangiozitoen isolamendua

Saguetatik eratorritako kolangiozito normalak (NMCs) gure ikerketa taldeak burutu zuen aurretik deskribatu bezala (305). Saguetatik eratorritako kolangiozitoen isolamendurako *in situ* perfusioa burutu zen protokolo berdina jarraituz, biana perfusiorako disoluzio desberdinak erabili ziren. Hasteko, gibela hurrengo osagiak zituen Hanks A disoluzioarekin perfunditu zen fluxua 5 ml/minutuko abiaduran jarriz: 120mM NaCl, 5mM KCl, 0.4 mM KH_2PO_4, 0.2 mM Na_2HPO_4, 25mM $NaHCO_3$, (denak Sigma-Aldrich) 0.1% D-Glucose (Sigma-Aldrich), 0.095% EGTA (Sigma-Aldrich) eta heparinaren 4 unitate. Ondoren, perfusioa hurrengo osagaiak zituen Hanks B disoluzioaz perfunditu ziren: 120mM NaCl, 5mM KCl, 0.4 mM KH_2PO_4, 0.2 mM Na_2HPO_4, 25mM $NaHCO_3$, 0.82mM $MgSO_4$, 1.07mM $MgCl_2$, 4mM $CaCl_2$, (denak from

Sigma-Aldrich) 0.1% D-Glucose, 5.1 µg/ml soybean trypsin inhibitor (STI) (Gibco), 0.025% Collagenase type IV. *In situ* perfusioa eta gero, gibela erauzi zen eta DMEM-az (Dulbecco's modified eagle médium) (Gibco) garbitu zen, gibelaren kapsula bota zen. Behazun zuhaitza pintza batzuen laguntzaz isolatu zen, eta hepatozitoez osatutako gainerako parenkima bota zen. Behazun zuhaitza isolatu eta gero, gibela Pronasa disoluzioaren 20 ml-z liseritu zen, %1 BSA (Sigma Aldrich), %0.025 Collagenase type IV, %0.034 pronasa, %0.006 DNasa eta P/S dituena, 37ºC-tara, 30 minutuz 140 rpm-tara nahastuz. Inkubazioa eta gero, kolangiozitoak 100 µm-ko filtro batean zehar filtratu zen. Berriki isolatutako NMCs-ak kolageno lodiaz estalitako plaketan eta aberastutako flask medioan hazi ziren. Flask medioak ondorengo osagaiak ditu: DMEM/F12, ondorengo osagaiekin aberastuta, %5 FBS (Gibco) %1 NEAA (Lonza), %1 lipid mixture (Sigma), %1 MEM vitamine solution (Gibco), %1 P/S (Gibco), %1 Insulin Transferrin Selenium (Gibco), 0.05 mg/ml STI (Gibco), 30 µg/ml Bovine Pituitary Extract (Gibco), 393 ng/ml Dexamethasone (Sigma), 3.4 µg/ml 3, 3' 5-triiodo-L-thyronine (T3) (Sigma), 25 ng/ml Epidermal Growth Factor (EGF) (Gibco) eta 4.11 mg/ml Forskolin (Ascent-Scientific). Kolangeno lodia prestatzeko azido azetikoa (50 µL) MilliQ urarekin (50 ml) nahastu zen arratoiaren isatseko I motako kolagenoarekin (BD) 1.5 mg/l-ko kontzentrazioan. Nahastea 0.22 µm poro tamaina zuen filro batean (Corning) zehar filtratu zen.

M.3.4. Saguetatik eratorritako KCs-en eta HSC-en isolamendua

In situ perfusioa eta gero, gibela gehiago digeritu zen *in vitro*, F-12 medioari 200 mg/ml pronasaren 10 µl eta 2 mg/ml DNasaren 50 µl gehitu zitzaizkion eta gibelak medio honetan inkubatu ziren 37ºC-tara 20 minutuz. Ondoren, gibelak homogenizatu, 70 µm-tako zelula filtro batean zehar filtratu, eta zentrifugazio (800 g-tara RT-ra 6 minutuz) eta F-12 medioan bersuspentsioan oinarritutako garbiketak egin ziren. Honen ostean, Nycodenz (Sigma-Aldrich) konposatuan oinarritutako dentsitate gradiente bat prestatu zen (%11 %16.5-ren gainean) eta zelula suspentsioa dentsitate gradientearen gainean gehitu zen. Gradientea 1500 g-tan RT-ra 22 minutuz eta balaztarik gabe zentrifugatu zen. Zentrifugazioa eta gero, zelulak dentsitate geruza egokietatik kontu handiz erauzi ziren. Euren dentsitatean dauden desberdintasunak direla eta, KC-ak % 16.5-eko geruzatik erautzten dira, HSC-ak % 11-ko geruzan aurkitzen diren bitartean. Hemendik Aurrera, KC-ak 10^6 zelula/ml-tako dentsitatean plakeatu ziren 6 putzutako plaketan (Corning) eta %10 FBS-az eta %1 P/S-az aberastutako RPMI (roswell park memorial institute medium 1640) mediotan hazi ziren. KC-ak plaketara itsasi zitezen utzi ziren 20 minutuz, ondoren, medioa aldatuz, zelula endotelial kutsakorrak garbitu ziren.

Isolatutako KC-en purutasuna gibel-zelulen markatzaile espezifikoak aztertuz egiaztatu zen, eta esperimentu guztiak 24 orduren buruan egin ziren. HSCs-ak 10^5 zelula/ml-tako dentsitatean plakeatu ziren 6 putzutako plaketan (Corning) eta %10 FBS-az eta %1 P/S-az aberastutako DMEM mediotan hazi ziren. HSC-en purutasuna isolamenduaren hurrengo egunean egiaztatu zen autofluoreszentzia aztertuz, eta beti %95-a baino altuagoa zen. HSC-en *in vitro* aktibazioa, zelula hauek zelula-hazkuntzarako erabilitako plastikoan 7 egunez 37ºC-tara eta %5 CO_2-rekin haziz lortu zen. KC-ak 100 ng/ml LPS-arekin (Sigma-Aldrich) edota UDCA-aren 100 µM edo 200 µM-rekin inkubatu ziren denbora puntu desberdinetan. Tratamendua eta gero, zelulak RNA-ren erauzketa egiteko prozesatu eta -80ºC-tara gorde ziren.

M.4. Gibelaren histologia eta tindaketa

Gibel ehuneko laginak jaso eta %4 paraformaldehidotan fijatu ziren 24 orduz, ondoren ehunak MTM ehun prozesadorearekin (Slee Medical GmbH) prozesatu ziren, parafinatan (Thermo fisher scientific) inkluitu eta HM355S mikrotomoaren (Thermo fisher scientific) laguntzaz 4-5 µm-tako mozketak egin ziren.

M.4.1. Haematoxilina eta eosina tindaketa (H&E) eta ebaluazio sistema

H&E tindaketa ehunaren morfologia aztertzeko helburuaz burutu zen. Hasteko, mozketak de-parafinatu eta ber-hidratatu ziren. Horretarako, mozketak xilenotan (VWR) 2 minutuz (2 inkubazio) eta gradualki txikitzen doan EtOH kontzentrazio desberdineko diluzioetan (100%, 96%, 70%, 50%) 5 minutuz murgildu ziren, azkenean, garbiketa pauso bat egin zen mozketak PBS-tan murgilduz. Hortik aurrera, mozketak Harris Haematoxilina-tan (Merck) murgildu ziren 5 minutuz, txorrotako urarekin garbitu, Eosina-tan (Merck) murgildu 5 minutuz, eta berriz ere txorrotako urarekin garbitu ziren. Azkenik, mozketei estalkia jarri zitzaien Pertex (Sigma-Aldrich) itsaskina erabiliz, eta Eclipse 80i (Nikon) mikroskopio batean aztertu ziren. Gibelaren histologia Madrileko Complutense unibertsitateko, albaitaritza fakultateko, animalia medikuntza eta kirurgiako departamentuko esperientziadun patologo batek burutu zuen. Laburbilduz, gibeleko inflamazioa honela ebaluatu zen: 0=inflamaziorik ez; 1=arina: isolatutako zelula inflamatorioak, foku inflamatorio definiturik gabe; 2=moderatua: fokuak eratzen dituzten zelula inflamatorioak; 3=larria: zelula inflamatorio asko, masak edo geruza anitzak eratuz. Bestalde, gibeleko nekrosiaren azterketa (306) argitalpena jarraituz burutu zen; 0=nekrosirik ez; 1=nekrosi zelular isolatua; 2= %5 baino gutxiago betetzen duten zonalde nekrotikoak; 3=%5-10 betetzen duten zonalde nekrotikoak; 4=

%10 baino gehiago betetzen duten zonalde nekrotikoak. Azkenik, behazun hodien hedapena modu itsuan ebaluatu eta puntuatu zen, 0= behazun hedapenik ez eta 5= behazun hedapen handiena behatu zen mozketa izanik.

M.4.2. Sirius red tindaketa

Sirius red tindaketa parafinan inkluitutako ehun mozketetan egin zen, kolageno zuntzak ikustarazteko. Mozketak aurreko atalean azaldutakoari jarraiki de-parafinatu eta ber-hidratatu ziren. Ber-hidratatu eta gero, mozketak % 2 azido fosfomolibdikotan (Sigma-Aldrich) 2 minutuz tindatu ziren eta dH_2O-rekin garbitu. Kolageno zuntzak tindatzeko mozketak 0.1% sirius red F3BA (Gibco)-tan murgildu ziren 3 orduz. Azkenik, mozketak 0.01 N HCl (Merck)-tan murgildu ziren 2 minutuz eta aurreko ataletan azaldu bezala deshidratatu eta gero, estalkia jarri zitzaien.

M.4.3. Inmunohistokimika (IHC) eta irudi analisia

IHC formalinan fixatu eta parafinan inkluitutako giza eta sagu gibelaren mozketetan egin zen. Hasteko, mozketak H&E-ren atalean azaldutako moduan de-parafinatu eta ber-hidratatu ziren. Gibelaren berezko peroxidasa aktibitatea blokeatu zen mozketak %0,6 hidrogeno peroxido (H_2O_2)-tan murgilduz 15 minutuz. Gero, kasuan kasuko antigeno berreskurapen metodoa burutu zen (**M.3. Taula**). Hoztu ondoren, mozketak sequenza sisteman egokitu ziren. Beharrezko kasuetan, ehunaren berezko abidina eta biotina tokiak blokeatu ziren 20 minutuz abidina eta biotinarekin (Vector laboratories) inkubatuz. Ondoren, mozketak kasuan kasuko blokeo sueroarekin blokeatu ziren 30 minutuz RT-ra. Blokeoen ondoren, kasuan kasuko antigorputz primarioen kontzentrazio egokiekin (**M.3. Taula**) inkubatu ziren mozketak 4ºC-tan gau osoan zehar. Hurrengo egunean, mozketak 1X PBS-arekin garbitu ostean, biotinilatutako antigorputz sekundarioekin inkubatu ziren (**M.3. Taula**). Ondoren, ABC erreaktibo tertziarioa (Vector laboratories) erabili genuen. IHC-ak DAB-az (Vector laboratories) errebelatu ziren. Azkenik, mozketak Haematoxilinarekin (Sigma-Aldrich) kontrastatu, deshidratatu eta DPX-arekin (Sigma-Aldrich) estali ziren.

Tindatutako zelulak eskuz kontatu ziren mozketa bakoitzeko handipen desberdinetako (10X, 20X edo 40X) 15 zonaldetan, eta zelula kopuru positiboen bataz bestekoa kalkulatu zen. Bestalde, CK19, αSMA, eta F4/80 IHC-en kasuan, irudi analisia mozketa bakoitzeko handipen desberdinetako (10X edo 20X) 15 zonaldetan egin zen Image J

software-a erabiliz. Irudi adierazarriak hartu ziren Eclipse 80i (Nikon) mikroskopio batean Digital sight DS-U2 kamara (Nikon) batean.

M.3. Taula. IHC-rako erabilitako antigorputzak.

Antigorputza	*Konpania*	*Referentzia*	*Diluzioa*	*Antigeno berreskurapena*
Rabbit polyclonal anti-CK19	Abcam	ab84632	1/200	Citrate buffer pH6 (Vector laboratories)
Mouse monoclonal anti-aSMA	Sigma-Aldrich	F3777	1/200	Citrate buffer pH6
Rat monoclonal anti-NIMP-R14	Abcam	ab2557	1/100	Citrate buffer pH6.0 followed by 2% trypsin in PBS 1X
Rat monoclonal anti-F4/80	Abcam	Ab6640	1/100	Proteinase K-EDTA pH 8
Rabbit monoclonal anti-CD3	Thermo scientific	RM-9107	1/500	EDTA pH 9
Rabbit polyclonal anti-Cl-Casp3	Cell Signaling	9661	1/750	EDTA pH 9
Swine anti-rabbit IgG biotinylated secondary antibody	Dako	E0353	1/200	-
Goat anti-rat IgG biotinylated secondary antibody	Serotec	STAR80B	1/200	-
Rabbit polyclonal anti-FITC HRP conjugate	Dako	P5100	1/200	-

αSMA, alpha smooth muscle actin; CD3, cluster of differentiation 3; Cl-Casp3, cleaved caspase 3; CK19, cytokeratin 19; EDTA, ethylenediaminetetraacetic acid; FITC, fluorescein isothiocyanate; HRP, horse radish peroxidase; IgG, immunoglobulin G; IHC, immunohistochemistry; PBS, phosphate buffered saline; PCNA, proliferating cell nuclear antigen.

M.5. Behazun azidoen neurketa

BDL edo sham ebakuntza egindako WT eta *Trem2*$^{-/-}$ saguen gibel edo serumeko BA-ak, etekin handiko kromotagrafia likidoa eta tandem masa espektrometria konbinatuz aztertu ziren, aurretik argitaratutako prozedura baten (308) egokitzapena jarraituz (307). Esperimentu hauek Salamankako unibertsitateko Jose J. G. Marin katedratikoaren ikerketa taldean burutu ziren.

Serumeko BA-ak azetonitriloaz egindako prezipitazio/erauzketaren ondoren neurtu ziren (309). Gutxi gora behera gibelaren 150 mg uraren 3 bolumenetan homogenizatu ziren. Nor-DCA gehitu zen eta gibel homogenatuak 65ºC-tara inkubatu ziren EtOH absolutuaren 2 bolumenekin 2 ordutako 2 periodoetan. Inkubazioen ondoko zentrifugazioaz EtOH erauzkinak lortu ziren, bi inkubazioetako erauzkinak bateratu ziren eta 0.1N NaOH-rekin nahastu ziren (1:4 bolumen:bolumen erlazioan) Silikan oinarritutako “Silica-based bonded phase cartridges”-etan(C18 Sep Pack cartridges, Waters-Millipore) aplikatu aurretik. Cartridge-ak uraz, %10 azetonaz eta uraz garbitu

ondoren, BA-ak metanolaz eluitu eta lehortu ziren. BA-ak serumetik erauzteko, 200 µl serum azetonitriloarekin nahastu ziren (1:3, bolumen:bolumen erlazioan), nahastea indarrez nahastu zen 1 minutuz eta 15 minutuz zentrifugatu zen 13 000 x G-tara eta 4ºC-tara. Gainjalkina bildu ondoren, prozesu hau jalkinarekin errepikatu zen. Bi gainjalkinak nahastu eta lehortu arte lurrundu ziren.

HPLC-a *Zorbax Eclipse XDB-C18* (150 mm x 4.6 mm, 5 µm) zutabe baten laguntzaz burutu zen. Kromatografiarako baldintzak honakoak izan ziren: i) disolbatzaileak metanola eta ura iza ziren, biak 5 mM amonio azetatoa eta % 0,01 azido formikoaz aberastuak, bukaerako pH-a 4,6-koa zen; ii) fluxuaren abiadura 0.5 ml/minutu-koa izan zen eta iii) kromatorafia 73:27 metanol/ur proportzioan hasi zen, hortik aurrera, metanolaren proportzioa linearki igotzen joan zen 10 minututan 93:7-ra igoz eta 73:27-ra itzuliz1 minututan. Electrospray ionizazio negatiboa (negative electrospray ionization (ESI)) honako baldintzetan burutu zen: gasaren tenperatura: 350ºC, gasaren fluxuaren abiadura: 11 l/min; nebulizatzailea: 45 psi, kapilarraren boltaia: 2500 V. Ioi aurrekariak filtratu eta gehiago zatikatu ziren MRM (multiple-reaction monitoring) metodoaren bidez, honela, zatiketaren ioi-produktuak intereseko BA bakoitzaren kantitatea neurtzeko erabili ziren (80,2 m/z taurinarekin konjugatutako BA-entzat; 74.0 m/z glizinarekin konjugatutako BA-entzat eta euren ioi aurrekariak BA libreentzat). Azido nor-dexikolikoa barne-estandar bezala erabili zen. BA honentzat 377.0 m/z to 331.3 m/z-ko trantsizioa jarraitu zen.

M.6. Kemokinen adierazpenaren neurketa Bio-Plex-aren bidez

MCP1 eta CXCL1 kemokinen adierazpena sham ebakuntza eta BDL-a jasandako WT eta *Trem2*$^{-/-}$ saguetan neurtu zen Tom Luedde doktorearen laborategian Uniklik Aachen-en (Aachen, Alemania). Horreatarako, neurrira diseinatutako Bio-Plex assay kit-a (Bio-Rad) eta FACS Canto II System-a (BD) erabili ziren ekoizlearen argibideak jarraituz. Kemokinen analisirako laginak 0.9 µg/µl-ko kontzentraziora prestatu ziren %0.5 BSA zuen lagin disolbatzailearekin.

M.7. Proteinen adierazpenaren neurketa immunoblotting bidez

M.7.1. Gibel ehunetik eratorritako proteinen erauzketa

Gibel ehuna (~20 mg) RIPA (radioimmunoprecipitation assay) tanpoiaren 400 µl-tan homogenizatu zen, zeinak honako osagaiak dituen: 150 mM NaCl, 50 mM Tris pH 7.5, 0.1% sodio dodecyl sulfatoa (SDS), 1% triton X100, 0.5% sodio deoxikolatoa, proteasen inhibitzaileak (Complete; Roche) eta fosfatasen inhibitzaileak (1 mM ortovanadatoa, 10 mM NaF, 100 mM β-glycerofosfatoa). Ondoren, homogenatuak rotatzaile batean inkubatu ziren 30 minutuz 4ºC-tara homogenzazioa errazteko. Gero, ehun homogenatuak 15 segundoko bi txandatan sonikatu (JP Selecta) eta 18000 g-tara zentrifugatu ziren 10 minutuz 4ºC-tara. Gainkalkina eppendorf berri batera pasa zen, horrela proteina homogenatuak lortuz.

M.7.2. Proteina totalaren kontzentrazioaren neurketa

Gibel ehunetatik eratorritako proteina kantitatea Pierce Bicinconic acid kit-aren (Thermo Scientific) bidez neurtu zen, ekoizlearen argibideak jarraituz. Laburbilduz, lagin bakoitzeko alikuota bat 1/40 diluitu zen dH_2O-arekin. Bitartean behiaren serumeko albuminan (bovine serum albumin, BSA) oinarritutako erreferentziazko estandar kurba bat prestatu zen. Laginen zein estandar kurbaren 25 µl pipeteatu ziren 96 putzuko plaka batean (Corning). A eta B erreaktiboak 50/1 erlazioan nahastu ziren eta putzu bakoitzeko nahasketaren 200 µl gehitu ziren. Plaka 30 minutuz iluntasunean 37 ºC-tara inkubatu zen eta xurgapena 570 nm-tara neurtu zen Haloled aparatu batean. Lagin bakoitzaren proteina kontzentrazioa kurba estandarraren extrapolaziotik lortu zen.

M.7.3. SDS poliakrilamida gel elektroforesia eta inmunobloting-a

Proteinen banaketarako, beharrezko proteina totalen kantitatea (60-100 µg artean detexkatu nahi zen proteinaren arabera) % 10 edo 12.5-eko SDS-PAGE-tan kargatu eta ondoren nitrozelulosa mintzetara (Sigma-Aldrich) transferitu zen. Ponceau tindatzailearekin (Sigma-Aldrich) tranferentzia egokia egiaztatu ondoren, mintzak %0.1 Tween-20 zuen Tris tanpoian (T-TBS) egindako %5 esnetan blokeatu ziren ordu betez. Antigorputz primario egokiak prestatu ziren (**M.4. Taula**) eta mintzak hauekin inkubatu ziren gau osoan zehar 4ºC-tara. Hurrengo egunean, mintzak T-TBS-arekin garbitu eta ordu betez kasuan kasuko, HPR-arekin konjugatutako antigorputz sekundarioen 1/5000

diluzioekin inkubatu ziren (**M.4. Taula**). Antigorputz sekundarioarekin inkubatu ondoren, mintzak T-TBS-arekin garbitu eta (ECL) HRP Chemiluminiscent Substrate Reagent Kit (Invitrogen)-rekin ikustarazi ziren iBright FL1000 (Invitrogen)biomolekular irudi egile batean, glizeraldehido-3-deshidrogenasa (GAPDH) edo β-aktina proteinen kargatze kontrola bezala erabili ziren.

M.4. Taula. Immunoblotting-ean erabilitako antigorputzak.

Antigorputza	*Konpania*	*Referentzia*	*Diluzioa*
Rabbit-polyclonal anti-RIP3	Pro Sci	2283	1/2000
Rabbit-polyclonal anti-Cleaved caspase-3 (Asp-175)	Cell signaling	9661	1/2000
Rabbit polyclonal anti-MLKL	Biorbyt	Orb32399	1/2000
Mouse-monoclonal anti-GAPDH	AbD Serotec	MCA-4739	1/2000
Anti-rabbit IgG HRP-linked antibody	Cell signaling	7074	1/5000
Anti-mouse IgG HRP-linked antibody	Sigma-Aldrich	A4416	1/5000

Asp, aspartate; GAPDH, glyceraldehyde-3-phosphate dehydrogenase; HRP, horse raddish peroxidase; IgG, immunoglobulin G; MLKL, mixed lineage kinase domain like; RIP3 receptor interacting protein 3; Thr, threonine.

M.8. RNA erauzketa eta qPT-PCR bidezko analisia

M.8.1. Gibel ehunetik eratorritako RNA-ren erauzketa

Gibel ehuna (~20 mg) Tri-reagent® (Sigma-Aldrich) erreaktiboren 1 ml-tan homogenizatu zen eta izozte-desizozte ziklo bat egin zitzaion homogenizazioa errazteko. RNA totalaren erauzketarako 200 µl of koroformo (Merck) gehitu ziren eta laginak nahastu eta 15 minutuz RT-ra inkubatu ziren. Honen ondoren, laginak 18000 g-tan 4ºC-tara zentrifugatu ziren 15 minutuz eta goiko fasea eppendorf berri batera pasa zen. RNA prezipitatzeko helburuarekin, 500 µl of isopropanol (AppliChem Panreac) gehitu eta laginak nahastu eta 10 minutuz RT-ra inkubatu ziren, ondoren 18000 g-tan 4ºC-tara zentrifugatu ziren 15 minutuz. Pauso hau eta gero jalkina sortu zen, gainjalkina bota eta jalkinak 1 ml %75 EtOH-az gabitu ziren 18000 g-tan 4ºC-tara zentrifugatuz 15 minutuz. Gainjalkina berriz bota eta jalkinak lehortzen utzi ziren. Azkenean, RNA jalkinak 200-300 µl Ultrapure™ DNase/RNase-free ur destilatutan (Gibco) bersuspenditu ziren eta RNA kontzentrazioa NanoDrop® ND-1000 apparatus (Thermo-Fisher Scientific) batean neurtu zen.

M.8.2. Giza gibel ehunetik eta isolatutako sagu zeluletatik eratorritako RNA-ren alderantzizko transkripzioa

Giza gibel ehunetik eta isolatutako sagu zeluletatik eratorritako RNA-ren alderantzizko transkripzioa egiteko SuperScript® VILO™ cDNA Synthesis Kit (Life technologies)-a erabili zen. Alderantzizko transkripzioa ekoizlearen argibideak jarraituz burutu zen. Laburki, 2 µl of 10X SuperScript® Enzyme Mix, 4 µl of 5X VILO™ Reaction Mix eta 20 µl osatzeko beharrezko DNase/RNase-free ur destilatua RNA laginen 200-500 ng-rekin nahastu ziren. Alderantzizko transkripzioa Verity 96 well thermal cycler (Applied biosystems) aparatu batean burutu zen, honako protokoloa jarraituz: i) 10 minutu 25ºC-tara, ii) 60 minutu 42ºC-tara, iii) 5 minutu 85ºC-tara. Sintetizatu berritako DNA osagarriari (complementary DNA, cDNA) DNase/RNase-free ur destilatua gehitu zitzaion 12,5 ng/ µl-ko kontzentrazioa lortu arte.

M.8.3. Sagu gibel ehunetik eratorritako RNA-ren alderantzizko transkripzioa

Erauzitako RNA 1 µg-ri DNasa tratamendua egin zitzaion DNA genomikoa garbitzeko. Honetarako, laginei 1 µl DNase I Amplification Grade (Invitrogen) eta 1 µl 10X DNase I Reaction Buffer (Invitrogen) gehitu zitzaizkien eta 37°C-tara 20 minutuz inkubatu ziren. Ondoren, 1 µl 25 mM azido ethylenediaminetetraacetic (EDTA) (Invitrogen) gehitu zitzaien laginei magnesioa kelatu eta DNasaren aktibitatea geldiarazteko, honetarako, laginak 65°C-tara 10 minutuz eta 90°C-tara 1 minutuz inkubatu ziren, azkenik, 4°C-tara mantendu ziren. cDNA-ren sintesia burutzeko, alderantzizko transkripziorako nahasketaren 30 µl prestatu ziren lagin bakoitzeko [8 µl Buffer 5X, 4 µl Random primers 100 ng/µl, 4 µl Deoxy-nucleotide-triphosphate mix (dNTPs), 2 µl DTT, 1.2 µl RNase OUT, 1.2 µl M-MLVRT (denak Invitrogen) eta 9.6 µl DNase/RNase-free ur destilatua] hau laginei gehitu zitzaien eta erreakzioa burutzeko, laginak 37°C-tara 60 minutuz eta 95°C-tara 1 minutuz inkubatu ziren eta 4°C-taraino hoztu ziren. Sintetizatu berritako DNA osagarriari (complementary DNA, cDNA) DNase/RNase-free ur destilatua gehitu zitzaion 12,5 ng/ µl-ko kontzentrazioa lortu arte.

M.8.4. RT-qPCR-aren bidezko gen adierazpenaren azterketa

Gen adierazpenaren azterketa SYBR teknologia eta primer espezifikoak erabiliz egin zen. RT-qPCR erreakziorako nahasketa prestatu zen 10 µl iQ™ SYBR® Green Supermix (Bio-Rad), 0.6 µl 10 µM beharrezko forward eta reverse primerrak (**M.5.**

Taula eta **M.6. Taula**) eta DNase/RNase-free ur destilatua nahastuz lagineko, 17 µl-ko bolumenean. Nahastea Hard-Shell PCR plates 96-well (Bio-Rad) plaka batean pipeteatu zen, ondoren, 12,5 ng/µl-kontzentraziora zeuden beharrezko cDNA laginen 2-3 µl gehitu ziren eta plaka estalki (Microseal "B" seal (Bio-Rad)) batekin estali zen. CFX 96 apparatus (Bio-Rad) makina bat erabili zen RT-qPCR erreakzioa eta DNA-ren anplifikazioaren detekziorako, iQ™ SYBR® Green Supermix-aren protokolo arrunta jarraituz. Laburki, cDNA desnaturalizazioa eta entzimaren aktibazioa hasierako 10 minutuko 95°C-tako pauso batekin lortu ziren. Hemendik aurrera, DNA-ren anplifikazioa 3 pausotako 40 ziklotan egin zen. Pausoak honakoak ziren: DNA-ren desnaturalizaziorako, 15 segundo 95ºC-tara, primerrak itsasteko, 30 segundo 60ºC-tara eta 45 segundo 72ºC-tara extensiorako. Disoziazio kurba bat ere egin zen, primerren espezifizitatea ziurtatzeko. Horretarako, temperatura 60°C-tatik 93ºC-tara igotzen joan zen gradualki. Kontrol bezala, *GAPDH* edo *HPRT1* (Hypoxanthine phosphoribosyltransferase 1) geneen adierazpen mailak erabili ziren. Geneen adierazpen maila erlatiboak kalkulatu ziren ΔCT kalkuluaren bidez, mRNA mailak unitate arbitrariotan edo horrela adierazten denean, kontrol egoerarekiko normalizatuta, erakusten dira.

M.5. Taula. qRT-PCR-an oinarritutako gen adierazpenaren azterketan erabilitako gizak primerrak.

Genea	*Forward primerraren sekuentzia (5´-3´)*	*Reverse primerraren sekuentzia (5´-3´)*
ACTA2	CGGGACTAAGACGGGAATCCT	GTCACCCACGTAGCTGTCTT
CD9	CAACAAGCTGAAAACCAAGGA	CAAACCACAGCAGTTCAACG
COL1A1	GATGGCTGCACGAGTCACAC	AACGTCGAAGCCGAATTCCT
GAPDH	CCAAGGTCATCCATGACAAC	TGTCATACCAGGAAATGAGC
HPRT1	TATGGCGACCCGCAGCCCT	CATCTCGAGCAAGACGTTC
IL6	AAAGAGGCACTGGCAGAAAA	AGCTCTGGCTTGTTCCTCAC
IL8	GTGCAGTTTTGCCAAGGAGT	ACTTGTCCACAACCCTCTGC
IL33	TTAATGGTAACCCTGAGTCC	TATGAAGGACAAAGAAGGCC
MCP1	CAGCCAGATGCAATCAATGCC	TGGAATCCTGAACCCACTTCT
TNF	CCTGCTGCACTTTGGAGTGA	CAGCTTGAGGGTTTGCTACA
TREM2	ACGAGATCTTGCACAAGGCA	GGTAGAGACCCGCATCATGG

Acta2, actin alpha 2, smooth muscle; *COL1A1*, collagen type 1 alpha 1;*GAPDH*, glyceraldehyde 3-phosphate dehydrogenase; *HPRT1*, hypoxanthine-guanine phosphoribosyltransferase; *IL*, interleukin; *MCP1*, monocyte chemoattractant protein 1; *TNF*, tumour necrosis factor; *TREM2* triggering receptor expressed on myeloid cells 2.

M.6. Taula. qRT-PCR-an oinarritutako gen adierazpenaren azterketan erabilitako sagu primerrak.

Genea	*Forward primerraren sekuentzia (5´-3´)*	*Reverse primerraren sekuentzia (5´-3´)*
Acta2	CTCAGCGCCTCCAGTTCCT	AAAAAAAACCACGAGTAACAAATCAA
Col1a1	TTCACCTACAGCACGCTTGTG	GATGACTGTCTTGCCCCAAGTT
Ck7	AGGAGTCAACCGACGCAC	GTCTCGTGAAGGGTCTTGAGG
Ck19	GGGGGTTCAGTACGCATTGG	GAGGACGAGGTCACGAAGC
Cxcl1	CTGGGATTCACCTCAAGAACATC	CAGGGTCAAGGCAAGCCTC
Cyp7a1	GGGATTGCTGTGGTAGTGAGC	GGTATGGAATCAACCCGTTGTC
Fxr	GGCTGAAAGGTTTCTTCG	CAGCCAACATCCCATCTCT
GAPDH	GCACAGTCAAGGCCGAGAAT	GCCTTCTCCATGGTGGTGAA
Hmox	AAGCCGAGAATGCTGAGTTCA	GCCGTGTAGATATGGTACAAGGA
Il6	TAGTCCTTCCTACCCCAATTTCC	TTGGTCCTTAGCCACTCCTTC
Mcp1	TTAAAAACCTGGATCGGAACCAA	GCATTAGCTTCAGATTTACGGGT
Nos2	GTTCTCAGCCCAACAATACAAGA	GTGGACGGGTCGATGTCAC
Tnf	CCCTCACACTCAGATCATCTTCT	GCTACGACGTGGGCTACAG
Trem1	ATGACCTAGTGGAGGGCCAG	GCACAACAGGGTCATTCGGAG
Trem2	TTGCTGGAACCGTCACCATC	CACTTGGGCACCCTCGAAAC

Acta2, actin alpha 2, smooth muscle; *Ck*, cytokeratin; *Col1a1*, collagen type 1 alpha 1; *Cxcl1*, C-XC motif ligand 1; *Cyp7a1*, cytochrome P450 family 7 subfamily A Member 1; *Fxr*, farnesoid X receptor; *Gapdh*, glyceraldehyde 3-phosphate dehydrogenase; *Hmox1*, heme oxygenase 1; *Hprt1*, hypoxanthine-guanine phosphoribosyltransferase; *Il*, interleukin; *Mcp1*, monocyte chemoattractant protein 1; *Nos2*, nitric oxide synthase 2; *Shp*, small heterodimer partner*; Tnf*, tumour necrosis factor; *Trem1*, triggering receptor expressed on myeloid cells 1; *Trem2*, triggering receptor expressed on myeloid cells 2.

M.9. Azterketa estatistikoa

GraphPad Prism 6.00 (GraphPad Software) programa erabili zen azterketa estatistikoa egiteko. Lehenik eta behin, aztertutako datu taldeak banaketa normala jarraitzen zuen ikusi zen Shapiro-Wilk testaren bidez. Banaketa normala jarraitzen zuten datuetan test parametrikoak egin ziren eta, datu ez-normalentzat, aldiz, test ez-parametrikoak erabili ziren. Bi talde independenteren konparaziorako Student-en *t* test parametrikoa edo Mann Whitney-ren test ez-parametrikoa erabili zen. Bi talde baino gehiago konparatu ziren kasuetan, ANOVA (one-way analysis of variance) eta Tukey-ren post hoc test parametrikoak edo Kruskal-Wallis eta Dunn-en post hoc test ez-parametrikoak erabili ziren. Korrelazioak aztertzeko, Person-en test parametrikoa eta Spearman-en test ez-parametrikoa erabili ziren. Datuak bataz bestekoa ± bataz bestekoaren errore estandar (standard error of the mean, SEM) bezala adierazten dira. Estatistikoki esanguratsuak diren konparazioak figuretan adierazten dira * edo # kodeen bidez, kasu bakoitzean egindako konparaketa bereizteko. * edo #, ** edo ##, *** edo ### eta **** edo #### *p* balioa <0.05, <0.01, < 0.001 and < 0.0001 dela adierazten dute, hurrenez hurren. Korrelazio azterketetan, korrelazio koefizientea (r) eta *p* balioa erakusten dira.

EMAITZAK

E.1.*TREM2*-ren adierazpena emendatuta dago giza kolestasian

E.1.1. TREM2-ren adierazpena emendatuta dago PBC eta PSC-dun gaixoen gibelean eta gaixotasunaren markatzaileekin positiboki korrelazionatzen du San Sebastian/Warsaw gaixo taldean

Gure ikerketa taldearen aurreko lanetan, jatorri desberdinetako zirrosia duten pazienteen gibelean (288) eta HCC tumoreak dituzten pazienteen gibelean (289), TREM2-ren adierazpena emendatuta dagoela behatu da, gibel osasuntsu kontrolarekin konparatuz. Lan honetan, TREM2-ren adierazpena giza kolestasian aztertu da.

Hasteko, TREM2-ren mRNA adierazpen maila San Sebastian/Warsaw gaixoen taldean aztertu zen, honetan, PBC eta PSC gaixotasun kolestatikoak (PBC n=10 eta PSC n=10) duten gaixoen gibeleko, kontrol osasuntsuen gibeleko (n= 218) eta jatorri desberdinetako zirrosia duten gaixoen gibeleko (n= 35) laginak daude. Gaixo talde honen ezaugarriak eta parametro klinikoak **E.1 Taulan** ageri dira. Aurretik deskribatutakoa konfirmatuz (288), *TREM2*-ren mRNA adierazpena emendatuta ageri da zirrosia duten gaixoen gibelean gibel kontrolarekin alderatuz. Aurkikuntza berria da, *TREM2*-ren mRNA adierazpena emendatuta dagoela PBC eta PSC duten gaixoen gibelean kontrol gibelarekin konparatuz. Halaber, *TREM2*-ren mRNA adierazpena ere handiagoa zen PBC eta PSC duten gaixoen gibelean zenbait jatorriko (jatorri alkoholikoa, hepatitis C birusak (HCV) hepatitis B birusak (HBV) edo jatorri idiopatikoa, hots identifikatu gabekoa, barne) zirrosia duten gaixoen gibelarekin konparatuz (**R.1A Irudia**).

Ondoren, *TREM2*-ren mRNA adierazpena gibeleko inflamazioaren eta fibrosiaren markatzaile desberdinekin korrelazionatzeko asmoz, PBC eta PSC-dun gaixoen datuak taldekatu genituen. Honela, *TREM2*-ren mRNA adierazpenak korrelazio positiboa du *IL6*, *IL8* eta *IL33* zitokina proinflamatorioen mRNA-rekin KCs-en markatzaile den *CD68*-rekin, gibel ehun zirrotikoan identifikatu berri den $TREM2^{+}CD9^{+}$ makrofagoen markatzaile den *CD9*-rekin (281) eta fibrosiaren markatzaile den COL1A1-ren mRNA-rekin, gaixotasun kolesetatiko kroniko desberdinak dituzten gaxioetan, PBC eta PSC barne (**R.1B Irudia**).

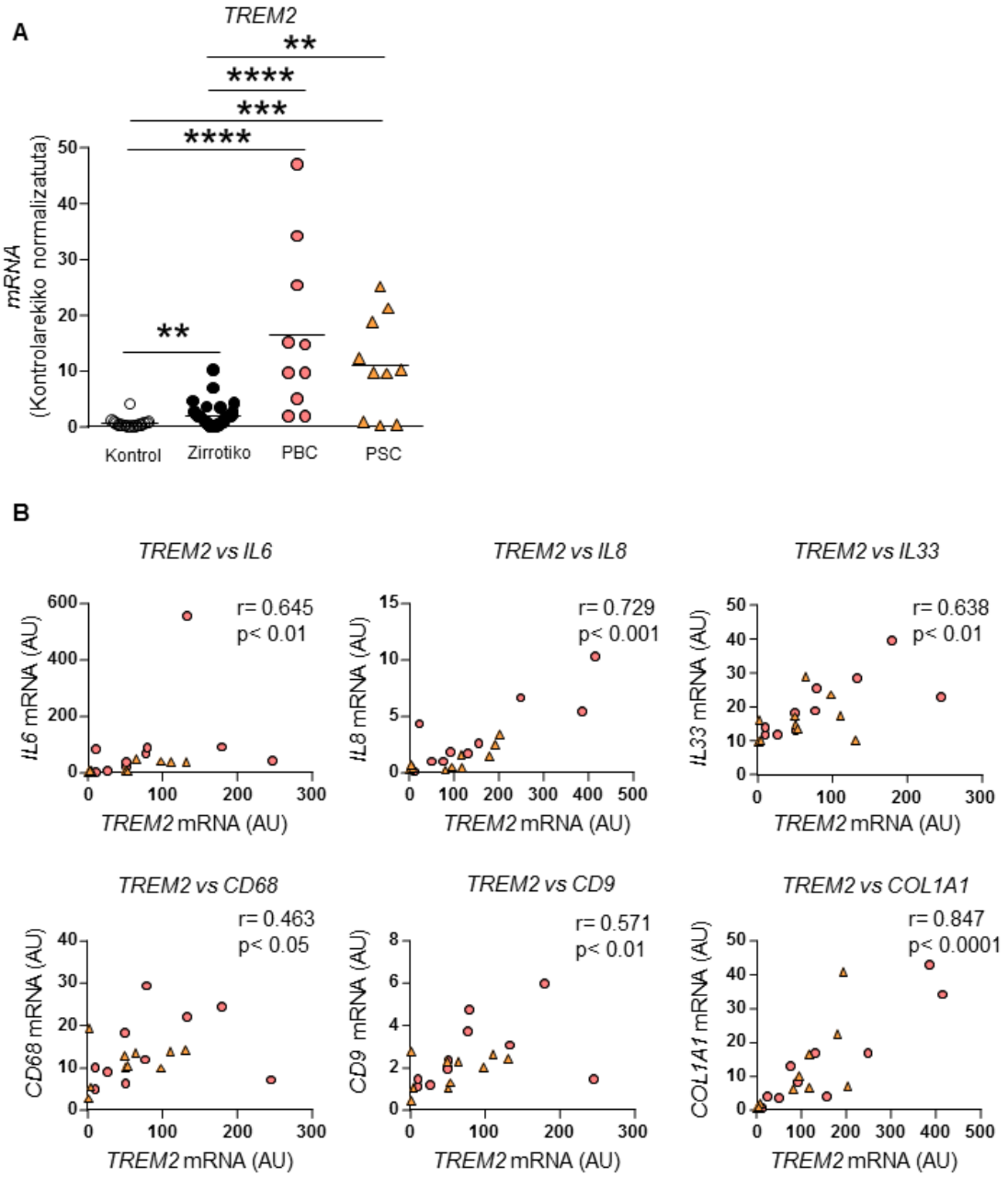

E.1. Irudia. TREM2 mRNA adierazpena giza gaixotasun kolestatikodun gaixoen gibeletan. (A) *TREM2* mRNA adierazpena indibiduo kontrolen (n=18), zirrosidun gaixoen (n=35) eta PBC (n=10) eta PSC (n=10)-dun gaixoen gibeletan. (**B**) *TREM2* mRNA adierazpenaren korrelazioa *IL6*, *IL8*, *IL33*, CD68, *CD9* eta *COL1A1* markatzaileekin gaixotasun kolestatiko kronikoak (PBC eta PSC) dituzten gaixoen gibelean. (**A**) Mann Whitney-ren test ez-parametrikoa erabili zen. (**B**) Spearman-en korrelazio test ez-parametrikoa erabili zen, korrelazioaren koefizientea (r) eta *p* balioa erakusten dira. **, *** eta **** *p* balorea <0.01, <0.001 eta 0.0001 adierazten dute, hurrenez hurren. AU, arbitrary units; *CD9*, cluster of differentiation 9; CD68, cluster of differentiation 68; *COL1A1*, collagen type 1 a 1; *IL6*, interleukin 6; *IL8*, interleukin 8; *IL33*, interleukin 33; PBC, primary biliary cholangitis; PSC, primary sclerosing cholangitis; *TREM2*, triggering receptor expressed on myeloid cells.

PBC eta PSC bakoitza bere patologia propioa duten bi gaixotasun desberdin direnez, korrelazioak era bananduan aztertu ziren, gaixotasun bakoitza bere aldetik, alegia. Ildo honetan, PBC-dun gaixoen kasuan, *TREM2*-ren mRNA adierazpenak positiboki korrelazionatzen du gibeleko minaren serumeko markatzaile diren AST eta ALT-ren mailarekin, baita kolestasiaren markaitzailea den bilirrubina maila serologikoekin ere (**R.2A Irudia**). Era berean, korrelazio positiboa behatu genuen *TREM2*-ren mRNA adierazpena eta MELD puntuazioaren artean PBC duten gaixoetan (**R.2A Irudia**). Emaitza hauek gibeleko inflamazio eta fibrosiaren markatzaile diren geneen adierazpen mailen korrelazioetan ere agerikoak ziren. Honela, *TREM2*-ren mRNA adierazpenak positiboki korrelazionatzen du *IL8*, *IL33* eta *COL1A1*-ren mRNA adierazpenarekin PBC duten gaixoetan, eta *IL6*, *IL8* eta *COL1A1*-rekin PSC duten gaixoetan (**R.2B Irudia**).

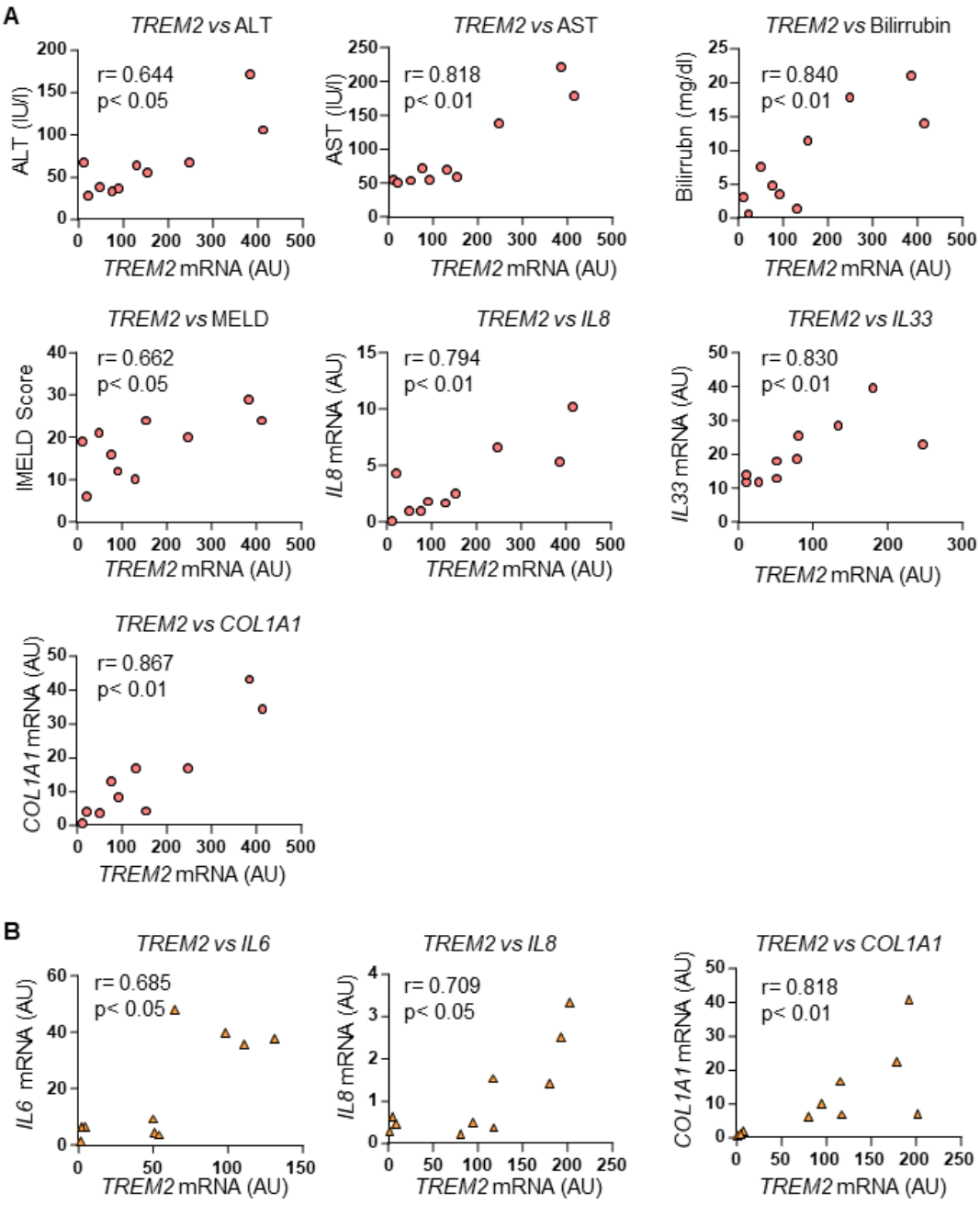

E.2. Irudia. PBC eta PSC-dun gaixoen gibeleko *TREM2* mRNA adierazpenaren korrelazioa gaixotasun kolestatikoaren garapenaren markatzaileekin. (A) PBC-dun (n=10) gaixoen gibeleko *TREM2* mRNA adierazpenaren korrelazioa serumeko ALT, AST eta bilirrubinarekin, MELD puntuazioarekin eta *IL8* eta *IL33* inflammazioaren markatzaileekin mRNA adierazpenarekin eta *COL1A1* fibrosiaren markatzailearen mRNA adierazpenarekin. (**B**) PSC-dun (n=10) gaixoen gibeleko TREM2 mRNA adierazpenaren korrelazioa *IL6* eta *IL8* inflamazioaren markatzaileen adierazpenarekin eta *COL1A1* fibrosiaren markatzailearen mRNA adierazpenarekin. Pearson-en korrelazio test parametrikoa (*TREM2*-Bilirrubin and *TREM2*-MELD) eta Spearman-en korrelazio test ez-parametrikoa erabili ziren, korreazioaren koefizientea (r) eta *p* balorea erakusten dira. ALT, alanine aminotransferase; AST, aspartate aminotransferase; AU, arbitrary units; *COL1A1*, collagen type 1 a 1; *IL6*, interleukin 6; *IL8*, interleukin 8; *IL33*, interleukin 33; MELD, model for end-stage liver disease; PBC, primary biliary cholangitis; PSC, primary sclerosing cholangitis; *TREM2*, triggering receptor expressed on myeloid cells.

E.1.2. TREM2-ren adierazpena emendatuta dago arrisku altuko PBC duten gaixoen gibelean eta positiboki korrelazionatzen du gaixotasunaren garapenaren markatzaileekin GSE79850 gaixo taldean

Ondoren, GEO (Gene Expression Omnibus) datu basean publikoki eskuragarri dauden datuak erabili genituen TREM2-ren adierazpena PBC-dun gaixoen talde independente batean aztertzeko asmoz. Gaixo talde honetan, diagnostikoaren momentuan, tratamendua jaso aurretik, lortutako laginak daude, arrisku bajuko eta arrisku altuko PBC-dun gaixoen laginak eta osasuntsuen talde kontrol baten laginak ere badaude (290). Arrisku bajuko PBC-dun gaixoek ondorengo irizpideak betetzen dituzte: 1) Paris 1 irizpidearen arabera UDCA-rekiko erabateko erantzuna erakusten dute; 2) 15 urteko jarraipenean zehar, osasuntsu jarraitzen dute eta UDCA-ri erantzuten jarraitzen diote; 3) ez dute gibelaren transplanterik behar izan. Arriku altuko PBC-dun gaixoen taldea sailkatzeko, berriz, honako irizpideak erabiltzen dira: 1) Paris 1 irizpidearen arabera, ez dute UDCA-ren 13–15 mg/Kg dosi batekiko erantzun osorik, 2) PBC gaixotasunaren arrazoi prognostikoak direla eta, gibeleko transplante baten beharra izan dute 15 urteko jarraipenean zehar momenturen batean.

Azpimarragarria da, *TREM2* genearen adierazpena emendatuta dagoela arrisku altuko PBC-dun gaixoen gibelean arrisku bajuko PBC-dun gaixoen eta gibel ehun kontrolarekin alderatuta. Ez zen desberdintasunik topatu, ordea, arrisku bajuko PBC-dun gaixoen gibelen eta gibel ehun kontrolaren artean (**R.3A Irudia**). *TREM2*-ren adierazpenak eta PBC gaixotasunaren garapenaren markatzaileek GSE79850 gaixo taldean duten korrelazioa aztertzeko asmoz, arrisku bajuko eta arrisku altuko PBC-dun pazienteak taldekatu genituen. San Sebastian/Warsaw gaixoen taldean behatutakoari jarraiki, gaixoen talde honetan ere, *TREM2*-ren gibeleko adierazpenak inflamazioaren markatzaile diren *IL6* eta *CXCL1*-rekin korrelazionatzen zuen (**R.3B Irudia**). Era berean, *TREM2*-ren gibeleko adierazpenak *CD9* markatzailearen adierazpenarekin ere korrelazionatzen zuen (**R.3B Irudia**), *CD9*-a gibeleko zirrosia duten gaixoetan aurkitzen den $TREM2^{+}CD9^{+}$ makrofagoen azpi-populazio bat definitzen duela aurkitu da berriki (280). Azkenik, TREM2-ren gibeleko adierazpenak *COL3A*1 fibrosiaren markatzailearen adierazpenarekin ere korrelazionatzen zuen.

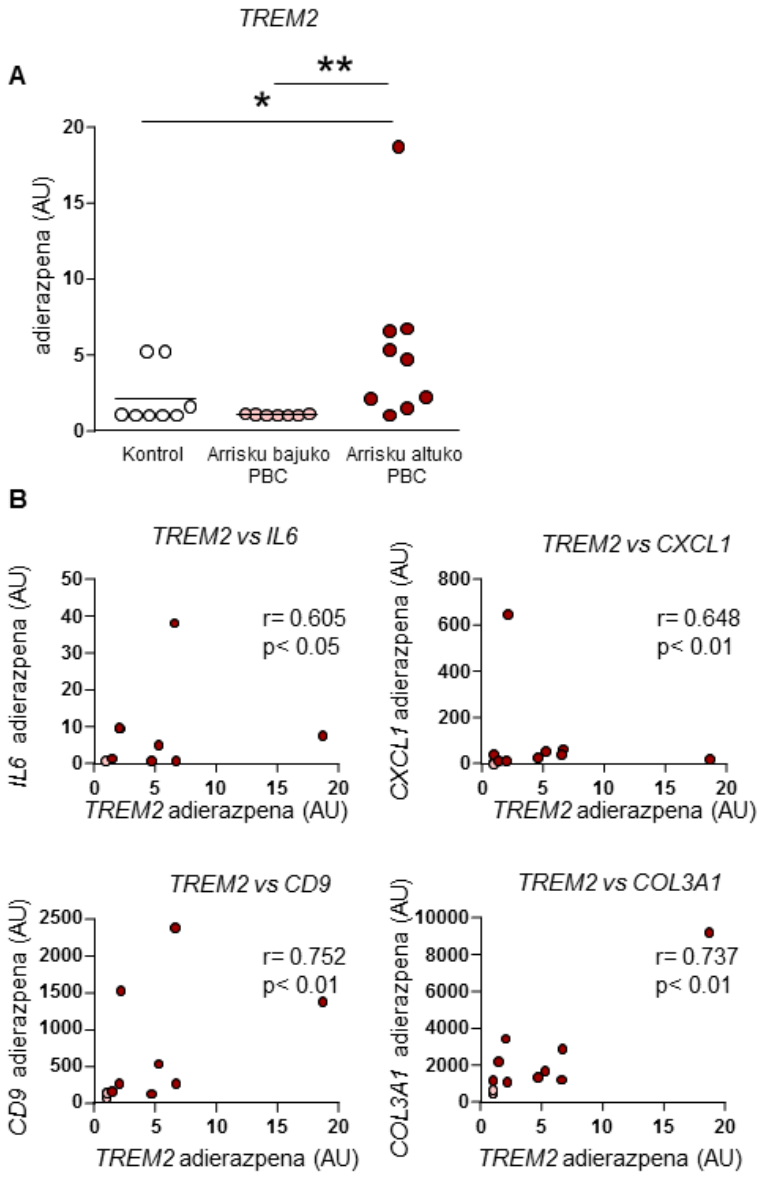

E.3 Irudia. *TREM2* genearen adierazpena eta korrelazioa markatzaile inflamatorio eta fibrotikoen adierazpenarekin GSE79850 gaixo taldean. (**A**) *TREM2* genearen adierazpen maila indibiduo kontrolen (n=8), eta arrisku bajuko (n=7) eta arrisku altuko (n=9) PBC-dun gaixoen gibelean. (**B**) *TREM2* genearen adierazpenaren korrelazioa inflamazioaren (*IL6* eta *CXCL*1), makrofagoen (*CD9*) eta fibrosiaren (*COL3A1*) markatzaileen adierazpenarekin PBC-dun pazienteen gibelean (arrisku bajuko eta arrisku altuko pazienteak taldekatu dira). (**A**) Mann Whitney-ren test ez-parametrikoa eta (**B**) Spearman-en korrelazio test ez-parametrikoa erabili dira, korrelazioaren koefizientea (r) eta *p* baloreak erakusten dira. * eta ** *p* balorea <0.05 eta <0.01 adierazten dute, hurrenez hurren. AU, arbitrary units; *CD9*, cluster of differentiation 9; *COL3A1*, collagen type 3 a 1; *CXCL1*, *Cxcl1*, C-X-C Motif Chemokine Ligand 1; *IL6*, interleukin 6; PBC, primary biliary cholangitis;*TREM2*, triggering receptor expressed on myeloid cells.

Orokorrean, datu hauek iradokitzen dute TREM2-ren adierazpena handituta dagoela kolestasia duten gaixoen gibeletan, beraz, hartzaile honek paper garrantzitsua bete lezake gaitz honen garapenean.

E.2.*TREM2*-ren adierazpena emendatuta dago kolestasiaren sagu ereduetan

TREM2-ren adierazpenaren emendioa giza eta sagu kolestasian kontserbatzen den fenomenoa den aztertzeko asmoz, ondoren, *Trem2*-ren gene adierazpena saguen ehunean aztertu genuen. Hasteko, *Trem2*-ren adierazpena sagu osasuntsuetatik isolatutako zelula mota desberdinetan ikertu genuen. HCC-dun gaixoen gibelean IHC bidez behatutakoa eta gure ikerketa taldeak aldez aurretik argitaratutako emaitzak baieztatuz (288, 289), *Trem2*-ren mRNA adierazpena zelula epitelialetan oso bajua zela behatu genuen, KCs eta aktibatutako HSCs-etan, aldiz, adierazpen hau asko emendatzen zen (**E.4A Irudia**). Hartzaile honek kolestasian izan lezakeen garrantzia aztertzeko asmoz, gure hurrengo urratsa, *Trem2*-ren adierazpena kolestasiaren sagu ereduetan aztertzea izan zen. Kolestasiaren sagu eredu desberdinak erabili genituen, gaitzaren ezaugarri desberdinak kontuan hartzeko asmoz. Zehazki, *Trem2*-ren adierazpena emendatuta dago BDL-an oinarritutako buxadurazko kolestasian “sham” ebakuntza egindako saguekin konparatuz (**E.4B Irudia**). Era berean, *Trem2*-ren adierazpena emendatuta dago kimikoki eragindako kolestasiaren bi sagu eredu desberdinetan, bat ANIT-aren eta bestea DDC-aren administrazioan oinarrituta, beti kontrol kondizioekin konparatuz, kasu honetan, oliba olioaren eta dieta kontrolaren administrazioan oinarritutakoak, hurrenez hurren (**E.4C,D Irudia**). Aipagarria da, beraz, *Trem2*-ren adierazpena aztertutako kolestasiaren sagu eredu guztietan emendatuta zegoela kondizio kontrolarekin konparatuz, kolestasi hori eragiten zuen estimulua edozein izanik ere (**E.4B-D Irudia**). Honek iradokitzen du *Trem2*-ren gainadierazpena fenomeno orokorra dela kolestasian

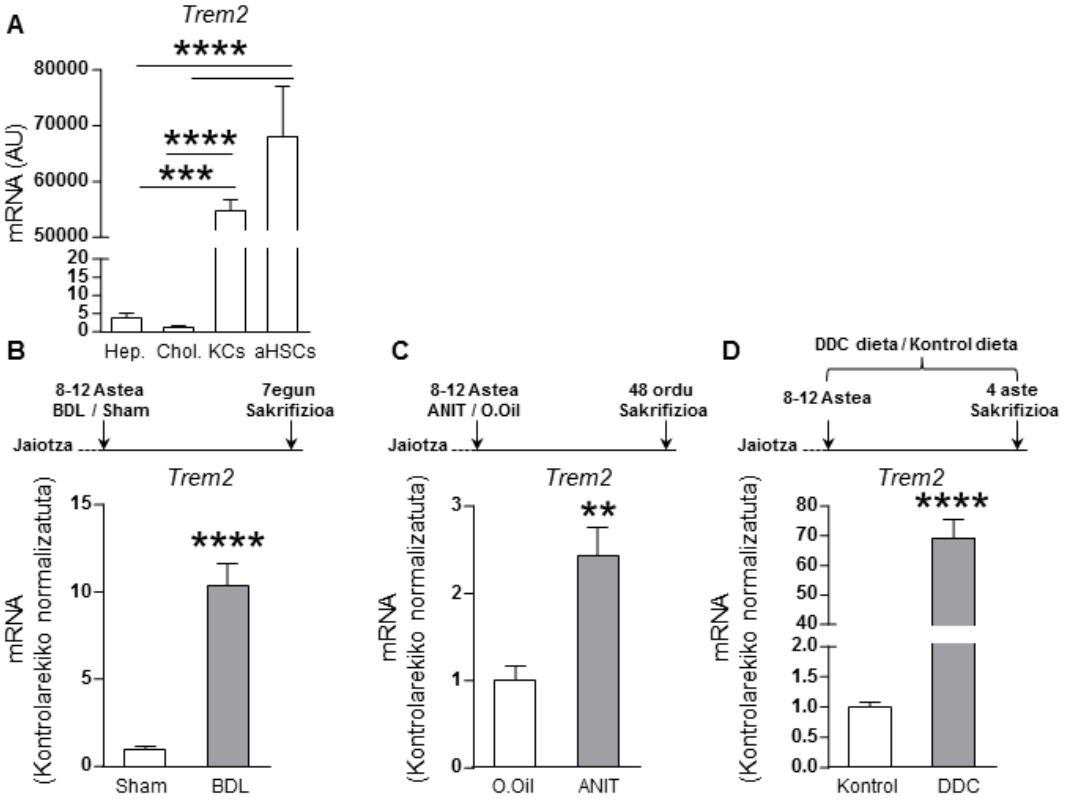

E.4. Irudia. *Trem2* mRNA adierazpena gibeleko zenbait zelula motatan eta kolestasiaren sagu ereduetan. (**A**) *Trem2* mRNA adierazpena sagu osasuntsuen gibeleko zleula primarioetan, zehazki, hepatozitoak (n=8), kolangiozitoak (n=6), KCs-ak (n=6) eta aktibatutako HSCs-ak (n=5) erakusten dira. (**B-D**) *Trem2* mRNA adierazpena kolestasiaren hainbat sagu ereduetan egoera kontrolarekin konparatuz, (**B**) behazun hodi komuneko lotura (n=6-9), (**C**) ANIT administrazioa (n=9-10) eta (**D**) DDC gehigarri duen dieta (n=9-11). (**A**) Sudent-en *t* test parametrikoa eta Mann Whitney-ren test ez-parametrikoa erabili ziren. (**B**,**C**) Sudent-en *t*-test parametrikoa erabili zen. (**D**) Mann Whitney-ren test ez-parametrikoa erabili zen. **, *** eta **** *p* balorea <0.01, <0.001 eta 0.0001 adierazten dute, hurrenez hurren. ANIT, α-Naphthylisothiocyanate; AU, arbitrary units; BDL, bile duct ligation; DDC, 3,5-Diethoxycarbonyl-1, 4-Dihydrocollidine; *Trem2*: triggering receptor expressed on myeloid cells 2.

Kolestasia duten gaixoen gibeletan behatutako emaitzei jarraiki, kasu hoentan ere, gibeleko *Trem2*-ren mRNA adierazpenak positiboki korrelazionatzen du gaixoatasunaren garapenaren markatzaileekin. Zehazki, *Trem2*-ren adierazpen mailak positiboki korrelazionatzen du behazun zuhaitzeko zelulen markatzaile diren *Ck19* eta *Ck7*-rekin (**E.5A Irudia**). Gainera, *Trem2*-ren adierazpenak positiboki korrelazionatzen du *Acta2* eta *Col1a1*-ren mRNA-ekin (**E.5B Irudia**), *Acta2* αSMA proteina kodetzen duen genea da eta, beraz, HSCs-en aktibazioaren markatzaile nagusia eta *Col1a1*, gibel fibrosian metatzen den fibra mota nagusia da.

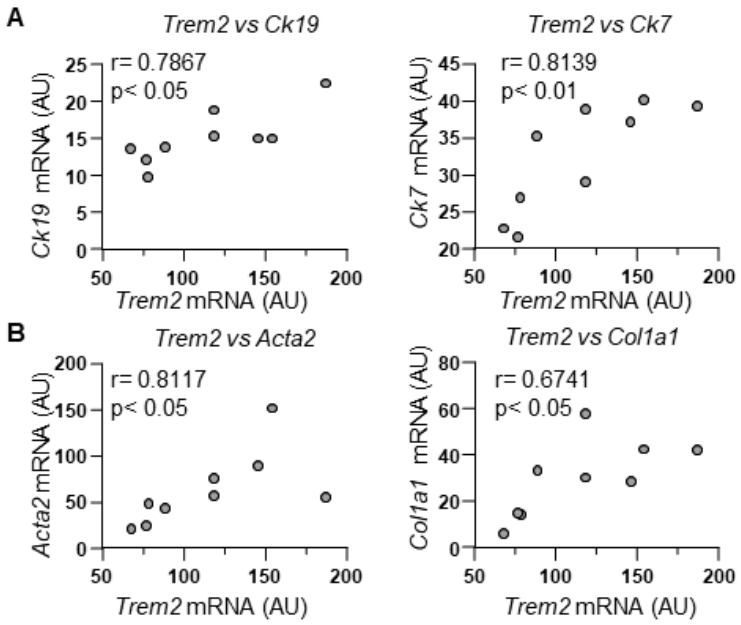

E.5. Irudia. *Trem2*-ren mRNA adierazpenaren korrelazioa gaixotasunaren garapenaren markatzaileekin BDL-aren sagu ereduan. (**A**) *Ck19* eta *Ck7* behazun zuhaitzeko markatzaileekin eta (**B**) *Acta2* eta *Col1a1* fibrosiaren markatzaileekin BDL sagu ereduaren saguen gibelean (n=9) **E**) Pearson-en korrelazio test parametrikoa eta (**F**) Spearman-en korrelazio test ez-parametrikoa (*Trem2* vs *Acta2*) erabili ziren (*Trem2* vs *Col1a1)* erabili ziren, korrelazioaren koefizientea (r) eta *p* baloreak erakusten dira. *Acta2*, actin alpha 2; AU, arbitrary units; *Ck7*, cytokeratin 7; *Ck19*, cytokeratin 19; *Col1a1*, collagen type 1a 1; *Trem2*: triggering receptor expressed on myeloid cells 2.

Datu hauek ikusita, TREM2-ren adierazpena giza gaixotasun kolestatiko zein kolestasiaren sagu ereduetan emendatzen dela esan genezake. Hortaz, TREM2-k kolestasiaren garapenean paper garrantzitsua bete lezakeela iradokiz. Era berean, saguen erabilera, TREM2-k kolestasian betetzen duen papera ikerketzeko aukera egokia dela ere adierazten dute emaitza hauek.

E.3. *Trem2*$^{-/-}$ saguek gehiegizko erantzuna garatzen dute behazun hodi komunaren lotura eta gero

E.3.1. Gibeleko kaltearen puntuazioaren eta behazun zuhaitzaren hedapenaren emendioa *Trem2*$^{-/-}$ saguetan WT saguekin alderatuta BDL-a eta gero

TREM-k kolestasian betetzen duen papera ulertzeko asmoz, lehenik BDL-an oinarritutako buxadurazko kolestasiaren sagu-ereduan jarri genuen arreta. WT eta *Trem2*$^{-/-}$ saguek BDL-arekiko duten erantzuna konparatzeko, bi genotipo hauetako

saguetan BDL-aren eredua burutu genuen. Kontrol taldeko saguei "Sham" ebakuntza egin zitzaien (**E.6A Irudia**).

BDL-ak kolestasiak eragindako gibel-kaltearen markatzaile diren serumeko fosfatasa alkalinoaren eta bilirrubinaren emendio handia eragin zuen, bai WT bai *Trem2*$^{-/-}$ saguetan ere (**E.6B Irudia**). Era berean, gibeleko kalte hepatozelularraren markatzaile diren trasaminasen (hots, AST eta ALT) maila ere altuagoa zen BDL-a jasandako animalietan "Sham" animalietan baino, bi genotipoen kasuan (**E.6B irudia**). Hala ere, ALT-ren kasuan sham *Trem2*$^{-/-}$ animaliek, sham WT animaliekin konparatuz aurkezten zuten emendioa salbu, ez zen desberdintasunik behatu serumeko gibel kaltearen markatzaile hauetan WT eta *Trem2*$^{-/-}$ saguen artean (**E.6B irudia**).

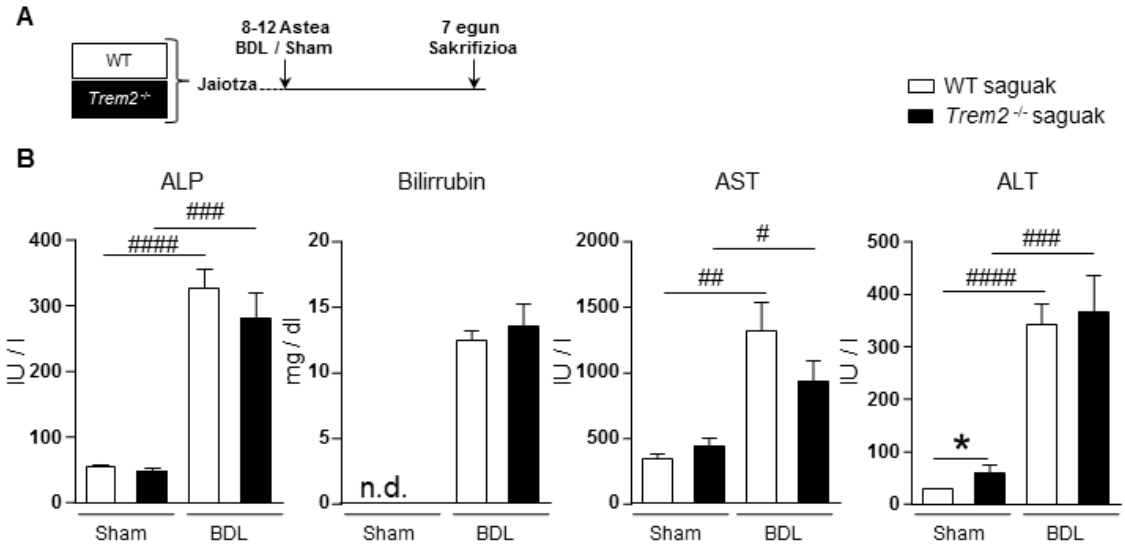

E.6. Irudia. Behazun zuhaitzeko zein kalte hepatozelularraren serumeko markatzeileak WT eta *Trem2* $^{-/-}$ saguetan BDL-a eta gero. (**A**) WT eta *Trem2* $^{-/-}$ saguetan BDL (WT n=9; *Trem2* $^{-/-}$ n=8) edo sham (WT n=6; *Trem2* $^{-/-}$ n=7) prozedimenduak burutu ziren eta saguak kirurgiatik 7 egunetara sakrifikatu ziren. (**B**) Gibeleko entzimen eta bilirrubinaren serumeko mailak aztertu ziren. (**B**) Sudent-en *t*-test parametrikoa eta Mann Whitney-ren test ez-parametrikoa erabili ziren. * *p* balorea <0.05 adierazten du tratamendu berdina jaso zuen WT saguekin konparatuz, #, ##, ### and #### *p* balorea <0.05, <0.01, <0.001 eta <0.0001 adierazten dute, hurrenez hurren, genotipo berdineko sham ebakuntza jaso zuten animaliekin konparatuz. AP, alkaline phosphatase; ALT, alanine aminotransferase; AST, aspartate aminotransferase; AU, arbitrary units; BDL, bile duct ligation; IU, international units; n.d., non-detected; *Trem2*, triggering receptor expressed on myeloid cells; WT, wild type.

Animalia hauen gibel mozketen, H&E tindaketan oinarritutako analisi histologikoak, agerian utzi zuen *Trem2*$^{-/-}$ saguek gehiegizko erantzuna zutela buxadurazko kolestasiarekiko. Gehiegizko erantzun honen ezaugarri ziren, inflamazio eta nekrosiaren emendioa eta behazun zuhaitzeko egituren hedapena, *Trem2*$^{-/-}$ saguetan WT saguekiko konparatuz BDL-a eta gero. (**E.7A Irudia**). Behazun zuhaitzeko egituren hedapenaren inguruko datuak zehatzago ikertu genituen, eta aurretik azaldutako datuekin batera, *Trem2*$^{-/-}$ saguetan BDL-a eta gero behazun hodietako zelulen markatzaile den CK19-ren tindaketan emendioa zegoela ikusi genuen (**E.7B Irudia**). mRNA mailak aztertzerakoan, *Ck19*, beraren eta *Ck7*, behazun hodietako beste markatzaile baten, mRNA-ren adierazpenaren maila altuagoak ikusi ziren bai WT bai *Trem2*$^{-/-}$ saguetan BDL-a eta gero, sham jasandako saguekin konparatuz (**E.7C Irudia**). Gainera, *Trem2*$^{-/-}$ saguetan WT saguekin konparatuz *Ck19* eta *Ck7*-ren adierazpenaren emendioa ere behatu genuen BDL-a eta gero (**E.7C Irudia**).

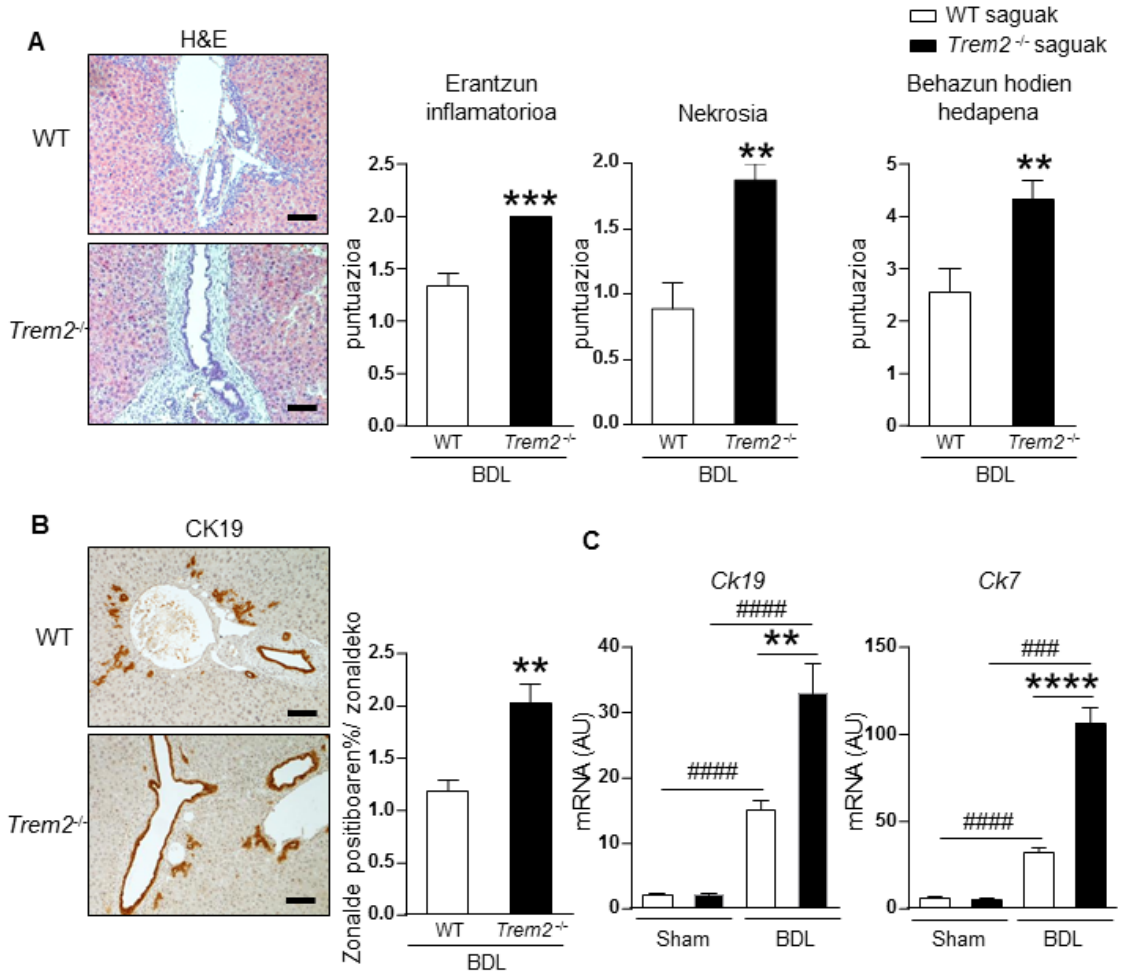

E.7. Irudia. Gibeleko kaltea eta behazun zuhaitzaren hedapena BDL-aren ondorioz WT eta *Trem2*$^{-/-}$ saguetan. (**A**) Gibeleko H&E tindaketa esperientziadun patologo batek aztertu zuen, irudi adierazgarriak eta erantzun inflamatorioaren, nekrosiaren eta behazun zuhaitzaren hedapenaren puntuazioak aurkezten dira. (**B**) Gibeleko IHC kolangiozitoen markatzaile den CK19-rentzat, irudi adierazgarriak eta kuantifikazioa aurkezten dira. (C) *Ck19* eta *Ck7* behazun zuhaitzeko markatzaileen mRNA adierazpena gibelean. (**A,B**) Eskalaren marrak 100 µm adierzten ditu. (**A**) Mann whitney-ren test ez-parametrikoa erabili zen. (**B**) Sudent-en *t*-test parametrikoa erabili zen. (**C**) Sudent-en *t*-test parametrikoa eta Mann Whitney-ren test ez-parametrikoa erabili ziren. **, *** eta **** *p* balorea <0.01, <0.001 <0.0001 adierazten dute, hurrenez hurren, tratamendu berdina jaso zuten WT saguekin konparatuz ### and #### *p* balorea <0.001 eta <0.0001 adierazten dute, hurrenez hurren, genotipo berdineko sham ebakuntza jaso zuten animaliekin konparatuz. AU, arbitrary units; BDL, bile duct ligation; *Ck7*, cytokeratin 7; *Ck19*, cytokeratin 19; H&E, hematoxylin and eosin; *Trem2*, triggering receptor expressed on myeloid cells; WT, wild type.

Trem2$^{-/-}$ saguen gibelek azalera nekrotiko handiagoak zituzten WT saguen gibelekin konparatuz BDL eta gero (**E.8A Irudia**). Honekin batera, estres oxidatiboko markatzaile diren *Hmox* eta *Nos2*-ren adierazpena emendatzen zen bi genotipoetako saguetan BDL-aren ondorioz, eta are altuagoa zen BDL jasandako *Trem2*$^{-/-}$ saguen gibelean WT saguen gibelarekin alderatuz (**R.8B Irudia**). Fenomeno honen atzean zegoen zelularen heriotzaren mekanismo zehatza aztertzeko asmoz, apoptosia eta nekroptosiaren markatzaileak aztertu ziren. IHC zein immunoblot bidez, apoptosiaren

markatzaile den Cl-Casp3-ren maila bajuak aurkitu ziren (kontrol positibo bezala LPS-ren dosi altua jaso zuen sagu bat gehitu zen) eta ez zen genotipoen arteko desberdintasunik behatu (**E.9A,B Irudia**). Aitzitik, nekroptosiaren markatzaile den RIP3-ren (receptor-interacting protein kinase 3) adierapzpen mailak goranzko joera nabarmena erakusten zuen BDL jasandako *Trem2*$^{-/-}$ saguen gibelean WT saguen gibelarekin alderatuz. MLKL nekroptosiaren efektore nagusiaren gibeleko adierazpen mailak altuagoak ziren *Trem2*$^{-/-}$ saguetan WT saguekin konparatuz BDL eta gero (**E.9C Irudia**).

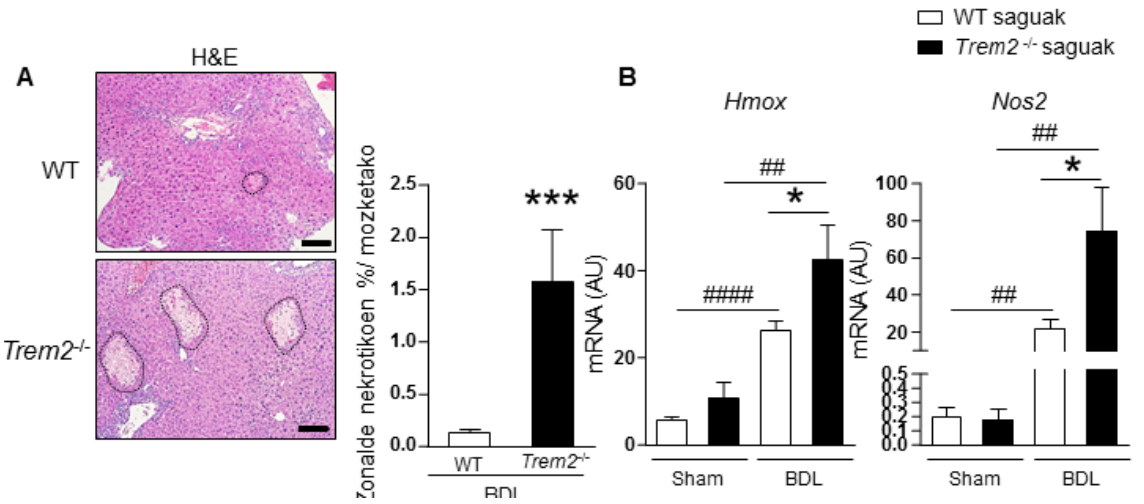

E.8. Irudia. BDL-aren ondoriozko zelularen heriotza WT eta *Trem2* $^{-/-}$ saguen gibelean. (**A**) H&E-az tindatutako mozketetan zonalde nekrotikoak neurtu ziren, irudi adierazgarriak eta kuatifikazioa aurkezten dira. (**B**) Gibeleko *Hmox* eta *Nos2* estres oxidatiboko markatzaileen mRNA adierazpena. Eskalaren marrak (**A**)-n 100 µm adierazten ditu (**A**) Student-en *t*-test parametrikoa erabili zen (**B**) Student-en *t*-test parametrikoa eta Mann Whitney-ren test ez-parametrikoa erabili ziren. * eta *** *p* balorea <0.05 eta <0.001 <0.0001 adierazten dute, hurrenez hurren, tratamendu berdina jaso zuten WT saguekin konparatuz ## eta ### *p* balorea <0.01 eta <0.001 adierazten dute, hurrenez hurren, genotipo berdineko sham ebakuntza jaso zuten animaliekin konparatuz. AU, arbitrary units; BDL, bile duct ligation; H&E, haematoxylin and eosin; *Hmox*, heme oxygenase; *Nos2*, nitric oxide synthase 2; *Trem2*, triggering receptor expressed in myeloid cells 2; WT, wild type.

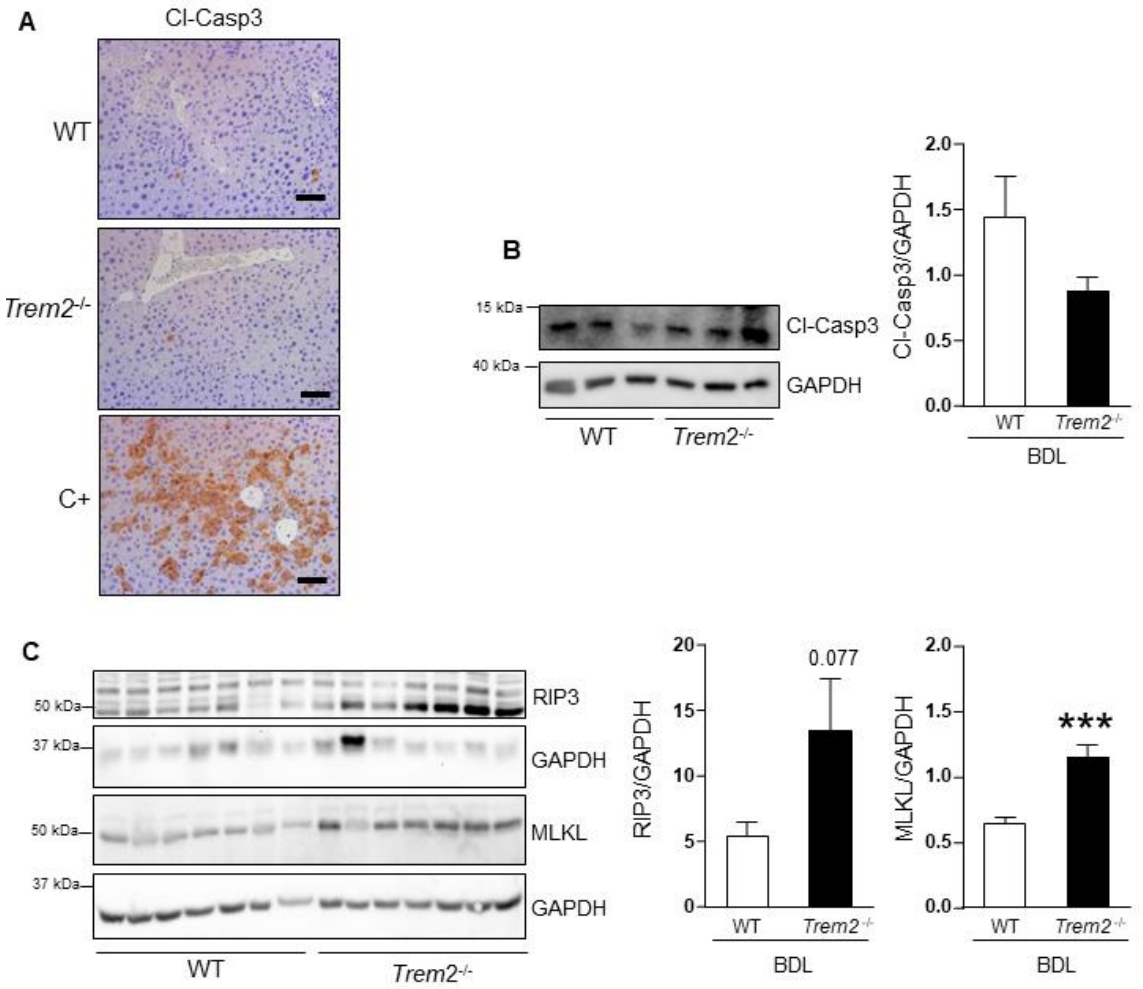

R.9. Irudia. Markatzaile apoptotiko eta nekroptotikoen adierazpena BDL-aren ondorioz WT eta *Trem2*$^{-/-}$ saguetan. (**A**) Cl-Casp3-ren IHC WT eta *Trem2*$^{-/-}$ saguetan BDL-a eta gero eta kontrol positibo batean, irudi adirazgarriak aurkezten dira. (**B**) Apoptosiaren markatzaile den Cl-Casp3-ren immunoblota, immunoblot adierazgarria eta GAPDH-arekiko kuantifikazio erlatiboa aurkezten dira. (**C**) RIP3 eta MLKL nekroptosiaren markatzaileen immunoblota, immunoblot adierazgarria eta GAPDH-arekiko kuantifikazio erlatiboa aurkezten dira. Eskalaren marrak (**C**)-n 50 µm adierazten ditu. (**B,C**) Student-en *t*-test parametrikoa erabili zen. *** p balorea <0.05 eta <0.001 <0.0001 adierazten du, tratamendu berdina jaso zuten WT saguekin konparatuz. AU, arbitrary units; BDL, bile duct ligation; Cl-Casp3, cleaved caspase 3; GAPDH, glyceraldehyde-3-phosphate dehydrogenase; RIP3, receptor-interacting protein kinase 3; *Trem2*, triggering receptor expressed in myeloid cells 2; WT, wild type.

E.3.2. Serumeko eta gibeleko BA-en kontzentrazioen aldaketak WT eta *Trem2*$^{-/-}$ saguetan BDL-a eta gero

BA-ak kolestasi bidezko gibel-kaltearen lehengo eragiletzat hartzen dira, hau beren efektu zitotoxiko zuzenen bidez (119) edo erantzun inflamatorioak areagotzeko duten gaitasunaren bidez eragin dezakete (117). Hau kontuan izanik, BDL eta "sham" ebakuntza jasandako sagu kontrolen serumeko eta gibeleko BA-en profila aztertu genuen masa espektrometria bidez.

BA-en osotasunean frakzio mespretxagarria osatzen dutela kontuan harturik, lan honetan ez ziren glizinarekin konjokatutako BA-k kontuan hartu BA-en analisian (12). Esperotako emaitzak konfirmatuz, serumeko BA-en kontzentrazioa asko handitu zen BDL-aren eraginez WT eta *Trem2*$^{-/-}$ saguetan (**E.10. Irudia**). Handipen hau BA primarioen kontzentrazioan behatutako emendioaren bidez azaltzen da (**E.10A Irudia**). BA primarioak gibeleko entzimak bakarrik parte hartuz sintetizatzen diren espeziak dira, saguetan CA, QDCA, αMCA, βMCA eta beren taurinarekin konjokatutako espezieak sailkatzen dira talde honetan (8, 12). BA di-hidroxilatu toxikoen espezieen, hots, DCA, QDCA eta bere taurinarekin konjokatutako espezieen (310), emendioa behatu zen bi genotipoetako saguen serumean BDL-a eta gero (**E.10B Irudia**). Era berean, BA koloretikoen familian sailkatzen diren UDCA eta TUDCA-ren kontzentrazioa ere emendatzen zen BDL-aren eraginez bi genotipoetako saguetan (**E.10B Irudia**), UDCA eta TUDCA BA primarioen taldean sailaktzen dira saguetan, gizakian BA sekundarioen taldean sailakatzen diren bitartean (12). BA sekundarioen kontzetrazioa, aldiz, murrizten zen BDL-aren eraginez bi genotipoetako saguen serumean (**E.10B Irudia**). BA sekundarioak hesteetako mikrobiotaren metabolismoaren ondorioz sortzen diren espezieak dira eta saguetan DC, LC eta beren taurinarekin konjokatutako espeziak daude talde honen barruan (8, 12). Aztertutako BA espezieetan ez zen WT eta *Trem2*$^{-/-}$ saguen arteko desberditasunik behatu, ez "Sham" sagu kontroletan ez BDL-a jasandako saguetan (**E.10. Irudia**).

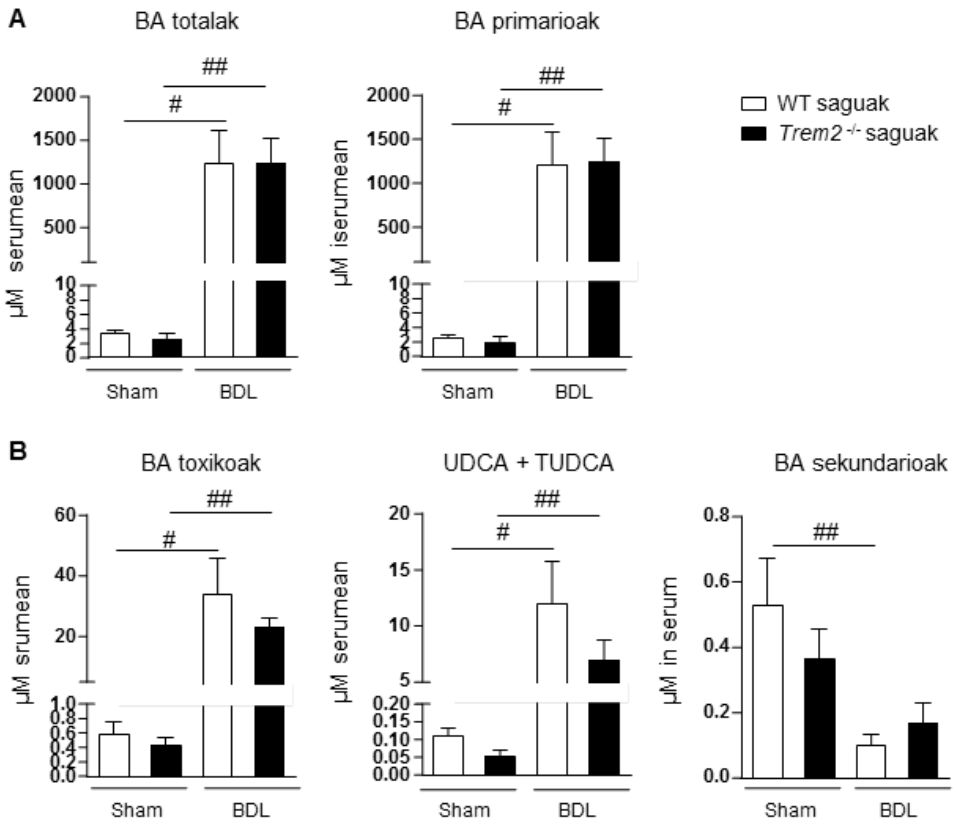

E.10. Irudia. Serumeko BA-en kontzentrazioa WT eta *Trem2*$^{-/-}$ saguetan BDL-a eta gero. Serumeko BA-en kontzentrazioak (Sham: WT n=5; *Trem2*$^{-/-}$ n=6 and BDL: WT n=7; *Trem2* $^{-/-}$ n=6) WT eta *Trem2*$^{-/-}$ saguetan sham edo BDL-a eta gero aztertu ziren. (**A**) Serumeko BA totalen eta primarioen kontzentrazioak. (**B**) Serumeko Ba toxikoen, UDCA eta TUDCA eta Ba sekundarioen kontzentrazioa. Sudent-en *t*-test parametrikoa eta Mann Whitney-ren test ez-parametrikoa erabili ziren. # and ## *p* balorea <0.05 eta <0.01 adierazten dute, hurrenez hurren, genotipo berdineko sham ebakuntza jaso zuten animaliekin konparatuz. AU, arbitrary units; BAs, bile acids; BDL, bile duct ligation; TUDCA, tauroursodeoxycholic acid; *Trem2*, triggering receptor expressed on myeloid cells; UDCA, ursodeoxycholic acid; WT, wild type.

Serumean behatutakoari jarraiki, gibeleko BA totalen kontzentrazioa ere asko emendatzen zen BDL-aren eraginez bi genotipoetan (**E.11A irudia**). Era berean, hau BA primarioen espezieetan behatutako aldaketen ondorioz azaltzen da (**E.11A irudia**). BA toxikoen eta UDCA familiaren kontzentrazioak ere emendatuta agertzen ziren BDL-aren eraginez bai WT bai *Trem2*$^{-/-}$ saguen gibeletan (**E.11B irudia**). BA sekundarioen espezieen kontzentrazioa, berriz, murrizten zen BDL-a eta gero bi genotipoetan (**E.11C irudia**). Serumean behatutakoari kontrajarriz, gibelaren analisiaren kasuan, desberdintasunak aurkitu ziren WT eta *Trem2*$^{-/-}$ animalien artean. Honela, *Trem2*$^{-/-}$ saguetan BA-en murrizpen orokorra behatu genuen "Sham" kontroletan WT saguen gibelekin konparatuz (**E.11. Irudia**). BDL-aren ondoren desberdintasun hauek ez ziren ikusten, eta WT eta *Trem2*$^{-/-}$ saguetan antzeko mailak ikusten ziren. Hala ere, garrantzitsua da azpimarratzea BDL-ak eragindako BA totalen, BA primarioen eta BA

toxikoen kontzentrazioaren emendioa nabarmenagoa zela *Trem2*$^{-/-}$ saguetan WT saguekin alderatuz (**E.11. Irudia**).

"Sham" taldeko WT eta *Trem2*$^{-/-}$ saguen artean behatutako desberdintasunak azaltzeko ahaleginean, BA-en metabolismoan parte hartzen duten gene garantzitsu batzuen adierazpena neurtu genuen. Honela, *Cyp7a1*-ren adierazpenak beheranzko ageriko joera zuen *Trem2*$^{-/-}$ saguetan WT saguekin konparatuz "sham" kontrol taldean, eta bi genotipoaetan emendatzen zen BDL-aren ondorioz (**E.11C Irudia**). Halaber, *Cyp7a1*-ren erregulatzaile negatibo nagusia den *Fxr*-k goranzko ageriko joera agerzen zuen *Trem2*$^{-/-}$ saguetan WT saguekin konparatuz "sham" kontrol taldean (**E.11C Irudia**).

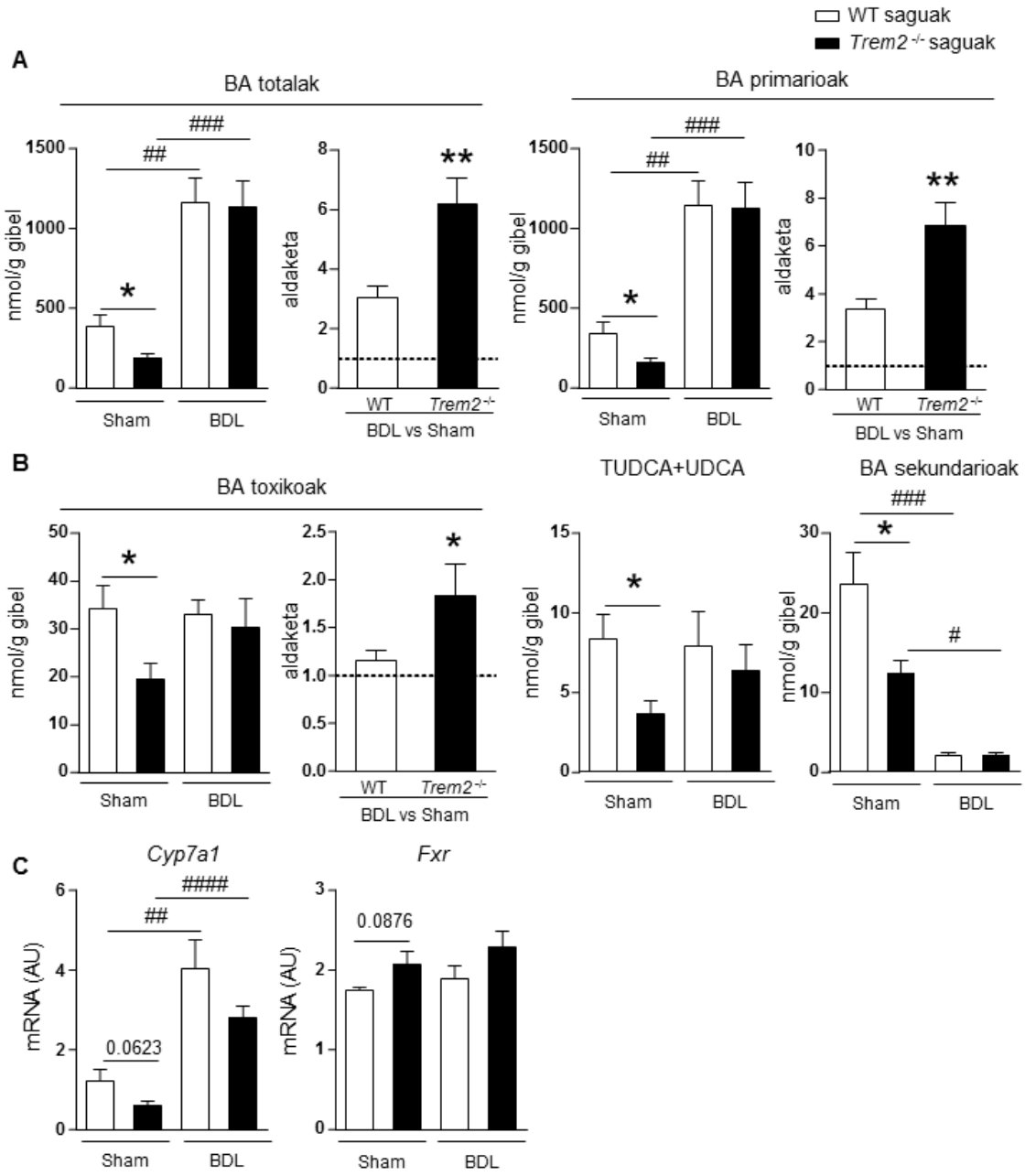

E.11. Irudia. Gibeleko BA-en kontzentrazioa eta gibeleko BA-en metabolismoan parte hartzen duten geneen adierazpen maila WT eta *Trem2*$^{-/-}$ saguetan BDL-aren ondoren. Gibeleko BA-en kontzentrazioa neurtu zen sham edo BDL (Sham: WT n=5; *Trem2*$^{-/-}$ n=6 and BDL: WT n=7; *Trem2* $^{-/-}$ n=6) eta gero WT eta *Trem2*$^{-/-}$ saguetan. (**A**) Gibeleko BA totalen eta BA primarioen kontzentrazioak eta sham-etik BDL-rako BA-en kontzentrazioaren emendioa WT eta *Trem2*$^{-/-}$ saguetan aurkezten dira. (**B**) BA toxikoen, UDCA+TUDCA espezieen eta BA sekundarioen gibeleko kontzentrazioa WT eta *Trem2*$^{-/-}$ saguetan sham eta BDL-a eta gero, kontzentrazioak eta sham-etik BDL-rako BA-en kontzentrazioaren emendioa WT eta *Trem2*$^{-/-}$ saguetan aurkezten dira. (**C**) Gibeleko *Cyp7a1* eta *Fxr* mRNA adierazpena. (**A**) Student-en *t*-test parametrikoa erabili zen. (**B**) Student-en *t*-test parametrikoa eta Mann Whitney-ren test ez-parametrikoa erabili ziren. (**C**) Student-en *t* test parametrikoa erabili zen. * eta ** *p* balorea <0.05 eta <0.01 adierazten dute, hurrenez hurren, tratamendu berdina jaso zuten WT saguekin konparatuz, ##, ### eta #### *p* balorea <0.01 <0.001 eta <0.0001 adierazten dute, hurrenez hurren, genotipo berdineko sham ebakuntza jaso zuten animaliekin konparatuz. AU, arbitrary units; BAs, bile acids; BDL, bile duct ligation; *Cyp7a1*; Cytochrome P450 family 7 subfamily A member 1; *Fxr*, farnesoid X receptor; *Trem2*, triggering receptor expressed on myeloid cells; TUDCA, tauroursodeoxycholic acid; UDCA, ursodeoxycholic acid.

E.3.3. Gibelean gehiegizko inflammazioa behatzen da *Trem2*$^{-/-}$ saguetan BDL-a eta gero

Bitartekari inflamatorioek paper garrantzitsua betetzen dute behazun hodietako gaixotasunen garapenean, orokorrean eta gaixotasun kolestatiko kronikoetan, zehazki. Bitartekari hauek zelulen arteko komunikazioa ahalbidetzen dute, eta beraz, gaixotasun kolestasiko kronikoen ezaugarri den zauri-sendatze erantzuna koordinatzen dute (6, 154). Era berean, erreakzio inflamatorioek berebiziko garrantzia dute BDL sagu-ereduean behatutako fenotipoan ere, sagu-eredu honen gibelean bitartekari inflamatorioen emendioa eta sistema inmuneko zelulen gibelerako erakarpena behatzen dira (293).

Orohar, BDL-ak *Il6, Tnf,* eta *Il33* zitokina pro-inflamatorioen eta, hurrenez hurren, neutrofilo eta makrofagoen gibelerako erakarpenaz arduratzen diren *Cxcl1* and *Mcp1* kemokinen mRNA adierazpena sustatu zuen bi genotipoetako saguetan "sham" ebakuntza jasandako kontrolekin konparatuz (**E.12 Irudia.**). Gainera, gure emaitzetan ikusten da *Il*6, *Il33* eta *Tnf* zitokina inflamatorioen, baita *Cxcl*1 eta *Mcp*1 kemokinen adierazpena ere emendatuta dagoela *Trem2*$^{-/-}$ saguen gibelean WT saguekin konparatuta BDL-a eta gero (**E.12A,B Irudia**). Emaitza hauekin batera, MCP1 eta CXCL1 kemokinen proteina mailako adierazpenaren emendioa ere behatu zen BDL-aren eraginez bi genotipoetako saguetan, eta emendio hau are handiagoa zen *Trem2*$^{-/-}$ saguetan WT saguekin konparatuz BDL eta gero (**E.12C Irudia**).

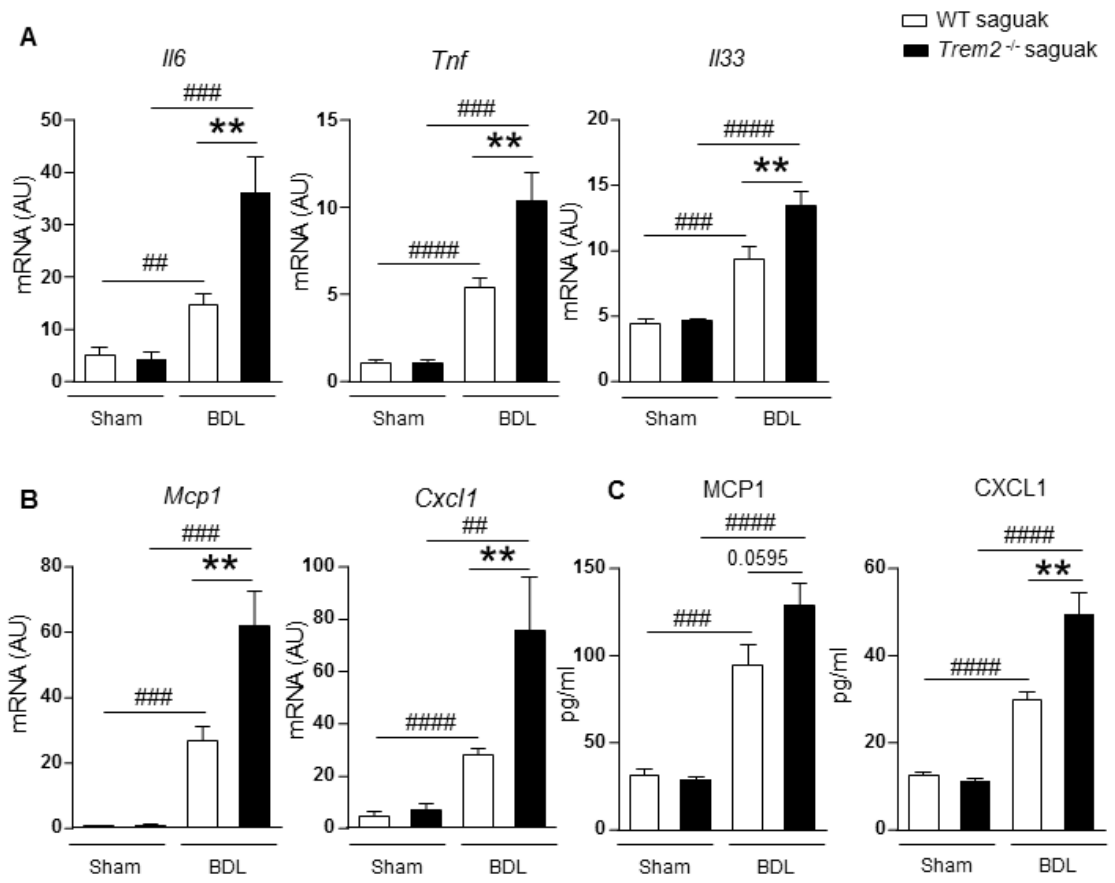

E.12. Irudia. Zitokina eta kemokina inflamatorioen adierazpena WT eta *Trem2*$^{-/-}$ saguen gibelean BDL-a eta gero. (**A**) *Il6*, *Tnf* eta *Il33* zitokina inflamatorioen mRNA adierazpena eta (**B**) *Mcp1* eta *Cxcl1* kemokinen mRNA adierazpena gibelean. (**C**) MCP1 eta CXCL1 kemokina inflamatorioen proteina mailako adierazpena gibelean. Student-en *t*-test parametrikoa erabili zen. ** *p* balorea <0.01 adierazten du, tratamendu berdina jaso zuten WT saguekin konparatuz, ##, ### eta #### *p* balorea <0.01 <0.001 eta <0.0001 adierazten dute, hurrenez hurren, genotipo berdineko sham ebakuntza jaso zuten animaliekin konparatuz. AU, arbitrary units; BDL, bile duct ligation; *Cxcl1*, C-X-C Motif Chemokine Ligand 1; *Il6*, interleukin 6; *Il33*, interleukin 33; *Mcp1*, monocyte chemoattractant protein 1; *Tnf*, tumour necrosis factor; *Trem2*, triggering receptor expressed on myeloid cells; WT, wild type.

Neutrofiloak bai giza kolestasisan bai kolestasiaren sagu ereduetan erantzun zitotoxikoak bideratzen dituzten sistema immuneko zelula nagusitzat hartzen dira (125-127). Behatutako *Cxcl1*-ren adierazpenaren emendioarekin batera, neutrofiloen markatzaile den NIMP-R14 proteina aztertu zen IHC bidez eta *Trem2*$^{-/-}$ saguen gibeletan neutrofilo kopuru handiagoa zela behatu genuen, WT saguen gibelekin konparatuz BDL eta gero (**E.13A Irudia**). Gibeleko makrofago eta T linfozitoen konpuruan ez zen desberdintasunik behatu WT eta *Trem2*$^{-/-}$ saguen artean BDL-aren ondorioz, hau F4/80 eta CD3 markatzaileen IHC bidez aztertu zen, hurrenez hurren (**E.13B,C Irudia**).

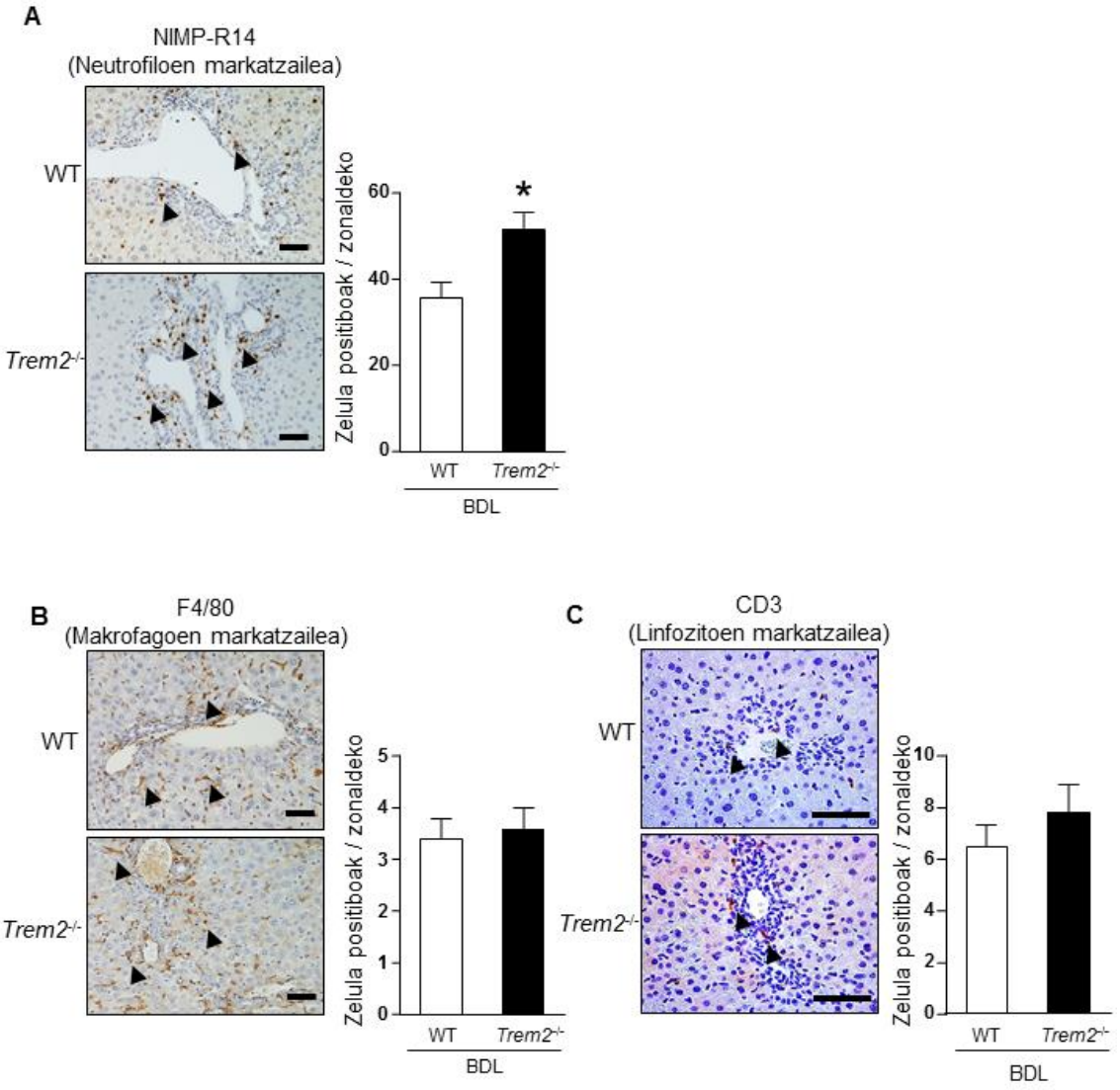

E.13. Irudia. Sistema immuneko zelulen erakarpena WT eta *Trem2*$^{-/-}$ saguetan BDL-a eta gero. (**A**) NIMP-R14 neutrofiloen markatzaileen IHC-a, irudi adierazgarriak eta kuantifikazioa aurkezten dira. (**B**) F4/80 makrofagoen markatzailearen IHC-a, irudi adierazgarriak eta kuantifikazioa aurkezten dira. (**C**) CD3 linfozitoen markatzailearen IHC-a, irudi adierazgarriak eta kuantifikazioa aurkezten dira. Eskalaren marrak (A,B)-n 50 µm adierazten ditu eta (**C**)-n 10 µm. Student-en *t*-test parametrikoa erabili zen. * *p* balorea <0.05 adierazten du, tratamendu berdina jaso zuten WT saguekin konparatuz. AU, arbitrary units; BDL, bile duct ligation; CD3,cluster of differentiation 3; *Hmox*, heme oxygenase; *Nos2*, nitric oxide synthase 2; *Trem2*, triggering receptor expressed on myeloid cells; WT, wild type.

E.3.4. *Trem2*$^{-/-}$ saguetan HSCs-en aktibazioaren emendioa ikusten da, baina desberdintasunik ez gibeleko fibrosis mailan WT saguekin konparatuz BDL-a eta gero

Lehenago aipatu moduan, bitartekari inflamatorioek zelulen arteko komunikazioa ahalbidetzen dute erreakzio duktularrean. Honela, komunikazio honen ondorio garrantzitsuenetako bat HSC-en eta PM-en erakarpena eta aktibazioa da. Zelula hauek erantzun inflamatorioan ere parte hartzen dute eta ECM-aren ekoizpenaren eta gibeleko fibrosiaren arduradun nagusiak dira (136, 176). Gure emaitzek iradokitzen dute *Trem2*$^{-/-}$ saguek gehiegizko erantzun inflamatorioa dutela WT-ekin konparatuz BDL-a eta gero emaitza hauek ikusita, gibeleko fibrosia aztertzera ekin genion.

Hasteko, HSCs-en aktibazioaren marktzailearen adierazpena emendatuta dago, bai proteina mailan bai *Acta2*, proteina hau kodetzen duen genearen adierazpen mailan ere, *Trem2*$^{-/-}$ saguetan WT saguekin konparatuz BDL eta gero (**E.14A Irudia**). *Col1a1* mRNA mailak ere handituta daude *Trem2*$^{-/-}$ saguetan WT saguekin konparatuta BDL eta gero (**E.14B Irudia**). *Acta2* zein *Col1a1* adierazpen mailak handitu ziren bi genotipoetan BDL-aren ondorioz sham kontrolekin alderatuta. Aitzitik, ez genuen desberdintasunik behatu gibeleko fibrosia tindatzen duen Sirius red tindaketan WT and *Trem2*$^{-/-}$ saguen artean BDL-aren ondorioz (**E.14C Irudia**).

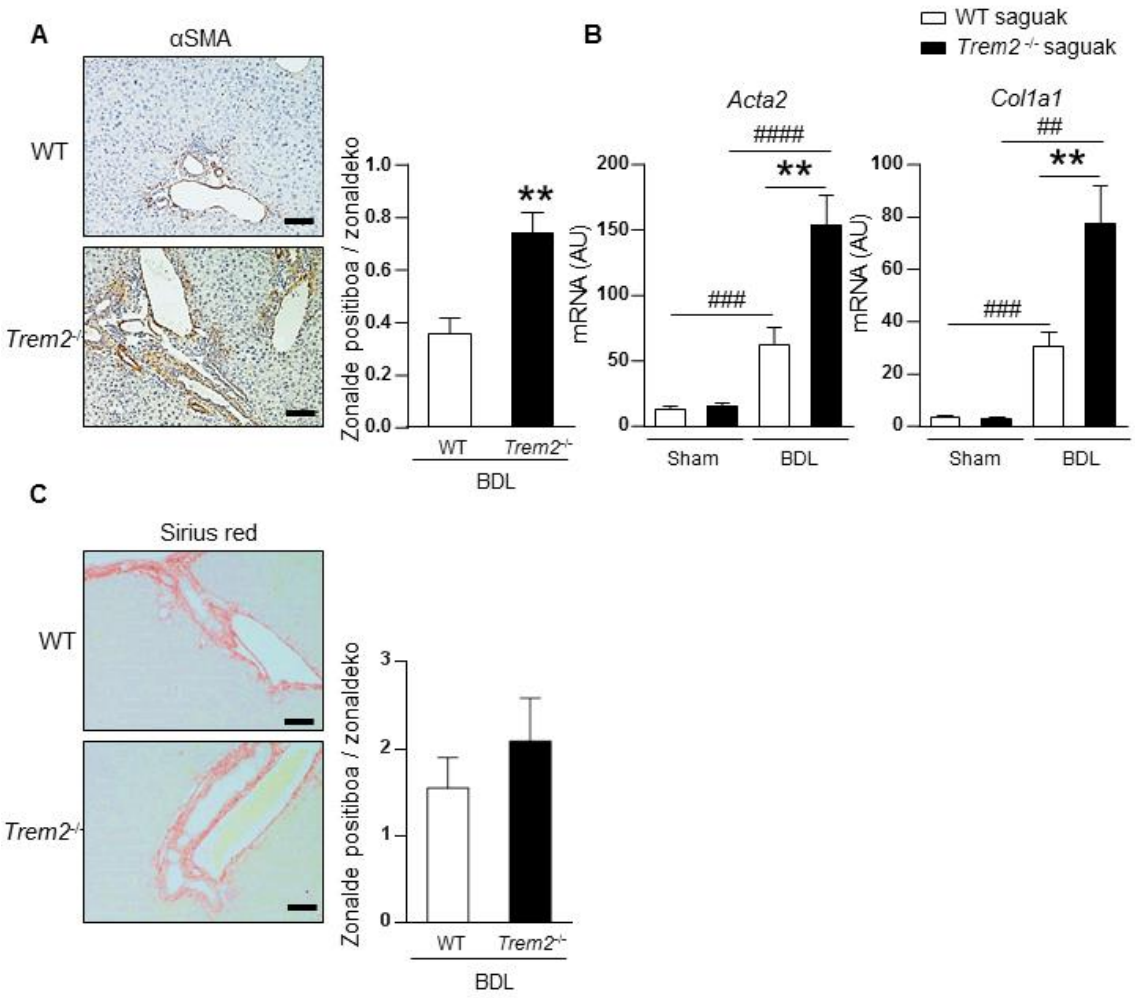

E.14. Irudia. Gibeleko fibrosia WT eta *Trem2*$^{-/-}$ saguetan BDL-a eta gero. (A) αSMA HSCs-en aktibazioaren markatzailearen IHC-a, irudi adierazgarriak eta kuantifikazioa erakusten dira. (**B**) *Acta2* eta *Col1a1* mRNA adierazpena gibelean. (**C**) Sirius red tindaketa, irudi adierazgarriak eta kuantifikazioa aurkezten dira. Eskalaren marrak (**A,C**)-n 100 µm adierazten ditu. (**A,C**) Student-en *t*-test parametrikoa erabili zen. (**B**) Student-en *t*-test parametrikoa eta Mann Whitney-ren test ez-parametrikoa erabili ziren. ** *p* balorea <0.01 adierazten du, tratamendu berdina jaso zuten WT saguekin konparatuz, ##, ### eta #### *p* balorea <0.01 <0.001 eta <0.0001 adierazten dute, hurrenez hurren, genotipo berdineko sham ebakuntza jaso zuten animaliekin konparatuz. *Acta2*, actin alpha 2, smooth muscle; αSMA, alpha smooth muscle actin; AU, arbitrary units; BDL, bile duct ligation; *Col1a1*, collagen type 1 A 1; *Trem2*, triggering receptor expressed on myeloid cells; WT, wild type.

Orokorrean, datu hauek adierazten dute TREM2-k erantzun inflamatorioen erregulatzaile negatibo bezala jokatzen duela kolestasiak eragindako gibeleko kaltean saguetan, azkenean, zauri-sendatze erantzun murriztuagoa eta kolestasiari loturiko fenotipo arinagoa sortuz.

E.4. Antibiotikoetan oinarritatuko tratamenduak BDL sagu ereduan behatzen diren TREM2-rekin lotutako efektuetako batzuk deuseztatzen ditu

Gaixotasun kolestatiko kronikoek hipertentsio portal eta disbiosia eragin dezakete etapa aurreratuetan, honek, azkenean, bakterien eta bakterietatik eratorritako produktuen porta zainean zeharreko lekualdaketa dakar, bakteriok eta eratorritako produktuok hesteetatik gibelera helduz. Fenomeno hau heste-gibel ardatza izenaz ezagutzen da, eta egun, seinale inflamatorioen iturrietako bat dela uste da, eta hortaz, kolestasi kronikoaren progresioan eragile garrantzitsu bat (204). BDL-aren sagu ereduan ere, ebakuntzatik 24 orduetara dagoeneko, bakterietatik eratorritako produktuen translokazioa behatu da (294). Lehenago aipatu bezala, gure ikerketa taldeak eta beste talde batzuek argitaratutako lanetan ikusi da TREM2 TLR-en bidezko seinaleztapenaren erregulatzaile negatibo bat dela (264, 265, 288, 289).

Bakterien gibeletik hesteetarako lekualdaketak TREM2-k kolestasian eragindako fenotipoan izan dezakeen parte hartzea aztertzeko asmoz, WT eta *Trem2*$^{-/-}$ saguak antibiotiko nahasketa batekin tratatu genituen 4 astez. Tratamenduaren 3. astean, BDL ebakuntza burutu genien saguei; antibiotikoen tratamendua beste aste betez ematen jarraitu genuen sakrifizioaren egunera arte, zeina BDL-aren ebakuntzatik 7 egunetara egin genuen (**E.15A Irudia**). Deigarria da, Abx-en tratamenduak BDL-an WT eta *Trem2*$^{-/-}$ saguen artean behatutako desberdintasunetako batzuk deuseztatu zituela.

Ez genuen desberdintasunik behatu inflamazio eta nekrosiaren puntuazioan Abx-en tratamendua eta gero, BDL-a bakarrik jasan zuten saguekin konparatuz (**E.15B Irudia**). Hala ere, BDL-a eta gero WT eta *Trem2*$^{-/-}$ saguen artean ikusten ziren desberdintasunak deuseztatzen ziren Abx-en tratamenduarekin, eta nekrosiaren puntuazioaren WT-*Trem2*$^{-/-}$-ren arteko aldea ere murrizten zen. Ildo honetan, estres oxidatiboaren markatzaile den *Nos2*-ren adierazpena murrizten zen *Trem2*$^{-/-}$ saguetan Abx-en tratamenduaren ondorioz, *Hmox* markatzailearen kasuan beheranzko joera nabarmena behatzen zen. BDL-a bakarrik jasandako sauetan WT eta *Trem2*$^{-/-}$ saguen artean behatutako desberdintasunak deuseztatzen ziren Abx-en tratamenduaren bidez. Are gehiago, Abx jasotako animalia taldeetan WT-*Trem2*$^{-/-}$-ren arteko aldea BDL soilik jasandako taldeetan baino txikiagoa zen *Nos2*-ren gibeleko adierazpenaren kasuan, eta beheranzko joera nabarmena behatu zen *Hmox*-en kasuan (**E.16. Irudia**).

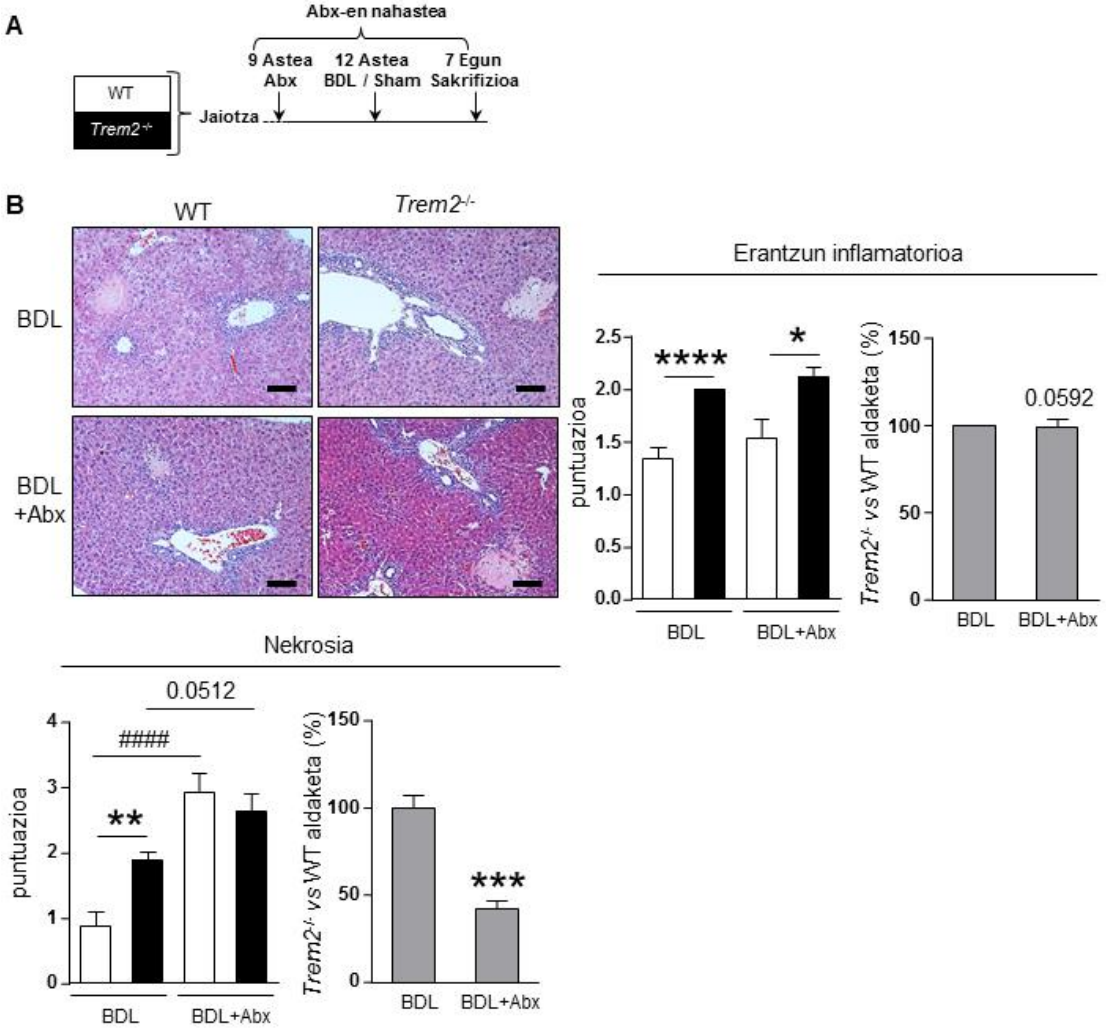

E.15. Irudia. Gibeleko kaltea BDL eta BDL + Abx-en tratamenduaren ondorioz WT eta *Trem2*$^{-/-}$ saguetan. (A) WT eta *Trem2*$^{-/-}$ saguak antibiotiko konbinazio batez tratatu ziren lau astez, tratamenduaren hirugarren astean BDL burutu zitzaien saguei eta animaliak BDL-tik 7 egunetara sakrifikatu ziren (WT n=13; *Trem2*$^{-/-}$ n=8). Sham ebakuntza (WT n=6; *Trem2*$^{-/-}$ n=7) eta BDL-a (WT n=9; *Trem2*$^{-/-}$ n=8) jasan zuten saguen datuak ere aurkezten dira konparazioak egiteko. (**B**) Gibeleko H&E tindaketaren esperientziadun patologo batek aztertu zuen, irudi adierazgarriak eta erantzun inflamatorioaren eta nekrosiaren puntuazioak aurkezten dira, balore totalak eta *Trem2*$^{-/-}$ eta WT-en arteko aldea BDL eta eta Abx+BDL tratamenduetan aurkezten dira. (**B**) Eskala marrak 100 µm adierazten ditu. (**B**) Mann Whitney test ez-parametrikoa erabili zen. *, **, *** eta **** *p* balorea <0.05, <0.01, <0.001 eta <0.0001 adierazten dute, hurrenez hurren, tratamendu berdina jaso zuten WT saguekin konparatuz (edo BDL-an behatutako *Trem2*$^{-/-}$ eta WT-en arteko aldearekin konparatuz) , #### *p* balorea <0.0001 adierazten du, genotipo berdineko sham ebakuntza jaso zuten animaliekin konparatuz. Abx, antibiotics; AU, arbitrary units; BDL, bile duct ligation; *Trem2*, triggering receptor expressed on myeloid cells; *vs*, versus; WT, wild type. *Sham eta BDL-an aurkezten diren datuak, aurreko irudietako datu berdinak dira.*

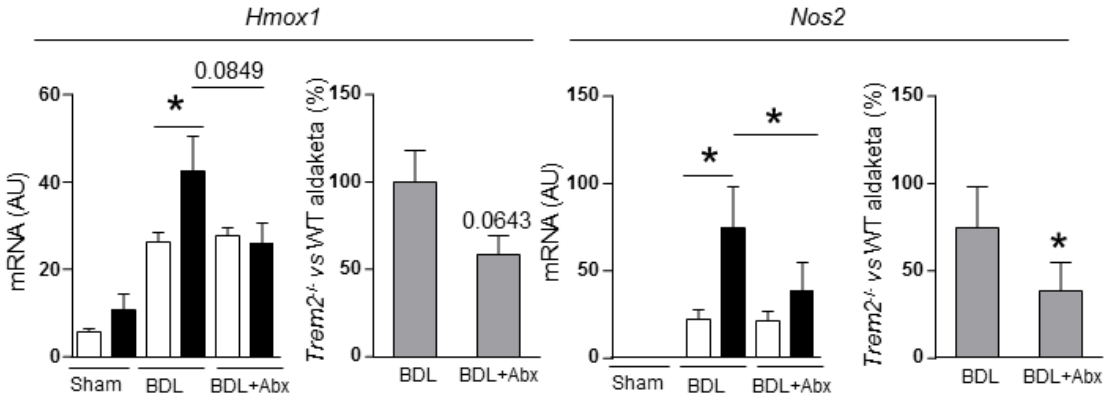

E.16. Irudia. Estrés oxidatiboaren markatzaileen adierazpena BDL edota BDL + Abx tratamendua jaso zuten WT eta *Trem2*$^{-/-}$ saguen gibelean. Gibeleko *Hmox* eta *Nos2* estres oxidatiboaren markatzaileen mRNA adierazpena, balore totalak eta *Trem2*$^{-/-}$ eta WT-en arteko aldea BDL eta Abx+BDL tratamenduetan aurkezten dira. Student-en *t*-test parametrikoa (*Hmox*) eta Mann Whitney-ren test ez-parametrikoa erabili ziren. * *p* balorea <0.05 adierazten du , tratamendu berdina jaso zuten WT saguekin konparatuz (edo BDL-an behatutako *Trem2*$^{-/-}$ eta WT-en arteko aldearekin konparatuz). Abx, antibiotics; AU, arbitrary units; BDL, bile duct ligation; *Hmox*, heme oxygenase; *Nos2*, nitric oxide synthase 2 *Trem2*, triggering receptor expressed on myeloid cells; *vs*, versus; WT, wild type. *Sham eta BDL-an aurkezten diren datuak, aurreko irudietako datu berdinak dira.*

Behazun zuhaitzaren hedapenarekin erlazionatutako aldaketak aztertzerakoan, CK19, behazun zuhaitzeko markatzailearen adierazpena bi genotipoetako saguetan murrizten zen Abx-en tratamenduaren ondorioz BDL bakarrik jasandako saguekin alderatuz. Gainera, adierazpen hau ez zen desberdina WT eta *Trem2*$^{-/-}$ saguen artean Abx-aren tratamenduaren ondorioz eta WT-*Trem2*$^{-/-}$-ren arteko aldeak beheranzko joera nabarmena aurkezten du (**E.17A Irudia**). *Trem2*$^{-/-}$ saguetan *Ck7*-ren mRNA adierazpena murrizten zen Abx-en ondorioz, BDL soilik jasandako taldeekin alderatuz, *Ck19*-ren mRNA adierazpena, aldiz ez zen aldatzen. Hala ere, *Ck19*-ren mRNA adierazpenaren WT-*Trem2*$^{-/-}$-ren arteko aldeak beheranzko joera nabarmena erakusten zuen Abx-en tratamenduaren ondorioz BDL bakarrik jasan zuten saguekin konparatuz, *Ck7*-ren kasuan beheranzko joera hau estatistikoki esanguratsua zen (**E.17B Irudia**).

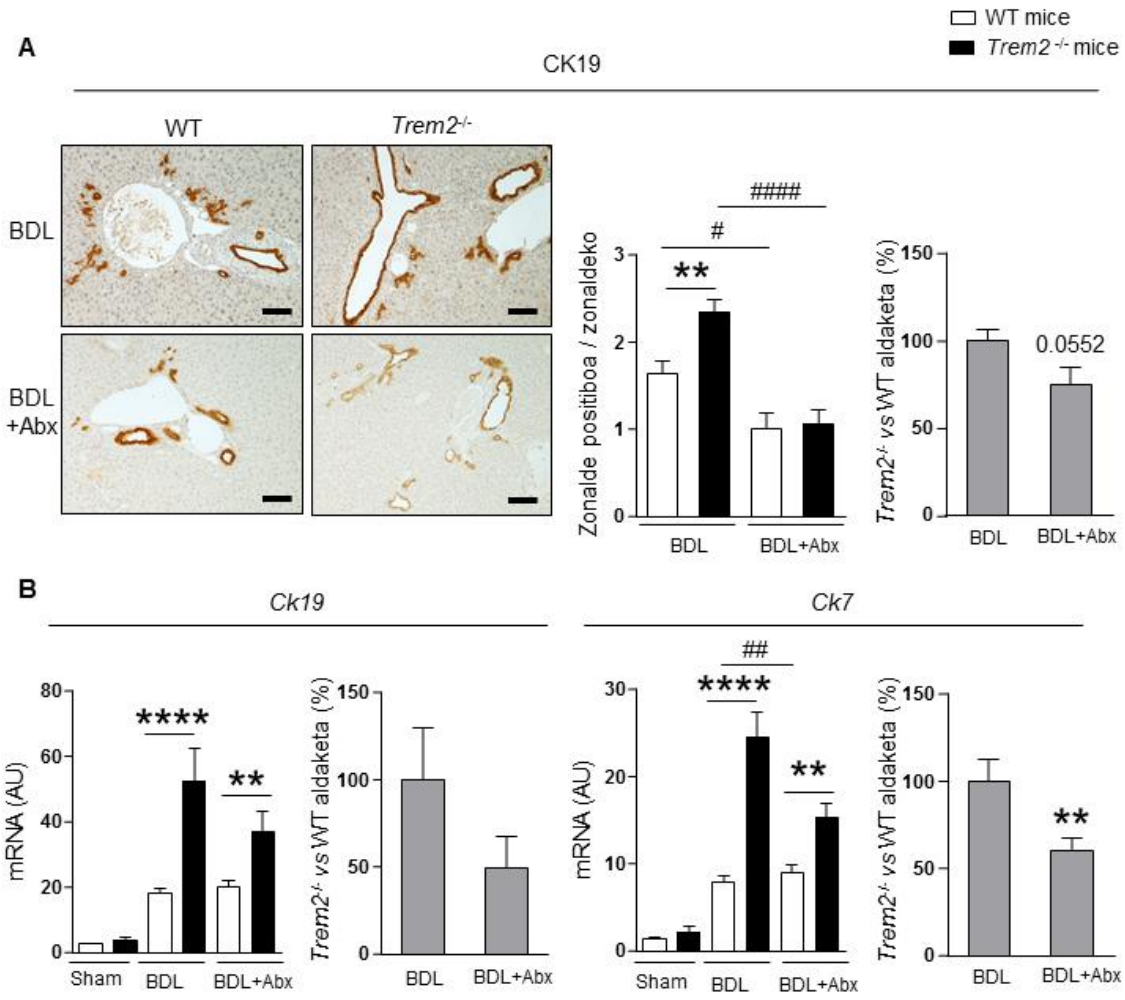

E.17. Behazun zuhaitzaren hedapena BDL eta BDL + Abx tratamenduaren ondorioz WT eta *Trem2*$^{-/-}$ saguetan. (A) CK19 kolangiozioen markailearen IHC-a, irudi adierazgarriak, kuantifikazioa eta *Trem2*$^{-/-}$ eta WT-en arteko aldea BDL eta eta Abx+BDL tratamenduetan aurkezten dira. (**B**) *Ck19* eta *Ck7* behazun zuhaitzeko markatzaileen mRNA adierazpena gibelean, balore totalak eta *Trem2*$^{-/-}$ eta WT-en arteko aldea BDL eta eta Abx+BDL tratamenduetan aurkezten dira. (**A**) Eskalaren marrak 100 µm adierazten ditu. (**A**) Student-en *t*-test parametrikoa erabili zen. (**B**) Student-en *t*-test parametrikoa eta Mann Whitney-ren test ez-parametrikoa erabili ziren. ** eta **** *p* balorea <0.01 eta <0.0001 adierazten dute, hurrenez hurren, tratamendu berdina jaso zuten WT saguekin konparatuz (edo BDL-an behatutako *Trem2*$^{-/-}$ eta WT-en arteko aldearekin konparatuz) , #, ## eta #### *p* balorea <0.05, <0.01 eta <0.0001 adierazten dute, hurrenez hurren, genotipo berdineko sham ebakuntza jaso zuten animaliekin konparatuz. Abx, antibiotics; AU, arbitrary units; BDL, bile duct ligation; *Ck7*, cytokeratin 7; *Ck19*, cytokeratin 19; *Trem2*, triggering receptor expressed on myeloid cells; vs, versus; WT, wild type. *Sham eta BDL-an aurkezten diren datuak, E.6. irudiko datu berdinak dira, IHC datu berdinak, qPCRs-ak, qPCR desberdinak baina lagin berdinak.*

Markatzaile inflamatorio batzuen gibeleko adierazpena murrizten zen Abx-en tratamenduari esker, horrela, WT saguetan *Tnf* eta *Mcp1*-ren adierazpena murrizten zen eta *Mcp1*-ren kasuan, bere adierazpena *Trem2*$^{-/-}$ saguetan ere murrizten zen Abx-en ondorioz (**E.18. Irudia**). *Cxcl1*, *Il6* eta *Il33* markatzaileen adierazpena, berriz, ez zen aldatzen Abx-en tratamenduaren ondorioz. Markatzaile hauetan, *Il33*-ren adierazpenaren WT-*Trem2*$^{-/-}$-ren arteko aldearen murrizketaz gain, ez zen beste aldaketarik behatu Abx-en tratamendua eta gero, BDL-a jasan zuten WT eta *Trem2*$^{-/-}$ saguen artean behatu zen desberdintasunekin alderatuz (**E.18. Irudia**).

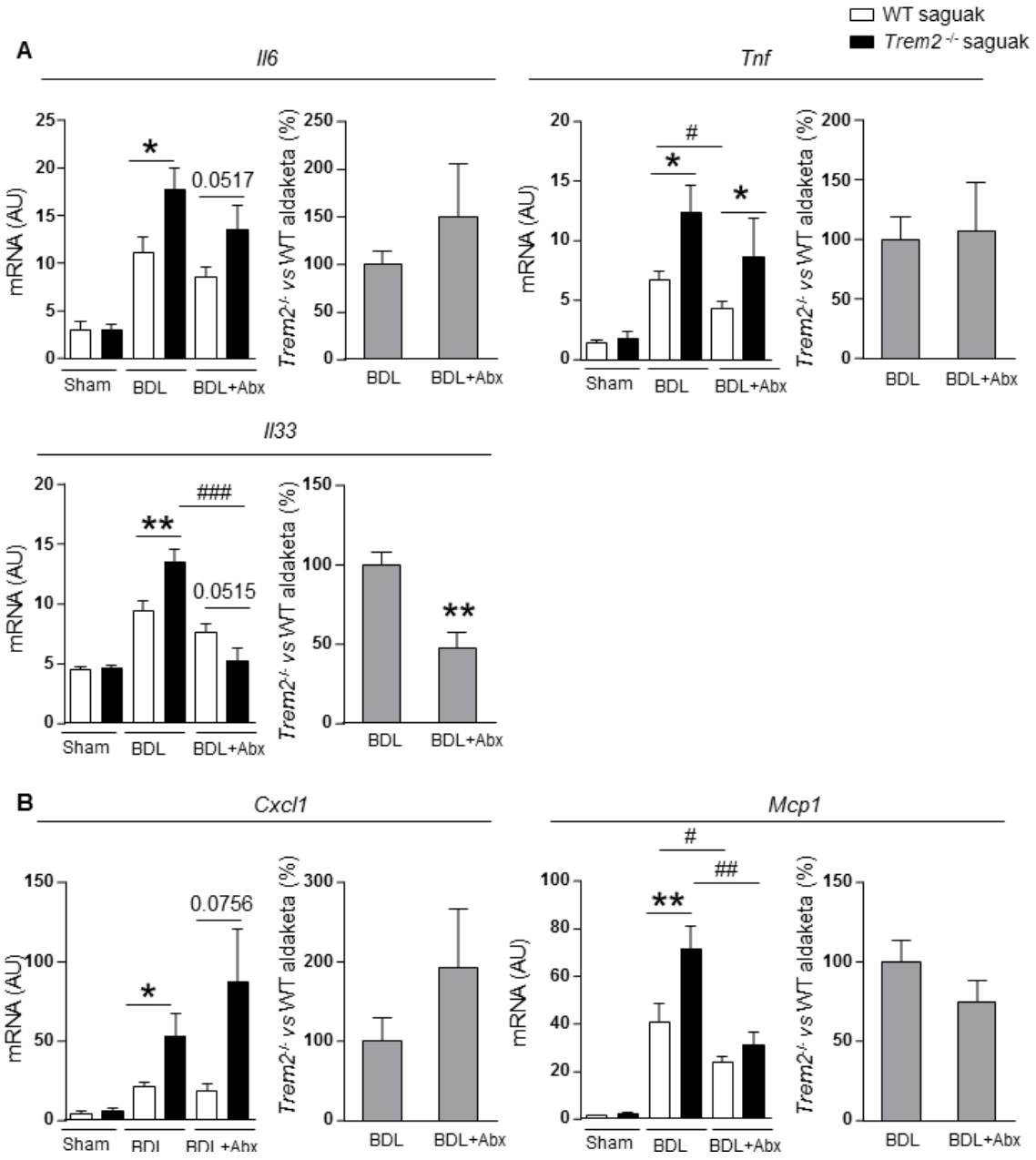

E.18. Irudia. Zitokina eta kemokina inflamatorioen adierazpena BDL eta BDL gehi Abx-en tratamendua eta gero WT eta *Trem2* $^{-/-}$ saguetan. (**A**) Gibeleko *Il6*, *Tnf* eta *Il33*zitokina inflamatorioen mRNA adierazpena, balore totalak eta *Trem2*$^{-/-}$ eta WT-en arteko aldea BDL eta eta Abx+BDL tratamenduetan aurkezten dira. (**B**) Gibeleko *Mcp1* eta *Cxcl1* kemokina inflamatorioen mRNA adierazpena, balore totalak eta *Trem2*$^{-/-}$ eta WT-en arteko aldea BDL eta eta Abx+BDL tratamenduetan aurkezten dira. Student-en *t*-test parametrikoa eta Mann Whitney-ren test ez-parametrikoa erabili ziren. * eta ** *p* balorea <0.05 eta <0.01 adierazten dute, hurrenez hurren, tratamendu berdina jaso zuten WT saguekin konparatuz (edo BDL-an behatutako *Trem2*$^{-/-}$ eta WT-en arteko aldearekin konparatuz) , #, ## eta ### *p* balorea <0.05, <0.01 eta <0.001 adierazten dute, hurrenez hurren, genotipo berdineko sham ebakuntza jaso zuten animaliekin konparatuz. Abx, antibiotics; AU, arbitrary units; BDL, bile duct ligation; *Cxcl1*, C-X-C Motif Chemokine Ligand 1; *Il6*, interleukin 6; *Il33*, interleukin 33; *Mcp1*, monocyte chemoattractant protein 1; *Tnf*, tumour necrosis factor; *Trem2*, triggering receptor expressed on myeloid cells; vs; versus; WT, wild type. *Sham eta BDL-an aurkezten diren datuak, aurreko irudietako datu berdinak dira, Il6, Tnf, Mc1 eta Cxcl1qPCR desberdina, Il33 qPCR bera.*

Neutrofiloen gibelerako erakarpenak goranzko joera nabarmena aurkeztu zuen Abx-ekin tratatutako WT saguetan BDL bakarrik jasandakoekin alderatuz, *Trem2*$^{-/-}$ aldatzen ez zen bitartean (**E.19. Irudia**). WT-*Trem2*$^{-/-}$-ren arteko aldea aztertu genuenean, Abx-aren tratamenduak, BDL bakarrik jasandako saguetan ikusitako aldaketak murrizten zituela behatu genuen (**E.19. Irudia**).

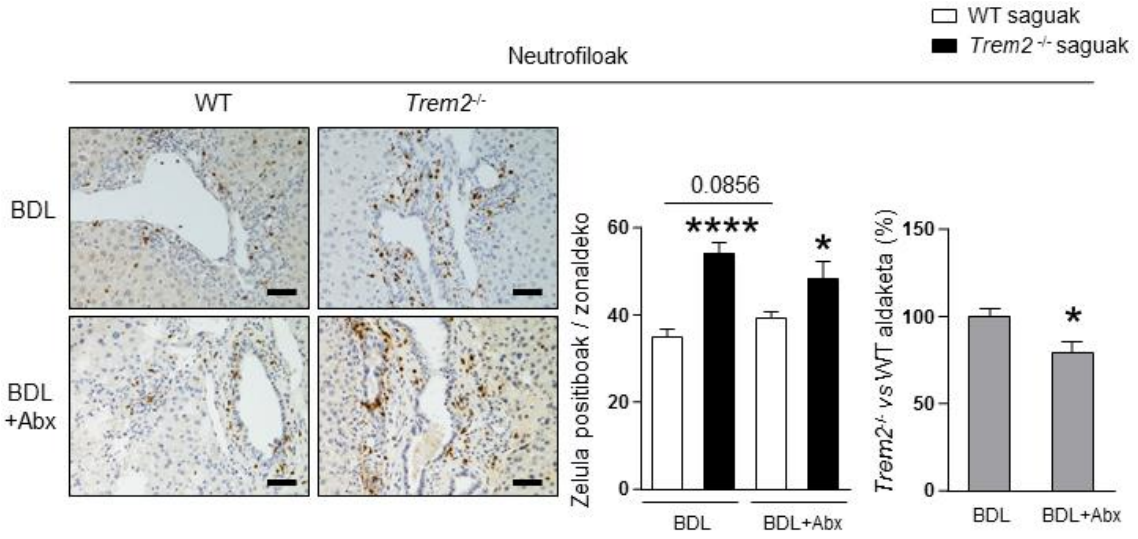

E.19. Irudia. Neutrofiloen gibelerako erakarpena BDL eta BDL gehi Abx-en tratamendua eta gero WT eta *Trem2*$^{-/-}$ saguetan. NIMP-R14 neutrofiloen markatzailearen IHC-a, irudi adierazgarriak, kuantifikazioa eta *Trem2*$^{-/-}$ eta WT-en arteko aldea BDL eta eta Abx+BDL tratamenduetan aurkezten dira. Eskalaren marrak 50 µm adierazten ditu. Student-en *t*-test parametrikoa eta Mann Whitney-ren test ez-parametrikoa erabili ziren. * eta **** *p* balorea <0.05 eta <0.0001 adierazten dute, hurrenez hurren, tratamendu berdina jaso zuten WT saguekin konparatuz (edo BDL-an behatutako *Trem2*$^{-/-}$ eta WT-en arteko aldearekin konparatuz). Abx, antibiotics, BDL, bile duct ligation; *Trem2*, triggering receptor expressed on myeloid cells; *vs*, versus; WT, wild type. *BDL-an aurkezten diren datuak, aurreko irudietako datu berdinak dira.*

E.5. *Trem2*$^{-/-}$ saguek gehiegizko gibeleko kaltea eta inflamazioa aurkezten dute ANIT-aren adiministrazioan oinarritutako kolestasi kimikoaren sagu eredu batean

E.5.1. Gehiegizko gibeleko kaltea *Trem2*$^{-/-}$ saguetan ANIT-aren adiministrazioan oinarritutako kolesetasi kimikoaren sagu eredu batean

BDL sagu ereduan lortutako emaitzek, jatorri desberdineko koletasiaren sagu ereduen gibelean behatutako *Trem2*-ren adierazpenaren emendioarekin batera, TREM2-ren papera kimikoki eragindako kolestasiaren sagu eredu batean aztertzera eraman gintuen. ANIT-aren administrazioan oinarritutako sagu eredua aukeratu genuen, ANIT-ak kolangiozitoetan dituen eraginengatik, izan ere, ahotik hartzeko dosi altu bakarrean ematen denean, kolangiozitoen galera larria, eta honen ondoriozko gibel barruko

kolestasia dakar (295, 296). Sagu eredu hau burutzeko, ANIT-a 50mg/kg-ko dosian edo O.Oil-a eman genizkien WT eta *Trem2*$^{-/-}$ saguei, eta animaliak administraziotik 48 orduetara sakrifikatu genituen (**E.20A Irudia**).

Hasteko, 50mg/kg-ko dosian ANIT-ak WT saguetan gibeleko kalterik ez zuela eragin behatu genuen. Izan ere, AP, serumeko kalte kolestasikoaren markatzailearen eta ALT eta AST serumeko gibel kaltearen markatzaileen mailak pareakoak ziren O.Oil eta ANIT-az tratatutako WT saguetan (**E.20B Irudia**). *Trem2*$^{-/-}$ saguetan aldiz, ANIT-ak markatzaile hauen mailen emendioa eragin zuen O.Oil-az tratatutako saguekin alderatuz. Gainera, *Trem2*$^{-/-}$ saguetan AP, ALT eta AST-ren mailak altuagoak ziren WT saguekin alderatuz ANIT-a eta gero.

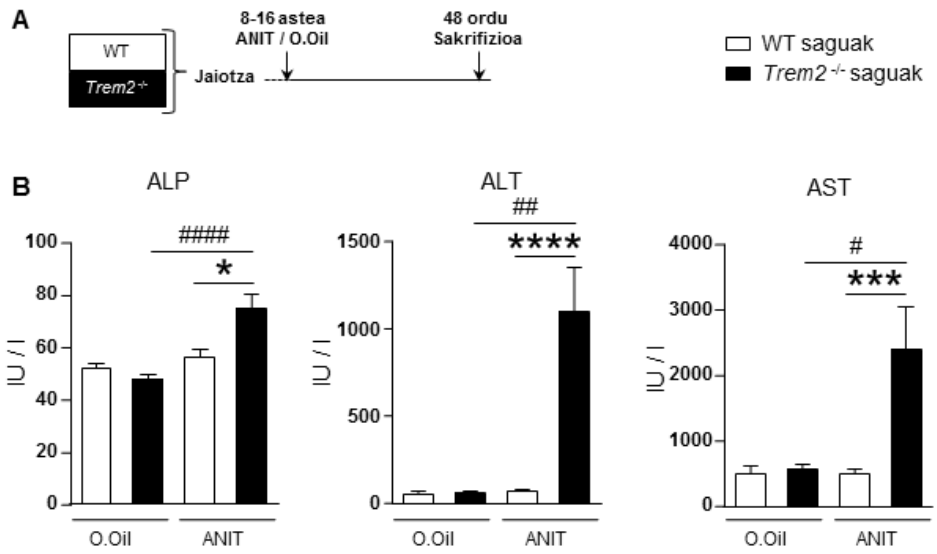

E.20. Irudia. Serumeko gibel eta behazun zuhaitzeko kaltearen markatzaileak ANIT-aren administrazioan oinarritutako, kimikoki eragindako kolestasiaren sagu eredu batean WT eta *Trem2* $^{-/-}$ saguetan. (**A**) WT eta *Trem2*$^{-/-}$ saguei O.Oil (WT n=8; *Trem2*$^{-/-}$ n=8) edo ANIT (WT n=11; *Trem2*$^{-/-}$ n=12) eman zitzaien eta saguak 48 ordutara sakrifikatu ziren. (**B**) Serumeko gibeleko entzimen mailak aztertu ziren. (**B**) Student-en *t*-test parametrikoa eta Mann Whitney-ren test ez-parametrikoa erabili ziren. *, *** eta **** *p* balorea <0.05, <0.001 eta <0.0001 adierazten dute, hurrenez hurren, tratamendu berdina jaso zuten WT saguekin konparatuz #, ## eta ### *p* balorea <0.05, <0.01 eta <0.0001 adierazten dute, hurrenez hurren, genotipo berdineko O.Oil jaso zuten animaliekin konparatuz. ALT, alanine aminotransferase; ANIT, α-naphthylisothiocyanate; ALP, alkaline phosphatase; AST, aspartate aminotransferase; AU, arbitrary units; BDL, bile duct ligation; *Ck7*, cytokeratin 7; *Ck19*, cytokeratin 19; H&E, hematoxylin and eosin; O.Oil, olive oil; *Trem2*, triggering receptor expressed on myeloid cells; WT, wild type.

Honekin batera, *Trem2*$^{-/-}$ saguek zonalde nekrotikoen emendioa aurkezten zuten ANIT-a eta gero WT saguekin konparatuz (**E.21A Irudia**). *Hmox* eta *Nos2* estres oxidatiboaren

markatzaileen adierazpena bi genotipoetako saguetan emendatzen zen ANIT-aren administrazioaren ondorioz, O.Oil-arekin konparatuz, are gehiago, emendio hau nabarmenagoa zen *Trem2*$^{-/-}$ saguetan WT-ekin alderatuz ANIT eta gero (**E.21B Irudia**). Era beran, *Ck7* eta *Ck19* behazun zuhaitzeko markatzaileen mRNA adierazpena handiagoa zen bi genotipoetako saguetan ANIT-aren ondorioz, eta are gehiago emendatzen zen *Trem2*$^{-/-}$ saguetan WT saguekin alderatuz ANIT-az tratatutako taldean (**E.21C Irudia**).

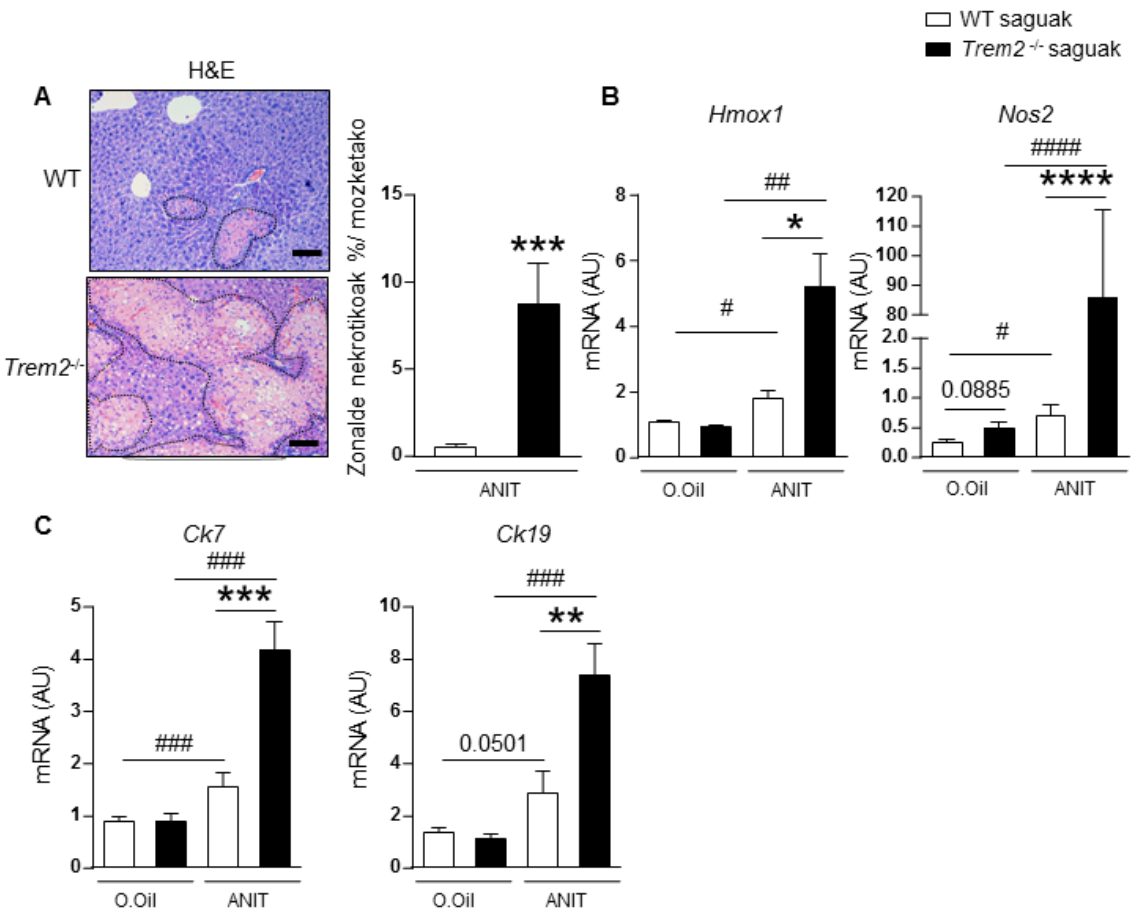

E.21. Irudia. Gibel kaltea ANIT-aren administrazioan oinarritutako, kimikoki eragindako kolestasiaren sagu eredu batean WT eta *Trem2* $^{-/-}$ saguetan. (**A**) Zonalde nekrotikoak H&E-az tindatutako gibelaren mozketetan, irudi adierazgarriak eta kuantifikazioa aurkezten dira. (**B**) *Hmox* eta *Nos2* estres oxidatiboko markatzaileen mRNA adierazpena gibelean. (**C**) *Ck7* eta *Ck19* kolangiozitoen markatzailen mRNA adierazpena gibelean. Student-en *t*-test parametrikoa eta Mann Whitney-ren test ez-parametrikoa erabili ziren *, **, *** eta **** *p* balorea <0.05 <0.01, <0.001 <0.0001 adierazten dute, hurrenez hurren, tratamendu berdina jaso zuten WT saguekin konparatuz #, ##, ### eta #### *p* balorea <0.05, <0.01 eta <0.0001 adierazten dute, hurrenez hurren, genotipo berdineko O.Oil jaso zuten animaliekin konparatuz. ANIT, α-naphthylisothiocyanate; AU, arbitrary units; *Ck7*, cytokeratin 7; *Ck19*, cytokeratin 19; H&E, hematoxylin and eosin; O.Oil, olive oil; *Trem2*, triggering receptor expressed on myeloid cells; WT, wild type.

E.5.2. Gehiegizko inflamazioa *Trem2*$^{-/-}$ saguetan ANIT-aren adiministrazioan oinarritutako kolesetasiaren sagu eredu batean

BDL sagu ereduan behatutako emaitzekin bat eginez, *Trem2*$^{-/-}$ saguek gehiegizko erantzun inflamatorioa aurkezten dute ANIT-aren administrazioan oinarritutako kimoki eragindako kolestasiaren sagu ereduan ere. Ildo honetan, *Trem2*$^{-/-}$ saguek *Il1β*, *Il6*, *Il33* eta *Tnf* zitokina inflamatorioen eta *Mcp1* kemokina inflamatorioaren adierazpenaren emendioa aurkezten zuten WT saguekin alderatuz ANIT-aren administrazioa eta gero. (**E.22. Irudia**). Azpimarragarria da ANIT-aren tratamenduak ez zuela eraginik izan markatzaile pro-inflamatorioen adierazpenean WT saguetan, O.Oil-az tratatutako saguekin alderatuz, *Trem2*$^{-/-}$ saguetan markatzaile guztien mRNA adierazpena emendatzen zituen bitartean. Era berean, ANIT-aren administrazioaren ondorioz, *Acta2* mRNA adierazpenak goranzko joera nabarmena aurkeztu zuen WT saguetan, eta emendio hau estatistikoki esanguratsua zen *Trem2*$^{-/-}$ saguen kasuan. *Acta2*-ren adierazpena gehiago emendatzen zen *Trem2*$^{-/-}$ saguetan WT saguekin alderatuz ANIT eta gero (**E.22. Irudia**).

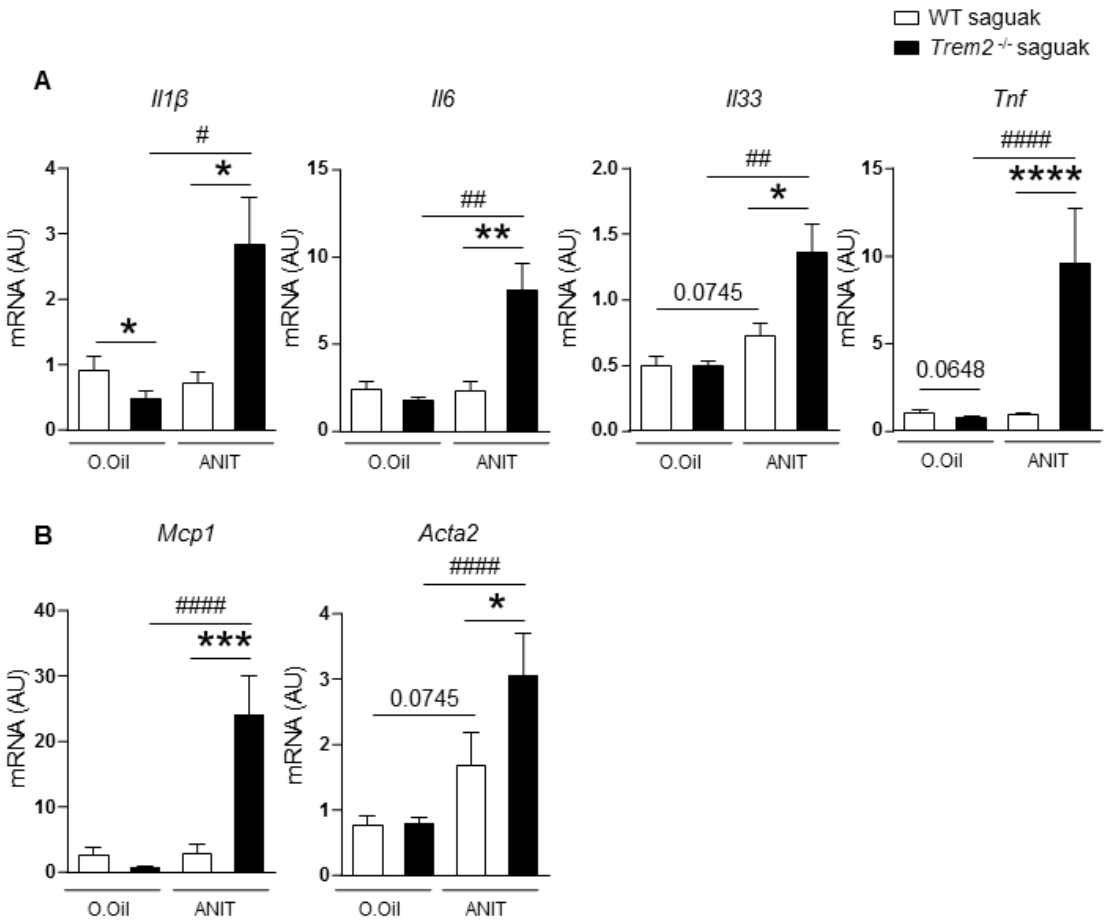

E.22. Irudia. Zitokina eta kemokina inflamatorioen mRNA adierazpena ANIT-aren administrazioan oinarritutako, kimikoki eragindako kolestasiaren sagu eredu batean WT eta *Trem2* $^{-/-}$ saguetan. (**A**) *Il1β*, *Il6*, *Il33* eta *Tnf* zitokina inflamatorioen mRNA adierazpena, (**B**) *Mcp1* kemokinaren mRNA adierazpena eta (**C**) *Acta2* HSCs-en aktibazioaren markatzailearen mRNA adierazpena. Student-en *t*-test parametrikoa eta Mann Whitney-ren test ez-parametrikoa erabili ziren. *, **, *** eta **** *p* balorea <0.05 <0.01, <0.001 <0.0001 adierazten dute, hurrenez hurren, tratamendu berdina jaso zuten WT saguekin konparatuz. #, ## eta #### *p* balorea <0.05, <0.01 eta <0.0001 adierazten dute, hurrenez hurren, genotipo berdineko O.Oil jaso zuten animaliekin konparatuz. *Acta2*, actin alpha 2, smooth muscle; ALT, alanine aminotransferase; ANIT, α-naphthylisothiocyanate; AP, alkaline phosphatase; AST, aspartate aminotransferase; AU, arbitrary units; BDL, bile duct ligation; *Cxcl1*, C-X-C Motif Chemokine Ligand 1; *Il6*, interleukin 6; *Il33*, interleukin 33; *Mcp1*, monocyte chemoattractant protein 1; O.Oil, olive oil; *Tnf*, tumour necrosis factor; *Trem2*, triggering receptor expressed on myeloid cells; WT, wild type.

BDL eta ANIT sagu ereduetan behatutako datu guztiak kontuan hartuta, jatorri desberdinetatik eratorritako kolestasiaren bidez eragindako gibel kaltearen testuinguruan, TREM2 gibela gehiegizko kalteaz eta inflamazioaz babesteko gai dela ematen du.

E.6. UDCA-k TREM1 eta TREM2-ren gene adierazpena erregulatzen ditu isolatutako KCs-etan

Lehenago aipatu bezala, KC-ak kolestasian zauri-sendatze erantzuna bideratzen duten zelula garrantzitsuak dira (27, 131). Are gehiago, lan honen E.2 (**E.4. Irudia**) atalean eta gure taldearen aurreko argitalpenetan (288, 289) ikusi dugun bezala, TREM2 gibelaren zelula mota hauetan adierazten da gehien bat. Aipagarria da, TREM1 eta TREM2-k kontrako efektuak eragiten dituztela, orokorrean, TREM1-ek TLR-en bidezko inflamazioa areagotzen du, TREM2-k bidezidor hau negatiboki erregulatzen duen bitartean (242). Efektu kontrajarri hauek hepatokartzinogenesian azaleratzen dira (261), non TREM1-ek gaixotasunaren progresioa bultzatzen duen, TREM2-k askotariko efektu babesleak eragiten dituen bitartean (289).

Hasteko, LPS-aren tratamenduaren ondorioz, *Trem1* eta *Trem2*-ren adierazpena isolatutako KCs WT-etan, analizatu genuen, denbora puntu desberdinetan. Esperimentu honen bidez, LPS-ak *Trem1*-en adierazpena emendatzen duela behatu genuen, adierazpen hau inkubaziotik 12 ordu ondoren altu mantentzen zela ikusi genuen eta 24 ordutara adierazpenaren murrizpena txiki bat behatu zen. Bestalde, *Trem2*-ren adierazpena era progresiboan murrizten zen LPS-aren inkubazioaren ondorioz (**E.23. Irudia**).

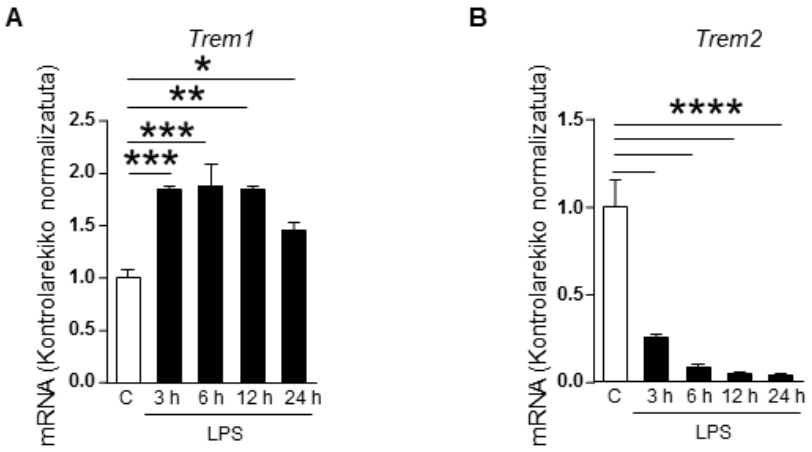

E.23. Irudia. *Trem1* eta *Trem2* mRNA adierazpena saguetatik isolatutako WT KCs-etan LPS-ren eraginez. (**A**) *Trem1* eta (**B**) *Trem2* mRNA adierazpen mailak saguetatik isolatutako KCs-etan LPS-aren inkubaziotik 3, 6, 12 eta 24 orduetara kontrol zelulekin konparatuz (n=3-5). ANOVA test parametrikoa eta Tukey-ren post hoc testa erabili ziren. *, **, ***, **** *p* balorea <0.05, <0.01, <0.001 and <0.0001 adierazten dute, hurrenez hurren. AU, arbitrary units; LPS, lipopolysaccharide *Trem1*, triggering receptor expressed on myeloid cells 1; *Trem2*, triggering receptor expressed on myeloid cells 2.

UDCA, BA koleretiko endogenoa, PBC-aren tratamenduan lehengo mailako terapia da eta PSC-aren tratamenduan ere erabiltzen da osasun zentro askotan. UDCA-ren koleresiaz gaindiko efektuen artean, efektu anti-apoptotikoak, bikarbonatoaren jariapena behazun zuhaitzean eta efektu anti-inflamatorioak daude, baina hauen azpiko mekanismo molekularrak ezagutzeke daude oraindik (311). UDCA-an oinarritutako tratamendua hartzen duten PBC-dun gaixoen %30-40-ak erantzun ez-osoa aurkezten dute eta, hortaz, gaixotasunaren garapenarekin lotutako egoera larriagoak aurkezteko eta gibeleko transplante baten beharra izateko arrisku handiaga dute (22). UDCA-k kolestasian dituen efektuak bideratzen dituzten mekanismo molekularrak zehatzago ulertzea arazo hau konpontzen lagun lezake, erantzun ez-osoa aurkezten duten gaixoentzako terapia optimizatzeko estrategiak proposatuz. Ildo honetan, gure hurrengo urratsa UDCA-k KCs-etan erantzun inflamatorioengan TREM2-ren menpeko efekturik izan lezakeen aztertzea izan zen.

Gure aurreko emaitzak baieztatuz, 6 orduetara, LPS-ak *Trem1*-en mRNA adierazpena sustatu zuen WT KCs-etan (**E.24A Irudia**). Denbora puntu honetan, UDCA-ren inkubazioak *Trem1*-en mRNA adierazpenaren murrizketa eragiten zuen WT KCs-etan kontrol egoerarekin alderatuz. LPS eta UDCA-ren konbinazioak *Trem1*-en mRNA adierazpena emendatzen zuen LPS-az bakarrik inkubatutako taldearekin alderatuz (**E.24A Irudia**). Ondoren, *Trem2*-ren adierazpena denbora puntu luzeagoetan aztertu genuen, LPS-ak eragindako *Trem2*-ren adierazpenaren murrizketa nabarmenena zen unean. Aurretik adierazi bezala. *Trem2*-ren adierazpena murrizten zen LPS-aren inkubaziotik 24 orduetara. UDCA-ren inkubazioak 200 μM dosian *Trem2* mRNA adierazpena emendatzen zuen kontrol taldearekin alderatuz. UDCA-ren gehiketa LPS-az tratatutako zeluletan, Trem2-ren adierazpenaren igoera eragin zuen, LPS-az bakarrik tratatutako zelulekin alderatuz (**E.24B Irudia**). Efektu hau ez zen esanguratsua ANOVA+Tukey´ren post hoc testa erabiliz, baina bai bi taldeen arteko konparaketa eginez Student-en t testarekin.

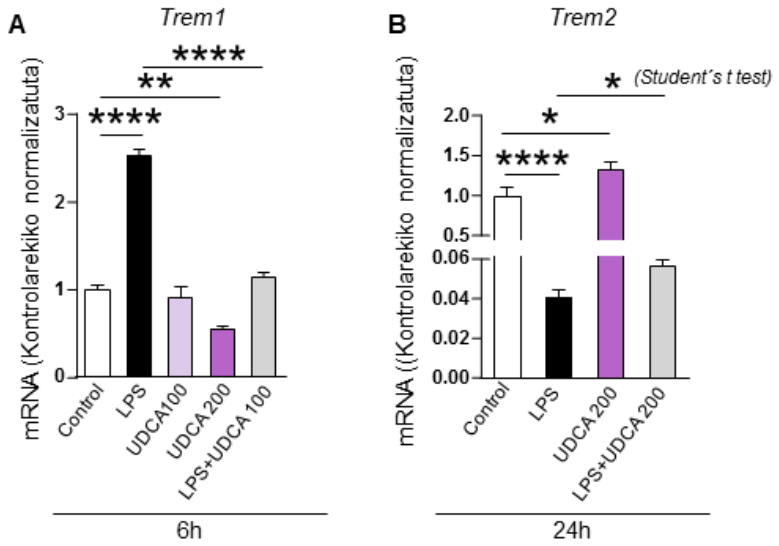

E.24. Irudia. KCs zeluletan UDCA-k *Trem1* eta *Trem2* mRNAadierazpenean duen eragina LPS edota UDCA-ren inkubazioa eta gero. *Trem1* eta *Trem2* mRNA adierazpen maila isoltutako KCs-etan LPS eta UDCA-ren inkubazioaren 6 eta 24 orduetara. ANOVA eta Tukey-ren post hoc test parametrikoak eta Student-en *t* test parametrikoa erabili ziren. *, **, ***, **** *p* balorea <0.05, <0.01, <0.001 eta <0.0001 adierazten dute. AU, arbitrary units; LPS, lipopolysaccharide *Trem1*, triggering receptor expressed on myeloid cells 1; *Trem2*, triggering receptor expressed on myeloid cells 2; UDCA, ursodeoxycholic acid.

E.7. UDCA-k gibeleko zelula ez-parenkimaletan dituen efektuak, partzialki behintzat, TREM2-ren menpekoak dira

Gure hurrengo helburua, *Trem*1 eta *Trem2*-ren gainean UDCA-k KCs-etan eragiten zituen efektuak aldaketa funtzionalen batekin lotuta zeuden aztertzea izan zen. Horretarako, KCs-ak WT eta *Trem2*$^{-/-}$ saguetatik isolatu genituen eta LPS edota LPS eta UDCA-ren konbinazioaz inkubatu. Gure aurreko lanetan argitaratu dugun moduan (288), LPS-ak *Il6, Tnf and Cxcl1* markatzaile inflamatorioen mRNA adierazpenaren emendio nabarmena eragin zuen, emendio hau are handiagoa zen *Trem2*$^{-/-}$ saguetatik eratorritako KCs-etan WT saguetatik eratorritakoekin alderatuz, eta emendio hau mantentzen zen UDCA-az inkubatutako zeluletan (**E.25.Irudia**). Halaber, deigarria da, UDCA-ren gehiketak, markatzaile hauen adierazpenaren murrizketa zekarrela WT zeluletan LPS-az bakarrik inkubatutako taldearekin konparatuz, *Trem2*$^{-/-}$ saguetan, ordea, UDCA-ren gehiketak ez zuen aldaketarik eragin markatzaile inflamatorio hauen mRNA adierazpenean (**E.25.Irudia**). Emaitza hauek UDCA-k markatzaile inflamatorioen adierazpenean dituen efektu babesleak *Trem2*-ren menpekoak direla iradokitzen dute.

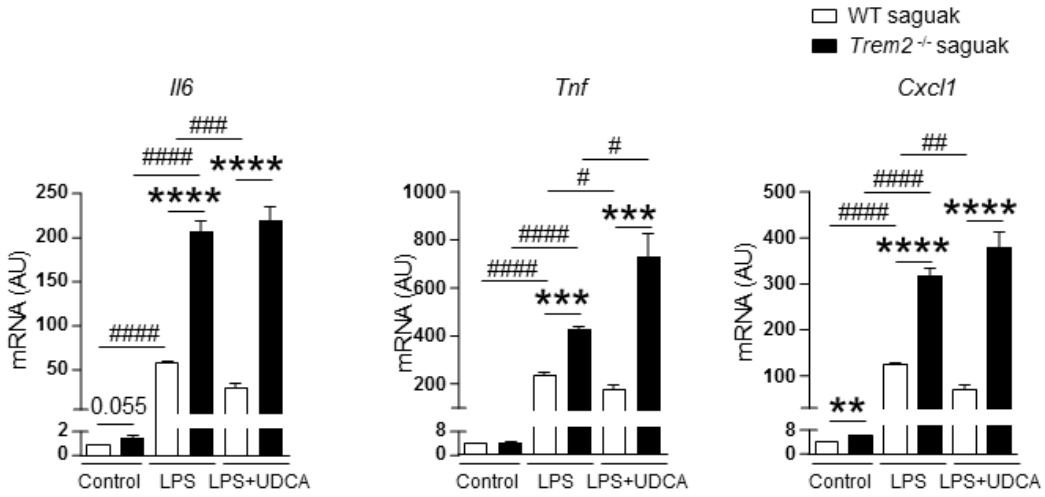

E.25. Irudia. UDCA-ren efektuak markatzaile inflamatorioen mRNA adierazpenean LPS-az tratatutako WT eta *Trem2*$^{-/-}$ KC–etan. *Il6, Tnf eta Cxcl1-en* mRNA adierazpen mailak WT eta *Trem2* $^{-/-}$ KC-etan LPS eta LPS gehi UDCA konbinazioaren inkubaziotik 3 orduetara. Student-en *t*-test parametrikoa erabili zen. **, *** eta **** *p* balorea <0.01, <0.001 eta <0.0001 adierazten dute tratamendu berdina jaso duten WT KCs-ekin alderatuz; #, ##, ### eta #### *p* balorea <0.05, <0.01, <0.001 eta <0.0001 adierazten dute, genotipo bereko WT edo LPS tratatutako KCs-ekin alderatuz. AU, arbitrary units; Cxcl1, C-X-C motif chemokine ligand 1, *Il6*, interleukin 6; *Tnf*, tumour necrosis factor; *Trem1*, triggering receptor expressed on myeloid cells 1; *Trem2*, triggering receptor expressed on myeloid cells 2; UDCA, ursodeoxycholic acid.

E.8. HCC-an, TREM2-ren adierazpena batez ere gibeleko bertako eta gibelera erakarritako makrofagoetan detektatzen da

Kolestasia eta gibel barruko BA-en metaketa estuki lotuta daude gibel eta behazun hodietako kartzinogenesiarekin (182). Gaixotasun kolestasiko kroniko aurreratu edo larriak dituzten pazienteek gibel eta behazun zuhaitzeko minbiziara garatzeko arrisku handiagoa dute. Honela, PBC-dun pazienteek HCC-a garatu dezakete (183) eta PSC-dun pazienteek HCC zein CCA garatzeko arrisku handiagoa dute (184-186). Kasu gehienetan, kartzinogenesia gaixotasunaren etapa aurreratuetan garatzen da, fibrosia eta zirrosia ezarri ondoren (180). Berriki argitaratutako ikerlan batean, TREM2 gibela hepatokartzinogenesiaz babesteko gaitasuna duela ikusi dugu (289). Lan horretan, bi gaixo talde debesberdinetan, giza HCC tumoreetan TREM2-ren adierazpena emendatuta dagoela behatu dugu, ehun kontrol osasuntsuarekin konparatuz (289).

R.8.1. TREM2-ren adierazpena makrofago itxura duten zelulaten behatzen da HCC tumoreetan.

Hasteko, TREM2-ren adierazpena IHC bidez aztertu genuen jatorri anitzetako HCC-dun gaixoen gibelean eta minbizi kolorrektala edo bularreko minbiziaren ondoriozko gibeleko metastasia duten kontrol indibiduoen gibel osasuntsuan. Azterketa honetan erabilitako gaixoen ezaugarriak eta aldagai klinikoak **M.2. Taulan** jasotzen dira. Gure aurreko datuekin bat eginez (289), TREM2-ren immuno-tindaketa handiagoa behatu genuen gibel ehun gaixoan ehun osasuntsuarekin alderatuz (**E.26. Irudia**). HCC-ren laginetan, TREM2-ren immuno-tindaketa tumorearen inguruko gibel ehun zirrotikoan eta tumorearen barnean aztertu genuen, bi ehun mota hauen artean tindaketaren intentsitatea antzekoa zela behatu gneuen. Azpimarragarria da, orokorrean ez genuela TREM2-ren immuno-tindaketarik behatu eraldatutako hepatozitoetan. Tumorearen inguruko ehun zirrotikoan TREM2-ren immuno-tindaketa porta zainaren inguruko gune inflamatorioetan eta septo fibrosoen ondoko ehunean behatu zen. Tumorearen barruan, immuno-tindaketa hau tumore-bertako zein tumorera erakarritako zeluletan ikusi zen, TREM2-ren tindaketa aurkezten zuten zelulek makrofago itxura zuten (**E.26. Irudia**).

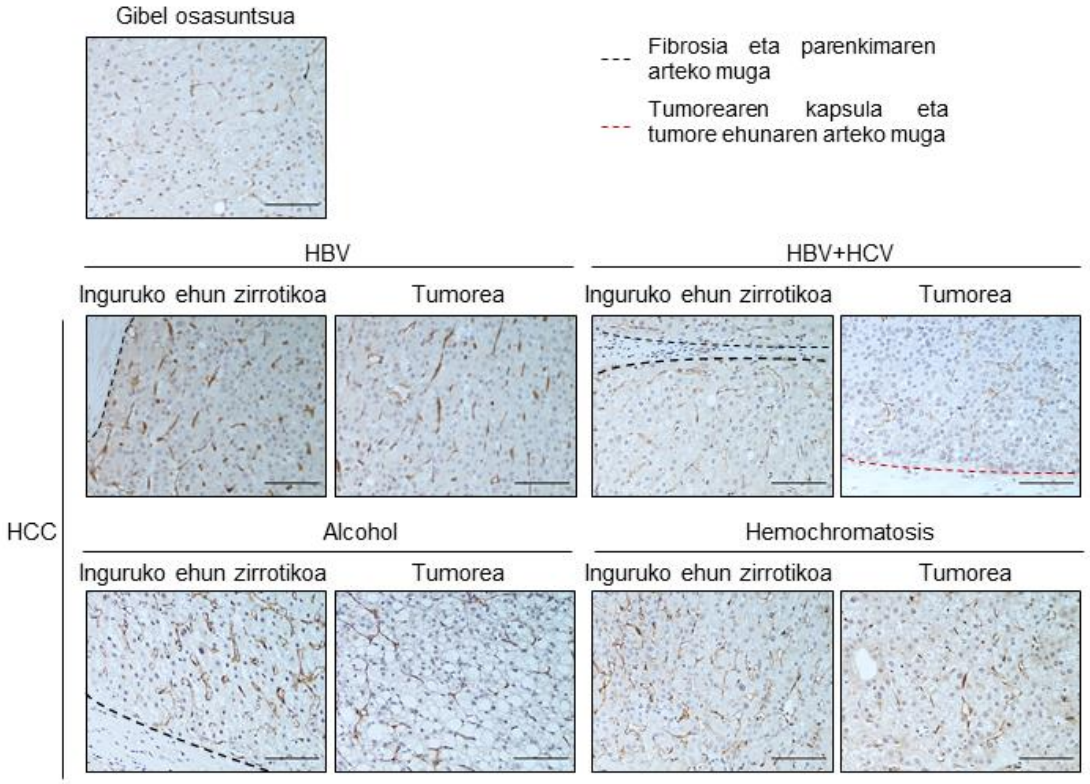

E.26. TREM2-ren adierazpena giza HCC-an eta tumorearen inguruko ehun zirrotikoan. TREM2-ren IHC-a gibel ehun osasuntsuan eta jatorri anitzetako HCC-dun gaixoen gibelean, irudi adierazgarriak aurkezten dira. HCC ehunetan, tumore inguruko ehun zirrotikoa eta tumore barnekoak aurkezten dira. Eskalaren barrak 100 µm adierazten ditu.

R.8.2. TREM2-ren adierazpena makrofago itxura duten zelulaten behatzen da HCC tumoreetan.

Giza HCC-an TREM2 adierazten duten zelula motak zeintzuk diren zehatzago aztertzeko, publikoki eskuragarri dagoen, 9 giza HCC-dun gibelen zelula bakarreko RNA sekuentziazo datuak erabili genituen (291). Prozesamendua eta gero, datuok t-SNE (t-distributed Stochastic Neighbor Embedding) grafikoen bidez aurkeztu genituen, Seurat T paketearen bidez. 6 zelula talde desberdin identifikatu genituen, talde hauek T zelula, B zelula, tumorearekin lotutako fibroblasto (CAFs), tumorearekin lotutako makrofago (TAMs), tumorearekin lotutako zelula endotelial (TECs) eta gibeleko zelula progenitore antzekoekin (HPC-like) bat egiten zuten (**E.27A Irudia**). HCC-aren zelula malignoak HPC-like taldearekin bat egiten zuten, eta hauek jatorrizko laneko, RNA-seq-etik eratorritako kromosomen kopia-kopuruko eraldaketa handien predikzioan oinarritu ziren (291). Zelula talde hauen artean, *TREM2*-ren adierazpena TAMs-etan aurkitu zen batez ere, gainerako zelula taldeetan adierazpen maila oso bajuak ikusten ziren bitartean (**E.27B Irudia**). Honek, aurretik HCC-en ehunaren sekzioetan IHC-az behatutakoarekin bat egiten du (289).

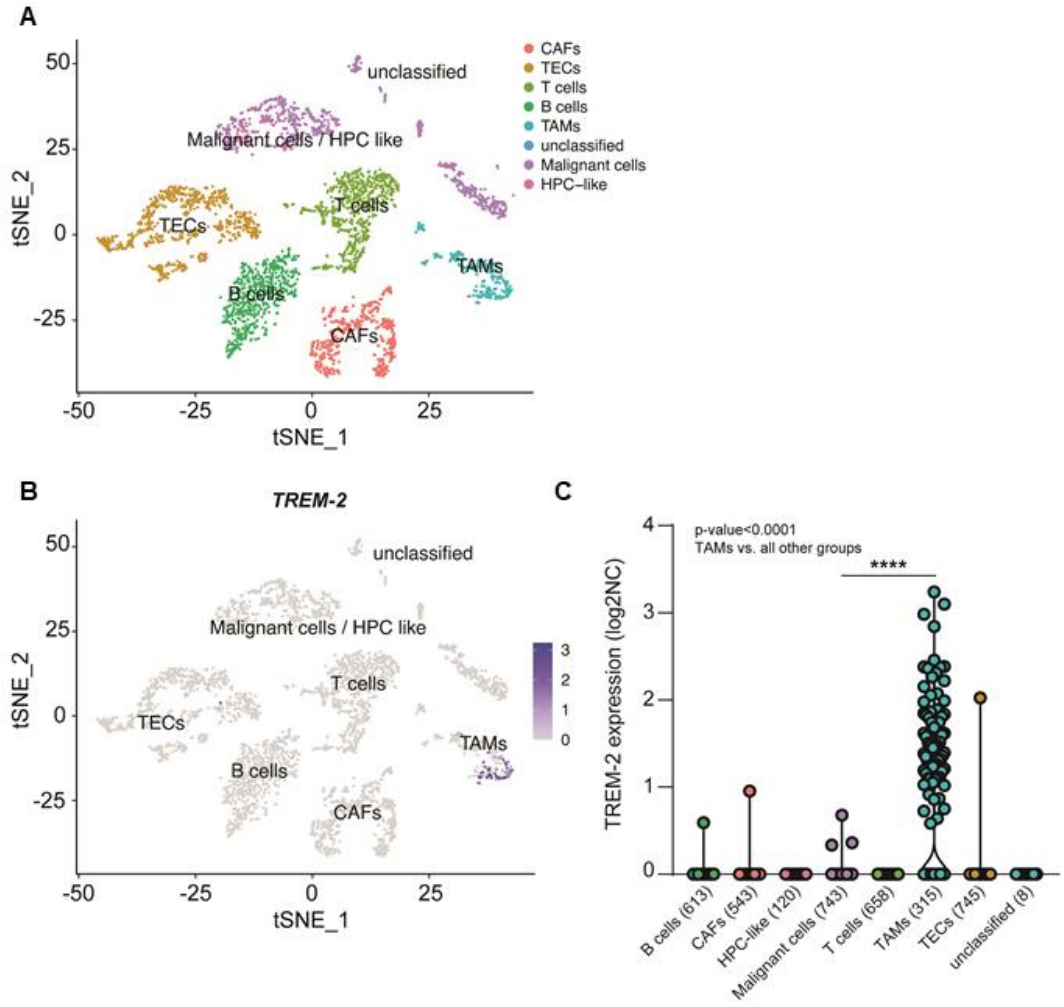

E.27. Irudia. *TREM2*-ren adierazpena HCC tumoreen zelula pupulazio desberdinetan. HCC tumoreen (n=9) publikoki eskuragarri dauden scRNAseq datuak erabili ziren *TREM2*-ren adierazpena aztertzeko. (**A**) t-SNE proiekzioak giza HCC tumoreen osagai zelularrak erakutsiz. Profil transkriptomiko antzekoak partekatzen dituzten zelulak koloreka taldekatuta daude eta jatorri zelularraren markatzaile espezifikoak erabiliz anotatu ziren. (**B**) *TREM2*-ren adierazpena TAMs-etan erakusten duen t-SNE proiekzioa. (**C**) *TREM2*-ren adierazpena tumorean aurkitzen diren zelula mota desberdinetan, Log2 normalizatutako kontaketak eran azalduta. Parentesi artean talde bakoitzeko analizatu zen zelula kopurua ageri da. (**C**) ANOVA test parametrikoa eta Tukey-ren post hoc testa erabili ziren, **** *p* balorea < 0.0001 adierazten du. CAFs, cancer associated fibroblasts; HPC-like, hepatic progenitor cell-like; TAMs, tumour associated macropghages; TECs, tumour associated endothelial cells; TREM2, triggering receptor expressed on myeloid cells; tSNE_2, t-distributed Stochastic Neighbor Embedding.

Identifikatuta talde bakoitza zelula mota zehatz batekin anotatu zen jatorri zelularraren markatzaileen adierazpenaren aberastasunaren aztertuz. Honela, T zeluletan CD3D eta CD2 hartzaile konplexuak aurkitu ziren, B zeluletan B zeluletako hartzailearen (BCR) osagaiak diren CD79A eta Fc receptor like 5 (FCRL5), TECs-ak von Willebrand factor (VWF) eta cadherin 5 (CDH5) faktore endotelialen adierazpenean aberastuta daude. TAMs taldea, aldiz, makrofagoen markatzaile diren CD163 eta CSFR1 adierazten dituzte, eta azkenik, CAFs-ak COL3A1 eta decorin (DCN) markatzaileen adierazpena erakusten dute (**E.28. Irudia**). Bestalde, hepatozito malignoak/HCC zelula

progenitoreak, HPC bezalako zelulekin batera agertzen ziren eta ama-zelulen ezaugarriak dituzten hepatozito transformatuen markatzaileen adierazpena erakusten zuten, hauen artean, alpha-fetoproteina (AFP), albumina (ALB), CD24 (cluster of differentiation 24), zitokeratina 19 (KRT19) eta SOX9 (SRY-box transcription factor 9) (**E.29. Irudia**).

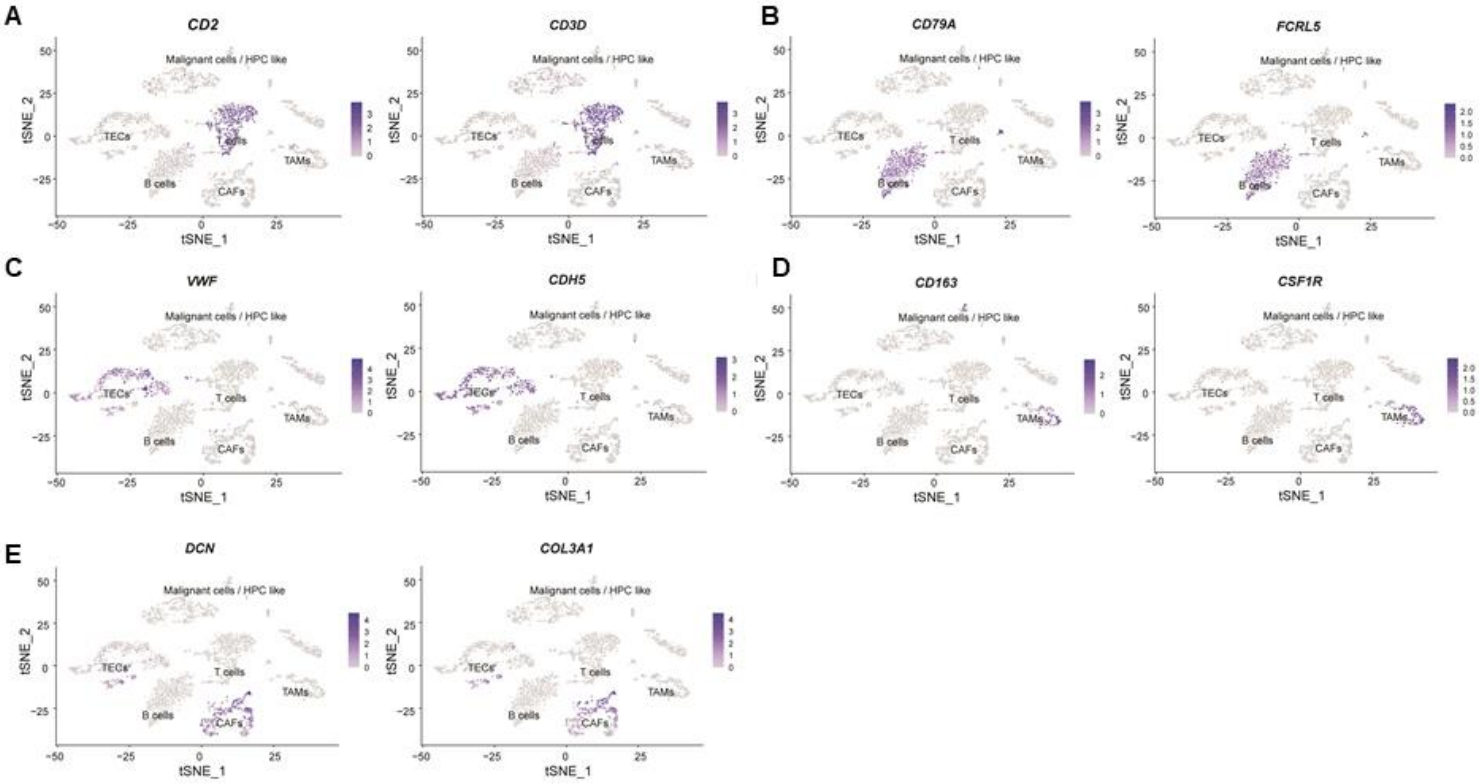

E.28. Irudia. Jatorri zelularraren markatzaileek scRNAseq datuen anotazioa ahalbidetzen dute. (**A**) T zeluletan, zelula hauetan hartzaile konplexuko osagaiak aurkitzen dira CD2 eta CD3D, besteak beste. (**B**) B zelulak BCR-aren seinaleztapenaren osagai diren CD79A eta FCRL5 adierazten dituzte. (**C**) TECs-ak markatzaile endotelialak diren VWF and CDH5-ren adierazpenean aberastuta daude. (**D**) TAMs-ek CD163 eta CSFR1 makrofagoen markatzaileen adierazpena aurkezten dute. (**E**) CAFs-ek COL3A1 eta DCN markatzaileen adierazpena dute. CAFs, cancer associated fibroblasts; CD, Cluster of Differentiation; CDH5, Cadherin 5; ; COL3A1, Collagen Type III Alpha 1 Chain; CSFR1, Colony Stimulating Factor 1 Receptor; DCN, Decorin; FCRL5, Fc Receptor Like 5; VWF, von Willebrand factor; TAMs, tumour-associated macrophages; TECs, tumour-associated endothelial cells; t-SNE_2, t-distributed Stochastic Neighbor Embedding.

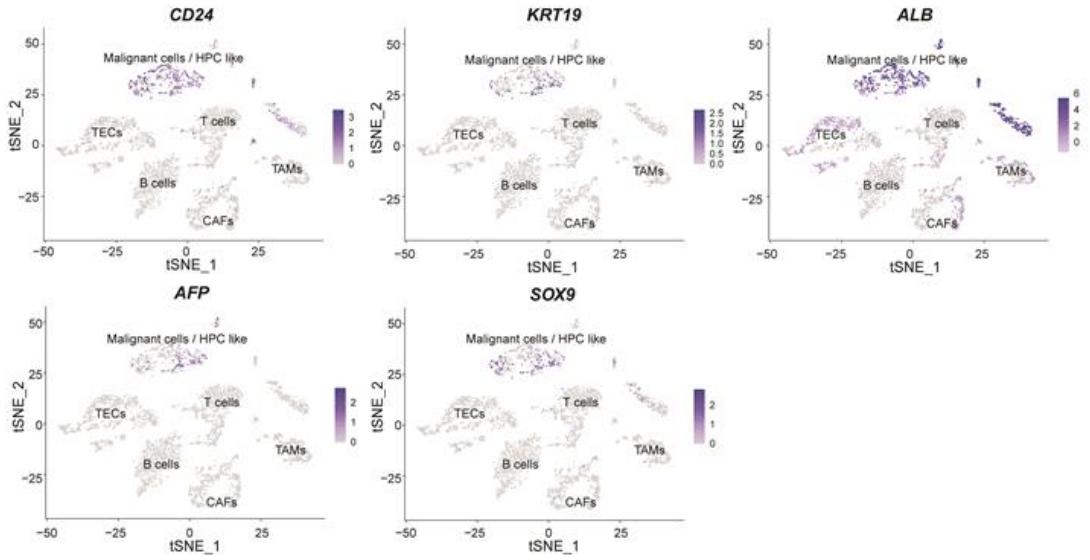

E.29. Irudia. Zelula maligno/HCC progenitoreen t-SNE taldea eraldatutako hepatozitoen markatzaileen adierazpenean aberastuta dago. Eraldatutako hepatozitoek adieraztu ohi dituzten markatzailetan aberastuta dago zelula talde hau, zehatz esanda, *AFP*, *ALB*, *CD24*, *KRT19* eta *SOX9* adierazten dituzte. *AFP*, Alpha-Feto protein; *ALB*, Albumin; *CD24*, CD24 molecule, *KRT19*; Keratin 19; *SOX9*, SRY-Box Transcription Factor 9; t-SNE_2, t-distributed Stochastic Neighbor Embedding.

Are gehiago, hurrengo urratsean TAMs-en taldea zehatzago aztertu genuen, talde honetako zelulak gehiago banatuz, honela, TAMs-en 5 azpi-populazio desberdin aurkitu genituen. Hauen artean, *TREM2*-ren adierazpena 1 eta 2 taldeetan zen nabarmenen (**E.30A Irudia**). Talde hauek ere KCs markatzaile den *CD68*-ren eta moozitoen markatzaile den *CD14*-ren adierazpena aurkezten zuten. Azpimarragarria da 1 eta 2 talde hauek ere *CD9*-ren adierazpena ezaugarri zutela (**E.30B Irudia**). Hau berriki argitaratutako ikerlan batekin bat dator, honetan fibrosiarekin lotzen diren eta $TREM2^{+}CD9^{+}$ fenotipoa duten makrofagoak aurkitzen dira zirrosidun gibeletan (281). Azkenik, GSEA analisiak burutu genituen, *TREM2* adierazten duten TAMs-en azpi-populazioetan. Hauek TLRs-en seinaleztapenaren eta lisosomarekin lotutako bidezidorretako geneen adierazpenean aberastuta daude (**E.30C Irudia**).

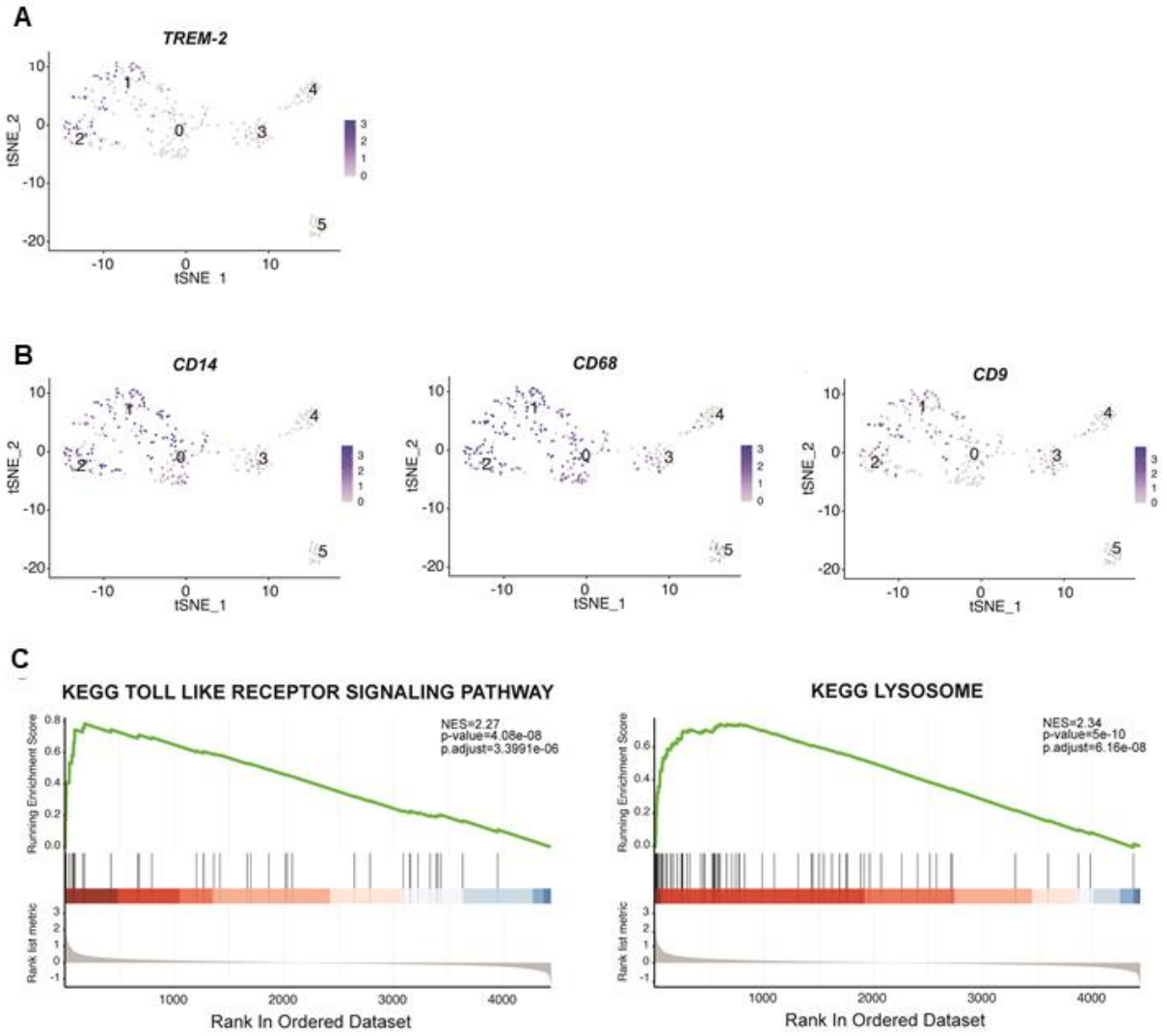

E.30. Irudia. TAMs-en taldekatzea eta ezaugarriak. (**A,B**) t-SNE proiekzioak TAMs-en bir-taldekatzea eta gero (**A**) *TREM2* eta (**B**) *CD14*, *CD68* eta *CD9*-ren adierazpena azalduz. (**C**) GSEA proekzioak TLRs-en seinaleztapena eta lisosomekin lotutako bidezidorren aberastasuna azalduz TREM2 adierazten duten TAMs-etan. y ardatzean aberastasunaren puntuazioa agertzen da eta x ardatzeko marra beltz bertikalek bidezidor bakoitzarekin lotutako geneak ordenatutako geneen zerrendan non agertzen den adierazten dute. Koloretako marrak ES baloreak adierazten ditu (gorria positivo eta urdina negativo). CD, cluster of differentiation; KEGG, Kyoto encyclopedia of genes and genomes; t-SNE_2, t-distributed Stochastic Neighbor Embedding.

E.9. TREM2-k paper babeslea betetzen du fibrosiarekin lotutako kartzinogenesian

TREM2-k kolestasi kronikoaren progresioan dituen efektu babesleen inguruko gure hipotesia indartzeko, eta hartzaile honek fibrosiarekin lotutako gibeleko kartzinogenesian izan lezakeen efektuak aztertzeko, fibrosiarekin lotutako gibeleko kartzinogenesiaren bi sagu eredu garatu genituen.

E.9.1. DEN+ CCl_4-aren administrazioan oinarritutako sagu eredu batean, *Trem2*$^{-/-}$ saguek kartzinogenesi areagotua agertzen dute

CCl_4-ak gibeleko fibrosia eragiten du eta maiz, DEN-aren administrazioarekin konbinatzen da fibrosiarekin lotutako HCC-a aztertzeko (300). Honela, WT eta *Trem2*$^{-/-}$ saguetan, DEN kronikoa, asteroko CCl_4-aren ziztadekin konbinatu genuen, fibrosiarekin lotutako HCC-aren sagu eredua burutzeko (**E.31A Irudia**). DEN gehi CCl4-aren administrazioaren eraginez, tamaina txikiko (≤ 2mm) tumore gehiago behatu genituen *Trem2*$^{-/-}$ saguen gibeletan WT saguekin konparatuz, DEN-aren administraziotik 30 asteetara, tamaina handiagoko tumoreen kasuan ez zen desberdintasunik behatu (**E.31B Irudia**). Gibeleko fibrosia Sirius red tindaketaren bidez aztertu genuen eta, *Trem2*$^{-/-}$ saguetan tumorigenesiaren emendioa detektatu genuen arren, animalia hauek gibeleko fibrosi gutxiago agertzen zuten (**E.31C Irudia**). Gainera, DEN+CCl4 tratamendua eta gero, zelulen proliferazioaren markatzaile den *Pcna*-ren mRNA maila altuagoa zen *Trem2*$^{-/-}$ saguen gibeletan WT saguen gibelekin konparatuz (**E.31D Irudia**).

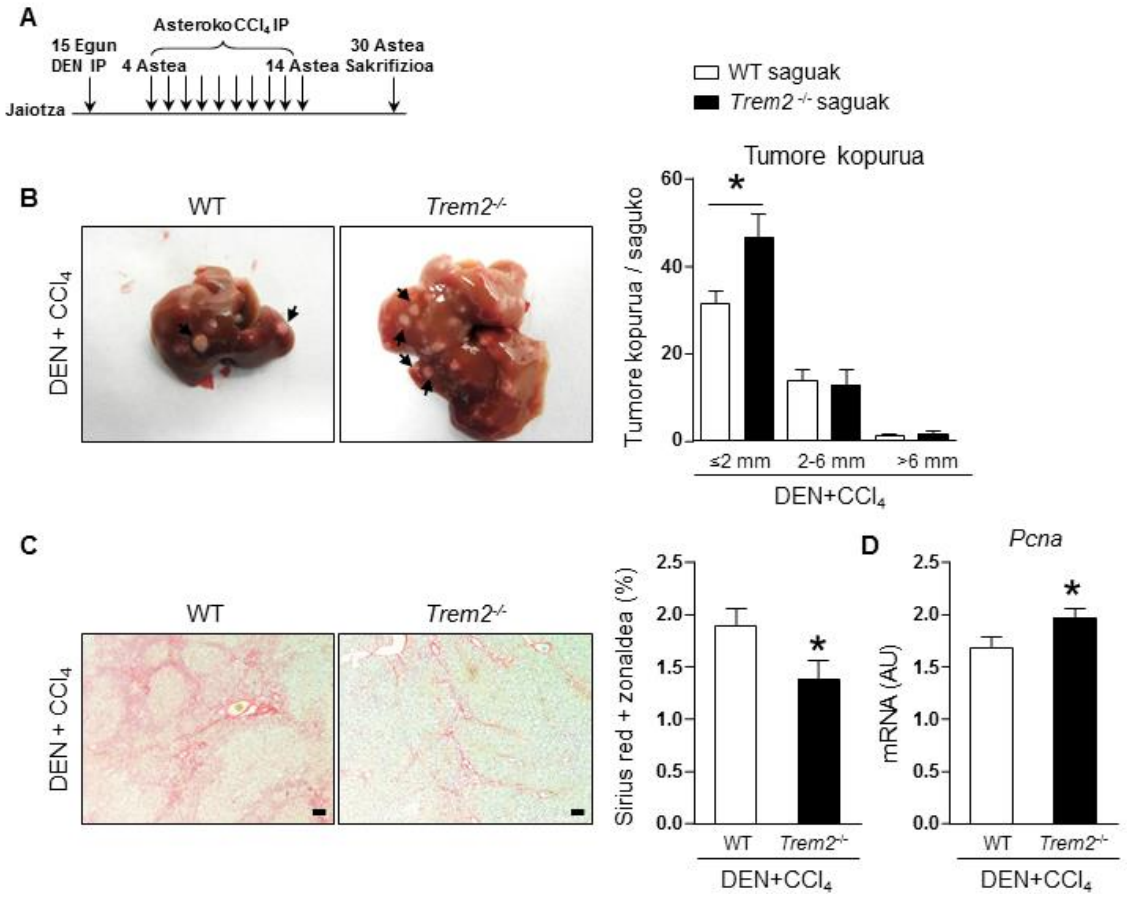

E.31. Irudia. WT eta *Trem2*$^{-/-}$ saguetan fibrosiarekin lotutako hepatokartzinogenesia DEN gehi CCl_4 sagu ereduan. (**A**) WT eta *Trem2*$^{-/-}$ saguei DEN ziztatu zitzaiden jaiotzetik 15 egunetara 30mg/kg-ko dosian, ondoren, asteroko 10 CCl_4 ziztada egin zitzaizkien eta saguak DEN ziztadatik 30 asteetara sakrifikatu ziren (WT n=13;*Trem2*$^{-/-}$ n=14). (**B**) Gibeleko tumoreen kopurua tamainaren arabera sailkatuta, gibelen irudi adierazgarriak eta tumoreen kuantifikazioak aurkezten dira. (**C**) Sirius red tindaketa, irudi adierazgarriak eta kuantifikazioak aurkezten dira. (**D**) *Pcna* mRNA adierazpena gibelean. (**C**) Eskalaren marrak 100 µm adierazten ditu. (**A**) Student-en *t*-test parametrikoa eta Mann Whitney-ren test ez-parametrikoa erabili ziren. (**B,C**) Student-en *t*-test parametrikoa erabili zen. * *p* balorea <0.05 adierazten du. AU, arbitrary units; CCl4 carbon tetrachloride; DEN, diehylnitrosamine; IP, intraperitoneal; *Pcna*, proliferating cell nuclear antigen*; Trem2*, Triggering receptor expressed on myeloid cells; WT, wild type.

E.9.2. TAA-aren administrazioan oinarritutako sagu eredu batean, *Trem2*$^{-/-}$ saguek kartzinogenesi areagotua agertzen dute

Fibrosiarekin lotutako HCC-aren eredu gehigarri bezala, WT eta *Trem2*$^{-/-}$ saguak thioazetamida (TAA)-rekin tratatu genituen, TAA edateko uretan disolbatu zen eta tratamendua 40 astez luzatu zen (302) (**E.32A Irudia**). *Trem2*-rik gabeko animalien gibeletan tumoreek betetzen zuten bolumenaren emendio bat behatu zen WT aniamaliekin alderatuz (**E.32B Irudia**). Era berean, DEN+CCl_4 sagu ereduan bezala, TAA-an oinarritutakoan ere, WT saguekin alderatuz gero, *Trem2*$^{-/-}$ saguek gibeleko

fibrosiaren murrizpena (**E.32C Irudia**) eta *Pcna*-ren mRNA adierazpenaren emendioa agertzen zuten (**E.32D Irudia**).

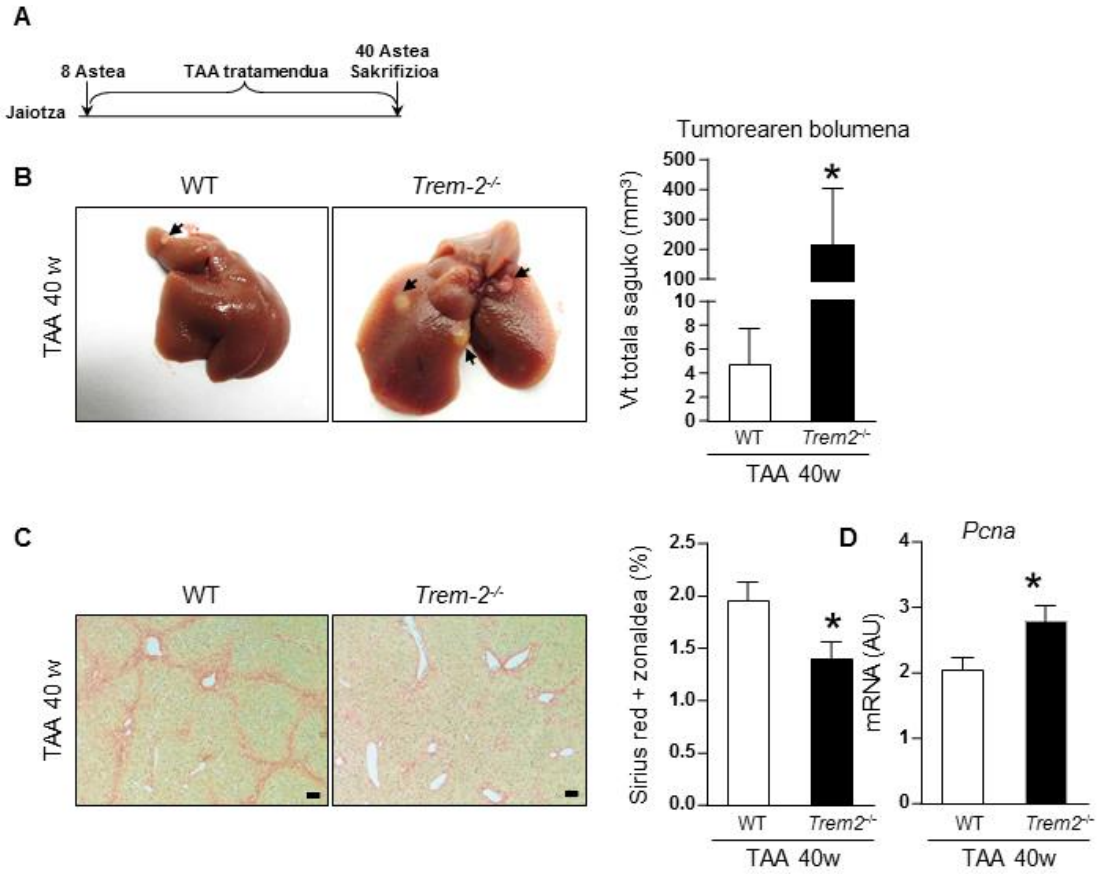

E.32. Irudia. WT eta *Trem2*$^{-/-}$ saguetan fibrosiarekin lotutako hepatokartzinogenesia TAA sagu ereduan. (**A**) WT eta *Trem2*$^{-/-}$ saguak edateko uretan disolbatutako TAA-z tratatu ziren 40 astez (WT n=9; *Trem2*$^{-/-}$ n=9). (**B**) Gibeleko tumoreek hartzen zuren bolumena, gibelen irudi adierazgarriak eta tumoreen kuantifikazioak aurkezten dira. (**C**) Sirius red tindaketa, irudi adierazgarriak eta kuantifikazioak aurkezten dira. (**D**) *Pcna* mRNA adierazpena gibelean. (**C**) Eskalaren marrak 100 µm adierazten ditu. (**A**) Mann Whitney-ren test ez-parametrikoa erabili zen. (**B,C**) Student-en *t*-test parametrikoa erabili zen. * *p* balorea <0.05 adierazten du. AU, arbitrary units; *Pcna*, proliferating cell nuclear antigen; TAA, thioacetamide; *Trem2*, triggering receptor expressed on myeloid cells; WT, wild-type.

Era batera, sagu eredu desberdinetatik eratorritako datu hauek guztiek aditzera ematen dute TREM2-k gaixotasun kolestatiko kronikoen garapenetik eta fibrosiarekin lotutako hepatokartzinogenesitik babesten duela gibela.

EZTABAIDA

Kolestasia kolangiopatia desberdinek amankomunean duten ezaugarri patologikoa da, kolangiopatia hauen artean, PBC eta PSC daude, hauek, helduetan ematen diren gaixotasun kolestasiko kroniko ohikoenak dira (74). Kolestasi kronikoa hainbat etapetan zehar garatzen da, hauen artean, inflamazioa, erreakzio duktularra, fibrosia, zirrosia, eta kasu batzuetan gibeleko zein behazun zuhaitzeko minbiziaren garapenean ere buka daiteke (312). Inflamazioak berebiziko garrantzia du garapen honetan eta zelulen arteko komunikazioa zuzentzen du, hortaz, zauri-sendatze prozesu akastuna eta, ondorioz, gaixotasunaren garapena bultzatzen ditu (136). Gaixotasun kolestasikoak erantzun egokirik gabeko erronka dira osasun arloan, izan ere, gaixo hauentzako estrategia terapeutikoak mugatuak dira eta, kasu askotan, gaixotasunak aurrera egiten du, gibeleko transplantea sendatzeko aukera bakarra den egoeretara (181). Era berean, hepatokartzinogenesia, gibeleko gaixotasun kronikoen garapenaren azken urrats bezala gibel zirrotikoetan garatzen dena, osasun erronka bat da. Izan ere, tumore mota honen heterogenizitate handiak eta bere izaera kimioerresistenteak, bere tratamendua zailtzen dute (192). Hori dela eta, kolestasi kronikoaren eta hepatokartzinogenesiaren garapena zuzentzen duten mekanismo molekularrak aztertzen dituzten ikerlanen beharra dago, hauen bidez gaixotasun hauentzako itu terapeutiko berriak aurkituko direlakoan.

Kolestasiaren eta hepatokartzinogenesiaren fisiopatologian parte hartzen duten prozesuen artean, heste-gibel ardatza fenomeno garrantzitsutzat aitortu da azken urteotan (204, 205). Honela, hesteetatik gibelera translokatutako bakterietatik eratorritako produktuak KCs, HSCs-etan eta gibelera erakarritako sistema immuneko zeluletan adierazten diren TLR-etara lotzen dira eta hauetan gene inflamatorioen transkripzioa areagotzen dute (217). Heste-gibel ardatzaren gainean estrategia desberdinen bidez eragiteak efektu onuragarriak dakartza gibeleko kaltearen hainbat testuingurutan (213, 232-234). Ildo honetan, TREM hartzaileen familia TLR-bidezko seinaleztapenaren modulatzaile bezala deskribatu zen (235, 236). Oro har, TREM1-k TLR-bidezko seinaleztapena sustatzen du, TREM2-k TLR-aren seinaleztapenak eragindako gene inflamatorioen transkripzioa murrizten duen bitartean (235, 264, 265). Gure aurreko lanetan, TREM2 KCs, HSCs, eta gibelera erakarritako makrofagoetan adierazten dela deskribatu dugu, hauetan, hartzaile anti-inflamatorio baten papera betetzen du TREM2-k, gibela kalte akutu, zein kronikoaz eta hepatokartzinogenesiaz babestuz (288, 289). Datu hauek aintzat hartuta, ikerlan honen hipotesia da, TREM2-k erantzun inflamatorioak erregulatu ditzakeela kolestasiaren eta fibrosiarekin lotutako hepatokartzinogenesiaren testuinguruan, hortaz, hartzaile hau gaitz hauek pairatzen dituzten gaixoentzako itu terapeutiko berria izan liteke.

D.1. TREM2-ren adierazpena emendatuta dago giza kolestasian eta kolestasiaren sagu ereduetan

Lan honetan, TREM2-ren adierazpenaren emendioa erakutsi dugu kolestasidun pazienteen gibeleko laginetan, ehun kontrol osasuntsuarekin alderatuz. Joera hau, kolestasia era esperimentalean eragindako sagu ereduen gibelean ere behatu zen. Guk dakigula, hau da giza eta sagu ereduen kolestasian TREM2-ren adierazpena aztertzen duen lehengo ikerlana. Gure emaitzak aurretik argitaratutako lanekin bat datoz, zeinetan, gibeleko TREM2-ren adierazpenaren emendioa behatzen den inflamazioarekin lotutako jatorri anitzetako gaixotasun hepatozelularretan, eta hauen sagu-ereduetan (288, 289). Halaber, gure emaitzaten ikusi daitekeen moduan, *TREM2* mRNA mailak kolestasidun pazienteen gibeletan beste jatorrietatik eratorritako zirrosidun pazienteetan baino altuagoak dira.

Aurretik argitaratu dugu *TREM2*-ren adierazpenak gaixotasunaren garapenarekin korrelazionatzen duela, hain zuzen ere, *TREM2*-ren gibeleko adierazpenak serumeko transaminasen mailarekin, gibeleko inflamazioarein eta fibrosiarekin korrelazionatzen du (288, 289). Ikerlan honetan kontzeptu hau kolestasian ere betetzen dela baieztatu dugu. Honela, *TREM2*-ren adierazpenak gaixotasun kolestastikoen garapenaren hainbat markatzailerekin korrelazionatzen du gaixoen bi talde desberdinetan. Honela, San Sebastian/Waraw gaixoen taldean, kolestasidun pazienteek (PBC zein PSC) serumeko transaminasen, AP-aren eta bilirrubinaren balio altuak dituzte beste jatorriko zirrosidun gaixoekin konparatuz. Hau gaixotasunaren etapa aurreratuago baten erakusle izan liteke, eta, era berean, beste jatorrietako zirrosidun gaixoekin alderatuz, PBC eta PSC-dun pazienteen gibelean behatu ditugun TREM2-ren adierazpen maila altuagoak azaldu ditzake. Are gehiago, GSE79850 gaixoen taldean, TREM2-ren adierazpena bereziki emendatuta dago arrisku-altuko PBC-dun pazienteen gibelean arrisku-txikiko gaixoekin eta kontrol lagin osasuntsuekin alderatuz. Arrisku handiko PBC-dun gaixoek gaixotasunaren fenotipo aurreratuagoa erakusten dute diagnostikoaren momentuan. Era berean, gaixo hauetan T zelulen aktibazioarekin eta apoptosiarekin, INF-γ seinaleztapenarekin eta leukozioen migrazioarekin lotutako geneen adierazpen maila altuagoa da arrisku txikiko PBC-dun gaixoekin konparatuz (290). Datu hauek aditzera ematen dutenez, TREM2-ren adierazpena gaixotasunaren fenotipo aurreratuago batean emendatzen da, eta hartzaile honen adierazpena gaixoatasunaren garapenaren erakusle izan liteke. Are gehiago, TREM2-ren adierazpena gehiago emendatzen da gaixotasunaren progresioarekin, hori del eta, gure hipotesia da TREM2-ren adierazpena

sustatzen dela mekanismo konpensatorio bat bezala, gaixotasunaren etapa aurreratuetan ematen den gehiegizko inflamazioa geldiarazteko ahaleginean.

Lehenago aipatu bezala, *TREM2* genearen gainadierazpena jatorri desberdinetako gaixotasun kolestatikoetan, hau da PBC eta PSC-an, PBC-ren bi gaixo-talde desberdinetan, eta buxadurazko (BDL model) zein kimikoki eragindako (ANIT and DDC models) kolestasi esperimentalean ere behatu genuen. Hori dela eta, *TREM2*-ren gainadierazpeana kolestasian ematen den fenomeno orokorra dela esan genezake. PBC eta PSC-ren jatorria ezezaguna bada ere, biak lotzen dira sistema inmune innato zein adaptatiboko bidezidorren eraldaketekin (81, 91). Ildo honetan, berriki argitaratutako lan batean PBC, PSC eta BA gaixotasun pediatrikoak partekatzen dituzten eraldaketa genetikoen eta ehuneko adierazpen mailen aldaketen azterketa egin zuten, eta honela, gaixotasun hauen konektoma aurkezten dute. Lan honetan, inflamazio edota immunitatearekin lotutako hainbat generen garrantzia azpimarratzen da, hauen artean, TNF, IL10, FOXP3 (forkhead box P3), TGFB1, IL2, IL17A, NFKB1, STAT3 (Signal transducer and activator of transcription 3), TP53, SMAD3, HIF1A (hypoxia inducible factor 1 A), PTGS2 (prostaglandin-endoperoxide synthase 2) IL6 eta TLR4, hiru kolangiopatiek amankomunean dituzten geneen artean nabarmentzen dira (313). Aurretik aipatu bezala, TREM2 hartzaileak TLR-bidezko seinaleztapena modulatzen du (242) eta, zehazki, gene hauetako batzuen adierazpena, IL6 eta TNF, esaterako, erregulatzen duela ikusi da, hemen eta gure taldearen aurreko lanetan ere (288, 289). Hortaz, datu hauek iradokitzen dute TREM2-ren azterketa interesgarria izan litekeela, behintzat PBC eta PSC gaixotasunen konektoman entidade bereizgarri berri bat bezala.

Saguetatik isolatutako zeluletan *Trem2*-ren adierazpena KCs eta HSCs-etan nabarmenki altuagoa dela behatu dugu hepatozito eta kolangiozitoekin alderatuz. Datu hauek aldez aurretik aurkeztutako datuekin bat datoz, zeinetan TREM2-ren adierazpena gibeleko zelula ez-parenkimaletara mugatzen dela behatu den (253, 279, 288, 289). Kolestasi kronikoa inflamazio iraunkorraz lagunduta dago eta bere ezaugarrietako bat da sistema immuneko zelulen erakarpena eta KC eta HSC-en aktibazio eta hazkuntza (131). Hortaz, TREM2-ren adierazpenaren emendioa eta honek gaixotasunaren garapenaren markatzaileekin agertzen duen korrelazioa bi mekanismo paraleloen bidez azaldu liteke. Alde batetik, gibeleko kaltearen ondorioz, zelula mota hauen erakarpen eta hazkuntza ematen da, hau TREM2-ren adierazpearen emendioaren atzean egon liteke. Bestalde, KC-en, HSC-en eta monozitoetatik eratorritako makrofagoen aktibazioaren ondorioz, TREM2-ren adierazpena mekanismo konpentsatorio bat bezala emendatu liteke, zelula

hauen aktibazio iraunkorra dela eta emaen den gene inflamatorioen gehiegizko transkripzioa geldiarazteko ahaleginean.

Lan honen emaitzen esanahia mugatu dezakeen ezaugarrietako bat da, gaixoetan egindako analisietan erabili den laginaren tamaina txikia, bereziki, kolestasidun gaixoen taldeetan. Kolestasidun gaixoen gibel laginak lortzeko zailtasuna, gaixotasun hauen diagnostikorako biopsiaren erabileraren murrizketa dela eta azaltzen da, izan ere, egun, gaixotasun hauen diagnostikoa serumeko markatzaileen eta gibelaren irudi tekniken bidez burutzen da (77, 92) Hala ere, gure emaitzak bi gaixo-talde independenteetan baieztatzen dira, eta kolestasiaren sagu ereduetan ere behatzen dira, honela, TREM2-ren gainadierazpena kolestasian gertatzen den fenomeno orokor eta kontserbatuta dela dirudi.

Zelula bakarreko RNA sekuentziazio teknikek gibeleko gaixoatasun kronikoen garapenean paper garrantzitsua betetzen duen zelulen azpi-populazioak identifikatu dituzte. Ildo honetan, berriki argitaratutako zelula bakarrreko RNA sekuentziazioko analisiek TREM2 adierazten duten makrofagoen azpipoluzioak identifikatu dituzte, obesitatea (278), NAFLD (280) eta zirrosia (281) duten gaixoetan. Gure datuek erakusten dute TREM2-ren gainadierazpena fenomeno garrantzitsua dela kolestasian, hala ere, PBC eta PSC-dun pazienteen gibel laginak lortzeko zailtasunak eta teknika aurreratuen gabezia dela eta, ikerlan honetan ezin izan ditugu TREM2 adierazten duten sistema immuneko azpi-populazio zehatzak aztertu. Era honetako azterketek berebiziko garrantzia izan lezakete gaixotasun kolestasikoen testuinguruan, hauetan sistema immune innato zein adaptatiboak paper garrantzitsua betetzen baitute, eta hipotetikoki, azterketa hauen bidez, kolestasiarekin lotutako eta TREM2 adierazten duten zelula talde berriak aurki litezke.

D.2. TREM2-k gibela babesten du kolestasiaren garapenaz

Gure emaitzek azaleratzen dutenez, TREM2-ren adierazpena emendatuta dago gaixotasun kolestatikoak dituzten gaixoen gibelean eta fenomeno hau saguetan ere ikusten da, *Trem2*-ren adierazpena emendatzen baita jatorri desberdinetako kolestasiaren sagu ereduen gibeletan ere. Emaitza hauek TREM2-k kolestasiaren garapenean betetzen duen papera aztertzera bultzatu gintuzten.

Lan honetan behatutako emaitzen arabera, TREM2-k inflamazioaren erregulatzaile bezala jokatzen du jatorri desberdinetako gaixotasun kolesetatikoetan. Hemen, TREM2-

ren papera kolestasiaren bi sagu eredu desberdinetan aztertu dugu, hain zuzen ere, BDL ebakuntza eta ANIT tratamendua eta gero. BDL-a buxadurazko kolestasiaren sagu eredua da, behazun hodien buxadura, erreakzio duktularra eta fibrosi biliarra ezaugarri dituena (293). ANIT-aren tratamenduak kolangiozitoen galera larria dakar, nagusiki gibel barneko kolangiozitoei eragiten diena, honela PBC-ren ezaugarri batzuekin antzekotasuna du sagu eredu honek (296). Beraz, emaitza hauek, TREM2-en bidezko babesa kolestasian, kolestasiaren etiologia edozein izanik ere, fenomeno orokor bat izatearen hipotesia indartzen dute. Sagu eredu hauetan, *Trem2*$^{-/-}$ saguetan kolestasiarekiko gehiegizko erantzuna behatzen da, BDL zein ANIT-aren testuinguruan. Bi sagu ereduek aurkeztutako fenotipoek zenbait ezaugarrietan bat egiten dute, ezaugarri bereizgarri batzuk ere aurkezten dituzten bitartean.

Hemen aurkeztutako ANIT-ean oinarritutako sagu-ereduak muga batzuk azaltzen ditu. Honela, ANIT-aren tratamenduak, lan honetan aukeratutako dosian, ez zuen eraginik izan gibeleko kalte eta inflamazioaren markatzaile gehienetan WT saguetan. Hauetan bakarrik *Ck19* eta *Ck7* behazun zuhaitzeko markatzaileen, *Hmox* eta *Nos2* estres oxidatiboko markatzaileen eta *Acta2*, HSCs-en aktibazioko markatzaileen emendioa edo emendiorako joera nabarmena ikusten da ANIT-aren eraginez. Gainerako markatzaileen adierazpena, ordea, ez zen aldatu ANIT-aren ondorioz O.Oil-az tratatutako saguekin alderatuz. Eztabaida dago ANIT-aren tratamenduan oinarritutako sagu-eredua burutzerakoan, honela, argitaratutako lanetan ANIT-a 50mg/kg eta 100mg/kg dosien artean erabiltzen da (295, 296, 314-316). Lan honetan, behazun zuhaitzeko kaltea sortzen duen dosirik txikiena (50mg/kg) erabili genuen, izan ere, *Trem2*$^{-/-}$ saguetan fenotipo okerragoa behatzea espero genuen eta ez genituen sagu eredua gainasetu eta WT eta *Trem2*$^{-/-}$ saguen artean egon zitezkeen desberdintasunak galdu nahi.

BDL eta ANIT sagu ereduen fenotipoetan aurkitutako antzekotasunen artean, zelula epitelialen heriotzaren emendioa behatzen da *Trem2*$^{-/-}$ saguen gibelean WT saguekin alderatuz bi sagu ereduetan. Honekin batera, nekroptosiaren marktzaileen emendioa ere ikusten da, apoptosiaren marktzailean desberdintasunik ikusten ez den bitartean, BDL sagu ereduan. ANIT sagu ereduaren kasuan, serumeko gibel kaltearen markatzaileen maila ere altuagoa zen *Trem2*$^{-/-}$ saguetan WT saguekin alderatuz. Aurkikuntza hauekin bat eginez, PBC-dun gaixoetan eta BDL-an oinarritutako segu ereduetan, zelula heriotza eragiten duen mekanismo nagusia nekroptosia dela ikusi da (317, 318). Are gehiago, RIP3-k, nekroptosiaren bitartekari molekular nagusiak, kolestasi bidezko gibel kaltea eragiten du saguetan (317, 319). TNF-ak zelularen nekroptosi bidezko heriotzaren eragile bezala joka dezake (320), eta hau gainadierazita dago *Trem2*$^{-/-}$ saguen gibelean

BDL-a eta ANIT-aren eraginez WT saguekin alderatuz. Hala ere, DEN-ak eragindako hepatokartzinogenesiaren fase akutuetan ere *Tnf*-ren gainadierazpena behatu genuen *Trem2*$^{-/-}$ saguetan, DEN-ak eragindako epe luzeko hepatokartzinogenesiaren ereduan, aldiz, ez genuen nekroptosiaren markatzaileen adierazpenean desberdintasunik behatu (289). Aipagarria da, kolangiozitoak nekroptosiaren bidezko zelularen heriotzari sentikorragoak direla, RIP3-ren adierazpen maila altuagoak aurkezten baitituzte (321), honek iradokitzen duenez, zelularen nekroptosi bidezko heriotzaren marktzaileen emendioa kolangiozitoen heriotzatik erator liteke.

BAs-ek berebiziko garrantzia hartzen dute gaixotasun kolestatikoen garapenean. Ildo honetan, gibel barneko BA-en metaketak efektu zitotoxiko zuzeneak eragin ditzake gibeleko zelula epitelialetan (119), era berean, BA-en gibel barneko metaketak erantzun inflamatorioak piztu eta areagotu ditzakete (117). Testuinguru honetan, gure datuek azaleratzen dute sham ebakuntza jasandako saguetan, *Trem2*$^{-/-}$ saguen gibelean BA-en kontzentrazioa baxuagoa dela WT saguekin alderatuz. Emaitza hauekin batera, *Cyp7a1* BA-en sintesiaz arduratzen den entzimaren eta *Fxr*, honen inhibitzaile nagusiaren adierazpenaren beheranzko joera nabarmena behatu genuen. Honela, datu hauen arabera, *Trem2*$^{-/-}$ saguek BA-en maila bajuak mantentzeko mekanismoa garatu dutela dirudi. BDL-ak eragiten duen BA-en kontzentrazioaren emendio nabarmenak mekanismo hau gaindituko luke, honela, BDL-aren ondoren BA-en kontzentrazioa konparagarria da WT eta *Trem2*$^{-/-}$ saguetan. Hala ere, BDL-aren ondoriozko BA-en kontzentrazioaren emendioa nabarmenagoa *Trem2*$^{-/-}$ saguetan WT saguekin alderatuz. Hau aurreko atalean azaldutako, *Trem2*$^{-/-}$ saguen gibelean behatu den zelularen heriotzaren emendioarekin bat dator, *Trem2*$^{-/-}$ saguak BA-en bidezko heriotz zelularrarekiko sentikorragoak direla iradokiz.

Berez, TREM2 eta hartzaile nuklearren arteko lotura aurretik proposatu izan da, *Trem2*-rik gabeko mikrogliak CE-en kontzentrazioaren emendioa aurkezten baitu, zeina LXR-ren agonista batekin deuseztatzen den (322). Are gehiago, hesteetan TLR-aren aktibitateak FXR-ren adierazpena erregulatzen duela ikusi da (323). Honela, TLR2,4,5 eta 6-ren aktibazioak FXR eta SHP-ren adierazpena murrizten dute, TLR3,7 eta 9-k, aldiz, FXR eta SHP-ren adierazpena emendatzen duten bitartean. Beraz, gure hipotesia da TREM2-k TLR-en bidezko seinaleztapenean eragiten dituen efektuak, FXR-ren adierazpen edota aktibitatean ere eragina izan ditzaketela. Honela, TREM2 eta BA-en arteko lotura molekularra eta honek gibeleko gaixotasunen garapenean bete lezakeen papera, oraindik argitzeke daude, eta ikerketarako aukera interesgarria dira.

BA-en gibel barneko metaketa zein zelularen heriotza erantzun inflamatorioen sustapenarekin lotzen dira. Zehazki, nekroptosia estuki lotuta dago inflamazioarekin (111), nekroptosiaz hildako zelulek jariatutako DAMPs-ek mikroingurune pro-inflamatorioan parte hartzen dute mekanismo autokrino eta parakrinoen bidez. Are gehiago, RIP3, nekroptosian parte hartzen duen proteina nagusietako batek, NF-κB aktibatu eta zuzenean erantzun inflamatorioak piztu ditzake (324). Aurretik azaldu bezala, gibel barneko BAs-en metaketak erantzun inflamatorioak piztu ditzake (117). Hori dela eta, BDL eta ANIT sagu ereduetan *Trem2*$^{-/-}$ saguetan behatu den zelularen heriotzaren emendioak eta BDL sagu ereduan, sham-etik BDL-ra behatu den BA-en kontzentrazioaren aldaketaren emendioak, erantzun inflamatorioekin lotu daitezke.

Honekin bat eginez, mikroingurune pro-inflamatorioa areagotuta dago BDL-aren zein ANIT-aren sagu ereduan *Trem2*$^{-/-}$ saguetan. Gainadierazitako bitartekari inflamatorioen artean gibeleko kaltean parte hartzen duten zitokina eta kemokina nagusiak aurkitzen ditugu, zehazki, *Il1β*, *Il6*, *Tnf*, *Il33 Mcp1* and *Cxcl*. Aurkikuntza hau gure ikerketa taldearen aurreko emaitzekin bat dator, non *Il6*, *Tnf*, *Mcp1* eta *Cxcl1*-ren adierazpenaren emendioa behatu den gibeleko kalte akutu zein kronikoaren, gibeleko birsortzearen eta hepatokartzinogenesiaren sagu ereduetan *Trem2*$^{-/-}$ saguetan WT saguekin alderatuz (288, 289). Beraz, emaitza guzti hauek aditzera ematen dute TREM2-k gibeleko inflamazioa geldiarazten duela, kaltea sustatu duen estimulua edozein izanik ere. Gainera, bitartekari inflamatorio hauek paper garrantzitsua betetzen dute giza gaixotasun kolestatikoen garapenean, baita hauen sagu ereduetan ere (325). Izan ere, bitartekari hauen adierazpena emendatuta dago PBC-dun (164, 326) eta PSC-dun gaixoetan (327, 342) eta DRCs-etatik eratorritako mikroingurune inflamatorioaren faktore gakoak dira (6). Are gehiago, IL6 eta TNF PBC, PSC eta BA gaixotasunen konektomaren gene garrantzitsuen artean daude (313). Ildo honetan, PBC-dun gaixoetatik eratorritako monozito periferikoek LPS-rekiko gehiegizko erantzuna aurkezten dute, beste batzuen artean, IL1β, IL6, IL8 eta TNF zitokinen maila altuagoak jariatzen baitituzte (328). Bestalde, IL33-k kolangiozitoen hazkuntza sustatzen du behazun hodietako kaltearen sagu ereduetan (329) eta gainadierazita dago PBC-dun pazienteen serumean (330). Halaber, IL8-ren adierazpena, zeina CXCL1-en homologotzat hartzen den bere funtzio gehienetan (331), emendatuta dago PSC-dun gaixoen behazunean eta kolangiozitoen hazkuntza sustatzen du *in vitro* (153). Beraz, TREM2-k zitokina eta kemokina hauen guztien adierazpena murrizten du, kolestasiak eragindako gibel kaltearen garapenean hartzaile honek paper babeslea bete lezakeela iradokiz.

Gure emaitzetan azaleratzen denez, bitartekari inflamatorioen adierazpenaren emendioa bakarrik neutrofiloen erakarpenean eragiten zuen, makrofagoen eta T linfozitoen erakarpenean, berriz, ez zen genotipoen arteko desberdintasunik behatu. Honela, aurretik deskribatu izan da gibelaren kaltearen eraginez organo honetara erakartzen diren sistema immuneko zelula mota kaltearen eta gaixotasunaren testuinguruaren araberako dela (39). Gainera, neutrofiloek berebiziko garrantzia dute kolestasian, non zelula zitotoxiko nagusitzat hartzen diren (125-127). Era berean, CXCL1-CXCR2 ardatzak, zeinak neutrofiloen gibelerako erakarpena zuzentzen duen, kolestasian duen garrantziaren erakusle, *Cxcr2*$^{-/-}$ saguak BDL-aren bidezko gibeleko kalteaz babestuta daudela deskribatu da (332). Honela, TREM2-k biriketan neutrofiloen erakarpena zuzentzeko gai dela ikusi da (274). Gainera, azken aldian makrofagoen azpi-klaseen aniztasuna deskribatzen hasi da zelula bakarreko RNA sekuntziatzioko teknikei esker (333). BDL-aren ondorioz WT eta *Trem2*$^{-/-}$ saguen gibelean makrofagoen kopurua konparagarria izan arren, desberdintasuna gibelera erakarritako makrofagoen azpi-klaseetan ere egon daiteke. Izan ere, TREM2 adierazten duten eta obesitate (278), zirrosia (281) eta NAFLD-arekin (280) lotzen diren makrofagoen azpi-klaseak deskribatu dira azken urteotako lanetan. Lan honetan aurretik aipatu bezala, kolestasiarekin lotutako makrofago azpi-klase bereizgarriak aurkitzeko helburua duten ikerlanak interesgarriak izan daitezke zentzu honetan.

Gibel kaltearen ondorioz sortzen den zauri-sendatze prozesuan, organoaren birsortze erantzunak eta erantuzn fibrotikoak aktibatzen dira galdutako ehuna berreraikitzeko asmoz (111). Inflamazioak eta gehiegizko zelularen heriotzatik eratorritako produktuek hepatozito eta kolangiozitoen hazkuntza sustatzen dute (111). Honekin bat eginez, zelularen gehiegizko heriotza behatu genuen *Trem2*$^{-/-}$ saguetan kolestasiaren eraginez, gainera, sagu hauek behazun zuhaitzeko egituren hedapenaren emendioa aurkezten zuten WT saguekin alderatuz BDL-a eta gero, eta behazun hodietako markatzaileen adierazpenaren emendioa ANIT-a eta gero. TREM2-k kolestasiaren ondoriozko erantzun fibrogenikoetan bete lezakeen paperari dagokionez, HSCs-en aktibazioaren emendioa behatu zen *Trem2*$^{-/-}$ saguetan BDL-a eta gero, efektu hau bitartekari inflamatorioen maila altuagoekin lotzen da. Hala ere, Sirius red tindaketa bidez neurtutako gibeleko fibrosia, antzekoa da WT and *Trem2*$^{-/-}$ saguen artean BDL-a eta gero. Fenomeno hau, sagu eredua burutzeko aukeratutako denbora puntuarengatik azal liteke. Izan ere, BDL sagu ereduan ez da igoera nabarmenik behatzen gibeleko kolageno kantitatean BDL-tik 14 egunera arte (334, 335).

TREM2-k kolestasian dituen efektuen atzean egon litezkeen mekanismo molekularrei dagokienez, hesteetatik translokatutako bakterietatik eratorritako produktuak gibeleko kaltearen forma desberdinen garapenean bitartekari garrantzitsutzat hartzen dira. Kolestasian kontzeptu hau ezarrita dago jadanik (204) eta azken aldian indartzen jarraitzen da. Berriki, hesteetatik eratorritako produku bakterianoek hepatozitoak BA-en bidezko kaltearekiko sentikorrago egiten dituztela, eta kolestasiaren bidezko kaltea ezartzeko beharrezkoak direla ikusi da bi sagu eredutan (316). TREM2 TLR-aren bidezko seinaleztapenaren inhibitzaile bat da, ideia honekin bat eginez, antibiotikoen bidezko hesteen esterilizazioak, BDL-aren ondorioz WT eta *Trem2*$^{-/-}$ saguen arteko desberdintasunetako batzuk deuseztatzen ditu. Emaitza hauek gure aurreko lanetan behatutakoarekin bat datoz, non CCl_4-ren bidezko gibel kaltean TREM2-k dituen efektuak hesteetatik eratorritako PAMPs-en ondoriozkoak direla aurkezten zen (288). Hala eta guztiz ere, doktoretza tesi honetan aurkeztutako azterketan, azalekoa da WT eta *Trem2*$^{-/-}$ saguen arteko desberdintasunetako batzuk ez direla deuseztatzen antibiotikoen tratamenduari esker. Honek iradokitzen du TREM2-ren efektuak kolestasian, PAMP-ez gaineko TLR-en ligandoen loturaren ondorioz gerta litezkeela, hauen artean hildako zeluletatik eratorritako DAMPs-ak leudeke (111, 210). Bestalde, TREM2-k kolestasian dituen efektu babesleak TLR-en gaindiko, mekanismo independente baten bidezkoak ere izan litezke. Honela, TREM2-k neurona apoptotikoetan aurkitzen diren lipidoak detektatu (269) eta estimulu hauen ondorioz zelula barneko seinaleztapen mekanismoak pizteko gai dela deskribatu da (336). Hortaz, TREM2-k kolestasian erantzun inflamatorioak TLR-en independente den mekanismo baten bidez erregulatu ditzakeela iradokiz.

D.3. TREM2 UDCA-k zelula ez-parenkimaletan dituen efektuen bitartekari berri bezala

UDCA, BA koleretiko endogenoa, PBC-dun gaixoentzako lehenengo lerroko aukerako tratamendua da. PSC-aren tratamendurako, ez daude hain ongi zehaztuta UDCA-ren efektu onuragarriak eta, egun, ez dago adostasunik bere erabilerari dagokionez. Honela, EASL-ak bere erabilera onartzen du, AASLD-k, ordea, erabilera honen kontrako gomendioa egiten du (105). UDCA-ren efektuen artean, efektu anti-apoptotikoak, kolangiozitoen bikarbonatoaren jariapena eta efektu anti-inflamatorioak deskribatu izan dira, baina efektu hauek bideratzen dituzten mekanismo molekularrak aztertzeke daude oraindik (311). UDCA-az tratatutako gaixoen % 30 inguruk erantzun partziala aurkezten dute, honela, gibeleko gaixotasun larriagoak garatu eta gibeleko transplantearen beharra izateko arrisku handiagoa dute gaixo hauek (22). UDCA-ak

kolestasian eragiten dituen efektuen gaineko ikerketa sakonagoek arazo hau konpontzen lagunduko lukete, erantzun partziala aurkezten duten pazienteentzako aukera terapeutiko optimizatuak bilatzeko aukera emanez. KCs eta HSCs-ek, hots, gibeleko zelula ez-parenkimalek paper garrantzitsua betetzen dute gaixotasun kolestasikoen garapenean (131), hortaz, zelula mota hauek itu dituzten estrategia terapeutikoek askotariko efektu onuragarriak eragin litzakete gaixotasunaren garapenean.

Ildo honetan, oso gutxi ezagutzen da UDCA-k KC eta HSC-etan dituen efektu onuragarrien inguruan. Egun, UDCA-k gibeleko fibrosia murrizten duela ikusi da, hain zuzen ere, CCl_4-aren administrazioan oinarritutako sagu eredu batean. Efektu hau UDCA-k *in vitro* eragiten dituen aldaketekin lotzen da. Honela, LX2, HSC-en lerro zelular batean, UDCA-k TGFβ1-en efektuak kontrajartzen ditu, LX2-en aktibazioa murriztuz eta hauen heriotza eraginez (337). Era berean, UDCA-k fibrosian dituen efektuak mastozitoen aktibazioa modulatzeko duen gaitasunarekin lotzen dira (338). Are gehiago, UDCA eta lisofosfatidieletanolamidaren (UDCA-LPE) arteko konjokatuak LPS-ak eragindako zitokina pro-inflamatorioen ekoizpena murrizten du KC-etan, eta *in vivo*, galaktosamina eta LPS-aren administrazioan oinarritako gibeleko kaltearen sagu eredu batean. Gainera, UDCA-LPE-az tratatutako KC-en medioak fibrosia geldiarazten du HSC-etan (339). Halaber, UDCA-k hesteen mikrobiotatik eratorritako seinaleak erregulatu litzakeela dioten lanak argitaratu dira berriki. Ildo honetan, UDCA-k hesteetako mikrobiota *Bacteroidetes* anduietan aberasten duela ikusi da haurdunaldiko kolestasian, efektu hauek FGF15/19-FXR seinaleztapen ardatzaren emendioa, eta honek gibelean betetzen duen paper babeslearekin lotu dira (340). NAFLD-dun gaixekin egindako lan batean, UDCA-k mibrobioma eta bidezidor metabolikoak modulatzeko gai dela ikusi da gibelaren funtzioaren hobekuntza eraginez (341).

Lan honetan, UDCA-k zelula ez-parenkimalen biologian duen eraginaren inguruko mekanismo berri bat aurkeztu dugu. Gure emaitzen arabera, UDCA LPS-aren efektuak gainditzeko gai da KC-etan. Zehazki, UDCA-k *Trem1* hartzaile pro inflamatorioaren adierazpena murrizten du, *Trem2* hartzaile anti-inflamatorioaren adierazpena emendatzen duen artean, beti LPS-arekin bakarrik tratatutako zelulekin konparatuz. Azpimarragarria da, UDCA-az bakarrik tratatzerakoan *Trem1*-en adierazpena murriztu eta *Trem2*-ren adierazpena ere emendatzen direla KC-etan control egoerarekin alderatuz. Guk berri dugula, hau da UDCA-k TREM1 eta TREM2-ren adierazpenean eragin litzakeen efektuak aztertzen dituen lehenengo ikerlana. Era berean, UDCA-k KC-etan eragiten dituen efektu anti-inflamatorioak TREM2-ren menpekoak direla ere

adierazten dute gure emaitzek. Izan ere, WT zeluletan UDCA-k eragiten duen *Il6*, *Tnf* eta *Cxcl1*-en adierazpenaren murrizketa, ez zen *Trem2*$^{-/-}$ zeluletan behatu.

Bitartekari inflamatorio hauek garrantzitsuak dira kolestasiaren garapenean. Lehen aipatu bezala, bere adierazpena emendatuta dago PBC-dun gaixoetan, baita PSC-dun gaixoetatik eratorritako zeluletan ere (327, 342), eta DRC-en mikroingurune inflamatorioan (6). IL6-ak eta TNF-ak efektu mitogenikoak dituzte kolangiozito (343) eta hepatozitoetan (344) eta CXCL1-k ezinbesteko papera du neutrofiloen gibelerako erakarpenean, hauek zelula zitotoxiko nagusiak izanik kolestasian (332). Are gehiago, UDCA-LPE konjokatuak IL6-ren eta TNF-ren ekoizpena murrizten du KCs-etan (339). Emaitza hauek iradokitzen dute UDCA-k TREM1 eta TREM2-ren adierazpenean aldaketak eragin litzakeela eta honek UDCA-rekiko erantzuna zuzendu lezake PBC eta PSC-dun gaixoetan. Honela, interesgarria litzateke TREM1 eta TREM2-ren adierazpena neurtzea UDCA-az tratatutako gaixoetan, UDCA-rekiko erantzun totala eta partziala erakusten duten gaixoen arteko desberdintasunean arreta jarriz. Beraz, aurkikuntza hauek UDCA-k KCs-etan dituen efektuen inguruan mekanismo berri bat identifikatzen dute, eta UDCA-an oinarritutako tratamenduaren inguruan ikerketarako alor berriak zabaltzen dituzte.

D.4. HCC tumoreetan, TREM2 gibeleko bertako eta gibelera erakarritako makrofagoetan adierazten da nagusiki

Gure ikerketa taldearen aurreko lanetan, HCC-dun pazienteen gibelean TREM2-ren adierazpenaren emendioa ematen dela aurkeztu dugu (289). Lan honetan, adierazpen honen jatorri zelularra aztertu dugu sakonki. Gure IHC emaitzek adierazten dutenez, TREM2 ez da adierazten eraldatutako hepatozitoetan, TREM2-ren adierazpena agerikoa zen makrofago itxura zuten zeluletan tumorearen inguruko ehunean eta tumorearen barnean. Gure zelula bakarreko RNA sekuentziazioko analisiek azaleratzen dute TREM2-ren adierazpena gibeleko bertako zein gibelera erakarritako TAMs-etan ematen dela nagusiki. Aurkikuntza honek azken aldian argitaratutako zelula bakarreko RNA sekuentzioa egiten duten beste lanekin bat egiten du, lan hauetan, TREM2 adierazten duten makrofagoen azpi-klaseak deskribatzen dira NAFLD-an (280), giza eta sagu zirrosian (281) eta gaixo obesoen ehun adipotsuan (278). Are gehiago, lan honetan, HCC-ko tumoreetan identifikatutako, TREM2 adierazten duten TAM-ek CD68 eta CD9-ren adierazpena ere ezaugarri dute, honela, zirrosiarekin lotutako makrofagoekin antzekotasunak dituztela azaleratuz (280). Era berean, NASH-dun gaixoetan identifikatutako *Trem2*^{high} KCs-en azpipopulazioa CD9-ren gainadierazpena du

ezaugarritzat (280). Are gehiago, gure datuek erakusten dutenez, TREM2 adierazten duten TAMs-etan TLR seinaleztapenarekin eta lisosomekin lotutako bidezidorreko geneen adierazpenak aberastuta dadue, TAMs hauek TLR-bidezko erantzun inflamatorioen erregulazioan parte hartzen dutela iradokiz (288). Halaber, NASH-ean deskribatutako *Trem2*^{high} KC-ak ere lisosomarekin lotutako bidezidorreko geneen adierazpenean aberastuta daude (280).

D.5. TREM2-k gibela babesten du fibrosiarekin lotutako kartzinogenesiaz

Trem2$^{-/-}$ saguetan behatu dugun kolestasiak eragindako kaltearekiko gehiegizko erantzunak, zelularen heriotzaren, inflamazioaren eta neutrofiloen erakarpenaren emendioa ditu ezaugarri nagusi. Prozesu hauek inflamazioa eta zelularen heriotza kateatu eta elkar sustatzen duten zikloa ekar lezakete, eta epe luzera, zelula epitelialen transformazioa eta, beraz, HCC-a (192) eta CCA-ren (185) garapena lagundu.

Ildo honetan, gure emaitzetan ikusi dugu IL6 eta TNF zitokina inflamatorioen adierazpena emendatuta dagoela *Trem2*$^{-/-}$ saguetan kolestasiaren ondorioz. Interesgarria da zitokina hauen gainadierazpena kalte hepatozelular akutu zein kronikoaren ondorioz zein DEN-aren administrazio akutuaren ondoriozko hepatokartzinogenesiaren fase goiztiarretan ere behatu direla *Trem2*$^{-/-}$ saguetan (288, 289). Era berean, IL6 eta TNF-k kolangiozitoen hazkuntza eragiten dute (343). Hain zuzen ere, IL6-ren adierazpena bereizgarriki emendatuta dago PSC-dun pazienteetan sortzen diren CCA-etan (345). IL6 eta TNF zitokinek ere berebiziko garrantzia dute hepatokartzinogenesian, inflamazioa eta minbiziaren garapenaren arteko lotura molekularra ezartzen baitute (346, 347). Mutazioak eragiten dituzten DEN edo TAA bezalako estimulu baten menpean, hazkuntzaren emendioak eta inflamazio iraunkorrak hepatozitoen eraldaketa malignoa ekar lezake (348). Berez, *Trem2*$^{-/-}$ saguetan hepatokartzinogenesiaren emendioa behatzen dugu fibrosiarekin lotutako HCC-aren sagu ereduak diren DEN+CCl_4 eta TAA ereduetan, hauetan, zelularen hazkuntzaren markatzaile den *Pcna*-ren adierazpenaren emendioa ere behatu dugu.

Honez gain, WT eta *Trem2*$^{-/-}$ saguetan BDL-a eta gero gibel barneko BA kontzentrazioak antzekoak diren arren, sham ebakuntzatik BDL-ra ematen den BA-en kontzentrazioaren emendioa nabarmenagoa da *Trem2*$^{-/-}$ saguetan. Ildo honetan, BA-en metaketak efektu kaltegarriak dituzte gibelean, hauen artean, DNA-ren kaltea, estres oxidatiboa eta inflamazioaren loop autokrino eta parakrinoak sustatzen dituzte, eta efektu hauek denek HCC eta CCA-ren garapena errazten dute (349). Berriki, BA-ek

hepatokartzinogenesia sustatzeko gai direla ikusi da gibelerako NKT-en erakarpenaren bidez (350). CCA-n, konjokatutako BA-ek AKT eta ERK1/2-en seinaleztapena eragiten dute CCA zeluletan, azkenean CCA-ren hazkuntza eta inbasioa eragitenez (351). Gainera, BA-ak kartzinogenesiarekin lotzen dira FXR-an dituzten efektuak direla eta. BA-en metaketak FXR-ren adierazpenaren murrizketa dakar (352), era berean, *Fxr*$^{-/-}$ saguek berezko HCC-a garatzen dute (353), prozesu honetan, *Fxr*-ren galera bere hortan, ez da kartzinogenesia sustatzeko nahikoa, aitzitik, prozesu hau BA-en gibelearen barneko metaketaren menpekoa da (354). Bestalde, FXR-ren aktibazioak gibela babesten du HCC (25) eta CCA-ren (355) garapenaz. Laburbilduz, BA-ak faktore ko-kartzinogenikoak dira, eta beraz, kolestasiarekiko gehiegizko erantzuna eta ondorengo fibrosiaren lotutako kartzinogenesiaren arteko lotura izan litezke.

Epe luzeko erantzun fibrotikoei dagokienez, fibrosiarekin lotutako HCC ereduetan, gibeleko fibrosi gutxiago aurkezten zuten *Trem2*$^{-/-}$ saguek WT saguekin alderatuz. Orokorrean, fibrosia hepatokartzinogenesiaren bultzatzailetzat hartzen den arren, testuinguru batzuetan, bi fenomeno hauen disoziazioa ere behatu da (356). Ildo honetan, TREM2-k paper pro-fibrogenikoa betetzen du zirrosiarekin lotutako markofagoetan (281). Hortaz, TREM2-k efektu banatuak eragin ditzake HSCs-en aktibazioan eta fibrogenesian, eta hau mekanismo molekular desberdinen bidez azal liteke. Hasteko, makrofagoek fibrosian metatzen diren zuntzak fagozitatzen dituzte, honela fibrosiaren erresoluzioan lagunduz (357). TREM2 fagozitosiarekin lotu izan da, non makrofagoen azpipopulazio desberdinetan testuinguruaren araberako aurkikuntzak egin diren. Hain zuzen ere, CNS sistemaren makrofagoetan TREM2-k gorputz apoptotikoen fagozitosia sustatzen du (358, 359), makrofago albeolarretan bakterien opsonizazioa eta garbiketa geldiarazten dituen bitartean (274). Beraz, hau kontuan hartuta, gure hipotesia da TREM2-k fibrosian metatzen diren zuntzen fagozitosia ere modulatu lezakeela, hala ere, hipotesi hau frogatu gabe dago oraindik. Gainera, berriki argitaratutako lan batean iradokitzen denez, TREM2-k bere efektu anti-inflamatorio eta fagozitikoak zelula barneko seinaleztapen bidezidor independenteen bidez eragin litzake (360). Hau da, TREM2-k era desberdinean erregulatu litzake inflamazioa eta fagozitosia, eta honek, fibrosiko zuntzen metaketan ustekabezko efektuak ere eragin litzake. Izatez, makrofagoek fibrosiaren erresoluzioan berebiziko garrantzia dute, eta espezializatutako makrofago azpi-klaseek bideratzen dute fenomeno hau (361). Aurretik aipatu den moduan, TREM2-k makrofagoen azpi-klaseen erakarpenean duen efektua zehazki aztertzeak TREM2 eta fibrosiaren arteko loturaren mekanismo molekularren berri ere ekar lezake.

D.6. TREM2-ren aktibazioak estrategia terapeutiko berria izan daiteke kolestasia zein HCC-dun gaixoentzat

Laburbilduz, kalte kolestatikoak zauri-sendatze erantzuna pizten du, zeinetan zelula epitelial zein ez-epitelialak elkarlanean aritzen diren, galdutako gibelaren parenkima eta honen funtzioak berreskuratzeko ahaleginean. Testuinguru honetan, hesteetako bakterietatik eratorritako produktuak TLR-etara lotzen dira KC eta HSC-etan, eta hauetan, gene inflamatorioen adierazpena sustatzen dute. Bitartekari inflamatorioek era autokrino eta parakrinoan, zelula epitelialen heriotza eta erantzun inflamatorioaren areagotzea eragiten dute. Epe luzean, eraldaketa hauek hepatozitoen transformazioa eta, beraz, fibrosiarekin lotutako HCC-aren agerpena laguntzen dute. TREM2-ren ezean, TLR-en bidezko seinaleztapenaren muga naturala desagertzen da, beraz, KCs eta HSCs-etan TLR-bidezko seinaleztapena areagotzen da, azkenean, kolestasiaren garapena eta fibrosiarekin lotutatako HCC-aren agerpena sustatuz (**D.1. Irudia**). Antibiotikoen bidez hesteetatik eratorritako produktuen parte hartzea mugatzeak, TREM2-ren efektuak, behintzat partzialki, bidezidor honen araberakoak direla azaleratzen du. Are gehiago, gure dautuen arabera, TREM2 UDCA-k gibeleko zelula ez-parenkimaletan dituen efektu anti-inflamatorioen eragileetako bat izan daitekeela dirudi.

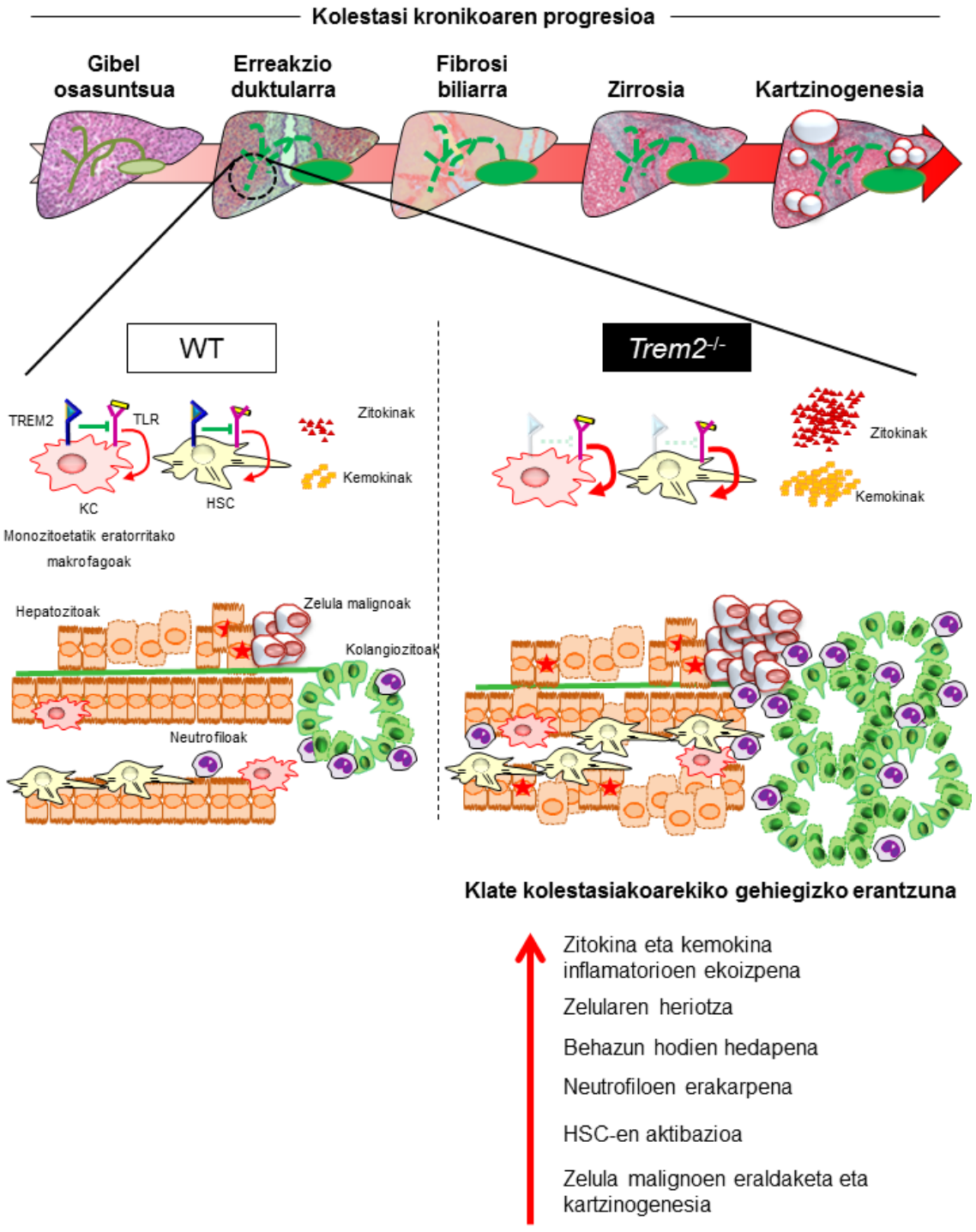

D.1 Irudia. TREM2-k kolestasiak eragindako gibel kaltean betetzen duen paperaren inguruko proposamena. Gaixotasun kolestatiko kronikoak erreakzio duktularra, fibrosia eta zirrosia bezalako urratsetan garatzen dira eta kartzinogenesia ere ekar lezakete. Garapen honetan, PAMPs eta DAMPs-ak TLRs-etara lotzen dira KCs, monozitoetatik eratorritako makrofago eta HSCs bezalako zelula ez-parenkimaletan, hauetan zitokina eta kemokina pro-inflamatorioen adierazpena sustatuz. TREM2-ren ezean, TLR-en bidezko seinaleztapenaren muga naturala desagertzen da, honek zitokina eta kemokina inflamatorioen ekoizpena eragiten du. Ondorioz, kolestasiak eragindako gibel kaltearekiko gehiegizko erantzuna ematen da, honen ezaugarriak dira zelulen gehiegizko heriotza, behazun zuhaitzeko egituren hedapena, neutrofiloen erakarpena gibelera, HSCs-en aktibazioa eta fibrosiarekin lotutako

hepatokartzinogenesia. KCs, kupffer cells; HSCs, hepatic stellate cells; TLR, toll like receptors; TREM2, triggering receptor expressed on myeloid cells 2; WT, wild type.

Inflamazioa gibeleko gaixotasun gehienen garapenaren erdigunean dago. Ideia honek, eta lan honetan eta gure taldeko aurreko lanetan aurkeztutako datuek (288, 289) aditzera ematen dutenez, TREM2-k gibelean betetzen duen efektu anti-inflamatorioak, iradokitzen dute TREM2-k zauri-sendatze erantzunaren erregulatzaile nagusi bezala joka dezakeela jatorri desberdinetako gibeleko gaixotasunetan. Kontzeptu honek, garrantzi berezia ematen dio bidezidor honi, izan ere, TREM2-ren seinaleztapena emendatzea bilatzen duten estrategia terapeutikoek, gaixotasun desberdin askotan efektu onuragarriak izan litzakete.

Hartzaile honen bidezko seinaleztapena sustatzeko molekula txikiak oraindik garatu ez diren arren, estrategia alternatiboak deskribatu dira azken aldian CNS-eko gaixotasunetan, batez ere AD-an. Honela, TREM2 disolbagarriak mikrogliaren funtzioak hobetu eta, hortaz, gaixotasunaren garapena geldiarazteko gai dela ikusi da AD-aren sagu ereduetan (362). Berriki argitaratutako beste lan batzuetan, TREM2-ren seinaleztapena antigorputzen bidez aktibatzeko estrategiak aztertu dituzte. Lanetako batean, antigorputz monoklonal batek TREM2-ren mozketa entzimatikoa ekidin eta hau zelulen kanpoaldean egonkortzen du, azkenenik, AD-arekin lotutako fenotipoaren hobetzea eraginez mikroglian (363). Hala ere, estrategia honek TREM2 disolbagarriaren murrizketa ere ekarri zuen, eta honek kontrako efektuak eragin dizake mikrogliaren aktibazioan. Beste estrategia gehigarri batean, garunean zeharreko AL002a-aren ziztadak, AL002a TREM2-ren zelula kanpoko domeinuari lotu eta seinaleztapena pizten duen antigorputza izanik, efektu onuragarriak eragin zituen mikroglian, azkenean amiloidearen metaketan murrizpena eta kognizioaren hobetzea zekarrena (364). Orokorrean, estrategia berriztatzaileak garatzen ari diren arren, TREM2-ren seinaleztapena sustatzen duten estrategia optimoak aurkitzekotan, TREM2 eta TREM2 disolbagarriari buruzko ikerketa gehiago behar dira oraindik. Ildo honetan, aurretik aipatu bezala, UDCA-k TREM“-ren adierazpena emendatzen du KC-etan eta BA koleretiko honek kolestasian eragiten dituen efektuetako batzuk TREM2-ren bidezko mekanismoen bidez gertatu litezke.

Erantzun inflammatorio eta immuneak modulatzeko duen gaitasuna dela eta, TREM2-k tumorearen mikroingurunean bete lezakeen papera ikertzen hasi da azken aldian. Honela, berriki argitaratutako bi lanetan TREM2-k sistema immuneko zelulen eta hauek tumorearen hazkuntzarekiko duten erantzunean zeresana duela erakutsi dute (365, 366). *Trem2*-ren gabezian tumorearen hazkuntza handiagoa ematen dela behatu dute. Lan

hauetako batean, sagu fibrosarkoma MCA205 zeluletatik eratorritako tumoreetan, *Arg1* eta *Trem2* adierazten dituzten zelula mieloideen bi azpi-populazio berri identifikatu dituzte, zelula mieloide supresoreak eta TAM-ak, hain zuzen ere. Zelula hauen eta CD8+ linfozito akastunen kopurua nabarmenki murrizten da *Trem2*-ren ezean, eta honek, sistema immuneko zelula zitotoxikoen biraktibazioa, hauen artean NK zelulak eta T linfozito zitotoxikoak, eta, ondorioz, tumorearen hazkuntzaren geldiaraztea dakar (365). Beste lan batean antzeko emaitzak deskribatzen dira, hoentan, *Trem2*-ren gabeziaren ondorioz fibrosarkoma, minbizi kolorrektal eta bularreko minbiziaren zelula lerroetatik eratorritako tumorearen hazkuntza geldiarazten da. Hau, *Trem2*-ren ezean gertatzen den sistema immuneko zelulen azpi-populazioen eraldaketaren bidez azaltzen da. Honela, *Trem2*$^{-/-}$ saguen tumoreen mikroingurunean, zelula mieloide supresore gutxiago eta zelula mieloide estimulatorio gehiago aurkitzen dira. Era berean, NK eta T zeluletan aberastuta daude *Trem2*$^{-/-}$ saguak eta CD4+ eta CD8+ zelulek PD1 gehiago adierazten dute. Azken efektu hau, anti-PD1 immunoterapiarekiko erantzun eraginkorrago batekin lotzen da. Antzeko efektuak lortzen dituzte WT saguak TREM2 inhibitzen duen antigorputz batekin tratatzean. Gainera, ikerlan honetan, hainbat tumoreren motatan, tumore barruan TREM2-ren adierzpena makrofagoetan ematen dela behatzen dute (366).

Datu hauek aditzera ematen dute TREM-ren bidezko erantzun inflamatorio eta immuneen modulazioak testuinguru eta denboraren araberako ondorioak izan litzakeela. Ildo honetan, TREM2 inflamazio iraunkorra geldiarazten duen mekanismo naturala da. Beraz, TREM2-ren agonismoak inflamazioa geldiaraziko luke gibeleko zelula ez-parenkimaletan eta gibelera erakarritako monozitoetatik eratorritako makrofagoetan. Honela, orokorrean kolestasiaren garapenean onuragarria izango litzateke efektu hau, bai eta garapenaren fase aurreratuagoetan ere, hepatokartzinogenesia barne (**D.2. Irudia**). Aitzitik, behin tumorea garatu denean, TREM2-ren aktibazioak tumorea itu duten erantzun immuneen inhibizioa eragin lezake, eta beraz, kaltegarria izan liteke gaxioentzat. Testuinguru honetan, TREM2-ren inhibizioak sisema immuneko populazio mieloide eta linfoideak eraldatu litzake, tumorearen kontrako erasoa ahalbidetuz eta hnen hazkuntza geldiaraziz (**D.2. Irudia**). Zehazki, *Trem2*-ren galera genetikoa edo bere inhibizioa antigorputz espezifiko baten bidez, zelula mieloide supresoreen murrizketa eta zelula mieloide eta linfoide estimulatorioen emendioa dakar, era berean, PD1-en gainadierazpenarekin eta immune-terapiarekiko erantzun eraginkorragoarekin ere lotzen da TREM2-ren galera. Hortaz, gibeleko eta behazun zuhaitzeko gaixotasunen garapenean TREM2-k betetzen duen papera zehatz-mehatz ezagutzeko, hartzaile honek zelula azpipopulazio desberdinetan betetzen duen funtzioa aztertu behar da, oraindik.

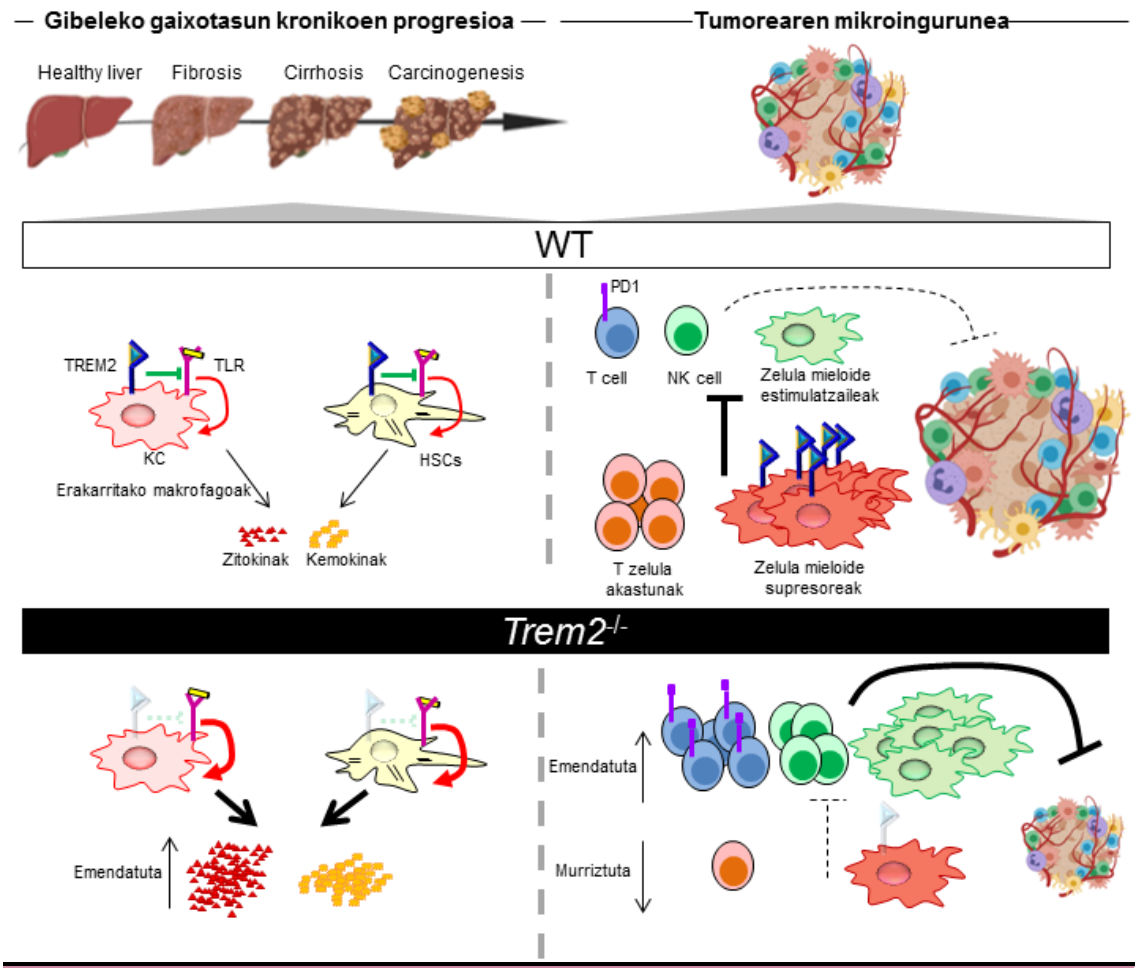

TREM2-ren galera genetikoaren edo honen inhibizioaren ondorioz behatutako efektuak	
Gibeleko gaixotasun kronikoen garapena	**Tumorearen mikroingurunea**
Zitokina eta kemokinen ekoizpenaren emendioa	Zelula mieloide supresoreen murrizketa eta zelula mieloide eta linfoide estimulatorioen emendioa
Zelularen heriotza eta estres oxidatiboaren emendioa	Zelula zitotoxikoen aktibazioaren eta kopuruaren emendioa, PD1-en adierazpenaren emendioa
Gehiegizko gibeleko kaltea	Immuno-terapiarekiko erantzun eraginkorragoa
Hepatokartzinogenesiaren emendioa	Tumorearen hazkuntzaren murrizketa

D.2. Irudia. TREM2-ren galera genetikoa edo inhibizioaren ondorioz behatutako efektuak gibeleko gaixotasun kronikoetan eta tumorearekiko erantzun immuneetan. *Ezkerreko irudia*. Gibeleko gaixotasun kronikoen garapena, fibrosia, zirrosia eta gibeleko kartzinogensia bezalako etapetan gertatzen da. Garapen honetan zehar, KC-ak, monozitoetatik eratorritako makrofagoek eta HSC-ek inflamazio, zauri-sendatze eta organoaren birsortze prozesuak bideratzen dituzte. Testuinguru honetan, TREM2-k TLR-en bidezko seinaleztapena inhibitzen du, ondorioz gene inflamatorioen adierazpena geldiaraziz. Trem2-ren ezean, TLR-ek bideratutako gene inflamatorioen transkripzioa emendatuta dago, gibeleko kaltearekiko eta hepatokartzinogenesiarekiko gehiegizko erantzuna emanez. Eskuineko irudia. Tumorearen mikroingurunean, zelula mieloide supresore estimulatorioak aurkitzen ditugu, eta hauen elakrrekintzat tumorearen hazkuntza mugatzen du. TREM2 zelula mieloide supresoreetan adierazten da batez ere, hauek T, NK eta zelula mieloide estimulatorioek eragindako tumorearen kontrako erantzun zitotoxikoak inhibitzen dituzte. Trem2-ren ezean, edo honen inhibizioaren bidez, zelula mieloide supresore eta estimulatorioen arteko oreka eraldatzen da, zelula mieloide supresore gutxiago eta zelula mieloide estimulatorio gehiago aurkitzen dira. Gainera, PD1-en adierazpenaren emendioa gertatzen da zelula linfoideetan, honek immuno-terapiarekiko erantzun eraginkorragoa eragiten du, Trem2-ren aurkako antigorputz inhibitorio batekin batera ematen demean.

ONDORIOAK

1. *TREM2*-ren mRNA adierazpena emendatuta dago PBC eta PSC bezalako gaixotasun kolestatikoak dituzten gaixoen gibelean gibel ehun osasuntsuarekin alderatuz.

2. *TREM2*-ren mRNA adirazpenak positiboki korrelazionatzen du markatzaile inflamatorio eta fibrotikoen mRNA adierazpenarekin PBC eta PSC bezalako gaixotasun kolestatikoak dituzten gaixoen gibelean.

3. PBC-dun gaixoen gibelean, , *TREM2*-ren mRNA adierazpenak positiboki korrelazionatzen du serumeko gibel kaltearen markatzaileekin eta gaixotasunaren garapena neurtzen duten puntuazioekin

4. Saguen gibelean, *Trem2*-ren mRNA adirazpena minimoki adirazpen da zelula epitelialetan (hepatozito eta kolangiozitoak) eta adirazpen hau nabarmenki emendatzen da KCs-etan eta aktibatutako HSC bezalako zelula ez-parenkimaletan.

5. Gibeleko *Trem2*-ren mRNA adirazpena emendatzen da kolestasiaren hainbat sagu eredutan egoera kontrolarekin alderatuz.

6. *Trem2*$^{-/-}$ saguek BDL-an oinarritutako kalte kolestatikoarekiko gehiegizko erantzuna aurkezten dute, behazun hodien hedapena eta zelulen heriotzaren emendioa ezaugarri dituena.

7. *Trem2*$^{-/-}$ saguetan gibeleko BA-en metabolismoaren asaldura basala behatzen da, honela, BA-en kontzentrazio murriztuagoa dute gibelean eta BA-en metabolismoan parte hartzen duten geneen adierazpenaren aldaketarako joera nabarmena erakusten dituzte sagu hauek.

8. *Trem2*$^{-/-}$ saguetan behatzen den BDL-an oinarritutako kalte kolestatikoarekiko gehiegizko erantzuna inflamazioarekin eta neutrofiloen gibelerako erakarpenaren emendioarekin lotzen da.

9. Abx-en konbinazioan oinarritutako tratamenduak, WT eta *Trem2*$^{-/-}$ saguen arteko desberdintasunetako batzuk deuseztatzen ditu. Honela, TREM2-k buxadurazko kolestasiaren kontra dituen efektu babesleak, partzialki behintzat,

hartzaile honek hesteetatik lekualdatutako bakteriek gibelean dituzten efektuengan eragiten duen erregulazioarengatik ematen da.

10. TREM2-ren efektu babesleak kimikoki eragindako kolestasian ere agerikoak dira, izan ere, *Trem2*$^{-/-}$ saguek gehiegizko gibeleko kaltea, zelularen heriotza eta inflamazioaren emendioa aurkezten dituzte.

11. Saguetatik isolatutako KCs-etan UDCA-k *Trem1*-ren mRNA adierazpena murrizten du *Trem2*-rena emendatzen duen bitartean.

12. UDCA-k LPS-ak eragindako efektuak kontrajartzen ditu KCs-etan, honela, *Trem1* hartzaile pro-inflamatorioaren mRNA adierazpena murrizten du, *Trem2* hartzaile anti-inflamatorioarena emendatzen duen bitartean.

13. UDCA-k LPS-ak emendatutako *Il6*, *Tnf* eta *Cxcl1*-en mRNA adierazpena murrizten ditu KCs-etan TREM2-ren menpeko mekanismo baten bidez.

14. *TREM2* gibeleko bertako eta gibelera erakarritako TAM-etan adierazten da HCC tumoreetan.

15. *TREM2*$^{+}$ TAM-ak *CD68, CD14* eta *CD9* markatzaileen adierazpena ezaugarri dute, era berean, TLR eta lisosomekin lotutako bidezidorretan aberastatuta daude.

16. TREM2-k gibela babesten du fibrosiarekin lotutako hepatokartzinogenesiaz, hau zelularen hazkuntzaren adierazpenaren murrizpenarekin eta fibrosiaren emendioarekin lotzen da.

Laburbilduz, TREM2-k erantzun inflamatorioak erregulatzen ditu kolestasiaren garapenean eta paper babeslea betetzen du fibrosiarekin lotutako hepatokartzinogenesian. Hori dela eta, TREM2-ren aktibazioa estrategia terapeutiko itxaropentsua izan liteke kolestasidun pazienteentzat. Gainera, UDCA-k kolestasian eragiten dituen efektu onuragarriak, zelula ez-parenkimaletan TREM1 eta TREM2-ren adierazpenaren modulazioarekin lotu daitezke. Aitzitik, TREM2-ren aktibazioak kolestasiak eragindako gibeleko kaltea eta hepatokartzinogenesia ekidin litzakeen arren, egun, gibeleko fibrosian eta tumorearen hazkuntzarekiko sistema immunearen erantzunean egun oraindik aurreikusi ezin diren efektuak eragin litzake.

SUMMARY IN SPANISH

Fisiología y anatomía hepática

El hígado es un órgano que cumple una función vital en el mantenimiento de la homeostasis metabólica del organismo, a la vez que se encarga de la detoxificación de sustancias potencialmente nocivas (1, 2). El hígado está formado por distintos tipos celulares, entre ellos destacan las células parenquimales o hepatocitos las cuales conforman el 70-80 del volumen hepático y cumplen la gran mayoría de las funciones metabólicas del órgano (1). Los colangiocitos, son las células epiteliales que cubren los conductos biliares y, pese a representar únicamente el 3-5% del volumen hepático, cumplen una función clave en la producción y regulación de la bilis, siendo responsables de hasta el 30-40% del flujo biliar (6).

La bilis es un biofluido generado por la acción coordinada de enzimas hepatocitarias y de la microbiota intestinal (8). Las sales o ácidos biliares (BAs) representan el componente más importante de la bilis y se generan por la acción de distintos enzimas en los hepatocitos, entre las cuales CYP7A1 es el enzima limitante (10). La bilis se genera inicialmente en los hepatocitos, posteriormente se secreta al canalículo hepático, de donde se drena a través de los conductos biliares (8) y finalmente se libera en el duodeno, donde es objeto de modificaciones por la acción de la microbiota intestinal (18). Una vez en el intestino, la bilis también puede ser reabsorbida y tansportada nuevamente a los hepatocitos en una ciclo denominado transporte enterohepático (17). Cabe destacar que los BAs son capaces de regular su propia síntesis, por su unión sobre FXR, el cual activa SHP, el principal regulador transcripcional negativo de CYP7A1 (10).

Entre las células no parenquimales hepáticas destacan las células de Kupffer (KCs) y las células estrelladas hepáticas (HSCs). En un hígado sano, todas ellas colaboran con hepatocitos y colangiocitos en el mantenimiento de la función hepática, mientras que en situaciones de daño hepático las células no parenquimales adquieren un papel crucial en la coordinación de la respuesta “wound-healing” o respuesta reparativa (27).

Las KCs y los macrófagos derivados de monocitos que se reclutan al hígado, son la primera línea de la defensa inmune innata en este órgano (28). Estas células actúan de manera coordinada y responden a microorganismos, productos bacterianos y derivados de muerte celular epitelial fagocitándolos y generando una gran cantidad de mediadores pro- y anti-inflamatorios, los cuales actúan de manera autocrina y paracrina perpetuando su respuesta y atrayendo y alertando a otras poblaciones inmunes (39). Las HSCs, por

su parte, en presencia de daño hepático se activan y sufren un proceso de transdiferenciación, mediante el cual se convierten en miofibroblastos. Las HSCs activadas adquieren capacidades proliferativas, contráctiles, quemotácticas y también la capacidad de producir grandes cantidades de proteínas de matriz extracelular (ECM) (44). En consecuencia, esta es la población celular más importante en la fibrogénesis hepática (45).

Enfermedades hepáticas crónicas y su progresión

Al ser un órgano complejo y jugar un papel clave en el metabolismo y detoxificación de diversas moléculas en el organismo, el hígado también es diana de una gran variedad de enfermedades de diversos orígenes. Las enfermedades hepáticas pueden clasificarse de acuerdo a la población epitelial que sufre el daño inicial (62). Así, se distinguen enfermedades hepatocelulares que tienen como diana principal los hepatocitos y entre las que se encuentran infecciones por virus de la hepatitis B o C (HCV, HBV), enfermedad hepática alcohólica, enfermedad hepática no-alcoholica o el hepatocarcinoma (62). Por su parte, las enfermedades que tienen como diana inicial el colangiocito se denominan colangiopatías (71).

Enfermedades colestásicas

La colestasis es una condición patológica que se caracteriza por la disminución o la interrupción del flujo biliar, lo cual conlleva la acumulación de BAs y otras sustancias tóxicas de la bilis en el hígado (75). Entre las enfermedades colestásicas, las más comunes en adultos son colangitis biliar primaria (PBC) y la colangitis esclerosante primaria (PSC), dos enfermedades crónicas asociadas con procesos auto-immunes contra la vía biliar (74). Las estrategias terapéuticas para PBC y PSC se basan en la administración del ácido ursodeoxicólico (UDCA), un ácido biliar endógeno con propiedades coleréticas, hepatoprotectora anti-apoptóticas y anti-inflamatorias (22, 101). En el caso de los pacientes con PBC es el tratamiento de primera línea, aunque aproximadamente un 30% de los pacientes con PBC presenta una respuesta incompleta y puede evolucionar a cuadros clínicos más graves en los que el transplante hepático es la única opción terapéutica curativa (102). En el caso de los pacientes con PSC, existe cierta controversia en el uso del UDCA, ya que algunos estudios reportan efectos adversos importantes a dosis altas de UDCA (104). En consecuencia, no existe un consenso por parte de las asociaciones internacionales en cuanto al uso del UDCA, así la "European association for the Study of the Liver (EASL)" aprueba el uso del UDCA

en enfermos con PSC, mientras que la "American Association for the Study of Liver Diseases (AASLD)" no lo recomienda.

La progresión de las enfermedades hepáticas crónicas presenta un curso similar, independiente de su origen (27). Esta progresión se inicia con la muerte del hepatocito o colangiocito, lo cual inicia una respuesta reparadora en un esfuerzo por restaurar el tejido hepático dañado (110).

Progresión de las enfermedades colestásicas

En el caso de las enfermedades colestásicas, hay controversia en cuanto a la iniciación del daño. Los BAs tienen propiedades membranolíticas, y pueden provocar la muerte de hepatocitos y colangiocitos, aunque a concentraciones mayores de las detectadas en pacientes con colestasis (119, 120). Por lo tanto, se cree que los BAs pueden iniciar el daño hepático por su acción en hepatocitos dónde estimulan la producción de mediadores pro-inflammatorios (119). Además, en la iniciación de enfermedades como la PBC y la PSC participan procesos auto-inmunes y se observa el reclutamiento de linfocitos T que atacan a la vía biliar (114).

Tras el daño inicial, se desencadena la reacción ductular, en un intento por recuperar las estructuras biliares dañadas y aumentar la superficie que elimine los BAs acumulados (132). En este proceso se observa la proliferación y expansión de estructuras biliares, a la vez que se genera un micro-ambiente pro-inflamatorio con la secreción de citoquinas y quemoquinas pro-inflammatorias, el reclutamiento y activación de poblaciones immunes, la angiogénesis, y la activación de poblaciones mesenquimales (15, 131). Aunque su origen celular exacto aún no se ha establecido, en la reacción ductular, las célular reactivas ductulares (DRCs) adquieren un papel clave (6, 136). Las DRCs proliferan y adquieren un fenotipo mixto biliar-mesenquimal, además de secretar citoquinas pro-inflamatorias, quemoquinas y factores de crecimiento como IL1β, IL6, IL8, MCP1, CXCL1, EGF, o VEGF, entre otros que activan y atraen a las células del sistema immune, tales como KCs, macrófagos y HSCs, perpetuando la respuesta y el micro-ambiente inflamatorio (154).

La fibrosis hepática se caracteriza por la acumulación de proteínas de ECM, pero también por cambios cualitativos en la misma (156). En este caso la fibrosis biliar se desarrolla a consecuencia de la comunicación intercelular entre DRCs y HSCs o PM, y comienza a generarse en la proximidad de los conductos biliares y progresando hasta

abarcar el lóbulo hepático y desarrollar puentes fibrosos (148). En estadios avanzados la fibrosis biliar progresa a cirrosis biliar, un estadio de punto final en el que la acumulación masiva de ECM sustituye el parénquima hepático y los hepatocitos se organizan en nódulos regenerativos (177). La cirrosis hepática y biliar representa el mico-ambiente óptimo para la transformación de células malignas y la carcinogénesis, y es además una de las principales indicaciones de transplante hepático (180).

La colestasis está íntimamente asociada con la carcinogénesis hepatobiliar (182); concretamente, los pacientes con PBC presentan un mayor riesgo de padecer hepatocarcinoma (HCC) (183), y la enfermedad de PSC es un factor de riesgo para el desarrollo de colangiocarcinoma (CCA), o HCC (185, 186). El HCC es una enfermedad que en el 80% de los casos se desarrolla en hígados cirróticos. En la progression del daño hepático crónico, los factores mitogénicos que estimulan la proliferación compensatoria inicial se perpetúan y llevan a la proliferación descontrolada, situación en la que también se propicia la acumulación de mutaciones, y por lo tanto, la transformación maligna de los hepatocitos y/o colangiocitos (192).

El eje intestino-hígado y la translocación bacteriana

En los últimos años, el eje intestino-hígado ha adquirido considerable atención como una fuente importante de mediadores pro-inflamatorios que favorecen la progresión del daño hepático crónico. En situaciones de enfermedad hepática avanzada, la barrera epitelial del intestino presenta disfunciones, a la vez que se da la disbiosis de la microbiota con crecimiento selectivo de cepas patógenas. Estas alteraciones facilitan la translocación de microorganismos y/o productos bacterianos del intestino al hígado (202). En el hígado, estos productos se unen principalmente a TLRs expresados en KCs y en HSCs, células en las que potencian la expresión de genes pro-inflammatorios y contribuyen, así a la progresión de distintas enfermedades hepáticas (58, 211, 212). En este contexto, se ha visto que el limitar o regular la contribución de las señales derivadas del intestino frena la progresión de distintas enfermedades hepátobiliares (232-234).

Los receptores TREM

La familia de los receptores TREM se ha descrito como moduladora de la señalización mediada por TLRs (235, 236). En términos generales, aunque existen respuestas específicas de tipos celulares concretos, se ha descrito el papel de TREM1 como potenciador de la señalización por TLRs, aumentando la expresión de genes pro-

inflamatorios. Por el contrario, se sugiere que TREM2 tendría una función opuesta, modulando negativamente la señalización mediada por TLRs, y disminuyendo, así la expresión de genes pro-inflamatorios (242).

Cabe destacar que en estudios anteriores, hemos descrito el papel protector del receptor TREM2 en respuesta a daño hepatocelular agudo y crónico, así como en la hepatocarcinogénesis. En estos estudios hemos observado que la expresión de TREM2 se encuentra aumentada en el hígado de pacientes con cirrosis de diversos orígenes, así como en tumoures de HCC y en modelos murinos de ambas patologías. Asimismo, ratones deficientes en *Trem2* (*Trem2*$^{-/-}$) muestran daño hepático exacerbado en respuesta a injurias agudas y crónicas, caracterizado por mayor inflamación, estrés oxidativo, peroxidación lipídica, y mayores tasas de mortalidad en un modelo de DILI. Estos resultados se asocian con mayores niveles de expresión de citoquinas y quemoquinas pro-inflamatorias en las KCs y HSCs aisladas de ratones *Trem2*$^{-/-}$ en respuesta a la activación de TLR4 por LPS (288). En fases iniciales de hepatocarcinogénesis, los ratones *Trem2*$^{-/-}$ muestran más daño en el DNA, proliferación y expresión de genes inflamatorios, y en fases crónicas mayor tumorigénesis hepática. Además, estas observaciones se asocian con el efecto que tiene TREM2 en la regulación de la inflamación y en consecuencia en la comunicación entre HSCs y células de HCC (289).

HIPÓTESIS Y OBJETIVOS

Teniendo en cuenta el papel del receptor TREM2 como regulador de respuestas inflamatorias en respuesta a daños hepáticos agudos y crónicos, y también durante la hepatocarcinogénesis, trabajamos en la hipótesis que TREM2 también podría regular las respuestas inflamatorias durante la colestasis y el HCC asociado a fibrosis. Con esta hipótesis, nos propusimos los siguientes objetivos específicos:

1. Evaluar los niveles de expresión del receptor TREM2 en el hígado de pacientes con enfermedades colestásicas en comparación a tejido hepático sano y a tejido hepático cirrótico de distintas etiologías.

2. Evaluar los niveles de expresión de *Trem2* en modelos animales de colestasis.

3. Caracterizar el papel de TREM2 en el desarrollo y progresión del daño biliar en un modelo de colestasis obstructiva.

4. Determinar la contribución de las señales derivadas de la translocación bacteriana en el fenotipo mediado por TREM2 en un modelo de colestasis obstructiva.

5. Caracterizar el papel de TREM2 en el desarrollo de daño biliar en un modelo de colestasis inducida por estímulo químico.

6. Analizar el papel de TREM2 como nuevo mediador de los efectos beneficiosos del UDCA en células no parenquimales hepáticas.

7. Analizar las subpoblaciones immunológicas que expresan TREM2 en tumores de pacientes con HCC.

8. Caracterizar el papel del receptor TREM2 en la hepatocarcinogénesis asociada a fibrosis.

MATERIALES Y MÉTODOS

Expresión génica del receptor TREM2 en muestras de tejido hepático de pacientes con enfermedades colestásicas, individuos control y pacientes con cirrosis

En primer lugar, se analizó la expresión de TREM2 a nivel de mRNA en tejido hpeático de la cohorte San Sebastian/Varsovia. En esta cohorte se incluyeron muestras de tejido hepático de pacientes con enfermedades colestásicas (i.e. PBC y PSC), así como tejido hepático sano de individuos control e hígado con cirrosis de distintas etiologías. Las muestras de tejido hepático de PBC y PSC se obtuvieron en colaboración con los Drs. Piotr Milkiewicz y M. Milkiewicz de la universidad de Varsovia y Sczein, respectivamente. Las muestras de tejido hepático sano de individuos control se obtuvieron a través del Biobanco Vasco. Asimismo, también se utilizaron datos públicamente accesibles en la base de datos GEO (Gene Expression Omnibus) para analizar la expresión de TREM2 en una cohorte adicional de pacientes con PBC y controles sanos (290).

Análisis de la expresión génica del receptor TREM2 en distintos tipos celulares del sistema inmune en tumores de HCC mediante secuenciación de RNA en células individuales (scRNAseq)

Se obtuvieron datos de "single cell RNA sequencing" (scRNAseq) de 9 tumores de HCC, accesible públicamente en GSE125449 (291). La información clínica sobre los pacientes incluidos así como el protocolo empleado y el control de calidad han sido previamente descritos en el artículo original. Los datos organizados en clusters o grupos se visualizaron mediante t-distributed Stochastic Neighbor Embedding (t-SNE) con el programa Seurat de R.

Modelos experimentales murinos de colestasis y HCC asociado a fibrosis

En esta tesis se han realizado modelos experimentales de daño hepático inducido por colestasis y de generación de HCC asociada a fibrosis con el objetivo de determinar el papel de TREM2 en el desarrollo de estas condiciones patológicas. Así, empleamos ratones deficientes en *Trem2* (*Trem2*$^{-/-}$) y comparamos su respuesta en los contextos anteriormente citados con su efecto en ratones control o "wild-type". En todos los casos en el momento del sacrificio de los animales, al tiempo indicado, se obtuvieron muestras de sangre, que posteriormente se procesaron para obtener suero y analizar niveles de marcadores serológicos de daño hepático. Asimismo, se obtuvieron muestras de tejido hepático que se procesaron para su análisis histológico o se almacenaron a -80ºC para diversos análisis moleculares. Todos los procedimientos fueron aprobados por el comité ético de experimentación animal (CEEA) del Instituto de Investigación Sanitaria Biodonostia.

Se realizó un modelo de colestasis obstructiva basado en la ligadura del conducto biliar común (BDL), en el cuál se anestesiaron los animales, se les realizó una escisión abdominal, y a continuación se realizó una ligadura del conducto biliar común con sutura doble; posteriormente, se suturó el tejido muscular y la piel de los animales. A los ratones control se les realizó el mismo procedimiento, en este caso sin la ligadura. Se empleó analgesia en las horas posteriores a la cirugía. Los animales se sacrificaron a los 7 días tras la cirugía.

Para determinar el papel que cumplen las señales derivadas de la translocación bacteriana del eje intestino-hígado en el papel del receptor TREM2 durante la colestasis, se acopló el modelo de BDL con un protocolo de esterilización intestinal a base de

antibióticos. Para ello, se empleó una combinación de antibióticos previamente descrita, se trataron los animales durante 3 semanas previas al BDL, y se continuó una semana más con el tratamiento hasta el sacrificio de los ratones a los 7 días tras la cirugía.

Además, se realizaron modelos de colestasis inducida químicamente. Así, se empleó el hepatotóxico ANIT, el cual se secreta en la bilis y sufre varios ciclos de reabsorción-secreción, concentrándose en la bilis e induciendo muerte en los colangiocitos. Se administró ANIT a una dosis de 50 mg/kg por sondaje orogástrico y se sacrificaron los animales a las 48 horas tras la administración; a los ratones control se les administró aceite de oliva. Adicionalmente, se realizó otro modelo consistente en la administración de una dieta enriquecida en DDC, el cual afecta al metabolismo de las porfirinas y produce un fenotipo de colestasis intrahepática. Se alimentaron los ratones con una dieta que contiene 0.1% DDC durante 4 semanas, mientras que a los ratones control se alimentaron con la misma dieta sin DDC, y los ratones se sacrificaron a tras 4 semanas.

Modelos de HCC asociado a fibrosis

El HCC se desarrolla en la mayoría de los casos en pacientes que presentan un hígado cirrótico y enfermedades hepatobiliares previas. Por ello, se realizaron dos modelos de HCC asociado a fibrosis. En el primero se combinó la administración del hepatocarcinógeno DEN con inyecciones semanales de CCl_4 y se sacrificaron los animales a las 30 semanas de la inyección de DEN. En el segundo modelo, se les administró a los ratones TAA en agua de bebida durante 40 semanas.

Perfusión hepática, aislamiento y tratamiento de células primarias hepáticas

Se aislaron las distintas poblaciones celulares del hígado de ratones WT y *Trem2*$^{-/-}$. El protocolo empleado para el aislamiento se basa en la digestión *in situ* del hígado mediante perfusión a través de la vena porta con distintas solucionen que contienen las enzimas pronasa y colagenasa (Roche). Tras la perfusión se obtuvo el hígado y tras un paso adicional de digestión con DNasa y pronasa (Roche) se filtró y la suspensión celular se separó mediante centrifugación en gradiente de densidad con Nycodenz (Axis-Shield). Posteriormente, las células fueron incubadas con LPS y/o UDCA.

Análisis estadístico

Los parámetros cuantitivos obtenidos en el curso de este estudio se recogieron y analizaron en documentos MS Excell, y posteriormente se analizaron y visualizaron por medio del programa GraphPad Prism 6.00 (GraphPad Software). Se realizaron análisis de normalidad en los datos y se emplearon test paramétricos en el caso de que los datos mostraran una distribución normal y no paramétrico en el caso de que no se cumplieran criterios de normalidad. Para comparaciones entre dos grupos independientes se empleó el test paramétrico de la *t* de Student o el test no paramétrico de Mann Whitney. Para comparaciones entre más de dos grupos se emplearon el test paramétrico de análisis de varianza unidireccional seguido del test *pos hoc* de Bonferroni o del test no paramétrico Kruskal Wallis seguido del test *post hoc* Dunns. Para los análisis de correlación se utilizó el test paramétrico de Pearson o el no paramétrcio de Spearman.

RESULTADOS Y DISCUSIÓN

TREM2 se encuentra sobreexpresado en el hígado de pacientes con colestasis y en modelos murinos de daño hepático por colestasis

La expresión de TREM2 se encontró aumentada en el hígado de pacientes con PBC y PSC en comparación con tejido hepático sano y con tejido hepático de pacientes con cirrosis en la cohorte de San Sebastián/Varsovia. Esta expresión correlaciona positivamente con distintos marcadores pro-inflamatorios y pro-fibrogénicos de la progresión de la enfermedad. Adicionalmente, la expresión de TREM2 también se encuentra aumentada en el hígado de pacientes con PBC de riesgo alto en comparación al hígado de individuos control y pacientes con PBC de riesgo bajo. La misma tendencia se observó en diversos modelos murinos de colestasis, donde la expresión hepática de *Trem2* se vio aumentada en comparación a tejido de ratones control. Adicionalmente, el análisis de la expresión de *Trem2* en distintos tipos celulares del hígado en ratón, reveló que este receptor se expresa principalmente en las poblaciones celulares no parenquimales, tales como KCs y HSCs, mientras que su expresión en hepatocitos y colangiocitos es mínima. Estos datos están en consonancia con estudios anteriores que muestran un aumento de la expresión de TREM2 en enfermedades hepáticas con un fuerte componente inflamatorio, independientemente de su origen y que esta expresión aumenta con la progresión de la enfermedad (288, 289). Además, indican que la sobreexpresión de TREM2 es un evento central en la colestasis y por lo tanto que este receptor podría desempeñar un papel clave en su desarrollo y progresión.

Papel del receptor TREM2 en el desarrollo y progresión de daño hepático inducido por colestasis

Los datos obtenidos tras la realización de modelos de daño hepático por colestasis y de HCC asociado a fibrosis en ratones WT y *Trem2*$^{-/-}$ sugieren que TREM2 desempeña un papel protector frente al desarrollo de estas condiciones patológicas. Así ratones los *Trem2*$^{-/-}$ mostraron una respuesta exacerbada ante el daño hepático inducido por colestasis; en el caso del modelo de BDL, esta respuesta estuvo caracterizada por mayores niveles de muerte celular, expansión biliar, expresión de citoquinas y quemoquinas pro-inflamatorias, reclutamiento de neutrófilos, y activación de HSCs tras el BDL en comparación con ratones WT. Además, la administración de una combinación de antibióticos hizo que desaparecieran algunas de las diferencias observadas entre ratones WT y *Trem2*$^{-/-}$ tras el BDL. En el modelo basado en la administración de ANIT, los ratones *Trem2*$^{-/-}$ presentaron niveles elevados de marcadores serológicos de daño hepático, muerte celular y también mayor expresión de citoquinas y quemoquinas pro-inflamatorias. Estos datos sugieren que TREM2 regula negativamente la respuesta inflamatoria en el desarrollo y progresión del daño hepático inducido por colestasis, de manera que afecta a la expresión de citoquinas inflamatorias como IL6, IL33, TNF o CXCL1, las cuales se ha descrito anteriormente que juegan un papel clave en pacientes con PBC y PSC (81, 91, 313). Adicionalmente, nuestras observaciones indican que, si bien la contribución de la señalización derivada de productos bacterianos translocados desde el intestino al hígado media algunos de los efectos asociados a TREM2 en colestasis, no todos ellos dependen de este mecanismo. De hecho, en estudios anteriores hemos observado que TREM2 podría regular respuestas inflamatorias mediadas por otro tipo de ligandos de TLRs o incluso por mecanismos independientes a esta vía (269, 336).

UDCA ejerce sus efectos en las células no-parenquimales hepáticas por un mecanismo dependiente de TREM2

El UDCA es la estrategia terapéutica de primera línea para el tratamiento de pacientes con PBC y también se utiliza en muchos centros para el tratamiento de PSC. No obstante, más allá de su acción colerética, los mecanismos por los que UDCA ejerce sus efectos hepatoprotectores en el contexto de las enfermedades colestásicas aún no se han definido en detalle. En este trabajo mostramos que el UDCA es capaz de disminuir la expresión de *Trem1* mientras que aumenta la expresión de *Trem2* en células de KCs. Además, al añadir UDCA a células incubadas con LPS se revierten los efectos de este

producto bacteriano, con una disminución de la expresión de *Trem1* y un aumento de la expresión de *Trem2* respecto a las células incubadas únicamente con LPS. De manera importante, el UDCA es capaz de disminuir la expresión de las citoquinas pro-inflamatorias *Il6, Tnf* y *Cxcl1* en KCs de células WT, mientras que estos efectos no se observan en KCs derivadas de ratones *Trem2*$^{-/-}$. Estos resultados están en línea con publicaciones recientes en las que se describen los efectos del tratamiento con UDCA y un conjugado LPE-UDCA en KCs y HSCs (339). Adicionalmente, cabe destacar que estos marcadores pro-inflamatorios juegan un papel clave en el desarrollo de las enfermedades colestásicas (6), y el hecho de que TREM2 medie los efectos de UDCA sobre estas citoquinas cobra una especial importancia.

El receptor TREM2 se expresa en macrófagos asociados al tumor en muestras tumorales de pacientes con HCC

Mediante los análisis de scRNAseq identificamos 6 grupos diferentes de células, los cuales se caracterizan por el enriquecimiento en la expresión de marcadores de cada uno de los tipos celulares. Entre estos grupos, TREM2 se expresa prominentemente en macrófagos asociados al tumor. Al separar la población de macrófagos en distintos grupos, TREM2 se identifica en el grupo 1 y 2 de macrófagos, los cuales se caracterizan por la expresión de CD68, CD14 y CD9. Estos resultados van en línea con nuestras observaciones en un estudio anterior donde por IHC identificábamos la expresión de TREM2 en células que parecían macrófagos. Además, en estudios recientes de scRNAseq en pacientes obesos (278) , pacientes de NAFLD (281)y pacientes con cirrosis hepática (280), se han identificado subpoblaciones de macrófagos que se caracterizan por la expresión de TREM2.

En modelos de HCC asociados a fibrosis, los ratones *Trem2*$^{-/-}$ desarrollaron mayor tumorigénesis hepática, lo que se asoció con un aumento de expresión del marcador de proliferación *Pcna*. Sorprendentemente, estos ratones también muestran menores niveles de fibrosis hepática. El aumento de la muerte celular, el incremento de BAs y los mediadores inflamatorios observados en el hígado de ratones *Trem2*$^{-/-}$ pueden actuar como inductores de proliferación descontrolada y transformación maligna de las células epiteliales, estableciendo el nexo entre la progresión del daño hepático por colestasis y el desarrollo de carcinogénesis hepatobiliar (345-347). El hecho de que los ratones *Trem2*$^{-/-}$ muestren mayor tumorigénesis hepática pero menores niveles de fibrosis, se explica por mecanismos de desacoplamiento de ambas respuestas que han sido descritos en estudios recientes (356).

La activación de TREM2 representa una nueva estrategia terapéutica potencial para el tratamiento de pacientes con colestasis y con HCC

En conclusión, los datos presentados en este trabajo sugieren que TREM2 cumple un papel protector en el desarrollo y progresión de la colestasis y el HCC asociado a fibrosis. Así, el daño hepático inducido por colestasis se inicia con la muerte de las células epiteliales que secretan señales pro-inflammatorias al entorno. Esto activa la respuesta de las células no parenquimales como KCs y HSCs, las cuales responden a esas señales coordinando la respuesta "wound-healing". En este contexto, productos bacterianos translocados en del eje intestino-hígado se unen a TLRs principalmente en KCs y en HSCs, y aquí fomentan la expresión de genes inflamatorios. Los mediadores inflamatorios actúan de manera autocrina y paracrina, induciendo más muerte celular epitelial y perpetuando la respuesta inflamatoria. A largo plazo, estas alteraciones favorecen la transformación maligna de hepatocitos y la generación de HCC asociado a fibrosis. En ausencia de TREM2, el freno natural de la inflamación mediada por TLRs desaparece. Por lo tanto, la expresión de genes pro-inflamatorios mediada por TLRs en KCs y en HSCs se amplifica, y esto resulta en una respuesta exagerada como consecuencia del daño hepático por colestasis y hepatocarcinogénesis asociada a fibrosis.

El desarrollo de estrategias terapéuticas que activen la señalización mediada por TREM2 es todavía un campo muy incipiente. Sin embargo, cabe destacar que el desarrollo de estas estrategias podría representar una estrategia terapéutica interesante para un amplio rango de pacientes con enfermedades hepáticas, incluidos pacientes con colestasis, ya que protegería al hígado de respuestas inflamatorias exacerbadas ante estímulos de diversa naturaleza. No obstante, la activación del receptor TREM2 en el desarrollo de la fibrosis podría estar asociado con efectos negativos. En el contexto del HCC asociado a fibrosis, TREM2 desempeña un papel protector frente al desarrollo de la hepatocarcinogenesis, ya que frena respuestas inflamatorias que favorecen estos procesos. No obstante, una vez establecido el tumor, al tener efectos moduladores negativos en la inflamación y distintas poblaciones inmunes, TREM2 actuaría como freno ante la respuesta inmune contra el tumor, tal y como se muestra en dos publicaciones recientes en las que se reporta un mayor crecimiento tumoral en ratones *Trem2*$^{-/-}$, lo cual está asociado también con una mayor respuesta a inmunoterapia y abriendo así un nuevo abanico de posibilidades de tratamiento immuno-incológico (365, 366)

Por lo tanto, es preciso esclarecer en detalle el papel del receptor TREM2 en las distintas poblaciones del hígado en distintos contextos de enfermedad con el objetivo de determinar los beneficios de la regulación de este receptor como nueva estrategia terapéutica.

CONCLUSIONES

1. La expresión de TREM2 esta aumentada en el tejido hepático de pacientes con PBC y PSC en comparación a tejido hepático de individuos sanos o pacientes con cirrosis.

2. La expresión de TREM2 correlaciona positivamente con la expresión de marcadores inflamatorios y fibróticos en el hígado de pacientes con enfermedades colesetaticas, como PBC y PSC.

3. En el hígado de pacientes con PBC, la expresión de TREM2 también correlaciona positivamente con marcadores serológicos de daño hepático así como con los valores de una escala de puntuación que determina el grado de progresión de las enfermedades hepáticas.

4. En el hígado de ratones sanos, Trem2 se expresa mínimamente en las poblaciones epiteliales (hepatocitos y colangiocitos), mientras que su expresión es prominente en las células no parenquimales tales como KCs y HSCs.

5. La expresión hepática de *Trem2* se induce en modelos experimentales de cholestasis de diversos orígenes en comparación a condiciones control.

6. Los ratones *Trem2*$^{-/-}$ presentan una respuesta exacerbada en un modelo de daño hepático inducido por colestasis basado en el BDL, y esta respuesta se caracteriza por un aumento en la expansión biliar, inflamación y mayor muerte celular.

7. La respuesta exacerbada detectada en ratones *Trem2*$^{-/-}$ en el modelo de BDL se asocia con mayores niveles de inflamación y reclutamiento de neutrófilos al hígado de estos ratones.

8. Los ratones *Trem2*$^{-/-}$ muestran una alteración basal del metabolismo de BAs en el hígado, caracterizada por una menor concentración de BAs en el hígado y una tendencia a cambios de expresión de genes involucrados en el metabolismo de BAs.

9. El tratamiento con Abx rescata algunas de las diferencias observadas entre ratones WT y *Trem2*$^{-/-}$ tras BDL. Por lo tanto, parte de los efectos protectores de TREM2 en la colestasis obstructiva son parcialmente mediados por la señalización de productos bacterianos translocados mediante el eje intestino-hígado.

10. TREM2 también cumple un papel protector en un modelo de colestasis inducida químicamente basado en la administración de ANIT. Así, ratones *Trem2*$^{-/-}$ muestran mayores niveles de muerte celular e inflamación.

11. El tratamiento con UDCA reduce la expresión de *Trem1* mientras que aumenta la de *Trem2* en KCs aisladas de ratón.

12. El tratamiento con UDCA disminuye los efectos inducidos por LPS en KCs. En este sentido, el UDCA disminuyó la expresión de *Trem1* mientras que aumentó la de *Trem2* en comparación a células incubadas únicamente con LPS.

13. El tratamiento con UDCA disminuye la expresión de *Il6, Tnf* y *Cxcl1* en KCs aisladas de ratón mediante un mecanismo dependiente de *Trem2*.

14. *TREM2* se expresa en TAMs residentes y reclutados en tumores de HCC.

15. Los TAMs que expresan *TREM2* también se caracterizan por la expresión de CD68 y CD9, así como por el enriquecimiento en la expresión de genes asociados a la señalización mediada por TLR y a lisosomas.

16. TREM2 protege al hígado de la hepatocarcinogénesis asociada a fibrosis, lo cual se ve asociado con una menor expresión de marcadores proliferativos y mayor fibrosis hepática.

En conclusión, TREM2 se erige como un nuevo regulador negativo de la inflamación en situaciones de colestasis y también juega un papel protector en hepatocarcinogénesis

asociada a fibrosis. En consecuencia, la activación de TREM2 podría representar una prometedora estrategia terapéutica para los pacientes con colestasis. No obstante, pese a que la activación de TREM2 podría prevenir el daño hepático por colestasis y también la hepatocarcinogenesis, también podría estar asociado con efectos contraproducentes en la fibrosis hepática y la regulación de respuestas de la inmunidad innata contra el crecimiento tumoral.

REFERENCES

1. Juza RM, Pauli EM. Clinical and surgical anatomy of the liver: a review for clinicians. Clinical anatomy. 2014;27(5):764-9.
2. Racanelli V, Rehermann B. The liver as an immunological organ. Hepatology. 2006;43(2 Suppl 1):S54-62.
3. Miyajima A, Tanaka M, Itoh T. Stem/progenitor cells in liver development, homeostasis, regeneration, and reprogramming. Cell stem cell. 2014;14(5):561-74.
4. Gebhardt R, Matz-Soja M. Liver zonation: Novel aspects of its regulation and its impact on homeostasis. World journal of gastroenterology. 2014;20(26):8491-504.
5. Banales JM, Prieto J, Medina JF. Cholangiocyte anion exchange and biliary bicarbonate excretion. World journal of gastroenterology. 2006;12(22):3496-511.
6. Banales JM, Huebert RC, Karlsen T, Strazzabosco M, LaRusso NF, Gores GJ. Cholangiocyte pathobiology. Nature reviews Gastroenterology & hepatology. 2019;16(5):269-81.
7. Masyuk AI, Masyuk TV, LaRusso NF. Cholangiocyte primary cilia in liver health and disease. Developmental dynamics : an official publication of the American Association of Anatomists. 2008;237(8):2007-12.
8. Boyer JL. Bile formation and secretion. Comprehensive Physiology. 2013;3(3):1035-78.
9. Russell DW. The enzymes, regulation, and genetics of bile acid synthesis. Annual review of biochemistry. 2003;72:137-74.
10. Marin JJ, Macias RI, Briz O, Banales JM, Monte MJ. Bile Acids in Physiology, Pathology and Pharmacology. Current drug metabolism. 2015;17(1):4-29.
11. de Aguiar Vallim TQ, Tarling EJ, Edwards PA. Pleiotropic roles of bile acids in metabolism. Cell metabolism. 2013;17(5):657-69.
12. Li J, Dawson PA. Animal models to study bile acid metabolism. Biochimica et biophysica acta Molecular basis of disease. 2019;1865(5):895-911.
13. Qi Y, Jiang C, Cheng J, Krausz KW, Li T, Ferrell JM, et al. Bile acid signaling in lipid metabolism: metabolomic and lipidomic analysis of lipid and bile acid markers linked to anti-obesity and anti-diabetes in mice. Biochimica et biophysica acta. 2015;1851(1):19-29.
14. Saxena R, Theise N. Canals of Hering: recent insights and current knowledge. Seminars in liver disease. 2004;24(1):43-8.
15. Roskams TA, Theise ND, Balabaud C, Bhagat G, Bhathal PS, Bioulac-Sage P, et al. Nomenclature of the finer branches of the biliary tree: canals, ductules, and ductular reactions in human livers. Hepatology. 2004;39(6):1739-45.
16. Tabibian JH, Masyuk AI, Masyuk TV, O'Hara SP, LaRusso NF. Physiology of cholangiocytes. Comprehensive Physiology. 2013;3(1):541-65.
17. Hofmann AF. The enterohepatic circulation of bile acids in mammals: form and functions. Frontiers in bioscience. 2009;14:2584-98.
18. Hofmann AF, Hagey LR. Bile acids: chemistry, pathochemistry, biology, pathobiology, and therapeutics. Cellular and molecular life sciences : CMLS. 2008;65(16):2461-83.
19. Chen ML, Takeda K, Sundrud MS. Emerging roles of bile acids in mucosal immunity and inflammation. Mucosal immunology. 2019;12(4):851-61.
20. Halilbasic E, Fiorotto R, Fickert P, Marschall HU, Moustafa T, Spirli C, et al. Side chain structure determines unique physiologic and therapeutic properties of norursodeoxycholic acid in Mdr2-/- mice. Hepatology. 2009;49(6):1972-81.
21. Halilbasic E, Claudel T, Trauner M. Bile acid transporters and regulatory nuclear receptors in the liver and beyond. Journal of hepatology. 2013;58(1):155-68.
22. Beuers U, Trauner M, Jansen P, Poupon R. New paradigms in the treatment of hepatic cholestasis: from UDCA to FXR, PXR and beyond. Journal of hepatology. 2015;62(1 Suppl):S25-37.
23. Inagaki T, Choi M, Moschetta A, Peng L, Cummins CL, McDonald JG, et al. Fibroblast growth factor 15 functions as an enterohepatic signal to regulate bile acid homeostasis. Cell metabolism. 2005;2(4):217-25.

24. Modica S, Petruzzelli M, Bellafante E, Murzilli S, Salvatore L, Celli N, et al. Selective activation of nuclear bile acid receptor FXR in the intestine protects mice against cholestasis. Gastroenterology. 2012;142(2):355-65 e1-4.
25. Degirolamo C, Modica S, Vacca M, Di Tullio G, Morgano A, D'Orazio A, et al. Prevention of spontaneous hepatocarcinogenesis in farnesoid X receptor-null mice by intestinal-specific farnesoid X receptor reactivation. Hepatology. 2015;61(1):161-70.
26. Shapiro H, Kolodziejczyk AA, Halstuch D, Elinav E. Bile acids in glucose metabolism in health and disease. The Journal of experimental medicine. 2018;215(2):383-96.
27. Pellicoro A, Ramachandran P, Iredale JP, Fallowfield JA. Liver fibrosis and repair: immune regulation of wound healing in a solid organ. Nature reviews Immunology. 2014;14(3):181-94.
28. Krenkel O, Tacke F. Liver macrophages in tissue homeostasis and disease. Nature reviews Immunology. 2017;17(5):306-21.
29. Scott CL, Zheng F, De Baetselier P, Martens L, Saeys Y, De Prijck S, et al. Bone marrow-derived monocytes give rise to self-renewing and fully differentiated Kupffer cells. Nature communications. 2016;7:10321.
30. Ingersoll MA, Spanbroek R, Lottaz C, Gautier EL, Frankenberger M, Hoffmann R, et al. Comparison of gene expression profiles between human and mouse monocyte subsets. Blood. 2010;115(3):e10-9.
31. Bogdanos DP, Gao B, Gershwin ME. Liver immunology. Comprehensive Physiology. 2013;3(2):567-98.
32. Jenne CN, Kubes P. Immune surveillance by the liver. Nature immunology. 2013;14(10):996-1006.
33. Thomson AW, Knolle PA. Antigen-presenting cell function in the tolerogenic liver environment. Nature reviews Immunology. 2010;10(11):753-66.
34. Heymann F, Peusquens J, Ludwig-Portugall I, Kohlhepp M, Ergen C, Niemietz P, et al. Liver inflammation abrogates immunological tolerance induced by Kupffer cells. Hepatology. 2015;62(1):279-91.
35. Willekens FL, Werre JM, Kruijt JK, Roerdinkholder-Stoelwinder B, Groenen-Dopp YA, van den Bos AG, et al. Liver Kupffer cells rapidly remove red blood cell-derived vesicles from the circulation by scavenger receptors. Blood. 2005;105(5):2141-5.
36. Kristiansen M, Graversen JH, Jacobsen C, Sonne O, Hoffman HJ, Law SK, et al. Identification of the haemoglobin scavenger receptor. Nature. 2001;409(6817):198-201.
37. Bieghs V, Verheyen F, van Gorp PJ, Hendrikx T, Wouters K, Lutjohann D, et al. Internalization of modified lipids by CD36 and SR-A leads to hepatic inflammation and lysosomal cholesterol storage in Kupffer cells. PloS one. 2012;7(3):e34378.
38. Wang Y, van der Tuin S, Tjeerdema N, van Dam AD, Rensen SS, Hendrikx T, et al. Plasma cholesteryl ester transfer protein is predominantly derived from Kupffer cells. Hepatology. 2015;62(6):1710-22.
39. Heymann F, Tacke F. Immunology in the liver--from homeostasis to disease. Nature reviews Gastroenterology & hepatology. 2016;13(2):88-110.
40. Li P, He K, Li J, Liu Z, Gong J. The role of Kupffer cells in hepatic diseases. Molecular immunology. 2017;85:222-9.
41. Theurl I, Hilgendorf I, Nairz M, Tymoszuk P, Haschka D, Asshoff M, et al. On-demand erythrocyte disposal and iron recycling requires transient macrophages in the liver. Nature medicine. 2016;22(8):945-51.
42. Tacke F, Zimmermann HW. Macrophage heterogeneity in liver injury and fibrosis. Journal of hepatology. 2014;60(5):1090-6.
43. Liaskou E, Zimmermann HW, Li KK, Oo YH, Suresh S, Stamataki Z, et al. Monocyte subsets in human liver disease show distinct phenotypic and functional characteristics. Hepatology. 2013;57(1):385-98.

44. Puche JE, Saiman Y, Friedman SL. Hepatic stellate cells and liver fibrosis. Comprehensive Physiology. 2013;3(4):1473-92.
45. Friedman SL. Evolving challenges in hepatic fibrosis. Nature reviews Gastroenterology & hepatology. 2010;7(8):425-36.
46. Xu J, Liu X, Koyama Y, Wang P, Lan T, Kim IG, et al. The types of hepatic myofibroblasts contributing to liver fibrosis of different etiologies. Frontiers in pharmacology. 2014;5:167.
47. Mederacke I, Hsu CC, Troeger JS, Huebener P, Mu X, Dapito DH, et al. Fate tracing reveals hepatic stellate cells as dominant contributors to liver fibrosis independent of its aetiology. Nature communications. 2013;4:2823.
48. Taura K, Miura K, Iwaisako K, Osterreicher CH, Kodama Y, Penz-Osterreicher M, et al. Hepatocytes do not undergo epithelial-mesenchymal transition in liver fibrosis in mice. Hepatology. 2010;51(3):1027-36.
49. Scholten D, Osterreicher CH, Scholten A, Iwaisako K, Gu G, Brenner DA, et al. Genetic labeling does not detect epithelial-to-mesenchymal transition of cholangiocytes in liver fibrosis in mice. Gastroenterology. 2010;139(3):987-98.
50. Chu AS, Diaz R, Hui JJ, Yanger K, Zong Y, Alpini G, et al. Lineage tracing demonstrates no evidence of cholangiocyte epithelial-to-mesenchymal transition in murine models of hepatic fibrosis. Hepatology. 2011;53(5):1685-95.
51. Tsuchida T, Friedman SL. Mechanisms of hepatic stellate cell activation. Nature reviews Gastroenterology & hepatology. 2017;14(7):397-411.
52. Friedman SL. Hepatic stellate cells: protean, multifunctional, and enigmatic cells of the liver. Physiological reviews. 2008;88(1):125-72.
53. Wallace MC, Friedman SL, Mann DA. Emerging and disease-specific mechanisms of hepatic stellate cell activation. Seminars in liver disease. 2015;35(2):107-18.
54. Canbay A, Taimr P, Torok N, Higuchi H, Friedman S, Gores GJ. Apoptotic body engulfment by a human stellate cell line is profibrogenic. Laboratory investigation; a journal of technical methods and pathology. 2003;83(5):655-63.
55. Zhan SS, Jiang JX, Wu J, Halsted C, Friedman SL, Zern MA, et al. Phagocytosis of apoptotic bodies by hepatic stellate cells induces NADPH oxidase and is associated with liver fibrosis in vivo. Hepatology. 2006;43(3):435-43.
56. Henderson NC, Arnold TD, Katamura Y, Giacomini MM, Rodriguez JD, McCarty JH, et al. Targeting of alphav integrin identifies a core molecular pathway that regulates fibrosis in several organs. Nature medicine. 2013;19(12):1617-24.
57. Olaso E, Ikeda K, Eng FJ, Xu L, Wang LH, Lin HC, et al. DDR2 receptor promotes MMP-2-mediated proliferation and invasion by hepatic stellate cells. The Journal of clinical investigation. 2001;108(9):1369-78.
58. Seki E, De Minicis S, Osterreicher CH, Kluwe J, Osawa Y, Brenner DA, et al. TLR4 enhances TGF-beta signaling and hepatic fibrosis. Nature medicine. 2007;13(11):1324-32.
59. Krizhanovsky V, Yon M, Dickins RA, Hearn S, Simon J, Miething C, et al. Senescence of activated stellate cells limits liver fibrosis. Cell. 2008;134(4):657-67.
60. Kisseleva T, Cong M, Paik Y, Scholten D, Jiang C, Benner C, et al. Myofibroblasts revert to an inactive phenotype during regression of liver fibrosis. Proceedings of the National Academy of Sciences of the United States of America. 2012;109(24):9448-53.
61. Troeger JS, Mederacke I, Gwak GY, Dapito DH, Mu X, Hsu CC, et al. Deactivation of hepatic stellate cells during liver fibrosis resolution in mice. Gastroenterology. 2012;143(4):1073-83 e22.
62. Van Haele M, Snoeck J, Roskams T. Human Liver Regeneration: An Etiology Dependent Process. International journal of molecular sciences. 2019;20(9).
63. Sebastiani G, Gkouvatsos K, Pantopoulos K. Chronic hepatitis C and liver fibrosis. World journal of gastroenterology. 2014;20(32):11033-53.

64. Suhail M, Abdel-Hafiz H, Ali A, Fatima K, Damanhouri GA, Azhar E, et al. Potential mechanisms of hepatitis B virus induced liver injury. World journal of gastroenterology. 2014;20(35):12462-72.
65. Osna NA, Donohue TM, Jr., Kharbanda KK. Alcoholic Liver Disease: Pathogenesis and Current Management. Alcohol research : current reviews. 2017;38(2):147-61.
66. Younossi Z, Anstee QM, Marietti M, Hardy T, Henry L, Eslam M, et al. Global burden of NAFLD and NASH: trends, predictions, risk factors and prevention. Nature reviews Gastroenterology & hepatology. 2018;15(1):11-20.
67. Tujios S, Fontana RJ. Mechanisms of drug-induced liver injury: from bedside to bench. Nature reviews Gastroenterology & hepatology. 2011;8(4):202-11.
68. Brissot P, Pietrangelo A, Adams PC, de Graaff B, McLaren CE, Loreal O. Haemochromatosis. Nature reviews Disease primers. 2018;4:18016.
69. Bray F, Ferlay J, Soerjomataram I, Siegel RL, Torre LA, Jemal A. Global cancer statistics 2018: GLOBOCAN estimates of incidence and mortality worldwide for 36 cancers in 185 countries. CA: a cancer journal for clinicians. 2018;68(6):394-424.
70. Younossi ZM, Koenig AB, Abdelatif D, Fazel Y, Henry L, Wymer M. Global epidemiology of nonalcoholic fatty liver disease-Meta-analytic assessment of prevalence, incidence, and outcomes. Hepatology. 2016;64(1):73-84.
71. Lazaridis KN, Strazzabosco M, Larusso NF. The cholangiopathies: disorders of biliary epithelia. Gastroenterology. 2004;127(5):1565-77.
72. Cheung AC, Lorenzo Pisarello MJ, LaRusso NF. Pathobiology of biliary epithelia. Biochimica et biophysica acta Molecular basis of disease. 2018;1864(4 Pt B):1220-31.
73. Lazaridis KN, LaRusso NF. The Cholangiopathies. Mayo Clinic proceedings. 2015;90(6):791-800.
74. Karlsen TH, Vesterhus M, Boberg KM. Review article: controversies in the management of primary biliary cirrhosis and primary sclerosing cholangitis. Alimentary pharmacology & therapeutics. 2014;39(3):282-301.
75. Trauner M, Meier PJ, Boyer JL. Molecular pathogenesis of cholestasis. The New England journal of medicine. 1998;339(17):1217-27.
76. de Vries E, Beuers U. Management of cholestatic disease in 2017. Liver international : official journal of the International Association for the Study of the Liver. 2017;37 Suppl 1:123-9.
77. Griffiths L, Dyson JK, Jones DE. The new epidemiology of primary biliary cirrhosis. Seminars in liver disease. 2014;34(3):318-28.
78. Surh CD, Coppel R, Gershwin ME. Structural requirement for autoreactivity on human pyruvate dehydrogenase-E2, the major autoantigen of primary biliary cirrhosis. Implication for a conformational autoepitope. Journal of immunology. 1990;144(9):3367-74.
79. Lindor KD, Gershwin ME, Poupon R, Kaplan M, Bergasa NV, Heathcote EJ, et al. Primary biliary cirrhosis. Hepatology. 2009;50(1):291-308.
80. Rodrigues PM, Perugorria MJ, Santos-Laso A, Bujanda L, Beuers U, Banales JM. Primary biliary cholangitis: A tale of epigenetically-induced secretory failure? Journal of hepatology. 2018;69(6):1371-83.
81. Gulamhusein AF, Hirschfield GM. Primary biliary cholangitis: pathogenesis and therapeutic opportunities. Nature reviews Gastroenterology & hepatology. 2020;17(2):93-110.
82. Kita H, Lian ZX, Van de Water J, He XS, Matsumura S, Kaplan M, et al. Identification of HLA-A2-restricted CD8(+) cytotoxic T cell responses in primary biliary cirrhosis: T cell activation is augmented by immune complexes cross-presented by dendritic cells. The Journal of experimental medicine. 2002;195(1):113-23.
83. Shimoda S, Miyakawa H, Nakamura M, Ishibashi H, Kikuchi K, Kita H, et al. CD4 T-cell autoreactivity to the mitochondrial autoantigen PDC-E2 in AMA-negative primary biliary cirrhosis. Journal of autoimmunity. 2008;31(2):110-5.

84. Bettelli E, Oukka M, Kuchroo VK. T(H)-17 cells in the circle of immunity and autoimmunity. Nature immunology. 2007;8(4):345-50.
85. Banales JM, Saez E, Uriz M, Sarvide S, Urribarri AD, Splinter P, et al. Up-regulation of microRNA 506 leads to decreased Cl-/HCO3- anion exchanger 2 expression in biliary epithelium of patients with primary biliary cirrhosis. Hepatology. 2012;56(2):687-97.
86. Mao TK, Lian ZX, Selmi C, Ichiki Y, Ashwood P, Ansari AA, et al. Altered monocyte responses to defined TLR ligands in patients with primary biliary cirrhosis. Hepatology. 2005;42(4):802-8.
87. Zhao J, Zhao S, Zhou G, Liang L, Guo X, Mao P, et al. Altered biliary epithelial cell and monocyte responses to lipopolysaccharide as a TLR ligand in patients with primary biliary cirrhosis. Scandinavian journal of gastroenterology. 2011;46(4):485-94.
88. Molodecky NA, Kareemi H, Parab R, Barkema HW, Quan H, Myers RP, et al. Incidence of primary sclerosing cholangitis: a systematic review and meta-analysis. Hepatology. 2011;53(5):1590-9.
89. Jepsen P, Gronbaek L, Vilstrup H. Worldwide Incidence of Autoimmune Liver Disease. Digestive diseases. 2015;33 Suppl 2:2-12.
90. Tanaka A, Takikawa H. Geoepidemiology of primary sclerosing cholangitis: a critical review. Journal of autoimmunity. 2013;46:35-40.
91. Karlsen TH, Folseraas T, Thorburn D, Vesterhus M. Primary sclerosing cholangitis - a comprehensive review. Journal of hepatology. 2017;67(6):1298-323.
92. Chung BK, Karlsen TH, Folseraas T. Cholangiocytes in the pathogenesis of primary sclerosing cholangitis and development of cholangiocarcinoma. Biochimica et biophysica acta Molecular basis of disease. 2018;1864(4 Pt B):1390-400.
93. Liu JZ, Hov JR, Folseraas T, Ellinghaus E, Rushbrook SM, Doncheva NT, et al. Dense genotyping of immune-related disease regions identifies nine new risk loci for primary sclerosing cholangitis. Nature genetics. 2013;45(6):670-5.
94. Ji SG, Juran BD, Mucha S, Folseraas T, Jostins L, Melum E, et al. Genome-wide association study of primary sclerosing cholangitis identifies new risk loci and quantifies the genetic relationship with inflammatory bowel disease. Nature genetics. 2017;49(2):269-73.
95. Sabino J, Vieira-Silva S, Machiels K, Joossens M, Falony G, Ballet V, et al. Primary sclerosing cholangitis is characterised by intestinal dysbiosis independent from IBD. Gut. 2016;65(10):1681-9.
96. Alvaro D, Gigliozzi A, Attili AF. Regulation and deregulation of cholangiocyte proliferation. Journal of hepatology. 2000;33(2):333-40.
97. Lemoinne S, Cadoret A, Rautou PE, El Mourabit H, Ratziu V, Corpechot C, et al. Portal myofibroblasts promote vascular remodeling underlying cirrhosis formation through the release of microparticles. Hepatology. 2015;61(3):1041-55.
98. Dyson JK, Hirschfield GM, Adams DH, Beuers U, Mann DA, Lindor KD, et al. Novel therapeutic targets in primary biliary cirrhosis. Nature reviews Gastroenterology & hepatology. 2015;12(3):147-58.
99. Beuers U, Boyer JL, Paumgartner G. Ursodeoxycholic acid in cholestasis: potential mechanisms of action and therapeutic applications. Hepatology. 1998;28(6):1449-53.
100. Rodrigues CM, Fan G, Ma X, Kren BT, Steer CJ. A novel role for ursodeoxycholic acid in inhibiting apoptosis by modulating mitochondrial membrane perturbation. The Journal of clinical investigation. 1998;101(12):2790-9.
101. Takigawa T, Miyazaki H, Kinoshita M, Kawarabayashi N, Nishiyama K, Hatsuse K, et al. Glucocorticoid receptor-dependent immunomodulatory effect of ursodeoxycholic acid on liver lymphocytes in mice. American journal of physiology Gastrointestinal and liver physiology. 2013;305(6):G427-38.
102. Carbone M, Mells GF, Pells G, Dawwas MF, Newton JL, Heneghan MA, et al. Sex and age are determinants of the clinical phenotype of primary biliary cirrhosis and response to ursodeoxycholic acid. Gastroenterology. 2013;144(3):560-9 e7; quiz e13-4.

103. Beuers U, Spengler U, Kruis W, Aydemir U, Wiebecke B, Heldwein W, et al. Ursodeoxycholic acid for treatment of primary sclerosing cholangitis: a placebo-controlled trial. Hepatology. 1992;16(3):707-14.
104. Lindor KD, Kowdley KV, Luketic VA, Harrison ME, McCashland T, Befeler AS, et al. High-dose ursodeoxycholic acid for the treatment of primary sclerosing cholangitis. Hepatology. 2009;50(3):808-14.
105. Wiencke K, Boberg KM. Current consensus on the management of primary sclerosing cholangitis. Clinics and research in hepatology and gastroenterology. 2011;35(12):786-91.
106. Pellicciari R, Fiorucci S, Camaioni E, Clerici C, Costantino G, Maloney PR, et al. 6alpha-ethyl-chenodeoxycholic acid (6-ECDCA), a potent and selective FXR agonist endowed with anticholestatic activity. Journal of medicinal chemistry. 2002;45(17):3569-72.
107. Hirschfield GM, Mason A, Luketic V, Lindor K, Gordon SC, Mayo M, et al. Efficacy of obeticholic acid in patients with primary biliary cirrhosis and inadequate response to ursodeoxycholic acid. Gastroenterology. 2015;148(4):751-61 e8.
108. Nevens F, Andreone P, Mazzella G, Strasser SI, Bowlus C, Invernizzi P, et al. A Placebo-Controlled Trial of Obeticholic Acid in Primary Biliary Cholangitis. The New England journal of medicine. 2016;375(7):631-43.
109. Goldstein J, Levy C. Novel and emerging therapies for cholestatic liver diseases. Liver international : official journal of the International Association for the Study of the Liver. 2018;38(9):1520-35.
110. Schwabe RF, Luedde T. Apoptosis and necroptosis in the liver: a matter of life and death. Nature reviews Gastroenterology & hepatology. 2018;15(12):738-52.
111. Luedde T, Kaplowitz N, Schwabe RF. Cell death and cell death responses in liver disease: mechanisms and clinical relevance. Gastroenterology. 2014;147(4):765-83 e4.
112. Taub R. Liver regeneration: from myth to mechanism. Nature reviews Molecular cell biology. 2004;5(10):836-47.
113. Sasaki M, Nakanuma Y. Stress-induced cellular responses and cell death mechanisms during inflammatory cholangiopathies. Clinics and research in hepatology and gastroenterology. 2017;41(2):129-38.
114. Borchers AT, Shimoda S, Bowlus C, Keen CL, Gershwin ME. Lymphocyte recruitment and homing to the liver in primary biliary cirrhosis and primary sclerosing cholangitis. Seminars in immunopathology. 2009;31(3):309-22.
115. Faubion WA, Guicciardi ME, Miyoshi H, Bronk SF, Roberts PJ, Svingen PA, et al. Toxic bile salts induce rodent hepatocyte apoptosis via direct activation of Fas. The Journal of clinical investigation. 1999;103(1):137-45.
116. Rust C, Wild N, Bernt C, Vennegeerts T, Wimmer R, Beuers U. Bile acid-induced apoptosis in hepatocytes is caspase-6-dependent. The Journal of biological chemistry. 2009;284(5):2908-16.
117. Woolbright BL, Jaeschke H. Inflammation and Cell Death During Cholestasis: The Evolving Role of Bile Acids. Gene expression. 2019;19(3):215-28.
118. Fickert P, Wagner M. Biliary bile acids in hepatobiliary injury - What is the link? Journal of hepatology. 2017;67(3):619-31.
119. Li M, Cai SY, Boyer JL. Mechanisms of bile acid mediated inflammation in the liver. Molecular aspects of medicine. 2017;56:45-53.
120. Pinzani M, Luong TV. Pathogenesis of biliary fibrosis. Biochimica et biophysica acta Molecular basis of disease. 2018;1864(4 Pt B):1279-83.
121. Allen K, Jaeschke H, Copple BL. Bile acids induce inflammatory genes in hepatocytes: a novel mechanism of inflammation during obstructive cholestasis. The American journal of pathology. 2011;178(1):175-86.
122. Cai SY, Ouyang X, Chen Y, Soroka CJ, Wang J, Mennone A, et al. Bile acids initiate cholestatic liver injury by triggering a hepatocyte-specific inflammatory response. JCI insight. 2017;2(5):e90780.

123. Wen Y, Jeong S, Xia Q, Kong X. Role of Osteopontin in Liver Diseases. International journal of biological sciences. 2016;12(9):1121-8.
124. Reich M, Deutschmann K, Sommerfeld A, Klindt C, Kluge S, Kubitz R, et al. TGR5 is essential for bile acid-dependent cholangiocyte proliferation in vivo and in vitro. Gut. 2016;65(3):487-501.
125. Gujral JS, Farhood A, Bajt ML, Jaeschke H. Neutrophils aggravate acute liver injury during obstructive cholestasis in bile duct-ligated mice. Hepatology. 2003;38(2):355-63.
126. Kodali P, Wu P, Lahiji PA, Brown EJ, Maher JJ. ANIT toxicity toward mouse hepatocytes in vivo is mediated primarily by neutrophils via CD18. American journal of physiology Gastrointestinal and liver physiology. 2006;291(2):G355-63.
127. Cai SY, Boyer JL. The Role of Inflammation in the Mechanisms of Bile Acid-Induced Liver Damage. Digestive diseases. 2017;35(3):232-4.
128. Gulubova MV. Intercellular adhesion molecule-1 (ICAM-1) expression in the liver of patients with extrahepatic cholestasis. Acta histochemica. 1998;100(1):59-74.
129. Gulubova M, Vlaykova T, Manolova I, Hadjipetkov P, Popharitov A. Implication of adhesion molecules in inflammation of the common bile duct in patients with secondary cholangitis due to biliary obstruction. Hepato-gastroenterology. 2008;55(84):836-41.
130. Crosby HA, Hubscher S, Fabris L, Joplin R, Sell S, Kelly D, et al. Immunolocalization of putative human liver progenitor cells in livers from patients with end-stage primary biliary cirrhosis and sclerosing cholangitis using the monoclonal antibody OV-6. The American journal of pathology. 1998;152(3):771-9.
131. Sato K, Marzioni M, Meng F, Francis H, Glaser S, Alpini G. Ductular Reaction in Liver Diseases: Pathological Mechanisms and Translational Significances. Hepatology. 2019;69(1):420-30.
132. Vartak N, Damle-Vartak A, Richter B, Dirsch O, Dahmen U, Hammad S, et al. Cholestasis-induced adaptive remodeling of interlobular bile ducts. Hepatology. 2016;63(3):951-64.
133. Gadd VL, Skoien R, Powell EE, Fagan KJ, Winterford C, Horsfall L, et al. The portal inflammatory infiltrate and ductular reaction in human nonalcoholic fatty liver disease. Hepatology. 2014;59(4):1393-405.
134. Lorenzini S, Bird TG, Boulter L, Bellamy C, Samuel K, Aucott R, et al. Characterisation of a stereotypical cellular and extracellular adult liver progenitor cell niche in rodents and diseased human liver. Gut. 2010;59(5):645-54.
135. Gouw AS, van den Heuvel MC, Boot M, Slooff MJ, Poppema S, de Jong KP. Dynamics of the vascular profile of the finer branches of the biliary tree in normal and diseased human livers. Journal of hepatology. 2006;45(3):393-400.
136. Fabris L, Spirli C, Cadamuro M, Fiorotto R, Strazzabosco M. Emerging concepts in biliary repair and fibrosis. American journal of physiology Gastrointestinal and liver physiology. 2017;313(2):G102-G16.
137. Scrushy M, O'Brien A, Glaser S. Recent advances in understanding bile duct remodeling and fibrosis. F1000Research. 2018;7.
138. Strazzabosco M, Fabris L. Development of the bile ducts: essentials for the clinical hepatologist. Journal of hepatology. 2012;56(5):1159-70.
139. Libbrecht L, Roskams T. Hepatic progenitor cells in human liver diseases. Seminars in cell & developmental biology. 2002;13(6):389-96.
140. Michalopoulos GK, Barua L, Bowen WC. Transdifferentiation of rat hepatocytes into biliary cells after bile duct ligation and toxic biliary injury. Hepatology. 2005;41(3):535-44.
141. Yovchev MI, Locker J, Oertel M. Biliary fibrosis drives liver repopulation and phenotype transition of transplanted hepatocytes. Journal of hepatology. 2016;64(6):1348-57.
142. Ader T, Norel R, Levoci L, Rogler LE. Transcriptional profiling implicates TGFbeta/BMP and Notch signaling pathways in ductular differentiation of fetal murine hepatoblasts. Mechanisms of development. 2006;123(2):177-94.

143. Apte U, Thompson MD, Cui S, Liu B, Cieply B, Monga SP. Wnt/beta-catenin signaling mediates oval cell response in rodents. Hepatology. 2008;47(1):288-95.
144. Rygiel KA, Robertson H, Marshall HL, Pekalski M, Zhao L, Booth TA, et al. Epithelial-mesenchymal transition contributes to portal tract fibrogenesis during human chronic liver disease. Laboratory investigation; a journal of technical methods and pathology. 2008;88(2):112-23.
145. Omenetti A, Porrello A, Jung Y, Yang L, Popov Y, Choi SS, et al. Hedgehog signaling regulates epithelial-mesenchymal transition during biliary fibrosis in rodents and humans. The Journal of clinical investigation. 2008;118(10):3331-42.
146. Fiorotto R, Raizner A, Morell CM, Torsello B, Scirpo R, Fabris L, et al. Notch signaling regulates tubular morphogenesis during repair from biliary damage in mice. Journal of hepatology. 2013;59(1):124-30.
147. Panciera T, Azzolin L, Cordenonsi M, Piccolo S. Mechanobiology of YAP and TAZ in physiology and disease. Nature reviews Molecular cell biology. 2017;18(12):758-70.
148. Ehrlich L, Scrushy M, Meng F, Lairmore TC, Alpini G, Glaser S. Biliary epithelium: A neuroendocrine compartment in cholestatic liver disease. Clinics and research in hepatology and gastroenterology. 2018;42(4):296-305.
149. Marra F, DeFranco R, Grappone C, Milani S, Pastacaldi S, Pinzani M, et al. Increased expression of monocyte chemotactic protein-1 during active hepatic fibrogenesis: correlation with monocyte infiltration. The American journal of pathology. 1998;152(2):423-30.
150. Saito JM, Maher JJ. Bile duct ligation in rats induces biliary expression of cytokine-induced neutrophil chemoattractant. Gastroenterology. 2000;118(6):1157-68.
151. Sedlaczek N, Jia JD, Bauer M, Herbst H, Ruehl M, Hahn EG, et al. Proliferating bile duct epithelial cells are a major source of connective tissue growth factor in rat biliary fibrosis. The American journal of pathology. 2001;158(4):1239-44.
152. Zimmermann HW, Seidler S, Gassler N, Nattermann J, Luedde T, Trautwein C, et al. Interleukin-8 is activated in patients with chronic liver diseases and associated with hepatic macrophage accumulation in human liver fibrosis. PloS one. 2011;6(6):e21381.
153. Zweers SJ, Shiryaev A, Komuta M, Vesterhus M, Hov JR, Perugorria MJ, et al. Elevated interleukin-8 in bile of patients with primary sclerosing cholangitis. Liver international : official journal of the International Association for the Study of the Liver. 2016;36(9):1370-7.
154. Fabris L, Strazzabosco M. Epithelial-mesenchymal interactions in biliary diseases. Seminars in liver disease. 2011;31(1):11-32.
155. Medina J, Sanz-Cameno P, Garcia-Buey L, Martin-Vilchez S, Lopez-Cabrera M, Moreno-Otero R. Evidence of angiogenesis in primary biliary cirrhosis: an immunohistochemical descriptive study. Journal of hepatology. 2005;42(1):124-31.
156. Friedman SL. Mechanisms of hepatic fibrogenesis. Gastroenterology. 2008;134(6):1655-69.
157. Park SM. The crucial role of cholangiocytes in cholangiopathies. Gut and liver. 2012;6(3):295-304.
158. Lua I, Li Y, Zagory JA, Wang KS, French SW, Sevigny J, et al. Characterization of hepatic stellate cells, portal fibroblasts, and mesothelial cells in normal and fibrotic livers. Journal of hepatology. 2016;64(5):1137-46.
159. Carruthers JS, Kalifat SR, Steiner JW. The ductular cell reaction of rat liver in extrahepatic cholestasis. II. The proliferation of connective tissue. Experimental and molecular pathology. 1962;1:377-96.
160. Popper H, Uenfriend S. Hepatic fibrosis. Correlation of biochemical and morphologic investigations. The American journal of medicine. 1970;49:707-21.
161. Schaffner F, Barka T, Popper H. Hepatic Mesenchymal Cell Reaction in Liver Disease. Experimental and molecular pathology. 1963;2:419-41.
162. Kinnman N, Housset C. Peribiliary myofibroblasts in biliary type liver fibrosis. Frontiers in bioscience : a journal and virtual library. 2002;7:d496-503.

163. Matsumoto K, Fujii H, Michalopoulos G, Fung JJ, Demetris AJ. Human biliary epithelial cells secrete and respond to cytokines and hepatocyte growth factors in vitro: interleukin-6, hepatocyte growth factor and epidermal growth factor promote DNA synthesis in vitro. Hepatology. 1994;20(2):376-82.
164. Yasoshima M, Kono N, Sugawara H, Katayanagi K, Harada K, Nakanuma Y. Increased expression of interleukin-6 and tumor necrosis factor-alpha in pathologic biliary epithelial cells: in situ and culture study. Laboratory investigation; a journal of technical methods and pathology. 1998;78(1):89-100.
165. Kinnman N, Francoz C, Barbu V, Wendum D, Rey C, Hultcrantz R, et al. The myofibroblastic conversion of peribiliary fibrogenic cells distinct from hepatic stellate cells is stimulated by platelet-derived growth factor during liver fibrogenesis. Laboratory investigation; a journal of technical methods and pathology. 2003;83(2):163-73.
166. Kruglov EA, Nathanson RA, Nguyen T, Dranoff JA. Secretion of MCP-1/CCL2 by bile duct epithelia induces myofibroblastic transdifferentiation of portal fibroblasts. American journal of physiology Gastrointestinal and liver physiology. 2006;290(4):G765-71.
167. Pereira TA, Syn WK, Machado MV, Vidigal PV, Resende V, Voieta I, et al. Schistosome-induced cholangiocyte proliferation and osteopontin secretion correlate with fibrosis and portal hypertension in human and murine schistosomiasis mansoni. Clinical science. 2015;129(10):875-83.
168. Fiorucci S, Baldelli F. Farnesoid X receptor agonists in biliary tract disease. Current opinion in gastroenterology. 2009;25(3):252-9.
169. He Y, Wu GD, Sadahiro T, Noh SI, Wang H, Talavera D, et al. Interaction of CD44 and hyaluronic acid enhances biliary epithelial proliferation in cholestatic livers. American journal of physiology Gastrointestinal and liver physiology. 2008;295(2):G305-12.
170. Jung Y, McCall SJ, Li YX, Diehl AM. Bile ductules and stromal cells express hedgehog ligands and/or hedgehog target genes in primary biliary cirrhosis. Hepatology. 2007;45(5):1091-6.
171. Yang L, Wang Y, Mao H, Fleig S, Omenetti A, Brown KD, et al. Sonic hedgehog is an autocrine viability factor for myofibroblastic hepatic stellate cells. Journal of hepatology. 2008;48(1):98-106.
172. Tanaka A, Leung PS, Kenny TP, Au-Young J, Prindiville T, Coppel RL, et al. Genomic analysis of differentially expressed genes in liver and biliary epithelial cells of patients with primary biliary cirrhosis. Journal of autoimmunity. 2001;17(1):89-98.
173. Shackel NA, McGuinness PH, Abbott CA, Gorrell MD, McCaughan GW. Identification of novel molecules and pathogenic pathways in primary biliary cirrhosis: cDNA array analysis of intrahepatic differential gene expression. Gut. 2001;49(4):565-76.
174. Sackett SD, Gao Y, Shin S, Esterson YB, Tsingalia A, Hurtt RS, et al. Foxl1 promotes liver repair following cholestatic injury in mice. Laboratory investigation; a journal of technical methods and pathology. 2009;89(12):1387-96.
175. Monga SP. beta-Catenin Signaling and Roles in Liver Homeostasis, Injury, and Tumorigenesis. Gastroenterology. 2015;148(7):1294-310.
176. Glaser SS, Gaudio E, Miller T, Alvaro D, Alpini G. Cholangiocyte proliferation and liver fibrosis. Expert reviews in molecular medicine. 2009;11:e7.
177. Tsochatzis EA, Bosch J, Burroughs AK. Liver cirrhosis. Lancet. 2014;383(9930):1749-61.
178. Iwakiri Y. Pathophysiology of portal hypertension. Clinics in liver disease. 2014;18(2):281-91.
179. Poordad FF. Presentation and complications associated with cirrhosis of the liver. Current medical research and opinion. 2015;31(5):925-37.
180. Zhang DY, Friedman SL. Fibrosis-dependent mechanisms of hepatocarcinogenesis. Hepatology. 2012;56(2):769-75.
181. Adam R, Karam V, Cailliez V, JG OG, Mirza D, Cherqui D, et al. 2018 Annual Report of the European Liver Transplant Registry (ELTR) - 50-year evolution of liver transplantation.

Transplant international : official journal of the European Society for Organ Transplantation. 2018;31(12):1293-317.
182. Li T, Apte U. Bile Acid Metabolism and Signaling in Cholestasis, Inflammation, and Cancer. Advances in pharmacology. 2015;74:263-302.
183. Liang Y, Yang Z, Zhong R. Primary biliary cirrhosis and cancer risk: a systematic review and meta-analysis. Hepatology. 2012;56(4):1409-17.
184. Song J, Li Y, Bowlus CL, Yang G, Leung PSC, Gershwin ME. Cholangiocarcinoma in Patients with Primary Sclerosing Cholangitis (PSC): a Comprehensive Review. Clinical reviews in allergy & immunology. 2020;58(1):134-49.
185. Banales JM, Cardinale V, Carpino G, Marzioni M, Andersen JB, Invernizzi P, et al. Expert consensus document: Cholangiocarcinoma: current knowledge and future perspectives consensus statement from the European Network for the Study of Cholangiocarcinoma (ENS-CCA). Nature reviews Gastroenterology & hepatology. 2016;13(5):261-80.
186. Lleo A, de Boer YS, Liberal R, Colombo M. The risk of liver cancer in autoimmune liver diseases. Therapeutic advances in medical oncology. 2019;11:1758835919861914.
187. Choi J, Ghoz HM, Peeraphatdit T, Baichoo E, Addissie BD, Harmsen WS, et al. Aspirin use and the risk of cholangiocarcinoma. Hepatology. 2016;64(3):785-96.
188. Bergquist A, Ekbom A, Olsson R, Kornfeldt D, Loof L, Danielsson A, et al. Hepatic and extrahepatic malignancies in primary sclerosing cholangitis. Journal of hepatology. 2002;36(3):321-7.
189. Fattovich G, Stroffolini T, Zagni I, Donato F. Hepatocellular carcinoma in cirrhosis: incidence and risk factors. Gastroenterology. 2004;127(5 Suppl 1):S35-50.
190. Bertuccio P, Turati F, Carioli G, Rodriguez T, La Vecchia C, Malvezzi M, et al. Global trends and predictions in hepatocellular carcinoma mortality. Journal of hepatology. 2017;67(2):302-9.
191. Forner A, Reig M, Bruix J. Hepatocellular carcinoma. Lancet. 2018;391(10127):1301-14.
192. Llovet JM, Zucman-Rossi J, Pikarsky E, Sangro B, Schwartz M, Sherman M, et al. Hepatocellular carcinoma. Nature reviews Disease primers. 2016;2:16018.
193. Barash H, E RG, Edrei Y, Ella E, Israel A, Cohen I, et al. Accelerated carcinogenesis following liver regeneration is associated with chronic inflammation-induced double-strand DNA breaks. Proceedings of the National Academy of Sciences of the United States of America. 2010;107(5):2207-12.
194. Berasain C, Castillo J, Perugorria MJ, Latasa MU, Prieto J, Avila MA. Inflammation and liver cancer: new molecular links. Annals of the New York Academy of Sciences. 2009;1155:206-21.
195. Zucman-Rossi J, Villanueva A, Nault JC, Llovet JM. Genetic Landscape and Biomarkers of Hepatocellular Carcinoma. Gastroenterology. 2015;149(5):1226-39 e4.
196. Kelleher FC, Fennelly D, Rafferty M. Common critical pathways in embryogenesis and cancer. Acta oncologica. 2006;45(4):375-88.
197. Yang JD, Hainaut P, Gores GJ, Amadou A, Plymoth A, Roberts LR. A global view of hepatocellular carcinoma: trends, risk, prevention and management. Nature reviews Gastroenterology & hepatology. 2019;16(10):589-604.
198. Yang JD, Larson JJ, Watt KD, Allen AM, Wiesner RH, Gores GJ, et al. Hepatocellular Carcinoma Is the Most Common Indication for Liver Transplantation and Placement on the Waitlist in the United States. Clinical gastroenterology and hepatology : the official clinical practice journal of the American Gastroenterological Association. 2017;15(5):767-75 e3.
199. Shiina S, Sato K, Tateishi R, Shimizu M, Ohama H, Hatanaka T, et al. Percutaneous Ablation for Hepatocellular Carcinoma: Comparison of Various Ablation Techniques and Surgery. Canadian journal of gastroenterology & hepatology. 2018;2018:4756147.
200. Rimassa L, Pressiani T, Merle P. Systemic Treatment Options in Hepatocellular Carcinoma. Liver cancer. 2019;8(6):427-46.

201. Zhu AX, Kang YK, Yen CJ, Finn RS, Galle PR, Llovet JM, et al. Ramucirumab after sorafenib in patients with advanced hepatocellular carcinoma and increased alpha-fetoprotein concentrations (REACH-2): a randomised, double-blind, placebo-controlled, phase 3 trial. The Lancet Oncology. 2019;20(2):282-96.
202. Wiest R, Lawson M, Geuking M. Pathological bacterial translocation in liver cirrhosis. Journal of hepatology. 2014;60(1):197-209.
203. Balmer ML, Slack E, de Gottardi A, Lawson MA, Hapfelmeier S, Miele L, et al. The liver may act as a firewall mediating mutualism between the host and its gut commensal microbiota. Science translational medicine. 2014;6(237):237ra66.
204. Kummen M, Hov JR. The gut microbial influence on cholestatic liver disease. Liver international : official journal of the International Association for the Study of the Liver. 2019;39(7):1186-96.
205. Gupta H, Youn GS, Shin MJ, Suk KT. Role of Gut Microbiota in Hepatocarcinogenesis. Microorganisms. 2019;7(5).
206. Schwabe RF, Jobin C. The microbiome and cancer. Nature reviews Cancer. 2013;13(11):800-12.
207. Albillos A, de Gottardi A, Rescigno M. The gut-liver axis in liver disease: Pathophysiological basis for therapy. Journal of hepatology. 2020;72(3):558-77.
208. Beutler BA. TLRs and innate immunity. Blood. 2009;113(7):1399-407.
209. Kiziltas S. Toll-like receptors in pathophysiology of liver diseases. World journal of hepatology. 2016;8(32):1354-69.
210. Huebener P, Schwabe RF. Regulation of wound healing and organ fibrosis by toll-like receptors. Biochimica et biophysica acta. 2013;1832(7):1005-17.
211. Gabele E, Muhlbauer M, Dorn C, Weiss TS, Froh M, Schnabl B, et al. Role of TLR9 in hepatic stellate cells and experimental liver fibrosis. Biochemical and biophysical research communications. 2008;376(2):271-6.
212. Hartmann P, Haimerl M, Mazagova M, Brenner DA, Schnabl B. Toll-like receptor 2-mediated intestinal injury and enteric tumor necrosis factor receptor I contribute to liver fibrosis in mice. Gastroenterology. 2012;143(5):1330-40 e1.
213. Dapito DH, Mencin A, Gwak GY, Pradere JP, Jang MK, Mederacke I, et al. Promotion of hepatocellular carcinoma by the intestinal microbiota and TLR4. Cancer cell. 2012;21(4):504-16.
214. Rivera CA, Adegboyega P, van Rooijen N, Tagalicud A, Allman M, Wallace M. Toll-like receptor-4 signaling and Kupffer cells play pivotal roles in the pathogenesis of non-alcoholic steatohepatitis. Journal of hepatology. 2007;47(4):571-9.
215. Hua J, Qiu DK, Li JQ, Li EL, Chen XY, Peng YS. Expression of Toll-like receptor 4 in rat liver during the course of carbon tetrachloride-induced liver injury. Journal of gastroenterology and hepatology. 2007;22(6):862-9.
216. Pinero P, Juanola O, Caparros E, Zapater P, Gimenez P, Gonzalez-Navajas JM, et al. Toll-like receptor polymorphisms compromise the inflammatory response against bacterial antigen translocation in cirrhosis. Scientific reports. 2017;7:46425.
217. Seki E, Schnabl B. Role of innate immunity and the microbiota in liver fibrosis: crosstalk between the liver and gut. The Journal of physiology. 2012;590(3):447-58.
218. Verdier J, Luedde T, Sellge G. Biliary Mucosal Barrier and Microbiome. Viszeralmedizin. 2015;31(3):156-61.
219. Tang R, Wei Y, Li Y, Chen W, Chen H, Wang Q, et al. Gut microbial profile is altered in primary biliary cholangitis and partially restored after UDCA therapy. Gut. 2018;67(3):534-41.
220. Dhillon AK, Kummen M, Troseid M, Akra S, Liaskou E, Moum B, et al. Circulating markers of gut barrier function associated with disease severity in primary sclerosing cholangitis. Liver international : official journal of the International Association for the Study of the Liver. 2019;39(2):371-81.

221. Umemura T, Sekiguchi T, Joshita S, Yamazaki T, Fujimori N, Shibata S, et al. Association between serum soluble CD14 and IL-8 levels and clinical outcome in primary biliary cholangitis. Liver international : official journal of the International Association for the Study of the Liver. 2017;37(6):897-905.
222. Henao-Mejia J, Elinav E, Thaiss CA, Licona-Limon P, Flavell RA. Role of the intestinal microbiome in liver disease. Journal of autoimmunity. 2013;46:66-73.
223. Yu LX, Yan HX, Liu Q, Yang W, Wu HP, Dong W, et al. Endotoxin accumulation prevents carcinogen-induced apoptosis and promotes liver tumorigenesis in rodents. Hepatology. 2010;52(4):1322-33.
224. Jing YY, Han ZP, Sun K, Zhang SS, Hou J, Liu Y, et al. Toll-like receptor 4 signaling promotes epithelial-mesenchymal transition in human hepatocellular carcinoma induced by lipopolysaccharide. BMC medicine. 2012;10:98.
225. Yoshimoto S, Loo TM, Atarashi K, Kanda H, Sato S, Oyadomari S, et al. Obesity-induced gut microbial metabolite promotes liver cancer through senescence secretome. Nature. 2013;499(7456):97-101.
226. Yamada S, Takashina Y, Watanabe M, Nagamine R, Saito Y, Kamada N, et al. Bile acid metabolism regulated by the gut microbiota promotes non-alcoholic steatohepatitis-associated hepatocellular carcinoma in mice. Oncotarget. 2018;9(11):9925-39.
227. Nakamura K, Kageyama S, Ito T, Hirao H, Kadono K, Aziz A, et al. Antibiotic pretreatment alleviates liver transplant damage in mice and humans. The Journal of clinical investigation. 2019;129(8):3420-34.
228. Liu R, Kang JD, Sartor RB, Sikaroodi M, Fagan A, Gavis EA, et al. Neuroinflammation in Murine Cirrhosis Is Dependent on the Gut Microbiome and Is Attenuated by Fecal Transplant. Hepatology. 2020;71(2):611-26.
229. Bajaj JS, Salzman N, Acharya C, Takei H, Kakiyama G, Fagan A, et al. Microbial functional change is linked with clinical outcomes after capsular fecal transplant in cirrhosis. JCI insight. 2019;4(24).
230. Moratalla A, Caparros E, Juanola O, Portune K, Puig-Kroger A, Estrada-Capetillo L, et al. Bifidobacterium pseudocatenulatum CECT7765 induces an M2 anti-inflammatory transition in macrophages from patients with cirrhosis. Journal of hepatology. 2016;64(1):135-45.
231. Leifer CA, Medvedev AE. Molecular mechanisms of regulation of Toll-like receptor signaling. Journal of leukocyte biology. 2016;100(5):927-41.
232. Feng W, Gu YF, Nie L, Guo DY, Xiang LX, Shao JZ. Characterization of SIGIRR/IL-1R8 Homolog from Zebrafish Provides New Insights into Its Inhibitory Role in Hepatic Inflammation. Journal of immunology. 2016;197(1):151-67.
233. Sun YY, Fan YC, Wang N, Xia HH, Xiao XY, Wang K. Increased A20 mRNA Level in Peripheral Blood Mononuclear Cells is Associated With Immune Phases of Patients With Chronic Hepatitis B. Medicine. 2015;94(52):e2428.
234. Wang Y, Hu Y, Chao C, Yuksel M, Colle I, Flavell RA, et al. Role of IRAK-M in alcohol induced liver injury. PloS one. 2013;8(2):e57085.
235. Bouchon A, Dietrich J, Colonna M. Cutting edge: inflammatory responses can be triggered by TREM-1, a novel receptor expressed on neutrophils and monocytes. Journal of immunology. 2000;164(10):4991-5.
236. Paloneva J, Manninen T, Christman G, Hovanes K, Mandelin J, Adolfsson R, et al. Mutations in two genes encoding different subunits of a receptor signaling complex result in an identical disease phenotype. American journal of human genetics. 2002;71(3):656-62.
237. Pelham CJ, Agrawal DK. Emerging roles for triggering receptor expressed on myeloid cells receptor family signaling in inflammatory diseases. Expert review of clinical immunology. 2014;10(2):243-56.
238. Genua M, Rutella S, Correale C, Danese S. The triggering receptor expressed on myeloid cells (TREM) in inflammatory bowel disease pathogenesis. Journal of translational medicine. 2014;12:293.

239. Sharif O, Knapp S. From expression to signaling: roles of TREM-1 and TREM-2 in innate immunity and bacterial infection. Immunobiology. 2008;213(9-10):701-13.
240. Kober DL, Brett TJ. TREM2-Ligand Interactions in Health and Disease. Journal of molecular biology. 2017;429(11):1607-29.
241. Turnbull IR, Colonna M. Activating and inhibitory functions of DAP12. Nature reviews Immunology. 2007;7(2):155-61.
242. Ford JW, McVicar DW. TREM and TREM-like receptors in inflammation and disease. Current opinion in immunology. 2009;21(1):38-46.
243. Konishi H, Kiyama H. Microglial TREM2/DAP12 Signaling: A Double-Edged Sword in Neural Diseases. Frontiers in cellular neuroscience. 2018;12:206.
244. Bouchon A, Facchetti F, Weigand MA, Colonna M. TREM-1 amplifies inflammation and is a crucial mediator of septic shock. Nature. 2001;410(6832):1103-7.
245. Gibot S, Kolopp-Sarda MN, Bene MC, Bollaert PE, Lozniewski A, Mory F, et al. A soluble form of the triggering receptor expressed on myeloid cells-1 modulates the inflammatory response in murine sepsis. The Journal of experimental medicine. 2004;200(11):1419-26.
246. Netea MG, Azam T, Ferwerda G, Girardin SE, Kim SH, Dinarello CA. Triggering receptor expressed on myeloid cells-1 (TREM-1) amplifies the signals induced by the NACHT-LRR (NLR) pattern recognition receptors. Journal of leukocyte biology. 2006;80(6):1454-61.
247. Gibot S, Massin F, Marcou M, Taylor V, Stidwill R, Wilson P, et al. TREM-1 promotes survival during septic shock in mice. European journal of immunology. 2007;37(2):456-66.
248. Schenk M, Bouchon A, Seibold F, Mueller C. TREM-1--expressing intestinal macrophages crucially amplify chronic inflammation in experimental colitis and inflammatory bowel diseases. The Journal of clinical investigation. 2007;117(10):3097-106.
249. Zysset D, Weber B, Rihs S, Brasseit J, Freigang S, Riether C, et al. TREM-1 links dyslipidemia to inflammation and lipid deposition in atherosclerosis. Nature communications. 2016;7:13151.
250. Murakami Y, Akahoshi T, Aoki N, Toyomoto M, Miyasaka N, Kohsaka H. Intervention of an inflammation amplifier, triggering receptor expressed on myeloid cells 1, for treatment of autoimmune arthritis. Arthritis and rheumatism. 2009;60(6):1615-23.
251. Saurer L, Zysset D, Rihs S, Mager L, Gusberti M, Simillion C, et al. TREM-1 promotes intestinal tumorigenesis. Scientific reports. 2017;7(1):14870.
252. Sigalov AB. A novel ligand-independent peptide inhibitor of TREM-1 suppresses tumor growth in human lung cancer xenografts and prolongs survival of mice with lipopolysaccharide-induced septic shock. International immunopharmacology. 2014;21(1):208-19.
253. Chen LC, Laskin JD, Gordon MK, Laskin DL. Regulation of TREM expression in hepatic macrophages and endothelial cells during acute endotoxemia. Experimental and molecular pathology. 2008;84(2):145-55.
254. Liao R, Sun TW, Yi Y, Wu H, Li YW, Wang JX, et al. Expression of TREM-1 in hepatic stellate cells and prognostic value in hepatitis B-related hepatocellular carcinoma. Cancer science. 2012;103(6):984-92.
255. Duan M, Wang ZC, Wang XY, Shi JY, Yang LX, Ding ZB, et al. TREM-1, an inflammatory modulator, is expressed in hepatocellular carcinoma cells and significantly promotes tumor progression. Annals of surgical oncology. 2015;22(9):3121-9.
256. Hyun J, McMahon RS, Lang AL, Edwards JS, Badilla AD, Greene ME, et al. HIV and HCV augments inflammatory responses through increased TREM-1 expression and signaling in Kupffer and Myeloid cells. PLoS pathogens. 2019;15(7):e1007883.
257. Kozik JH, Trautmann T, Carambia A, Preti M, Lutgehetmann M, Krech T, et al. Attenuated viral hepatitis in Trem1-/- mice is associated with reduced inflammatory activity of neutrophils. Scientific reports. 2016;6:28556.
258. Tornai D, Furi I, Shen ZT, Sigalov AB, Coban S, Szabo G. Inhibition of Triggering Receptor Expressed on Myeloid Cells 1 Ameliorates Inflammation and Macrophage and Neutrophil Activation in Alcoholic Liver Disease in Mice. Hepatology communications. 2019;3(1):99-115.

259. Rao S, Huang J, Shen Z, Xiang C, Zhang M, Lu X. Inhibition of TREM-1 attenuates inflammation and lipid accumulation in diet-induced nonalcoholic fatty liver disease. Journal of cellular biochemistry. 2019.
260. Nguyen-Lefebvre AT, Ajith A, Portik-Dobos V, Horuzsko DD, Arbab AS, Dzutsev A, et al. The innate immune receptor TREM-1 promotes liver injury and fibrosis. The Journal of clinical investigation. 2018;128(11):4870-83.
261. Wu J, Li J, Salcedo R, Mivechi NF, Trinchieri G, Horuzsko A. The proinflammatory myeloid cell receptor TREM-1 controls Kupffer cell activation and development of hepatocellular carcinoma. Cancer research. 2012;72(16):3977-86.
262. Wu Q, Zhou W, Yin S, Zhou Y, Chen T, Qian J, et al. Blocking Triggering Receptor Expressed on Myeloid Cells-1-Positive Tumor-Associated Macrophages Induced by Hypoxia Reverses Immunosuppression and Anti-Programmed Cell Death Ligand 1 Resistance in Liver Cancer. Hepatology. 2019;70(1):198-214.
263. Cella M, Buonsanti C, Strader C, Kondo T, Salmaggi A, Colonna M. Impaired differentiation of osteoclasts in TREM-2-deficient individuals. The Journal of experimental medicine. 2003;198(4):645-51.
264. Turnbull IR, Gilfillan S, Cella M, Aoshi T, Miller M, Piccio L, et al. Cutting edge: TREM-2 attenuates macrophage activation. Journal of immunology. 2006;177(6):3520-4.
265. Hamerman JA, Jarjoura JR, Humphrey MB, Nakamura MC, Seaman WE, Lanier LL. Cutting edge: inhibition of TLR and FcR responses in macrophages by triggering receptor expressed on myeloid cells (TREM)-2 and DAP12. Journal of immunology. 2006;177(4):2051-5.
266. Jonsson T, Stefansson H, Steinberg S, Jonsdottir I, Jonsson PV, Snaedal J, et al. Variant of TREM2 associated with the risk of Alzheimer's disease. The New England journal of medicine. 2013;368(2):107-16.
267. Cady J, Koval ED, Benitez BA, Zaidman C, Jockel-Balsarotti J, Allred P, et al. TREM2 variant p.R47H as a risk factor for sporadic amyotrophic lateral sclerosis. JAMA neurology. 2014;71(4):449-53.
268. Borroni B, Ferrari F, Galimberti D, Nacmias B, Barone C, Bagnoli S, et al. Heterozygous TREM2 mutations in frontotemporal dementia. Neurobiology of aging. 2014;35(4):934 e7-10.
269. Wang Y, Cella M, Mallinson K, Ulrich JD, Young KL, Robinette ML, et al. TREM2 lipid sensing sustains the microglial response in an Alzheimer's disease model. Cell. 2015;160(6):1061-71.
270. Ulland TK, Song WM, Huang SC, Ulrich JD, Sergushichev A, Beatty WL, et al. TREM2 Maintains Microglial Metabolic Fitness in Alzheimer's Disease. Cell. 2017;170(4):649-63 e13.
271. Song WM, Joshita S, Zhou Y, Ulland TK, Gilfillan S, Colonna M. Humanized TREM2 mice reveal microglia-intrinsic and -extrinsic effects of R47H polymorphism. The Journal of experimental medicine. 2018;215(3):745-60.
272. N'Diaye EN, Branda CS, Branda SS, Nevarez L, Colonna M, Lowell C, et al. TREM-2 (triggering receptor expressed on myeloid cells 2) is a phagocytic receptor for bacteria. The Journal of cell biology. 2009;184(2):215-23.
273. Gawish R, Martins R, Bohm B, Wimberger T, Sharif O, Lakovits K, et al. Triggering receptor expressed on myeloid cells-2 fine-tunes inflammatory responses in murine Gram-negative sepsis. FASEB journal : official publication of the Federation of American Societies for Experimental Biology. 2015;29(4):1247-57.
274. Sharif O, Gawish R, Warszawska JM, Martins R, Lakovits K, Hladik A, et al. The triggering receptor expressed on myeloid cells 2 inhibits complement component 1q effector mechanisms and exerts detrimental effects during pneumococcal pneumonia. PLoS pathogens. 2014;10(6):e1004167.
275. Wu K, Byers DE, Jin X, Agapov E, Alexander-Brett J, Patel AC, et al. TREM-2 promotes macrophage survival and lung disease after respiratory viral infection. The Journal of experimental medicine. 2015;212(5):681-97.

276. Seno H, Miyoshi H, Brown SL, Geske MJ, Colonna M, Stappenbeck TS. Efficient colonic mucosal wound repair requires Trem2 signaling. Proceedings of the National Academy of Sciences of the United States of America. 2009;106(1):256-61.
277. Correale C, Genua M, Vetrano S, Mazzini E, Martinoli C, Spinelli A, et al. Bacterial sensor triggering receptor expressed on myeloid cells-2 regulates the mucosal inflammatory response. Gastroenterology. 2013;144(2):346-56 e3.
278. Jaitin DA, Adlung L, Thaiss CA, Weiner A, Li B, Descamps H, et al. Lipid-Associated Macrophages Control Metabolic Homeostasis in a Trem2-Dependent Manner. Cell. 2019;178(3):686-98 e14.
279. Goncalves LA, Rodrigues-Duarte L, Rodo J, Vieira de Moraes L, Marques I, Penha-Goncalves C. TREM2 governs Kupffer cell activation and explains belr1 genetic resistance to malaria liver stage infection. Proceedings of the National Academy of Sciences of the United States of America. 2013;110(48):19531-6.
280. Xiong X, Kuang H, Ansari S, Liu T, Gong J, Wang S, et al. Landscape of Intercellular Crosstalk in Healthy and NASH Liver Revealed by Single-Cell Secretome Gene Analysis. Molecular cell. 2019;75(3):644-60 e5.
281. Ramachandran P, Dobie R, Wilson-Kanamori JR, Dora EF, Henderson BEP, Luu NT, et al. Resolving the fibrotic niche of human liver cirrhosis at single-cell level. Nature. 2019;575(7783):512-8.
282. Nakao T, Ono Y, Dai H, Nakano R, Perez-Gutierrez A, Camirand G, et al. DNAX Activating Protein of 12 kDa/Triggering Receptor Expressed on Myeloid Cells 2 Expression by Mouse and Human Liver Dendritic Cells: Functional Implications and Regulation of Liver Ischemia-Reperfusion Injury. Hepatology. 2019;70(2):696-710.
283. Yao Y, Li H, Chen J, Xu W, Yang G, Bao Z, et al. TREM-2 serves as a negative immune regulator through Syk pathway in an IL-10 dependent manner in lung cancer. Oncotarget. 2016;7(20):29620-34.
284. Zhang X, Wang W, Li P, Wang X, Ni K. High TREM2 expression correlates with poor prognosis in gastric cancer. Human pathology. 2018;72:91-9.
285. Wang XQ, Tao BB, Li B, Wang XH, Zhang WC, Wan L, et al. Overexpression of TREM2 enhances glioma cell proliferation and invasion: a therapeutic target in human glioma. Oncotarget. 2016;7(3):2354-66.
286. Zhang H, Sheng L, Tao J, Chen R, Li Y, Sun Z, et al. Depletion of the triggering receptor expressed on myeloid cells 2 inhibits progression of renal cell carcinoma via regulating related protein expression and PTEN-PI3K/Akt pathway. International journal of oncology. 2016;49(6):2498-506.
287. Tang W, Lv B, Yang B, Chen Y, Yuan F, Ma L, et al. TREM2 acts as a tumor suppressor in hepatocellular carcinoma by targeting the PI3K/Akt/beta-catenin pathway. Oncogenesis. 2019;8(2):9.
288. Perugorria MJ, Esparza-Baquer A, Oakley F, Labiano I, Korosec A, Jais A, et al. Non-parenchymal TREM-2 protects the liver from immune-mediated hepatocellular damage. Gut. 2018.
289. Esparza-Baquer A, Labiano I, Sharif O, Agirre-Lizaso A, Oakley F, Rodrigues PM, et al. TREM-2 defends the liver against hepatocellular carcinoma through multifactorial protective mechanisms. Gut. 2020.
290. Hardie C, Green K, Jopson L, Millar B, Innes B, Pagan S, et al. Early Molecular Stratification of High-risk Primary Biliary Cholangitis. EBioMedicine. 2016;14:65-73.
291. Ma L, Hernandez MO, Zhao Y, Mehta M, Tran B, Kelly M, et al. Tumor Cell Biodiversity Drives Microenvironmental Reprogramming in Liver Cancer. Cancer cell. 2019;36(4):418-30 e6.
292. Mariotti V, Cadamuro M, Spirli C, Fiorotto R, Strazzabosco M, Fabris L. Animal models of cholestasis: An update on inflammatory cholangiopathies. Biochimica et biophysica acta Molecular basis of disease. 2019;1865(5):954-64.

293. Tag CG, Sauer-Lehnen S, Weiskirchen S, Borkham-Kamphorst E, Tolba RH, Tacke F, et al. Bile duct ligation in mice: induction of inflammatory liver injury and fibrosis by obstructive cholestasis. Journal of visualized experiments : JoVE. 2015(96).
294. Fouts DE, Torralba M, Nelson KE, Brenner DA, Schnabl B. Bacterial translocation and changes in the intestinal microbiome in mouse models of liver disease. Journal of hepatology. 2012;56(6):1283-92.
295. Xu J, Lee G, Wang H, Vierling JM, Maher JJ. Limited role for CXC chemokines in the pathogenesis of alpha-naphthylisothiocyanate-induced liver injury. American journal of physiology Gastrointestinal and liver physiology. 2004;287(3):G734-41.
296. Santamaria E, Rodriguez-Ortigosa CM, Uriarte I, Latasa MU, Urtasun R, Alvarez-Sola G, et al. The Epidermal Growth Factor Receptor Ligand Amphiregulin Protects From Cholestatic Liver Injury and Regulates Bile Acids Synthesis. Hepatology. 2019;69(4):1632-47.
297. Sachar M, Anderson KE, Ma X. Protoporphyrin IX: the Good, the Bad, and the Ugly. The Journal of pharmacology and experimental therapeutics. 2016;356(2):267-75.
298. Pose E, Sancho-Bru P, Coll M. 3,5-Diethoxycarbonyl-1,4-Dihydrocollidine Diet: A Rodent Model in Cholestasis Research. Methods in molecular biology. 2019;1981:249-57.
299. Fickert P, Stoger U, Fuchsbichler A, Moustafa T, Marschall HU, Weiglein AH, et al. A new xenobiotic-induced mouse model of sclerosing cholangitis and biliary fibrosis. The American journal of pathology. 2007;171(2):525-36.
300. Caviglia JM, Schwabe RF. Mouse models of liver cancer. Methods in molecular biology. 2015;1267:165-83.
301. Kim YO, Popov Y, Schuppan D. Optimized Mouse Models for Liver Fibrosis. Methods in molecular biology. 2017;1559:279-96.
302. Wallace MC, Hamesch K, Lunova M, Kim Y, Weiskirchen R, Strnad P, et al. Standard operating procedures in experimental liver research: thioacetamide model in mice and rats. Laboratory animals. 2015;49(1 Suppl):21-9.
303. Faustino-Rocha A, Oliveira PA, Pinho-Oliveira J, Teixeira-Guedes C, Soares-Maia R, da Costa RG, et al. Estimation of rat mammary tumor volume using caliper and ultrasonography measurements. Lab animal. 2013;42(6):217-24.
304. Perugorria MJ, Murphy LB, Fullard N, Chakraborty JB, Vyrla D, Wilson CL, et al. Tumor progression locus 2/Cot is required for activation of extracellular regulated kinase in liver injury and toll-like receptor-induced TIMP-1 gene transcription in hepatic stellate cells in mice. Hepatology. 2013;57(3):1238-49.
305. Uriarte I, Banales JM, Saez E, Arenas F, Oude Elferink RP, Prieto J, et al. Bicarbonate secretion of mouse cholangiocytes involves Na(+)-HCO(3)(-) cotransport in addition to Na(+)-independent Cl(-)/HCO(3)(-) exchange. Hepatology. 2010;51(3):891-902.
306. Isayama F, Hines IN, Kremer M, Milton RJ, Byrd CL, Perry AW, et al. LPS signaling enhances hepatic fibrogenesis caused by experimental cholestasis in mice. American journal of physiology Gastrointestinal and liver physiology. 2006;290(6):G1318-28.
307. Nytofte NS, Serrano MA, Monte MJ, Gonzalez-Sanchez E, Tumer Z, Ladefoged K, et al. A homozygous nonsense mutation (c.214C->A) in the biliverdin reductase alpha gene (BLVRA) results in accumulation of biliverdin during episodes of cholestasis. Journal of medical genetics. 2011;48(4):219-25.
308. Ye L, Liu S, Wang M, Shao Y, Ding M. High-performance liquid chromatography-tandem mass spectrometry for the analysis of bile acid profiles in serum of women with intrahepatic cholestasis of pregnancy. Journal of chromatography B, Analytical technologies in the biomedical and life sciences. 2007;860(1):10-7.
309. LeniLek M, Vecka M, Zizalova K, Vitek L. Comparison of simple extraction procedures in liquid chromatography-mass spectrometry based determination of serum 7alpha-hydroxy-4-cholesten-3-one, a surrogate marker of bile acid synthesis. Journal of chromatography B, Analytical technologies in the biomedical and life sciences. 2016;1033-1034:317-20.

310. Munoz-Garrido P, Marin JJ, Perugorria MJ, Urribarri AD, Erice O, Saez E, et al. Ursodeoxycholic acid inhibits hepatic cystogenesis in experimental models of polycystic liver disease. Journal of hepatology. 2015;63(4):952-61.
311. Khanna A, Jones DE. Novel strategies and therapeutic options for the management of primary biliary cholangitis. Therapeutic advances in gastroenterology. 2017;10(10):791-803.
312. Mariotti V, Strazzabosco M, Fabris L, Calvisi DF. Animal models of biliary injury and altered bile acid metabolism. Biochimica et biophysica acta Molecular basis of disease. 2018;1864(4 Pt B):1254-61.
313. Luo Z, Jegga AG, Bezerra JA. Gene-disease associations identify a connectome with shared molecular pathways in human cholangiopathies. Hepatology. 2018;67(2):676-89.
314. Rudraiah S, Moscovitz JE, Donepudi AC, Campion SN, Slitt AL, Aleksunes LM, et al. Differential Fmo3 gene expression in various liver injury models involving hepatic oxidative stress in mice. Toxicology. 2014;325:85-95.
315. Yu L, Liu X, Yuan Z, Li X, Yang H, Yuan Z, et al. SRT1720 Alleviates ANIT-Induced Cholestasis in a Mouse Model. Frontiers in pharmacology. 2017;8:256.
316. Isaacs-Ten A, Echeandia M, Moreno-Gonzalez M, Brion A, Goldson A, Philo M, et al. Intestinal microbiome-macrophage crosstalk contributes to cholestatic liver disease by promoting intestinal permeability. Hepatology. 2020.
317. Afonso MB, Rodrigues PM, Simao AL, Ofengeim D, Carvalho T, Amaral JD, et al. Activation of necroptosis in human and experimental cholestasis. Cell death & disease. 2016;7(9):e2390.
318. Afonso MB, Rodrigues PM, Simao AL, Gaspar MM, Carvalho T, Borralho P, et al. miRNA-21 ablation protects against liver injury and necroptosis in cholestasis. Cell death and differentiation. 2018;25(5):857-72.
319. Vucur M, Reisinger F, Gautheron J, Janssen J, Roderburg C, Cardenas DV, et al. RIP3 inhibits inflammatory hepatocarcinogenesis but promotes cholestasis by controlling caspase-8- and JNK-dependent compensatory cell proliferation. Cell reports. 2013;4(4):776-90.
320. Brenner C, Galluzzi L, Kepp O, Kroemer G. Decoding cell death signals in liver inflammation. Journal of hepatology. 2013;59(3):583-94.
321. Krishna-Subramanian S, Singer S, Armaka M, Banales JM, Holzer K, Schirmacher P, et al. RIPK1 and death receptor signaling drive biliary damage and early liver tumorigenesis in mice with chronic hepatobiliary injury. Cell death and differentiation. 2019;26(12):2710-26.
322. Nugent AA, Lin K, van Lengerich B, Lianoglou S, Przybyla L, Davis SS, et al. TREM2 Regulates Microglial Cholesterol Metabolism upon Chronic Phagocytic Challenge. Neuron. 2020;105(5):837-54 e9.
323. Renga B, Mencarelli A, Cipriani S, D'Amore C, Carino A, Bruno A, et al. The bile acid sensor FXR is required for immune-regulatory activities of TLR-9 in intestinal inflammation. PloS one. 2013;8(1):e54472.
324. Moriwaki K, Chan FK. Necroptosis-independent signaling by the RIP kinases in inflammation. Cellular and molecular life sciences : CMLS. 2016;73(11-12):2325-34.
325. Cannito S, Milani C, Cappon A, Parola M, Strazzabosco M, Cadamuro M. Fibroinflammatory Liver Injuries as Preneoplastic Condition in Cholangiopathies. International journal of molecular sciences. 2018;19(12).
326. Nagano T, Yamamoto K, Matsumoto S, Okamoto R, Tagashira M, Ibuki N, et al. Cytokine profile in the liver of primary biliary cirrhosis. Journal of clinical immunology. 1999;19(6):422-7.
327. Tabibian JH, O'Hara SP, Splinter PL, Trussoni CE, LaRusso NF. Cholangiocyte senescence by way of N-ras activation is a characteristic of primary sclerosing cholangitis. Hepatology. 2014;59(6):2263-75.
328. Honda Y, Yamagiwa S, Matsuda Y, Takamura M, Ichida T, Aoyagi Y. Altered expression of TLR homolog RP105 on monocytes hypersensitive to LPS in patients with primary biliary cirrhosis. Journal of hepatology. 2007;47(3):404-11.

329. Li J, Razumilava N, Gores GJ, Walters S, Mizuochi T, Mourya R, et al. Biliary repair and carcinogenesis are mediated by IL-33-dependent cholangiocyte proliferation. The Journal of clinical investigation. 2014;124(7):3241-51.
330. Sun Y, Zhang JY, Lv S, Wang H, Gong M, Du N, et al. Interleukin-33 promotes disease progression in patients with primary biliary cirrhosis. The Tohoku journal of experimental medicine. 2014;234(4):255-61.
331. Hol J, Wilhelmsen L, Haraldsen G. The murine IL-8 homologues KC, MIP-2, and LIX are found in endothelial cytoplasmic granules but not in Weibel-Palade bodies. Journal of leukocyte biology. 2010;87(3):501-8.
332. Konishi T, Schuster RM, Goetzman HS, Caldwell CC, Lentsch AB. Cell-specific regulatory effects of CXCR2 on cholestatic liver injury. American journal of physiology Gastrointestinal and liver physiology. 2019;317(6):G773-G83.
333. MacParland SA, Liu JC, Ma XZ, Innes BT, Bartczak AM, Gage BK, et al. Single cell RNA sequencing of human liver reveals distinct intrahepatic macrophage populations. Nature communications. 2018;9(1):4383.
334. Abshagen K, Konig M, Hoppe A, Muller I, Ebert M, Weng H, et al. Pathobiochemical signatures of cholestatic liver disease in bile duct ligated mice. BMC systems biology. 2015;9:83.
335. Georgiev P, Jochum W, Heinrich S, Jang JH, Nocito A, Dahm F, et al. Characterization of time-related changes after experimental bile duct ligation. The British journal of surgery. 2008;95(5):646-56.
336. Shirotani K, Hori Y, Yoshizaki R, Higuchi E, Colonna M, Saito T, et al. Aminophospholipids are signal-transducing TREM2 ligands on apoptotic cells. Scientific reports. 2019;9(1):7508.
337. Ye HL, Zhang JW, Chen XZ, Wu PB, Chen L, Zhang G. Ursodeoxycholic acid alleviates experimental liver fibrosis involving inhibition of autophagy. Life sciences. 2020;242:117175.
338. Meng F, Kennedy L, Hargrove L, Demieville J, Jones H, Madeka T, et al. Ursodeoxycholate inhibits mast cell activation and reverses biliary injury and fibrosis in Mdr2(-/-) mice and human primary sclerosing cholangitis. Laboratory investigation; a journal of technical methods and pathology. 2018;98(11):1465-77.
339. Ludwig JM, Zhang Y, Chamulitrat W, Stremmel W, Pathil A. Anti-inflammatory properties of ursodeoxycholyl lysophosphatidylethanolamide in endotoxin-mediated inflammatory liver injury. PloS one. 2018;13(5):e0197836.
340. Ovadia C, Perdones-Montero A, Fan HM, Mullish BH, McDonald JAK, Papacleovoulou G, et al. Ursodeoxycholic acid enriches intestinal bile salt hydrolase-expressing Bacteroidetes in cholestatic pregnancy. Scientific reports. 2020;10(1):3895.
341. Kim DJ, Yoon S, Ji SC, Yang J, Kim YK, Lee S, et al. Ursodeoxycholic acid improves liver function via phenylalanine/tyrosine pathway and microbiome remodelling in patients with liver dysfunction. Scientific reports. 2018;8(1):11874.
342. Tabibian JH, Trussoni CE, O'Hara SP, Splinter PL, Heimbach JK, LaRusso NF. Characterization of cultured cholangiocytes isolated from livers of patients with primary sclerosing cholangitis. Laboratory investigation; a journal of technical methods and pathology. 2014;94(10):1126-33.
343. O'Hara SP, Splinter PL, Trussoni CE, Gajdos GB, Lineswala PN, LaRusso NF. Cholangiocyte N-Ras protein mediates lipopolysaccharide-induced interleukin 6 secretion and proliferation. The Journal of biological chemistry. 2011;286(35):30352-60.
344. Tao Y, Wang M, Chen E, Tang H. Liver Regeneration: Analysis of the Main Relevant Signaling Molecules. Mediators of inflammation. 2017;2017:4256352.
345. Carpino G, Cardinale V, Folseraas T, Overi D, Grzyb K, Costantini D, et al. Neoplastic Transformation of the Peribiliary Stem Cell Niche in Cholangiocarcinoma Arisen in Primary Sclerosing Cholangitis. Hepatology. 2019;69(2):622-38.

346. Bergmann J, Muller M, Baumann N, Reichert M, Heneweer C, Bolik J, et al. IL-6 trans-signaling is essential for the development of hepatocellular carcinoma in mice. Hepatology. 2017;65(1):89-103.
347. Villanueva A, Luedde T. The transition from inflammation to cancer in the liver. Clinical liver disease. 2016;8(4):89-93.
348. Saviano A, Roehlen N, Virzi A, Roca Suarez AA, Hoshida Y, Lupberger J, et al. Stromal and Immune Drivers of Hepatocarcinogenesis. In: Hoshida Y, editor. Hepatocellular Carcinoma: Translational Precision Medicine Approaches. Cham (CH)2019. p. 317-31.
349. Di Ciaula A, Wang DQ, Molina-Molina E, Lunardi Baccetto R, Calamita G, Palmieri VO, et al. Bile Acids and Cancer: Direct and Environmental-Dependent Effects. Annals of hepatology. 2017;16(Suppl. 1: s3-105.):s87-s105.
350. Ma C, Han M, Heinrich B, Fu Q, Zhang Q, Sandhu M, et al. Gut microbiome-mediated bile acid metabolism regulates liver cancer via NKT cells. Science. 2018;360(6391).
351. Liu R, Zhao R, Zhou X, Liang X, Campbell DJ, Zhang X, et al. Conjugated bile acids promote cholangiocarcinoma cell invasive growth through activation of sphingosine 1-phosphate receptor 2. Hepatology. 2014;60(3):908-18.
352. Maroni L, Alpini G, Marzioni M. Cholangiocarcinoma development: the resurgence of bile acids. Hepatology. 2014;60(3):795-7.
353. Yang F, Huang X, Yi T, Yen Y, Moore DD, Huang W. Spontaneous development of liver tumors in the absence of the bile acid receptor farnesoid X receptor. Cancer research. 2007;67(3):863-7.
354. Kong B, Zhu Y, Li G, Williams JA, Buckley K, Tawfik O, et al. Mice with hepatocyte-specific FXR deficiency are resistant to spontaneous but susceptible to cholic acid-induced hepatocarcinogenesis. American journal of physiology Gastrointestinal and liver physiology. 2016;310(5):G295-302.
355. Erice O, Labiano I, Arbelaiz A, Santos-Laso A, Munoz-Garrido P, Jimenez-Aguero R, et al. Differential effects of FXR or TGR5 activation in cholangiocarcinoma progression. Biochimica et biophysica acta Molecular basis of disease. 2018;1864(4 Pt B):1335-44.
356. Filliol A, Schwabe RF. Contributions of Fibroblasts, Extracellular Matrix, Stiffness, and Mechanosensing to Hepatocarcinogenesis. Seminars in liver disease. 2019;39(3):315-33.
357. Ramachandran P, Iredale JP, Fallowfield JA. Resolution of liver fibrosis: basic mechanisms and clinical relevance. Seminars in liver disease. 2015;35(2):119-31.
358. Kim SM, Mun BR, Lee SJ, Joh Y, Lee HY, Ji KY, et al. TREM2 promotes Abeta phagocytosis by upregulating C/EBPalpha-dependent CD36 expression in microglia. Scientific reports. 2017;7(1):11118.
359. Garcia-Reitboeck P, Phillips A, Piers TM, Villegas-Llerena C, Butler M, Mallach A, et al. Human Induced Pluripotent Stem Cell-Derived Microglia-Like Cells Harboring TREM2 Missense Mutations Show Specific Deficits in Phagocytosis. Cell reports. 2018;24(9):2300-11.
360. Yao H, Coppola K, Schweig JE, Crawford F, Mullan M, Paris D. Distinct Signaling Pathways Regulate TREM2 Phagocytic and NFkappaB Antagonistic Activities. Frontiers in cellular neuroscience. 2019;13:457.
361. Ramachandran P, Pellicoro A, Vernon MA, Boulter L, Aucott RL, Ali A, et al. Differential Ly-6C expression identifies the recruited macrophage phenotype, which orchestrates the regression of murine liver fibrosis. Proceedings of the National Academy of Sciences of the United States of America. 2012;109(46):E3186-95.
362. Zhong L, Xu Y, Zhuo R, Wang T, Wang K, Huang R, et al. Soluble TREM2 ameliorates pathological phenotypes by modulating microglial functions in an Alzheimer's disease model. Nature communications. 2019;10(1):1365.
363. Schlepckow K, Monroe KM, Kleinberger G, Cantuti-Castelvetri L, Parhizkar S, Xia D, et al. Enhancing protective microglial activities with a dual function TREM2 antibody to the stalk region. EMBO molecular medicine. 2020;12(4):e11227.

364. Price BR, Sudduth TL, Weekman EM, Johnson S, Hawthorne D, Woolums A, et al. Therapeutic Trem2 activation ameliorates amyloid-beta deposition and improves cognition in the 5XFAD model of amyloid deposition. Journal of neuroinflammation. 2020;17(1):238.
365. Katzenelenbogen Y, Sheban F, Yalin A, Yofe I, Svetlichnyy D, Jaitin DA, et al. Coupled scRNA-Seq and Intracellular Protein Activity Reveal an Immunosuppressive Role of TREM2 in Cancer. Cell. 2020;182(4):872-85 e19.
366. Molgora M, Esaulova E, Vermi W, Hou J, Chen Y, Luo J, et al. TREM2 Modulation Remodels the Tumor Myeloid Landscape Enhancing Anti-PD-1 Immunotherapy. Cell. 2020;182(4):886-900 e17.

APPENDIX

Publications wthin the PhD

Esparza-Baquer A, **Labiano I**, Sharif O, Agirre-Lizaso A, Oakley F, Rodrigues PM, Zhuravleva E, O'Rourke CJ, Hijona E, Jimenez-Agüero R, Riaño I, Landa A, La Casta A, Zaki MYW, Munoz-Garrido P, Azkargorta M, Elortza F, Vogel A, Schabbauer G, Aspichueta P, Andersen JB, Knapp S, Mann DA, Bujanda L, Maria Banales JM, Perugorria MJ. TREM-2 defends the liver against hepatocellular carcinoma through multifactorial protective mechanisms. **Gut** 2020. gutjnl-2019-319227. *Shared first authorship.*

Maroni L, Pinto C, Giordano DM, Saccomanno S, Banales JM, Spallacci D, Albertini MC, Orlando F, Provinciali M, Milkiewicz M, Melum E, **Labiano I**, Milkiewicz P, Rychlicki C, Trozzi L, Scarpelli M, Benedetti A, Svegliati Baroni G, Marzioni M. Aging-Related Expression of Twinfilin-1 Regulates Cholangiocyte Biological Response to Injury. **Heaptology**.2019 Sep;70(3):883-898.

Perugorria MJ, Olaizola P, **Labiano I**, Esparza-Baquer A, Marzioni M, Marin JJG, Bujanda L, Banales JM. Wnt–β-catenin signalling in liver development, health and disease. **Nat Rev Gastroenterol Hepatol**. 2019 Feb;16(2):121-136. *Review.*

Perugorria MJ, Esparza-Baquer A, Oakley O, **Labiano I**, Korosec A, Jais A, Mann J, Tiniakos D, Santos-Laso A, Arbelaiz A, Gawish R, Sampedro A, Fontanellas A, Hijona E, Jiménez-Agüero R, Esterbauer H, Stoiber D, Bujanda L, Banales JM, Knapp S, Sharif O, and Mann DA. Non-parenchymal TREM-2 protects the liver from immune-mediated hepatocellular damage. **Gut** 2018. pii: gutjnl-2017-314107.

- Nature Reviews Gastroenterology and Hepatology did an editorial about this paper: Ray K. Liver: A protective role for TREM2 in liver injury. **Nat Rev Gastroenterol Hepatol**. 201815(3):130-131. *Editorial*

Erice O, **Labiano I**, Arbelaiz A, Santos-Laso A, Munoz-Garrido P, Jimenez-Agüero R, Olaizola P, Caro-Maldonado A, Martín-Martín N, Carracedo A, Lozano E, Marin JJ, O'Rourke CJ, Andersen JB, Llop J, Gómez-Vallejo V, Padro D, Martin A, Marzioni M, Adorini L, Trauner M, Bujanda L, Perugorria MJ, Banales JM. Differential effects of FXR or TGR5 activation in cholangiocarcinoma progression. **Biochim Biophys Acta Mol Basis Dis**. 2018 Apr;1864(4 Pt B):1335-1344.

Perugorria MJ, **Labiano I**, Esparza-Baquer A, Marzioni M, Marin JJ, Bujanda L, Banales JM. Bile Acids in Polycystic Liver Diseases: Triggers of Disease Progression and Potential Solution for Treatment. **Dig Dis**. 2017;35(3):275-281. *Review*.

Esparza-Baquer A, **Labiano I**, Bujanda L, Perugorria MJ, Banales JM. MicroRNAs in cholangiopathies: Potential diagnostic and therapeutic tools. **Clin Res Hepatol Gastroenterol**. 2016 40(1):15-27. *Review*.